Enantioenriched Cyclic Boronates as Versatile Building Blocks: Synthesis, Mechanism and Applications

by

Helen Clement

A thesis submitted in partial fulfillment of the requirements for the degree of

Doctor of Philosophy

Department of Chemistry
University of Alberta

Abstract

Since the discovery and development of the famed Suzuki-Miyaura cross-coupling reaction, organoboron compounds have gained increasing attention as small molecule building blocks in organic synthesis and drug discovery efforts. In this regard, enantioenriched alkyl boronic esters are ideal synthetic intermediates due to their low toxicity, configurational stability and versatile reactivity. As a result, catalytic enantioselective approaches to boronic esters have seen remarkable advancements within the past decade. Although a variety of enantioenriched boronic ester scaffolds continue to accumulate in the organoboron literature, the number of catalytic methodologies to afford linear, hydrocarbon-based scaffolds with limited functionality other than the boronate group has become pervasive. In this regard, this thesis focuses on the development of methodologies to access novel enantioenriched cyclic and heterocyclic chiral boronates with increased functionality. The products obtained have potential to be versatile building blocks in medicinal chemistry.

Chapter 2 describes efforts to expand the substrate scope of a powerful methodology previously reported by the Hall Group, namely the borylative migration of enol sulfonates. To-date the borylative migration had only been applied to the synthesis of pyranyl and piperidinyl allylic boronates. The substrate scope expansion of the palladium-catalyzed enantioselective borylative migration reaction is explored for five different novel electrophiles. An optimization for the 7-membered nitrogen-containing azepane ring is achieved. The applicability of the allylic boronate product is displayed in the synthesis of a small set of novel α-hydroxyalkyl dehydroazepanes upon aldehyde allylboration. The utility of the developed approach is portrayed in the synthesis of the azepane derivative of the biologically active piperidine-based amino alcohol, β-conhydrine.

Considering the difficulty in expanding the borylative migration to new electrophiles, a better mechanistic understanding of this reaction is desirable. In this regard, Chapter 3 describes efforts to decipher a reasonable catalytic pathway by which the unique borylative migration reaction of pyranyl and piperidinyl electrophiles may occur using a combined experimental and computational approach. In a collaborative effort with an expert of computational chemistry, a detailed discussion of the potential steps in the catalytic cycle is presented. Key insights throughout this study suggest a rate-limiting oxidative addition, a substrate-controlled palladium hydride alkene isomerization and that the amine base has multiple roles in the reaction. In the end, a new mechanistic perspective of the borylative migration reaction is provided.

The focus of Chapter 4 moves to the synthesis of four membered rings, specifically the synthesis of novel cyclobutylboronates. An optimization of the first catalytic enantioselective approach to tertiary cyclobutylboronates is described, using copper-catalyzed borylation of α,β-disubstituted cyclobutenones. The project includes the development of a novel reliable synthetic approach to the cyclobutenone substrates. In a collaborative effort with chemists from Pfizer Inc., a high-throughput-ligand screening study reveals an appropriate starting point for the challenging borylation of interest. Optimization of the conjugate borylation allows a general approach to enantioenriched tertiary cyclobutylboronates. The utility of the products is displayed by chemoselective functional group manipulations of both the ketone and boronic ester moieties.

Preface

Chapter 2 (omitting Section 2.3) of this thesis was published as H. A. Clement, D. G. Hall, "Synthesis of α-hydroxyalkyl dehydroazepanes *via* catalytic enantioselective borylative migration of an enol nonaflate" *Tetrahedron Letters* **2018**, *59*, 4334–4339. I was responsible for the reaction optimization, study of the substrate scope, data collection, analysis and writing of the supporting information. T. Adele (NSERC Undergraduate Student Research Award scholarship recipient) was an undergraduate student under my supervision and assisted in the synthesis of some precursors relevant to Chapter 2, all of which are specified in Chapter 2. I also wrote the manuscript with assistance from D. G. Hall. D. G. Hall was the supervisory author and was involved with concept formation and manuscript composition.

Chapter 3 is a collaborative effort with Dr. Claude Y. Legault from Université de Sherbrooke. I was responsible for all of the experimental research described in Chapter 3, while C. Y. Legault was responsible for all DFT calculations regarding the borylative migration. I was responsible for data collection and compound characterization. I wrote the manuscript with assistance from D. G. Hall and C. Y. Legault. C. Y. Legault and D. G. Hall were the supervisory authors and were involved with concept formation and manuscript composition.

Chapter 4 of this thesis was published as H. A. Clement, M. Boghi, R. M. McDonald, L. Bernier, J. W. Coe, W. Farrell, C. J. Helal, M. R. Reese, N. W. Sach, J. C. Lee, D. G. Hall "High-Throughput Ligand Screening Enables the Enantioselective Conjugate Borylation of Cyclobutenones to Access Synthetically Versatile Tertiary Cyclobutylboronates" *Angew. Chem. Int. Ed.* **2019**, *58*, 18405–18409. I was the sole investigator responsible for the reaction

optimization and product functionalization. I was also responsible for the development of half of the substrate scope, data collection, analysis and writing of the supporting information with assistance from Rory McDonald, MSc. The examples that R. McDonald was responsible for is specified in each table. I assisted in writing the manuscript in collaboration with D. G. Hall and J. C. Lee. D. G. Hall and J. C. Lee were the supervisory authors and were involved with project conception and initiation.

Acknowledgements

The past five years have been a very fulfilling and rewarding experience at the University of Alberta. There are a number of people that have had incredibly positive impacts on my experience as a PhD candidate, and for which I am very grateful.

Firstly I would like to acknowledge my supervisor Prof. Dennis Hall for his inspirational interest in fundamental organic chemistry, his patience and his commitment throughout my degree. He always puts his students' learning first and goes above and beyond the standard requirements of running an academic lab. He has believed in my capabilities when I've been in doubt and has offered more opportunities to learn and grow as a scientist than I ever expected. Attending numerous well-organized group meetings, conferences and involvement in collaborative research projects were all highlights that I will remember fondly when looking back on this experience.

I also extend my gratitude to the collaborators who have made two of the projects described in this thesis possible. I am particularly indebted to Dr. Jack C. Lee, Dr. Christopher J. Helal, Mr. Matthew Reese and Prof. Claude Y. Legault for taking the time out of their busy schedules for meetings and emails regarding our collaborative projects. These projects would not have come to fruition without their support and continued interest.

I would like to acknowledge my Supervisory Committee and Examination Committee members: Prof. Frederick West, Prof. Rylan Lundgren, Prof. James Takacs, Prof. Mariusz Klobukowski, Prof. Florence Williams and Prof. Eric Rivard. Their advice and insight have been very helpful and I feel I have benefitted greatly from their generous contributions.

My appreciation is also extended to the excellent administrative and research service staff at the University of Alberta. I am grateful for the help of the NMR, mass spectrometry, analytical labs, glass shop, chemistry shipping/receiving and the storeroom for their continued contributions. I would particularly acknowledge Mark Miskolzie for his NMR help and Ed Fu for all of his help with chiral HPLC purification and characterization.

Of course, I must thank all of the awesome Hall Group members and friends in the department that have helped make these five years an exceptional experience. I would like to specifically thank Carmanah Hunter and Michele Boghi – they both have offered continued and vital support and I am very grateful to have met them. I have had the opportunity to work with exceptional group members and would like to further acknowledge Timothy Morgan, Xiaobin Mo, Samantha Kwok, Jason Rygus, Carl Estrada, Hwee Ting Ang and Rory McDonald. I would also like to thank Jeffrey Wong, Vitor Cunha, Ryan Sweeney and Jeremy Nortoff for many refreshing discussions and their continued support.

Finally I would like to recognize my parents, Pierre and Sarah Clement and my brothers Nicky and Sam Clement for their interest and understanding over the past five years. Thanks to my family, I have had the foundational support to be able to take on demanding challenges and follow my genuine interests. Thank you.

Table of Contents

Chapter 1 : Cyclic Chiral Boronates as Versatile Synthetic Building Blocks 1

1.1 Chiral boronic esters as synthetic intermediates 1

1.1.1 Chirality in medicinal chemistry 1

1.1.2 Introduction to boronic esters and common protecting groups 2

1.2 Catalytic enantioselective approaches to cyclic boronates 4

1.2.1 The increasing influence of organoboronates in the literature 4

1.2.2 Borylation of non-polarized alkenes 5

1.2.3 Borylation of electron-deficient alkenes 16

1.2.4 Borylation methods to afford cyclic allylic boronates 19

1.3 Synthetic applications of chiral boronic esters 25

1.3.1 The unique reactivity of organoboron compounds 25

1.3.2 Carbon-carbon bond forming reactions 26

1.3.3 Oxidation methods – oxygenation and amination 30

1.3.4 Protodeboronation 32

1.4 Thesis objective 32

1.5 References 34

Chapter 2 : Expanding of the Substrate Scope of the Borylative Migration 40

2.1 Introduction 40

2.2 Objective 42

2.3 Initial screening of new alkenyl nonaflate substrates 43

2.3.1 Synthesis of the alkenyl nonaflate starting materials 43

2.3.2 Initial borylative migration results of the alkenyl nonaflate derivatives 46

2.4 Synthesis of α-hydroxyalkyl dehydroazepanes *via* catalytic enantioselective borylative migration of a dehydroazepanyl nonaflate 50

2.4.1 Overview of synthetic approaches to azepane scaffolds and their precedence in medicinal chemistry 50

2.4.2 Optimization of the borylative migration reaction conditions 53

2.4.3 Substrate scope of the aldehyde allylboration with **2-14** 58

2.4.4 Determination of the absolute and relative stereochemistry of the α-hydroxyalkyl dehydroazepanes 61
2.4.5 Synthesis of the 7-membered ring analogue of β-conhydrine 65
2.5 Summary 66
2.6 Experimental 67
2.6.1 General information 67
2.6.2 Procedure and characterization of alkenyl nonaflates **2-5**, **2-7**, **2-8**, **2-10** 69
2.6.3 General procedure A – racemic borylative migration 75
2.6.4 General procedure B – enantioselective borylative migration 75
2.6.5 Initial borylative migration results of nonaflates **2-5**, **2-6** and **2-7b** 76
2.6.6 General procedure C: *N*-protection of 4-perhydroazepinone precursors 78
2.6.7 Characterization of the *N*-protection of 4-perhydroazepinone precursors 79
2.6.8 General procedure D: synthesis of azepenyl nonaflates 83
2.6.9 Characterization of allylboration products **2-32** to **2-35** 91
2.6.10 Racemic borylative migration for product characterization of **2-14**, **2-36** and **2-37** .. 94
2.6.11 General procedure E: enantioselective borylative migration–aldehyde allylboration sequence 96
2.6.12 Separation and characterization of the diastereomers of compound **2-39** 100
2.6.13 Synthesis of HCl salt **2-41** 102
2.6.14 General procedure F: synthesis of carbamates **2-41a**, **2-42b** and **2-43** 103
2.6.15 Synthesis of HCl salt **2-45**: the azepane derivative of β-conhydrine 105
2.7 References 108
Chapter 3 : Mechanistic Investigations of the Palladium-Catalyzed Borylative Migration Reaction 111
3.1 Introduction 111
3.2 Plausible pathways of the borylative migration reaction 116
3.2.1 Overview of hydropalladation and Miyaura borylation pathways 116
3.2.2 Feasibility of the hydropalladation pathway 118
3.2.3 Feasibility of the Miyaura borylation pathway 119

3.3 Borylation of the alkenyl nonaflate....121
3.3.1 Cationic vs neutral palladium pathway 121
3.3.2 Synthesis of the pyranyl alkenyl iodide.... 122
3.3.3 Borylative migration with the alkenyl iodide substrate.... 123
3.3.4 Effect of iodide additive 125
3.3.5 DFT calculations of the borylation step 127
3.3.6 Probing for a dissociative Pd-H source 129
3.4 Alkene isomerization....131
3.4.1 Protic *vs* hydridic pathways.... 131
3.4.2 Influence of the heteroatom.... 133
3.4.3 Reductive elimination and product release.... 138
3.5 Kinetic studies....139
3.5.1 Method development 139
3.5.2 Reaction orders of the reagents 142
3.5.3 Kinetics results of the catalyst.... 146
3.5.4 Summary of kinetics data to-date 148
3.6 Effect and proposed roles of the base....149
3.6.1 Dependence of the enantioselectivity on the base.... 149
3.6.2 Kinetic resolution of the cationic palladium hydride **Int-II-C**.... 150
3.6.3 Conformational change from Taniaphos amine protonation.... 154
3.7 Proposed catalytic cycle....155
3.8 Mechanistic considerations for the novel electrophiles in Chapter 2....157
3.8.1 Correlating a new mechanistic understanding with experimental observations.... 157
3.8.2 A precautionary note from the optimization of the azepanyl system.... 157
3.8.3 Complex mixtures with the methylated nonaflate.... 158
3.8.4 Analysis of the potential reduction mechanisms of the alkenyl nonaflate 159
3.9 Summary....161
3.10 Experimental....162
3.10.1 General information.... 162

3.10.2 Synthesis of borylative migration substrates 163
3.10.3 General procedure A: enantioselective borylation migration 168
3.10.4 General procedure B: racemic borylative migration 169
3.10.5 Characterization of allylic and alkenyl boronates 170
3.10.6 General procedure for the kinetic experiments 174
3.10.7 Details of the DFT calculations 176
3.11 References 178
Chapter 4 : Enantioselective Conjugate Borylation to Access Synthetically Versatile Cyclobutylboronates 183
4.1 Introduction 183
4.2 Project objective 187
4.3 Synthesis of unsymmetrical α,β-unsaturated cyclobutenones 187
4.3.1 Developed procedure 187
4.3.2 Acetonitrile activation – Jiao's [2+2] approach to cyclobutenones 191
4.4 Optimization of the conjugate borylation reaction 192
4.4.1 High throughput ligand screening results 192
4.4.2 Optimization of the alcohol and base 197
4.4.3 Optimization of the solvent 198
4.4.4 Brief screening of the copper source, ligand and diboron reagent 199
4.5 Substrate scope 200
4.5.1 Electronic and steric effects of the β-aryl ring 202
4.5.2 α-Alkyl and β-alkyl variation 202
4.5.3 *para* Nitrile substrate: proposals for the observed alkene reduction 203
4.6 Functionalization of cyclobutylboronate 4-24 204
4.6.1 Potential for keto-cyclobutylboronates as versatile synthetic building blocks 204
4.6.2 Ketone functionalization 205
4.6.3 Boron oxidation 208
4.6.4 Boron to carbon bond formation to afford carbon quaternary centers 209
4.6.5 Protodeboronation 212

4.6.6 Summary of successful applications 213
4.7 Proposed rational for the observed diastereoselectivity 214
4.8 Conjugate borylation of cyclobutenoates 216
4.8.1 Project design 216
4.8.2 Development of a novel cyclobutenoate substrate 217
4.8.3 Initial conjugate borylation results 218
4.9 Summary 219
4.10 Experimental 220
4.10.1 General methods 220
4.10.2 General procedure A: synthesis of α,β-disubstituted cyclobutenones (Table 4-1) 221
4.10.3 Characterization of the α,β-disubstituted cyclobutenones **4-1** to **4-19** 223
4.10.4 Synthesis of tosyl indole aryl acetylene **4-21** 233
4.10.5 Synthesis of dialkyl cyclobutanone **4-23** 235
4.10.6 HTS screening procedure and analysis 237
4.10.7 General procedure B: enantioselective cyclobutenone conjugate borylation 238
4.10.8 Characterization of the cyclobutylboronate products **4-24** to **4-42** 239
4.10.9 Ketone functionalization products 254
4.10.10 Products from boron functionalizations 258
4.10.11 Synthesis of cyclobutenoate substrates 269
4.10.12 Borylated benzhydrol ester 272
4.11 References 273
Chapter 5 : Conclusions and Future Perspectives 279
Bibliography 283
Appendix 1 : Selected copies of NMR spectra 300
Appendix 2 : Select chromatograms for HPLC measurements 332
Appendix 3 : X-ray crystal structure report 340

List of Tables

Table 2-1. Synthesis of azepanyl nonaflate derivatives. 53

Table 2-2. Optimization of the nitrogen protecting group (PG). 55

Table 2-3. Optimization of the reaction solvent. 56

Table 2-4. Optimization of the base. 57

Table 2-5. Brief screening of the ligand and temperature. 58

Table 2-6. Scope of the borylative migration, aldehyde allylboration sequence. 60

Table 3-1. Borylative migration attempts with alkenyl iodide **3-9**. 125

Table 3-2. Effect of Bu_4NI additive in the reaction. 126

Table 3-3. Probing a dissociative alkene isomerization pathway. 130

Table 3-4. Effect of the heteroatom on the product distribution. 134

Table 3-5. Effect of the base on the reaction. 150

Table 4-1. Substrate scope for the synthesis of α,β-disubstituted cyclobutenones. 190

Table 4-2. List of ligands that led to no observable conversion of **4-1**. 193

Table 4-3. List of ligands that led to observable conversion of **4-1**. 195

Table 4-4. Variation of the alcohol and base. 197

Table 4-5. Variation of the solvent. 198

Table 4-6. Variation of the copper source, ligand and diboron reagent. 200

Table 4-7. Substrate scope of the stereoselective conjugate borylation. 201

Table 4-8. Optimization of the ketone reduction to obtain the boryl alcohol epimer. 206

List of Figures

Figure 1-1. Chiral boronic esters as building block templates to increase chemical complexity..... 2

Figure 1-2. Brief overview of organoboron compounds (a) oxygen-containing organoboron nomenclature (b) common boron protecting groups. 3

Figure 1-3. The number of references provided by Scifinder that were found containing the concept "enantioselective borylation" per year. 4

Figure 1-4. General representation of the borylation process to obtain cyclic boronates. 5

Figure 1-5. Directed catalytic asymmetric hydroboration developed by Takacs and co-workers. ... 7

Figure 1-6. (a) Hydroboration of cyclic dienes (b) explanation of the observed regioselectivity..... 8

Figure 1-7. Simplified catalytic cycle of copper-catalyzed borylations with diboron reagents. 10

Figure 1-8. The regio- and stereoselectivity possibilities of allylic boronates. 20

Figure 1-9. The β-alkoxy elimination step in the copper-catalyzed allylic borylation..... 20

Figure 1-10. (a) Enantioconvergent copper-catalyzed allylic borylation (b) source of the observed enantioconvergency. 21

Figure 1-11. Brief overview of (a) boronic ester reactivity and (b) synthetic transformations..... 26

Figure 1-12. Allylboration of α-substituted enantioenriched allylic boronates..... 27

Figure 1-13. The traditional Matteson homologation of boronic esters. 27

Figure 1-14. General mechanistic steps of the Zweifel olefination of boronic esters. 28

Figure 1-15. (a) The general palladium-catalyzed Suzuki-Miyaura cross-coupling reaction of alkylboronates (b) selected examples of alkylboronate coupling substrates. 30

Figure 1-16. Simplified overview of stereospecific oxygenation and amination of boronic esters. 31

Figure 1-17. Proposed stereospecificity of Aggarwal's protodeboronation of benzylic substrates. 32

Figure 2-1. Catalytic enantioselective borylative migration for the preparation of various piperidine and pyran derivatives 40

Figure 2-2. Previously published applications of piperidine **2-4** for the syntheses of bioactive molecules. 41

Figure 2-3. Novel nonaflates targeted for the borylative migration reaction screening. 43

Figure 2-4. Examples of azepane-containing natural products and drugs. 51

Figure 2-5. Common synthetic approaches to azepane scaffolds. 52

Figure 2-6. The potential competing transition states during the aldehyde allylboration step with aliphatic aldehydes. 61

Figure 2-7. Detailed chart of the 2D correlations of carbamates **2-42a** and **2-42b** for stereochemical assignment of their relative configurations. 65

Figure 3-1. (a) Summary of the borylative migration reaction (b) mechanistic proposal from the original report. 112

Figure 3-2. (a) Miyaura borylation with pinacolborane and proposed catalytic cycles by (b) Masuda (c) Lin and Marder and their co-workers. 114

Figure 3-3. The two general mechanistic pathways under consideration. 117

Figure 3-4. Potential neutral and cationic borylation pathways. 122

Figure 3-5. Formation of alkenyl iodide **3-9**. 126

Figure 3-6. General representation of the enantiodetermining σ-bond metathesis step. 131

Figure 3-7. Comparison of the β-hydride elimination in the pyranyl (left) and cyclohexyl (right) systems. 137

Figure 3-8. Formation of **3-5** over time using the conditions in Scheme 3-10. 140

Figure 3-9. Reaction profile for the standard reaction conditions used for kinetics..... 141

Figure 3-10. Reaction profiles for the doubling of concentration of (a) HBpin and (b) $PhNMe_2$. 143

Figure 3-11. Rate dependence of alkenyl nonaflate **3-4**. 146

Figure 3-12. Consumption profile of **3-4** with 3 mol% and 6 mol% $Pd_2(dba)_3 \bullet CHCl_3$. 147

Figure 3-13. Consumption of alkenyl nonaflate **3-4** with 0.3 mol% and 0.6 mol% $Pd_2(dba)_3 \bullet CHCl_3$. 148

Figure 3-14. Hayashi's asymmetric Heck arylation (a) conditions (b) mechanistic steps. 152

Figure 3-15. Kinetic resolution model to rationalize the effect of the base on the *ee*. 153

Figure 3-16. Proposed mechanism of the borylative migration. 156

Figure 3-17. Generalized summary of the results in Section 2.3. 157

Figure 3-18. Possible borylated products from the methylated nonaflate. 159

Figure 4-1. Examples of stereochemically complex cyclobutane-containing natural products and pharmaceutical drugs. 183

Figure 4-2. Stoichiometric approaches to enantioenriched cyclobutylboronates. 185

Figure 4-3. Catalytic enantioselective approaches to cyclobutylboronates. 186

Figure 4-4. Envisioned conjugate borylation of α,β-disubstituted cyclobutenones. 187

Figure 4-5. Summary of HTS results for ligand optimization. 196

Figure 4-6. Potential rational for alkene reduction by (a) β-borylation or (b) α-borylation. 204

Figure 4-7. Recently reported catalytic enantioselective approaches to trisubstituted cyclobutanones. 205

Figure 4-8. (a) Rh-catalyzed addition to *p*-NO_2-benzaldehyde (b) confirmation of the relative stereochemistry. 210

Figure 4-9. Summary of successful synthetic applications of **4-24**. 214

Figure 4-10. General mechanistic steps for the conjugate borylation of ketones. 215

Figure 4-11**.** Proposed stereochemical model of the proto-decupration step. 216

Figure 4-12. Project design for the conjugate borylation of cyclobutenoates. 217

List of Schemes

Scheme 1-1. Original catalytic enantioselective hydroboration with Wilkinson's catalyst. 6

Scheme 1-2. Examples of copper-catalyzed hydroboration of heterocyclic substrates (a) borylative dearomatization (b) 2*H* chromene hydroboration. 9

Scheme 1-3. Examples of copper-catalyzed carboboration methodologies with intermolecular trapping. 11

Scheme 1-4. Copper-catalyzed intramolecular borylative cyclization. 12

Scheme 1-5. Tandem hydroboration-borylative cyclization. 13

Scheme 1-6. Examples of diboration conditions developed by Morken and co-workers. 15

Scheme 1-7. Enantioselective aminoboration of cyclic strained alkenes. 16

Scheme 1-8. (a) Metal-free conjugate borylation (b) formation of the chiral nucleophilic boron source. 17

Scheme 1-9. Copper-catalyzed conjugate borylation conditions reported by Shibasaki and co-workers. 18

Scheme 1-10. Conjugate borylation of indole-2-carboxylates. 19

Scheme 1-11. Copper-catalyzed allylic borylation to access secondary and tertiary cyclic boronates. 22

Scheme 1-12. Hall and co-workers' hetero-Diels-Alder approach to dihydro-pyranyl allylic boronates. 23

Scheme 1-13. Borylative migration approach to pyranyl and piperidinyl allylic boronates. 24

Scheme 2-1. Multigram-scale borylative migration-allylboration sequence. 42

Scheme 2-2. Proposed opportunities for expansion of the borylative migration substrate scope. .. 43

Scheme 2-3. Previously reported syntheses of pyran and piperidine alkenyl sulfonates. 44

Scheme 2-4. Synthesis of nonaflates **2-5** and **2-6**. 45

Scheme 2-5. Synthesis of azocanyl nonaflate **2-7**. 45

Scheme 2-6. Synthesis of methyl and ester substituted nonaflates **2-6** and **2-12**. 46

Scheme 2-7. Attempted borylative migration of 5-membered alkenyl nonaflate **2-5**. 47

Scheme 2-8. Initial borylative migration result of the azepane scaffold. 48

Scheme 2-9. Borylative migration attempt of 8-membered azocanyl nonaflate **2-7**. 49

Scheme 2-10. Initial borylative migration results of (a) methylated nonaflate **2-8** and (b) ethyl ester nonaflate **2-12**. 50

Scheme 2-11. (a) Confirmation of the stereochemistry of **2-14** (b) rationale of the stereochemistry of allylic boronate **2-14**. 62

Scheme 2-12. Synthesis of carbamates and coupling constant analysis. 63

Scheme 2-13. Synthesis of compound 2-45; the azepane derivative of β-conhydrine. 66

Scheme 3-1. D-labelling study with D-Bpin. 119

Scheme 3-2. Energy diagram of the oxidative addition process. 120

Scheme 3-3. Synthesis of alkenyl iodide **3-9**. 123

Scheme 3-4. Subjection of alkenyl iodide **3-9** to Masuda's borylation conditions. 125

Scheme 3-5. Energy diagram of the σ-bond metathesis process. 128

Scheme 3-6. Comparison of hydridic and protic alkene isomerization pathways. 133

Scheme 3-7. Synthesis of previously unreported alkenyl nonaflates. 134

Scheme 3-8. Alkene isomerization for the cyclohexyl manifold. 135

Scheme 3-9. Proposed D-labelling experiment to explain the racemic cyclohexyl allylic boronate. 137
Scheme 3-10. DFT calculations of the product release of allylic boronate **3-5**. 138
Scheme 3-11. Initial conditions for the kinetic profiling of pyranyl nonaflate **3-2**. 140
Scheme 3-12. Optimized conditions used for direct NMR-based kinetic profiling of the borylative migration. 141
Scheme 3-13. Evidence of the importance for the amine of Taniaphos and potential reasoning. 155
Scheme 3-14. Proposals for the observed reduced products by (a) protodeboronation (b) inversion of regioselectivity of the transmetallation or (c) protodematalation. 160
Scheme 4-1. Literature precedence of (a) ketenium 2+2 cycloaddition with phenylacetylene and hydrolysis (b) cyclobutenone alkene isomerization. 188
Scheme 4-2. Synthesis of the tosyl indole acetylene precursor. 190
Scheme 4-3. (a) [2+2] Cycloaddition of acetonitrile reported by Jiao and co-workers (b) application of Jiao's method for the synthesis of dialkyl cyclobutenone **4-23**. 192
Scheme 4-4. Diastereoselective ketone reduction with L-selectride and ORTEP of ester **4-44**. .. 206
Scheme 4-5. Chemoselective Grignard addition of **4-24**. 207
Scheme 4-6. Oxygenation attempts of (a) conjugate borylation product **4-24** (b) boryl alcohol **4-43**. 208
Scheme 4-7. Zweifel olefination and acetylation of boryl ketal **4-52**. 211
Scheme 4-8. (a) Optimization of the elimination step (b) optimized process for acetylene **4-57**. 212
Scheme 4-9. (a) Protodeboronation of **4-24** (b) synthesis of the *syn* diastereomer for confirmation of relative stereochemistry. 213

Scheme 4-10. Epimerization control experiment. 215

Scheme 4-11. Synthesis of cyclobutenoate starting material. 218

Scheme 4-12. Initial (a) racemic and (b) enantioselective conjugate borylation results of cyclobutenoate **4-63**. 219

Scheme 5-1. Opportunities for further functionalization of the enantioenriched allylic boronic ester. 280

Scheme 5-2. Potential diversification of the borylative migration. 281

Scheme 5-3. Avenues for expansion of the developped conjugate borylation reaction. 282

List of Abbreviations

A	Angstrom
AA	Acetic acid
Ac	Acetyl
AIBN	Azobisisobutyronitrile
APAO	acetyl-protected aminomethyl oxazoline
aq.	Aqueous
Ar	Aryl
BARF	Tetrakis[3,5-bis(trifluoromethyl)phenyl]borate
BDPP	2,4-Bis(diphenylphosphino)pentane
BINAP	(1,1′-Binaphthalene-2,2′-diyl)bis(diphenylphosphine)
BINOL	1,1′-Bi-2-naphthol
Bn	Benzyl
Boc	*tert*-Butyloxycarbonyl
br	Broad
Bz	Benzoyl
calcd	Calculated
cat.	Catalytic
cat	Catechol
Cbz	Benzyl chloroformate
cm^{-1}	Wavenumbers

COD	1,5-Cyclooctadiene
CPME	Cyclopentyl methyl ether
Cy	Cyclohexyl
d	Day
dan	1,8-Diaminonaphthyl
dba	Dibenzylideneacetone
DBU	1,8-Diazabicyclo[5.4.0]undec-7-ene
DCM	Dichloromethane
DFT	Density functional theory
DIBALH	Diisobutylaluminium hydride
DIPEA	*N*,*N*-Diisopropylethylamine
DMAP	4-Dimethylaminopyridine
DMF	*N*,*N*-Dimethylformamide
DMP	Dess–Martin periodinane
DM*p*T	*N,N*-Dimethyl-*p*-toluidine
DMSO	Dimethylsulfoxide
dppf	1,1′-Ferrocenediyl-bis(diphenylphosphine)
Bn	Benzyl
DMF	Dimethylformamide
DPEPhos	Bis[(2-diphenylphosphino)phenyl] ether
DTBM	Di-*tert*-butyl methoxy
E	Electrophile

ee	Enantiomeric excess
EI	Electron Impact
equiv	Equivalents
er	Enantiomeric Ratio
ESI	Electrospray Ionization
Et	Ethyl
FA	Formic acid
FG	Functional group
h	hour
HPLC	High performance liquid chromatography
HRMS	High resolution mass spectrometry
Hz	Hertz
IBX	2-Iodoxybenzoic acid
Ipc	Diisopinocampheylborane
*i*Pr	*iso*-propyl
IR	Infrared spectroscopy
kcal	kilocalorie
K_a	Acid dissociation constant
KHMDS	Potassium bis(trimethylsilyl)amide
L	Litre
L*	Chiral ligand
Ln	Undefined ligand

LDA	Lithium diisopropylamide
LiHMDS	Lithium bis(trimethylsilyl)amide
LUMO	Lowest Unoccupied Molecular Orbital
M	molarity
m	Multiplet
Me	Methyl
Mes	Mesityl
MIDA	*N*-Methyliminodiacetic
ms	Molecular sieves
min	Minute
mg	Milligram
mL	Millilitre
mol	Mole
MTBE	Methyl *tert*-butyl ether
NBS	*N*-Bromosuccinimide
nbd	2,5-Norbornadiene
*n*Bu	Normal butyl
neop	Neopentyl
Nf	Nonaflate
NHC	*N*-Heterocyclic carbene
NMR	Nuclear Magnetic Resonance
Nu	Nucleophile

ORTEP	Oak Ridge thermal ellipsoid plot
p	*para*
PG	Protecting group
Ph	Phenyl
pin	Pinacol
Pn	Pentoxide
Prophos	Bis(diphenylphosphino)propane
PTSA	*p*-Toluenesulfonic acid
pyr	Pyridine
q	Quartet
rt	Room temperature
R	Alkyl
RDS	Rate-determining step
sep	Septet
sex	Sextet
S_N	Nucleophilic substitution
TADDOL	α,α,α',α'-Tetraaryl-2,2-disubstituted 1,3-dioxolane-4,5-dimethanol
*t*Bu	*tert*-Butyl
TMEDA	Tetramethylethylenediamine
TBAF	Tetrabutylammonium fluoride

Temp.	Temperature
Tf	Tiflate
TES	Triethylsilane
TFA	Trifluoroacetic acid
THF	Tetrahydrofuran
TLC	Thin layer chromatography
Tos	Tosyl
μ	Micro
UV	Ultraviolet
xs	Excess

Chapter 1: Cyclic Chiral Boronates as Versatile Synthetic Building Blocks

1.1 Chiral boronic esters as synthetic intermediates

1.1.1 Chirality in medicinal chemistry

Drug development is an arduous and expensive endeavor. Despite many advances in regard to the synthesis and understanding of molecular structure, attrition rates at the clinic trial stage remain high. In particular, toxicity is the cause of many development projects failing, which stem from undesired off-target protein interactions inducing unwanted pharmacological effects (aka drug promiscuity).[1] From a medicinal chemistry perspective, many drug development projects focus on flat, aromatic compounds due to the ease of synthesis of these scaffolds and the advent of convenient high-throughput screening approaches. However, with increased complexity the receptor-ligand complementarity can in theory be improved leading to more specific interactions and a more desirable toxicity profile. Lovering and co-workers indeed found a correlation between complexity and clinic progression of a drug candidate, as well as improved toxicity profiles. The authors modelled complexity by the number of saturated carbons and chiral centers.[2] Furthermore, the term diversity-oriented synthesis has been described in the literature to promote the exploration of more structurally complex and diverse molecular scaffolds.[3] Clearly, the idea of accessing greater and more complex chemical space for medicinal chemistry purposes has become an essential topic in drug development research.

Enantioselective catalysis is an attractive and well-established approach to access complex and diverse three-dimensional scaffolds. From a synthetic diversity perspective, ideally the enantioenriched products are suitable for further elaboration without erosion of the stereochemical

information. In this respect, enantioenriched organoboronic esters are ideal targets for accessing versatile small molecular building blocks. Organoboron compounds are more stable and less toxic than other common organometallic reagents, such as organotin, zinc and magnesium.[4] Furthermore, the configurational stability of C-B bonds allow opportunities for subsequent stereoselective transformations. The types of possible stereospecific C-B bond functionalizations are diverse and continue to grow (see Section 1.3). Therefore, the boronyl functional group can be used as a potential handle to install enantioenriched complexity into various scaffolds (Figure 1-1). As a general example, template boronic ester **1-1** could undergo a stereoretentive or invertive C-C bond formation directly (e.g. Suzuki-Miyaura cross coupling) to afford **1-2** or **1-3**, respectively. Alternatively, oxidation to the alcohol or amine would furnish **1-4**, which now contains a nucleophilic handle with a different reactivity profile than **1-1**.

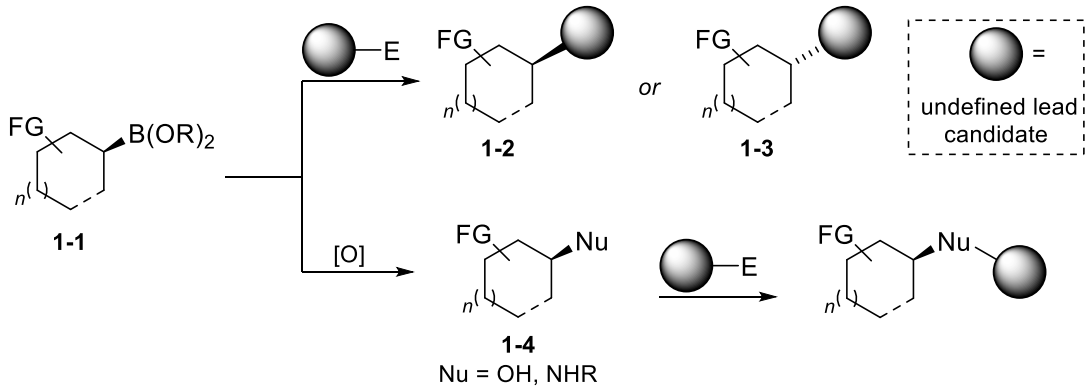

Figure 1-1. Chiral boronic esters as building block templates to increase chemical complexity.

1.1.2 Introduction to boronic esters and common protecting groups

The reactivity and utility of organoboron compounds originate from the inherent Lewis acidity of tricoordinate boron from the empty p-orbital of the atom (Figure 1-2a).[5] As expected, the relative Lewis acidity depends on a combination of resonance, inductive effects and ring strain at the boron

center. Organoboron compounds are commonly oxygen-bound due to the strong dissociation energy of a B-O bond (124 kcal mol^{-1} in the tricoordinate form). In particular, boronic esters are a great compromise between stability and reactivity and are products of interest in modern enantioselective catalysis. In many cases, the boronic ester will be oxidized to the corresponding alcohol for purification purposes. Since boronic esters and their reagents can generally be made by simple condensation reactions between the protecting group and boronic acid, many derivatives exist in the literature. A few of the more common boronic ester protecting groups are outlined in Figure 1-2b.[6] In particular, the pinacol-based protecting group (Bpin) is the most frequently used due to its high kinetic stability from the presence of *gem*-dimethyl groups and the commonly observed stability of these derivatives towards chromatographic purification. Furthermore, the commercial availability of the pinacolborane and bis(pinacolato)diboron reagents make pinacolboronates more accessible by synthetic means. However, a number of other variations such as neopentyl (Bneop), are being utilized in the literature with increasing regularity.

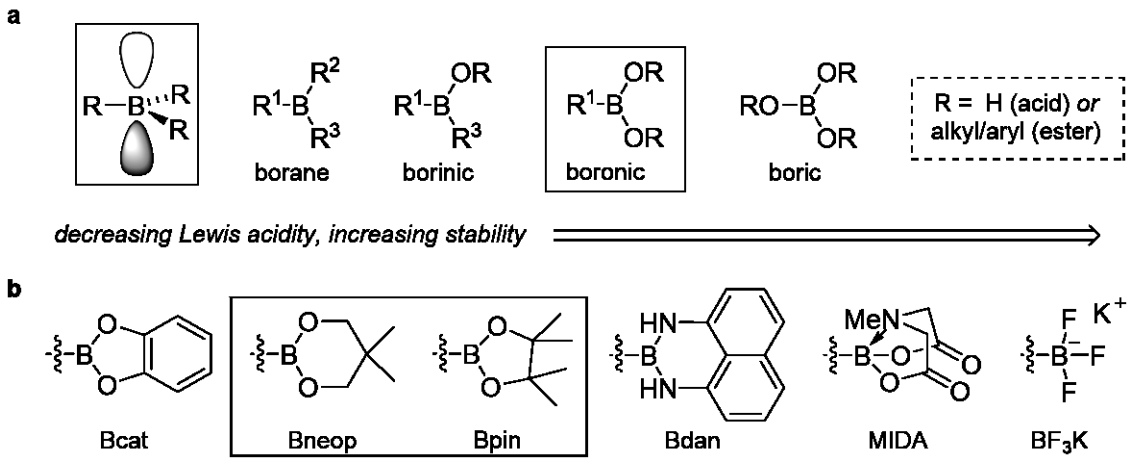

Figure 1-2. Brief overview of organoboron compounds (a) oxygen-containing organoboron nomenclature (b) common boron protecting groups. The Lewis acidity of the boron atom decreases from left to right.

1.2 Catalytic enantioselective approaches to cyclic boronates

1.2.1 The increasing influence of organoboronates in the literature

As the Suzuki-Miyaura cross-coupling reaction has become one of the most powerful Csp^2-Csp^2 bond forming reactions in organic chemistry,[7] the general interest in organoboron compounds has expanded. Correspondingly, the types of catalytic enantioselective methods to access secondary and tertiary boronates has continued to grow over the past decade as well (Figure 1-3). There have been many impressive advances in the field of catalytic enantioselective borylation and these developments have recently been reviewed.[8]

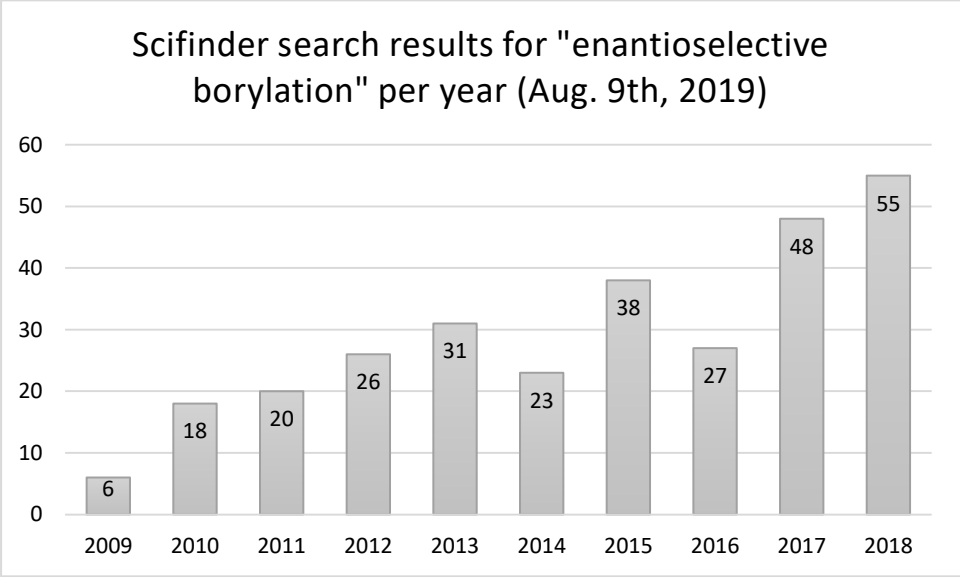

Figure 1-3. The number of references provided by Scifinder that were found containing the concept "enantioselective borylation" per year.

Upon review of the current literature, a notable theme is that many alkene borylation methods are limited to linear hydrocarbon or styrenyl substrates. Moreover, many of the products lack more functionality than solely a boronate group. In the interest to use chiral boronates as a handle to

introduce complexity in molecular scaffolds, the development of synthetic methods to access novel, enantioenriched cyclic boronates with increased functionality is a beneficial endeavor (Figure 1-4). Therefore, a brief overview of catalytic enantioselective approaches that are applicable to cyclic boronates will be covered in this chapter.

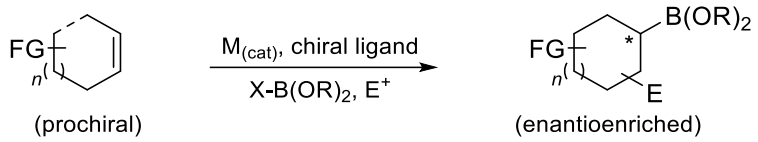

Figure 1-4. General representation of the borylation process to obtain cyclic boronates.

Due to the focus on cyclic boronates, some state-of-the-art catalytic enantioselective borylation methodologies that are currently limited to linear substrates will be omitted. These approaches include hydrogenation and conjugate reduction of alkenyl boronates and β-borylated Michael acceptors, respectively,[9] 1,2-borylation of carbonyl derivatives,[10] Suzuki-Miyaura desymmetrization of 1,1-bisboronates,[11] and the recently developed conjunctive cross coupling.[12] For an overview of these and other methodologies, the reader is referred to an excellent and more comprehensive recent review by Aggarwal and co-workers.[8]

1.2.2 Borylation of non-polarized alkenes

1.2.2.1 *Hydroboration*

Hydroboration methodologies have led the way in the field of catalytic enantioselective approaches to boronates. The first metal-catalyzed hydroboration was reported by Männig and Nöth using catecholborane and Wilkinson's catalyst (Scheme 1-1).[13] Interestingly, the authors found that the catalyzed reaction favoured alkene reduction of **1-5** to obtain **1-6**, whereas the non-catalyzed process favoured ketone reduction. Initial studies in the early 2000's continued to focus on rhodium catalysts

for the hydroboration of unsubstituted styrenes and terminal alkenes.[14] The reaction mechanism is proposed to undergo oxidative addition of catecholborane to the rhodium(I) catalyst, followed by alkene coordination to obtain **1-7** (Scheme 1-1). Alkene insertion into the Rh-H bond and subsequent C-B reductive elimination furnishes the product and regenerates the catalyst. More recently, many advances in the field of enantioselective hydroboration have been made particularly with rhodium, copper, and cobalt catalysts, along with challenging substrates such as sterically congested styrenes[15] and unactivated terminal alkenes.[16]

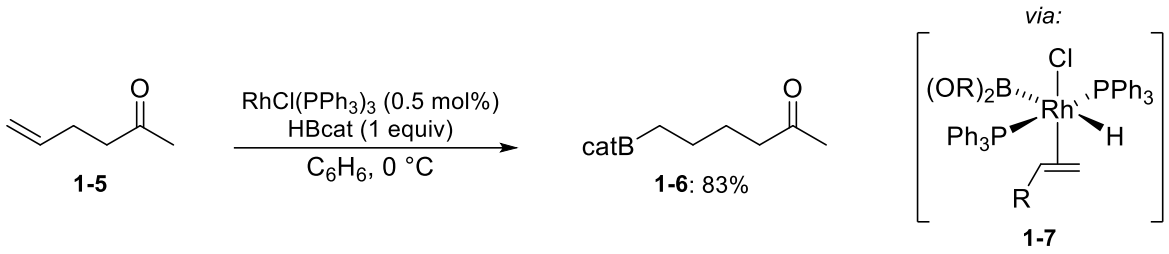

Scheme 1-1. Original catalytic enantioselective hydroboration with Wilkinson's catalyst.

Internal dialkyl-substituted alkenes are more challenging due to issues regarding regioselectivity. Some of these limitations have been addressed by substrate directed hydroboration approaches using rhodium, copper, cobalt and palladium catalysts.[17] Most notably in the field of directed hydroboration is the work of Takacs and co-workers, who have reported catalytic asymmetric hydroboration (CAHB) approaches with rhodium and BINOL or TADDOL-based phosphoramidite or phosphite ligands. The CAHB approach has been developed for various directing groups including amides, oximes and phosphonates furnishing alkyl tertiary boronates in high enantioselectivity in many cases (Figure 1-5).[18] An illustration of such a system is shown in Figure 1-5, where a carbonyl-directed hydroboration allowed the desymmetrization of γ,δ-unsaturated amides **1-8** to furnish cylopentanols **1-9** in high enantioselectivity as a single diastereomer after C-

B oxidation.[19] DFT calculations suggest that the mechanism likely proceeds by catalyst coordination to **1-8**, oxidative addition of the borane and Rh-H alkene insertion to obtain rhodium (III) intermediate **1-11**. Subsequent amide rotation, then reductive elimination affords the borylated product and regenerates the active rhodium(I) catalyst. Furthermore, the borylated products were competent Suzuki-Miyaura cross-coupling partners after conversion to the corresponding cesium or potassium trifluoroborate salt.

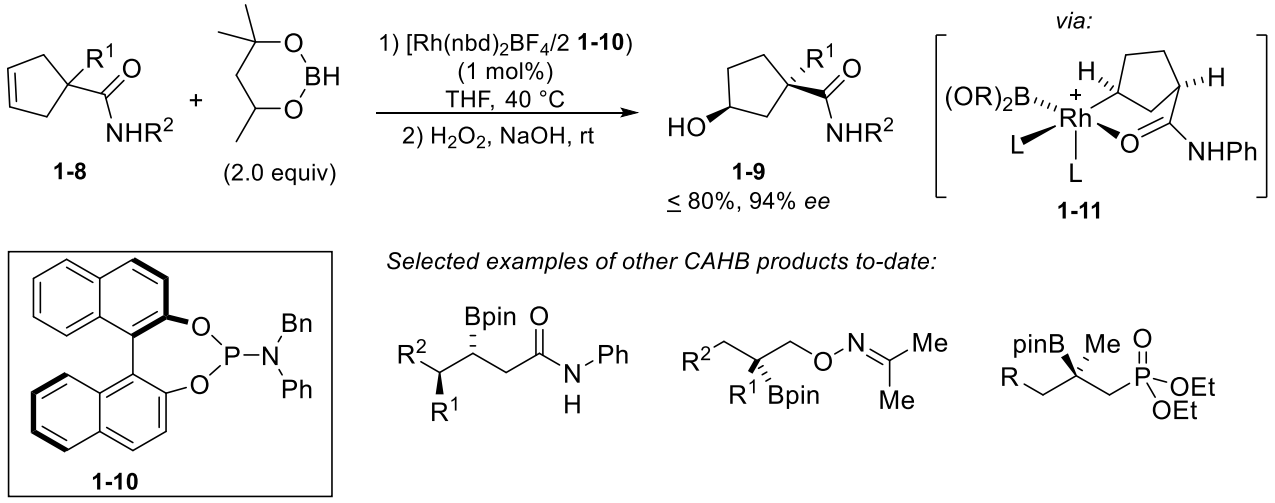

Figure 1-5. Directed catalytic asymmetric hydroboration developed by Takacs and co-workers.[19]

As is the case with rhodium systems, copper-catalyzed hydroboration has seen extensive expansion in the last decade. In 2010, Ito and co-workers reported a copper-catalyzed hydroboration of cyclic dienes **1-12** to obtain the homoallylic or allylic cyclic boronates **1-13** in high enantioselectivity (Figure 1-6a).[20] Mechanistic studies indicated that a *syn*-1,2-borylcupration leads to formation of σ-allylcopper species **1-15**, which undergoes thermodynamic isomerization to afford the 1,4-borylated cuprate **1-16**. An S_E2' protonation of intermediate **1-16** furnishes the homoallylic boronate. Indeed, it was shown that when the reaction was performed at –40 °C, the allylic boronate product **1-17** (*n*

= 0) was formed preferentially in high enantioselectivity, presumably due to a lack of isomerization at low temperature.

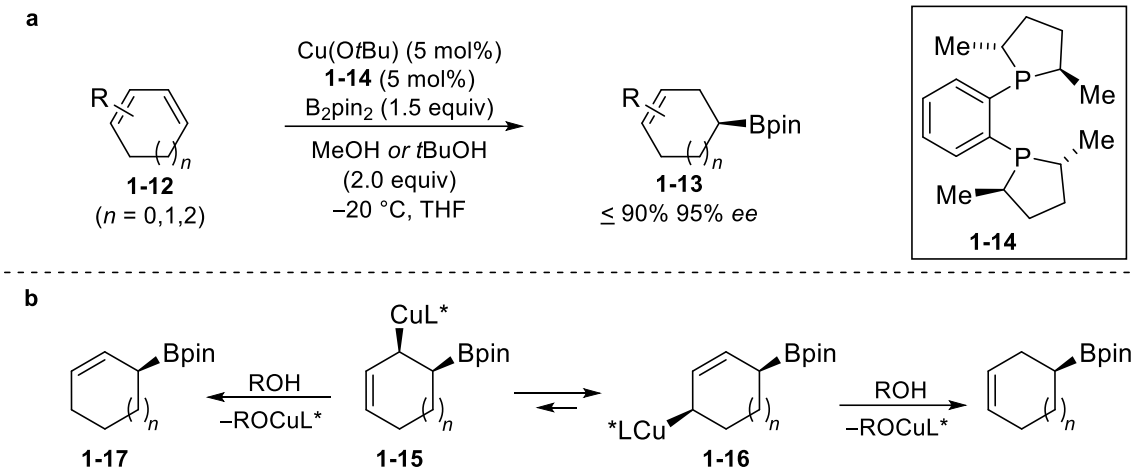

Figure 1-6. (a) Hydroboration of cyclic dienes (b) explanation of the observed regioselectivity.

More recently, the same group has expanded this chemistry to a two-step borylative dearomatization of substituted pyridines **1-18**, through an acylpyridinium reduction followed by borylation of the resulting 1,2-dihydropyridines **1-19** (Scheme 1-2a).[21] The ability to use pyridines directly to furnish highly novel and functionalized enantioenriched 3-boryl-tetrahydropyridines **1-20** is quite useful. However, three different ligands were used in the substrate scope, suggesting tuning is required in many cases for consistent results. The same approach was developed for tetrahydroquinolines to access 3-boryl-tetrahydroquinolines.[22] Similarly, Hou and co-workers reported related conditions for the hydroboration of 1,2-dihydroquinolines and 2*H*-chromene derivatives. The conditions for the hydroboration of 2*H*-chromenes **1-24** to afford heterocyclic boronates **1-25** are shown in Scheme 1-2b.[23]

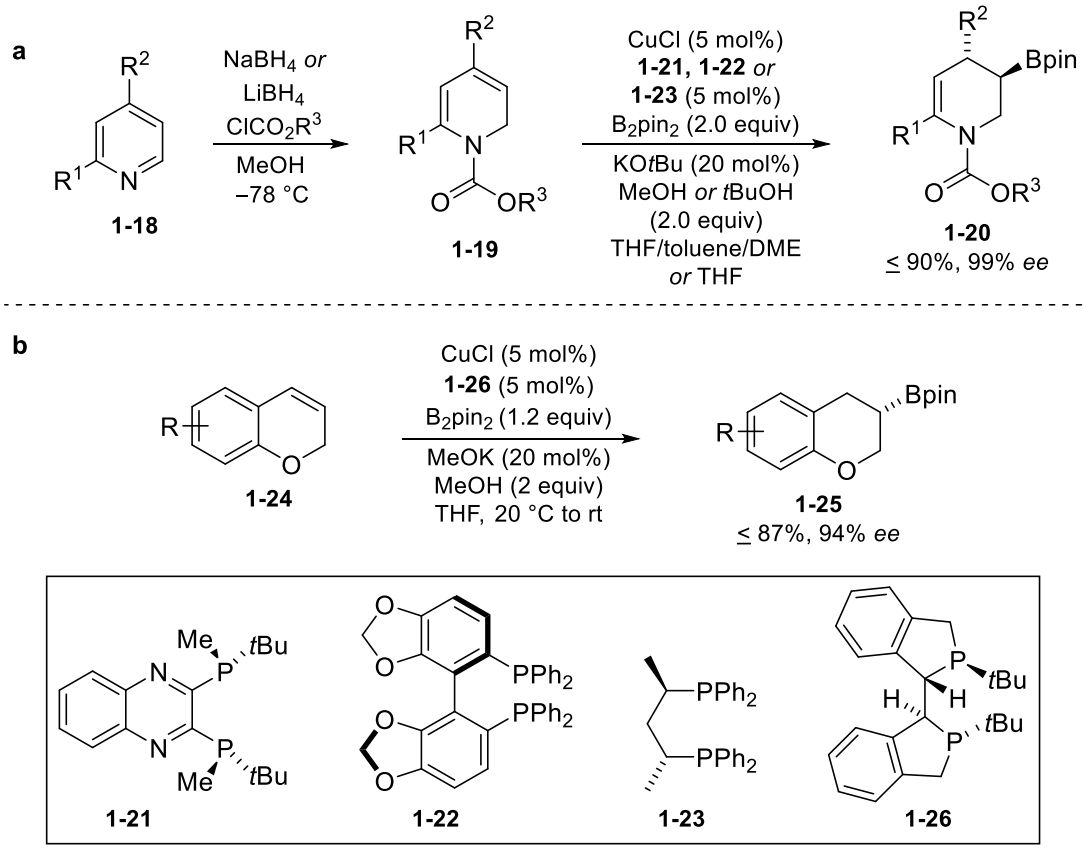

Scheme 1-2. Examples of copper-catalyzed hydroboration of heterocyclic substrates (a) borylative dearomatization (b) 2*H* chromene hydroboration.

1.2.2.2 *Carboboration*

The copper-catalyzed hydroboration of non-polarized alkenes can be modified to allow various borylative difunctionalization approaches.[24] Standard conditions for copper-catalyzed hydroboration involve the use of a diboron reagent, alkoxide base and a proton source. Mechanistically, an active copper(I)-alkoxide catalyst forms (**1-27**) from a copper(I) source, chiral ligand and a base (Figure 1-7). σ-Bond metathesis of **1-27** with the diboron reagent followed by a Cu-B alkene insertion affords the configurationally stable borylated copper species **1-28**. In the presence of an alcohol, protodecupration allows release of the hydroboration product and

regeneration of the active catalyst **1-27**. However, as would be expected from the mechanism shown in Figure 1-7, the nucleophilic copper species **1-28** can be trapped with a non-protic electrophile, such as carbon and amine sources to obtain carboboration and aminoboration products, respectively. In these cases, excess base is required to regenerate the active alkoxide catalyst **1-27**.

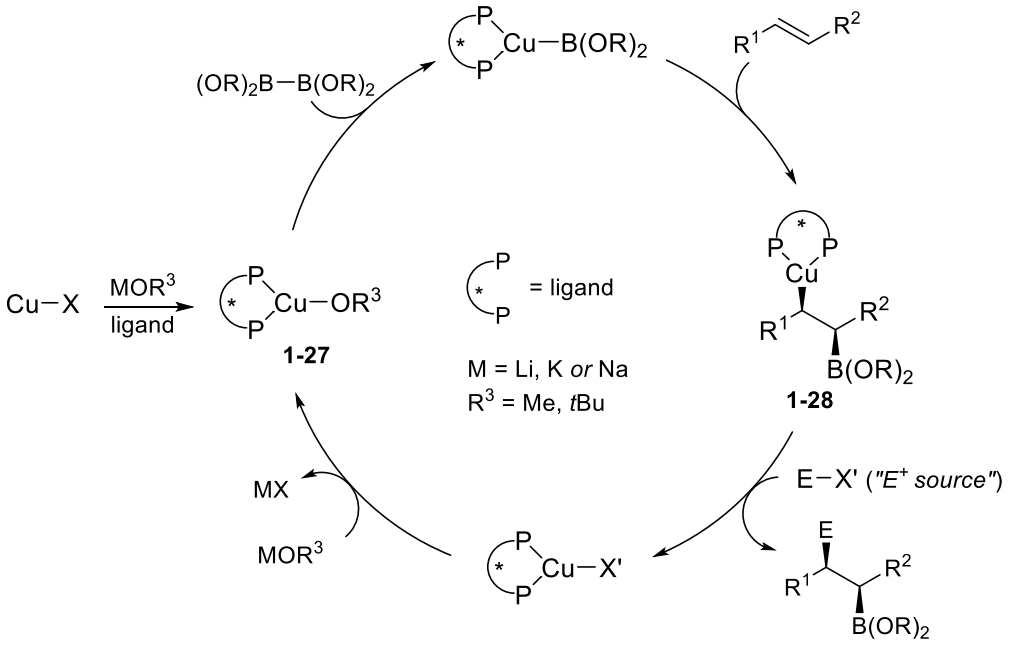

Figure 1-7. Simplified catalytic cycle of copper-catalyzed borylations with diboron reagents.

A few examples do exist of enantioselective carboboration of cyclic alkenes with intermolecular electrophilic trapping. For example, enantioenriched secondary boronates were reported in the methylation of β-substituted styrenes and aliphatic olefins with high enantioselectivity (Scheme 1-3a). The high diastereoselectivity stems from the expected *syn* addition of the copper boronate catalyst and electrophilic trapping with methyl iodide. The only cyclic example from this methodology utilized 1,2-dihydronaphthalene (**1-29**) to afford the methylated secondary alcohol **1-30** in high enantioselectivity after oxidation (Scheme 1-3a).[25] Alternatively, the electrophilic carbon

source can be more elaborate and general than methyl iodide. Brown and co-workers have developped a dual catalytic approach in which the benzylic alkyl-copper intermediate that is generated from the 1,2-borylcupration of **1-31** is trapped by transmetallation with an electrophilic aryl-palladium(II) oxidative addition intermediate (Scheme 1-3b).[26] The authors showed that highly enantioenriched cyclic styrenyl arylboration products could be achieved in moderate to good yields and high enantioenrichment. Interestingly, either inversion or retention could be achieved in the transmetallation step, depending on the palladium catalyst used. Brown and co-workers have extended this copper-palladium dual-catalysis system to cyclic dienes, but the system was largely limited to racemic reactions (only 3 enantioselective examples were reported).[27] Furthermore, a related nickel system was reported for a regiodivergent arylboration of various unactivated alkenes, yet only the racemic system has been reported to-date.[28]

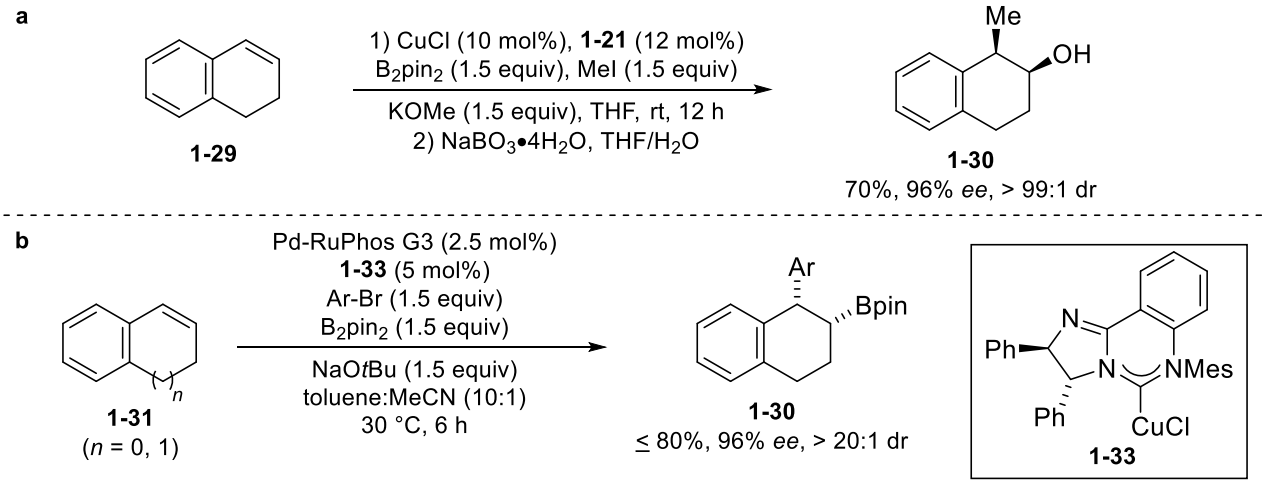

Scheme 1-3. Examples of copper-catalyzed carboboration methodologies with intermolecular trapping.

In contrast, intramolecular trapping during the carboboration process can allow for the formation of cyclic boronates from linear precursors. In many cases, the enantioenriched products contain a primary boronate.[29] However, Meek and co-workers have displayed the utility of a borylative

cyclization approach to secondary boronates using alkenyl boronates **1-34** to afford diboryl alcohols (**1-35**) or triols (**1-36**) with three contiguous stereocentres after oxidation (Scheme 1-4).[30] The products are formed from intramolecular trapping of the boryl-cuprate intermediate with an aldehyde or ketone. Interestingly, stereodivergence was observed depending on the type of carbonyl electrophile. In the case of ketones, transition state structure **1-40** was proposed to be preferred instead of **1-39** due to the relatively lower reactivity and increased steric hindrance of the electrophile in the transition state. Notably, a novel densely functionalized diboryl-piperidinol **1-41** was obtained in moderate yield and high enantioenrichment.

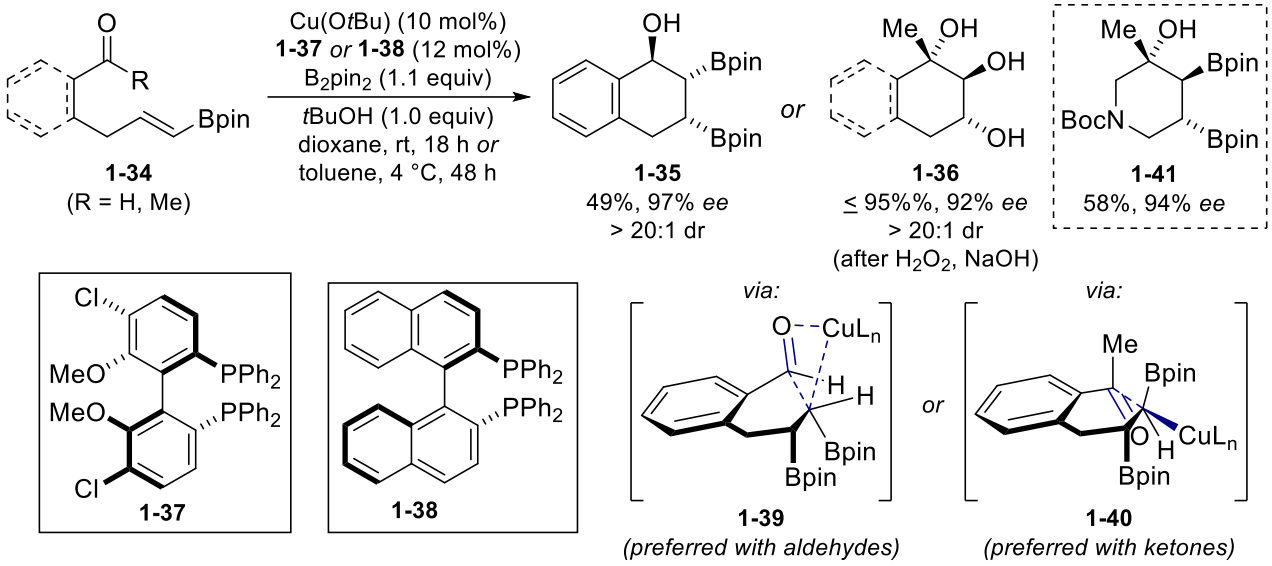

Scheme 1-4. Copper-catalyzed intramolecular borylative cyclization.

The methodology was further extended to a tandem hydroboration borylative cyclization of acetylenic diketones **1-42** (Scheme 1-5). The corresponding alkenyl boronate of substrate **1-42** is made efficiently *in situ* by hydroboration, which then undergoes a borylative cyclization similar to Scheme 1-4 to afford diboranols **1-43** or **1-44** with four contiguous stereocenters. As above, the

difference in diastereoselectivity between **1-43** and **1-44** stems from either a stereoinvertive or stereoretentive alkyl copper addition to the ketone. The observed diastereoselectivity was proposed to be due to a combination of steric considerations, which could be inverted by varying the ligand, although with only a moderate 70% *ee*.

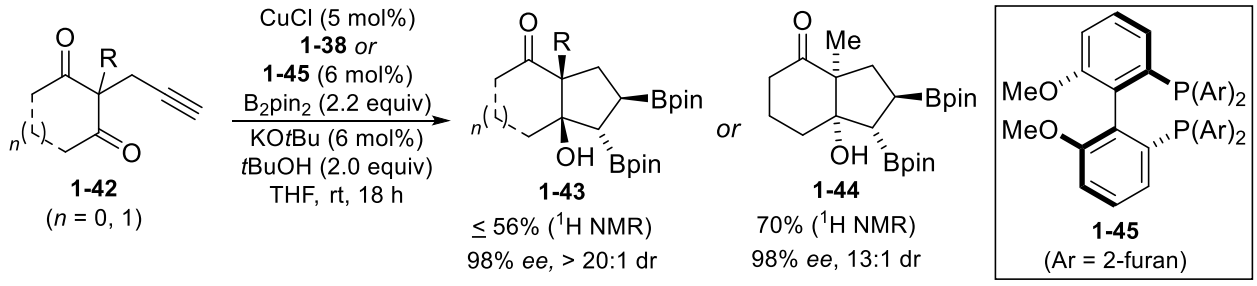

Scheme 1-5. Tandem hydroboration-borylative cyclization.

1.2.2.3 *Diboration*

Similarly to hydroboration, the first example of a metal-catalyzed diboration was reported using rhodium catalysis. Morken and co-workers provided a seminal report of alkene diboration with rhodium and B_2cat_2, yet the reaction was quite limited to simple substrates.[31] Nishiyama and Toribatake reported a rhodium system enabling the use of B_2pin_2; however, once again the diboration was limited to vinylic and styrenyl systems.[32] More recently, Morken and co-workers have developed a platinum-catalyzed system with B_2pin_2 and a TADDOL-derived phosphite ligand (**1-48**) to afford cyclic allylic boronates from a 1,4-diboration of substituted cyclic dienes (**1-46**), which were oxidized to the corresponding allylic diols **1-47** (Scheme 1-6a).[33] The hexyl allyl-diboronates were found to undergo a sterically-controlled regioselective allylboration when isovaleraldehyde was added in a one-pot protocol, with predictable diastereoselectivity. Furthermore, a two-step diboration of alkenyl boronates **1-49** under similar conditions, followed by

a deborylative alkylation afforded cyclic vicinal diboryl product **1-50** in moderate yield and high enantioselectivity over two steps (Scheme 1-6b).[34] Based on the observed *anti* diastereoselectivity of the deborylative alkylation, a stereochemical model was proposed which involves $\sigma_{C\text{-}B}$ to $\pi_{C\text{-}B}$ overlap, enhancing the nucleophilicity of the carbonanion (the enantiomer is shown for simplicity). Finally, the same group has recently developed a novel metal-free carbohydrate-catalyzed enantioselective diboration system. Although enantioselectivities above 90% *ee* are generally limited to vinylic substrates, the diboration of indene (**1-52**) was achieved in 86% *ee* (Scheme 1-6c).[35] The mechanism is proposed to involve transesterification of **1-53** with B_2pro_2 to afford a chiral diboron reagent which then undergoes a DBU-promoted diboration.

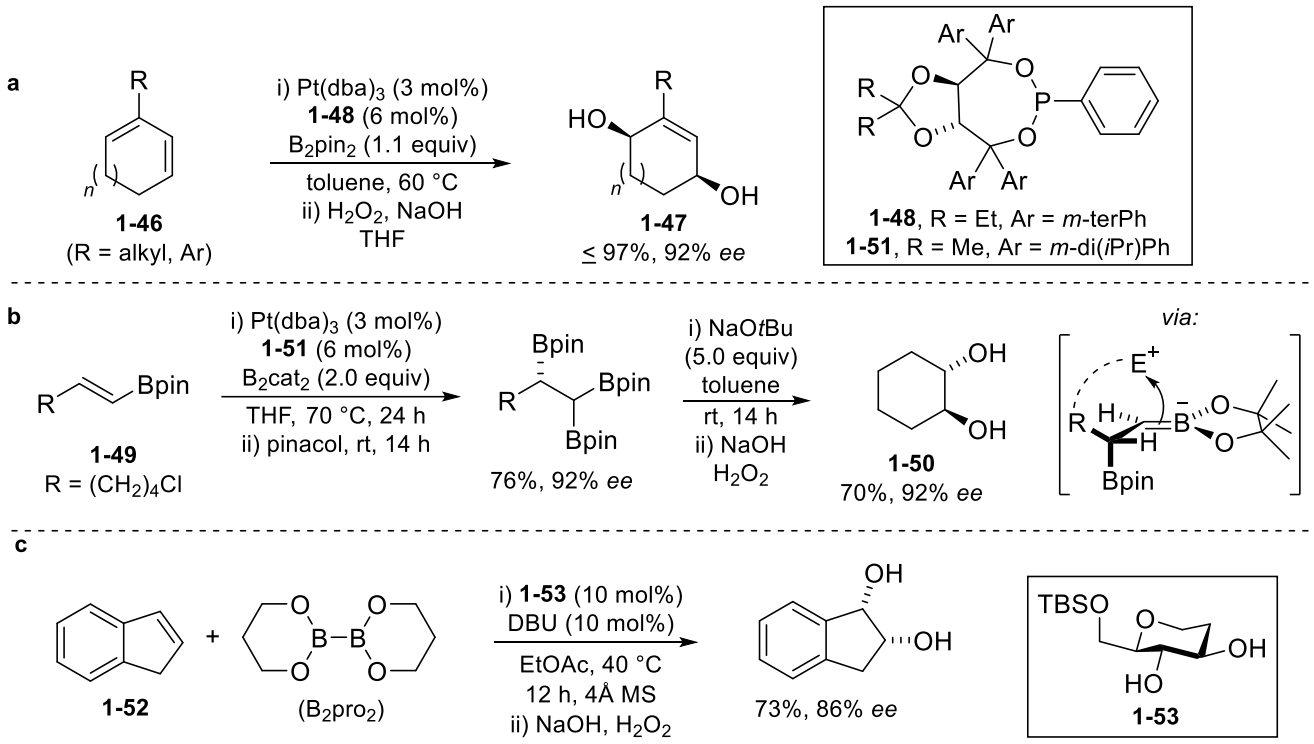

Scheme 1-6. Examples of diboration conditions developed by Morken and co-workers.

1.2.2.4 *Aminoboration*

Similarly to carboboration and diboration, boryl-cupration in the presence of an electrophilic amine source would allow overall aminoboration to furnish functionalized β-aminoboronates. Miura and co-workers have developed an approach to aminoboronates using O-benzoyl-*N*,*N*-dialkylhydroxylamines as the electrophilic amine source with disubstituted alkenyl Bdan substrates.[36] Although a few enantioselective examples exist, most aminoboration methodologies reported to-date have been focused on the racemic process. One exception, however, is the work of Miura and co-workers who have reported a small scope for the enantioselective aminoboration of strained alkenes **1-54** to furnish bicyclic amino alcohols **1-55** with over 90% *ee* after oxidation (Scheme 1-7).[37] Conversely, enantioenriched linear α-aminoboronates can be accessed by

hydroamination of alkenyl-Bdan substrates, where the Bdan efficiently controls the regioselectivity of the copper hydride addition.[38,15d]

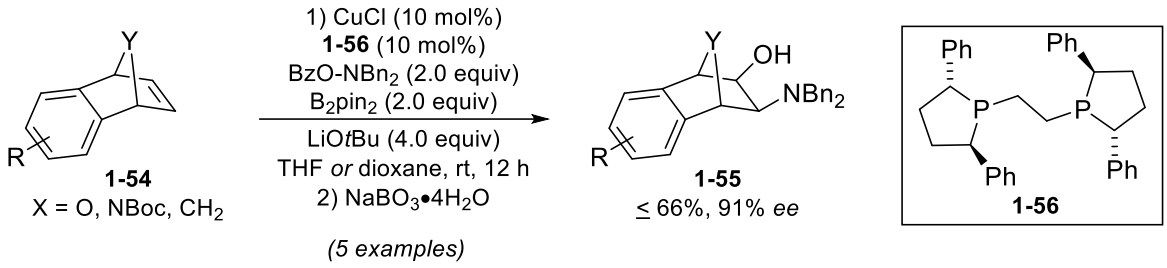

Scheme 1-7. Enantioselective aminoboration of cyclic strained alkenes.

1.2.3 Borylation of electron-deficient alkenes

1.2.3.1 *Conjugate borylation*

Conjugate borylation involves the addition of a nucleophilic boron-source to various types of Michael acceptors. From a synthetic perspective, inherent benefits in regard to conjugate borylation are two-fold: issues of regioselectivity are avoided from polarization of the alkene electrophilic partner and the borylated products have the increased functionality of the remaining 1,2-polar unsaturation. The first racemic copper-catalyzed borylation of α,β-unsaturated ketones was reported by Hosomi and co-workers almost two decades ago.[39] Although copper(I) remains the most common system, rhodium, nickel, palladium, platinum, phosphines and chiral NHCs have all been reported for the catalytic asymmetric borylation of a variety of Michael acceptors, including α,β-unsaturated ketones, imines, esters, amides and nitriles. Furthermore, copper(II) systems in water have also been developed.[40]

Conjugate borylation provided some of the first syntheses of tertiary cyclic boronates. Highly efficient metal-free conjugate borylation conditions were reported by Hoveyda and Radomkit for

the borylation of cyclic and acyclic unsaturated ketones using a chiral NHC imidazolinium salt **1-59** (Scheme 1-9a).[41] The system was applicable to numerous β-substituted enones **1-57**, including 5-, 6-, 7- and 8-membered rings furnishing enantioselectivities of borylated products (**1-58**) in over 90% *ee* in many cases. Although careful temperature modifications were required, the reaction does not require an inert atmosphere, whereas many metal-catalyzed processes commonly do. Linear trisubstituted α,β-unsaturated enoates were also applicable with a different NHC catalyst. Mechanistically, the chiral nucleophilic boron source was found to form from a DBU-promoted break-down of B_2pin_2 with methanol leading to formation of the active nucleophilic NHC boron source **1-60** (Scheme 1-9b).

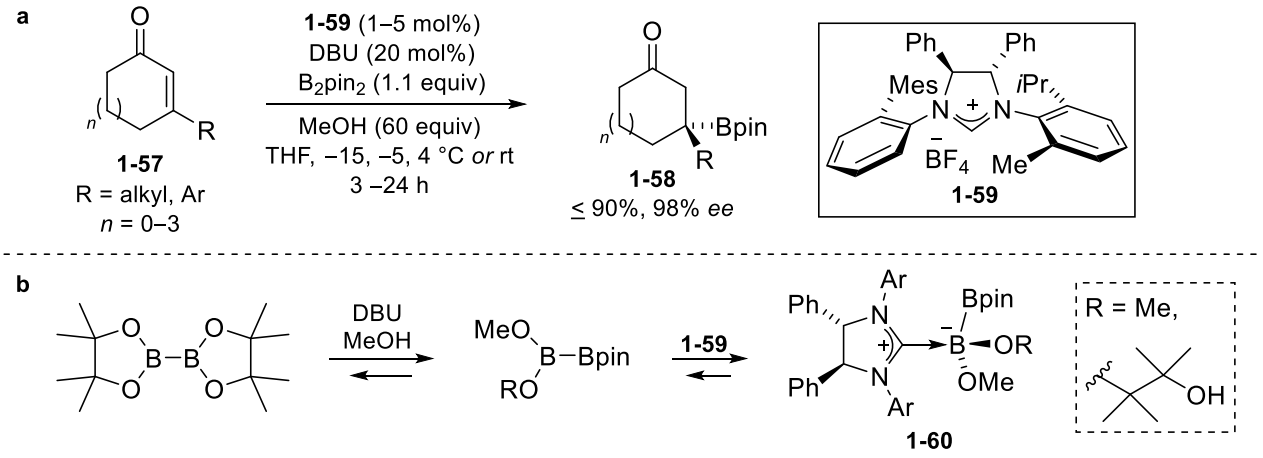

Scheme 1-8. (a) Metal-free conjugate borylation (b) formation of the chiral nucleophilic boron source.

The majority of the conjugate borylation systems reported to-date have been copper(I)-catalyzed. For example, Shibasaki and co-workers developed conditions for the borylation of similar trisubstituted 5-, 6- and 7-memebered cyclic enones **1-57** to furnish tertiary boronates **1-58** in high yield and enantioselectivity (Scheme 1-9).[42] Interestingly, an alcohol additive was not required in this system. The authors suggested that under the reported conditions a catalytic amount of $LiPF_6$

generated from formation of the active catalyst was able to efficiently accelerate the catalyst regeneration step. Furthermore, slightly modified reaction conditions in the presence of benzaldehyde furnished diol **1-61** after oxidation with 3-contiguous stereocenters and moderate diastereoselectivity after oxidation.

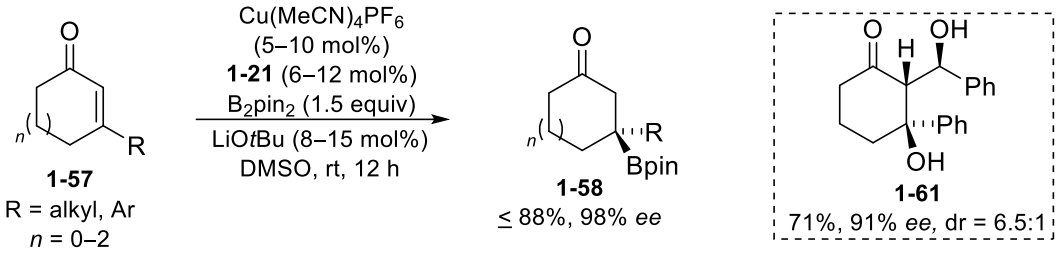

Scheme 1-9. Copper-catalyzed conjugate borylation conditions reported by Shibasaki and co-workers.

Finally, as an extension of the borylative dearomatization, Ito reported a highly diastereoselective borylation of indole-2-carboxylates **1-62** to afford novel borylated indoline esters **1-63** in high yield and enantioselectivity (Scheme 1-10).[43] The diastereoselectivity of the protonation step was proposed to favour a top-face attack to avoid the sterically bulky pinacol boronate group on the bottom face of the copper enolate in the stereochemical model **1-66**.

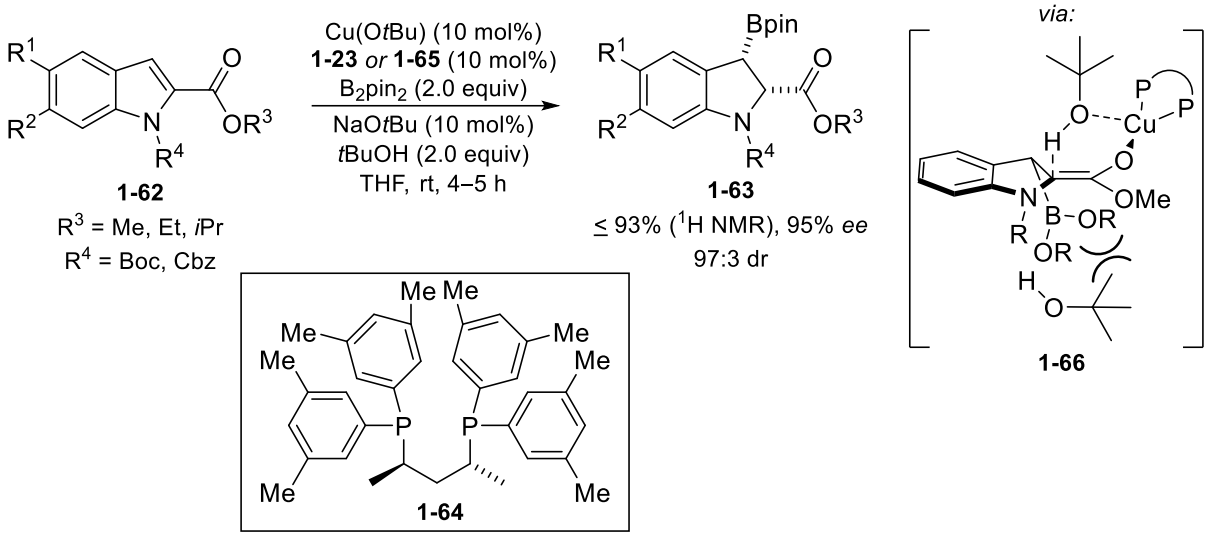

Scheme 1-10. Conjugate borylation of indole-2-carboxylates.

1.2.4 Borylation methods to afford cyclic allylic boronates

1.2.4.1 *Increased synthetic appeal of allylic boronates*

Organoboronic esters containing an allylic unsaturation have the increased synthetic appeal of having two sites of reactivity (α or γ, Figure 1-8). Although allylic boronates are configurationally stable and easy to handle, it is common for the allylic boronate to be subjected directly to aldehyde allylation for purification purposes. As would be expected, some approaches to allylic boronates are related to that of alkylboronates mentioned above, such as conjugate borylation of extended α,β,γ,δ-unsaturated systems or hydro/diboration involving allenyl substrates or products.[44,45] However, due to a lack of cyclic examples, these and some other methodologies will not be covered in this chapter and only a small number of well-established methodologies to access cyclic allylic boronates will be outlined. The synthesis and application of allylboron reagents has recently been reviewed in more extensive detail.[46]

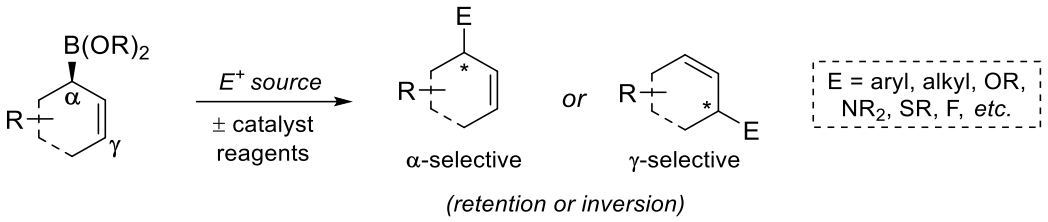

Figure 1-8. The regio- and stereoselectivity possibilities of allylic boronates.

1.2.4.2 *Allylic borylation*

One prominent methodology to access α-substituted allylic boronates is the copper-catalyzed γ-borylation of allylic carbonates. The reaction is mechanistically similar to that of the other copper borylation chemistry mentioned above (c.f. Figure 1-7); however, in this case the catalyst is regenerated from β-alkoxy elimination after the alkene insertion step to obtain allylic boronates of type **1-67** (Figure 1-9).[47] Ito and co-workers disclosed the first example of a copper(I)-catalyzed enantioselective γ-borylation of *Z*-allylic carbonates to obtain chiral α-substituted linear allylic boronates in high enantioselectivities and moderate yield.[48] Although no cyclic examples were reported at the time, Hoveyda and McQuade subsequently reported related copper-NHC approaches with improved substrate variability.[49,50]

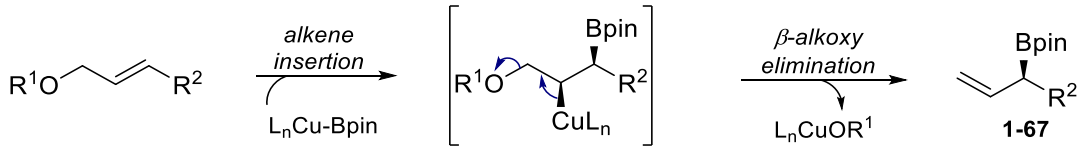

Figure 1-9. The β-alkoxy elimination step in the copper-catalyzed allylic borylation.

Since the initial reports outlined above, Ito's system has been extended to various substrates, including cyclic and linear *Z*-allylic acetals and cyclic *meso*-2-alkene-1,4-diols.[51] Notably, the chemistry has been recently expanded to allylic trifluoromethanes and *E*- or *Z*-allyl difluorides,

which undergo a β-fluoro elimination instead of β-alkoxy elimination step.[52] One of the relatively few cyclic allylic borylations is shown in Figure 1-10a, where an enantioconvergent γ-allylic borylation of racemic allylic ethers **1-68** affords cyclic allylic boronates **1-69** and homoallylic alcohols **1-70** in up to 98% *ee* after aldehyde allylboration.[53] Moreover, this work is particularly important from a more conceptual standpoint. The methodology represents the first example of an enantioconvergent transformation that is not biocatalytic and which proceeds without racemization or symmetrization. The enantioconvergence of the reaction originates from an opposite facial selectivity for each enantiomer of the copper(I)-Bpin nucleophilic attack (Figure 1-10b). The (*S*)-substrate preferentially undergoes an *anti*-S_N2' pathway in high enantioselectivity, whereas the enantiomeric (*R*)-substrate preferentially undergoes *syn*-S_N2' in a slightly lower enantioselectivity.

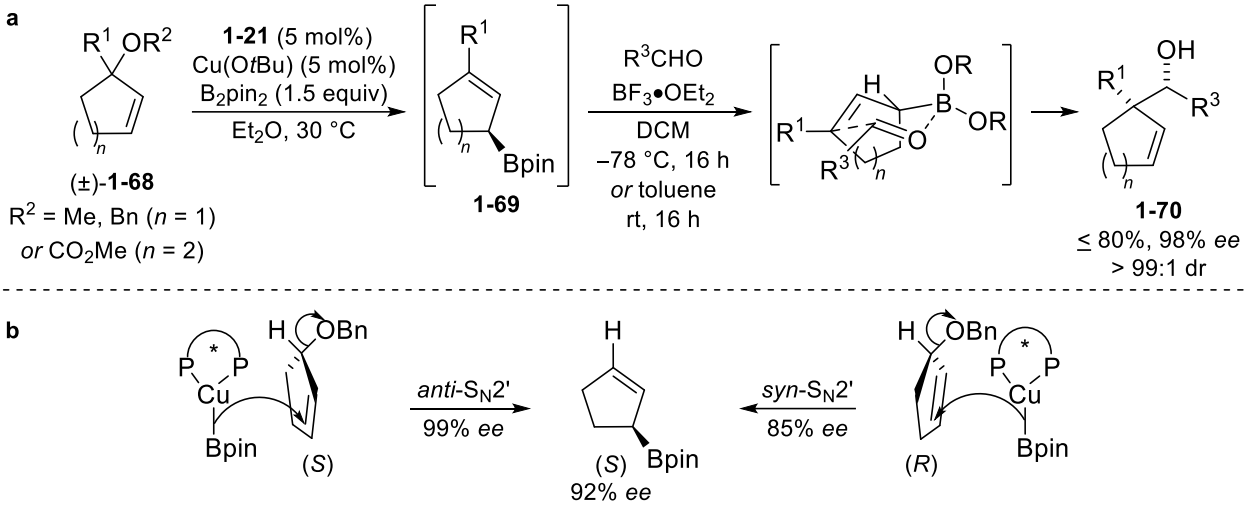

Figure 1-10. (a) Enantioconvergent copper-catalyzed allylic borylation (b) source of the observed enantioconvergency.

Tan and co-workers recently reported a similar enantioconvergent copper-catalyzed γ-allylic borylation process, however the reaction conditions are drastically different. In this case, racemic secondary allylbromides **1-71** and **1-72** were borylated with a rare chiral copper guanidine catalyst

in a biphasic mixture with saturated aqueous carbonate base to afford secondary (**1-73**) or tertiary (**1-74**) allylic boronates, respectively, in high enantioselectivity (Scheme 1-11).[54] Furthermore, this methodology is one of the few known catalytic enantioselective methods to access cyclic tertiary allylic boronates. The reaction yields improved results under air and requires the use of aqueous carbonate for significant conversion. Based on electron paramagnetic resonance (EPR) studies, the authors propose that the active borylation catalyst is a mono-ligated copper(I) catalyst which undergoes a similar enantioconvergent process as that of Ito and co-workers (c.f. Figure 1-10).

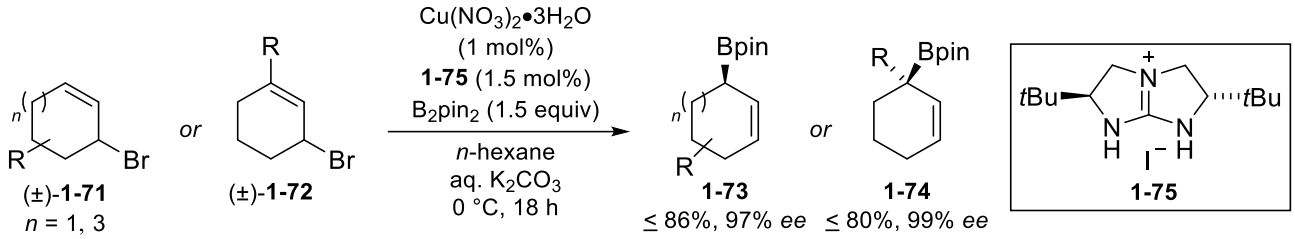

Scheme 1-11. Copper-catalyzed allylic borylation to access secondary and tertiary cyclic boronates.

1.2.2.1. Inverse electron-demand hetero Diels-Alder

Heterocyclic chiral allylic boronates are of particular interest as synthetic intermediates due to their relevance as building blocks in medicinal chemistry. However, there are only three reported methodologies for the enantioselective synthesis of heterocyclic allylic boronates. One example is from the copper-catalyzed γ-allylic borylation previously mentioned by Tan and co-workers (c.f. Scheme 1-11), where the corresponding 3,6-dihydro-2H-pyranyl allylic boronate is produced in 78% *ee*.[54]

The first established catalytic enantioselective approach to access heterocyclic allylic boronates was reported by Hall and co-workers using a chromium-catalyzed [4+2] Diels–Alder cycloaddition of 3-boronoacrolein and ethyl vinyl ether to provide a novel heterocyclic allylic boronate **1-76** in 96%

ee. The allylic boronate **1-76** could be utilized in a one pot aldehyde allylboration reaction to obtain novel α-hydroxyalkyl dihydropyrans **1-77** with high enantio- and diastereoselectivity (Scheme 1-12).[55] This highly efficient three-component one-pot reaction sequence was the basis for a number of subsequent natural product syntheses including thiomarinol **1-79**, and has recently been reviewed.[56] Alternatively, allylic boronate **1-76** can be utilized in ligand-controlled α- or γ-selective Suzuki-Miyaura cross coupling with aryl halides, which was recently reported as a key step in the total synthesis of Diospongin B.[57]

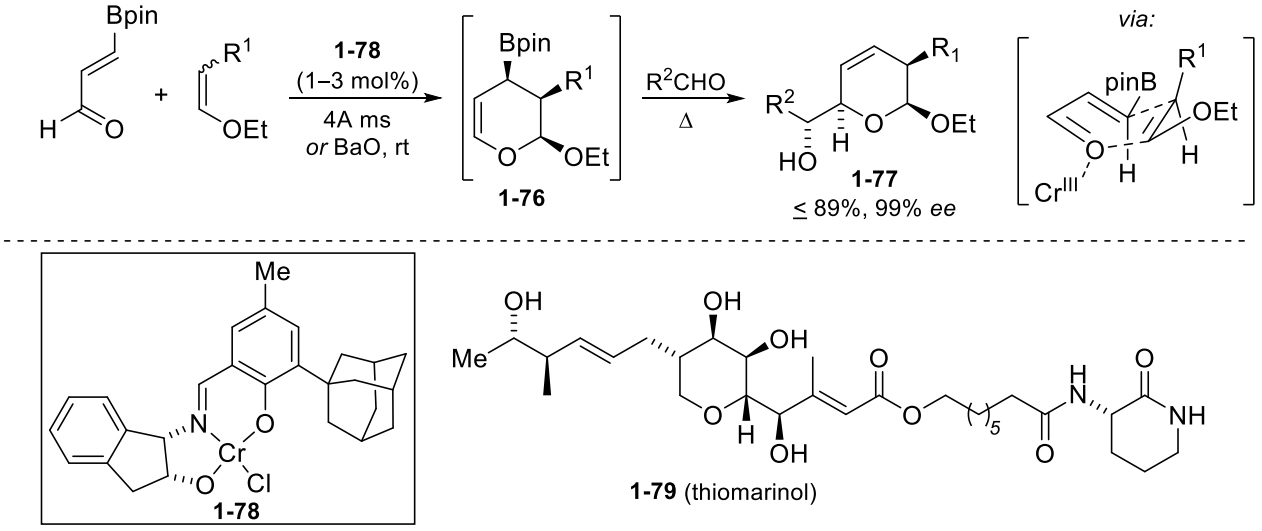

Scheme 1-12. Hall and co-workers' hetero-Diels-Alder approach to dihydro-pyranyl allylic boronates.

Surprisingly, the methodology outlined in Scheme 1-12 is the only catalytic enantioselective cycloaddition approach to access heterocyclic boronates in high enantioselectivity.[58] Although a Diels-Alder reaction may be the only type of cycloaddition amenable to accessing heterocylic allylic boronates, it seems that the area of catalytic enantioselective cycloadditions to access these important intermediates is vastly unexplored to-date.

1.2.4.3 *Borylative migration*

A conceptually different approach for the enantioselective synthesis of hetereocyclic allylic boronates is the borylative migration methodology developed by Hall and co-workers.[59] In the borylative migration, a cyclic alkenyl triflate or nonaflate is transformed to pyranyl or piperidinyl allylic boronates (**1-80**) using palladium catalysis, pinacolborane and an amine base (Scheme 1-13).[59] Similarly to allylic boronate **1-76**, the pyranyl or piperidinyl allylic boronate **1-80** can be utilized in both aldehyde allylboration or in ligand-controlled α- or γ-selective Suzuki-Miyaura cross coupling to obtain α-hydroxyalkyl heterocycles or arylated heterocycles in over 90% *ee*, respectively. For example, concise total syntheses of mefloquine, paroxetine and anabasine were achieved in high enantioselectivity and low step count from piperidinyl allylic boronate **1-80**. Details regarding the borylative migration reaction are presented in Chapters 2 and 3 of this thesis.

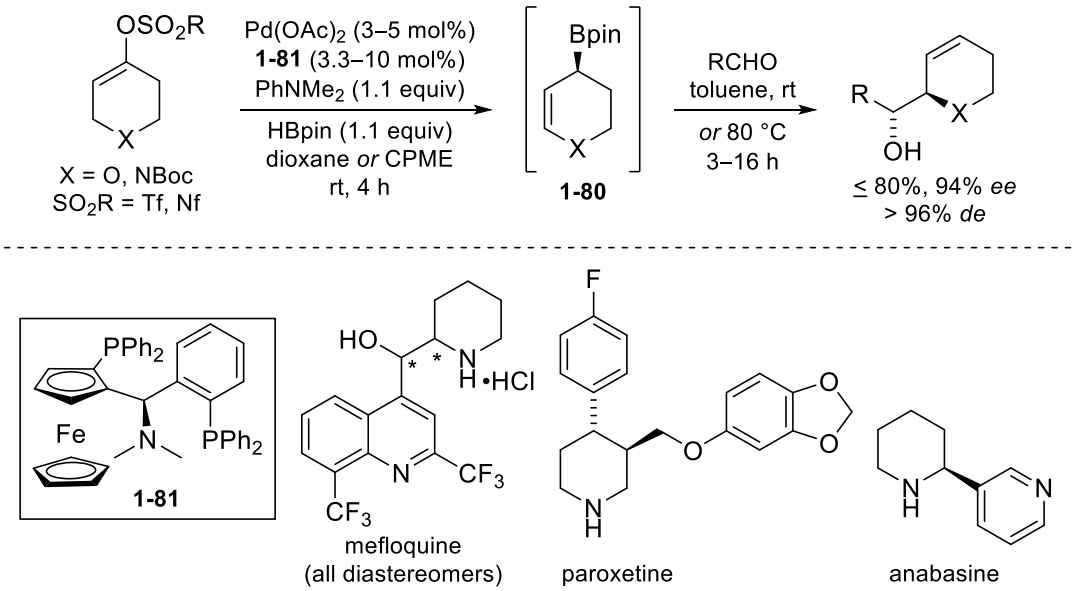

Scheme 1-13. Borylative migration approach to pyranyl and piperidinyl allylic boronates.

1.3 Synthetic applications of chiral boronic esters

1.3.1 The unique reactivity of organoboron compounds

Boron atoms are Lewis acidic in the tricoordinate state and electron rich in the tetracoordinate state (Figure 1-11a).[5] In regard to boronic esters, the high B-O bond strength results in the remaining σ-C-B bond becoming electron-rich and nucleophilic, thus with various electrophiles upon borate formation. This umpolung nature of boronates makes boronic esters remarkably versatile functional groups in organic chemistry (Figure 1-11b). Although there are numerous methodologies to utilize enantioenriched secondary and tertiary boronates in a stereospecific manner, limitations still exist in regard to the broad general for some of these transformation. Tertiary boronic esters suffer from limitations in reactivity due to increased steric hindrance around the boron atom, particularly in the case of pinacol-protected boronates. A very brief overview of the most common and general approaches to boronate functionalization is described in this chapter. For thorough coverage, the reader is directed to a recent more comprehensive review.[60]

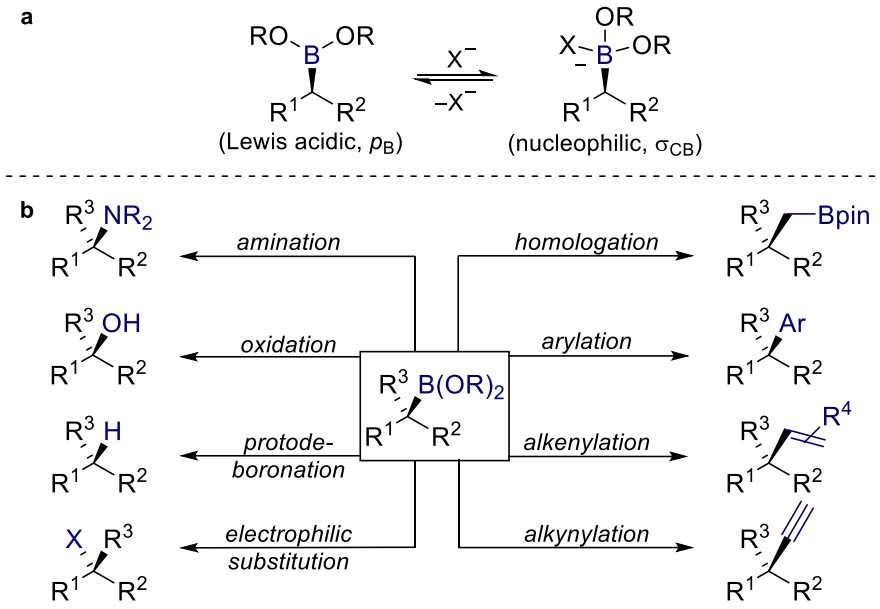

Figure 1-11. Brief overview of (a) boronic ester reactivity and (b) synthetic transformations.

1.3.2 Carbon-carbon bond forming reactions

1.3.2.1 *Allylboration*

The addition of allylic boronates to carbonyl compounds has continued to remain an invaluable synthetic tool for the stereocontrolled formation of carbon-carbon bonds in synthetic organic chemistry.[61] Allylic boronates belong to the Type I class of allylation reagents, which are characterized by a closed, Zimmerman-Traxler chair-like transition state involving carbonyl activation by the boron atom (**1-82**). The use of optically active α-substituted allylic boronates is an attractive method for the diastereoselective synthesis of *E*- or *Z*-homoallylic alcohols (**1-83**). Ketone allylborations are more challenging and are generally limited to catalytic enantioselective approaches using achiral non-substituted allylic boronates and methyl substituted ketones/acetophenone derivatives to aid with diastereoselectivity issues. Notably, Aggarwal and co-

workers have recently developed conditions allowing for the addition of enantioenriched allylic boronates to ketones by preforming a more reactive borinic ester intermediate *in situ*.[62]

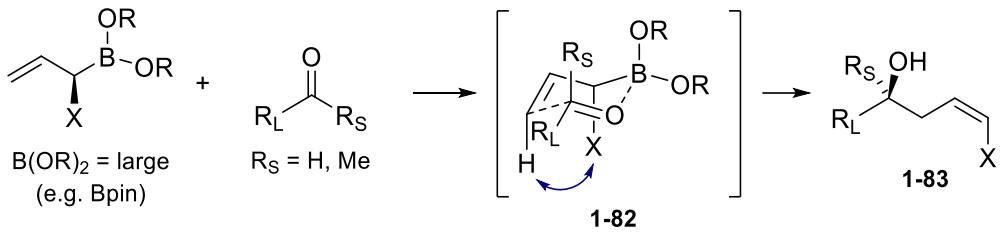

Figure 1-12. Allylboration of α-substituted enantioenriched allylic boronates.

1.3.2.2 *Matteson Homologation and Zweifel olefination*

Both the Matteson homologation and Zweifel olefination are well-established carbon-carbon bond forming reactions that utilize the 1,2-metallate rearrangement of borates promoted by a carbon-based nucleophile containing an α-leaving group.[60,63] These reactions have shown to be generally applicable to secondary and tertiary boronic esters. Furthermore, a variety of lithiated nucleophiles have been used in this process, including enantioenriched lithiated carbamates. The standard Matteson homologation involves coordination of lithiated dichloro- or dibromomethane, which will undergo a 1,2-shift upon warming of the reaction mixture to afford the homologated boronic ester **1-84** (Figure 1-13).

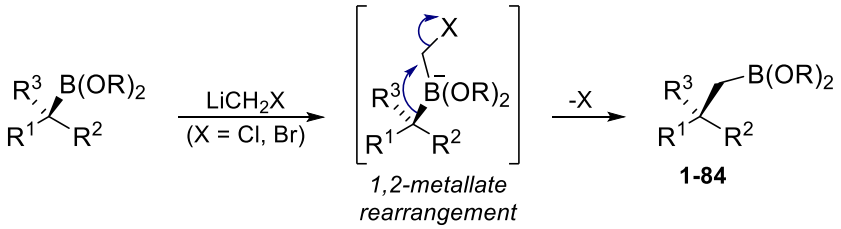

Figure 1-13. The traditional Matteson homologation of boronic esters.

The Zweifel olefination involves *in situ* formation of a vinylborate intermediate, which undergoes a 1,2-metallate rearrangement upon iodination (Figure 1-14). Alkoxide-induced *anti* elimination furnishes the vinylated product **1-86**. Under conditions involving reacting boronic esters with excess vinylmagnesium bromide, it has been found that complete dissociation of the pinacol boron protecting group occurs before iodination, and therefore forming alkyl-iodide **1-85** upon iodination and rearrangement. The ability to fully dissociate the pinacol group may be one reason why this reaction has seen extensive application with sterically congested alkyl boronates and in natural product syntheses.[63]

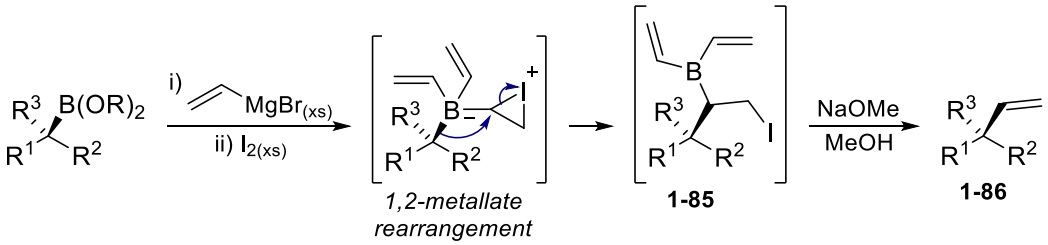

Figure 1-14. General mechanistic steps of the Zweifel olefination of boronic esters.

Furthermore, a number of other stereospecific reactions have been developed by Aggarwal and co-workers by varying the nucleophile and taking advantage of various elimination pathways. These variations allow for the stereospecific formation of specific C-C, C-N and C-X (X = halogen) bonds. Many of these processes require borate-formation followed by activation to an appropriate leaving group, similar to the Zweifel olefination. The methods developed by Aggarwal and co-workers are quite specific in terms of the lithiated nucleophile and the type of boronic ester used, and have recently been reviewed.[60]

1.3.2.3 *Suzuki-Miyaura cross-coupling*

Although the Suzuki-Miyaura cross-coupling reaction is one of the most powerful approaches to form Csp^2-Csp^2 bonds in organic chemistry, the corresponding process with secondary boronates to form Csp^3-Csp^2 bonds has been relatively limited to-date (Figure 1-15).[64] Mechanistically, only the oxidative addition step is not affected by the use of an alkylboronate.[65] The transmetallation can be a retentive or an invertive process (**1-87** vs **1-88**, Figure 1-15a) and is slow in the case of alkylboronates due to high steric-hindrance around the boron atom. Furthermore, if transmetallation succeeds, β-hydride elimination can compete with the desired reductive elimination process. To-date, substrates typically require activation by various means, including amide or alcohol coordination, a germinal/vicinal boronate group, or a π-conjugation (i.e. allylic or benzylic boronates). Select examples of enantioenriched substrates that were successfully employed in Suzuki-Miyaura cross-coupling conditions are shown in Figure 1-15b. Notably, conversion to the tetrafluoroborate salt is commonly required for an efficient reaction. Furthermore, conditions for the cross-coupling of simple, yet seemingly unactivated potassium trifluoroborate salts and boronic acids **1-89** and **1-90** have recently been reported, yet are currently limited to substrates containing an α-methyl group.[66]

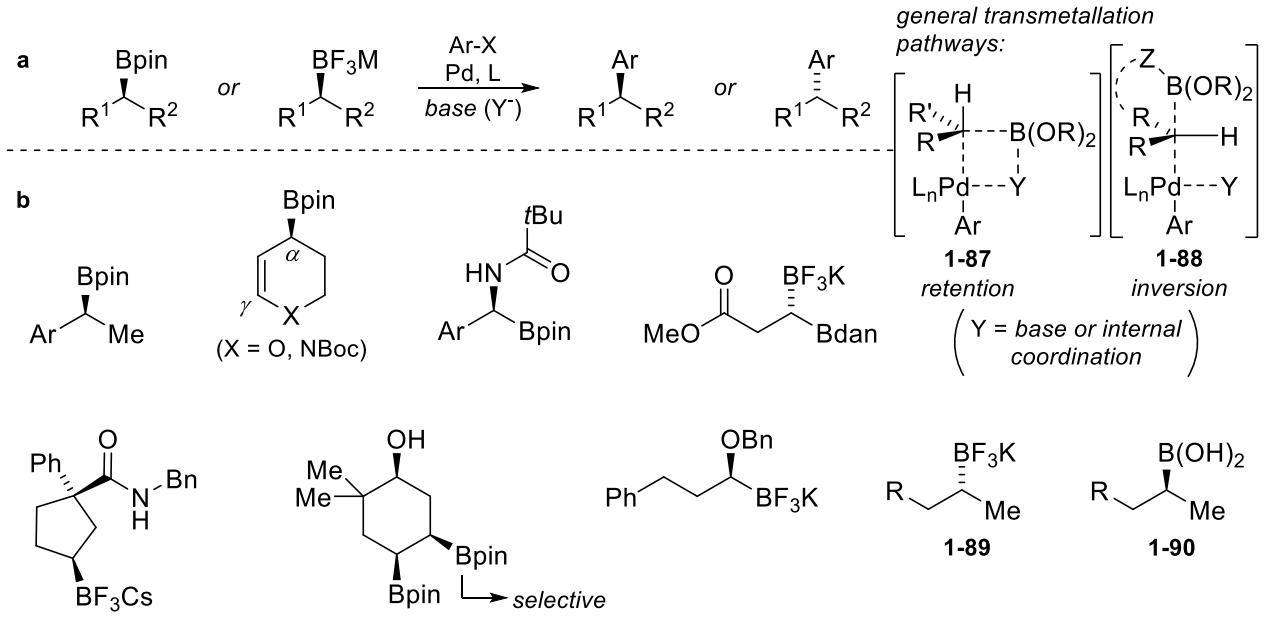

Figure 1-15. (a) The general palladium-catalyzed Suzuki-Miyaura cross-coupling reaction of alkylboronates (b) selected examples of alkylboronate coupling substrates.

1.3.3 Oxidation methods – oxygenation and amination

Alkylboronic esters are slowly oxidized to boric acid under ambient conditions.[5] Therefore, it is not surprising that promoting the oxygenation of C-B bonds has long been known and is an extremely robust reaction. Traditional conditions for the oxidation of alkylboronates are a mixture of organic solvent (commonly THF) and an alkaline solution of hydrogen peroxide. Furthermore, the milder sodium perborate oxidant can also be used, which can allow selective oxidation specific boron protecting groups.[67] Furthermore, more sophisticated methods with amine oxides have recently shown to be able to achieve site-selective oxidation of vicinal boronates.[68]The oxygenation reaction mechanism involves coordination of a hydroperoxide anion to form the common tetracoordinated borate. The borate undergoes the expected 1,2-metallate rearrangement to afford the corresponding alcohol **1-91** stereospecifically upon work-up of **1-92** (Figure 1-16).

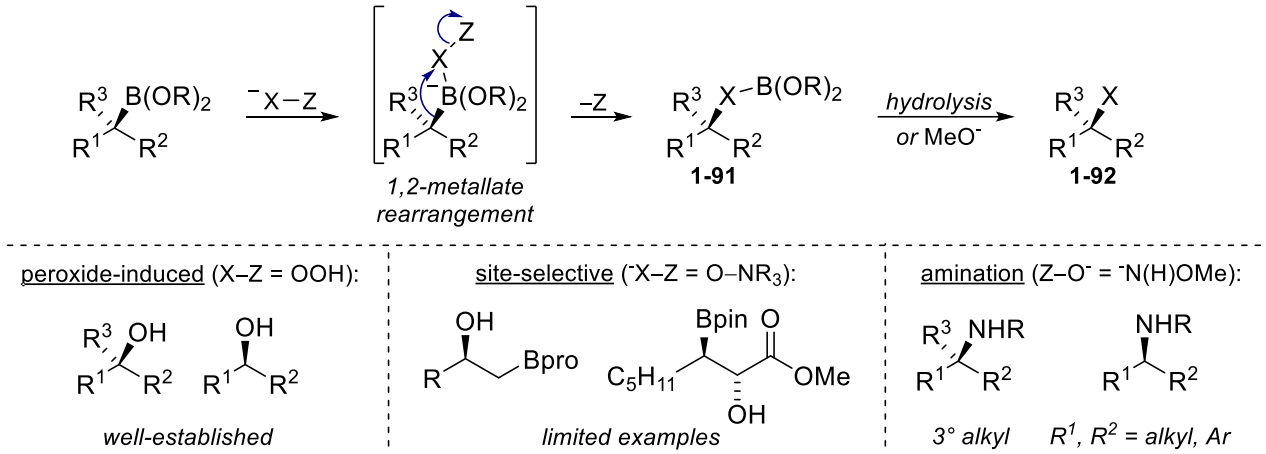

Figure 1-16. Simplified overview of stereospecific oxygenation and amination of boronic esters.

Considering the oxidation mechanism in Figure 1-16, one can easily envision an amination protocol following a similar pathway. Although conceptually the functionalization should be equivalent, the lack of forming a strong B-O bond renders the process much less thermodynamically favourable.[69] Morken and co-workers have overcome this obstacle by using a methoxamine nucleophile which can aminate secondary boronates and non-benzylic tertiary boronates stereospecifically.[70] With benzylic tertiary boronates, protodeboronation competes. The chosen nucleophile is likely kinetically reactive due its small size and the process may be thermodynamically favourable from overall formation of a B-O bond in the by-product pinBOMe. To-date all other amination protocols of secondary and tertiary boronic esters require formation of a more reactive borinic ester or dichloroborane *in situ* using relatively harsh reaction conditions.[60] Notably, a mild amination protocol for tertiary benzylic boronic esters still lacks in the literature.

1.3.4 Protodeboronation

Although protodeboronation is typically an undesired side reaction, stereospecific protodeboronation of tertiary boronates can unlock an avenue to enantioenriched methine stereocenters. Unlike many of the lithiation methodologies outlined above, a reagent for an intramolecular 1,2-metallate rearrangement is not possible for a protodeboronation pathway. Aggarwal and co-workers have reported a general stereoretentive protodeboronation pathway for diaryl and benzylic boronates using fluoride sources (Figure 1-17).[71] Mechanistic studies of benzylic substrates **1-93** suggest that the stereoselectivity arises from a hydrogen bonded boronate complex **1-94** to afford the corresponding methine product stereoretentively. Although this useful procedure has found applicability in methodology and natural product syntheses, a general approach for the stereospecific protodeboronation of tertiary non-benzylic boronates is still an unmet need in the literature.[60]

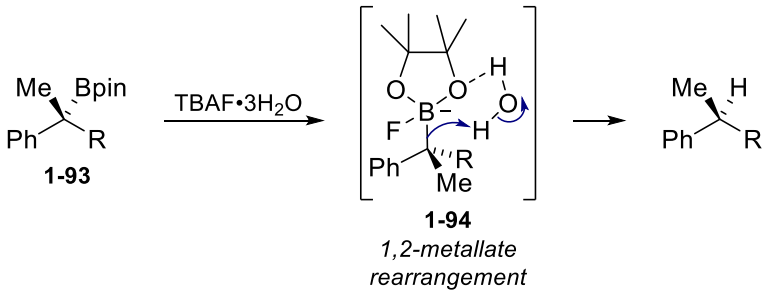

Figure 1-17. Proposed stereospecificity of Aggarwal's protodeboronation of benzylic substrates.

1.4 Thesis objective

Enantioenriched boronates are becoming increasingly valuable and versatile building blocks in organic chemistry. Although many catalytic approaches exist for the enantioselective synthesis of linear hydrocarbon-based boronates, the important move toward more functionalized cyclic and

heterocylic boronates is an unmet need. The opportunity to access more biologically-relevant chiral boronates would allow entry into novel 3-dimensional chemical space for medicinal chemistry purposes. In this regard, the primary goal of this thesis is to improve and expand the field of catalytic enantioselectivity approaches novel and versatile cyclic alkylboronates.

Considering the established synthetic utility of the pyranyl and piperidinyl allylic boronates obtained from the borylative migration reaction, our group is interested in expanding the scope of this unique borylation methodology to new, more functionalized substrates of pharmaceutical interest. Chapter 2 will present efforts towards expanding the substrate scope of the borylative migration from unsubtituted piperidinyl and pyranyl electrophiles. The optimization of the borylative migration reaction to the 7-memebered azepane ring system is described, allowing access novel enantioenriched α-hydroxyalkyl dehydroazepanes.

In light of the modest success in improving the generality of the borylative migration, deciphering the mechanism of this reaction is a beneficial endeavour. Chapter 3, will describe a detailed mechanistic investigation of the borylative migration, in a collaborative effort combining both experimental and computational work. Some key questions to be addressed include the nature of the Miyaura-type borylation with pinacolborane, the precise role(s) of the amine base and understanding the alkene isomerization step. With the information obtained, a mechanistic proposal is presented in regard to the most conceivable pathway whereby this overall Miyaura borylation and formal alkene isomerization reaction may occur.

Although cyclobutane rings are important in medicinal chemistry, very few catalytic enantioselective approaches to cyclobutylboronates exist. In this regard, Chapter 4 will present the development of a copper-catalyzed conjugate borylation to provide the first examples of

enantioennriched tertiary cyclobutylboronates. The unique reactivity of the borylated cyclobutanone products as versatile synthetic intermediates is displayed.

1.5 References

[1] N. A. Meanwell, *Chem. Res. Toxicol* **2016**, *29*, 564.

[2] a) F. Lovering, *Med. Chem. Commun.* **2013**, *4*, 515.; b) F. Lovering, J. Bikker, C. Humblet, *J. Med. Chem.* **2009**, *52*, 6752.

[3] a) B. J. Huffman, R. A. Shenvi, *J. Am. Chem. Soc.* **2019**, *141*, 3332.; (b) S. L. Schreiber, *Science* **2000**, *287*, 1964.

[4] C-Y., Wang, J. Derosa, M. R. Biscoe, *Chem. Sci.* **2015**, *6*, 5105.

[5] D. G. Hall, *Boronic Acids*, 2nd Edition, Wiley: Weinheim, 2011.

[6] Q. I. Churches, C. A. Hutton in *Boron Reagents in Synthesis*, Adiel Coca, Chapter 11, Oxford University Press, 2011, 357–377.

[7] D. G. Brown, J. Boström, *J. Med. Chem.* **2016**, *59*, 4443.

[8] B. S. Collins, C. M. Wilson, E. L. Myers, V. K Aggarwal, *Angew. Chem. Int. Ed.* **2017**, *56*, 11700.

[9] a) J. C. Lee, D. G. Hall, *J. Am. Chem. Soc.* **2010**, *132*, 5544.; b) Z. Han, G. Liu, X. Zhang, A. Li, X-Q. Dong, X. Zhang, *Org. Lett.* **2019**, *21*, 3923.; c) I. G. Smilović, E. Casas-Arcé, S. J. Roseblade, U. Nettekoven, A. Zanotti-Gerosa, M. Kovačevič, Z. Časar, *Angew. Chem. Int. Ed.* **2012**, *51*, 1014.

[10] K. Kubota, S. Osaki, M. Jin, H. Ito, *Angew. Chem. Int. Ed.* **2017**, *56*, 6646.

[11] a) B. Potter, A. A. Szymaniak, E. K. Edelstein, J. P. Morken, *J. Am. Chem. Soc.* **2014**, *136*, 17918.; b) H-Y. Sun, K. Kubota, D. G. Hall, *Chem. Eur. J.* **2015**, *21*, 19186.

[12] S. Namirembe, J. P. Morken, *Chem. Soc. Rev.* **2019**, *48*, 3464.

[13] D. Männig, H. Nöth, *Angew. Chem. Int. Ed.* **1985**, *10*, 878.

[14] C. M. Crudden, D. Edwards, *Eur. J. Org. Chem.* **2003**, 4695.

[15] Select examples: a) A. J. Bochat, V. M. Shoba, J. M. Takacs, *Angew. Chem. Int. Ed.* **2019**, *58*, 9434.; b) N. Hu, G. Zhao, Y. Zhang, X. Liu, G. Li, W. Tang, *J. Am. Chem. Soc.* **2015**, *137*, 6746.; c) L. Zhang, Z. Zuo, X. Wan, Z., *J. Am. Chem. Soc.* **2014**, *136*, 15501.; d) X. Feng, H. Jeon, J. Yun, *Angew. Chem. Int. Ed.* **2013**, *52*, 3989.

[16] a) W. J. Jang, S. M. Song, J. H. Moon, J. Y. Lee, J. Yun, *J. Am. Chem. Soc.* **2017**, *139*, 13660.; b) Y. Cai, X-T. Yang, S-Q. Zhang, F. Li, Y-Q. Li, L-X. Ruan, X. Hong, S-L. Shi, *Angew. Chem. Int. Ed.* **2018**, *57*, 1376.

[17] a) S. Chakrabarty, H. Palencia, M. D. Morton, R. O. Carr, J. M. Takacs, *Chem. Sci.*, **2019**, *10*, 4854.; b) Y. Xi, J. F. Hartwig, *J. Am. Chem. Soc.* **2016**, *138*, 6703.; (b) X. Chen, Z. Cheng, J. Guo, Z. Lu, *Nat. Commun.* **2018**, *9*, 3939.; c) Z. Bai, S. Zheng, Z. Bai, F. Song, H. Wang, Q. Peng, G. Chen, G. He, *ACS Catal.* **2019**, *9*, 6502.

[18] a) V. M. Shoba, N. C. Thacker, A. J. Bochat, J. M. Takacs, *Angew. Chem. Int. Ed.* **2016**, *55*, 1465.; b) S. Chakrabarty, J. M. Takacs, *ACS Catal.* **2018**, *8*, 10530.; c) G. L. Hoang, J. M. Takacs, *Chem. Sci.* **2017**, *8*, 4511.

[19] a) G. L. Hoang, Z-D. Yang, S. M. Smith, R. Pal, J. L. Miska, D. E. Pérez, L. S. Pelter, X. C. Zeng, J. M. Takacs, *Org. Lett.* **2015**, *17*, 940.; b) Z-D. Yang, R. Pal, G. L. Hoang, X. C. Zeng, J. M. Takacs, *ACS Catal.* **2014**, *4*, 763.

[20] Y. Sasaki, C. Zhong, M. Sawamura, H. Ito, *J. Am. Chem. Soc.* **2010**, *132*, 1226.

[21] K. Kubota, Y. Watanabe, K. Hayama, H. Ito, *J. Am. Chem. Soc.* **2016**, *138*, 4338.

[22] a) K. Kubota, Y. Watanabe, H. Ito, *Adv. Synth. Catal.* **2016**, *358*, 2379.; b) H. Ito, *Pure Appl. Chem.* **2018**, *90*, 703.

[23] a) X. Li, C. Wang, J. Song, Z. Yang, G. Zi, G. Hou,*J. Org. Chem.* **2019**, *84*, 8638.; b) D. Kong, S. Han, G. Zi, G. Hou, J. Zhang, *J. Org. Chem.* **2018**, *83*, 1924.

[24] K. Semba, T. Fujihara, J. Terao, Y. Tsuji, *Tetrahedron* **2015**, *71,* 2183.

[25] B. Chen, P. Cao, Y. Liao, M. Wang, J. Liao, *Org. Lett.* **2018**, *20*, 1346.

[26] K. M. Logan, M. K. Brown, *Angew. Chem. Int. Ed.* **2017**, *56*, 851.

[27] S. R. Sardini, M. K. Brown, *J. Am. Chem. Soc.* **2017**, *139*, 9823.

[28] L-A. Chen, A. R. Lear, P. Gao, M. K. Brown, *Angew. Chem. Int. Ed.* **2019**, *58*, 10956.

[29] For selected examples, see: a) A. Whyte, K. I. Burton, J. Zhang, M. Lautens, *Angew. Chem. Int. Ed.* **2018**, *57*, 13927.; b) L. Jiang, P. Cao, M. Wang, B. Chen, B. Wang, J. Liao, *Angew. Chem. Int. Ed.* **2016**, *55*, 13854.; c) N. Kim, J. T. Han, D. H. Ryu, J. Yun, *Org. Lett.* **2017**, *19*, 6144.; d) P. Zheng, X. Han, J. Hu, X. Zhao, T. XU, *Org. Lett.* **2019**, *21*, 6040.

[30] J. C. Green, M. V. Joannou, S. A. Murray, J. M. Zanghi, S. J. Meek, *ACS Catal.* **2017**, *7*, 4441.

[31] a) J. B. Morgan, S. P. Miller, J. P. Morken, *J. Am. Chem. Soc.* **2003**, *125*, 8702.; b) S. Trudeau, J. B. Morgan, M. Shrestha, J. P. Morken, *J. Org. Chem.* **2005**, *70*, 9538.

[32] K. Toribatake, H. Nishiyama, *Angew. Chem. Int. Ed.* **2013**, *52*, 11011.

[33] K. Hong, J. P. Morken, *J. Org. Chem.* **2011**, *76*, 9102.

[34] J. R. Coombs, L. Zhang, J. P. Morken, *J. Am. Chem. Soc.* **2014**, *136*, 16140.

[35] L. Yan, Y. Meng, F. Haeffner, R. M. Leon, M. P. Crockett, J. P. Morken, *J. Am. Chem. Soc.* **2018**, *140*, 3663.

[36] N. Matsuda, K. Hirano, T. Satoh, M. Miura, *J. Am. Chem. Soc.* **2013**, *135*, 4934.

[37] a) R. Sakae, K. Hirano, T. Satoh, M. Miura, *Angew. Chem. Int. Ed.* **2015**, *54*, 613; b) For a small scope of linear alkenyl silanes with over 90% *ee*, see: K. Kato, K. Hirano, M. Miura, *Angew. Chem. Int. Ed.* **2016**, *55*, 14400.

[38] D. Nishikawa, K. Hirano, M. Miura, *J. Am. Chem. Soc.* **2015**, *137*, 15620.

[39] a) H. Ito, H. Yamanaka, J. Tateiwa, A. Hosomi, *Tetrahedron Lett.* **2000**, *41*, 6821.; b) J. A. Schiffner, K. Müther, M. Oestreich, *Angew. Chem. Int. Ed.* **2010**, *49*, 1194.

[40] a) S. Lee, J. Yun, in *Synthesis and Application of Organoboron Compounds*, E. Fernández, A. Whiting, Chapter 3, Springer, 2015, 73–92.; b) J-B. Chen, A. Whiting, *Synthesis* **2018**, *50*, 3843.

[41] S. Radomkit, A. H. Hoveyda, *Angew. Chem. Int. Ed.* **2014**, *53*, 3387.

[42] I-H. Chen, L. Yin, W. Itano, M. Kanai, M. Shibasaki, *J. Am. Chem. Soc.* **2009**, *131*, 11664.

[43] K. Kubota, K. Hayama, H. Iwamoto, H. Ito, *Angew. Chem. Int. Ed.* **2015**, *54*, 8809.

[44] a) Y. Luo, S. M. Wales, S. E. Korkis, I. D. Roy, W. Lewis, H. W. Lam, *Chem. Eur. J.* **2018**, *24*, 8315.; b) H. Lee, J. Yun, *Org. Lett.* **2018**, *20*, 7961.

[45] a) H. L. Sang, S. Yu, S. Ge, *Org. Chem. Front.* **2018**, *5*, 1284.; b) D-W. Gao, Y. Xiao, M. Liu, Z. Liu, M. K. Karunananda, J. S. Chen, K. M. Engle, *ACS Catal.* **2018**, *8*, 3650.

[46] C. Diner, K. J. Szabó, *J. Am. Chem. Soc.* **2017**, *139*, 2.

[47] H. Ito, T. Miya, M. Sawamura, *Tetrahedron Lett.* **2012**, *68*, 3423.

[48] H. Ito, S. Ito, Y. Sasaki, K. Matsuura, M. J. Sawamura, *J. Am. Chem. Soc.* **2007**, *129*, 14856.

[49] A. Guzman-Martinez, A. H. Hoveyda, *J. Am. Chem. Soc.* **2010**, *132*, 10634.

[50] J. K. Park, H. H. Lackey, B. A. Ondrusek, D. T. McQuade, *J. Am. Chem. Soc.* **2011**, *133*, 2410.

[51] a) H. Ito, T. Okura, K. Matsuura, M. Sawamura, *Angew. Chem. Int. Ed.* **2010**, *49*, 560.; b) E. Yamamoto, Y. Takenouchi, T. Ozaki, T. Miya, H. Ito, *J. Am. Chem. Soc.* **2014**, *136*, 16515.; c) Y. Takenouchi, R. Kojima, R. Momma, H. Ito, *Synlett* **2017**, *28*, 270.

[52] a) R. Kojima, S. Akiyama, H. Ito, *Angew. Chem. Int. Ed.* **2018**, *57*, 7196.; b) S. Akiyama, K. Kubota, M. S. Mikus, P. H. Paioti, F. Romiti, Q. Liu, Y. Zhou, A. H. Hoveyda, H. Ito, *Angew. Chem. Int. Ed.* **2019**, *58*, 11998.

[53] H. Ito, S. Kunii, M. Sawamura, *Nat. Chem.* **2010**, *2*, 972.

[54] Y. Ge, X-Y. Cui, S. M. Tan, H. Jiang, J. Ren, N. Lee, R. Lee, C-H. Tan, *Angew. Chem. Int. Ed.* **2019**, *58*, 2382.

[55] X. Gao, D. G. Hall, *J. Am. Chem. Soc.* **2003**, *125*, 9308.

[56] D. G. Hall, T. Rybak, T. Verdelet, *Acc. Chem. Res.* **2016**, *49*, 2489.

[57] T. Rybak, D. G. Hall, *Org. Lett.* **2015**, *17*, 4156.

[58] A 1,3-dipolar cycloaddition was reported to access functionalized borylated pyrroles in 60% *ee*: a) A. López-Pérez, M. Segler, J. Adrio, J. C. Carretero, *J. Org. Chem.* **2011**, *76*, 1945.; For a single example of a stoichiometric hydrogen-bond promoted 2+2 cycloaddition approach to an enantioenriched cyclobutylboronate in 98% *ee*: b) S. C. Coote, T. Bach, *J. Am. Chem. Soc.* **2013**, *135*, 14948.; During revision of this thesis, a new report of a cobalt-catalyzed enantioselective [2+2] cycloaddition of cyclobutenylboronates was disclosed: c) M. M. Parsutkar, V. V. Pagar, T. V. RajanBabu, *J. Am. Chem. Soc.* **2019**, *141*, 15367.

[59] a) S. Lessard, F. Peng, D. G. Hall, *J. Am. Chem. Soc.* **2009**, *131*, 9612.; b) Y-R. Kim, D. G. Hall, *Org. Biomol. Chem.* **2016**, *14*, 4739.

[60] C. Sandford, V. K. Aggarwal, *Chem. Commun.* **2017**, *53*, 5481.

[61] a) H. Lachance, D. G. Hall, *Org. React*. **2008**, ***73***, 1–574.; b) P. V. Ramachandran, P. D. Gagare, D. R. Nicponski, in *Comprehensive Organic Synthesis II*, 2nd Edition, P. Knochel, Allylborons, Elsevier, 2014, 1–71.

[62] J. L.-Y. Chen, V. K. Aggarwal, *Angew. Chem. Int. Ed.* **2014**, *53*, 10992.

[63] R. J. Armstrong, V. K. Aggarwal, *Synthesis* **2017**, *49*, 3323.

[64] J. P. Rygus, C. M. Crudden, *J. Am. Chem. Soc.* **2017**, *139*, 18124.

[65] H-Y. Sun, D. G. Hall in *Synthesis and Application of Organoboron Compounds*, E. Fernández, A. Whiting, Chapter 7, Springer, 2015, 221–242.

[66] a) S. Zhao, T. Gensch, B. Murray, Z. L. Niemeyer, M. S. Sigman, M. R. Biscoe, *Science* **2018**, *362*, 670.; b) J. W. Lehmann, I. T. Crouch, D. J. Blair, M. Trobe, P. Wang, J. Li, M. D. Burke, *Nat. Commun.* **2019**, *10*, 1263.

[67] a) A. McKillop, W. R. Sanderson, *Tetrahedron* **1995**, *51*, 6145.; b) S. Radomkit, Z. Liu, A. Closs, M. S. Mikus, A. H. Hoveyda, *Tetrahedron* **2017**, *73*, 5011.

[68] a) L. Yan, J. P. Morken, *Org. Lett.* **2019**, *21*, 3760.; b) E. W. Ng, K-H. Low, P. Chiu, *J. Am. Chem. Soc.* **2018**, *140*, 3537.

[69] Calculated bond dissociation energies ($\Delta H f_{298}$) for B-C, B-N and B-O bonds are reported to be 107, 93 and 124 kcal mol^{-1}, respectively. Sources: see reference [5]; https://labs.chem.ucsb.edu/zakarian/armen/11---bond dissociationenergy.pdf, accessed August 5th, 2019.

[70] a) S. N. Mlynarski, A. S. Karns, J. P. Morken, *J. Am. Chem. Soc.* **2012**, *134*, 16449.; b) E. K. Edelstein, A. C. Grote, M. D. Palkowitz, J. P. Morken, *Synlett* **2018**, *29*, 1749.

[71] S. Nave, R. P. Sonawane, T. G. Elford, V. K. Aggarwal, *J. Am. Chem. Soc.* **2010**, *132*, 17096.

Chapter 2: Expanding of the Substrate Scope of the Borylative Migration

2.1 Introduction

As discussed in Chapter 1, synthetic approaches to enantioenriched alkylboronic esters are receiving increasing attention due to the synthetic versatility of the resulting C-B bond. Furthermore, allylic boronic esters have the increased synthetic appeal of increased reactivity as well as being able to undergo α- or β-regioselective reactions.[1] Particularly useful carbon-carbon bond forming reactions of allylic boronates include the famous Suzuki-Miyaura cross-coupling and allylboration reactions.[2,3] In this regard, the Hall group has previously developed a novel palladium-catalyzed enantioselective borylative migration reaction of 6-membered cyclic enol perfluorosulfonates **2-1** and **2-2**, leading to optically enriched piperidinyl and pyranyl allylic boronates **2-3** and **2-4**, respectively.[4,5] These products have proven to be versatile synthetic intermediates in stereospecific aldehyde allylboration and α- or γ-regiocontrolled allylic Suzuki-Miyaura cross-coupling chemistry (Figure 2-1).[6,7]

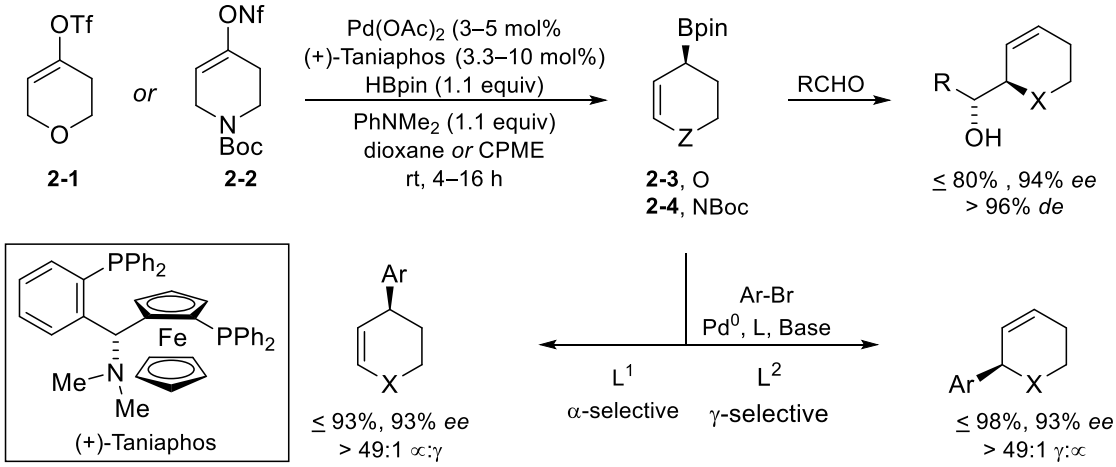

Figure 2-1. Catalytic enantioselective borylative migration for the preparation of various piperidine and pyran derivatives

Heterocyclic boronate **2-4** is particularly appealing considering the piperidine-based scaffold. Non-aromatic nitrogen-containing heterocycles are structural constituents of a vast number of natural products and pharmaceutical drugs. It has been reported that 59% of small molecule drugs contain a nitrogen atom and that the piperidine ring is the most common nitrogen heterocycle and the third most frequent ring system overall.[8] Therefore, the development of stereocontrolled methodologies to access enantioenriched piperidine rings is an important objective for medicinal chemistry purposes. In this regard, our laboratory has shown the synthetic utility of **2-4** for the synthesis of numerous piperidine-based scaffolds (Figure 2-2). Most notably, the first concise enantioselective synthesis of mefloquine was achieved, a feat which confirmed the configuration of each stereoisomer for the first time using a chemical approach.[7]

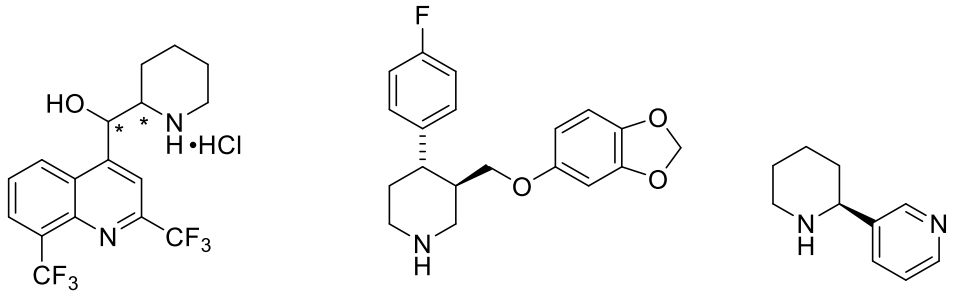

mefloquine stereoisomers
(antimalarial)
3 to 4 steps
99% *ee*

(+)-paroxetine
(antidepressant)
formal synthesis
4 steps, 91% *ee*

(+)-anabasine
(insecticide)
formal synthesis
3 steps, 90% *ee*

Figure 2-2. Previously published applications of piperidine **2-4** for the syntheses of bioactive molecules.

Recognizing the importance of allylic boronate **2-4** as a synthetic building block, the borylative migration methodology was further optimized with **2-2** for the first time to allow for more practical large-scale utility with a slightly improved yield (> 70%) and enantioselectivity (> 90%).[5] Notable improvements include the use of an alkenyl nonaflate instead of triflate, which displays improved stability and ease of synthesis. Furthermore, a catalyst loading of only 3 mol% palladium(II) acetate

and 3.3 mol% of the chiral ligand, Taniaphos, could be used without erosion of the yield nor enantioselectivity. The utility of the improved procedure was displayed with an 8.0 g large scale example of the borylative migration-allylboration sequence leading to an 80% yield and 91% *ee* (Scheme 2-1)

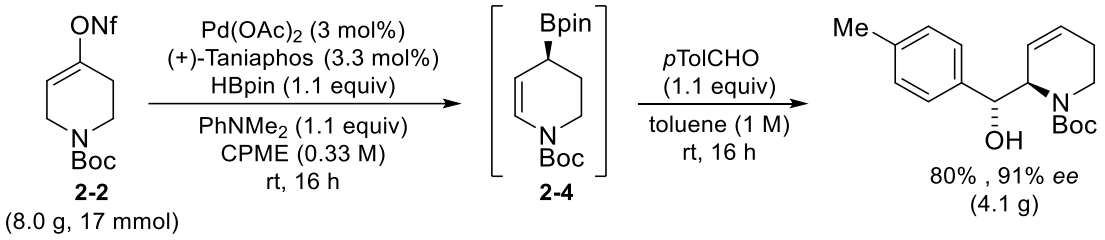

Scheme 2-1. Multigram-scale borylative migration-allylboration sequence.

2.2 Objective

Considering the effectiveness of the borylative migration methodogy in accessing 6-membered N- and O-containing boron heterocycles, our laboratory is interested in expanding the scope of this reaction. To-date, the reaction has only been developed for the 6-membered pyranyl and piperidinyl triflate and nonaflate, respectively, without further substitution on the alkene. The Hall Group is particularly interested in expanding the borylative migration reaction to various nitrogen-based heterocycles due to their high prevalence in drug scaffolds.[8] Therefore, two underlying opportunities for substrate modification of piperidinyl nonaflate **2-2** were identified (Scheme 2-2). Firstly, changing the ring size to the corresponding 5-, 7- and 8-membered nitrogen heterocycles would allow entry into new classes of important bioactive nitrogen ring systems. Secondly, a nonaflate which contains alkene substitution (i.e. a tetrasubstituted alkene) would lead to heterocyclic products involving a more useful synthetic handle for further elaboration post-allylboration or Suzuki-Miyaura cross-coupling.

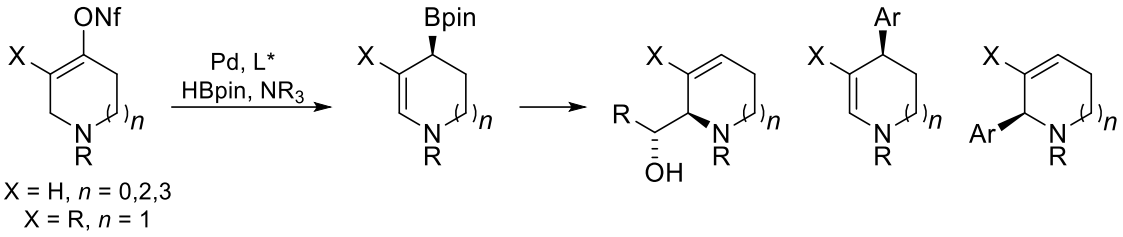

Scheme 2-2. Proposed opportunities for expansion of the borylative migration substrate scope.

In this regard, five different alkenyl nonaflates were targeted (Figure 2-3), which include the pyrrolidine, azepane and azocane-based ring systems that had yet to be properly explored in the borylative migration (**2-5**–**2-7**). In terms of alkene substitution, it was proposed that exploration of alkene substituents with varying electronic properties has the potential to provide different reactivity in the borylative migration. Therefore, alkenyl nonaflates containing a non-activated methyl substituent (**2-8**) and an electron-withdrawing ester substituent (**2-9**) were targeted.

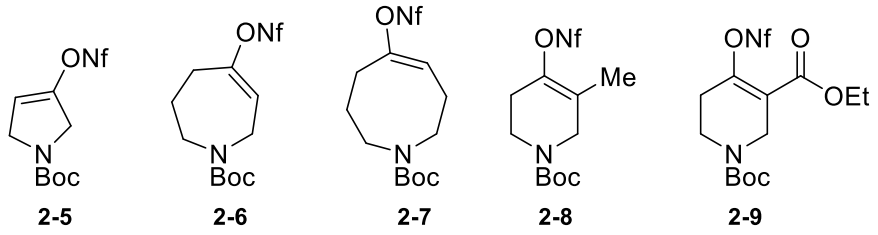

Figure 2-3. Novel nonaflates targeted for the borylative migration reaction screening.

2.3 Initial screening of new alkenyl nonaflate substrates

2.3.1 Synthesis of the alkenyl nonaflate starting materials

One appealing aspect of the borylative migration is that alkenyl nonaflates and triflates can be made in a single step from the corresponding ketone precursor by deprotonation and subsequent trapping with an electrophilic Nf or Tf source *in situ*.[9] For example, simple one step protocols to access the piperidine and pyran alkenyl nonaflates **2-1** and **2-2** have been previously reported by our group

(Scheme 2-3).[4,5] Thus, the borylative migration allows access to enantioenriched piperidine and pyran scaffolds without the requirement of a multistep synthetic approach of the corresponding precursor. Lengthy precursor syntheses are typically required for some of the more common unimolecular approaches to piperidine rings, such as intramolecular nucleophilic substitution and ring closing reactions.[5]

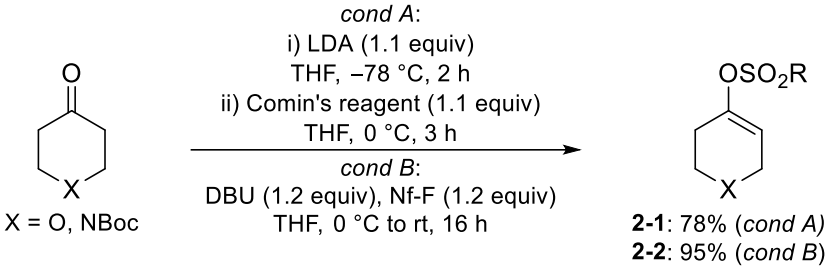

Scheme 2-3. Previously reported syntheses of pyran and piperidine alkenyl sulfonates.

However, when moving from a 6- to a 5- or 7-membered ring system, one new aspect to be considered is the potential for regioisomeric enolization during the preparation of the alkenyl nonaflate; a potential issue caused by the lack of symmetry of the ketone precursor. Fortunately, it was found by a previous Hall Group MSc graduate (Mrs. Samantha Kwok), that regioselective deprotonation of the corresponding *N*-Boc pyrrolidinone and azepinone could be achieved to obtain **2-5** and **2-6** using standard cryogenic conditions with lithium bis(trimethylsilyl)amide (LiHMDS) as the base (Scheme 2-4).[10] Although further experimental evidence is required for a conclusive rationale, the observed kinetically-controlled regioselective deprotonation for the pyrrolidinone could originate from the avoidance of steric interactions with the large *N*-Boc carbamate. On the other hand, the regioselectivity observed with the azepane scaffold could be attributed to a long range inductive effect of the homoallylic carbamate nitrogen. Overall, it was found that the

previously developed procedures for the synthesis of nonaflates **2-5** and **2-6** were reproducible in providing a single regioisomer in moderate yields on a large scale (Scheme 2-4).

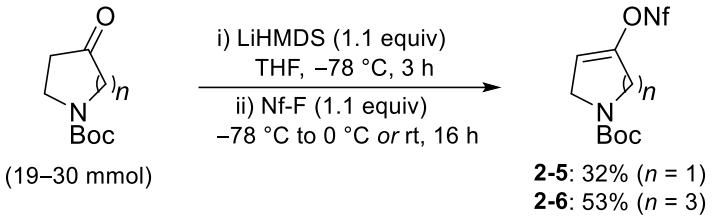

Scheme 2-4. Synthesis of nonaflates **2-5** and **2-6**.

Although the azocanone precursor for synthesis of the 8-membered ring nonaflate **2-7** is symmetrical, the reagent was not commercially available. Therefore, azocanone **2-11** was synthesized in three steps from commercially available *N*-Boc-hexahydro-1*H*-azepin-4-one according to a modified literature procedure by a Tiffeneau–Demjanov type ring expansion and subsequent decarboxylation.[11] The desired alkenyl nonaflate **2-7** was obtained by deprotonation, with LDA instead of DBU to ensure conversion, and trapping with an electrophilic nonaflate source (Scheme 2-5).

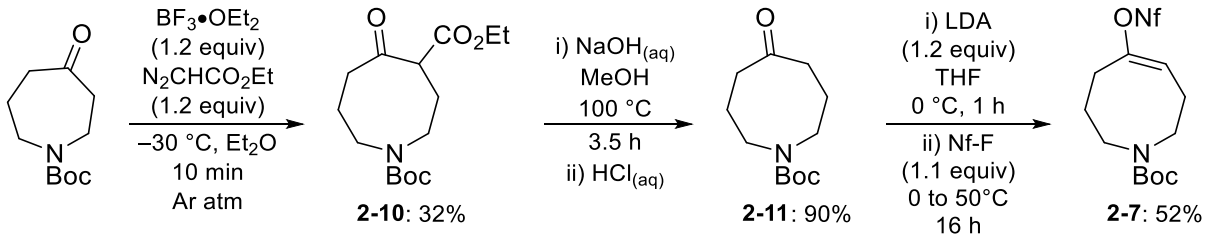

Scheme 2-5. Synthesis of azocanyl nonaflate **2-7**.

Both of the piperidine derivatives **2-8** and **2-9** were expected to be accessible in one step from commercially available piperidinone precursors (Scheme 2-6). The established protocol for the piperidine scaffold was directly applicable to the methyl piperidine derivative **2-8**. The DBU-

mediated nonaflation allowed isolation of the thermodynamically favoured alkenyl nonaflate **2-9** in a moderate yield (Scheme 2-6a).[5,†] In comparison, the ethyl ester precursor was found to be much less reactive towards the nonflate source. After a small screen of bases and electrophilic Nf /Tf sources, it was found that the corresponding triflate **2-10** could be made using KHMDS and phenyl triflimide. However, due to incomplete conversion of the starting material and similar polarities of the starting material and product, **2-12** was obtained as a mixture with about 10% of the starting material still present and was used in the interest of time (Scheme 2-6b).

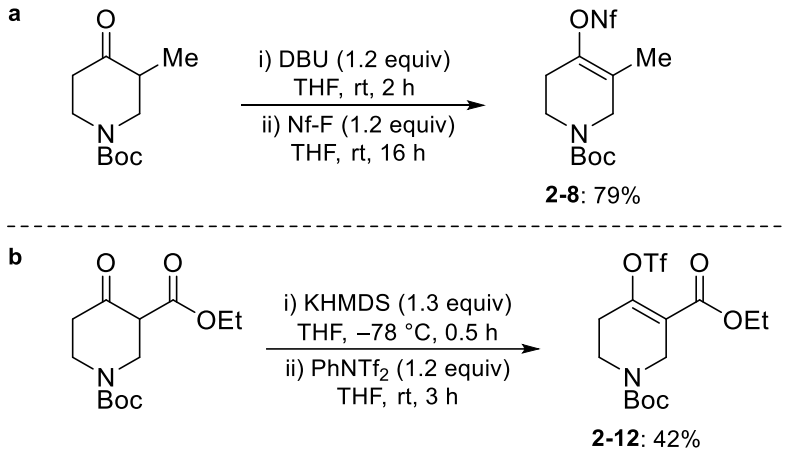

Scheme 2-6. Synthesis of methyl and ester substituted nonaflates **2-6** and **2-12**.

2.3.2 Initial borylative migration results of the alkenyl nonaflate derivatives

With the successful synthesis of the targeted alkenyl sulfonates, a brief screening **2-5** to **2-8** and **2-12** in the borylative migration reaction was undertaken using previously optimized racemic or enantioselective conditions.[5] Considering the established instability of the allylic boronate **2-4** to silica gel, in many cases the reaction was analyzed by crude ^{1}H NMR after the borylative migration

[†]Alkenyl nonaflate **2-6** was synthesized, purified and characterized by Tasmin Adel, who was an undergraduate researcher under the author's supervision.

before being submitted to thermal allylboration with *p*-tolualdehyde for proper characterization purposes.

Subjection of the 5-membered nonaflate **2-5** to the established racemic borylative migration conditions led to only 6% isolated yield of the allylboration product after purification (Scheme 2-7). Analysis of the crude ^{1}H NMR after the borylative migration step showed incomplete conversion and multiple side products present in relatively a large amount. The side products were identified based on partial purification and comparing with known literature spectra.[12] Changing the base to Et_3N or DBU and the solvent to CPME did not lead to any improvements, leading to only trace product formation and similarly messy crude reaction mixtures by ^{1}H NMR analysis. The low yield of the 5-membered allylic boronate in the borylative migration with nonaflate **2-5** is consistent with a previous chiral ligand screening with **2-5** undertaken by Samantha Kowk (MSc), in which the desired allylboration product could not be successfully isolated.[10] Re-analysis of previous ^{1}H NMR spectra from the ligand screen indicated that a large amount of the same side products shown in Scheme 2-7 accounted for the lack of a significant yield of product **2-13**. Considering that it seems forming the five membered allylic boronate product is quite unfavourable under the previously optimized conditions used, investigation of the borylative migration of **2-5** was discontinued.

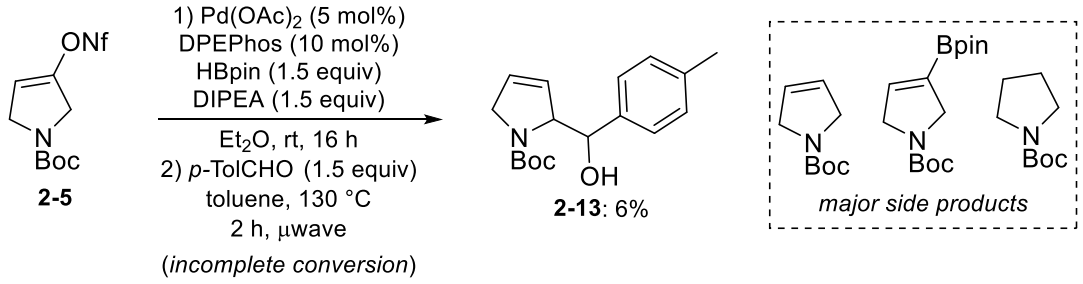

Scheme 2-7. Attempted borylative migration of 5-membered alkenyl nonaflate **2-5**.

In contrast, the 7-membered nonaflate **2-6** seemed to be a more promising substrate in the borylative migration. Subjection of **2-6** to the standard enantioselective borylative migration conditions resulted in formation of the desired allylic boronate **2-14** in 30% ^{1}H NMR yield and 80% *ee* of the allylboration product **2-15**. Furthermore, 70% conversion of **2-6** suggests the potential for further improvement of the reaction selectivity and conversion (Scheme 2-8). Dehydroazepane *N*-Boc nonaflate **2-6** was therefore viewed as a viable substrate for further investigation (see Section 2-4 for borylative migration studies with **2-6**).

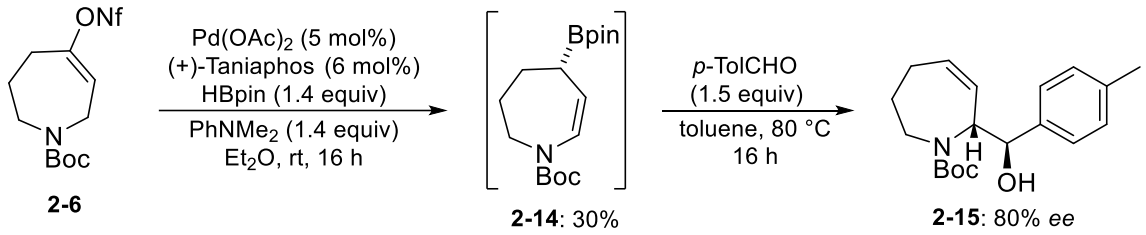

Scheme 2-8. Initial borylative migration result of the azepane scaffold.

On the other hand, the 8-membered nonaflate **2-7** did not lead to any observable amount of the desired allylic boronate. Upon exposure of **2-7** to the standard enantioselective borylative migration conditions, there was only 50% conversion of **2-7** and 36% yield of an undesired side product. The side product was identified as **2-16** by comparing with literature spectral data after partial purification (Scheme 2-9).[13] Notably, unlike **2-2**, **2-5** and **2-6**, azocanyl nonaflate **2-7** does not contain a homoallylic alkene. Based on these initial results, it seems that the homoallylic heteroatom may be important for obtaining borylation instead of reductive deoxygenation. This undesired deoxygenation process has also shown to occur under mild conditions in the presence of palladium(0) and a reductant, such as triethyl silane or dimethylamine borane.[14] The exact reason

for the discrepancy between borylation and reductive deoxygenation is unclear at this time. For a detailed discussion and mechanistic studies regarding the borylative migration, see Chapter 3.

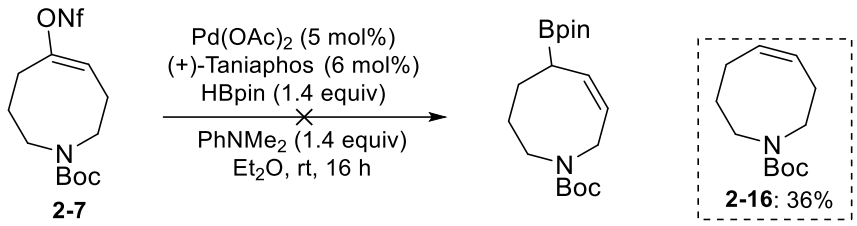

Scheme 2-9. Borylative migration attempt of 8-membered azocanyl nonaflate **2-7**.

As hypothesized, the borylative migration with neutral and electron-withdrawing alkenyl sulfonates (**2-8** and **2-12**) did lead to vastly different results, yet neither was promising. In the case of methylated nonaflate **2-8**, a complex mixture of at least four products formed along with remaining alkenyl nonaflate, all in around equivalent ratios. The products seemed to be a mixture of allyl- and alkenyl boronates, as well as protodeboronated/reduced side products, however proper identification of each individual product was not successfully pursued (Scheme 2-10a).[15] Slightly increasing the temperature in CPME did not improve the selectivity toward the thermodynamically favoured allyl- and/or alkenyl boronate and led to similar results. In contrast, the ethyl ester **2-12** resulted in clean conversion to the reductive deoxygenated product **2-17**, similarly to the azocane nonaflate **2-7** (Scheme 2-10b).[16]

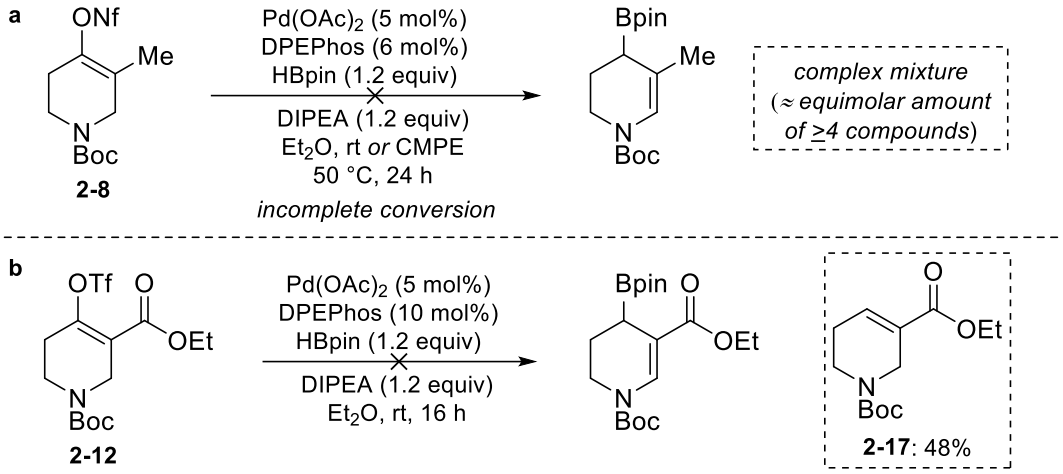

Scheme 2-10. Initial borylative migration results of (a) methylated nonaflate **2-8** and (b) ethyl ester nonaflate **2-12**.

Considering the results described in Scheme 2-7 to Scheme 2-10, the borylative migration with dehydroazepanyl nonaflate **2-6** seemed to be the most promising substrate, with potential for further development. Therefore, studies regarding the the borylative migration with the azepane-based scaffold **2-6** were pursued and are described in the rest of Chapter 2.

2.4 Synthesis of α-hydroxyalkyl dehydroazepanes *via* catalytic enantioselective borylative migration of a dehydroazepanyl nonaflate

2.4.1 Overview of synthetic approaches to azepane scaffolds and their precedence in medicinal chemistry

7-Membered saturated hydrocarbon rings containing one nitrogen atom are known as azepanes. Azepane-based motifs are quite common components of pharmaceutical drugs and natural products (Figure 2-4). Specifically, the azepane ring has been identified as one of the top 100 most prevalent ring systems in small molecule drugs.[17] Furthermore, a recent analysis of FDA-approved drugs revealed that, in addition to a large number of fused systems, single-ring azepanes and tetrahydro

azepines appeared in the top-5 of the most frequent 7-membered non-aromatic ring systems.[8] The azepane motif is also receiving increasing attention at the drug discovery level. Structure activity relationship (SAR) studies have revealed that the incorporation of an azepane scaffold can be essential in various motifs for a broad range of biological activities including anti-cancer, anti-microbial, anti-tubercular and anti-Alzheimer's disease.[18] Moreover, the synthesis of azepane analogues of piperidine compounds can be potentially beneficial in regard to potency and toxicity due to increased ring flexibility. For example, Sinaÿ and co-workers found that the azepane derivative of nojirimycin (an iminoheptitol, Figure 2-4) was found to be a potent α-galactosidase inhibitor.[19] Therefore, accessing 7-membered ring scaffolds using the borylative migration chemistry could allow access to novel chemical space which is relevant for medicinal chemistry purposes.

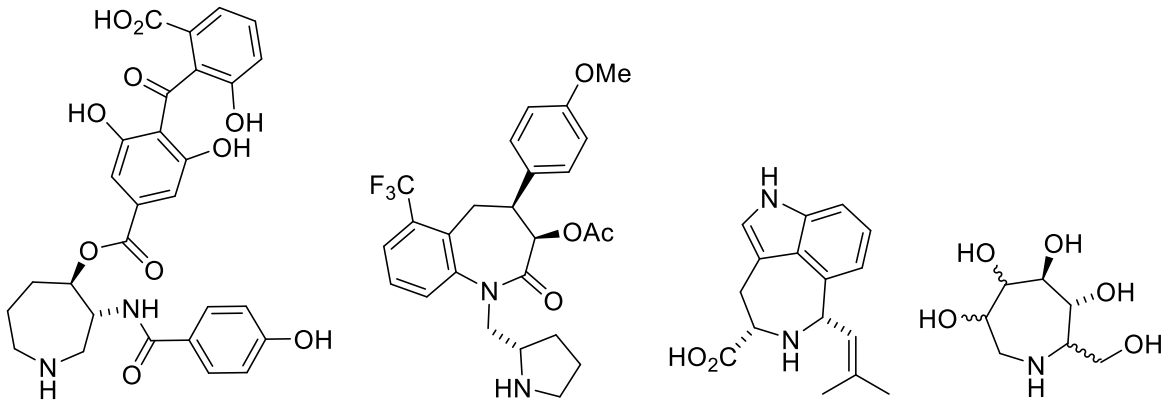

Figure 2-4. Examples of azepane-containing natural products and drugs.

Although 7-membered ring scaffolds are important in medicinal chemistry, stereoselective methods to access azepane rings have received much less attention than their piperidine and pyrrole counterparts.[20] A large number of methods and strategies for the preparation of polysubstituted 7-

membered nitrogen heterocycles are based on the cyclization of a linear precursor *via* N-C or C–C bond forming processes (Figure 2-5) such as alkene metathesis,[21] reductive amination[22] and intramolecular *N*-alkylation,[23] with subsequent nucleophilic trapping in the case of bicyclic intermediates.[24] Furthermore, ring-expansion and homologation approaches of functionalized nitrogen heterocyclic precursors have also been reported.[25] Many of these unimolecular approaches employ a pre-functionalized acyclic precursor, which is typically prepared through a multistep synthetic sequence in which the stereochemical information is embedded in the respective precursor or introduced at a later stage. An attractive, alternative approach consists of introducing the stereochemical information directly on a simple achiral azepane substrate to provide enantiomerically enriched products. Moreover, catalytic enantioselective borylation of a prochiral azepane substrate would provide a chiral secondary boronate with several avenues for further derivatization *via* either α- or γ-regioselective transformations of the resulting C–B bond.[1]

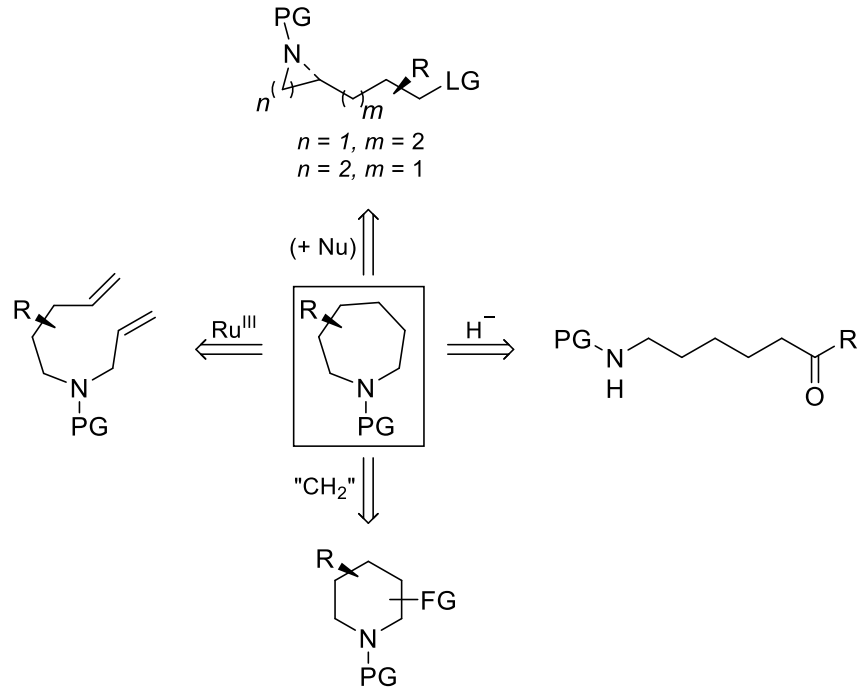

Figure 2-5. Common synthetic approaches to azepane scaffolds.

2.4.2 Optimization of the borylative migration reaction conditions

Considering that the initial results for the *N*-Boc nonaflate electrophile **2-6** in the borylative migration reaction were quite modest (c.f. Scheme 2-8), a short investigation on the effect of the nitrogen protecting group was undertaken. Since to-date only Cbz and Boc nitrogen protecting groups have been reported in the borylative migration for the piperidinyl substrate,[4,5] it was hypothesized that there could be a more desirable protecting group to improve the reaction with the azepane scaffold. Therefore, a small scope of dehydroazepanyl nonaflates were synthesized in two steps from azepinone hydrochloride by *N*-protection and subsequent nonaflation (Table 2-1). The approach was shown to be quite general for the regioselective synthesis of alkenyl nonaflates **2-25**–**2-31** with moderate to good yields. Notably, the phosphine oxide **2-29** and acetamide **2-31** could only be made in small amounts and were not investigated further. In regard to **2-29**, it was envisioned that the nucleophilicity of the phosphine oxide could cause catalyst binding/poisoning.

Table 2-1. Synthesis of azepanyl nonaflate derivatives.

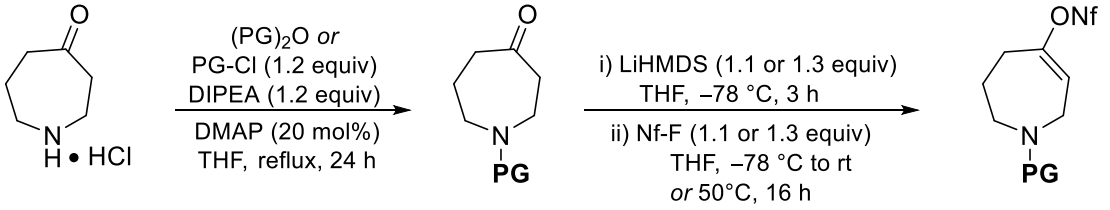

Entry	**PG**	Azepinone	Yield **2-15** (%)[a]	Nonaflate	Yield **2-4** (%)[a]
1	Cbz	**2-18**	72[b]	**2-25**	55[b]
2	CO_2Me	**2-19**	65[b]	**2-26**	58[b]
3	Ts	**2-20**	65[b]	**2-27**	36
4	$C(O)CF_3$	**2-21**	81[b]	**2-28**	52
5	$P(O)Ph_2$	**2-22**	65[b]	**2-29**	10[b]
6	Piv	**2-23**	59[b]	**2-30**	46[b]
7	Ac	**2-24**	—	**2-31**	20[c]

[a]Isolated yield after column chromatography. [b]The compound was synthesized, purified and characterized by Tasmin Adel, who was an undergraduate researcher under the author's supervision. [c]Isolated yield over two steps.

With the alkenyl nonaflates in hand, a small borylative migration screening was undertaken with the previously optimized enantioselective conditions. As briefly noted in the previous section, exposure of the novel nonaflate **2-6** to our previously developed borylative migration conditions led to incomplete conversion of the starting material and formation of the desired allylic boronate in 30% ^{1}H NMR yield, yet with a reasonable enantioselectivity of 80% *ee* (Table 2-2 entry 1). For both the corresponding carboxybenzyl (Cbz, **2-25**) and methyl carbamate (**2-26**) substrates, a lower yield of the corresponding allylic boronate (**A**) was observed with similar conversion and enantioselectivity (entries 2–3). Use of tosylamide (**2-27**) also led to a decreased yield of the allylic boronate relative to the Boc-protected substrate along with an *ee* of only 61% (entry 4). The strongly electron-withdrawing trifluoroacetamide resulted in full conversion of **2-28** with a cleaner reaction; the allylic boronate (**A**) was formed in 31% NMR yield, along with the undesired alkenyl boronate side product in 51% yield. Notably, the trifluoroacetamide allylboration product was unstable to silica gel purifyication and could only be partially purified using aluminum oxide to obtain a mixture of the allylboration product **2-35** with the undesired alkenyl boronate. Subsequent deprotection of the trifluoroacetamide group and Boc protection was required to isolate the pure allylboration product for *ee* determination as **2-15** with 14% yield over the three steps. Unfortunately, although the borylative migration with **2-28** was quite clean, the enantioselectivity decreased to only 57% *ee* (entry 5). Considering the results in Table 2-2, it seems that a carbamate nitrogen is important for maintaining a high enantioselectivity, however the rationalization of this effect is unclear at this time. Pivalate **2-30** was not extensively screened with the enantioselective borylative migration conditions, since it was found that none of the desired product formed under the standard racemic borylative migration conditions. Furthermore, the lack of deprotection methods for *N*-pivalamides

makes their use as precursors much less synthetically appealing. In the end, the *N*-Boc nonaflate substrate **2-6** was chosen for further reaction optimization due to the relatively high yield and enantioselectivity observed in the borylative migration, as well as the commercial availability of the corresponding *N*-Boc piperidinone starting material.

Table 2-2. Optimization of the nitrogen protecting group (PG).[a]

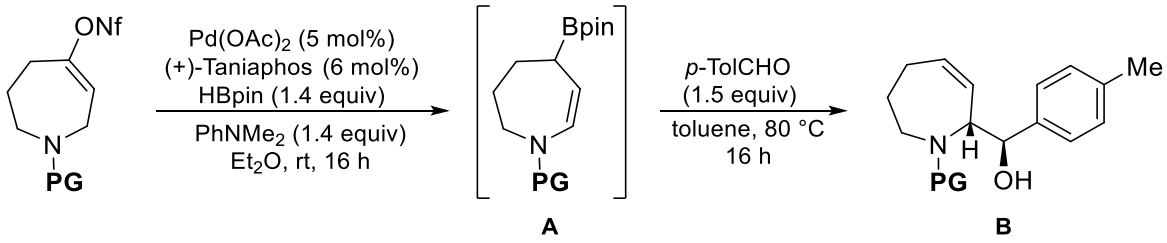

A **B**

Entry	PG	Substrate	Conversion (%)[b]	Yield **A** (%)[b]	**B**	Yield **B** (%)[b]	*ee*[c]
1	**Boc**	**2-6**	**70**	**30**	**2-15**	**23**	**80**
2	Cbz	**2-25**	75	11	**2-32**	10	84
3	CO_2Me	**2-26**	65	13	**2-33**	16	80
4[d]	Ts	**2-27**	90	12	**2-34**	5	61
5	$C(O)CF_3$	**2-28**	100	31	**2-35**	14[e]	57[e]

[a]All reactions were performed on a 0.3 mmol scale. [b]Estimated by crude ^1H NMR using 1,3,5-trimethoxybenzene as an internal standard. [c]Determined by chiral HPLC of the allylboration products **2-15**, **2-32**–**2-34**. [d]Reaction time: 24 h. Nf = $SO_2C_4F_9$; DMA = *N*,*N*-dimethylaniline. [e]The protecting group of the allylboration product was converted to a Boc protecting group for purification and *ee* determination as **2-15**.

Further optimization of the reaction conditions examining the solvent, concentration and temperature is summarized in Table 2-3. Notably, a significant amount of two main side products were observed in this reaction; alkenyl boronate **2-36** along with the deborylated enamide **2-37**. The reaction efficiency was found to be quite specific to using diethyl ether as the solvent. Other ethereal solvents that were previously shown to be effective with the piperidine ring system,[5] such as cyclopentyl methyl ether (CPME), dioxane, and *tert*-butyl methyl ether (MTBE) were ineffective with **2-6** (entries 2, 3, 5) with complex mixtures in many cases. Diluting the reaction by ten-fold

from 0.17 M to 0.017 M slightly increased the conversion and yield (entry 4), yet increasing the reaction temperature led to a diminished yield of only 16% (entry 12).

Table 2-3. Optimization of the reaction solvent.[a]

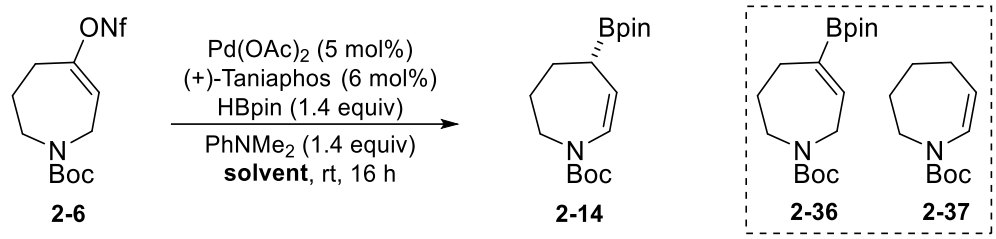

Entry	Solvent	Conv. **2-6** (%)[b]	**2-36** : **2-37** (%)[b]	**2-14** (%)[b]	ee (%)[c]
1[d]	Et_2O	70	5 : 14	30	80%
2[d]	CPME	58	8 : 10	15	—
3[d]	Dioxane	70	8 : 6	trace	—
4[e]	**Et_2O**	**89**	**12 : 22**	**41**	**79**
5[e]	MTBE	77	complex mix.	trace	—
6[e,g]	Et_2O	84	18 : 17	29	—
7[e]	THF	62	26 : 6	13	—
8[e]	Toluene	57	14 : 17	trace	—
9[e]	*t*BuOMe	77	16 : 10	trace	—
10[e]	1,2-dimethoxyethane	6	—	—	—
11[e]	Dibutyl ether	51	6 : 0	—	—
12[e,f]	Et_2O	78	9 : 9	16	—

[a]All reactions were performed on a 0.3 mmol scale. [b]Yields are estimated based on ^{1}H NMR of crude reaction mixture in C_6D_6 with 1,3,5-trimethoxybenzene as an internal standard. [c]Determined by chiral HPLC after thermal allylboration with *p*-tolualdehyde. [d]Concentration = 0.17 M, [e]Concentration = 0.017M, [f]Reaction was performed at 40 °C. [g]24 h reaction time.

With the optimal solvent in hand, the effect of the base was investigated (Table 2-4). On the basis of previous optimization of the borylative migration,[4,26] it was expected that the amine base should have a significant effect on the product distribution and enantioselectivity. Compared to the use of $PhNMe_2$ (entry 1), standard alkylamine bases such as *N*,*N*-diisopropylethylamine (DIPEA) and triethylamine led to diminished yields of **2-14** to 10 and 17%, respectively (entries 2–3). Introduction of steric hindrance on the aniline nitrogen, or near the nitrogen center, lowered the conversion of **2-6** and was detrimental to the yield of the desired product (entries 4–6). Methyl substitution at both

meta positions of the phenyl ring led to a slightly lowered yield of 31% and had no significant effect on the enantioselectivity (entry 7). Fortuitously, when a methyl group was introduced at the *para* position the reaction went to completion and the ^{1}H NMR yield increased to 57% without eroding the enantioselectivity of the process (entry 8). Further attempts to introduce *para* electron-donating substituents on the aniline ring were unsuccessful in improving the reaction; *para* methoxy substitution was ineffective (entry 10), while dimethylamine substitution (Tetramethyl-*p*-phenylenediamine, TM*p*PD) led to a comparable yield of 30%, yet the enantioselectivity was decreased to only 55% (entry 11).

Table 2-4. Optimization of the base.[a]

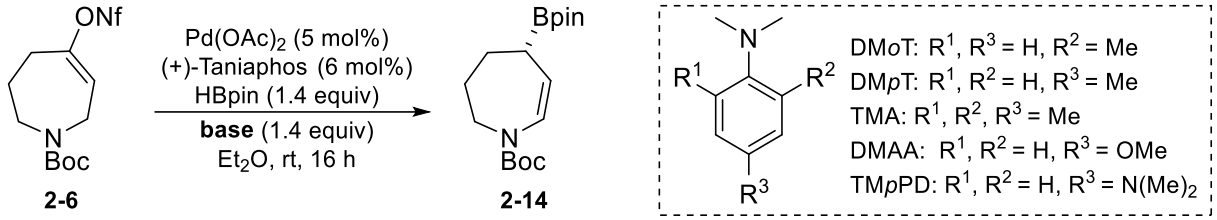

Entry	Base	Conv. **2-6** (%)[b]	**2-36** : **2-37** (%)[b]	**2-14** (%)[b]	*ee* (%)[c]
1	*N*,*N*-dimethylaniline (PhNMe$_2$)	89	12 : 2	41	79
2	DIPEA	100	18 : 0	10	—
3	NEt$_3$	87	15 : 0	17	—
4	4-Me-2,6-di-tBu-pyridine	40	22 : 17	trace	—
5	*N*,*N*-diethylaniline (DEA)	50	23 : 10	trace	—
6	*N*,*N*-dimethyl-*o*-toluidine (DM*o*T)	49	22 : trace	7	—
7	3,5,*N*,*N*-Tetramethylaniline (TMA)	95	17 : 18	31[b]	81
8	**N,N-dimethyl-*p*-toluidine (DM*p*T)**	**100**	**12 : 30**	**57**	**81**
9	*p*-bromo-*N*,*N*-dimethylaniline	70	17 : 12	trace	—
10	4-dimethylamino anisole (DMAA)	49	13 : 6	7	—
11	TM*p*PD	100	15 : 10	30	55

[a]All reactions were performed on a 0.3 mmol scale. [b]Estimated based on ^{1}H NMR of crude reaction mixture in C_6D_6 with 1,3,5-trimethoxybenzene as an internal standard. [c]Determined by chiral HPLC after thermal allylboration with *p*-tolualdehyde.

Finally, a brief ligand and temperature screening was undertaken with the newly optimal base (Table 2-5). It had previously been shown that obtaining a high enantioselectivity with the piperidine scaffold is specific to using Taniaphos and Walphos ligands.[5] However, with the 7-membered nonaflate **2-6**, both the cyclohexyl Taniaphos and Walphos ligands led to little or no formation of **2-14** (entries 2–3). Surprisingly, the enantioselectivity seems to be inversely proportional to temperature, although the yield decreased in both cases and therefore the effect of the temperature was not investigated further (entries 4–5).

Table 2-5. Brief screening of the ligand and temperature.[a]

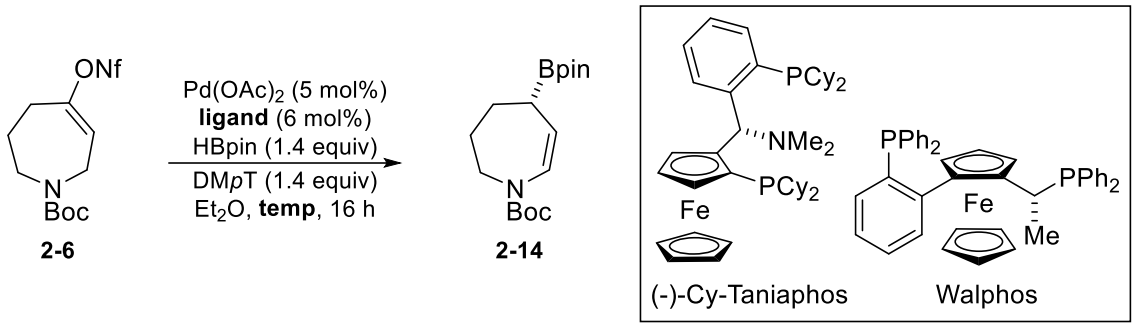

Entry	Ligand	Temp. (°C)	Conv. **2-6** (%)[b]	**2-36** : **2-37** (%)[b]	**2-14** (%)[b]	*ee* (%)[c]
1	**(+)-Taniaphos**	**rt**	**100**	**12 : 30**	**57**	**81**
2	(–)-Cy-Taniaphos	rt	68	6 : 3	—	—
3	Walphos	rt	100	10 : 2	trace	—
4	(+)-Taniaphos	0	100	13 : 25	45	68
5	(+)-Taniaphos	40	78	12 : 12	27	83

[a]All reactions were performed on a 0.3 mmol scale. [b]Estimated based on ^{1}H NMR of crude reaction mixture in C_6D_6 with 1,3,5-trimethoxybenzene as an internal standard. [c]Determined by chiral HPLC after thermal allylboration with *p*-tolualdehyde.

2.4.3 Substrate scope of the aldehyde allylboration with 2-14

The addition of allylboronates to carbonyl compounds remains an invaluable transformation in synthetic organic chemistry for the stereoselective synthesis of various homoallylic alcohols. The

use of allylic boronates is an exceptionally attractive tool, in part due to the stability of organoboron nucleophiles and the inherently high and predictable stereoselectivity consistently observed (see Chapter 1, Section 1.3.2.1). With the borylative migration reaction conditions optimized to an acceptable yield and enantioselectivity, the utility of novel allylic boronate **2-14** was displayed in the synthesis of a small set of α-hydroxyalkyl dehydroazepanes *via* subsequent thermal aldehyde allylboration (Table 2-6).[2,27] Representative aromatic (**2-15**), hetero-aromatic (**2-38**) and linear (**2-39**, **2-40**) aldehydes were applicable in this chemistry, leading to consistently moderate yields of 44–51% and good enantioselectivities (81–83%). Increasing the reaction scale slightly from a 0.3 to 0.5 mmol scale led to similar results of **2-14**. To our surprise, it was found that the linear allylboration products **2-39** and **2-40** from allylboration with aliphatic aldehydes were obtained as a mixture of diastereomers (dr ≈ 5.5 : 1). The absolute and relative stereochemistry of the α-hydroxyalkyl dehydroazepanes was confirmed and is discussed in Section 2.4.4.

Table 2-6. Scope of the borylative migration, aldehyde allylboration sequence.[a]

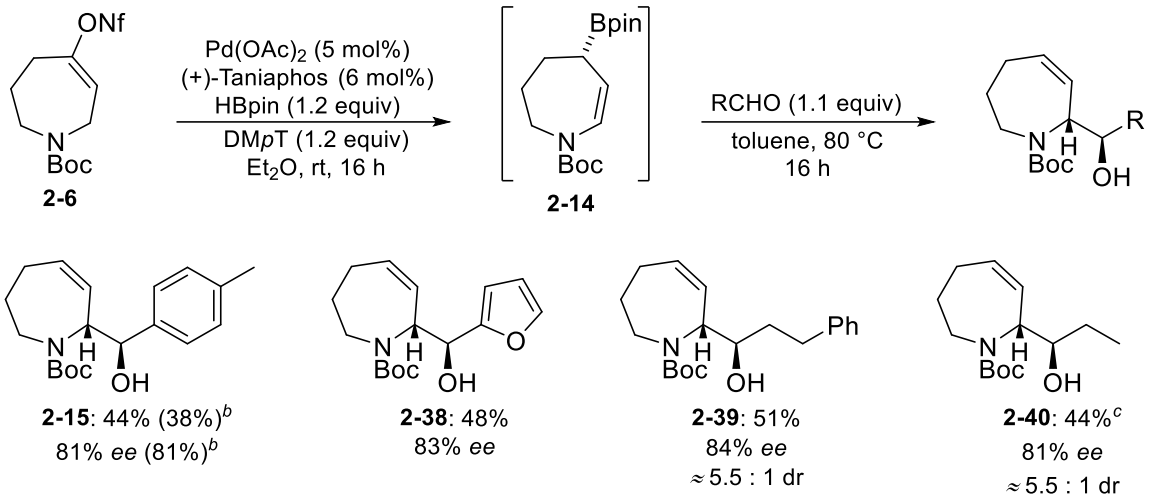

[a]Reaction sequence performed on a 0.3 mmol scale. Isolated yields reported over two steps. [b]Results from the reaction performed on a 0.5 mmol scale in parentheses. [c]0.5 mmol scale, allylboration conditions: C_2H_5CHO (2.0 equiv), toluene (1.0 M), rt, 1.5 d.

Usually, the stereoselectivity of aldehyde allylboration reactions are high due to a tight B–O coordination of the aldehyde carbonyl to the Lewis acidic boron atom resulting in a compact six-membered chair-like transition state (Figure 2-6, left).[2] Although further investigation would be required to rationalize the relatively low diastereoselectivity observed with linear aldehydes in this case, the small substrate scope in Table 2-6 suggests that the stereoselectivity of the aldehyde allylboration step is less efficient than that previously observed with the corresponding piperidine analogue.[5,7] It is proposed that the unexpectedly low diastereoselectivity is most likely due to a competing minor chair-like transition state with the aldehyde substituent placed in a pseudo-axial orientation to avoid steric interaction with the *N*-Boc group (Figure 2-6, middle). Such a transition state would be more accessible with aliphatic aldehydes due to the smaller substituent size compared to aromatic ones. However, the corresponding twist boat-like transition state cannot be

ruled out at this point (Figure 2-6, right). Only one example of a 7-membered ring allylboration reaction was found in the literature using $(Ipc)_2$B-cycloheptenyl borane.[2,28] Furthermore, a few examples do exist involving aldehyde allylboration reactions with relatively low diastereoselecivities (9:1 dr) from cyclic substrates.[29]

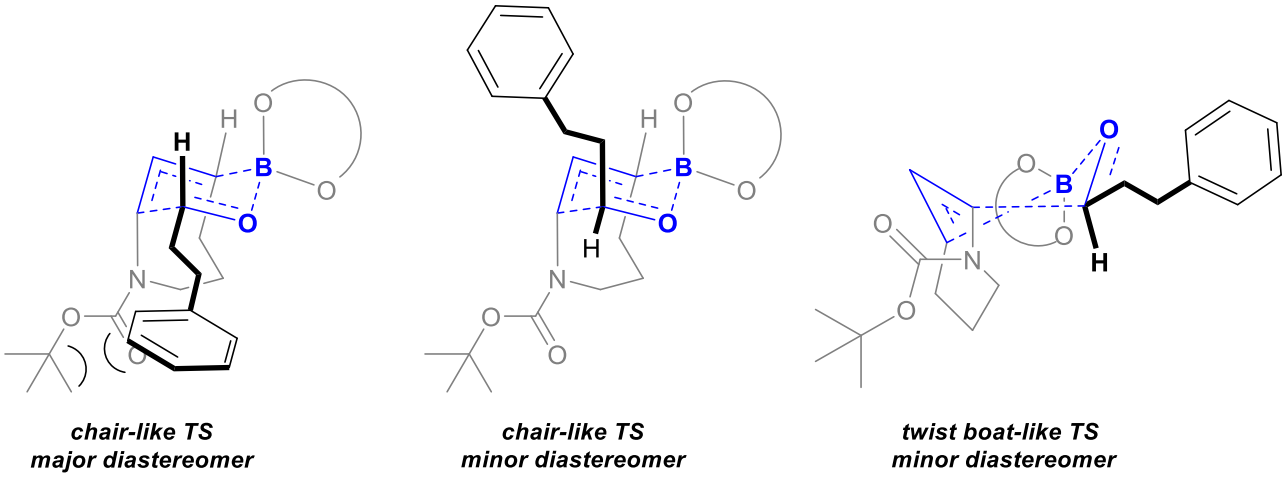

Figure 2-6. The potential competing transition states during the aldehyde allylboration step with aliphatic aldehydes.

2.4.4 Determination of the absolute and relative stereochemistry of the α-hydroxyalkyl dehydroazepanes

Although one would expect the 7-membered ring allylic boronate **2-14** to have the same absolute stereochemistry as with the piperidine analogue when using (+)-Taniaphos, confirmation of the stereochemistry is a valuable addition to this work. In a C-chiral allylboration reaction, the stereochemical information of the C-B bond is transferred to the absolute steoreochemistry of the product. Therefore, the stereochemistry of the allylic boronate **2-14** precursor can be rationalized in a logistical manner from the absolute stereochemistry of a diastereomerically pure α-hydroxyalkyl dehydroazepane from Table 2-6 (e.g. **2-15** or **2-38**). In this regard, enantioenriched *para* tolyl

derivative **2-15** was deprotected to obtain the corresponding HCl salt **2-41** using standard acidic conditions. X-ray crystallographic analysis of the salt **2-41** confirmed that the expected absolute and relative stereochemistry of **2-14** was obtained and therefore as with the 6-memebered ring, the (*S*)-allylic boronate **2-14** had been formed preferentially (Scheme 2-11).[4]

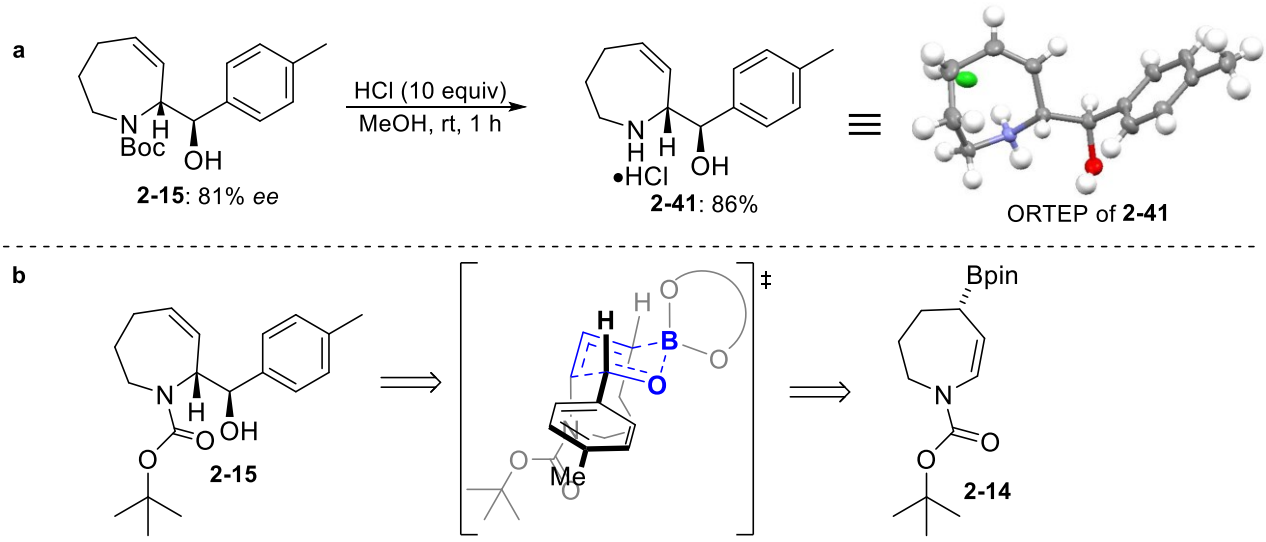

Scheme 2-11. (a) Confirmation of the stereochemistry of **2-14** (b) rationale of the stereochemistry of allylic boronate **2-14**.

Although the absolute configuration of **2-14** was confirmed by X-ray analysis, the relative stereochemistry of the major α-hydroxyalkyl dehydroazepane diastereomer obtained from allylboration with linear aldehydes (i.e. **2-39** and **2-40**) was still required, considering the unexpectedly low diastereoselectivity observed (see Section 2.4.3 for details). Separation of the two diastereomers of **2-39** was successfully achieved by semi-preparative HPLC purification to obtain the major (**2-39a**) and minor (**2-39b**) *N*-Boc amino alcohols for characterization purposes. Synthesis of the diastereomerically pure carbamates from **2-39a** and **2-39b** were targeted to allow for rigidification at the stereocenter of interest (C_1, Scheme 2-12). Synthesis of the corresponding

carbamate of each diastereomer (**2-42a** and **2-42b**) was efficiently achieved in a quantitative manner directly from the diastereomerically pure *N*-Boc amino alcohols using sodium hydride under mild conditions (Scheme 2-12).[30] Since the relative stereochemistry of the *para* tolyl allylboration product **2-15** was already known, the corresponding carbamate **2-43** was also accessed for reference. It was initially hoped that the vicinal coupling constant between the hydrogen at C_1 and the α-nitrogen hydrogen (in blue, Scheme 2-12) could provide insight into whether the relative configuration was *syn* or *anti* for **2-42a** and **2-42b** when compared to **2-43**. After proper assignment of each ^{1}H NMR signal by gCOSY NMR experiments, it was found that comparing the coupling constants for the hydrogens of interest was inconclusive – the control **2-43** displayed a coupling constant essentially halfway between that observed for **2-42a** and **2-42b** (**2-12**, Scheme 2-12).

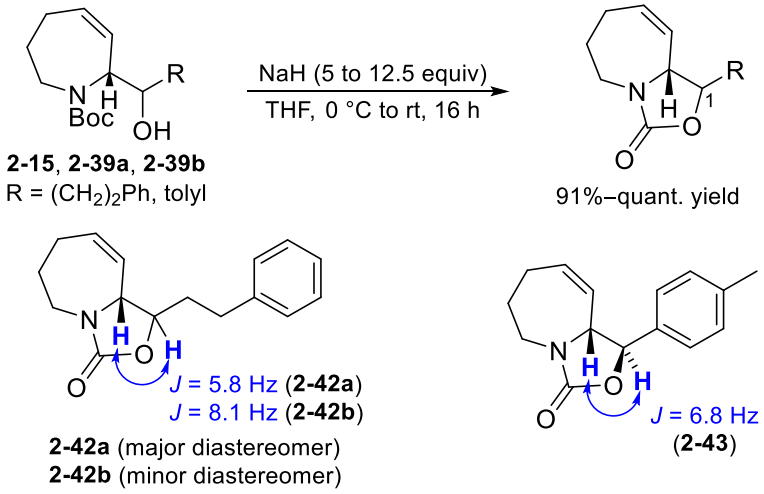

Scheme 2-12. Synthesis of carbamates and coupling constant analysis.

Since through-bond H-H coupling was found to be insufficient, further ROESY experimentation was undertaken to determine through-space interactions. The relative stereochemistry of each diastereomer was analyzed by 1D and 2D ROESY NMR experiments of the corresponding

carbamate derivatives **2-42a** and **2-42b**. A detailed correlation summary of the 2D NMR data of each diastereomer is summarized in Figure 2-7. A key through-space interaction was observed between the α-oxygen proton (H_C) and an α-nitrogen proton (H_E') in carbamate **2-42b** which was not present in **2-42a**. The key H_C to H_E' interaction in **2-42b** suggests that the minor diastereomer is indeed the one in which the carbamate is *anti* to the stereocenter, which is set by the borylative migration reaction (H_D). Notably, the corresponding tolyl carbamate **2-43** also did not display any through-space interaction across the azepane ring, similarly to the major diastereomer **2-42a**.The stereochemical assignment of **2-42a** and **2-42b** was further quantified using 1D ROESY experiments, in which the *syn* α-nitrogen proton (H_E') was selectively excited in each diastereomer. A small enhancement of about 10% is present between the α-nitrogen and oxygen proton in **2-42b** (H_C and H_E'). The equivalent interaction was not observed in the major diastereomer **2-42a** when the *syn* α-nitrogen proton (H_E') was excited. Therefore, the ROESY data obtained allowed conclusive evidence for the assignment of the relative configurations of **2-42a** and **2-42b**, as shown in Figure 2-7.

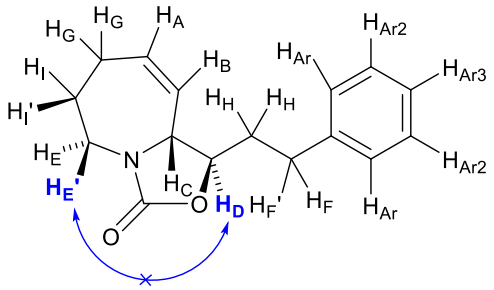

No ROESY interaction present

2-42a (major)

gCOSY:

- $H_A \leftrightarrow H_G$, H_B, H_C
- $H_B \leftrightarrow H_G$, H_C
- $H_C \leftrightarrow H_G$
- $H_D \leftrightarrow H_H$
- $H_E \leftrightarrow H_E'$
- $H_E/H_E' \leftrightarrow H_I/H_I'$
- $H_F \leftrightarrow H_F'$
- $H_F/H_F' \leftrightarrow H_H$
- $H_G \leftrightarrow H_I/H_I'$

ROESY:

- $H_{Ar} \leftrightarrow H_H$, H_F/H_F', H_B
- $H_A \leftrightarrow H_G$, H_B
- $H_B \leftrightarrow H_C$, H_D, H_G, H_H
- $H_C \leftrightarrow H_I/H_I'$, H_G, H_F/H_F', H_E', H_H
- $H_D \leftrightarrow H_H$, H_F/H_F'
- $H_E \leftrightarrow H_E'$, H_I/H_I'
- $H_E/H_E' \leftrightarrow H_G$
- $H_F/H_F' \leftrightarrow H_H$
- $H_G \leftrightarrow H_I/H_I'$

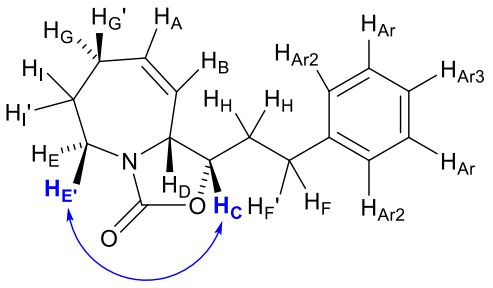

ROESY interaction present

2-42b (minor)

gCOSY:

- $H_{Ar2} \leftrightarrow H_F/H_F'$
- $H_A \leftrightarrow H_G/H_G'$, H_D, H_B
- $H_B \leftrightarrow H_G/H_G'$, H_D
- $H_C \leftrightarrow H_H/H_H'$
- $H_D \leftrightarrow H_G/H_G'$
- $H_E \leftrightarrow H_E'$
- $H_E/H_E' \leftrightarrow H_I/H_I'$
- $H_F \leftrightarrow H_F'$
- $H_F/H_F' \leftrightarrow H_H/H_H'$
- $H_G \leftrightarrow H_G'$
- $H_G/H_G' \leftrightarrow H_I/H_I'$
- $H_H \leftrightarrow H_H'$
- $H_I \leftrightarrow H_I'$

ROESY:

- $H_{Ar2} \leftrightarrow H_F/H_F'$
- $H_A \leftrightarrow H_G/H_G'$, H_B
- $H_B \leftrightarrow H_H/H_H'$, H_F/H_F', H_D, H_C
- **H_C** $\leftrightarrow H_H/H_H'$, H_F/H_F', H_D, **H_E'**
- $H_D \leftrightarrow H_H/H_H'$, H_F/H_F',H_E', H_D
- $H_E \leftrightarrow H_E'$, H_G
- $H_E/H_E' \leftrightarrow H_I/H_I'$
- $H_E' \leftrightarrow H_G$, H_G' (weaker)
- $H_F \leftrightarrow H_F'$
- $H_F/H_F' \leftrightarrow H_H/H_H'$
- $H_G \leftrightarrow H_G'$
- $H_G/H_G' \leftrightarrow H_I/H_I'$
- $H_H \leftrightarrow H_H'$

Figure 2-7. Detailed chart of the 2D correlations of carbamates **2-42a** and **2-42b** for stereochemical assignment of their relative configurations.

2.4.5 Synthesis of the 7-membered ring analogue of β-conhydrine

As a further demonstration of the developed methodology, a short synthesis of the 7-membered ring homolog of β-conhydrine was performed (Scheme 2-13). The piperidine-based 1,2-amino alcohol is a natural product obtained from hemlock and although it is of interest for displaying broad biological activity, its well-documented toxicity is a limiting factor. Surprisingly, even though the stereoselective synthesis of β-conhydrine has been completed numerous times with multiple different strategies,[31] the stereoselective synthesis of the 7-membered azepane homolog is lacking in the literature. Presumably, the additional conformational flexibility of the larger 7-membered ring

could lead to changes, and potentially improvements, in the therapeutic window of these compounds. The stereoselective synthesis of β-conhydrine analogue **2-45** was achieved in a high overall yield from allylboration product **2-40** *via* standard hydrogenation using Crabtree's catalyst to obtain the saturated azepane analogue **2-44** and subsequent *N*-Boc deprotection with excess hydrochloric acid.[7] The accomplishment of the synthesis of a diastereomeric mixture of ring-expanded β-conhydrine analogues **2-45** in only 5 steps from commercially available starting materials emphasizes how little these chiral α-hydroxyalkyl azepane scaffolds have been explored in the literature to-date, and suggests a potential for this borylative migration reaction to be utilized in alkaloid synthesis and drug discovery.

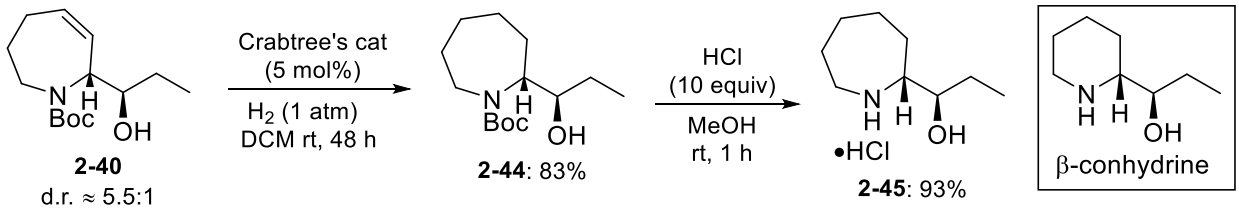

Scheme 2-13. Synthesis of compound 2-45; the azepane derivative of β-conhydrine.

2.5 Summary

This chapter describes efforts to expand the substrate scope of the palladium-catalyzed enantioselective borylative migration methodology. Five different *N*-Boc alkenyl nonaflates with varying ring sizes and alkene substitution were successfully synthesized. Initial evaluation of the new alkenyl nonafltes in the borylative migration indicate that the scope of this reaction is quite limited. Overall, the initial borylative migration results suggested that only the 7-membered azepane scaffold was promising enough to merit further investigation.

The borylative migration was successfully optimized to the corresponding 7-membered ring scaffold. The nitrogen protecting group proved to be a contributing factor to the product distribution, with carbamates being essential to avoid erosion of enantioselectivity. The novel enantioenriched azepanyl boronate was applied in aldehyde allylboration with linear and aromatic aldehydes to provide α-hydroxyalkyl dehydroazepanes in a low step count with good enantioselectivity and yields over two steps, albeit as a mixture of diastereomers with linear aldehydes. The azepane derivative of β-conhydrine was synthesized in only five steps, highlighting the new chemical space that can be accessed with the developed methodology.

2.6 Experimental

2.6.1 General information

Unless otherwise stated, all reactions were performed in flame-dried glassware under a nitrogen atmosphere. Diethyl ether (Et_2O) was distilled over sodium/benzophenone ketyl. Dioxane was distilled over sodium. Tetrahydrofuran (THF) and toluene were purified using an MBraun MS SPS* solvent system. All other anhydrous solvents were purchased from Sigma Aldrich and used as received. All liquid amine and aniline bases were purchased from Sigma Aldrich or Combi-Blocks, distilled from calcium hydride and stored over potassium hydroxide before use. Pinacolborane (98%, HBpin) was purchased from Oakwood Chemicals and stored in a flame-dried pear-shaped flask in a -20 °C freezer under nitrogen atmosphere. *N*-Boc-hexahydro-1*H*-azepin-4-one and 4-perhydroazepinone, HCl was purchased from Combi-Blocks and used as received. Palladium (II) acetate (99.95+%) was purchased from Strem. All other chemicals were purchased from Strem, Sigma Aldrich or Combi-Blocks and used as received. Thin layer chromatography (TLC) was

performed on silica gel 60 F254 plates and visualized using UV light, potassium permanganate ($KMnO_4$) and/or phosphomolybdic acid (PMA) stains. Flash chromatographic separations were performed with silica gel 60 using ACS grade solvents. Preparative thin-layer chromatography (pTLC) was performed on silica gel 60 F254 plates and visualized using UV light. ^{1}H NMR, ^{13}C NMR, ^{19}F NMR and ^{11}B NMR experiments were performed on 400 MHz, 500 MHz or 700 MHz instruments. The residual solvent ($CDCl_3$ or C_6H_6) protons (^{1}H) and carbons (^{13}C) were used as internal references. ^{1}H NMR data is presented as follows: chemical shift in ppm (δ) downfield from tetramethylsilane (multiplicity, coupling constant, integration). The following abbreviations are used in reporting the ^{1}H NMR data: s, singlet; br s, broad singlet; d, doublet; t, triplet; app t, apparent triplet; dd, doublet of doublet; m, multiplet. The error of coupling constants from ^{1}H NMR spectra is estimated to be 0.3 Hz. High-resolution mass spectra were recorded by the University of Alberta mass spectrometry services using electrospray ionization (ESI) techniques. Infrared (IR) experiments were performed using cast-film techniques with frequencies expressed in cm^{-1}. Optical rotations were measured using a 1 mL cell with a 10 cm length on a polarimeter by the University of Alberta analytical and instrumental laboratories. Melting points (mp) were measured on a melting point apparatus and uncorrected. The enantiomeric excess ratios for optically enriched compounds were determined using a HPLC Agilent instrument with a Chiralpak IC column.

2.6.2 Procedure and characterization of alkenyl nonaflates 2-5, 2-7, 2-8, 2-10

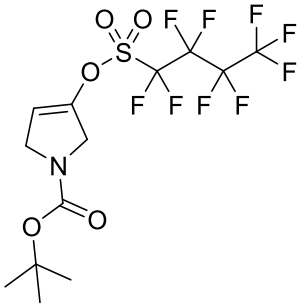

***tert*-butyl 3-(((perfluorobutyl)sulfonyl)oxy)-2,5-dihydro-1*H*-pyrrole-1-carboxylate (2-5):** *N*-Boc-3-pyrrolidinone (3.50 g, 19.0 mmol, 1.00 equiv) was dissolved in THF (70.0 mL, 0.270 M) and the reaction was cooled to -78 °C in a dry ice/acetone bath. Lithium bis(trimethylsilyl)amide (1 M in THF, 21.0 mL, 21.0 mmol, 1.10 equiv) was added dropwise at -78 °C and stirred for 3 hours. Perfluorobutanesulfonyl fluoride (6.61 g, 21.0 mmol, 1.10 equiv) was added dropwise and the reaction was then allowed to warm to 0 °C overnight. The reaction was quenched by addition of aqueous saturated sodium bicarbonate (70 mL) at room temperature and subsequently extracted with dichloromethane (70 mL) three times. The combined organic phases were washed with water and brine (70 mL) before being dried with anhydrous sodium sulfate. The solution was filtered, concentrated *in vacuo* and purified by column chromatography (30% Et_2O in hexanes) to afford yellow oil, which solidified upon standing to a white solid (2.80 g, 32% yield). All spectral data matched the literature:[10] **^{1}H NMR** (400 MHz, $CDCl_3$, rotamers are present): δ 5.89–5.63 (m, 1H), 4.35–4.11 (m, 4H), 1.47 (s, 9H); **^{13}C NMR** (176 MHz, $CDCl_3$, rotamers are present) δ 153.7, 153.6, 143.4, 142.9, 112.9, 112.7, 80.7, 80.5, 50.4, 50.1, 50.0, 49.8, 28.4; **IR** (microscope, cm^{-1}) 2980, 2935, 2874, 1711, 1671, 1433, 1409, 1350, 1241, 1204, 1144, 1112; **HRMS** (ESI-TOF) for $C_{13}H_{14}F_9NNaO_5S$ $(M + Na)^+$ calcd. 490.0341; found 490.0340.

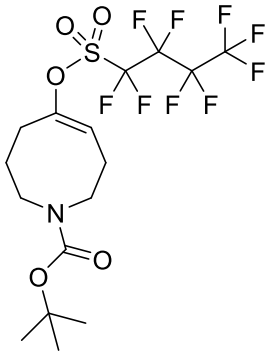

(*E*)-*tert*-butyl 5-(((perfluorobutyl)sulfonyl)oxy)-3,4,7,8-tetrahydroazocine-1(2*H*)-carboxylate (2-7): *n*-BuLi (2.5 M in hexanes, 0.63 mL, 1.6 mmol, 1.2 equiv) was added dropwise to a solution of diisopropylamine (0.24 mL, 1.7 mmol, 1.3 equiv) in THF (2.5 mL) at 0 °C. Azocanyl ketone **2-11** (294 mg, 1.3 mmol, 1.0 equiv) was dissolved in THF (3.0 mL, 0.24 M total) and added dropwise to the LDA solution at 0 °C. After stirring for 1 hour, perfluorobutanesulfonyl fluoride (432 mg, 1.43 mmol, 1.2 equiv) was added dropwise and the reaction was stirred for two hours before warming to 50 °C overnight. The reaction was cooled back to room temperature, diluted in Et_2O and quenched by addition of saturated ammonium chloride (10 mL). The aqueous phase was subsequently extracted three times and the combined organic phases were washed with water and brine before being dried with anhydrous sodium sulfate. The solution was filtered, concentrated *in vacuo* and purified by column chromatography (10% Et_2O in hexanes) to afford a clear colourless oil (344 mg, 52% yield). All spectral data matched the literature:[10] **^{1}H NMR** (500 MHz, $CDCl_3$, rotamers are present) δ 5.93–5.54 (m, 1H), 3.68–3.47 (m, 2H), 3.38–3.17 (m, 2H), 2.63–2.42 (m, 2H), 2.12–2.01 (m, 2H), 1.99–1.82 (m, 2H), 1.52–1.41 (m, 9H); **^{13}C NMR** (126 MHz, $CDCl_3$, rotamers are present) δ 155.6, 154.7, 150.1, 149.5, 122.1, 121.2, 79.9, 79.8, 48.6, 48.1, 47.1, 46.4, 32.2, 28.5, 28.4 (2C), 27.0, 22.8, 22.2; **^{19}F NMR** (469 MHz, $CDCl_3$) δ–80.7, –110.1, –121.0, –125.9;

IR (microscope, cm^{-1}) 2977, 2944, 1698, 1413, 1240, 1202, 1145; **HRMS** (ESI-TOF) for $C_{16}H_{20}F_9NNaO_5S$ $(M + Na)^+$ calcd. 532.0811; found 532.0815.

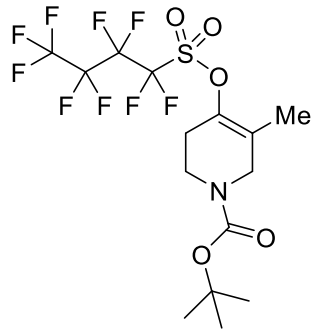

1-*tert*-butyl 3-methyl 4-(((trifluoromethyl)sulfonyl)oxy)-5,6-dihydropyridine-1(2*H*)-carboxylate (2-8): Following a modified literature procedure,[5] *tert*-butyl 3-methyl-4-oxopiperidine-1-carboxylate (320 mg, 1.5 mmol, 1.0 equiv) was dissolved in THF (7.5 mL, 0.20 M). DBU (0.22 mL, 1.80 mmol, 1.20 equiv) was added and the reaction was stirred at room temperature for two hours. Perfluorobutanesulfonyl fluoride (904 mg, 1.80 mmol, 1.20 equiv) was added dropwise and the reaction was stirred at room temperature for 16 hours. The reaction was diluted in Et_2O (10 mL) and water (10 mL), extracted with Et_2O three times 3 × 10 mL and the combined organic phases were washed with brine before being dried with anhydrous sodium sulfate. The solution was filtered, concentrated *in vacuo* and purified by column chromatography (15% EtOAc in hexanes) to afford a pale yellow oil (574 mg, 79% yield): **^{1}H NMR** (500 MHz, $CDCl_3$, rotamers are present) δ 3.93 (s, 2H), 3.68–3.53 (m, 2H), 2.50–2.35 (m, 2H), 1.82–1.76 (m, 3H), 1.48 (s, 9H); **^{13}C NMR** (126 MHz, $CDCl_3$, rotamers are present) δ 154.6, 154.3, 141.0, 124.6, 80.6, 46.8, 40.3, 33.6, 28.4, 28.4, 27.9, 15.3, 14.1; **^{19}F NMR** (376 MHz, $CDCl_3$): δ –80.7, –110.5, –120.9, –125.9; **IR** (microscope, cm^{-1}) 2980, 2933, 1703, 1420, 1244, 1203, 1175, 1144, 1033;

HRMS (ESI-TOF) for $C_{15}H_{18}F_9NNaO_5S$ $(M + Na)^+$ calcd. 518.0654; found 518.0655.

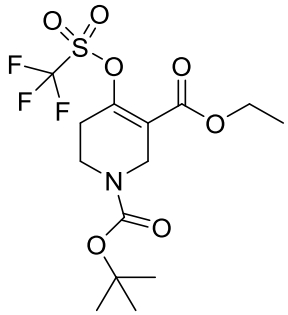

1-*tert*-butyl 3-ethyl 4-(((trifluoromethyl)sulfonyl)oxy)-5,6-dihydropyridine-1,3(2*H*)-dicarboxylate (2-12): Following a modified literature procedure,[32] *N*-Boc-3-carboethoxy-4-piperidone (265 mg, 1.00 mmol, 1.00 equiv) was dissolved in THF (1.3 mL, 0.80 M) and cooled to about –40 °C (dry-ice/acetonitrile bath) before KHMDS (0.50 M in toluene, 2.4 mL, 1.2 mmol, 1.2 equiv) was added dropwise. The reaction was stirred for 30 minutes before $PhNTf_2$ (429 mg, 1.20 mmol, 1.20 equiv) was added as a solid at –40 °C. The reaction was allowed to stir in an ice bath and warmed to room temperature overnight. The reaction was quenched with saturated sodium bicarbonate (10 mL) and extracted with DCM (3 × 10 mL). The combined organic phases were washed with brine (10 mL), dried with anhydrous magnesium sulphate, filtered and concentrated *in vacuo* and purified by column chromatography (10% MTBE in hexanes) to afford a yellow oil (169 mg, 42% yield, as a mixture with about 10% of the starting β-keto ester). All spectral data matched the literature:[33] **^{1}H NMR** (500 MHz, $CDCl_3$, rotamers are present) δ 4.39–4.19 (m, 4H), 3.61 (t, J = 5.7 Hz, 2H), 2.55–2.42 (m, 2H), 1.50–1.44 (m, 9H), 1.33 (t, J = 7.0 Hz, 3H); **IR** (microscope, cm^{-1}) 2982, 2936, 1708, 1425, 1369, 1295, 1244, 1213, 1166, 1142, 1081, 1081; **HRMS** (ESI-TOF) for $C_{14}H_{24}F_3N_2O_7S$ $(M + NH_4)^+$ calcd. 421.1251; found 421.1250; $C_{14}H_{20}NF_3NNaO_7S$ $(M + Na)^+$ calcd. 426.0805; found 426.0805.

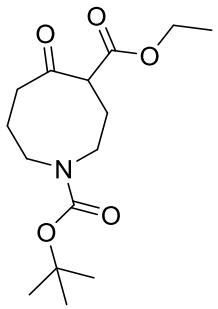

1-*tert*-butyl 4-ethyl 5-oxoazocane-1,4-dicarboxylate (2-10): Following a modified literature procedure,[11] *N*-Boc-hexahydro-1*H*-azepin-4-one (2.13 g, 10.0 mmol, 1.00 equiv) was dissolved in Et_2O (22 mL, 0.45 M) and cooled to about –40 °C (dry-ice/acetonitrile bath) before $BF_3{\bullet}OEt_2$ (1.50 mL, 12 mmol, 1.2 equiv) was added dropwise. Ethyl diazoacetate ($\geq$ 13 wt% in DCM, 1.5 mL, 12 mmol, 1.2 equiv) was added dropwise over 15 minutes as a solution in 7.0 mL in Et_2O. After 15 minutes, the reaction mixture was transferred to a separatory funnel containing ice and saturated sodium carbonate (30 mL, 0.33 M). Upon warming to room temperature, the aqueous phase was extracted with Et_2O (22 mL) three times. The combined organic phases were dried with anhydrous sodium sulphate, filtered and concentrated *in vacuo* and purified by column chromatography (EtOAc:hexanes = 1:8 to 1:4 to 1:3) to afford a pale yellow oil (948 mg, 32% yield). All spectral data matched the literature:[11] **^{1}H NMR** (500 MHz, $CDCl_3$, rotamers are present) δ 4.28–4.14 (m, 1H), 4.14–4.03 (m, 1H), 3.64– 2.94 (m, 5H), 2.71–2.14 (m, 4H), 2.13–1.64 (m, 2H), 1.47–1.32 (m, 9H), 1.31–1.13 (m, 3H); **^{13}C NMR** (126 MHz, $CDCl_3$, rotamers are present) δ 207.7 (2C), 177.0, 175.9, 172.5, 172.4, 171.0, 169.6 (2C), 155.5, 155.0, 98.3, 97.3, 80.2, 80.1, 79.3, 79.2, 61.4, 61.2 (2C), 60.5, 60.3, 56.6, 54.8, 53.4, 48.8, 48.7, 47.5, 47.3, 47.1, 46.7, 45.6, 45.1, 40.2, 38.3, 31.3, 30.6, 30.4, 29.2, 28.5, 28.4, 28.3 (2C), 27.6, 27.0, 25.8, 25.7, 25.6, 21.0, 14.2 (2C), 14.2, 14.0; **IR**

(microscope, cm^{-1}) 2975, 2867, 1696, 1644, 1469, 1413, 1367, 1245, 1191, 1171, 1073; **HRMS** (ESI-TOF) for $C_{15}H_{25}NNaO_5$ $(M + Na)^+$ calcd. 322.1625; found 322.1628.

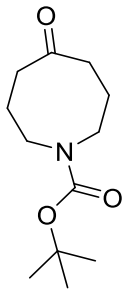

***tert*-butyl 5-oxoazocane-1-carboxylate (2-11)**: Following a modified literature procedure,[34] β-keto-ester **2-10** (435 mg, 1.50 mmol, 1.00 equiv) was dissolved in MeOH (3.0 mL, 0.50 M) and aqueous NaOH (4.0 M, 0.75 mL, 3.0 mmol, 2.0 equiv) was added dropwise. The reaction flask was equipped with a condenser and heated to 100 °C for 3.5 hours. The reaction was cooled to 0 °C and acidified to pH ≈ 2 with concentrated HCl the allowed to warm to room temperature. The reaction was diluted with DCM (10 mL) and extracted three times. The combined organic phases were washed with brine, dried with anhydrous sodium sulphate, filtered and concentrated *in vacuo* to afford a white solid which was used without further purification (296 mg, 90% yield). All spectral data matched the literature:[11] **^{1}H NMR** (700 MHz, $CDCl_3$, rotamers are present) δ 3.71–3.51 (m, 2H), 3.20–3.07 (m, 2H), 2.65–2.54 (m, 2H), 2.46–2.35 (m, 2H), 1.94–1.84 (m, 2H), 1.81–1.69 (m, 2H), 1.51–1.44 (m, 9H); **^{13}C NMR** (176 MHz, $CDCl_3$, rotamers are present) δ 216.6, 216.2, 206.3, 155.3, 154.6, 79.9, 79.8, 48.2, 48.2, 47.1, 46.6, 44.5, 43.9, 42.4, 41.5, 28.5 (2C), 27.8, 26.5, 21.7, 20.6; **IR** (microscope, cm^{-1}) 2971, 2945, 1693, 1482, 1419, 1322, 1253, 1168, 1124; **HRMS** (ESI-TOF) for $C_{12}H_{21}NNaO_3$ $(M + Na)^+$ calcd. 250.1414; found 250.1417.

2.6.3 General procedure A – racemic borylative migration

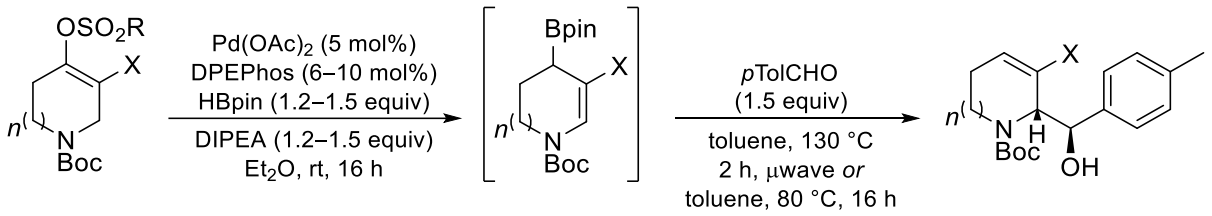

Following a modified literature procedure,[5] $Pd(OAc)_2$ (3.4 mg, 0.015 mmol, 5.0 mol%) and DPEPhos (9.7–16.2 mg, 0.018–0.030 mmol, 5.0–10 mol%) were dissolved in Et_2O (3.0 mL, 0.10 M) and stirred for 20 minutes. DIPEA (63– 80 μL, 0.36–0.45 mmol, 1.2–1.5 equiv), HBpin (41–66 μL, 0.36–0.45 mmol, 1.2–1.5 equiv) and the alkenyl nonaflate (0.30 mmol, 1.0 equiv) were sequentially added and the reaction was left to stir at room temperature for 16 hours. The crude reaction mixture was sequentially filtered through a short silica plug with Et_2O (80 mL) and the volatiles were removed *in vacuo*. For reactions in which the allylboration was performed, the crude reaction mixture was transferred to a new flame-dried flask using toluene (0.20 M total) and *p*-tolualdehyde (66 μL, 0.45 mmol, 1.5 equiv) was added. The reaction was stirred at 130 °C for two hours under microwave conditions or 80 °C for 16 hours. The volatiles were removed *in vacuo* and the crude reaction mixture was purified by column chromatography (eluent specified below).

2.6.4 General procedure B – enantioselective borylative migration

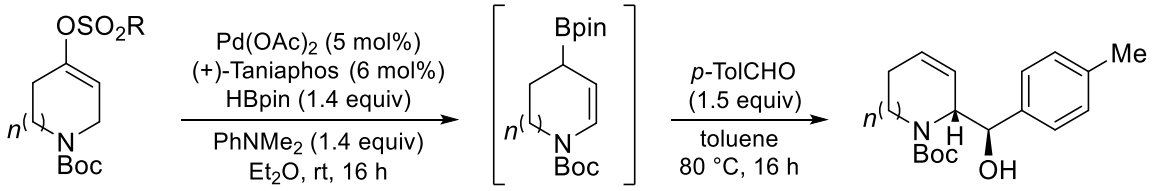

Following a modified literature procedure,[5] $Pd(OAc)_2$ (3.4 mg, 0.015 mmol, 5.0 mol%) and (+)-Taniaphos (12.4 mg, 0.018 mmol, 6.0 mol%) were dissolved in Et_2O (4.8 mL, 0.063 M) and stirred for 20 minutes. $PhNMe_2$ (53 μL, 0.44 mmol, 1.4 equiv), HBpin (61 μL, 0.42 mmol, 1.4 equiv) and

the alkenyl nonaflate (0.30 mmol, 1.0 equiv) were sequentially added and the reaction was left to stir at room temperature for 16 hours. The crude reaction mixture was sequentially filtered through a short silica plug with Et_2O (80 mL) and the volatiles were removed *in vacuo*. For reactions in which the allylboration was performed, the crude reaction mixture was transferred to a new flame-dried flask using toluene (0.20 M total) and *p*-tolualdehyde (66 μL, 0.45 mmol, 1.5 equiv) was added. The reaction was stirred at 80 °C for 16 hours. The volatiles were removed *in vacuo* and the crude reaction mixture was purified by column chromatography (eluent specified below).

2.6.5 Initial borylative migration results of nonaflates 2-5, 2-6 and 2-7b

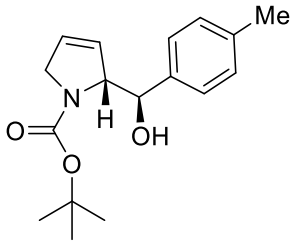

(±)-(*RS*)-tert-butyl 2-((*RS*)-hydroxy(*p*-tolyl)methyl)-2,5-dihydro-1*H*-pyrrole-1-carboxylate (2-13): Following general procedure A using nonaflate **2-5** (140 mg, 0.30 mmol, 1.00 equiv). After the allylboration step, the crude reaction mixture was purified by column chromatography (15 to 30% Et_2O in hexanes) to obtain a yellow oil (5 mg, 6% yield): **^{1}H NMR** (400 MHz, $CDCl_3$, rotamers are present) δ 7.23 (d, *J* = 7.8 Hz, 2H), 7.13 (d, *J* = 7.5 Hz, 2H), 5.95 (s, 1H), 5.76–5.44 (m, 1H), 5.11 (d, *J* = 6.5 Hz, 1H), 4.87–4.69 (m, 1H), 4.55 (d, *J* = 8.1 Hz, 1H), 4.21 (d, *J* = 15.0 Hz, 1H), 4.03 (d, *J* = 15.8 Hz, 1H), 2.33 (s, 3H), 1.52 (s, 9H); **^{13}C NMR** (126 MHz, $CDCl_3$, rotamers are present) δ 157.6, 138.7, 137.4, 128.9, 127.6, 127.0, 126.1, 81.1, 79.8, 71.6, 54.4, 29.7, 28.6, 28.6, 28.5, 24.8, 21.2, 14.2; **IR** (microscope, cm^{-1}) 3435, 2975, 2925, 1699, 1675, 1404, 1367, 1172, 1124; **HRMS** (ESI-TOF): for $C_{17}H_{24}NO_3$ $(M + H)^+$ calcd. 290.1751; found 290.1751.

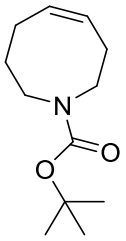

(*Z*)-*tert*-butyl 3,4,7,8-tetrahydroazocine-1(2*H*)-carboxylate (2-16): Following general procedure B using nonaflate **2-7** (150 mg, 0.30 mmol, 1.00 equiv). After the borylative migration step, 1,3,5-trimethoxybenzene was added (0.33 equiv) as an internal standard. The crude reaction mixture was then partially purified by column chromatography (5% EtOAc/Hex) to obtain a partially purified clear colourless oil for characterization purposes. All spectral data matched the literature: [13] **^{1}H NMR** (400 MHz, $CDCl_3$, rotamers are present) δ 5.87–5.57 (m, 2H), 3.37–3.24 (m, 2H), 3.24–3.11 (m, 2H), 2.27–2.14 (m, 2H), 2.11–1.95 (m, 2H), 1.86–1.65 (m, 2H), 1.46 (s, 9H).

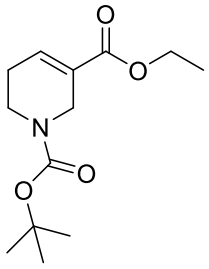

1-*tert*-butyl 3-ethyl 5,6-dihydropyridine-1,3(2*H*)-dicarboxylate (2-17): Following general procedure B using nonaflate **2-12** (118 mg, 0.30 mmol, 1.00 equiv). After the allylboration step, the crude reaction mixture was purified by column chromatography (5 to 10% EtOAc in hexanes) to obtain a clear colourless oil (36 mg, 48% yield). Notably, the crude ^{1}H NMR from the borylative migration to allylboration steps were the same. All spectral data matched the literature:[16] **^{1}H NMR** (400 MHz, $CDCl_3$, rotamers are present) δ 5.87–5.57 (m, 2H), 3.37–3.24 (m, 2H), 3.24–3.11 (m, 2H), 2.27–2.14 (m, 2H), 2.11–1.95 (m, 2H), 1.86–1.65 (m, 2H), 1.46 (s, 9H); **^{13}C NMR** (126 MHz,

$CDCl_3$, rotamers are present) δ 165.3, 154.8, 137.5, 128.5, 79.9, 60.5, 42.6, 39.8, 38.7, 28.4, 25.5, 14.2.

2.6.6 General procedure C: *N*-protection of 4-perhydroazepinone precursors

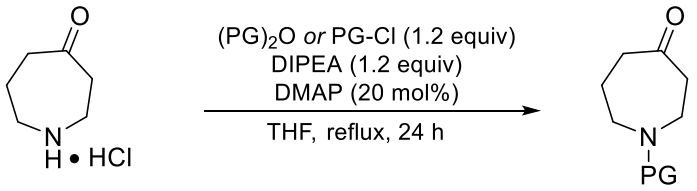

4-perhydroazepinone HCl (1.50 g, 10.0 mmol, 1.00 equiv) and *N*,*N*-dimethylaminopyridine (244 mg, 2.00 mmol) were dissolved in THF (50 mL) at room temperature. DIPEA (2.1 mL, 12.0 mmol) and the corresponding acid/tosyl chloride or anhydride (12.0 mmol) were sequentially added at room temperature or 0 °C. The reaction was heated to reflux for 24 hours before being allowed to cool back to room temperature. The solution was quenched with saturated aqueous ammonium chloride (50 mL) and extracted with dichloromethane (50 mL) three times. The combined organic phases were washed with brine (50 mL), dried with anhydrous sodium sulphate, filtered and concentrated *in vacuo*. The crude reaction mixture was purified by flash column chromatography (EtOAc:hexanes, ratios specified below) to afford the corresponding N-protected 4-perhydroazepinone product All spectral data matched the literature (the relevant precedence is referenced for each individual compound).

2.6.7 Characterization of the *N*-protection of 4-perhydroazepinone precursors

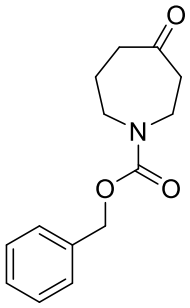

benzyl 4-oxo-1-azepanecarboxylate (2-18): Prepared according to general procedure C using 4-perhydroazepinone HCl (1.50 g, 10.0 mmol) and benzyl chloroformate (1.70 mL, 12.0 mmol). The crude reaction mixture was purified by flash chromatography (3:1 EtOAc:hexanes) to obtain a clear, colourless oil (1.79 g, 72% yield). All spectral data matched the literature:[35] **^{1}H NMR** (500 MHz, $CDCl_3$, rotamers are present) δ 7.42–7.27 (m, 5H), 5.12 (s, 2H), 3.75–3.49 (m, 4H), 2.85–2.50 (m, 4H), 1.91–1.65 (m, 2H); **^{13}C NMR** (126 MHz, $CDCl_3$, rotamers are present) δ 211.4, 211.3, 155.1, 136.5, 128.5, 128.1, 127.9, 67.4, 67.3, 49.5, 49.3, 43.9, 43.4, 43.3, 43.0, 42.9, 25.8, 25.4; **IR** (microscope, cm^{-1}) 3033, 2951, 1694, 1473, 1421, 1234, 1164, 1067; **HRMS** (ESI-TOF) for $C_{14}H_{17}NNaO_3$ $(M + Na)^+$ calcd. 270.1101; found 270.1096, for $C_{14}H_{21}N_2O_3$ $(M + NH_4)^+$ calcd. 265.1547; found 265.1545, for $C_{14}H_{18}NO_3$ $(M + H)^+$ calcd. 248.1281; found 248.1289.

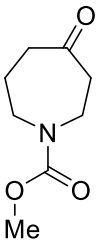

methyl 4-oxo-1-azepanecarboxylate (2-19): Prepared according to general procedure C using 4-perhydroazepinone HCl (1.50 g, 10.0 mmol) and methyl chloroformate (0.92 mmol, 12 mmol). The crude reaction mixture was purified by flash chromatography (36% EtOAc in hexanes) to obtain a

yellow oil (1.11 g, 65% yield). All spectral data matched the literature:[36] **^{1}H NMR** (400 MHz, $CDCl_3$, rotamers are present) δ 3.66 (s, 3H), 3.65–3.48 (m, 4H), 2.67–2.53 (m, 4H), 1.82–1.69 (m, 2H); **^{13}C NMR** (101 MHz, $CDCl_3$, rotamers are present) δ 211.4, 155.7, 52.8, 49.4, 49.3, 43.8, 43.3, 42.9, 25.8, 25.4; **IR** (microscope, cm^{-1}) 29567, 1698, 1480, 1443, 1243, 1193;

HRMS (ESI-TOF) for $C_8H_{13}NNaO_3$ $(M + Na)^+$ calcd. 194.0788; found 194.0794, for $C_8H_{17}N_2O_3$ $(M + NH_4)^+$ calcd. 189.1234; found 189.1239.

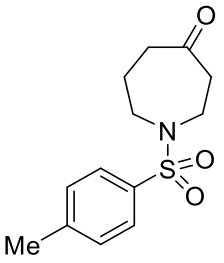

1-(4-methylphenyl)sulfonyl]-4-azepanone (2-20): Prepared according to general procedure C using 4-perhydroazepinone HCl (1.50 g, 10.0 mmol) and *p*-toluenesulfonyl chloride (2.30 g, 10.0 mmol). The crude reaction mixture was purified by flash chromatography (1:2 to 1:1 EtOAc:hexanes) to obtain a white solid (1.75 g, 65% yield): **mp** = 80.3–82.0 °C; ^{1}H NMR (500 MHz, $CDCl_3$) δ 7.67 (d, J = 8.2 Hz, 2H), 7.32 (d, J = 8.0 Hz, 2H), 3.40 (dt, J = 20.5, 5.6 Hz, 4H), 2.72–2.66 (m, 2H), 2.60–2.55 (m, 2H), 2.43 (s, 3H), 1.96–1.81 (m, 1H); **^{13}C NMR** (126 MHz, $CDCl_3$) δ 210.5, 143.7, 135.9, 129.9, 127.1, 50.9, 44.8, 44.6, 42.6, 24.9, 21.6; **IR** (microscope, cm^{-1}) 3071, 2951, 2926, 1706, 1347, 1332, 1178; **HRMS** (ESI-TOF) for $C_{13}H_{17}NNaO_3S$ $(M + Na)^+$ calcd. 290.0821; found 290.0817, for $C_{13}H_{21}N_2O_3S$ $(M + NH_4)^+$ calcd. 285.1267; found 285.1263.

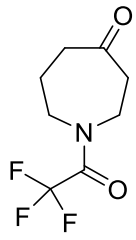

1-(trifluoroacetyl)-4-azepanone (2-21): Prepared according to general procedure C using 4-perhydroazepinone HCl (1.50 g, 10.0 mmol) and trifluoroacetic anhydride (0.92 mL, 12 mmol). The crude reaction mixture was purified by flash chromatography (35% EtOAc in hexanes) to obtain a yellow oil (1.68 g, 81% yield). All spectral data matched the literature:[37] **^{1}H NMR** (500 MHz, $CDCl_3$, rotamers are present) δ 3.85–3.63 (m, 4H), 2.78–2.57 (m, 4H), 1.92–1.78 (m, 2H); **^{13}C NMR** (126 MHz, $CDCl_3$, rotamers are present) δ 209.7, 209.2, 156.0 (q, J = 36 Hz), 116.4 (q, J = 288 Hz), 116.3 (q, J = 288 Hz), 50.6 (q, J = 4 Hz), 49.6, 44.4, 44.0, 43.7 (m), 42.6, 42.4, 41.6, 26.5, 23.5; **^{19}F NMR** (469 MHz, $CDCl_3$, rotamers are present): δ –69.1, –69.4; **IR** (microscope, cm^{-1}) 2959, 1690, 1464, 1438, 1200, 1136; **HRMS** (ESI-TOF) for $C_8H_{10}F_3NNaO_2$ $(M + Na)^+$ calcd. 232.0556; found 232.0554, for $C_8H_{14}F_3N_2O_2$ $(M + NH_4)^+$ calcd. 227.1002; found 227.0999.

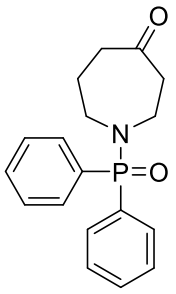

1-(diphenylphosphoryl)azepan-4-one (2-22): Prepared according to general procedure C using 4-perhydroazepinone HCl (1.50 g, 10.0 mmol) and diphenylphosphinic chloride (2.3 mL, 12 mmol). The crude reaction mixture was purified by flash chromatography (2% to 3% MeOH in DCM) to obtain a white solid (2.05 g, 65% yield), with minor unidentified aromatic impurities present: **^{1}H NMR** (400 MHz, $CDCl_3$) δ 7.89–7.81 (m, 4H), 7.56–7.39 (m, 6H), 3.32 (dd, J = 7.4, 6.0 Hz, 2H), 3.28–3.21 (m, 2H), 2.73–2.60 (m, 2H), 2.55–2.42 (m, 2H), 1.81–1.66 (dddd, J = 6.3, 6.3, 6.2, 6.2 Hz, 2H); **^{13}C NMR** (101 MHz, $CDCl_3$) δ 211.9, 132.2 (d, J = 9 Hz), 132.1 (d, J = 3 Hz), 128.8 (d, J = 13 Hz), 128.3 (d, J = 13 Hz) 50.8, 46.0 (d, J = 6 Hz), 44.0 (d, J = 3 Hz), 42.7, 26.5 (d, J = 8 Hz);

^{31}P NMR (162 MHz, $CDCl_3$) δ 31.6; **IR** (microscope, cm^{-1}) 3057, 2948, 2856, 1704, 1439, 1191, 1123, 960; **HRMS** (ESI-TOF) for $C_{18}H_{21}NO_2P$ $(M + H)^+$ calcd. 314.1304; found 314.1305, for $C_{18}H_{20}NNaO_2P$ $(M + Na)^+$ calcd. 336.1124; found 336.1124.

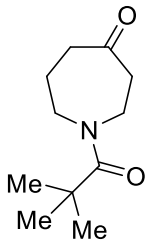

1-pivaloylazepan-4-one (2-23): Prepared according to general procedure C using 4-perhydroazepinone HCl (1.50 g, 10.0 mmol) and trimethylacetic anhydride (2.4 mL, 12 mmol). The crude reaction mixture was purified by flash chromatography (1.0:1.4 EtOAc:hexanes) to obtain a white solid (1.17 g, 59% yield): **^{1}H NMR** (400 MHz, $CDCl_3$) δ 3.77 (dd, J = 7.0, 5.4 Hz, 2H), 3.73 (dd, J = 5.7, 5.4 Hz, 2H), 2.73–2.61 (m, 4H), 1.91–1.82 (m, 2H), 1.28 (s, 9H); **IR** (microscope, cm^{-1}) 2985, 2978, 1696, 1613, 1485, 1419, 1202, 903; **HRMS** (ESI-TOF) for $C_{11}H_{20}NO_2$ $(M + H)^+$ calcd. 198.1489; found 198.1492, for $C_{11}H_{19}NNaO_2$ $(M + Na)^+$ calcd. 220.1308; found 220.1311.

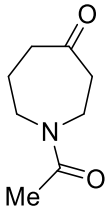

1-acetylazepan-4-one (2-24): Prepared according to general procedure C using 4-perhydroazepinone HCl (1.50 g, 10.0 mmol) and trimethylacetic anhydride (2.4 mL, 12 mmol). The crude orange oil was used in the following step without further purification. All spectral data matched the literature:[38] **^{1}H NMR** (500 MHz, $CDCl_3$) δ 3.74–3.63 (m, 4H), 2.70–2.57 (m, 4H), 2.06

(s, 3H), 1.87–1.70 (m, 2H); **HRMS** (ESI-TOF) for $C_8H_{14}NO_2$ $(M + H)^+$ calcd. 156.1019; found 156.1018, for $C_8H_{13}NNaO_2$ $(M + Na)^+$ calcd. 178.0838; found 178.0837.

2.6.8 General procedure D: synthesis of azepenyl nonaflates[10]

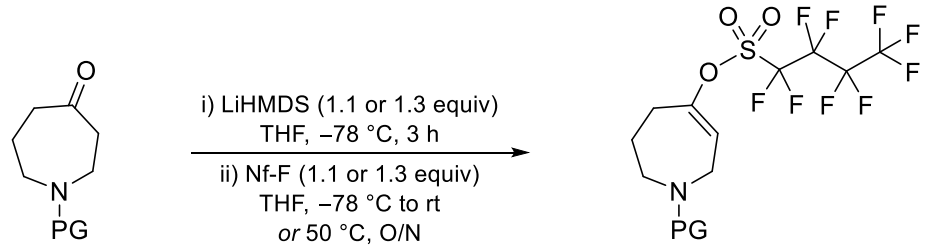

The *N*-protected azepinone (1.00 equiv) was dissolved in THF (0.24 M). Lithium bis(trimethylsilyl)amide (1.10 or 1.30 equiv) was added dropwise at –78 °C and stirred for 3 hours. Perfluorobutanesulfonyl fluoride (Nf-F, 1.10 or 1.30 equiv) was added dropwise and the reaction was then allowed to warm to room temperature or 50 °C overnight. The reaction was quenched by the addition of aqueous saturated sodium bicarbonate (0.20 M) at room temperature and subsequently extracted with dichloromethane (0.20 M) three times. The combined organic phases were washed with water and brine (0.20 M) before being dried with anhydrous sodium sulfate. The solution was filtered, concentrated in vacuo and purified by column chromatography (EtOAc:hexanes, ratios specified below) to afford the corresponding enol perfluorosulfonate.

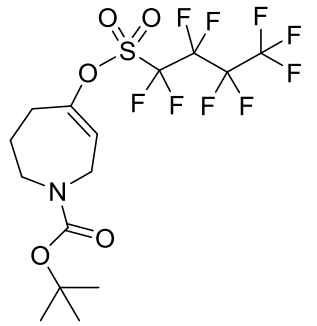

***tert*-butyl 5-(((perfluorobutyl)sulfonyl)oxy)-2,3,4,7-tetrahydro-1*H*-azepine-1-carboxylate (2-6)**: Prepared according to general procedure D with *N*-Boc-hexahydro-1*H*-azepin-4-one (6.40 g 30.0 mmol, 1.00 equiv), LiHMDS (33.0 mL, 33.0 mmol, 1.10 equiv) and Nf-F (10.4 g, 33.0 mmol, 1.10 equiv). The reaction was warmed to room temperature overnight and purified by flash chromatography (10% EtOAc in hexanes) to afford a clear colourless oil (7.90 g, 53% yield), which solidified to a white powder upon storing in a –20 °C freezer. All spectral data matched the literature:[10] **mp** = 30.2–31.5 °C; **^{1}H NMR** (400 MHz, $CDCl_3$, 60 °C, rotamers are present) δ 5.90 (dd, *J* = 5.8, 4.8 Hz, 1H), 3.96 (s, 2H), 3.57 (s, 2H), 2.62–2.51 (m, 2H), 2.03–1.88 (m, 2H), 1.47 (s, 9H); **^{13}C NMR** (101 MHz, $CDCl_3$, ^{19}F decoupled, 60 °C, rotamers are present) δ 154.2, 119.9, 116.3, 113.5, 109.1, 107.7, 79.4, 40.9, 30.2, 27.4, 23.8; **^{19}F NMR** (376 MHz, $CDCl_3$, 60 °C) δ –80.7, –109.6, –125.8, –125.7; **IR** (microscope, cm^{-1}) 2980, 2937, 1699, 1417, 1240, 1201, 1144; **HRMS** (ESI-TOF) for $C_{15}H_{18}F_9NNaO_5S$ $(M + Na)^+$ calcd. 518.0654; found 518.0646.

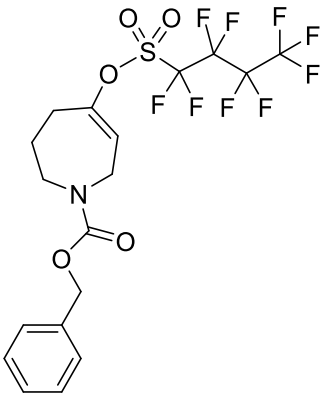

benzyl 5-(((perfluorobutyl)sulfonyl)oxy)-2,3,4,7-tetrahydro-1*H*-azepine-1-carboxylate (2-25): Prepared according to general procedure D with **2-18** (1.46 g, 5.90 mmol, 1.00 equiv), LiHMDS (7.70 mL, 7.70 mmol, 1.30 equiv) and Nf-F (2.32 g, 7.70 mmol, 1.30 equiv). The reaction was warmed to 50 °C overnight and purified by flash chromatography (15% EtOAc in hexanes) to afford a yellow oil (1.71 g, 55% yield): **^{1}H NMR** (400 MHz, $CDCl_3$, 60 °C, rotamers are present) δ 7.41–7.27 (m, 5H), 5.91 (br s, 1H), 5.16 (s, 2H), 4.06 (br s, 2H), 3.72–3.56 (m, 2H), 2.67–2.51 (m, 2H), 1.97 (br s, 2H); **^{13}C NMR** (101 MHz, $CDCl_3$, ^{19}F decoupled, 60 °C) δ 155.9, 152.8, 152.1, 136.7, 128.6, 128.2, 127.9, 120.4, 117.3, 114.5, 110.1, 108.7, 77.4, 77.1, 76.7, 67.7, 47.4, 41.7, 31.2, 24.5; **^{19}F NMR** (376 MHz, $CDCl_3$, 60 °C, rotamers are present) δ –80.8, –80.9, –109.6, –112.7, –120.7, –120.9, –125.6, –125.7; **IR** (microscope, cm^{-1}) 3183, 3071, 3037, 2948, 1703, 1420, 1353, 1238, 1201, 1143, 1037; **HRMS** (ESI-TOF) for $C_{18}H_{16}F_9NNaO_5S$ $(M + Na)^+$ calcd. 552.0498; found 552.0494, for $C_{18}H_{20}F_9N_2O_5S$ $(M + NH_4)^+$ calcd. 547.0944; found 547.0952.

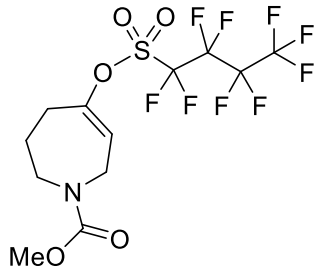

methyl 5-(((perfluorobutyl)sulfonyl)oxy)-2,3,4,7-tetrahydro-1*H*-azepine-1-carboxylate (2-26): Prepared according to the general procedure D with **2-19** (1.08 g, 6.30 mmol, 1.00 equiv), LiHMDS (8.20 mL, 8.20 mmol, 1.30 equiv) and Nf-F (2.47 g, 8.20 mmol, 1.30 equiv). The reaction was warmed to 50 °C overnight and purified by flash chromatography (15% EtOAc in hexanes) to afford a red oil (1.66 g, 58% yield): **^{1}H NMR** (400 MHz, $CDCl_3$, 60 °C, rotamers are present) δ 5.90 (dd, *J* = 6.0, 4.8 Hz, 1H), 4.02 (br s, 2H), 3.72 (s, 3H), 3.61 (br s, 2H), 2.77–2.40 (m, 2H), 1.96 (m, 2H); **^{13}C NMR** (101 MHz, $CDCl_3$, ^{19}F decoupled, 60 °C, rotamers are present) δ 156.5, 152.5, 152.1, 120.4, 117.3, 114.5, 110.1, 108.7, 77.4, 77.3, 77.1, 76.7, 52.9, 47.5, 41.8, 31.3, 24.5; **^{19}F NMR** (376 MHz, $CDCl_3$, 60 °C, defined rotamers, rot A/B, are present) δ –80.8 (rot A), –80.9 (rot B), –109.7 (rot A), –112.8 (rot B), –120.8 (rot A), –121.0 (rot B), –125.8 (rot A), –125.9 (rot B); **IR** (microscope, cm^{-1}) 3190, 3076, 2984, 2960, 1708, 1476, 1415, 1240, 1202, 1144; **HRMS** (ESI-TOF) for $C_{12}H_{12}F_9NNaO_5S$ $(M + Na)^+$ calcd. 476.0185; found 476.0185, for $C_{12}H_{16}F_9N_2O_5S$ $(M + NH_4)^+$ calcd. 471.0631; found 471.0639.

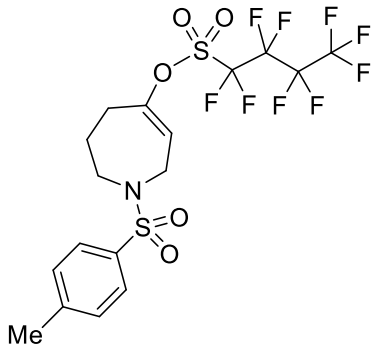

1-tosyl-2,5,6,7-tetrahydro-1*H*-azepin-4-yl 1,1,2,2,3,3,4,4,4-nonafluorobutane-1-sulfonate (2-27): Prepared according to general procedure D using **2-20** (1.74 g, 6.50 mmol, 1.00 equiv), LiHMDS (8.50 mL, 8.50 mmol, 1.30 equiv) and Nf-F (2.60 g, 8.50 mmol, 1.30 equiv). The reaction was warmed to room temperature overnight and purified by flash chromatography (15% to 20% EtOAc in hexanes) to afford a white solid (1.30 g, 36% yield): **mp** = 90.2–92.0 °C; **^{1}H NMR** (400 MHz, $CDCl_3$) δ 7.76–7.62 (m, 2H), 7.36–7.28 (m, 2H), 5.81 (dd, *J* = 5.5, 5.3 Hz, 1H), 3.94 (ddd, *J* = 5.4, 2.4, 1.6 Hz, 2H), 3.44–3.37 (m, 2H), 2.55–2.47 (m, 2H), 2.42 (s, 3H), 2.00–1.90 (m, 2H); **^{13}C NMR** (101 MHz, $CDCl_3$, ^{19}F decoupled) δ 152.8, 143.7, 135.9, 129.9, 127.2, 119.0, 117.1, 114.2, 109.9, 108.5, 48.4, 42.5, 31.0, 24.7, 21.5; **^{19}F NMR** (377 MHz, $CDCl_3$): δ –80.8, –110.0, –121.1, –126.0; **IR** (microscope, cm^{-1}) 30692, 2944, 2306, 1919, 1408, 1239, 1267, 1200, 1158, 1144, 1016; **HRMS** (ESI-TOF) for $C_{17}H_{16}F_9NNaO_5S_2$ $(M + Na)^+$ calcd. 572.0218; found 572.0218, for $C_{17}H_{20}F_9N_2O_5S_2$ $(M + NH_4)^+$ calcd. 567.0664; found 567.0677, for $C_{17}H_{17}F_9NO_5S_2$ $(M + H)^+$ calcd. 550.0399; found 550.0408.

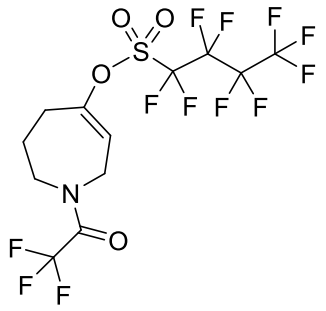

1-(2,2,2-trifluoroacetyl)-2,5,6,7-tetrahydro-1*H*-azepin-4-yl 1,1,2,2,3,3,4,4,4-nonafluorobutane-1-sulfonate (2-28): Prepared according to general procedure D with **2-21** (3.37 g, 16.1 mmol, 1.00 equiv), LiHMDS (17.7 mL, 17.7 mmol, 1.10 equiv) and Nf-F (5.35 g, 17.7 mmol, 1.10 equiv). The reaction was warmed to room temperature overnight and purified by flash chromatography (15% to 20% EtOAc in hexanes) to afford a white solid (4.15 g, 52% yield): **^{1}H NMR** (400 MHz, $CDCl_3$, 60 °C) δ 5.95 (ddd, *J* = 35.7, 6.4, 5.5 Hz, 1H), 4.17–4.14 (m, 2H), 3.85–3.68 (m, 2H), 2.67–2.62 (m, 2H), 2.22–1.92 (m, 2H); **^{13}C NMR** (101 MHz, $CDCl_3$, ^{19}F decoupled, 60 °C, rotamers are present) δ 153.4, 152.8, 118.8, 118.5, 117.3, 114.6, 110.1, 108.7, 48.7, 48.1, 42.4, 41.6, 31.2, 31.0, 25.0, 23.3; **^{19}F NMR** (377 MHz, $CDCl_3$, 60 °C, rotamers are present) δ –69.0, –69.4, –80.9, –81.0, –109.4, –112.7, –120.69, –120.9 , –125.6, –125.8; **IR** (microscope, cm^{-1}) 2958, 1696, 1422, 1203, 1143, 1021; **HRMS** (ESI-TOF) for $C_{12}H_9F_{12}NNaO_4S$ $(M + Na)^+$ calcd. 513.9953; found 513.9942, for $C_{12}H_{13}F_{12}N_2O_4S$ $(M + NH_4)^+$ calcd. 509.0399; found 509.0405.

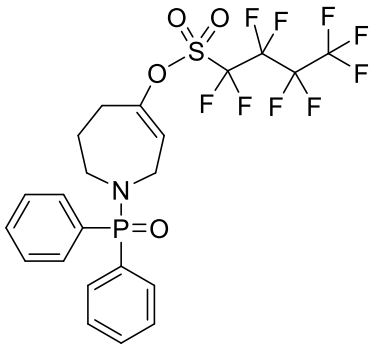

1-(diphenylphosphoryl)-2,5,6,7-tetrahydro-1i-azepin-4-yl 1,1,2,2,3,3,4,4,4-nonafluorobutane-1-sulfonate (2-29): Prepared according to general procedure D with **2-22** (1.95 g, 6.55 mmol, 1.00 equiv), LiHMDS (8.52 mL, 8.52 mmol, 1.30 equiv) and Nf-F (2.57 g, 8.52 mmol, 1.30 equiv). The reaction was warmed to 50 °C overnight and purified by flash chromatography (100% EtOAc) to afford a brown solid (265 mg, 10% yield): **^{1}H NMR** (500 MHz, $CDCl_3$) δ 7.92–7.86 (m, 4H), 7.55–7.42 (m, 6H), 5.71 (t, *J* = 5.3 Hz, 1H), 3.71–3.58 (m, 2H), 3.25 (ddd, *J* = 6.0, 6.0, 6.0 Hz, 2H), 2.73–2.64 (m, 2H), 1.94 (tt, *J* = 6.1, 6.2 Hz, 2H); **^{13}C NMR** (101 MHz, $CDCl_3$) δ 153.4, 132.4 (d, *J* = 9.3 Hz), 132.1 (d, *J* = 2.7 Hz), 131.3 (d, *J* = 129.4 Hz), 128.8 (d, *J* = 12.5 Hz), 121.9 (d, *J* = 6.9 Hz), 47.5 (d, *J* = 2.8 Hz), 42.3 (d, *J* = 4.2 Hz), 31.3, 25.65 (d, *J* = 7.8 Hz); **^{19}F NMR** (376 MHz, $CDCl_3$) δ –80.6, –109.9, –120.9, –125.8; **^{31}P NMR** (162 MHz, $CDCl_3$) δ –31.0; **IR** (microscope, cm^{-1}) 3432, 3060, 2955, 2858, 1686, 1418, 1353, 1240, 1201, 1144, 1122, 1011; **HRMS** (ESI-TOF) for $C_{22}H_{20}F_9NO_4PS$ $(M + H)^+$ calcd. 596.0701; found 596.0711, for $C_{22}H_{19}F_9NNaO_4PS$ $(M + Na)^+$ calcd. 618.0521; found 618.0517.

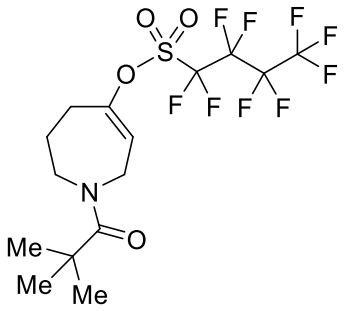

1-pivaloyl-2,5,6,7-tetrahydro-1*H*-azepin-4-yl 1,1,2,2,3,3,4,4,4-nonafluorobutane-1-sulfonate (2-30): Prepared according to general procedure D with **2-23** (1.16 g, 5.90 mmol, 1.00 equiv), LiHMDS (7.67 mL, 7.67 mmol, 1.30 equiv) and Nf-F (2.34 g, 7.67 mmol, 1.30 equiv). The reaction was warmed to 50 °C overnight and purified by flash chromatography (25% EtOAc in hexanes) to afford a light yellow solid (1.29 g, 46% yield): **^{1}H NMR** (500 MHz, $CDCl_3$) δ5.92 (t, *J* = 5.1 Hz,

1H), 4.11 (d, J = 5.0 Hz, 2H), 3.72 (t, J = 6.2 Hz, 2H), 2.60–2.49 (m, 2H), 2.03 (tt, J = 6.1, 6.0 Hz, 2H), 1.28 (s, 9H); **^{13}C NMR** (101 MHz, $CDCl_3$) δ 177.1, 152.4, 120.5, 48.6, 43.2, 39.1, 30.72, 28.6, 24.7; **^{19}F NMR** (377 MHz, $CDCl_3$) δ –80.8, –110.0, –121.1, –126.0; **IR** (microscope, cm^{-1}) 2977, 2878, 1630, 1416, 1240, 1202, 1144, 1013; **HRMS** (ESI-TOF) for $C_{15}H_{19}F_9NO_4S$ $(M + H)^+$ calcd. 480.0886; found 480.0891, for $C_{15}H_{18}F_9NNaO_4S$ $(M + Na)^+$ calcd. 502.0705; found 502.0705.

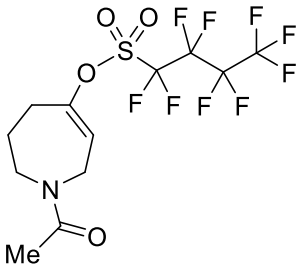

1-acetyl-2,5,6,7-tetrahydro-1*H*-azepin-4-yl 1,1,2,2,3,3,4,4,4-nonafluorobutane-1-sulfonate (2-31): Prepared according to general procedure D with crude **2-24** (1.91 g, 12.3 mmol, 1.00 equiv), LiHMDS (13.0 mL, 13.0 mmol, 1.05 equiv) and Nf-F (4.09 g, 13.5 mmol, 1.10 equiv). The reaction was warmed to rt overnight and purified by flash chromatography (1:6 EtOAc:hexanes) to afford a yellow oil (1.37 g, 25% yield over two steps): **^{1}H NMR** (400 MHz, $CDCl_3$, defined rotamers, rot A/B, are present) δ 5.95 (t, J = 5.4 Hz, 1H, rot A), 5.90 (t, J = 5.0 Hz, 1H, rot B), 4.12 (dt, J = 5.5, 1.5 Hz, 2H, rot A), 3.99 (dt, J = 5.1, 1.7 Hz, 2H, rot B), 3.71 (t, J = 6.3 Hz, 2H, rot A), 3.65–3.57 (m, 2H, rot B), 2.65–2.57 (m, 2H, rot A), 2.56–2.46 (m, 2H, rot B), 2.10 (s, 3H), 2.00 (tt, J = 6.1, 6.0 Hz, 2H); **^{13}C NMR** (101 MHz, $CDCl_3$, defined rotamers, rot A/B, are present) δ 170.3 (rot A), 169.7 (rot B), 153.4 (rot A), 151.6 (rot B), 120.4 (rot A), 119.1 (rot B), 49.2 (rot A), 45.1 (rot B), 43.3 (rot A), 39.4 (rot B), 31.2 (rot A), 30.7 (rot B), 24.8 (rot A), 24.0 (rot B), 21.5 (rot A), 21.3 (rot B); **^{19}F NMR** (377 MHz, $CDCl_3$) δ –81.03, –110.1, –121.2, –126.2; **IR** (microscope, cm^{-1}) 3462, 2946, 1649, 1418, 1353, 12337, 1201, 1010, 896, 868; **HRMS** (ESI-TOF) for $C_{12}H_{13}F_9NO_4S$ (M +

H)$^+$ calcd. 438.0416; found 438.0418, for $C_{12}H_{12}F_9NNaO_4S$ (M + Na)$^+$ calcd. 460.0236; found 460.0236.

2.6.9 Characterization of allylboration products 2-32 to 2-35

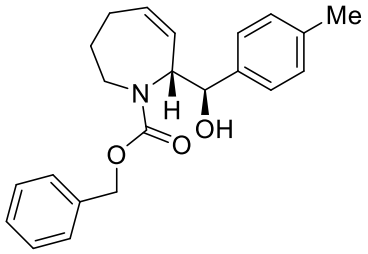

(*R*)-benzyl 7-((*R*)-hydroxy(*p*-tolyl)methyl)-2,3,4,7-tetrahydro-1*H*-azepine-1-carboxylate (2-32): Prepared according to general procedure B with **2-25** (157 mg, 0.300 mmol, 1.00 equiv). The crude reaction mixture was purified by flash chromatography (gradient 5 to 25% EtOAc in hexanes), followed by preparatory TLC (30% MTBE in hexanes) to afford a clear, colourless oil (10 mg, 10% yield): **^{1}H NMR** (700 MHz, $CDCl_3$, rotamers are present) 7.41–7.30 (m, 5H), 7.30–7.18 (m, 2H), 7.18–7.10 (m, 2H), 5.75–5.60 (m, 1H), 5.33–5.11 (m, 3H), 5.11–4.94 (m, 1H), 4.76–4.63 (m, 1H), 4.04–3.72 (m, 1H), 3.34–3.13 (m, 1H), 3.12–2.87 (br s, 1H), 2.34 (s, 3H), 2.31–1.83 (m, 3H), 1.77–1.49 (m, 1H); **^{13}C NMR** (176 MHz, $CDCl_3$, rotamers are present) δ 158.0, 156.5, 138.4, 137.8, 136.8, 130.6, 129.8, 129.2, 128.6, 128.0, 127.8, 127.7, 127.3, 127.1, 75.0, 74.5, 67.5, 67.3, 63.3, 63.0, 42.9, 29.8, 25.9, 24.6, 24.1, 21.2; **IR** (microscope, cm^{-1}) 3441, 3030, 2925, 2864, 1681, 1423, 1304, 1274, 1215; **HRMS** (ESI-TOF) for $C_{22}H_{25}NNaO_3$ (M + Na)$^+$ calcd. 374.1727; found 374.1726; **HPLC** (Chiralpak IC) 10:90 *i*PrOH/Hex, 20 °C, 0.5 mL/min, λ = 230 nm, T_{minor} = 23.4 min, T_{major} = 27.8 min, *er* = 92.2 : 7.8.

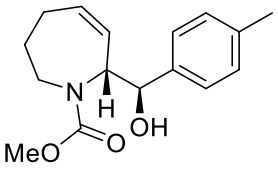

(*R*)-methyl 7-((*R*)-hydroxy(*p*-tolyl)methyl)-2,3,4,7-tetrahydro-1*H*-azepine-1-carboxylate (2-33): Prepared according to general procedure B with **2-26** (140 mg, 0.300 mmol, 1.00 equiv). The crude reaction mixture was purified by flash chromatography (gradient 10 to 25% EtOAc in hexanes), followed by preparatory TLC (40% MTBE in hexanes) to afford a clear, colourless oil (14 mg, 16% yield): **^{1}H NMR** (400 MHz, $CDCl_3$, rotamers are present) 7.32–7.21 (m, 2H), 7.16 (d, J = 7.9 Hz, 2H), 5.78–5.56 (m, 1H), 5.31–5.13 (m, 1H), 5.12–4.83 (m, 1H), 4.79–4.59 (m, 1H), 4.05–3.60 (m, 4H), 3.32–2.88 (m, 1H), 2.34 (s, 3H), 2.25 (dddd, J = 16.2, 10.9, 5.1, 2.8 Hz, 1H), 2.14–1.83 (m, 2H), 1.83–1.48 (m, 2H); **^{13}C NMR** (126 MHz, $CDCl_3$, rotamers are present) δ 158.6, 157.2, 138.4, 137.9, 137.7, 131.0, 130.6, 129.8, 129.2, 128.9, 127.4, 127.1, 74.9, 74.3, 63.2, 62.8, 61.6, 53.0, 52.9, 42.8, 29.7, 25.9, 24.7, 24.2, 21.2, 14.1; **IR** (microscope, cm^{-1}) 3433, 3024, 2952, 2923, 2863, 1696, 1681, 1446, 1407, 1306, 1276, 1198; **HRMS** (ESI-TOF) for $C_{16}H_{21}NNaO_3$ $(M + Na)^+$ calcd. 298.1414; found 298.1412; **$[\alpha]_D^{20}$** +35.2 (*c* 0.0500, $CHCl_3$); **HPLC** (Chiralpak IC) 2:98 *i*PrOH/Hex, 20 °C, 0.5 mL/min, λ = 230 nm, T_{minor} = 30.4 min, T_{major} = 34.2 min, *er* = 90.0 : 10.0.

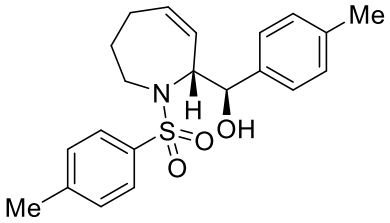

(*R*)-*p*-tolyl((*R*)-1-tosyl-2,5,6,7-tetrahydro-1*H*-azepin-2-yl)methanol (2-34): Prepared according to general procedure B with **2-27** (147 mg, 0.300 mmol, 1.00 equiv). The crude reaction mixture was purified by flash chromatography (gradient 10 to 20% EtOAc in hexanes), followed by

preparatory TLC (30% Et_2O in hexanes) to afford an orange oil (6.0 mg, 5% yield): **^{1}H NMR** (500 MHz, $CDCl_3$) 7.79–7.73 (m, 2H), 7.29–7.22 (m, 4H), 7.18–7.12 (m, 2H), 5.61 (dddd, *J* = 11.5, 6.3, 5.1, 1.2 Hz, 1H), 5.02 (dddd, *J* = 11.6, 5.6, 1.6, 1.6 Hz, 1H), 4.78 (dd, *J* = 9.6, 5.6 Hz, 1H), 4.69 (d, *J* = 9.4 Hz, 1H), 3.91 (ddd, *J* = 14.2, 6.5, 6.5 Hz, 1H), 3.38 (ddd, *J* = 14.6, 5.9, 5.9 Hz, 1H), 2.40 (s, 3H), 2.34 (s, 3H), 2.14–1.95 (m, 2H), 1.84–1.76 (m, 2H); **^{13}C NMR** (126 MHz, $CDCl_3$) δ 143.2, 138.1, 138.0, 137.9, 132.0, 129.6, 129.2, 127.6, 127.4, 127.1, 73.7, 63.7, 44.2, 27.4, 26.1, 21.6, 21.2; **IR** (microscope, cm^{-1}) 3508, 3027, 2975, 2928, 1451, 1435, 1305, 1154, 1102; **HPLC** (Chiralpak IC) 50:50 *i*PrOH/Hex, 20 °C, 0.5 mL/min, λ = 254 nm, T_{minor} = 15.1 min, T_{major} = 29.7 min, *er* = 80.5 : 19.5.

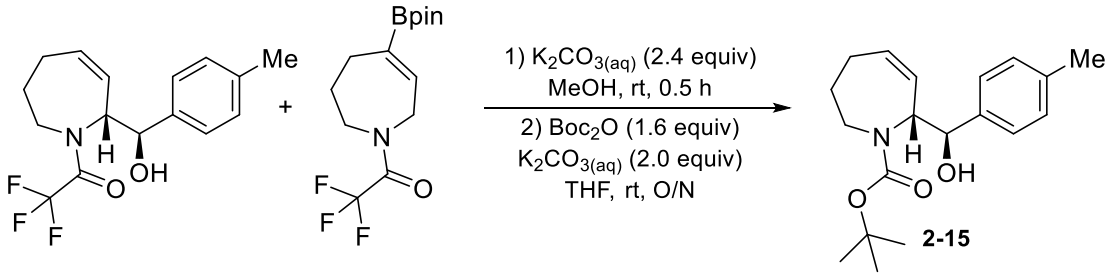

2,2,2-trifluoro-1-((*R*)-7-((*R*)-hydroxy(*p*-tolyl)methyl)-2,3,4,7-tetrahydro-1*H*-azepin-1-yl)ethanone (2-35): Prepared according to general procedure B with **2-28** (138 mg, 0.300 mmol, 1.00 equiv). The crude reaction mixture was partially purified by flash chromatography with Gr III AlO_2 (gradient 10 to 15% EtOAc in hexanes) to obtain **2-35** in about a 1:1 mixture with the corresponding alkenyl boronate. The residue was dissolved in MeOH (4.6 mL, 0.065 M) and aqueous potassium carbonate (3.1 M, 0.72 mmol, 2.4 equiv) was added dropwise at room temperature. The reaction was stirred for 30 minutes before the volatiles were removed *in vacuo*. The mixture was subsequently dissolved in THF (1.7 mL, 0.18 M) and more aqueous potassium carbonate (0.58 M, 0.30 mL, 2.0 equiv) followed by *N*-Boc anhydride (104 mg, 0.48 mmol, 1.6

equiv) in THF (1.0 mL, 0.11 M total). The reaction was left to stir at room temperature overnight. The reaction was diluted in EtOAc and saturated ammonium chloride (15 mL) and the aqueous phase was extracted with EtOAc (3 × 15 mL). The organic phase was washed with brine, dried with anhydrous sodium sulfate, filtered and the volatiles were removed *in vacuo*. The crude reaction mixture was purified by flash chromatography (10 to 15% EtOAc in hexanes) then preparatory TLC (30% Et_2O in hexanes) to afford a clear, colourless oil (16.2 mg, 14% yield over 3 steps). See Section 2.6.11 for characterization of **2-15**.

2.6.10 Racemic borylative migration for product characterization of 2-14, 2-36 and 2-37

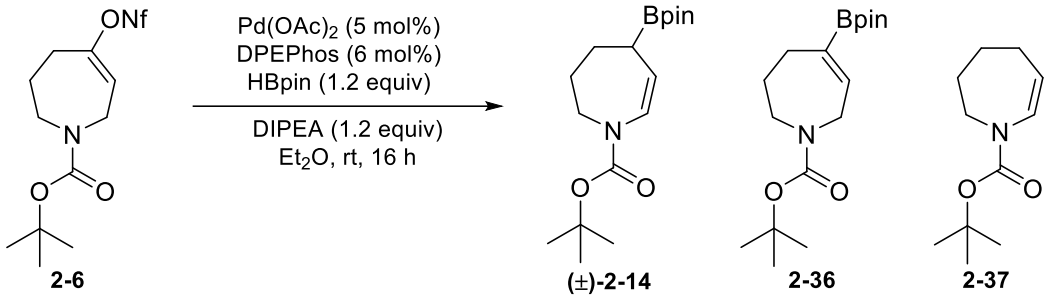

$Pd(OAc)_2$ (11 mg, 0.050 mmol, 5 mol%) and DPEPhos (32 mg, 0.060 mmol, 6 mol%) were dissolved in 3.0 mL of Et_2O and stirred for ten minutes at room temperature. DIPEA (0.21 mL, 1.2 mmol, 1.2 equiv) and pinacolborane (0.18 mL, 1.2 mmol, 1.2 equiv) were sequentially added, followed by **2-6** (495 mg, 1.00 mmol, 1.00 equiv) as a solution of Et_2O (1.0 mL). The round-bottom flask which contained **2-6** was rinsed further with Et_2O (1.0 mL × 2) for an overall reaction concentration of 0.17 M. The reaction was left to stir at room temperature for 16 hours. The crude reaction mixture was rinsed through a quick and short silica plug, which was further washed with 150 mL of Et_2O. The volatiles were removed *in vacuo*. The crude reaction mixture was quickly purified by flash chromatography (about 6 cm of silica, 7.5% MTBE in hexanes).

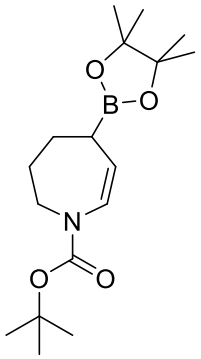

***tert*-butyl 5-(4,4,5,5-tetramethyl-1,3,2-dioxaborolan-2-yl)-2,3,4,5-tetrahydro-1*H*-azepine-1-carboxylate (2-14)**: Isolated as a white solid (65 mg, 20% yield): **mp** = 41.3–42.0 °C; **^{1}H NMR** (400 MHz, C_6D_6, rotamers are present) δ 7.10–6.6 (m, 1H), 5.21 (s, 1H), 4.00–3.55 (m, 2H), 2.10–1.80 (m, 4H), 1.68 (s, 1H) 1.42 (s, 9H), 1.00 (s, 12H); **^{13}C NMR** (126 MHz, C_6D_6) δ 153.5, 130.1, 115.1, 83.2, 79.6, 47.3, 28.3, 27.9, 27.1, 24.7, 24.7; **^{11}B NMR** (159 MHz, $CDCl_3$) δ 33.4; **IR** (microscope, cm^{-1}) 3446, 2978, 2933, 1703, 1368, 1323, 1168, 1144; **HRMS** (ESI-TOF) for $C_{17}H_{30}BNNaO_4$ $(M + Na)^+$ calcd. 346.2160; found 256.2160.

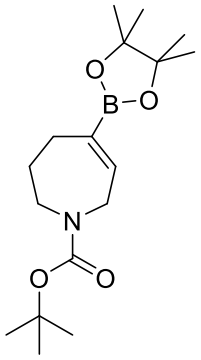

***tert*-butyl 5-(4,4,5,5-tetramethyl-1,3,2-dioxaborolan-2-yl)-2,3,4,7-tetrahydro-1*H*-azepine-1-carboxylate (2-36)**: An analytically pure sample was isolated as a white solid for characterization purposes: **mp** = 56.3–57.9 °C; **^{1}H NMR** (400 MHz, C_6D_6, rotamers are present) δ 6.86 (dd, J = 6.3, 4.1 Hz, 1H), 4.04 (s, 1H), 3.80 (s, 1H), 3.49 (dd, J = 7.9, 5.8 Hz, 1H), 3.29 (dd, J = 7.9, 5.9 Hz, 1H), 2.55 (s, 2H), 1.72–1.59 (m, 2H), 1.41 (s, 9H), 1.04 (s, 12H); **^{13}C NMR** (126 MHz, $CDCl_3$, rotamers

are present) δ 155.6, 142.8, 83.5, 79.3, 77.3, 77.1, 76.8, 47.5, 47.2, 29.7, 28.6, 28.5, 27.1, 26.8, 26.7, 26.2, 24.9; **^{11}B NMR** (128 MHz, $CDCl_3$) δ 30.2; **IR** (microscope, cm^{-1}) 3000, 2976, 2936, 1675, 1421, 1373, 1149, 1109; **HRMS** (ESI-TOF) for $C_{17}H_{30}BNNaO_4$ $(M + Na)^+$ calcd. 346.2160; found 346.2158.

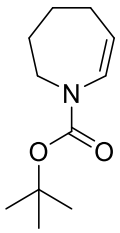

***tert*-Butyl 2,3,4,5-tetrahydro-1*H*-azepine-1-carboxylate (2-37):** An analytically pure sample was isolated as a clear, colourless oil for characterization purposes: **^{1}H NMR** (400 MHz, C_6D_6, rotamers are present) δ 7.05–6.50 (m, 1H), 4.86–4.73 (m, 1H), 3.78–3.40 (m, 2H), 1.87 (ddd, J = 8.4, 5.7, 5.4 Hz, 2H), 1.59–1.37 (m, 4H), 1.41 (s, 9H); **^{13}C NMR** (126 MHz, $CDCl_3$, rotamers are present) δ 153.5, 131.2, 113.6, 79.9, 53.3, 47.1, 28.4, 28.3, 26.4, 25.5; **IR** (microscope, cm^{-1}) 2978, 2932, 1705, 1653, 1455, 1389, 1367, 1163; **HRMS** (ESI-TOF) for $C_{11}H_{19}NNaO_2$ $(M + Na)^+$ calcd. 220.1308; found 220.1310.

2.6.11 General procedure E: enantioselective borylative migration–aldehyde allylboration sequence

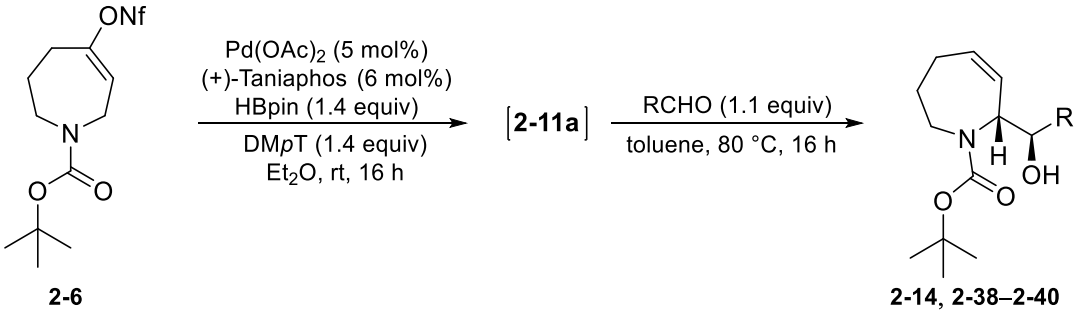

2-6 **2-14, 2-38–2-40**

$Pd(OAc)_2$ (3 mg, 0.02 mmol, 5 mol%) and (+)-Taniaphos (12 mg, 0.018 mmol, 6 mol%) were dissolved in 2.8 mL of Et_2O and stirred for ten minutes at room temperature. DM*p*T (60 μL, 0.40 mmol, 1.4 equiv) and pinacolborane (60 μL, 0.40 mmol, 1.4 equiv) were sequentially added, followed by **2-4a** (149 mg, 0.300 mmol, 1.00 equiv) as a solution of Et_2O (0.5 mL). The round-bottom flask which contained **2-6** was rinsed further with Et_2O (0.50 mL × 3) for an overall reaction concentration of 0.063 M. The reaction was left to stir at room temperature for 16 hours. The crude reaction mixture was rinsed through a quick and short silica plug, which was further washed with 150 mL of Et_2O. The volatiles were removed *in vacuo*. The crude reaction mixture was transferred in toluene (2.5 mL total, 0.20 M) to a new flask containing the aldehyde (0.33 mmol, 1.1 equiv). The reaction flask was sealed before being heated to 80 °C for 13 hours. The crude reaction mixture was once again filtered through a short silica plug and washed with Et_2O before being concentration and subsequently purified by column chromatography (EtOAc/Hex, ratios specified below) to obtain the desired α-hydroxy-dihydro-azeopane product.

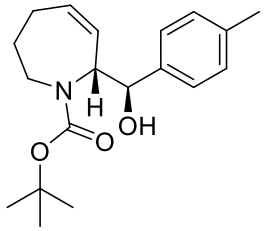

***tert*-butyl (*R*)-7-((*R*)-hydroxy(*p*-tolyl)methyl)-2,3,4,7-tetrahydro-1*H*-azepine-1-carboxylate (2-15)**: Prepared according to general procedure E and purified by flash chromatography (10% to 15% EtOAc in hexanes) to afford a clear, colourless oil (41 mg, 44% yield): **^{1}H NMR** (500 MHz, CD_3OD, rotamers are present) 7.26–7.17 (m, 2H), 7.13 (d, J = 7.9 Hz, 2H), 5.73–5.57 (m, 1H), 5.42–5.28 (m, 1H), 5.05–4.83 (m, 1H), 4.78–4.61 (m, 1H), 3.87–3.49 (m, 1H), 3.22–2.90 (m, 1H), 2.31 (s, 2H), 2.26–2.10 (m, 1H), 2.09–1.96 (m, 1H), 1.95–1.79 (m, 1H), 1.64–1.51 (m, 1H), 1.50–1.34 (m, 9H);

^{13}C NMR (126 MHz, CD_3OD, rotamers are present) δ 158.0, 157.4, 140.4, 140.2, 138.5, 138.4, 130.3, 130.1, 129.8, 129.5, 129.1, 128.3, 128.2, 81.0 (2 C), 75.7, 74.9, 64.1, 63.2, 43.5, 28.8, 28.6, 27.1, 26.5, 24.9, 24.8, 21.2; **IR** (microscope, cm^{-1}) 3429, 2974, 2928, 2863, 1691, 1670, 1414, 1366, 1167; **HRMS** (ESI-TOF) for $C_{19}H_{27}NNaO_3$ $(M + Na)^+$ calcd. 340.1883; found 340.1885; **[α]$_D^{20}$** +8.50 (*c* 0.220, $CHCl_3$); **HPLC** (Chiralpak IC) 5:95 *i*PrOH/Hex, 20 °C, 0.5 mL/min, λ = 230 nm, T_{major} = 19.2 min, T_{minor} = 23.3 min, *er* = 91 : 9.

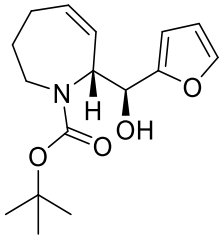

***tert*-butyl (*R*)-7-((*S*)-furan-2-yl(hydroxy)methyl)-2,3,4,7-tetrahydro-1*H*-azepine-1-carboxylate (2-38)**: Prepared according to general procedure E and purified by flash chromatography (15% to 25% EtOAc in hexanes) to afford a clear, yellow oil (41 mg, 48% yield): **^{1}H NMR** (500 MHz, CD_3OD, rotamers are present) 7.45 (ddd, *J* = 5.3, 1.8, 0.8 Hz, 1H), 6.39–6.34 (m, 1H), 6.30 (dd, *J* = 9.8, 3.1 Hz, 1H), 5.79–5.61 (m, 1H), 5.47–5.36 (m, 1H), 5.16–4.95 (m, 1H), 4.81–4.66 (m, 1H), 3.79–3.53 (m, 1H), 3.10–2.89 (m, 1H), 2.28–2.11 (m, 1H), 2.09–1.96 (m, 1H), 1.95–1.79 (m, 1H), 1.65–1.51 (m, 1H), 1.51–1.42 (m, 9H); **^{13}C NMR** (126 MHz, CD_3OD, rotamers are present) δ 157.9, 157.5, 156.0, 143.2, 130.7, 130.3, 129.0, 128.8, 111.3 (2C), 108.8, 108.7, 81.3, 81.1, 68.9, 68.5, 62.2, 61.4, 43.2, 42.9, 28.8, 28.7, 26.9, 26.5, 25.0, 24.7; **IR** (microscope, cm^{-1}) 3421, 2974, 2929, 2865, 1690, 1671, 1415, 1367, 1167; **HRMS** (ESI-TOF) for $C_{16}H_{23}NNaO_4$ $(M + Na)^+$ calcd. 316.1519; found 316.1523; **[α]$_D^{20}$** +30.6 (*c* 0.260, $CHCl_3$); **HPLC** (Chiralpak IC): 5:95 *i*PrOH/Hex, 20 °C, 0.5 mL/min, λ = 230 nm, T_{major} = 23.3 min, T_{minor} = 19.2 min, *er* = 91 : 9.

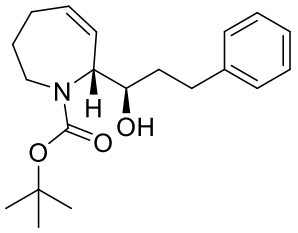

***tert*-butyl (*R*)-7-((*R*)-1-hydroxy-3-phenylpropyl)-2,3,4,7-tetrahydro-1*H*-azepine-1-carboxylate (2-39)**: Prepared according to general procedure E and purified by flash chromatography (15% to 20% EtOAc in hexanes) to afford a clear, yellow oil (51 mg, 51% yield, d.r. ≈ 5.5 : 1): **^{1}H NMR** (500 MHz, CD_3OD, rotamers are present) 7.29–7.03 (m, 5H), 5.82–5.70 (m, 1H), 5.63–5.51 (m, 1H), 4.78– 4.31 (m, 1H), 3.90–3.49 (m, 2H), 3.47–3.06 (m, 1H), 2.99–2.74 (m, 1H), 2.73–2.54 (m, 1H), 2.32–2.09 (m, 1H), 2.09–1.96 (m, 1H), 1.95–1.75 (m, 1H), 1.75–1.63 (m, 1H), 1.63–1.50 (m, 1H), 1.50–1.34 (m, 9H); **^{13}C NMR** (126 MHz, CD_3OD, rotamers are present) δ 158.1, 157.6, 143.5, 143.4, 131.1, 130.7, 130.4, 130.2, 129.6, 129.6, 129.5, 129.4, 129.3, 126.8, 126.7, 81.2, 81.1, 80.9, 73.8, 73.4, 73.0, 72.5, 63.3, 63.0, 62.3, 61.9, 44.4, 43.9, 37.2, 36.8, 33.1, 33.0, 32.9, 32.7, 28.8, 28.7, 27.2, 26.7, 26.6, 26.1, 25.5, 25.1, 24.8, 24.3; **IR** (microscope, cm^{-1}) 3443, 3026, 2973, 2929, 2863, 1690, 1669, 1455, 1414, 1366, 1166, 1112; **HRMS** (ESI-TOF) for $C_{20}H_{29}NNaO_3$ $(M + Na)^+$ calcd. 354.204; found 354.2044; **$[\alpha]_D^{20}$** +85.4 (*c* 0.370, $CHCl_3$); **HPLC** (Chiralpak IC) 5:95 *i*PrOH/Hex, 20 °C, 0.5 mL/min, λ = 220 nm, T_{major} = 19.4 min, T_{minor} = 11.4 min, *er* = 92 : 8.

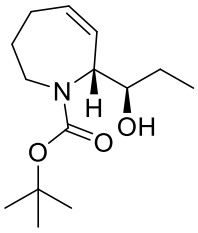

***tert*-butyl (*R*)-7-((*R*)-1-hydroxypropyl)-2,3,4,7-tetrahydro-1*H*-azepine-1-carboxylate (2-40)**: Prepared according to general procedure E with slight modifications. The reaction was performed

on a 0.50 mmol scale and the allylboration step was performed with excess propionaldehyde (50 µL, 1.0 mmol, 2.0 equiv) in toluene (0.50 mL, 1.0 M) at room temperature for 1.5 days. The crude reaction mixture was purified by flash chromatography (5% to 10% to 15% EtOAc in hexanes) to afford a clear, colourless oil (56 mg, 44% yield, d.r. ≈ 5.5:1):‡ **^{1}H NMR** (400 MHz, CD_3OD, rotamers are present) 5.83–5.71 (m, 1H), 5.65–5.53 (m, 1H), 4.71–4.40 (m, 1H), 3.90–3.68–3.50 (m, 1H), 3.42–3.20 (m, 1H), 2.28–2.12 (m, 1H), 2.12–1.98 (m, 1H), 1.98–1.82 (m, 1H), 1.69–1.52 (m, 2 H), 1.50–1.43 (m, 9 H), 1.45–1.35 (m, 1 H), 0.98 (td, J = 7.5, 4.4 Hz, 3 H); **^{13}C NMR** (126 MHz, CD_3OD, rotamers are present) δ 158.1, 157.8, 131.1, 130.6, 130.5, 130.4, 130.0, 129.6, 129.5, 81.1, 81.0, 80.9, 76.2, 76.0, 75.2, 74.8, 62.8, 62.7, 62.2, 61.9, 44.4, 44.0, 43.7, 28.8 (2 C), 28.0, 27.9, 27.7, 27.6, 27.3, 26.9, 26.7, 26.1, 25.6, 25.3, 24.8, 24.3, 10.7 (2C); **IR** (microscope, cm^{-1}) 3452, 2973, 2933, 1692, 1672, 1479, 1415, 1366, 1168; **HRMS** (ESI-TOF) for $C_{14}H_{25}NNaO_3$ $(M + Na)^+$ calcd. 278.1727; found 278.1726; **[α]$_D^{20}$** +70.1 (*c* 0.150, $CHCl_3$); HPLC (Chiralpak IC) 5:95 *i*PrOH/Hex, 20 °C, 0.5 mL/min, λ = 220 nm, T_{major} = 11.6 min, T_{minor} = 9.8 min, *er* = 90 : 10.

2.6.12 Separation and characterization of the diastereomers of compound 2-39

An analytically pure sample containing a 5.5 : 1 mixture of diastereomers was obtained by further purification using preperatory TLC (10% EtOAc in hexanes) to obtain 68 mg of a clear, colourless oil. The two diastereomers were separated by semi-preparatory HPLC (Agilent SB-C18): M.P.A: 0.1% AA/FA/TFA in H_2O, M.P.B: 0.1% AA/FA/TFA in MeCN, 40 °C, 0.6 mL/min, λ = 254 nm. The separated diastereomers were further purified by a short pipette column (15% EtOAc in hexanes) to afford a clear, colourless oil.

‡ The dr was estimated with consideration of the similarities of the spectra between compounds **2-39** and **2-40**.

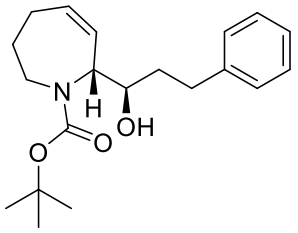

***tert*-butyl (*R*)-7-((*R*)-1-hydroxy-3-phenylpropyl)-2,3,4,7-tetrahydro-1*H*-azepine-1-carboxylate (2-39a)**: Separated by semi-preparatory HPLC (T_{major} = 10.24–10.67 min) to afford a clear, yellow oil (34 mg, 17% yield): **^{1}H NMR** (500 MHz, CD_3OD, rotamers are present) δ 7.27–7.21 (m, 2H), 7.21–7.16 (m, 2H), 7.16–7.10 (m, 1H), 5.84–5.71 (m, 1H), 5.65–5.52 (m, 1H), 4.76–4.53 (m, 1H), 3.91–3.64 (m, 2H), 3.46–3.25 (m, 1H), 2.91–2.76 (m, 1H), 2.74–2.60 (m, 1H), 2.26–2.10 (m, 1H), 2.09–1.95 (m, 1H), 1.93–1.76 (m, 2H), 1.74–1.64 (m, 1H), 1.63–1.51 (m, 1H), 1.52–1.34 (m, 9H); **^{13}C NMR** (126 MHz, CD_3OD, rotamers are present) δ 158.1, 157.6, 143.5, 143.4, 131.1, 130.7, 130.4, 130.2, 129.5, 129.4, 129.3, 126.8, 126.7, 81.2, 80.9, 73.0, 72.5, 63.0, 61.9, 49.5 (2 C), 49.4, 49.3, 49.2, 49.1, 49.0, 49.0, 48.8, 48.7, 48.5, 44.4, 43.9, 36.8, 33.1, 33.0, 30.7, 28.8, 28.7, 27.2, 26.6, 25.5, 25.1; **IR** (microscope, cm^{-1}) 3443, 2926, 1690, 1669, 1455, 1418, 1665, 1109, 1058, 1032; **HRMS** (ESI-TOF) for $C_{20}H_{29}NNaO_3$ $(M + Na)^+$ calcd. 354.204; found 354.2037; for $C_{20}H_{30}NO_3$ $(M + H)^+$ calcd. 332.222; found 332.222; **$[\alpha]_D^{20}$** +42.5 (*c* 0.120, $CHCl_3$).

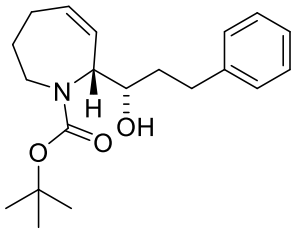

***tert*-butyl (*R*)-7-((*S*)-1-hydroxy-3-phenylpropyl)-2,3,4,7-tetrahydro-1*H*-azepine-1-carboxylate (2-39b)**: Separated by semi-preparatory HPLC (T_{minor} = 9.99–10.19 min) to afford a clear, yellow oil (6 mg, 3% yield): **^{1}H NMR** (500 MHz, CD_3OD, rotamers are present) 7.27–7.21 (m, 2H), 7.20–

7.10 (m, 3H), 5.83–5.69 (m, 2H), 4.65–4.36 (m, 1H), 3.71–3.50 (m, 2H), 3.24–3.08 (m, 1H), 2.83 (ddd, *J* = 14.0, 9.6, 4.9 Hz, 1H), 2.70–2.54 (m, 1H), 2.29–2.11 (m, 1H), 2.08–1.95 (m, 1H), 1.96–1.84 (m, 1H), 1.84–1.74 (m, 1H), 1.84–1.74 (m, 1H), 1.62–1.50 (m, 1H), 1.49–1.32 (m, 9H); **^{13}C NMR** (126 MHz, CD_3OD, rotamers are present) δ 157.8, 157.1, 143.6, 143.4, 130.2, 129.9, 129.6, 129.6, 129.5, 129.5, 129.4, 129.3, 126.8, 126.8, 81.3, 81.1, 73.8, 73.4, 63.3, 62.3, 44.1, 43.9, 37.2, 32.9, 32.7, 30.7, 28.8, 28.7, 26.7, 26.1, 24.9, 24.3; **IR** (microscope, cm^{-1}) 3434, 2925, 2855, 1692, 1669, 1455, 1414, 1166; **HRMS** (ESI-TOF) for $C_{20}H_{29}NNaO_3$ $(M + Na)^+$ calcd. 354.204; found 354.2037; for $C_{20}H_{30}NO_3$ $(M + H)^+$ calcd. 332.222; found 332.222; **$[\alpha]_D^{20}$** +55.8 (*c* 0.200, $CHCl_3$).

2.6.13 Synthesis of HCl salt 2-41

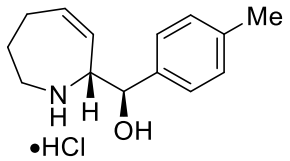

(*R*)-7-((*R*)-hydroxy(*p*-tolyl)methyl)-2,3,4,7-tetrahydro-1*H*-azepin-1-ium chloride (2-41): *N*-Boc amino alcohol **2-15** (32 mg, 0.10 mmol, 1.00 equiv, 81% *ee*) was subjected to the same protocol as for compound **2-45** to obtain **2-41** as a white solid (22 mg, 86% yield). X-ray quality crystals were obtained by vapour diffusion of Et_2O into a vial containing **2-41** dissolved in minimal $CHCl_3$: **^{1}H NMR** (500 MHz, CD_3OD) 7.32 (d, *J* = 7.8 Hz, 2 H), 7.21 (d, *J* = 7.7 Hz, 2 H), 6.08 (dddd, *J* = 11.7, 5.9, 1.9 Hz, 1 H), 5.29 (dd, *J* = 11.4, 4.3 Hz, 1 H), 4.60 (d, *J* = 10.0 Hz, 1 H), 4.16 (dd, *J* = 10.9, 4.2 Hz, 1 H), 3.62 (ddd, *J* = 13.4, 6.5, 3.3 Hz, 1 H), 3.38 (ddd, *J* = 13.2, 9.5, 3.1 Hz, 1 H), 2.39 (ddd, *J* = 5.8, 5.8, 5.6 Hz, 2 H), 2.33 (s, 3 H), 2.09–1.93 (m, 1H), 1.90–1.72 (m, 1 H); **^{13}C NMR** (126 MHz, CD_3OD) δ 139.9, 138.7, 137.9, 130.5, 128.6, 125.6, 74.3, 63.1, 50.0, 27.7, 24.8, 21.2;

IR (microscope, cm^{-1}) 3266, 3023, 2919, 2850, 1586, 1462, 1377; **HRMS** (ESI-TOF) for $C_{14}H_{20}NO^+$ (M^+) calcd. 218.1545; found 218.1539; **$[\alpha]_D^{20}$**: –53.8 (*c* 0.0900, MeOH).

2.6.14 General procedure F: synthesis of carbamates 2-41a, 2-42b and 2-43

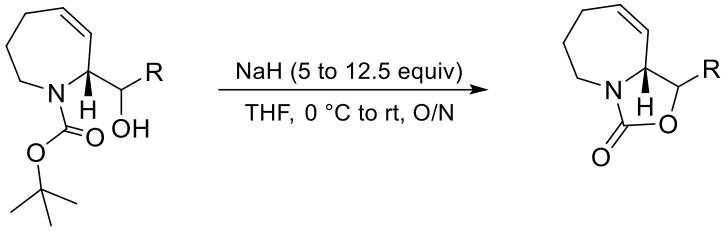

Following a procedure from Panda and co-workers with slight modifications,[30] the *N*-Boc protected amino alcohol (1.00 equiv) was dissolved in THF (0.10 M) and cooled to 0 °C before excess sodium hydride (60% dispersion in mineral oil, 5.0–2.5 equiv) was added. The RBF was capped with a glass stopper and the reaction was left to warm to room temperature overnight in an ice bath. The reaction was subsequently diluted with Et_2O, quenched with saturated ammonium chloride (5 mL) and the aqueous phase was extracted with Et_2O (3 × 5 mL). The combined organic phases were washed with brine (5 mL), dried with anhydrous sodium sulphate, filtered and concentrated *in vacuo*.

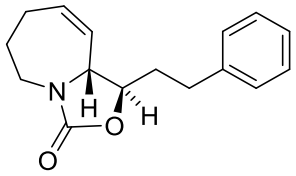

(1*R*,9aR)-1-phenethyl-1,6,7,9a-tetrahydrooxazolo[3,4-*a*]azepin-3(5*H*)-one (2-42a): Prepared using the general procedure F with **2-39a** (10 mg, 0.030 mmol, 1.0 equiv), sodium hydride (6 mg, 0.15 mmol, 5 equiv) and THF (0.40 mL, 0.075 M) to afford a clear, colourless oil (8 mg, quant. yield). The carbamate product **2-42a** was characterized without further purification: **^{1}H NMR** (500 MHz, CD_3OD) 7.31–7.24 (m, 2 H), 7.24–7.20 (m, 2 H), 7.20–7.14 (m, 1 H), 5.85 (dddd, *J* = 11.3,

5.7, 5.3, 2.6 Hz, 1 H), 5.44 (ddd, *J* = 11.5, 4.0, 1.8 Hz, 1 H), 4.27–4.21 (m, 1 H), 4.16 (ddd, *J* = 6.2, 6.2, 6.2 Hz, 1 H), 3.79 (ddd, *J* = 13.4, 9.1, 4.4 Hz, 1 H), 3.19 (ddd, *J* = 13.4, 6.5, 4.0 Hz, 1 H), 2.81 (ddd, *J* = 13.7, 7.8, 7.6 Hz, 1 H), 2.76–2.66 (m, 1 H), 2.31–2.23 (m, 2 H), 2.00 (ddd, *J* = 8.2, 7.5, 6.5 Hz, 2 H), 1.95–1.85 (m, 1 H), 1.83–1.73 (m, 1 H); **^{13}C NMR** (126 MHz, CD_3OD) δ 159.7, 142.2, 133.7, 130.5, 129.6, 129.5, 127.2, 81.5, 62.1, 46.1, 37.3, 31.9, 28.8, 27.5; **IR** (microscope, cm^{-1}) 3061, 3025, 2926, 2855, 1747, 1454, 1423, 1378, 1306, 1036; **HRMS** (ESI-TOF) for $C_{20}H_{29}NNaO_3$ $(M + Na)^+$ calcd. 280.1308; found 280.1306; for $C_{20}H_{30}NO_3$ $(M + H)^+$ calcd. 258.1489; found 258.1487; **[α]$_D^{20}$** +54.2 (*c* 0.170, $CHCl_3$).

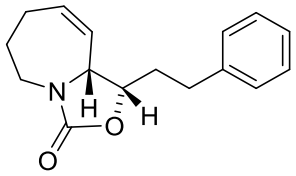

(1*S*,9a*R*)-1-phenethyl-1,6,7,9a-tetrahydrooxazolo[3,4-a]azepin-3(5*H*)-one (2-42b): Prepared using general procedure F using **2-39b** (5 mg, 0.020 mmol, 1.0 equiv), sodium hydride (10 mg, 0.250 mmol, 12.5 equiv) and THF (0.40 mL 0.050 M) to afford a clear, colourless oil (5 mg, quant. yield). The carbamate product **2-42b** was characterized without further purification: **^{1}H NMR** (600 MHz, $CDCl_3$) 7.33–7.28 (m, 2 H), 7.24–7.19 (m, 3 H), 5.90 (dddd, *J* = 11.5, 6.2, 4.9, 2.4 Hz, 1 H), 5.46 (ddd, *J* = 11.7, 4.7, 1.9 Hz, 1 H), 4.47 (ddd, *J* = 10.2, 8.1, 3.3 Hz, 1 H), 4.44–4.39 (m, 1 H), 3.94 (ddd, *J* = 13.5, 8.0, 5.3 Hz, 1 H), 3.10 (ddd, *J* = 13.7, 6.6, 4.8 Hz, 1 H), 2.92 (ddd, *J* = 14.1, 9.5, 4.8 Hz, 1 H), 2.72 (ddd, *J* = 13.8, 9.1, 7.5 Hz, 1 H), 2.40–2.28 (m, 1 H), 2.25–2.15 (m, 1 H), 2.03 (dddd, *J* = 14.0, 10.1, 9.1, 4.9 Hz, 1 H), 1.96–1.80 (m, 3 H); **^{13}C NMR** (126 MHz, $CDCl_3$) δ 157.9, 140.9, 133.5, 128.6, 128.6, 126.3, 124.8, 76.3, 59.5, 43.8, 32.6, 31.9, 29.8, 26.9; **IR** (microscope,

cm^{-1}) 3025, 2922, 2851, 1750, 1454, 1423, 1205, 1040; **HRMS** (ESI-TOF) for $C_{20}H_{29}NNaO_3$ (M + Na)$^+$ calcd. 280.1308; found 280.1307; for $C_{20}H_{30}NO_3$ (M + H)$^+$ calcd. 258.1489; found 258.1488; **[α]$_D^{20}$** –0.600 (*c* 0.110, $CHCl_3$).

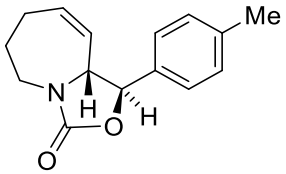

(1*R*,9*aR*)-1-(*p*-tolyl)-1,6,7,9a-tetrahydrooxazolo[3,4-a]azepin-3(5*H*)-one (2-43): Prepared using the general procedure using **2-15** (13 mg, 0.040 mmol, 1.0 equiv) sodium hydride (8 mg, 0.15 mmol, 5.0 equiv) and THF (0.40 mL, 0.10 M). The crude reaction mixture was purified by pipette flash chromatography (10 to 20% EtOAc in hexanes) to afford a clear, colourless oil (9 mg, 91% yield): **^{1}H NMR** (700 MHz, CD_3OD) 7.29 (d, *J* = 8.2 Hz, 2H), 7.23 (d, *J* = 7.9 Hz, 2H), 5.92 (dddd, *J* = 11.5, 5.3, 5.3, 2.5 Hz, 1H), 5.61 (dddd, *J* = 11.5, 1.8, 1.8, 1.8, 1.8 Hz, 1H), 5.12 (d, *J* = 6.8 Hz, 1H), 4.44 (ddddd, *J* = 6.8, 2.3, 2.3, 2.2, 2.2 Hz, 1H), 3.86 (ddd, *J* = 13.3, 8.9, 4.2 Hz, 1H), 3.24 (ddd, *J* = 13.4, 6.8, 3.8 Hz, 1H), 2.37–2.22 (m, 5H), 1.97–1.88 (m, 1H), 1.87–1.77 (m, 1H); **^{13}C NMR** (126 MHz, CD_3OD) δ 159.7, 140.3, 136.4, 133.9, 130.6, 129.4, 127.2, 83.0, 65.1, 46.3, 29.0, 27.5, 21.2; **IR** (microscope, cm^{-1}) 3380, 3022, 2924, 1757, 1420, 1376, 1308, 1282, 1178, 1039; **HRMS** (ESI-TOF) for $C_{15}H_{18}NO_2$ (M + H)$^+$ calcd. 244.1332; found 244.1331; **[α]$_D^{20}$** +8.46 (*c* 0.860, $CHCl_3$).

2.6.15 Synthesis of HCl salt 2-45: the azepane derivative of β-conhydrine[7]

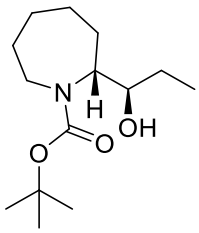

***tert*-butyl (*R*)-2-((*R*)-1-hydroxypropyl)azepane-1-carboxylate (2-45):** Crabtree's catalyst (7 mg, 0.009 mmol, 5 mol%) was added to a flame-dried flask and put under a nitrogen atmosphere. *N*-Boc amino alcohol **2-20** (43 mg, 0.17 mmol, 1.0 equiv) was added as a solution in DCM (3.4 mL, 0.050 M). Hydrogen was bubbled through the reaction mixture for 5 minutes before the needle was removed from the reaction mixture and left in the head space of the flask. The septum was sealed with polytetrafluoroethylene (PTFE) tape, electrical tape and parafilm to avoid solvent loss. The reaction was left to stir at room temperature for 48 hours. The volatiles were removed *in vacuo* and the crude reaction mixture was purified by column chromatography (20% EtOAc in hexanes) to afford compound a clear, colourless oil (36 mg, 83% yield, both diastereomers are present).

^{1}H NMR (400 MHz, CD_3OD, rotamers are present) 3.99–3.76 (m, 1H), 3.69 (dd, J = 23.6, 14.4 Hz, 1H), 3.55–3.32 (m, 1H), 3.08–2.90 (m, 1H), 2.14–1.91 (m, 1H), 1.09–1.73 (m, 2H), 1.70–1.43 (m, 4H), 1.46 (s, 9H), 1.43–1.09 (m, 3H), 1.02–0.91 (m, 3H); **^{13}C NMR** (126 MHz, CD_3OD, rotamers are present) δ 158.7, 158.0, 80.9, 80.6, 77.3, 77.2, 76.5, 76.3, 60.9, 60.2, 44.9, 44.3, 31.5, 31.3, 31.0, 30.8, 30.6, 30.3, 30.1, 29.6, 28.8, 28.8, 28.7, 28.3, 28.1, 27.7, 27.5, 26.4, 26.3, 11.0, 10.9, 10.8; **IR** (microscope, cm^{-1}) 3458, 2973, 2930, 2854, 1689, 1667, 1414, 1366, 1273, 1167; **HRMS** (ESI-TOF) for $C_{14}H_{27}NNaO_3$ $(M + Na)^+$ calcd. 280.1883; found 280.1884; **[α]$_D^{20}$** +31.1 (*c* 0.0700, $CHCl_3$).

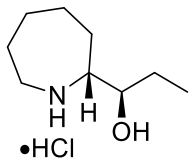

(*R*)-2-((*R*)-1-hydroxypropyl)azepan-1-ium chloride (2-45): Saturated *N*-Boc amino alcohol **2-44** (35 mg, 0.14 mmol, 1.0 equiv) was dissolved in methanol (1.4 mL, 0.10 M). Concentrated hydrogen chloride (0.13 mL, 1.4 mmol, 10 equiv) was added dropwise to the stirring solution at room

temperature. The reaction mixture was left to stir for one hour before the volatiles were removed *in vacuo* to afford compound a clear, colourless oil (25 mg, 93% yield, both diastereomers are present): **^{1}H NMR** (500 MHz, CD_3OD) 3.60–3.35 (m, 1H), 3.28–3.21 (m, 1H), 3.22–3.12 (m, 1H), 3.11–3.02 (m, 1H), 2.06–1.75 (m, 5H), 1.76–1.54 (m, 4H), 1.54–1.35 (m, 1H), 1.00 (t, J = 7.4 Hz, 3H); **^{13}C NMR** (126 MHz, CD_3OD, d_1 = major, d_2 = minor) δ 74.4 (d_2), 73.4 (d_1), 64.3 (d_1), 64.1(d_2), 47.7 (d_2) , 46.5 (d_1), 29.2 (d_1), 27.7 (d_1), 27.6 (d_1), 27.1 (d_2), 26.7 (d_2), 26.5 (d_2), 26.3 (d_1), 26.0 (d_2), 25.9 (d_1), 25.9 (d_2), 10.7 (d_2), 9.8 (d_1); **IR** (microscope, cm^{-1}) 3308, 2939, 2870, 1591, 1461, 1330, 1111; **HRMS** (ESI-TOF) for $C_9H_{20}NO^+$ (M^+): calcd. 158.1539; found 158.1538; **$[\alpha]_D^{20}$** +1.56 (*c* 0.0900, MeOH).

2.7 References

[1] C. Diner, K. J. Szabó, *J. Am. Chem. Soc.* **2016**, *139*, 2.

[2] a) H. Lachance, D. G. Hall, *Org. React*. **2008**, *73*, 1.; b) T. G. Elford, D. G. Hall in *Boronic Acids*, **2011**, 2nd edition, D. G. Hall, Chapter 8, Wiley-VCH Verlag & Co. KGaA, Weinheim, Germany, 393.

[3] J. P. G. Rygus, C. M. Crudden, *J. Am. Chem. Soc.* **2017**, *139*, 18124.

[4] S. Lessard, F. Peng, D. G. Hall, *J. Am. Chem. Soc.* **2009**, *131*, 9612.

[5] Y.-R. Kim, D. G. Hall, *Org. Biomol. Chem.* **2016**, *14*, 4739.

[6] J. Ding, T. Rybak, D. G. Hall, *Nat. Commun.* **2014**, *5*, 5474.

[7] J. Ding, D. G. Hall, *Angew. Chem. Int. Ed.* **2013**, *52*, 8069.

[8] E. Vitaku, D. T. Smith, J. T. Njardarson, *J. Med. Chem.* **2014**, *57*, 10257.

[9] J. Högermeier, H.-U. Ressig, *Adv. Synth. Catal.* **2009**, *351*, 2747.

[10] S. Kwok, M.Sc. Dissertation, University of Alberta, **2016**.

[11] X.-M. Zhang, Y.-Q. Tu, F.-M. Zhang, H. Shao, X. Meng, *Angew. Chem. Int. Ed.* **2011**, *50*, 3916.

[12] a) S. C. Söderman, A. L. Schwan, *J. Org. Chem.* **2012**, *77*, 10978. ; b) G. Barker, P. O'Brien, K. R. Campos, *Org. Lett.* **2010**, *12*, 4176. ; c) B. Subramanian, M. Jack, N. M. Leon, R. Roopa, S. Irina, T. Vincent, *Genelabs Tech Inc.* **2010**, *US2010204265 (A1).*

[13] M. Royzen, G. P. Yap, J. M. Fox, *J. Am. Chem. Soc.* **2008**, *130*, 3760.

[14] a) B. H. Lipshultz, D. J. Buzard, R. W. Vivian, *Tetrahedron Lett.* **1999**, *40*, 6871.; b) H. Kotsuki, P. K. Datta, H. Hayakawa, H. Suenaga, *Synthesis* **1995**, *11*, 1348.

[15] The reductive deoxygenation product was major: K. M. Kuhn, T. M. Champagne, S. H. Hong, W.-H. Wei, A. Nickel, C. W. Lee, S. C. Virgil, R. H. Grubbs, R. L. Pederson, *Org. Lett.* **2010**, *12*, 984. The non-isomerization alkenyl boronate was also obtained in a mixture and identified by low resolution mass spectrometry, but no characterization was found in the literature.

[16] J. M. Bentley, D. C. Brookings, J. A. Brown, T. P. Cain, P. T. Chovatia, A. M. Foley, E. O. Gallimore, L. J. Gleave, A. Heifetz, H. T. Horsley, M. C. Hutchings *et al.*, *UCB Pharma SA* **2014**, WO204009295 (A1).

[17] R. D. Taylor, M. MacCoss, A. D. Lawson, *J. Med. Chem.*, **2014**, *57*, 5854.

[18] G.-F. Zha, K. P. Rakesh, H.M. Manukumar, C. S. Shantharam, S. Long, *Eur. J. Med. Chem.* **2019**, *162*, 465.

[19] (a) H. Li, Y. Blériot, C. Chantereau, J.-M. Mallet, M. Sollogoub, Y. Zhang, E. Rodríguez-García, P. Vogel, J. Jiménez-Barbero, P. Sinaÿ, *Org. Biomol. Chem.* **2004**, *2*, 1492.; (c) I. Dragutan, V. Dragutan, C. Mitan, H. C. Vosloo, L. Delaude, A. Demonceau, *Belstein J. Org. Chem.* **2011**, *7*, 699.

[20] S. M. Thullen, D. M. Rubush, T. Rovis, *Synlett* **2017**, *28*, 2755.

[21] a) S. P. Roy, S. K. Chattopadhyay, *Tetrahedron Lett.* **2008**, *49*, 5498.; b) H. Wang, H. Matsuhashi, B. D. Doan, S. N. Goodman, X. Ouyang, W. M. Clark, *Tetrahedron* **2009**, *65*, 6921.

[22] E. Cini, G. Bifulco, G. Menchi, M. Rodriquez, M. Taddei, *Eur. J. Org. Chem.* **2012**, 2133.

[23] a) S. E. Denmark, H. M. Chi, *J. Am. Chem. Soc.* **2014**, *136*, 8915.; b) T. Seki; S. Tanaka, M. Kitamura, *Org. Lett.* **2012**, *14*, 608.

[24] a) B. Drouillat, I. V. Dorogan, M. Kletskii, O. N. Burov, F. Couty, *J. Org. Chem.* **2016**, *81*, 6677.; b) J. Zhou, Y.-Y. Yeung, *Org. Lett.* **2014**, *16*, 2134.

[25] a) D. G. Wishka, M. Bédard, K. E. Brighty, R. A. Buzon, R. K. A. Farley, M. W. Fichtner, G. S. Kauffman, J. Kooistra, J. G. Lewis, H. O'Dowd, I. J. Samardjiev, B. Samas, G. Yalamanchi, M. C. Noe, *J. Org. Chem.* **2011**, *76*, 1937.; b) A. Nortcliff, J. C. Moody, *Bioorg. Med. Chem.* **2015**, 2730.

[26] S. Lessard, M.Sc. Dissertation, University of Alberta, **2009**.

[27] S. C. Jonnalagadda, P. Suman, A. Patel, G. Jampana, A. Colfer, in *Boron Reagents in Synthesis*, **2016**, 1st Edition, A. Coca, Chapter 3, Oxford University Press: Washington DC, 67.

[28] H. C. Brown, K. S. Bhat, P. K. Jadhav, *J. Chem. Soc. Perkin Trans. 1* **1991**, 2633.

[29] a) J. Y. Renard, J. Y. Lallemand, *Bull. Soc. Chim. Fr.* **1996**, *133*, 143.; b) P. Y. Renard, P. Y. Lallemand, *Tetrahedron: Asymmetry* **1996**, *7*, 2523.; c) G. Ohanessian, Y. Six, J. Y. Lallemand, *Bull. Soc. Chim. Fr.* **1996**, *133*, 1143.

[30] P. Singh, S. K. Manna, G. Panda, *Tetrahedron*, **2014**, *70*, 1363.

[31] Conhydrine review: C. Bhat, S. T. Bugde, S. G. Tilve, *Synthesis* **2014**, *46*, 2551.

[32] K. Li, J. Ou, S. Gao, *Angew. Chem. Int. Ed.* **2016**, *55*, 14778.

[33] G. Zheng, A. M. Smith, X. Huang, K. L. Subramanian, K. B. Siripurapu, A. Deaciuc, C.-G. Zhan, L. P. Dwoskin, *J. Med. Chem.* **2013**, *56*, 1693.

[34] T. Kan, T. Fujimoto, S. Ieda, Y. Asoh, H. Kitaoka, T. Fukuyama, *Org. Lett.* **2004**, *16*, 2729.

[35] H. Liu, C. Sun, N.-K. Lee, R. F. Henry, D. L. Lee, *Chem. Eur. J.* **2012**, *18*, 11889.

[36] P. Krogsgaard-Larsen, H. Hjeds, *Acta Chem. Scand.* **1976**, *30b*, 884.

[37] N. Bailey, P. L. Pickering, D. M. Wilson, *Glaxo Group LTD.* **2006**, WO2006097691 (A1).

[38] N. Vicker, J. M. Day, H. V. Bailey, H. Wesley, A. M. R. Gonzalez, C. M. Sharland, J. M. Reed, A. Purohit, B V. Potter, *Sterix LTD* **2007**, WO2007003934 (A2).

Chapter 3: Mechanistic Investigations of the Palladium-Catalyzed Borylative Migration Reaction

3.1 Introduction

As described in Chapter 2, the borylative migration reaction has provided a platform for the concise enantioselective synthesis of numerous bioactive molecules through access to the novel enantioenriched heterocyclic allylic boronates, **3-5** and **3-7** (Figure 3-1a).[1] However, to-date expanding the reaction scope to other ring sizes and/or derivatives has been met with difficulty and limited success.[2] To further expand the scope and applications of this unique borylation chemistry, a sound understanding of the reaction mechanism is desirable. Although a mechanistic proposal was provided in the original disclosure of the borylative migration reaction in 2009, [3] extensive experimental evidence has yet to be reported.

A summary of the borylative migration reaction is shown in Figure 3-1a,[4] and the postulated mechanism from the original report is shown in Figure 3-1b.[3] The mechanistic cycle centers around a hydropalladation of enol triflate **3-1** followed by an allylic borylation of the resulting reactive allyl triflate intermediate. In theory, a catalytic palladium hydride complex **Int-I-A** could be generated *in situ* from oxidative addition of pinacolborane. The electron-deficient palladium(II) intermediate (**Int-I-A**) would be susceptible to alkene coordination with alkenyl triflate **3-1** to form a π- complex (**Int-I-B**) which could undergo an alkene insertion to form the key hydropalladation intermediate (**Int-I-C**). β-Hydride elimination from **Int-I-C** would furnish complex **Int-I-D**, which would subsequently release an allylic triflate intermediate. Oxidative addition of the allylic triflate to another equivalent of the palladium(0) catalyst would form allyl palladium(II) **Int-I-E**, which could undergo a transmetallation with pinacolborane to afford the borylated allyl palladium(II) **Int-I-F**, providing **3-5** upon a regioselective reductive elimination and subsequent product release. In theory,

the alkenyl boronate side product **3-6** could form from subsequent allyl to alkenyl boronate isomerization of product **3-5** with palladium hydride **Int-I-A** or a separate pathway altogether. Notably, the proposed mechanism is in agreement with a deteurium labelling study using DBpin, as well as a control suggesting that alkenyl boronate **3-6** is not an intermediate in the reaction.[3] Both of these issues will be discussed in more detail below.

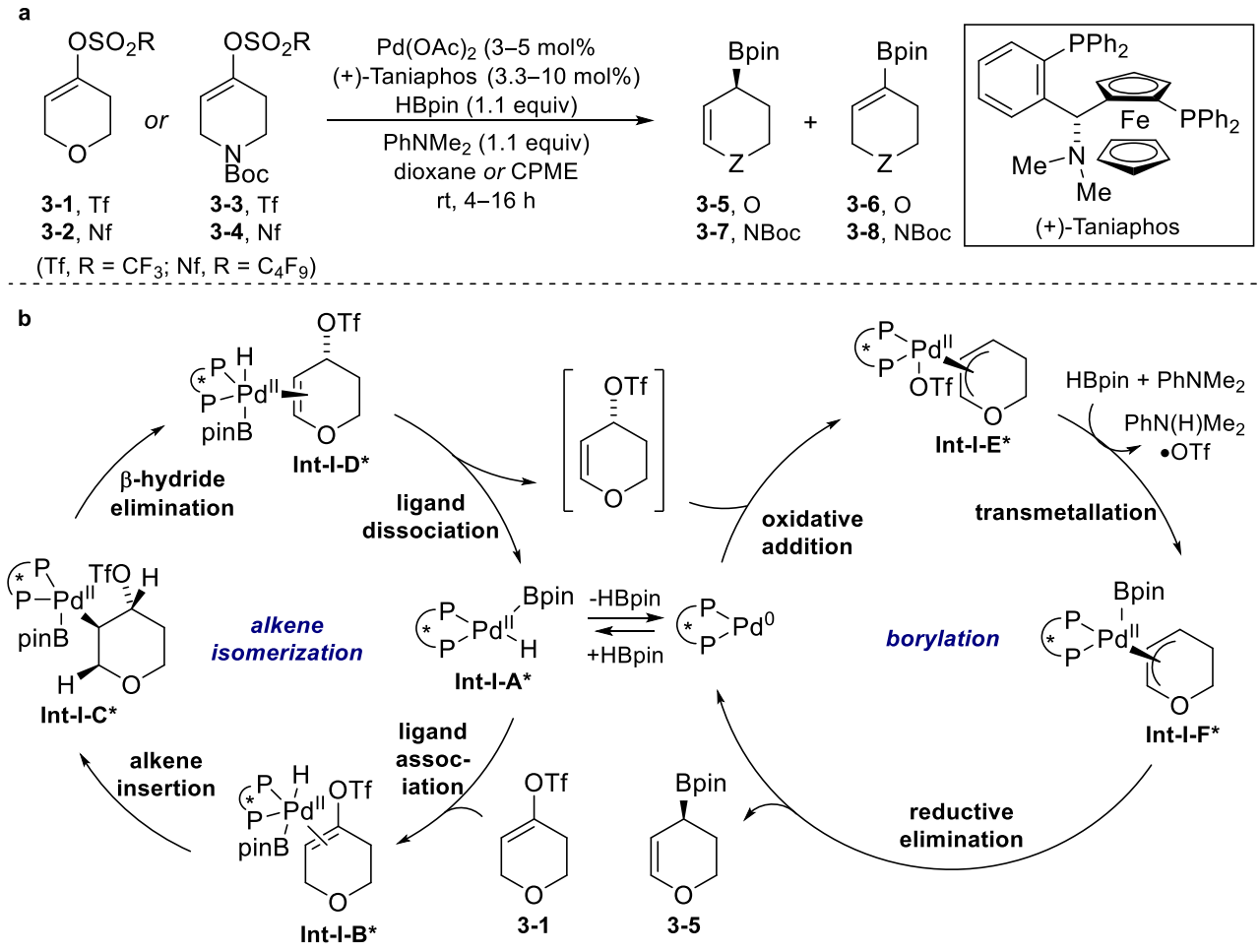

Figure 3-1. (a) Summary of the borylative migration reaction (b) mechanistic proposal from the original report.[3]

To gain further insight into other potential mechanistic pathways, a quick overview regarding the most relevant literature precedence of the borylative migration reaction is required. In 2009, the Hall

group was inspired from an undesired side product reported by Masuda and co-workers.[5] The authors developed a palladium-catalyzed Miyaura borylation using pinacolborane and an amine base, instead of the more traditional conditions employing a diboron source and potassium acetate base.[6] In a subsequent report regarding the extension of their developped chemistry from aryl to alkenyl triflate and iodide electrophiles, the authors found that in the case of pyranyl alkenyl triflate **3-1**, allylic boronate (±)-**3-5** was observed as an undesired major product instead of the expected Miyaura borylation product **3-6** (Figure 3-2a). The authors suggested that the undesired allylic boronate **3-5** forms from a palladium hydride-induced alkene isomerization, in which the palladium hydride was formed from the presence of pinacolborane and/or triethylamine. Furthermore, Masuda and co-workers did propose a catalytic cycle for the developed Miyaura borylation with pinacolborane (Figure 3-2b).[7] However, their catalytic cycle essentially attempts to rationalize a way by which the borylation could occur under the traditional oxidative addition, transmetallation and reductive elimination manifold of palladium cross-coupling chemistry with the reported reagents.[8] Specifically, the authors proposed oxidative addition of the aryl halide, although it was noted that oxidative addition of pinacolborane could not by entirely ruled-out. The transmetallation process was proposed to involve a ligand exchange with a boryl anion generated from the combination of triethylamine and pinacolborane. The boron-loaded aryl palladium(II) intermediate would then undergo reductive elimination furnishing the overall Miyaura borylation product and regenerate the catalyst.

The most questionable step of the Masuda mechanism shown in Figure 3-2b is the formation of the boride anion prior to the transmetallation step.[9] The deprotonation of pinacolborane by triethylamine to provide an ammonium boride ion pair has little precedence in the literature.[10] Considering that it is generally accepted that the hydrogen of pinacolborane is hydridic and not protic, this step is in

fact quite counter-intuitive. With this in mind, the type of transmetallation proposed by Masuda and co-workers will not be considered in this mechanistic study of the borylative migration.

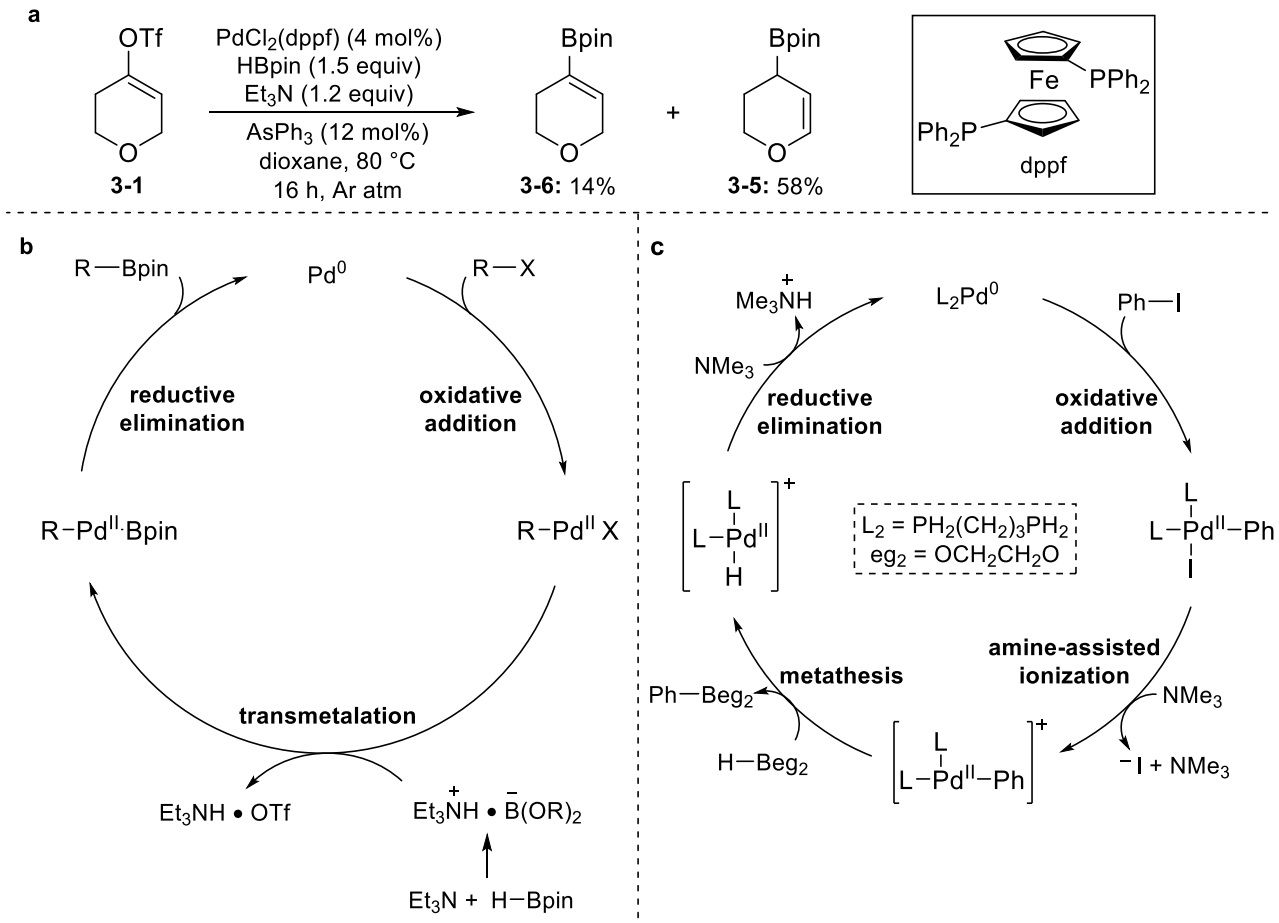

Figure 3-2. (a) Miyaura borylation with pinacolborane and proposed catalytic cycles by (b) Masuda[5] (c) Lin and Marder[9] and their co-workers.

With reference to the same concerns regarding Masuda's proposed mechanism described above, Lin and co-workers investigated the mechanism of the Miyaura borylation reaction with pinacolborane computationally using a simplified model reaction as shown in Figure 3-2c.[9] In the end, the authors concluded that the most favorable pathway relies upon a key σ-bond metathesis step between pinacolborane and a cationic aryl palladium(II) complex. Firstly, oxidative addition of phenyl iodide is followed by an ionization to a cationic palladium catalyst. The ionization step was assumed to be

amine-assisted and barrierless for the purpose of simplifying calculations. The resulting cationic palladium(II) intermediate can then undergo a σ-bond metathesis reaction with pinacolborane to furnish the borylation product and a cationic palladium hydride source, which is subsequently reduced by amine present in solution. Many of the mechanistic steps described by Lin and co-workers have the potential to be relevant in the borylative migration reaction. However, in our group's original report of the borylative migration,[3] it was found that the alkenyl boronate **3-6** is not an intermediate. It was expected that if a mechanism similar to Lin's was operating in the borylative migration, then one would expect that the alkenyl boronate **3-6** should be an intermediate in the reaction.

Clearly many questions regarding the mechanism of the borylative migration reaction remain unanswered to-date. Considering the variety of mechanistic considerations described above and the desire for rational design of this chemistry to new substrates, a thorough investigation of the borylative migration is warranted using both experimental and computational evidence. A number of fundamental aspects regarding the mechanism are in need of clarification, such as the controlling factor(s) of the alkene isomerization step, the role(s) of the base in the reaction, the basis of enantio-induction and the rate-determining step of the reaction. Herein, a comprehensive mechanistic study is described dedicated to address the aforementioned questions by combining experimental investigations along with a density functional theory calculations. Not only does such a study have the potential of helping understand the borylative migration and improve the substrate scope, but discoveries conclusions could have implications in palladium borylation chemistry in the future.[11]

3.2 Plausible pathways of the borylative migration reaction

3.2.1 Overview of hydropalladation and Miyaura borylation pathways

The general steps of the two most plausible mechanisms under consideration are shown in Figure 3-3. The two pathways differ by whether the alkene isomerization occurs before or after the borylation step, and are termed the hydropalladation and Miyaura borylation pathways, respectively. Since DPEPhos has shown to be an efficient ligand in the borylative migration of alkenyl nonaflate **3-4**, all calculations are modeled using DPEPhos as the ligand for simplification purposes.[4]. All DFT calculations were performed by Dr. Claude Legault (University of Sherbrooke) using the pyranyl alkenyl triflate substrate **3-1**. All free energies values are reported in kcal mol^{-1} relative to the dissociated alkenyl triflate **3-1** and palladium DPEPhos-bound catalyst (arbitrarilyset to 0 kcal mol^{-1}) using a M06-D3/6-31+G(d,p)/SDD(Pd)(SMD, Dioxane)//M06-D3/6-31G(d)/LANL2DZ(Pd) basis set (see Experimental Section 3.9.7 for details). The alkenyl triflate and nonaflate are considered interchangeable in this study. The experimental work was performed with the corresponding alkenyl nonaflate electrophiles due their improved ease of synthesis and stability relative to corresponding triflates.[4]

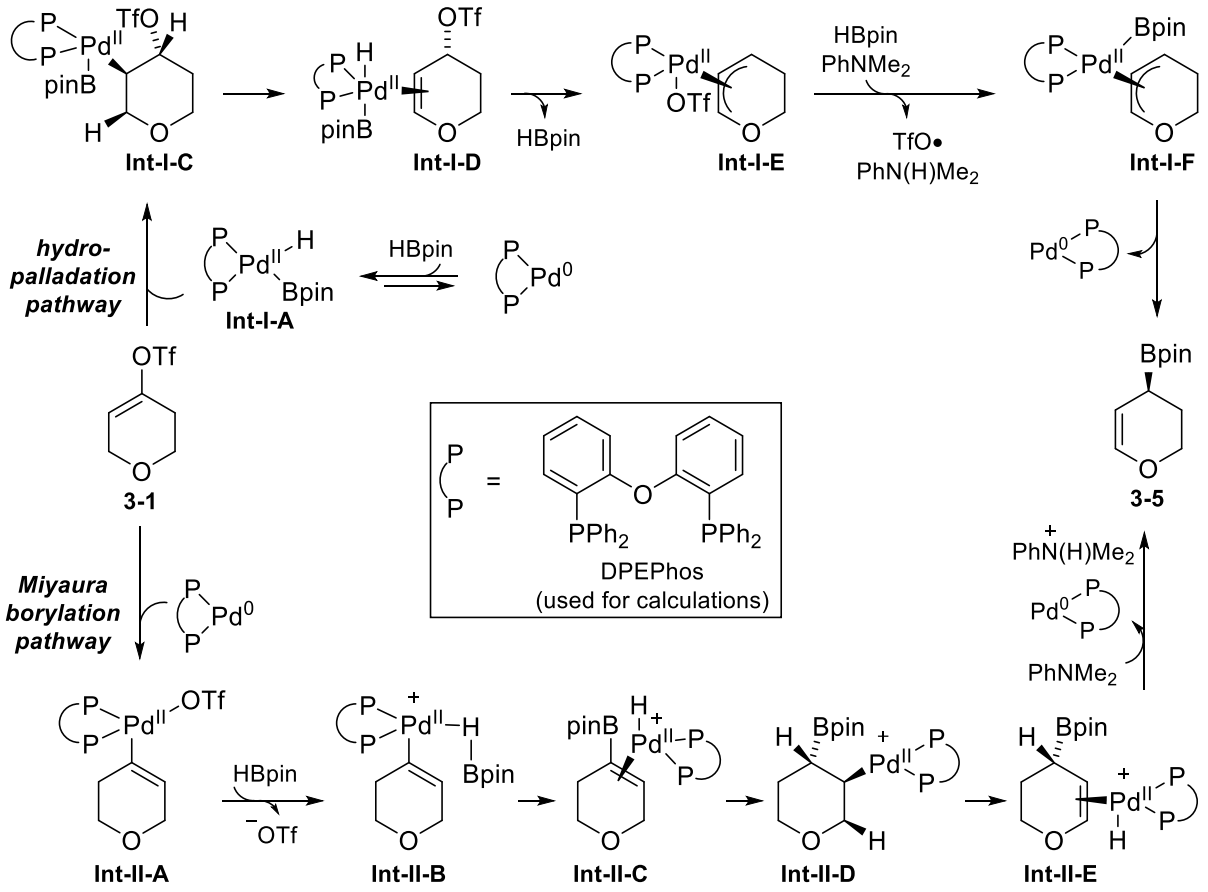

Figure 3-3. The two general mechanistic pathways under consideration.

The hydropalladation pathway is a simplified version of the catalytic cycle proposed in the original reported of the borylative migration,[3] as described above (c.f. Figure 3-1b). Upon a critical re-examination of the proposed steps of this mechanism, it is clear that many weaknesses exist. Although the oxidative addition of pinacolborane is a well-established process with a number of metal catalysts, such as rhodium and cobalt,[12] a strong precedence for the equivalent process with palladium(0) could not be found.[13] Furthermore, the reasoning is unclear in regard to the complete regioselectivity of the reductive elimination of the π-allyl palladium complex (**Int-I-F** to **3-5**).

In contrast, the Miyaura borylation pathway is inspired by calculations reported by Lin and co-workers regarding Masuda's borylation of phenyl iodide (Figure 3-3). A Miyaura-type borylation

would involve oxidative addition of alkenyl triflate **3-1** to form the corresponding palladium(II) complex **Int-II-A**. An overall ligand exchange and ionization process would furnish the hydride-bound palladium complex **Int-II-B**. The cationic palladium **Int-II-B** could then undergo an electronically-controlled, regioselective σ-bond metathesis with pinacolborane to form the alkenyl boronate-bound cationic palladium hydride (**Int-II-C**). At this stage, an off-cycle base-promoted reductive elimination of **Int-II-C** could explain the formation of the alkenyl boronate side product **3-6**. Conversely, a sterically-controlled regioselective alkene insertion into the Pd-H bond from **Int-II-C** would form the carbon-bound palladium complex (**Int-II-D**). **Int-II-D** could undergo a β-hydride elimination, which would afford the cationic π-bound palladium hydride complex **Int-II-E**. Finally, to end this "palladium-walking" scenario, a base-promoted reductive elimination with $PhNMe_2$ would regenerate the catalyst and furnish allylic boronate product **3-5**. Considering that the Miyaura borylation proposal is solely based on calculations for a significantly different reaction system, many questions and potential weaknesses exist for this pathway. For example, one may expect the alkenyl boronate **3-6** to be an intermediate in the reaction under these conditions.

3.2.2 Feasibility of the hydropalladation pathway

In our original report of the borylative migration, a deuterium labelling experiment was disclosed, showing that deuterium incorporation occurs mostly at the allylic position when DBpin is used (Scheme 3-1).[3] The position of the deuterium label agrees with both pathways shown in Figure 3-3. However, the high level of incorporation is somewhat questionable in regard to the hydropalladation pathway. One may expect the deuterium incorporation to be much lower than 85% if the hydropalladation pathway is operational, considering that non-deuterated pinacolborane wouuld be generated catalytically throughout the cycle. Specifically, upon release of the allylic triflate from **Int-I-D**, the pinacolborane released would re-enter the cycle to generate non-deuterated **Int-I-A**.

Furthermore, it is unclear how 8% incorporation could be achieved at the alkenyl site under both mechanistic models. Therefore, further studies with D-Bpin will be performed with both the piperidinyl and pyranyl nonaflates.

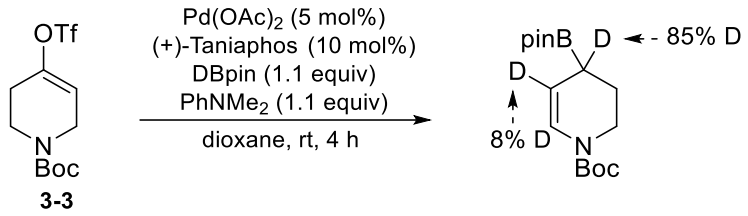

Scheme 3-1. D-labelling study with D-Bpin.

Furthermore, the hydropalladation pathway requires an initial oxidative addition of palladium(0) with pinacolborane. All attempts to calculate the pinacolborane oxidative addition complex **Int-I-A** were unsuccessful due to the unfavorable instability of the oxidative addition complex. The calculated unreacheable high energy barrier is in agreement with the lack of literature precedence for the oxidative addition of palladium(0) with pinacolborane. The most relevant examples found are limited to the oxidative addition of palladium with catecholborane in the presence of diene or enyne substrates.[14]

Considering both the high energy oxidative addition of pinacolborane and the high amount of allylic deuterium incorporation, it seems clear that the previously reported hydropalladation pathway is not be the most reasonable mechanism for the borylative migration reaction.

3.2.3 Feasibility of the Miyaura borylation pathway

In contrast to pinacolborane, the oxidative addition of alkenyl triflates and nonaflates with a palladium(0) catalyst is a well-established process in cross-coupling chemistry.[15] Indeed, it was found that the oxidative addition step is initiated by an energetically favourable association of **3-1** to form complex **Int-II-A'** (Scheme 3-2). A direct oxidative insertion of the bisligated catalyst leads

to the square-planar intermediate **Int-II-A**, with an overall energetic barrier of 13.4 kcal mol^{-1}. Calculations regarding formation of the mono-ligated phosphine complex show that the oxidative addition pathway involving an initial dissociation of one of the phosphine ligands is significantly less energetically favorable.

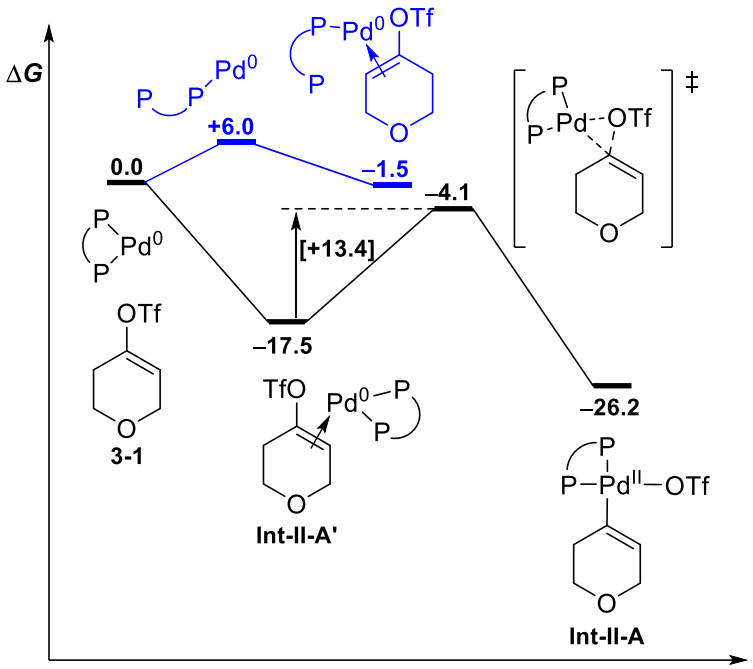

Scheme 3-2. Energy diagram of the oxidative addition process.

Considering the calculation results described above, it can be concluded that the oxidative addition of the catalyst is much more favorable with alkenyl triflate **3-1** than with pinacolborane. Therefore, the hydropalladation pathway is ruled-out from this point onward and all further studies are focused on the Miyaura borylation pathway shown in Figure 3-3. The overall process is devided into two steps – borylation and alkene isomerization.

3.3 Borylation of the alkenyl nonaflate

3.3.1 Cationic vs neutral palladium pathway

In theory, the borylation step could be occurring with either a neutral or cationic palladium pathway (Figure 3-4). To-date, the mechanism of the Miyaura borylation with pinacolborane has only been investigated computationally with aryl iodides by Lin and co-workers, as described above.[9] For a neutral borylation pathway, the oxidative addition complex (**Int-II-A**) would require a vacant coordination site by dissociation of one of the two phosphine ligands instead of the triflate anion. DFT calculations determined that the ligand dissociation process would be is +20 kcal mol^{-1}, suggesting a relatively high energy process under these reaction conditions. Alternatively, some sort of ionization process could lead to the cationic palladium complex **Int-II-A**$^{+}$, which would provide a vacant site available for the coordination of pinacolborane. However, there is a large error involved in calculating an ionization the process with palladium. Considering the aforementioned DFT limitaions and the fact that a +20 kcal mol^{-1} energy barrier is high but possible at room temperature, further experimental evidence to address whether a cationic or neutral palladium borylation pathway is occurring under the borylative migration conditions is required.

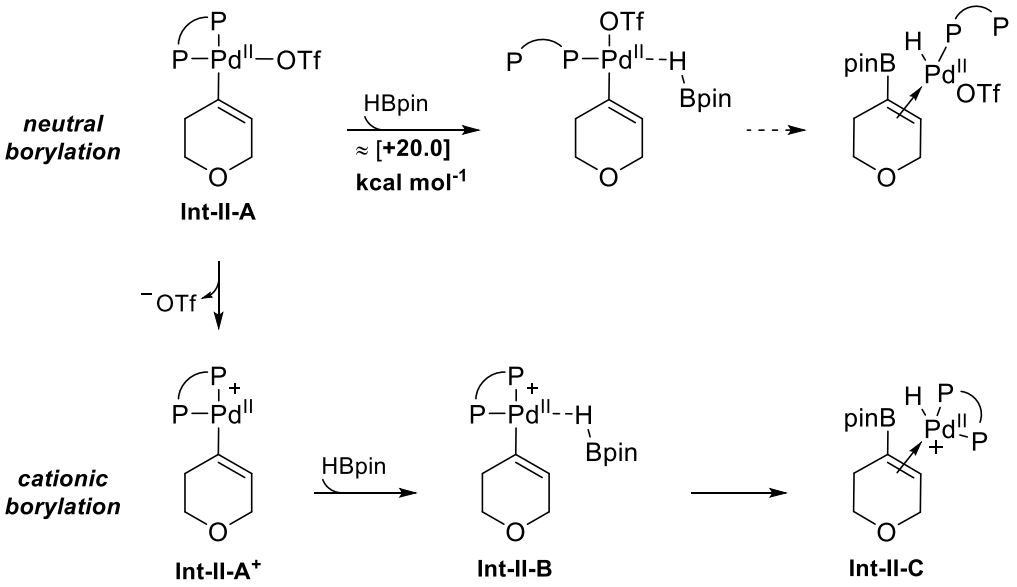

Figure 3-4. Potential neutral and cationic borylation pathways.

3.3.2 Synthesis of the pyranyl alkenyl iodide

Cationic palladium intermediates are frequently observed in palladium-catalyzed Heck reactions.[16] Under asymmetric conditions, it has been shown that cationic palladium pathways can be particular useful to improve enantioselectivity. Furthermore, it is common practice to promote cationic Heck reactions by adding silver(I) salts to reactions with alkenyl or aryl halides.[17] The additive promotes the cationic pathway by precipitation of silver halides from the oxidative addition intermediate. Therefore, we envisioned that further studies of the borylative migration with an alkenyl halide and silver salts could be useful in gaining experimental information regarding the nature of the active catalyst in the borylation. Considering the mild reaction temperature of the borylative migration, the pyranyl alkenyl iodide **3-9** was targeted as the ideal electrophile. Since the generally accepted relative reactivity for Pd(0) for oxidative addition with aryl electrophiles is Ar-I > Ar-Br ≈ Ar-OTf >> Ar-Cl, oxidative addition with the alkenyl iodide **3-9** is not an issue under the borylative migration conditions.[18]

Due to the limited commercial availability of alkenyl iodide **3-9**, the compound was synthesized. Although many approaches exist for the synthesis of acyclic alkenyl halides, general approaches for the synthesis of cyclic alkenyl iodides are more limited.[19] Specifically, alkenyl iodide **3-9** could not be found in the literature at the time of these investigations. The most common general approach to cyclic alkenyl iodides relies on the use of a hydrazine intermediate and an electrophilic iodine source, first reported by Barton and co-workers.[20] After a few unsuccessful attempts,[21] the alkenyl iodide **3-9** was accessed in high yield over two steps using hydrazine and iodine with a subsequent DBU-promoted elimination of the diiodide intermediate (Scheme 3-3). Notably, a similar approach to alkenyl iodide **3-9** has since been reported by Anderson and co-workers.[22]

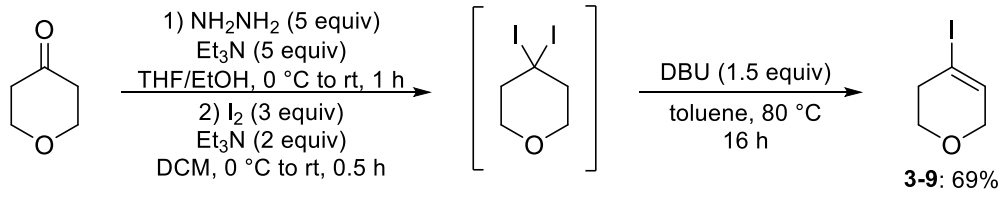

Scheme 3-3. Synthesis of alkenyl iodide **3-9**.

3.3.3 Borylative migration with the alkenyl iodide substrate

With alkenyl iodide **3-9** in-hand, experiments were undertaken with this electrophile under the borylative migration conditions to probe for evidence of a cationic palladium pathway. However, an initial control reaction revealed that silver triflate is not compatible with the standard borylative migration conditions with alkenyl nonaflate **3-2**. Immediate silver mirror formation upong the addition of pinacolborane suggested that the silver(I) is quickly reduced to silver(0) under the reaction conditions. A second control experiment was performed in which pinacolborane was added to a solution of silver triflate in d_6-benzene at room temperature for 15 mins. Once again silver mirror formation and a shift in the ^{11}B NMR signal from 28.5 to –2.5 ppm confirms that pinacolborane

reduces silver(I) triflate to silver(0) and is therefore incompatible with the borylative migration reaction conditions.

Nevertheless, it was expected that studies of the borylative migration with alkenyl iodide **3-9** could still be informative. Subjection of the alkenyl iodide **3-9** to the standard borylative migration reaction conditions with $PhNMe_2$ as a base resulted in no product formation (Table3-1, entry 1).[18] Since iodide is more strongly coordinating than triflate anions, it was reasoned that the alkenyl iodide **3-9** may be an unproductive substrate toward forming **3-5** due to issues in ionization of the palladium catalyst. Considering that literature precedence suggests that an amine-assisted ionization could be involved in the mechanism,[9] it was reasoned that displacement of the iodide may be possible with a more nucleophilic amine. Therefore, further studies were performed with alkenyl iodide **3-9** by increasing the temperature to 80 °C (Table 3-1, entry 2) and/or using a more nucleophilic base (entries 3–6). In general, it was found that the reaction was slightly more productive when the temperature was increased in dioxane (entries 2 and 5). However, in general all borylative migration attempts with the alkenyl iodide **3-9** were met with little to no product formation and moderate recovery of **3-9**, likely due to volatility of the compound. Furthermore, any attempts to-date of using other additives to promote the reaction with **3-9** in support of a cationic palladium pathway, such as the use of potassium triflate, have led to similarly low levels of product formation.[23]

Table 3-1. Borylative migration attempts with alkenyl iodide **3-9**.

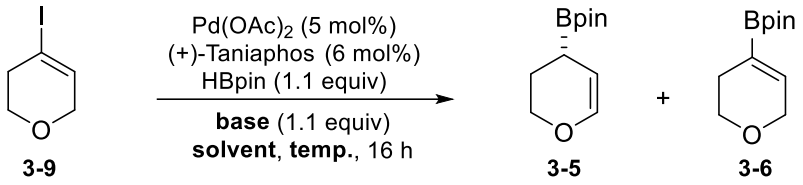

Entry	base	solvent	temp.	Yield of **3-5**[a]	Yield of **3-6**[a]
1	$PhNMe_2$	Et_2O	rt	—	—
2	$PhNMe_2$	dioxane	80 °C	4%	3%
3	NEt_3	Et_2O	rt	—	—
4	NEt_3	dioxane	rt	—	—
5	NEt_3	dioxane	80 °C	13%	6%
6	DABCO	dioxane	rt	—	—

[a]Determined by crude ^{1}H NMR using 1,3,5-trimethoxybenzene as an internal standard. "—" indicates not observed.

The specificity of the borylative migration reaction to the exclusive use of alkenyl triflates and nonaflates is suprising. As mentioned above, Masuda and co-workers employed aryl iodides as substrates in their Miyaura borylation conditions. Indeed, it was found that alkenyl iodide **3-9** was applicable in Masuda's Miyaura borylation conditions (Scheme 3-4), leading to a similar combined yield of the allylic boronate products (±)-**3-5** and **3-6** as was reported by the authors with the triflate (reportedly 72% yield).[5]

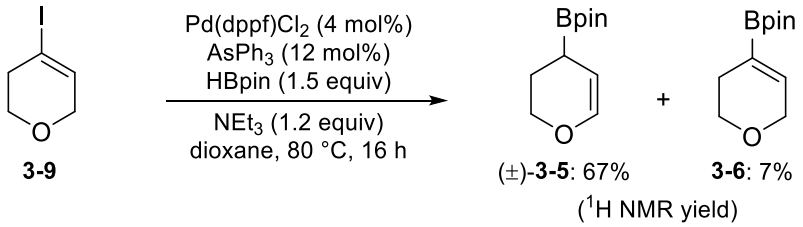

Scheme 3-4. Subjection of alkenyl iodide **3-9** to Masuda's borylation conditions.

3.3.4 Effect of iodide additive

To ensure that the presence of iodide anions is indeed why the alkenyl iodide **3-9** is an inefficient substrate in the borylative migration, the compatibility of the borylative migration reaction with

iodide anions was explored. A control reaction with pyranyl nonaflate **3-2** and one equivalent of tetrabutylammonium triflate afforded the allylic boronate product **3-5** in 70% yield, as expected (entry 1, Table 3-2). In contrast, addition of only 6 mol% tetrabutylammonium iodide hindered the reaction leading to the formation of both boronate products **3-5** and **3-6** in relatively small amounts (entry 2). Furthermore, the addition of a stoichiometric amount of iodide additive furnished similar results, but with 15% of alkenyl iodide **3-9** (entry 3). The formation of iodide **3-9** confirms that the nucleophilicity of the iodide anion affects the palladium catalyst. The formation of iodide **3-9** under the reaction conditions can be easily rationalized by an oxidative addition of **3-2**, followed by ligand exchange of the nonaflate anion with iodide. Reductive elimination would then afford the alkenyl iodide side product **3-9** (Figure 3-5). Based on the results in Table 3-2, it appears that a highly electrophilic palladium catalyst is required for the borylative migration reaction. Altogether, these results are therefore supportive of a cationic palladium intermediate.

Table 3-2. Effect of Bu_4NI additive in the reaction.

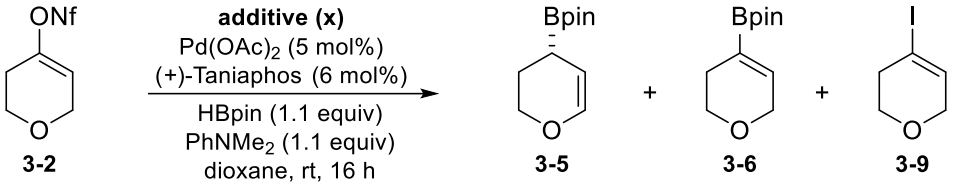

Entry	Additive	x	Yield of **3-5**[a]	Yield of **3-6**[a]	Yield of **3-9**[a]
1	Bu_4NOTf	1 equiv	70%	10%	—
2	Bu_4NI	6 mol%	≈ 3%	≈ 5%	—
3	Bu_4NI	1 equiv	≈ 4%	≈ 2%	15%

[a]Determined by crude ^1H NMR using 1,3,5-trimethoxybenzene as an internal standard. "—" indicates not observed.

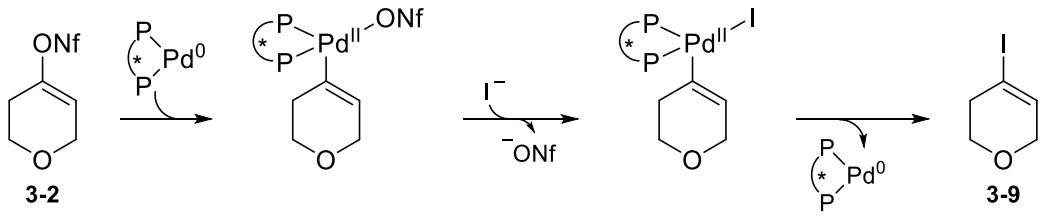

Figure 3-5. Formation of alkenyl iodide **3-9**.

3.3.5 DFT calculations of the borylation step

With the presence of a cationic palladium pathway confirmed experimentally, an appropriate approach to calculating the ionization process was addressed. Considering that the borylative migration reaction requires and a non-coordinating triflate/nonaflate anion for a productive reaction, it may be the case that a spontaneous ionization process is involved in the mechanism.[24] However, a spontaneous ionization process was found to be extremely endergonic by DFT calculations under the theory and solvation model used (+32.8 kcal mol^{-1}), similarly to the work of Lin and co-workers.[9] Therefore, the dissociation was addressed computationally by assuming a barrierless amine-promoted ionization process.[9,25] Notably, the ionization of an aryl-Pd(II)-OTf complex by DBU was recently described as a key intermediate in the Buchwald-Hartwig amination.[26] Furthermore, Hartwig, Buchwald and their co-workers have previously characterized oxidative addition complexes by X-ray crystallography, in which the triflate was displaced with a primary amine.[27] Although further experimental evidence is required for a conclusive determination of whether amine binding after the oxidative addition step actually occurs in the case of the borylative migration reaction, for the sake of this discussion the ionization process is modelled computationally as a barrierless amine-promoted ionization process to form amine-bound **Int-II-A**$^+$ (Scheme 3-5).

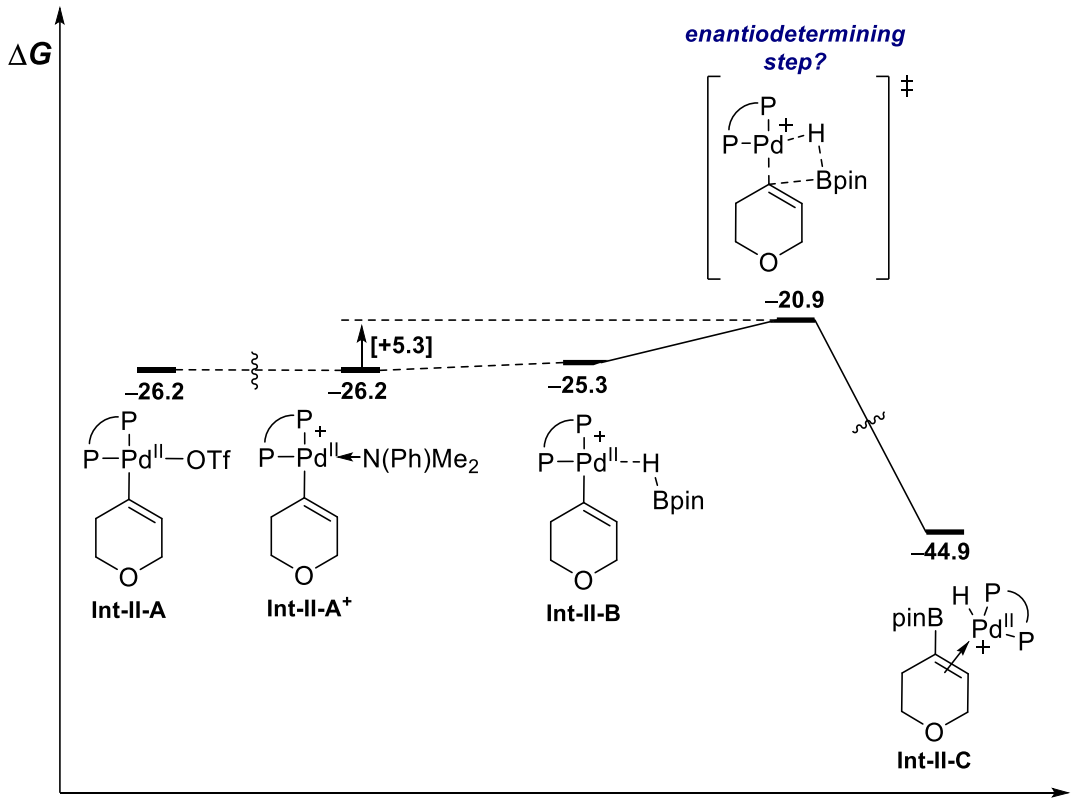

Scheme 3-5. Energy diagram of the σ-bond metathesis process.

For introduction of the boron unit, a ligand exchange between the amine from **Int-II-A**$^{+}$ and pinacolborane is required to form **Int-II-B** (Scheme 3-5). The ligand exchange process with pinacolborane has a low energy barrier of less than 1 kcal mol^{-1}. The regioselectivity of the ensuing σ-bond metathesis process to furnish the borylated product follows the predictable regioselectivity based on both electronics and sterics – the boron and palladium centers are relatively electropositive and large. Overall, the σ-bond metathesis process from **Int-II-A** to the palladium π-bound alkenyl boronate (**Int-II-B**) has a low energy barrier of 5.3 kcal mol^{-1}.

Mechanistically, the σ-bond metathesis of the pinacolborane palladium complex **Int-II-B** proceeds through a a spiro-like 4-membered transition state, which is well-established and has been reported with palladium(II) complexes (Scheme 3-5).[28] However, an intriguing aspect of this step in the borylative migraton is that the borylation may be the enantiodetermining step of the reaction when

the chiral Taniaphos ligand is used. For the σ-bond metathesis to be the enantiodetermining step in the borylative migration, the palladium hydride in complexes **Int-II-C** and/or **Int-II-E** must not dissociate throughout the rest of the reaction mechanism. Therefore, probing for a dissociative or non-dissociative palladium hydride source is required. Notably, the most relevant precedence found to-date involving an enantioselective σ-bond metathesis with pinacolborane is a manganese-catalyzed reduction of acetophenone reported by Gade and co-workers.[29]

3.3.6 Probing for a dissociative Pd-H source

Throughout this discussion, the reaction mechanism has been portrayed as a non-dissociative pathway, in which each catalytic intermediate completes the catalytic cycle to eventually release **3-5** before re-entering the process. However, the alkene isomerization step can instead be a dissociative process involving the release of alkenyl boronate **3-6**.[30] Intermediate **3-6** could subsequently lead to allylic boronate **3-5** from ligand exchange with either **Int-II-E** or with another catalytic Pd-H source present in solution (c.f. Figure 3-3).[31,32] Establishing whether palladium hydride dissociation is occurring is important in regard to the enantiodetermining step of the reaction, as described above.

To investigate the possibility of a dissociative pathway, a competition experiment was undertaken by subjecting nonaflate **3-2** to the reaction conditions in the presence of a fixed stoichiometric amount of alkenyl boronate **3-6** (Table 3-3). In the event, the reaction proceeded with similarly high efficiency in both cases (entries 1–2). Although there was a small increase by 9% in NMR yield of allylic boronate **3-5** between the two experiments, the enantiomeric excess of 90% *ee* was unchanged. Therefore, it was concluded that little to none of the alkenyl boronate was converted to the allylic boronate. Notably, the reaction was found to be incompatible with less than one equivalent of $PhNMe_2$, potentially due to competing protodeboronation of **3-5** under the resulting highly acidic media.

Table 3-3. Probing a dissociative alkene isomerization pathway.

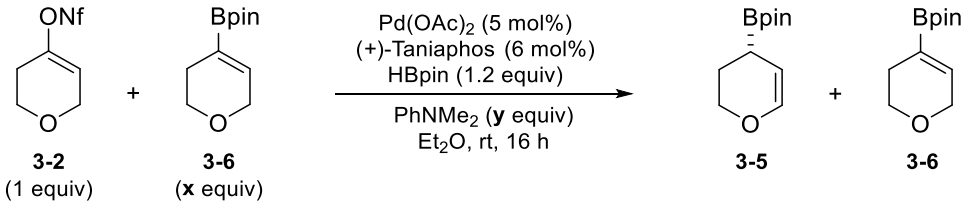

Entry	y	x	Yield of **3-5** (%)[a]	*ee* of **3-5** (%)[b]	Yield/recovery of **3-6** (%)[a]
1	1.2	none	72	90	9
2	1.2	1.0	81	90	92
3	0.75	none	3	—	10

[a]Yield and product ratios are estimated by crude ^{1}H NMR using 1,3,5-trimethoxybenzene as an internal standard. [b]*ee* is determined by chiral HPLC after thermal allylboration with *p*-tolualdehyde

The fact that little to no amount of **3-5** isomerized to **3-6** is in agreement with a non-dissociative isomerization pathway. Furthermore, monitoring of the reaction by ^{1}H NMR shows no significant build-up of **3-6** followed by consumption as would be expected if **3-6** was an intermediate in the reaction (see Section 3.5). Consequently, in this mechanistic scenario the alkenyl boronate **3-6** is not an intermediate in the reaction, the palladium hydride is substrate-bound throughout the reaction, and the σ-bond metathesis is the enantiodetermining step of the reaction.

Mechanistically, it is well-established that the σ-bond metathesis step occurs through a spiro-4-membered transition state (Figure 3-6).[9] Therefore, the enantio-induction is determined by the relative activation energies of the diastereomeric σ-bond metathesis transition states, which determine the enantiofacial selectivity of the process by the formation of a stereogenic center in the process. Considering the complexity of the Taniaphos ligand used, calculations regarding the facial selectivity are exceptionally challenging, although they are currently underway. Furthermore, adding to this complexity is the possibility that the dimethylamine functionality of the Taniaphos ligand may be protonated during this process (see Section 3.6).

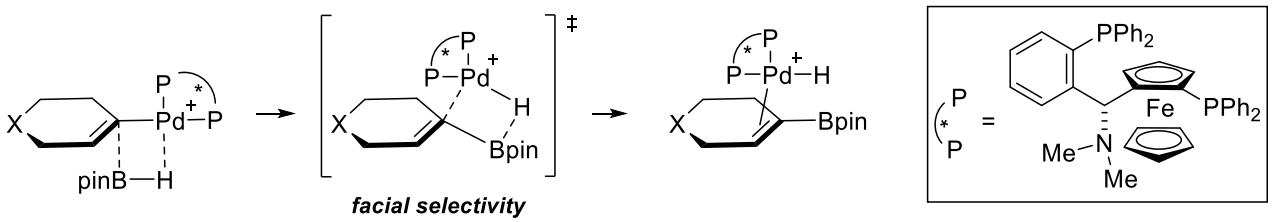

Figure 3-6. General representation of the enantiodetermining σ-bond metathesis step.

Notably, the steps of the alkene isomerization in the borylative migration mechanism is in contrast with many other metal-catalyzed alkenyl to allylic boronate isomerization processes, in which association of a pre-formed metal-hydride is required.[33,34] However, similar cationic palladium hydride species are commonly proposed in relay Suzuki coupling reactions developed by Sigman and co-workers.[35] Finally, any attempts to make a stoichiometric palladium hydride-DPEPhos complex *in situ* or to isomerize **3-6** to **3-5** by other means have been unsuccessful to-date.[36]

3.4 Alkene isomerization

3.4.1 Protic *vs* hydridic pathways

In terms of the mechanistic details regarding the alkene isomerization process, it was hypothesized that the isomerized allylic boronate **3-5** could be accessed by either an alkene insertion into the Pd-H bond, followed by a β-hydride elimination (inner sphere 1,2-hydride shift) or a deprotonation pathway (outer sphere, 1,2-proton shift) as shown in Scheme 3-6 (black and red pathways, respectively).[37] It was envisioned that since the alkene in **Int-II-C** is π-bound to the cationic palladium(II) catalyst and therefore quite electron-deficient, it may be possible that deprotonation of the allylic hydrogen could occur by the dimethylaniline base.[38] One appealing aspect of the alkene isomerization process occurring via deprotonation is that it would allow for a clear rationale in regard to the large effect of the base on the enantioselectivity of the process (see Section 3.6).

However, the energy barrier for the deprotonation of **Int-II-C** was calculated to be too high to be a competing pathway under the reaction conditions (Scheme 3-6, deprotonation pathway, in red). In comparison, a regioselective hydropalladation is essentially barrierless to form the σ-bound **Int-II-D** (Scheme 3-6, hydropalladation pathway in black). The observed regioselectivity of the hydropalladation step is hypothesized to be due to steric considerations, however calculations regarding formation of the opposite regioisomer are currently underway. Subsequent β-hydride elimination from **Int-II-D'** furnishes **Int-II-E**, which subsequently leads to **Int-II-F**, the Pd(0)-bound complex of the desired product **3-5**. Alternatively, deprotonation of the Pd-H bond from **Int-II-C** leads to overall reductive elimination and formation of the Pd(0)-bound alkenyl botonate product, **Int-II-G** (Scheme 3-6, blue pathway). A more detailed discussion of the controlling factors regarding the alkenyl:allyl boronate ratio is discussed in the following section.

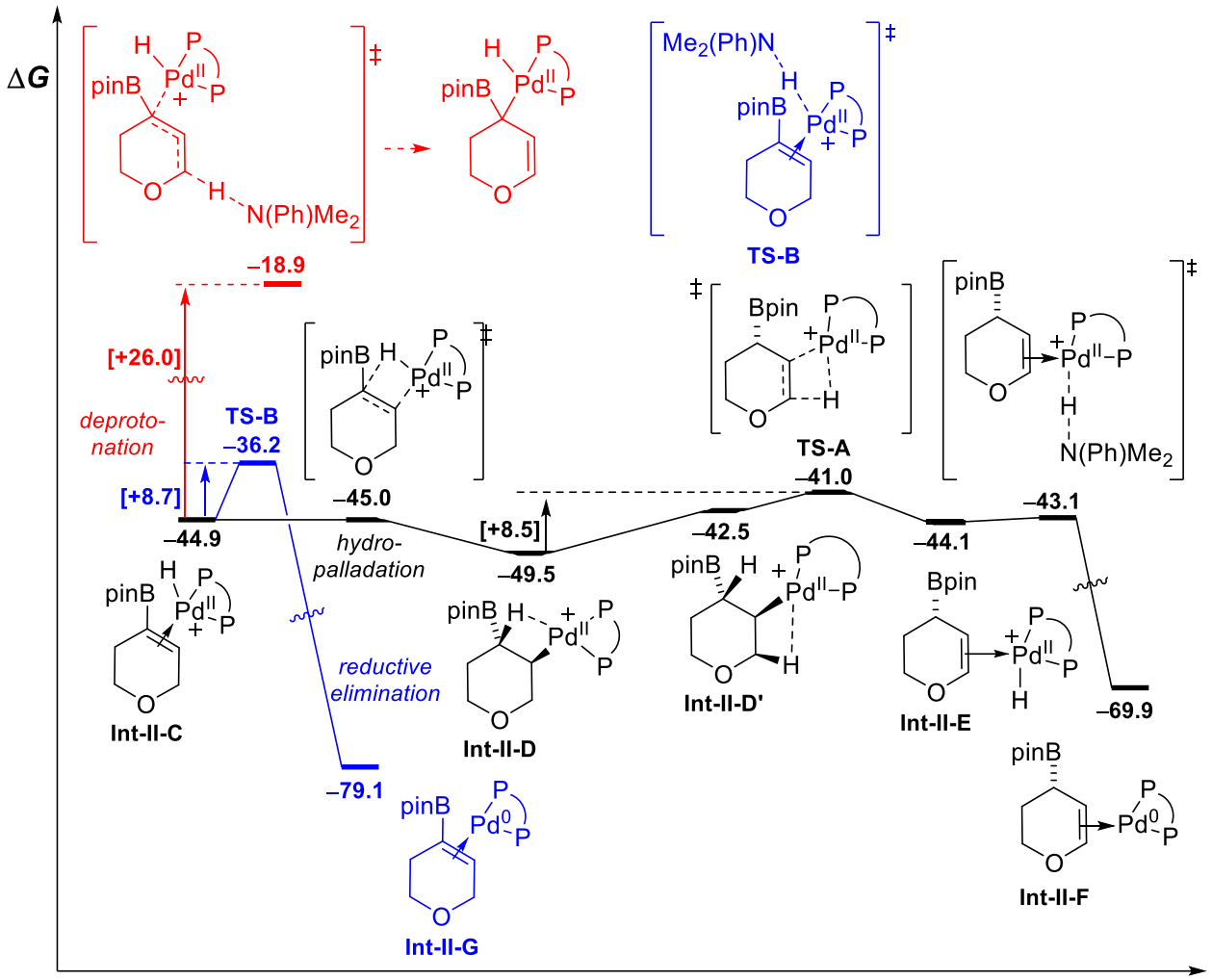

Scheme 3-6. Comparison of hydridic and protic alkene isomerization pathways.

3.4.2 Influence of the heteroatom

The effectiveness of the borylative migration relies on a favorable alkene isomerization to produce the allylic boronate **3-5** over reductive elimination of **Int-II-C**, which would otherwise result in the forming the alkenyl boronate **3-6**. Based on the data described above, the mechanism of the alkene isomerization follows an alkene insertion, β-hydride elimination pathway (Scheme 3-6). Considering the position of the β-hydrogen on the ring, it was proposed that the ratio of allylic boronate:alkenyl boronate (**A**:**B**) may be affected by the nature of the atom at the homoallylic position of the alkenyl sulfonate.[16,39] To gain more insight regarding the effect of the heteroatom on

the observed ratio of **A**:**B**, a brief study of four different alkenyl nonaflates was undertaken. To this end, two new alkenyl nonaflates were synthesized using modified standard literature procedures (Scheme 3-7).[2]

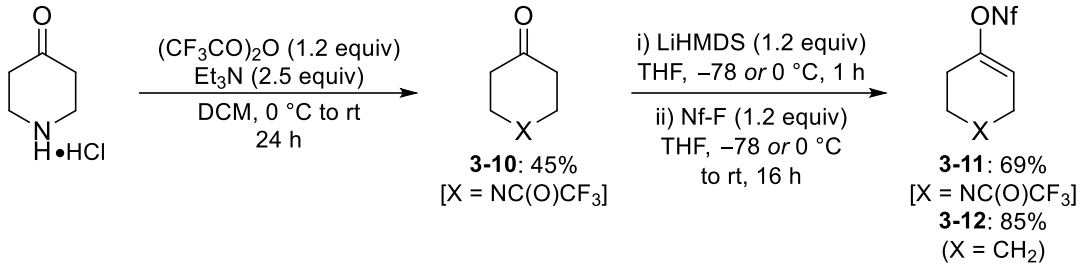

Scheme 3-7. Synthesis of previously unreported alkenyl nonaflates.

The results of the borylative migration using substrates with different heteroatoms are shown in Table 3-4. Indeed, the ratio of **A**:**B** varied substantially with the electronic nature of the heteroatom (**X**) with the relative amount of allylic boronate (**A**) decreasing from X = O > NBoc > $NC(O)CF_3$ > CH_2 (entries 1–4). Interestingly, the cyclohyexyl system favours the formation of the alkenyl boronate **3-16** and the allylic boronate was formed in a racemic fashion, potentially due to a Pd-H "chain-walking" around the ring. Overall, the relative amount of allylic boronate (**3-5**) seems to increase with the expected extent of lone-pair donation to the alkene in **A**.

Table 3-4. Effect of the heteroatom on the product distribution.

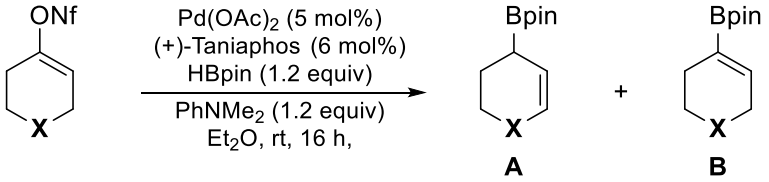

Entry	**X**	Substrate	**A**	**B**	Yield of **A**[a]	Ratio **A** : **B**[a]	*ee*[b]
1	O	**3-2**	**3-5**	**3-6**	72%	8 : 1	90%
2	NBoc	**3-4**	**3-7**	**3-8**	80%	4 : 1	89%
3	$NC(O)CF_3$	**3-11**	**3-13**	**3-14**	57%	2.5 : 1	89%[d]
4	CH_2	**3-12**	**3-15**	**3-16**	34%	1 : 2	0%

[a]Yield and product ratios are estimated by crude ^{1}H NMR using 1,3,5-trimethoxybenzene as an internal standard. [b]*ee* is determined by chiral HPLC after thermal allylboration with *p*-tolualdehyde to furnish products **3-17**, **3-18** and **3-19**

for X = O, NBoc, CH_2, respectively. [d]The allylboration product was converted to **3-18** before purification and *ee* determination.

To gain more insight into reasoning behind the observed ratios of **A**:**B**, the steps of the alkene isomerization was also calculated for the cyclohexyl manifold (Scheme 3-8). The key relative energy differences and controlling factors in the isomerization between the pyran and cyclohexyl manifolds in Schemes 3-6 and 3-8, respectively, are discussed below.

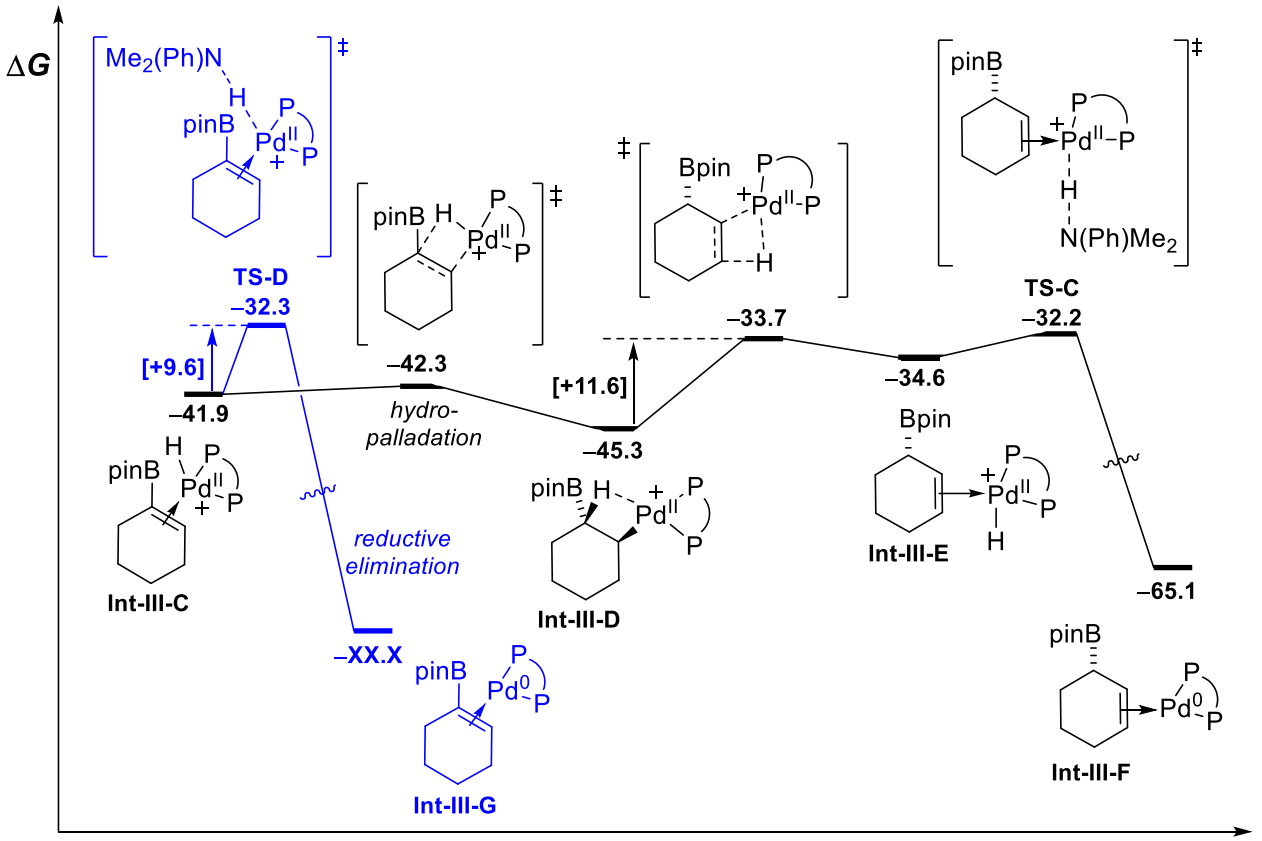

Scheme 3-8. Alkene isomerization for the cyclohexyl manifold. The energy for **Int-III-G** will be reported in due course.

It is important to note that although the absolute energies of the intermediates shown in the pathways of Schemes 3-6 and 3-8 cannot be compared directly, the relative energy barriers between the intermediates are comparable values for further analysis. Considering that the reductive elimination step is irreversible in all cases, the observed ratios of **A**:**B** in Table 3-4 in each case should

correspond with the difference in energy of the highest transition states in forming the allyl and alkenyl boronate in each manifold, which are **TS-A**/**TS-B** and **TS-C**/**TS-D** for the pyranyl and cyclohexyl substrates, respectively. Overall, the pyranyl system favours the allylic boronate by 6.9 kcal mol^{-1}, whereas the alkenyl boronate is slightly favoured in the case of the alkenyl boronate by only 0.2 kcal mol^{-1}. The aforementioned energy differences are in good agreement with the observed ratios in Table 3-4, yet a more thorough analysis of important steps in the alkene isomerization pathway is required to understand the reasoning as to why there is such an overall energy different between these two pathways.

The energy barriers for the deprotonation step for overall reductive elimination to the Pd-bound alkenyl boronate products, **Int-II-G** and **Int-III-G** (temporarily reported as –**XX.X** kcal mol^{-1}) are similar, yet the former is favoured by 0.8 kcal mol^{-1}. A weak long range inductive effect of the pyranyl oxygen is a simple explanation for the slight favourability towards deprotonation in **TS-B** vs **TS-D** (Schemes 3-6 and 3-8, respectively). Furthermore, in terms of the ease of alkene isomerization, the pyranyl system undergoes the Pd-H alkene insertion step to afford **Int-II-E**, which is 3.1 kcal mol^{-1} lower than the barrier to form **Int-III-E**. Finally, the deprotonation of the allyl-bound Pd-H intermediates **Int-II-E** and **Int-III-E** are quite similar.

Careful consideration of the various energy differences suggest that the overall primary contributing factor leading to the differing energy barriers in **TS-A**/**TS-B** and **TS-C**/**TS-D** is the relative energy cost for the β-hydride elimination of H_α (Figure 3-7). The formation of **Int-II-E** has a 5.2 kcal mol^{-1} lower energy barrier than **Int-III-E** because of the relatively stronger σ-donation to the electron-deficient Pd-H in **Int-II-E** from conjugation of the pyranyl oxygen. Although further analysis would be required for general extension of this theory to the two piperidinyl manifolds, the calculations described herein suggest that lone-pair donation to stabilize the allylic-bound Pd-H is a

key factor contributing to the large effect of changing the hetero atom on the allyl- to alkenyl boronate ratios shown in Table 3-4.

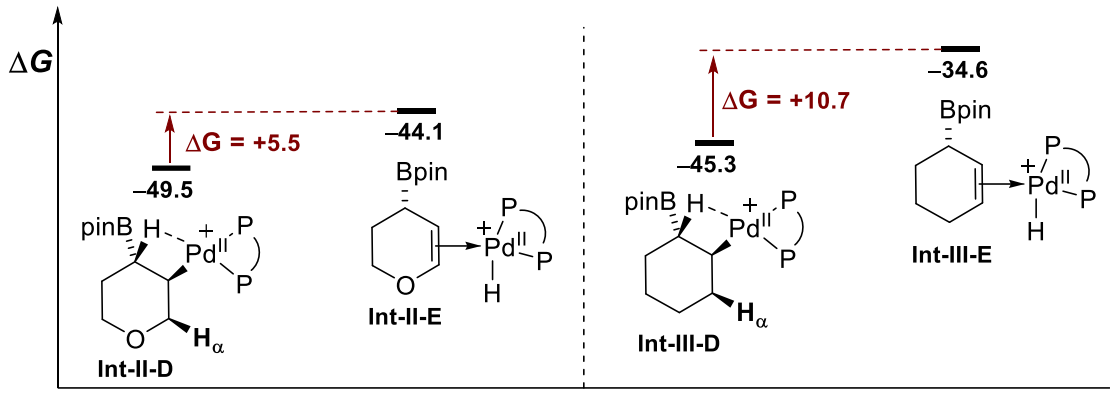

Figure 3-7. Comparison of the β-hydride elimination in the pyranyl (left) and cyclohexyl (right) systems.

Finally, it is notable that the enantioselectivity was seemingly unaffected by the nature of the heteroatom, yet in the case of cyclohexyl substrate **3-12** the reaction proceeded in a racemic fashion (Table 3-4). The lack of enantioenrichment in **3-15** could suggest that a heteroatom may be important for enantio-discrimination of the pro-chiral alkene in the borylation step to form **Int-II-C**. Alternatively, it could be that with the cyclohexyl scaffold the palladium hydride has a propensity to "chain walk" around the ring to form the enantiomeric product from the same diastereomeric intermediate. In the case of the other alkenyl nonaflates screened, the position X is blocked by a heteroatom and therefore the isomerization cannot continue around the ring. In this regard, a deteurium labelling study of the cyclohexyl alkenyl nonaflate could be very telling to whether the Pd-H chain-walking is occurring around the ring, as shown in Scheme 3-9.

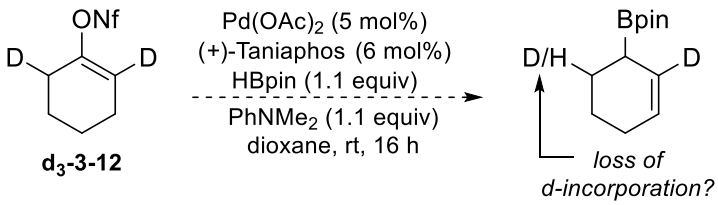

Scheme 3-9. Proposed D-labelling experiment to explain the racemic cyclohexyl allylic boronate.

3.4.3 Reductive elimination and product release

The outcome of DFT calculations regarding the product release of the allylic boronate **3-5** from **Int-II-E** is shown in Scheme 3-9. The process is relatively high in energy, with a barrier of 12.7 kcal mol^{-1} for release of the allylic boronate product **3-5** and formation of **Int-II-J**. Howvever, many intermediates with conformational flexibility exist along the pathway shown in Scheme 3-9, and therefore further refinement of the calculations may be required. Release of the alkenyl boronate side product **3-6** was also calculated following the same steps in the product release as for the allylic boronate **3-5**, however the product release is less favourable for the alkenyl boronate with an energy cost of 18.3 kcal mol^{-1}. Comparatively, the oxidative addition of palladium(0) into **3-2** has a well-defined energy barrier of 13.4 kcal mol^{-1}. Therefore, the calculations suggest that the oxidative addition is the rate-determining step in the catalytic cycle, yet release of **3-6** may cause product inhibition, which is in agreement with kinetic studies described in the next section.

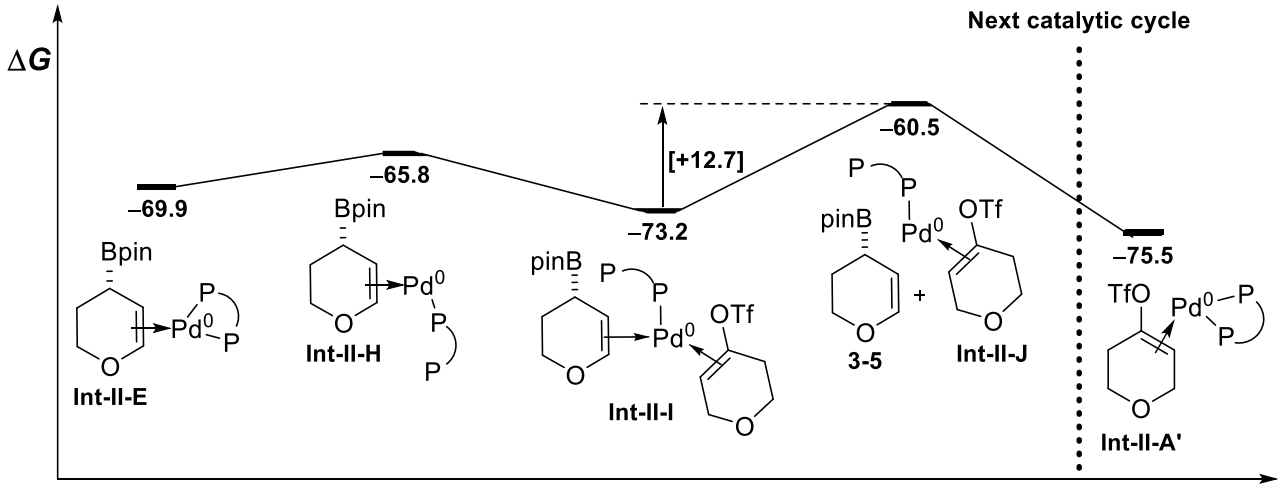

Scheme 3-10. DFT calculations of the product release of allylic boronate **3-5**.

3.5 Kinetic studies

3.5.1 Method development

Based on the calculations to-date, the rate-determining step (RDS) of the borylative migration is the oxidative addition of substrate **3-2**, yet that final product release of **3-5** and **3-6** are comparatively high energy processes. Important insight for both the RDS and the possibility of product inhibition can be probed experimentally using kinetic analysis.[40] Recent advances in visual kinetics analysis developed by Blackmond, Burés and their co-workers allows for the ability to obtain general rate dependence information in relatively few experiments.[41] The utility of the visual kinetic analysis approach stems from the ability to compare concentration against time data directly to gain information regarding rate-dependence. Furthermore, the kinetic data can be obtained by various readily-accessible means such as NMR, FTIR, UV, Raman, GC and HPLC analysis. The approach can elucidate general kinetic parameters in which high precision is not required while avoiding the use of counter-intuitive mathematical transformations. The simplicity of the visual kinetic analysis has allowed this approach to become an influential mechanistic tool in academia and industrial laboratories.[41]

In this regard, we sought to probe the RDS of the borylative migration experimentally using visual kinetics analysis. The first step of the process of acquiring kinetic data is the development of a reliable analytical method. Considering that the allylic boronate **3-5** has limited stability, it was proposed that direct NMR monitoring would be desirable. Although it has been previously reported by our group that the reaction with the piperidinyl nonaflate is complete within 4 hours, we were surprised to find that the reaction is complete very quickly with pyranyl nonaflate **3-2** in various solvents, such as diethyl ether, toluene, dioxane and benzene. For example, when the reaction was observed by ^{1}H NMR with 0.5 mol% palladium acetate at 12 °C in dioxane (Scheme 3-10), about

50% conversion of **3-2** occurred within one minute (Figure 3-8). Furthermore, in this experiment the data points were obtained by removing aliquots by syringe, diluting in diethyl ether (about 5 mL) and filtering through a short silica plug (about 800 mg). Considering that this process was overly time-consuming and that the speed of the reaction lead to inaccuracies, other conditions and analytical methods were evaluated.

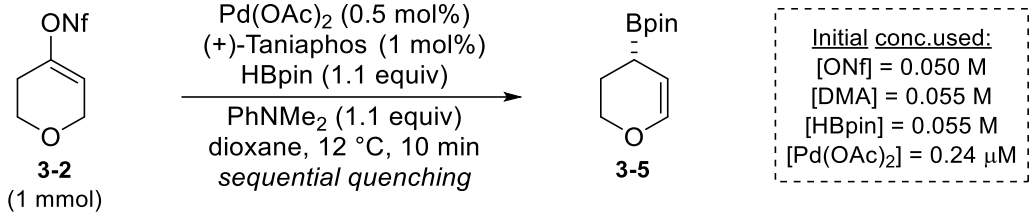

Scheme 3-11. Initial conditions for the kinetic profiling of pyranyl nonaflate **3-2**.

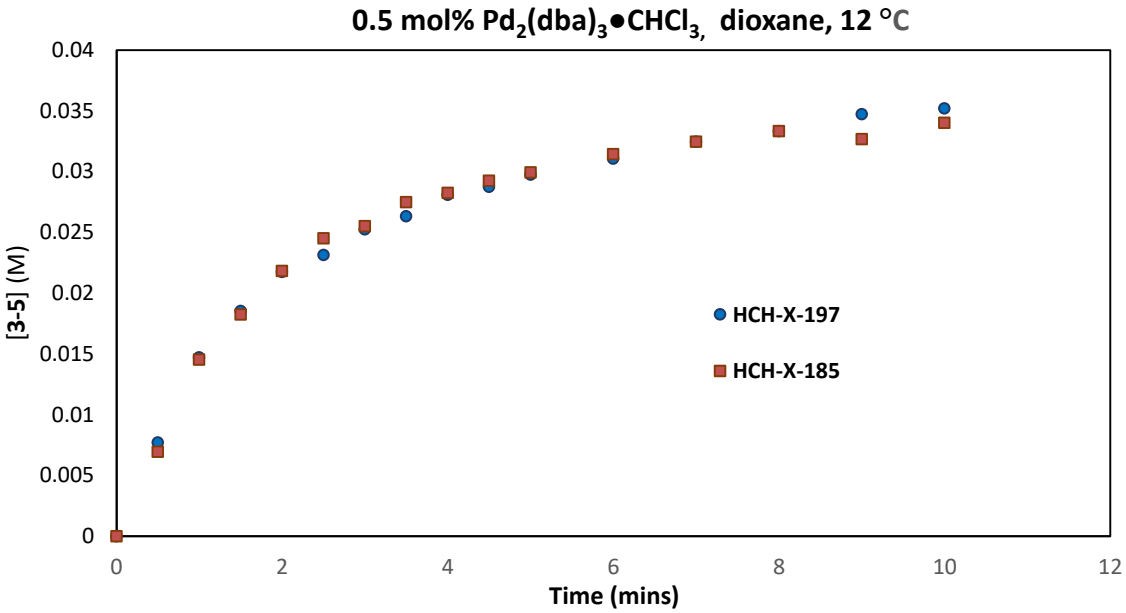

Figure 3-8. Formation of **3-5** over time using the conditions in Scheme 3-10.

After screening a few solvents and with reference to previous preliminary results by Ms. You-Ri Kim (Hall Group MSc graduate), a procedure was developed for kinetic analysis of the borylative migration using the piperidinyl nonaflate **3-4** in d_2-dichloromethane with $Pd_2(dba)_3$●$CHCl_3$ (Scheme 3-11). The reaction was set-up in an oven-dried J-Young NMR tube under argon atmosphere and

monitored by ^{1}H NMR as a spectral array every 0.5 or 1.0 minute (see the experimental section for details). Although it is not ideal to use significantly different conditions in kinetics experiments than that employed in the standard borylative migration reaction, this method was found to be reproducible and furnished a clean reaction with minimal side product formation. The resulting profile shows the expected reaction kinetics over a more reasonable timeframe, with about 50% conversion after 10 minutes instead of about 1 minute with the previous method (Figure 3-9).

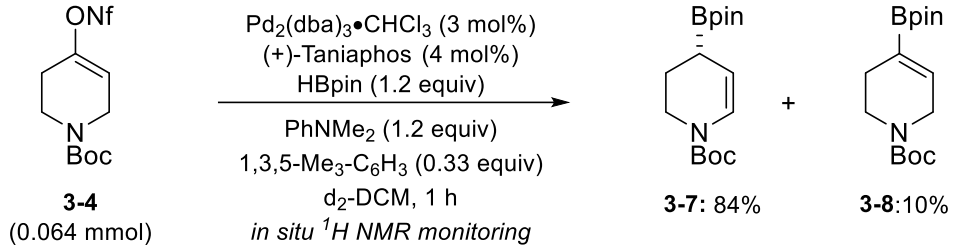

Scheme 3-12. Optimized conditions used for direct NMR-based kinetic profiling of the borylative migration.

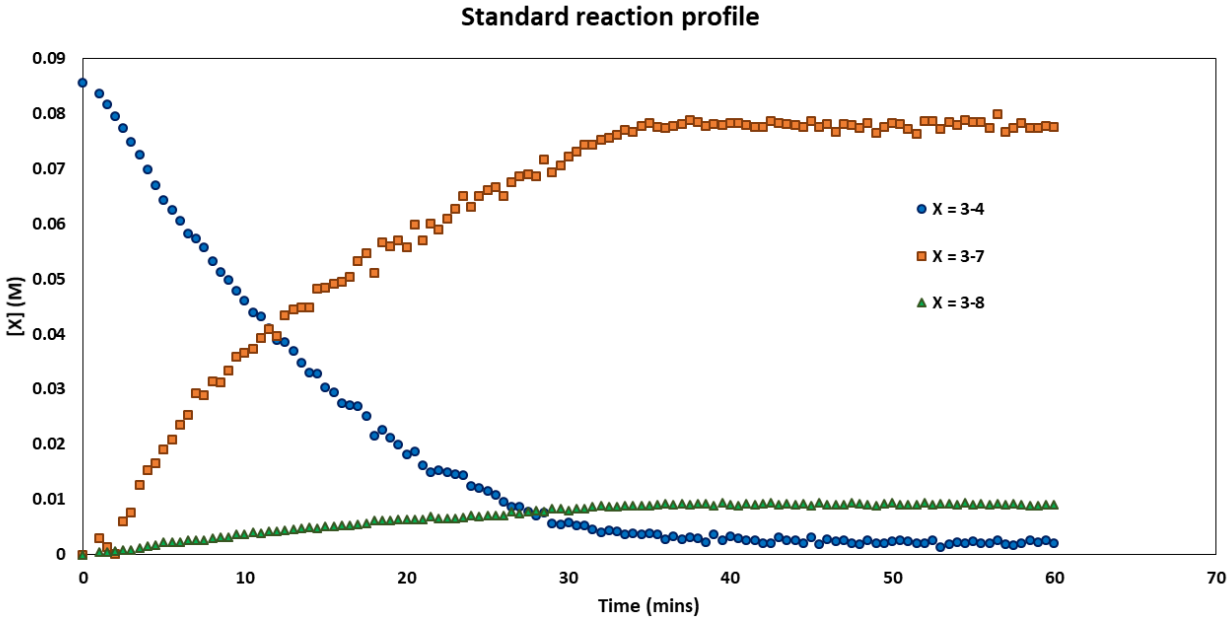

Figure 3-9. Reaction profile for the standard reaction conditions used for kinetics.

One notable point about the conditions used for the kinetic experiments is the excess palladium source compared to the ligand. The reaction was found to be consistently quite clean using these conditions. Although it was not expected that $Pd_2(dba)_3$ would be able to catalyze the reaction alone,[4] a control experiment confirmed that this is indeed the case. An experiment using the same conditions as in Scheme 3-12 without the addition of Taniaphos led to no observable product formation after one hour and 98% recovery of the alkenyl nonaflate **3-4** by ^{1}H NMR.

3.5.2 Reaction orders of the reagents

Using the modified reaction conditions shown in Scheme 3-12, the dependence of the reaction on the concentration of the alkenyl nonaflate **3-4**, HBpin, $PhNMe_2$ and catalyst were investigated.[42] For both pinacolborane and dimethylaniline, the reaction was found to be zero-order; doubling the concentration of both reagents led to an insignificant change in the rate of consumption of **3-4** (Figure 3-10). These results indicate that the rate-determining step of the borylative migration reaction occurs before any involvement of the base or pinacolborane.

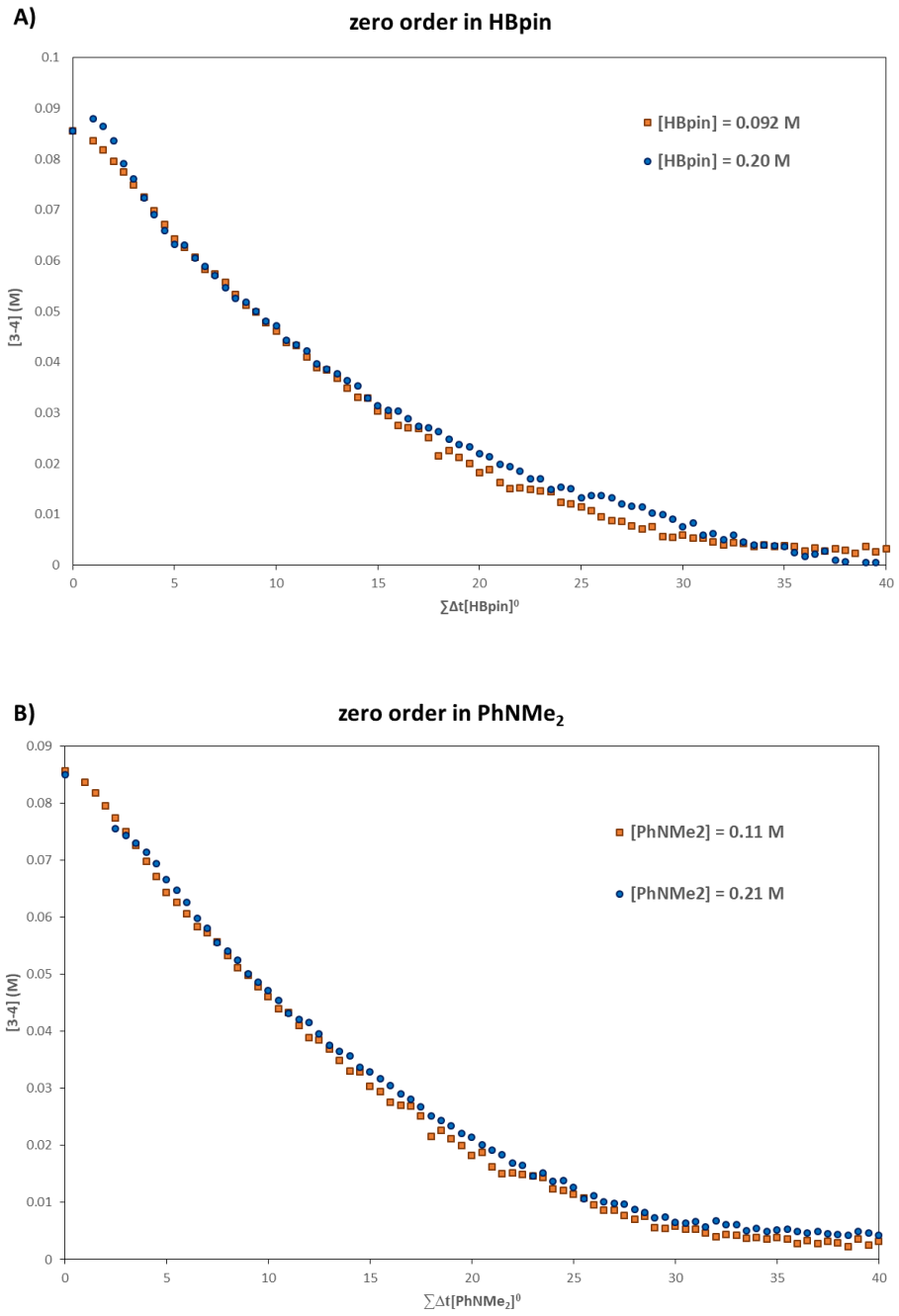

Figure 3-10. Reaction profiles for the doubling of concentration of (a) HBpin and (b) $PhNMe_2$.

Conversely, a non-zero order rate-dependence was observed in the case of the alkenyl nonaflate **3-4** (Figure 3-11A). When the reaction is non-zero order in a reagent, the Burés method involves fitting the exponent of the equation shown on the x-axis. The x-axis is modified by the change in concentration of the reagent over time, i.e. $\sum\Delta t[A]^{\beta}$, where the exponent (β) is the order of the

reagent of interest. Essentially, the value for β is changed until a best fit is found between the two (or more) curves, which indicates the order in reagent A by the value found for β. As can be seen in Figure 3-3, the borylative migration does not show a first or inverse first order dependence of the nonaflate **3-4** (graphs B and C). The best fit for the rate dependence of the alkenyl nonaflate was found to be a 0.6 rate order dependence (graph D). A partial first order suggests that alkenyl nonaflate **3-4** is involved in the reaction before or during the RDS, however there may be product inhibition of the catalyst, a commonly observed phenomenon in palladium catalysis.[43] Considering the calculations of the product release (Scheme 3-9), it is expected that the allylic boronate **3-7** and/or the alkenyl boronate **3-8** could be involved in inhibition of the catalyst. To further confirm this hypothesis, kinetic evidence for product inhibition of both the allylic boronate **3-7** and alkenyl boronate **3-8** will be investigated in due course.

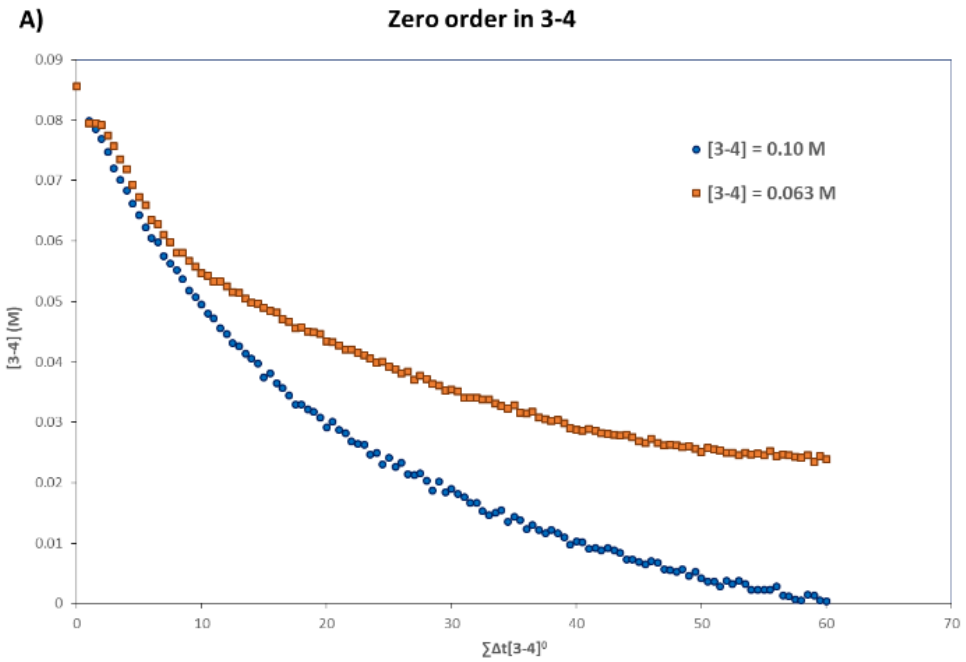

B)

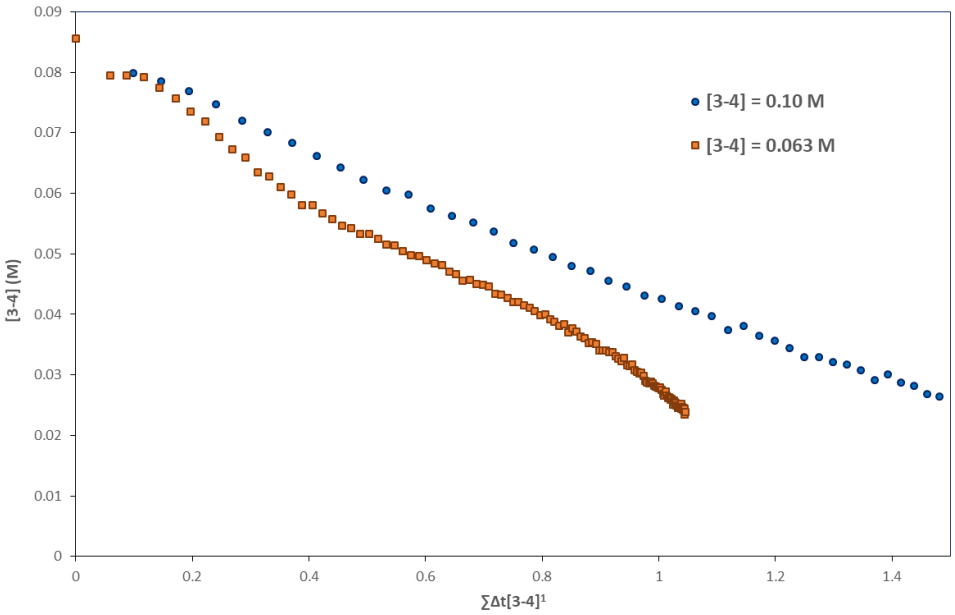
First order in 3-4
[3-4] = 0.10 M
[3-4] = 0.063 M
[3-4] (M)
∑Δt[3-4]¹
0.09
0.08
0.07
0.06
0.05
0.04
0.03
0.02
0.01
0
0.2
0.4
0.6
0.8
1
1.2
1.4

C)

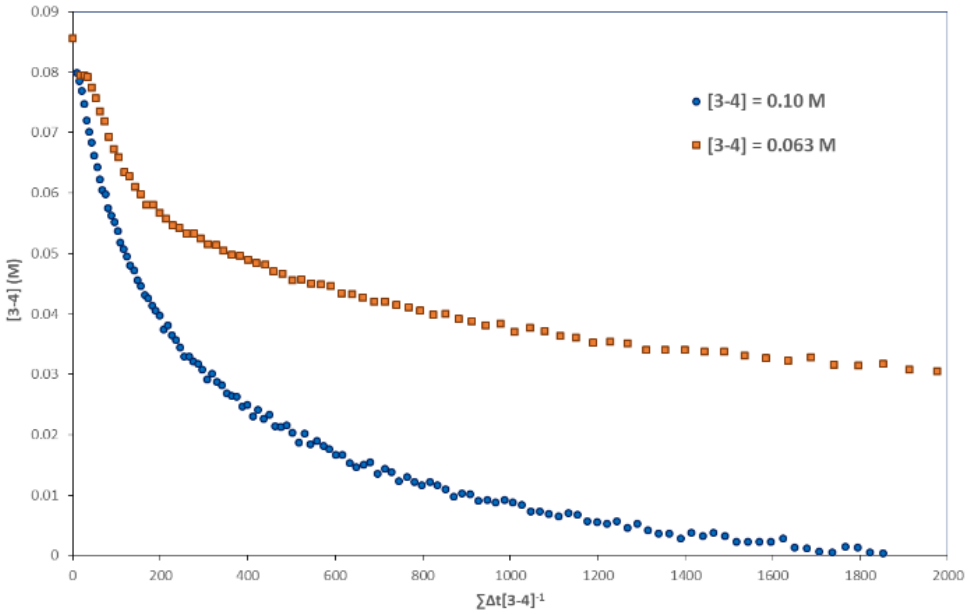
Inverse first order in 3-4
[3-4] = 0.10 M
[3-4] = 0.063 M
[3-4] (M)
∑Δt[3-4]⁻¹
0.09
0.08
0.07
0.06
0.05
0.04
0.03
0.02
0.01
0
200
400
600
800
1000
1200
1400
1600
1800
2000

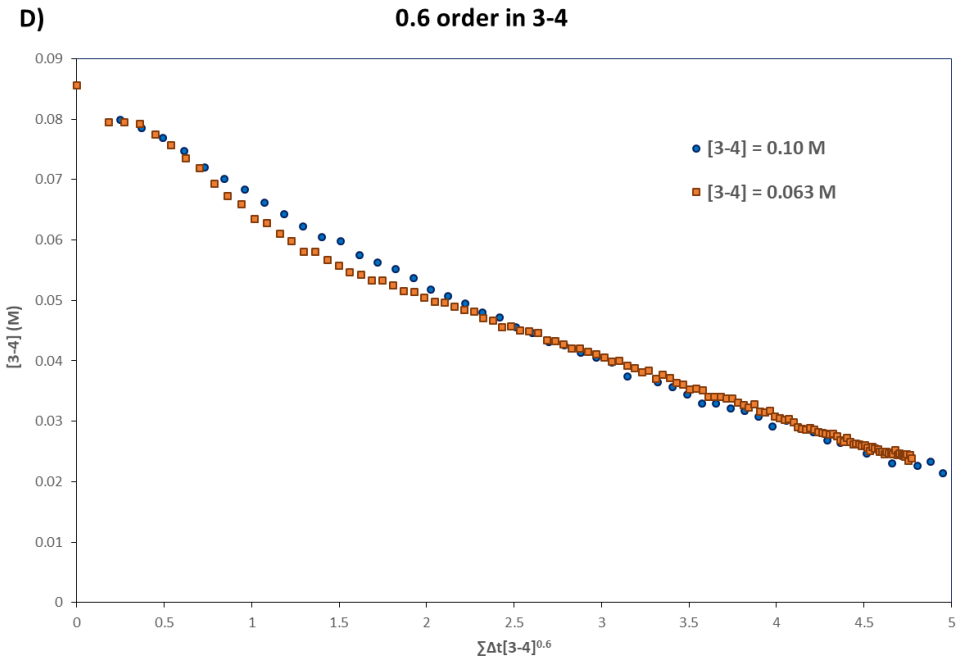

Figure 3-11. Rate dependence of alkenyl nonaflate **3-4**.

3.5.3 Kinetics results of the catalyst

The order in catalyst was also investigated using a related approach also reported by Burés.[44] In these experiments, the reported catalyst concentration is assumed to be equivalent to the initial concentration of Taniaphos used. Surprisingly, it was found that doubling the catalyst loading seemed to have no observable effect on the rate of the reaction (Figure 3-12). However, considering that the catalyst is involved in all steps of the reaction, the reaction cannot be zero-order in catalyst. Therefore, the apparent zero order in catalyst is rationalized to be due to the formation of inactive palladium dimers, a phenomenon also commonly seen in palladium catalysis and which is more likely to occur at a higher catalyst concentration.[44,45]

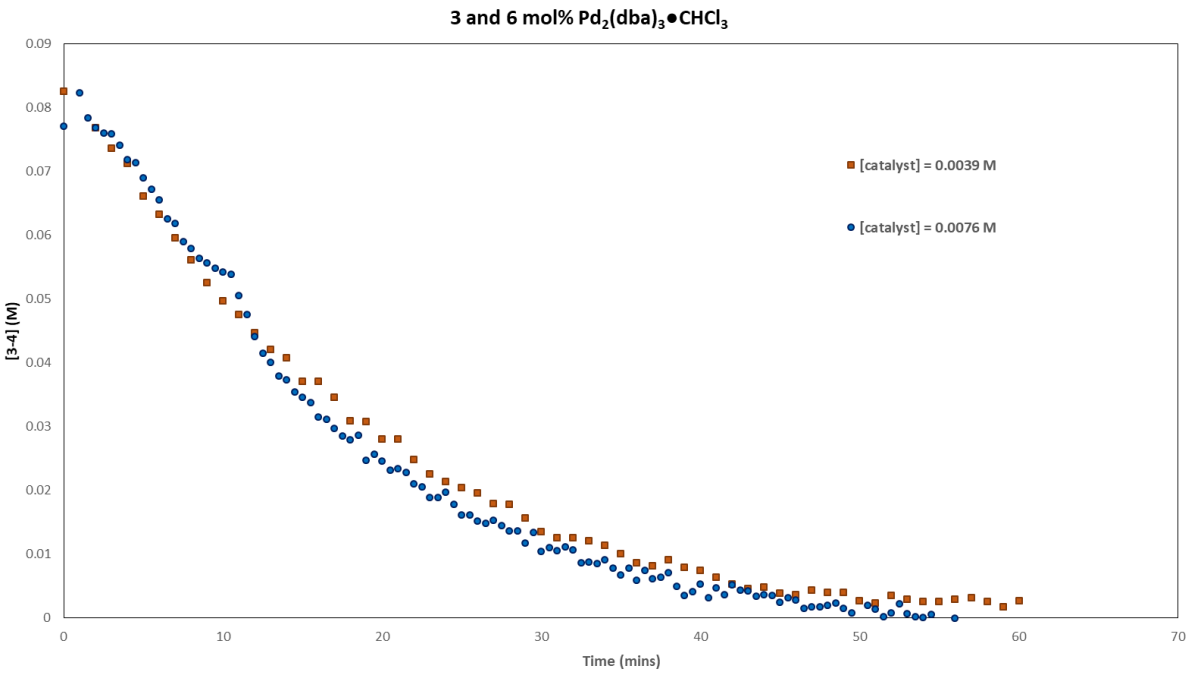

Figure 3-12. Consumption profile of **3-4** with 3 mol% and 6 mol% $Pd_2(dba)_3$●$CHCl_3$.

Therefore, the kinetics of the catalyst were investigated further using the same conditions, however, with ten times less catalyst (0.3 and 0.6 mol% palladium source) with the expectation that under lower palladium catalyst concentration dimerization may not significantly impact the kinetic profile.[44] Indeed, the results of nonaflate consumption under the lower catalyst loading was more informative (Figure 3-13, graph A). The consumption profile of substrate **3-4** had the best fit for first order kinetics agreeing with a monomeric active catalyst (graph B). It is notable that the formation of dimers is solvent-dependent and therefore cannot be directly correlated to the experimental reaction conditions since the borylative migration is commonly performed in dioxane, diethyl ether or CPME.

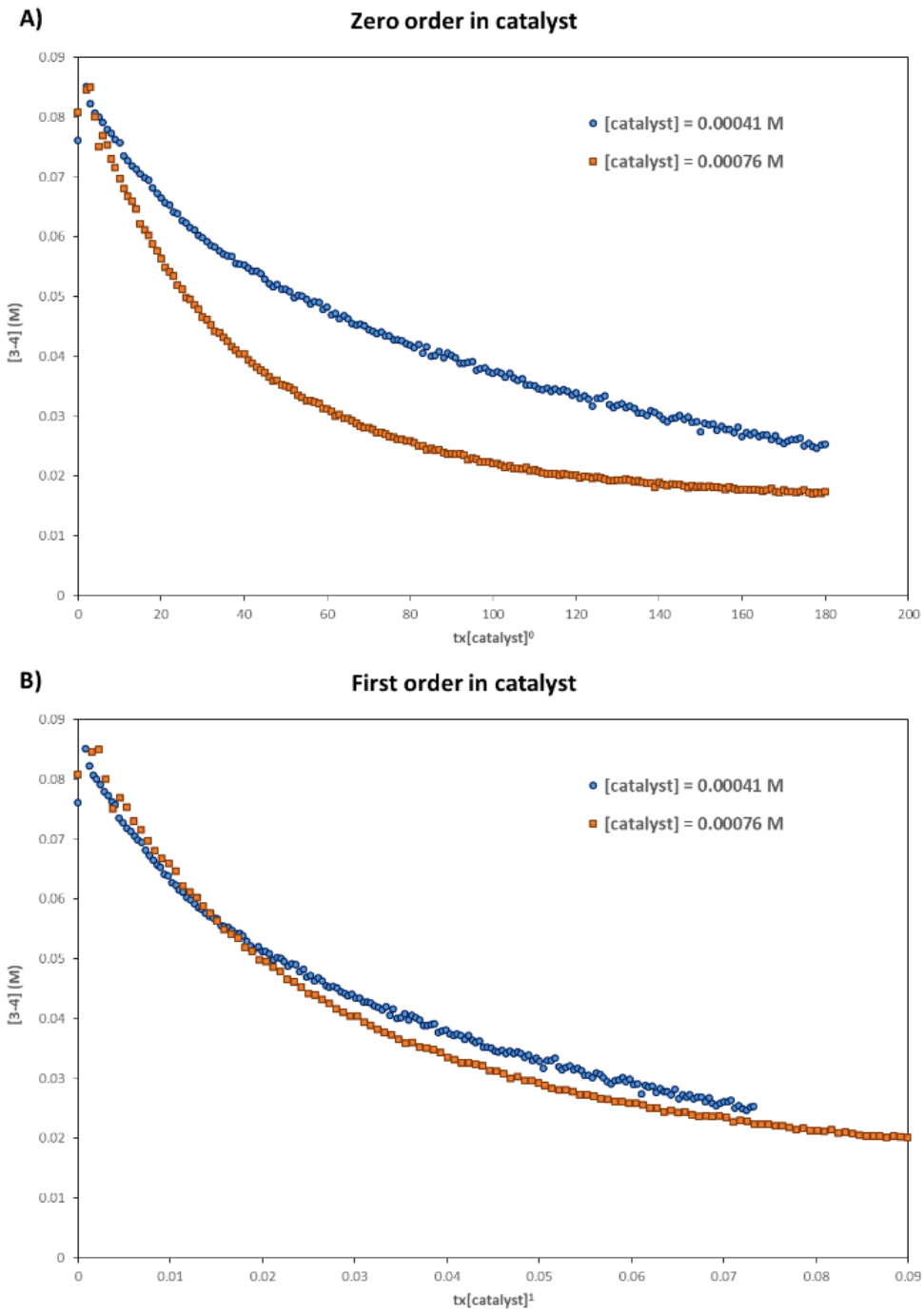

Figure 3-13. Consumption of alkenyl nonaflate **3-4** with 0.3 mol% and 0.6 mol% $Pd_2(dba)_3$●$CHCl_3$.

3.5.4 Summary of kinetics data to-date

Overall, the kinetic experiments suggest that oxidative addition onto the alkenyl sulfonate is the RDS of the catalytic cycle, which is in good agreement with the DFT calculations. The reaction

displays a zero-order dependence of the pinacolborane and base, suggesting that neither reagent is involved in the reaction until after the rate-determining step. The rate dependence in nonaflate **3-4** is a partial positive dependence, suggesting that it is involved in a step before or during the RDS. The current rationalization for the reaction having a 0.6 order dependence instead of first order fit is product inhibition of the catalyst. Based on the calculations of the product release alone, it seems more likely that formation of the alkenyl boronate **3-8** inhibits the reaction, although product inhibition studies will be performed for both the allylic boronate **3-7** and alkenyl boronate **3-8**. The borylative migration displays a first order rate dependence of the catalyst under lower catalyst loadings, suggesting that a monomeric catalyst is involved in the RDS. Finally, if oxidative addition is indeed the RDS, then by ^{31}P NMR the catalyst resting state should be the ligand-bound Pd^0 catalyst, **Int-II-A'** during the course of the reaction. Attempts to observe and partially characterize **Int-II-A'** are currently underway.

3.6 Effect and proposed roles of the base

3.6.1 Dependence of the enantioselectivity on the base

A limited study of the effect of different bases in the borylative migration reaction is shown in Table 3-5, ordered by decreasing enantioselectivity. Clearly, both the reaction efficiency and enantioselectivity are strongly affected by the specific amine base present. The reason for the yield being lower with stronger bases is unclear at this time and still under investigation. Furthermore, at first glance, it is not clear why the specific amine base would have such a profound effect on the enantioselectivity. In most palladium-catalyzed cross-coupling reactions, the base is thought to only be involved in the reductive elimination step.[16] Based on calculations previously discussed, the enantio-determining step is most likely the borylation to form **Int-II-C** (Scheme 3-5). Therefore, with the reasonable assumption that the borylation to form **Int-II-C** is an irreversible step, the face

of which the palladium hydride is bound to the prochiral alkene in **Int-II-C** should determine the enantioselectivity.

Interestingly, based on the results in Table 3-5 the enantioselectivity is inversely proportional to the pK_a of the conjugate ammonium (pK_{aH}) of the amine base. Therefore, it is clear that under more acidic conditions the enantioselectivity of the reaction is improved. Although a conclusive rationale to explain the effect of the base on enantioslectivity is still under consideration, two preferred speculative proposals to explain the effect of the base on the enantioselectivity are presented below.

Table 3-5. Effect of the base on the reaction.

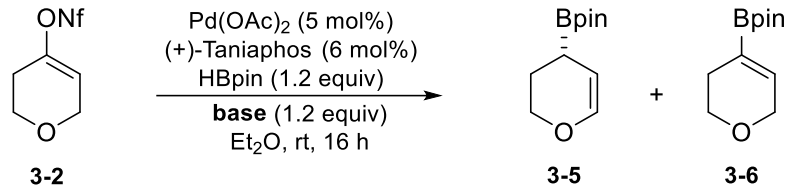

3-2 **3-5** **3-6**

Entry	**Base**	Yield of **3-5**[a]	Ratio **3-5**:**3-6**[a]	*ee*[b]	pK_{aH}[c]
1	$PhNMe_2$	72%	8 : 1	90%	5.2
2	TMPD	40%	7 : 1	75%	—[d]
3	*sym*-collidine	41%	>10 : 1	72%	7.4
4	DABCO	15%	trace **3**	66%	8.8
5	NEt_3	31%	≈ 8 : 1	56%	10.8

[a]Yield and product ratios are estimated by crude ^{1}H NMR using 1,3,5-trimethoxybenzene as an internal standard. [b]*ee* is determined of **3-16** by chiral HPLC after thermal allylboration with *p*-tolualdehyde. [c]pK_{aH} in water.[46] [d]An experimentally determined pK_{aH} for TMPD has not been found in the literature to-date.

bases screened:

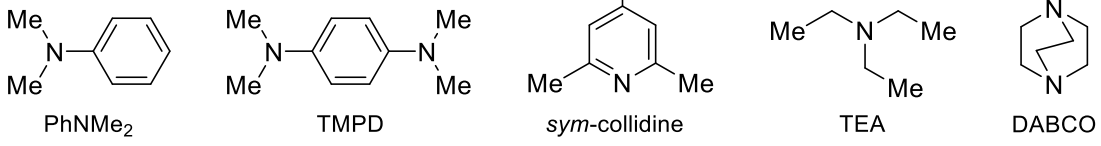

3.6.2 Kinetic resolution of the cationic palladium hydride Int-II-C

The most relevant literature precedence found to-date regarding an amine base affecting the enantioselectivity of a palladium-catalyzed cross-coupling reaction is the asymmetric Heck arylation of 2,3-dihydrofuran, first reported by Hayashi and co-workers.[16,47] The arylation reaction provides

two regioisomeric products (major and minor) that have the opposite preferred absolute stereochemistry (Figure 3-13a). It was found experimentally that stronger bases resulted in increased enantioselectivity. Based on these results, it was determined that a kinetic resolution scenario is operational (Figure 3-13b). Detailed characterization of catalytic intermediates by Brown and co-workers led to a reasonable rationale for why a kinetic resolution is observed.[48] The resolution under Hayashi's arylation system stems from the two diastereomeric palladium hydride species (**Int-C** and **Int-C'**) having different propensities for alkene isomerization. The diastereomeric palladium hydride complex leading to the (*R*)-major product (**Int-C**) is more prone to alkene isomerization to the regioisomeric palladium hydride (**Int-E**) than the diastereomeric palladium hydride (**Int-C'**) on the other ring face. Furthermore, Brown and co-workers also confirmed that the amine base is responsible for the reduction of the cationic palladium hydrides and therefore the kinetic resolution process.

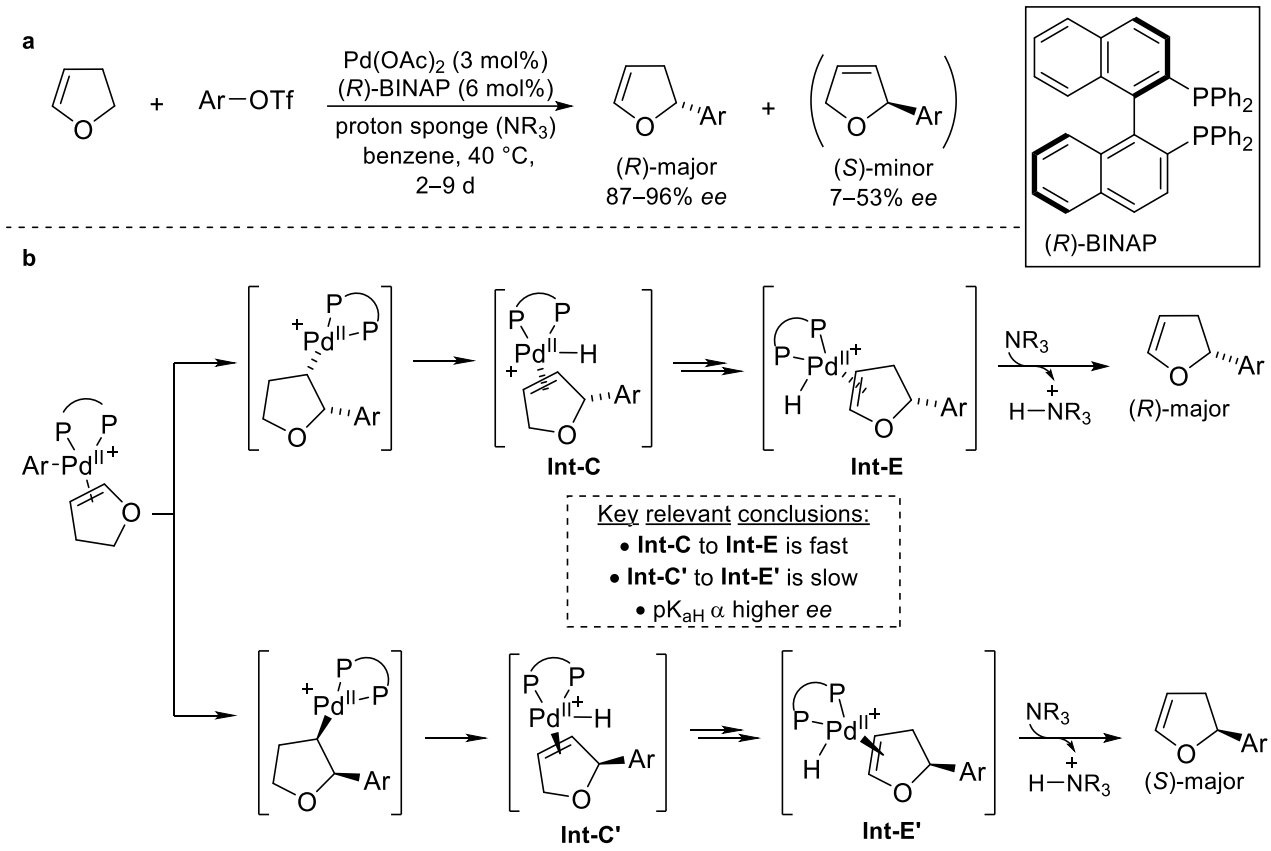

Figure 3-14. Hayashi's asymmetric Heck arylation (a) conditions (b) mechanistic steps.

Considering that more basic amines lead to a higher enantioselectivity,[47] it can be rationalized that a more basic amine can reduce **Int-C'** more efficiently. Since the propensity of **Int-C'** to isomerize to **Int-I-E'** is relatively slower than **Int-C** to **Int-E**, the (*R*)-major and (*S*)-minor form preferentially in the presence of a strong base. It is important to note that the authors did not propose the hypothesized connection between the relative base strength and propensity of alkene isomerization. Although this connection seems logical, it may be an oversimplification of the reaction system.

The work of Hayashi, Brown and their co-workers provides an important precedent for an amine-dependence of the enantioselectivity in an asymmetric palladium-catalyzed cross-coupling reaction. The results explained in Figure 3-13 suggest that it is not unreasonable to consider that a kinetic resolution of a cationic palladium hydride could be occurring in the borylative migration as well. In

the borylative migration, it could be the case that the propensity for alkene isomerization of the two diastereomeric palladium hydride species (**Int-II-C** and **Int-II-C'**) are not equivalent (Figure 3-14). For a kinetic resolution to be operating in this case, the assumption must be made that the borylation step is irreversible and that the two diastereomeric palladium hydride complexes, **Int-C** and **Int-II-C'** are not interconverting. These assumptions are reasonable based on our DFT calculations. It is important to note that the combined yield of allylboronates **3-5** and **3-6** is lower with more nucleophilic bases. Therefore, a correlation between the ratio of **3-5** to **3-6** to *ee* may not be very accurate by crude ^{1}H NMR in lower yielding reactions.

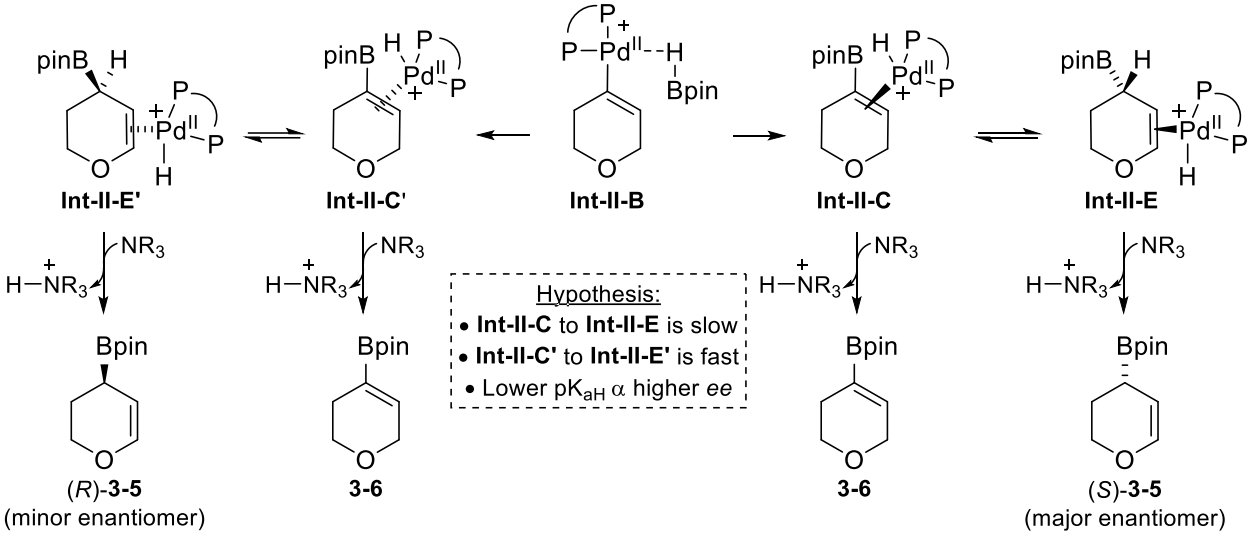

Figure 3-15. Kinetic resolution model to rationalize the effect of the base on the *ee*.

In terms of the borylative migration, the kinetic resolution model can be applied as follows (Figure 3-15). The major diastereomer **Int-II-C** would form in a much higher ratio than **Int-II-C'**, in a ratio that is independent of the base used. If the isomerization of **Int-II-C** to **Int-II-E** is slower than that of **Int-II-C'** to **Int-II-E'**, then with a weaker base less of **Int-II-C** will undergo reductive elimination to form alkenyl boronate **3-6**. Essentially, the process described is a kinetic resolution of the palladium hydride complexes **Int-II-C** and **Int-II-C'**, which is dependent on the pK$_{aH}$ of the amine base used. This would explain why there is an inverse correlation of pK$_{aH}$ to enantioselectivity.

To probe a kinetic resolution process, the enantioenrichment of the product will be determined after a short amount of conversion has occurred. In theory, if the *ee* is significantly different after a small amount of conversion, then this would be indicative of a kinetic resolution.

3.6.3 Conformational change from Taniaphos amine protonation

Based on the results shown in Table 3-5, it seems clear that a more acidic media leads to a more enantioselective reaction. Therefore, it may be possible that some sort of conformational change of the catalyst could occur at a lower pH. With this in mind, one logical hypothesis is that the amine subsitutent of the Taniaphos ligand could be protonated when the weaker base ($PhNMe_2$) is used. In theory, if the amine is protonated this would lead to a change in the catalyst that could increase the selectivity of the borylation step. Interestingly, during analysis of various Taniaphos derivatives by a previous group members (Ms. Stéphanie Lessard, MSc), it was seen that the amine is important for high enantio-induction with the Taniaphos scaffold.[49] Most notably, replacing the dimethylamine unit of Taniaphos with an isopropyl group led to formation of **3-5** in 56% *ee* (Scheme 3-12) similarly to the reaction with triethylamine (Table 3-5, entry 5). Furthermore, a 56% *ee* with Taniaphos and triethylamine was observed in dioxane as well.[49] Importantly, a precedence for the pK_{aH} of Taniaphos and this type of protonation has not been found in the literature to-date. However, NMR analysis of Taniaphos and/or its palladium complex in the presence of ammonium triflate salts is expected to be a valuable tool for further investigations. Furthermore, a useful control reaction would be to try the the *i*Pr-Taniaphos derivative with triethylamine. In theory the *ee* should be the same with triethylamine as with $PhNMe_2$ since protonation is not a factor with the *i*Pr-Taniaphos derivative.

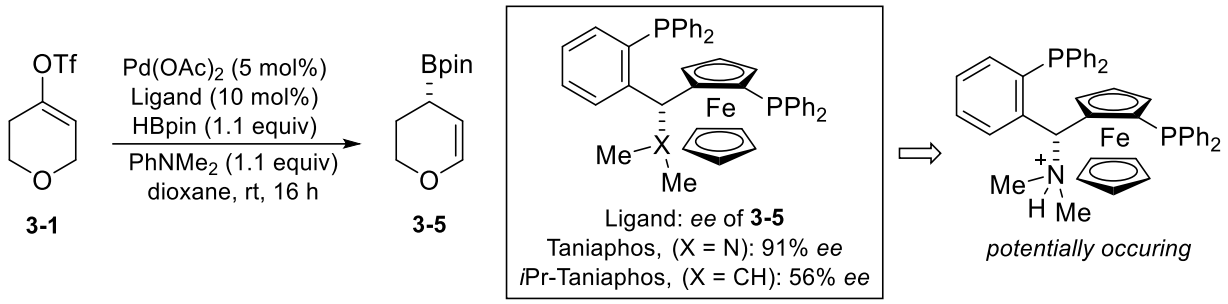

Scheme 3-13. Evidence of the importance for the amine of Taniaphos and potential reasoning.

3.7 Proposed catalytic cycle

According to the mechanistic studies described in this chapter, a full catalytic cycle of the borylative migration is proposed and shown in Figure 3-16. The experiments described suggest that the reaction mechanism involves a Miyaura-type borylation, followed by alkene isomerization pathway with an electrophilic cationic palladium. The first step is the oxidative addition to afford complex **Int-II-A**, which is most likely the RDS of the reaction. Ionization of the palladium complex affords the cationic palladium complex **Int-II-B** which may form from the spontaneous release of the non-coordinating triflate/nonaflate anion or an amine assisted ionization process. Coordination of cationic palladium complex with pinacolborane affords the hydride coordinated **Int-II-B**. The enantio-determining step is most likely the subsequent σ-bond metathesis with pinacolborane. An amine-promoted reductive elimination of palladium hydride-bound **Int-II-C** affords the observed alkenyl boronate side product **3-6**. Alternatively, alkene insertion results in the formation of the cationic complex **Int-II-D** which can undergo a β-hydride elimination to form a second cationic π-bound palladium hydride species (**Int-II-E**). A base-promote reductive elimination affords the allylic boronate product **3-5** after product release.

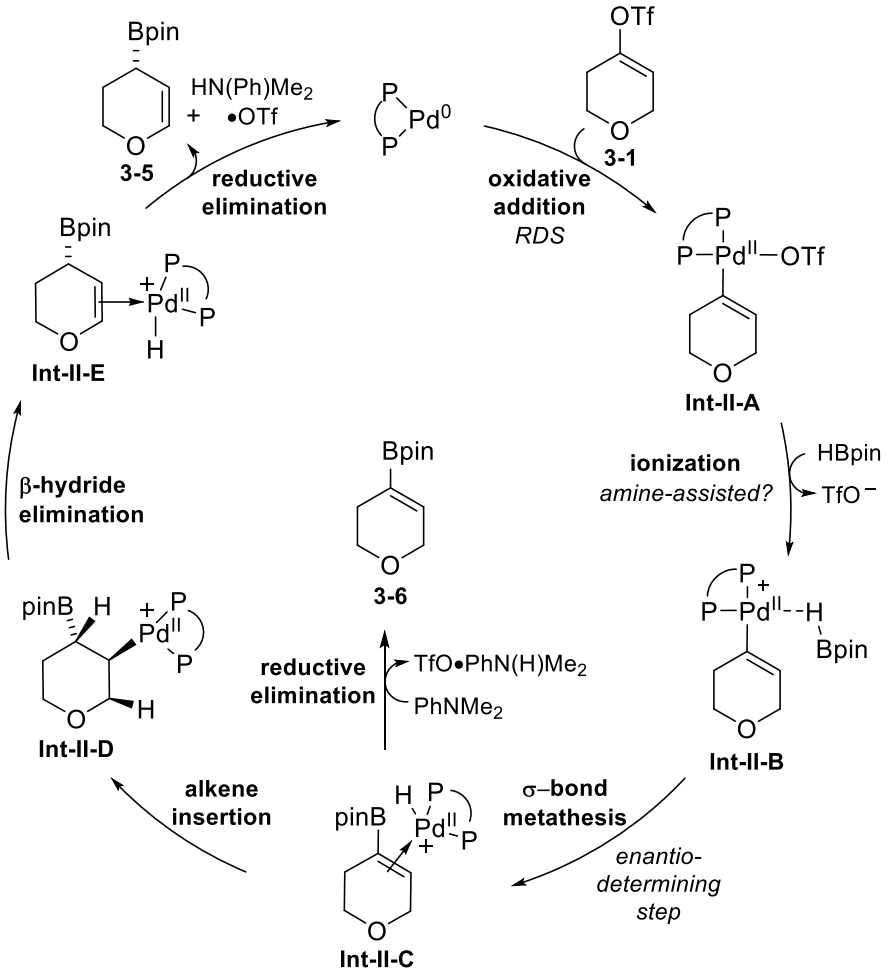

Figure 3-16. Proposed mechanism of the borylative migration.

The ratio of allylic boronate to alkenyl boronate formed depends on the heteroatom present and does not seem to be affected by the type of base present, but rather is thought to correlate with the hydricity of the allylic hydrogen in the alkenyl triflate/nonaflate electrophile. Conversely, the enantioselectivity appears to be inversely proportional to the pK_a of the conjugate acid of of the amine base used. Efforts to rationalize the relationship of the enantioselectivity to the amine and further characterize catalytic intermediates are currently underway.

3.8 Mechanistic considerations for the novel electrophiles in Chapter 2

3.8.1 Correlating a new mechanistic understanding with experimental observations

Section 2.3 of this thesis summarizes some initial results that were found during a screening of various nitrogen heterocycles as novel electrophiles in the borylative migration reaction. The initial test reactions were met with modest success using various substrates. A general summary of the results observed in the screening are recalled in Figure 3-17. Generally, the major product found throughout the screening was from an overall reductive deoxygenation of the alkenyl nonaflate. Considering the limited knowledge of the mechanism when this screening was performed, it was unclear how these major products could be forming. Moreover, attempting a thorough optimization from a starting point of little to no desired product was dauting considering the number of reagents in the borylative migration. However, in light of the new catalytic cycle described in the previous section, a brief analysis of the results from the unsucessful ring systems merits further discussion.

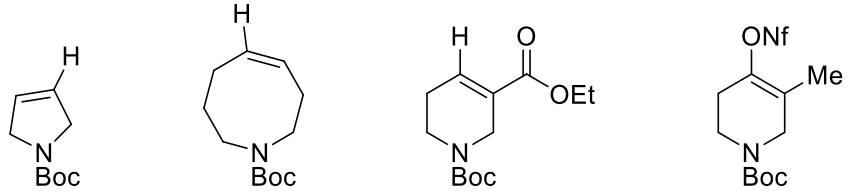

Figure 3-17. Generalized summary of the results in Section 2.3.

3.8.2 A precautionary note from the optimization of the azepanyl system

Considering that much more information was obtained during the optimization of the borylative migration with the azepanyl system, a few points regarding the results be highlighted as a precautionary point. Throughout the reaction optimization, the alkene-isomerized reduction product was observed as a consistent major by-product along with the alkenyl boronate (Tables 2-3 to 2-5). However, it is notable that complex mixtures were quite common as well, leading to the formation

of uncharacterized side products. Complex mixtures can be easily inferred by the fact that the sum of the alkenyl nonaflate, allylic boronate, alkenyl boronate and reduced side product was commonly quite low (c.f. Section 2.4.2, Tables 2-3 to 2-5). Furthermore, it was found that minor changes in the base, ligand and solvent led to detrimental results in many cases. Therefore, considering the complexity of the reaction mechanism and the varied results observed in the optimization of the azepanyl scaffold, it is important to appreciate that the analysis outlined in this section is by no means comprehensive. The primary purpose of this section is to provide guidance in further explorations of the borylative migration reaction and substrate scope expansions.

3.8.3 Complex mixtures with the methylated nonaflate

The mechanistic picture outlined in Section 3.7 provides a logical explanation for why a complex mixture could be observed with the methylated nonaflate. Although the products were not separable and could not be fully characterized, analysis of the crude ^{1}H and ^{11}B NMR suggested that a mixture of alkenyl and allylic boronates likely formed. Given the mechanism outlined in this chapter, the methylated scaffold has the opportunity to form three distinct borylated products (**3-17** to **3-19**) from the palladium hydride alkene insertion intermediate **Int-IV-D** (Figure 3-18a). Furthermore, if the steric hindrance from the methyl group allows for an inversion of regioselectivity during the alkene insertion step from **Int-IV-C** to **Int-IV-D'**, then a total of five borylated products can form from the methylated nonaflate including **3-20** and **3-21** (Figure 3-18b). However, proper characterization of the products formed in the reaction would be required for a more concrete determination of which borylated products form, which would be further complicated by the requirement of boronate oxidation to form stable allylic alcohols. Finally, it is important to note that only DPEPhos was tested in the reaction screening in Section 2.3.2 and that using Taniaphos as the ligand or a different amine base could lead to improved results.

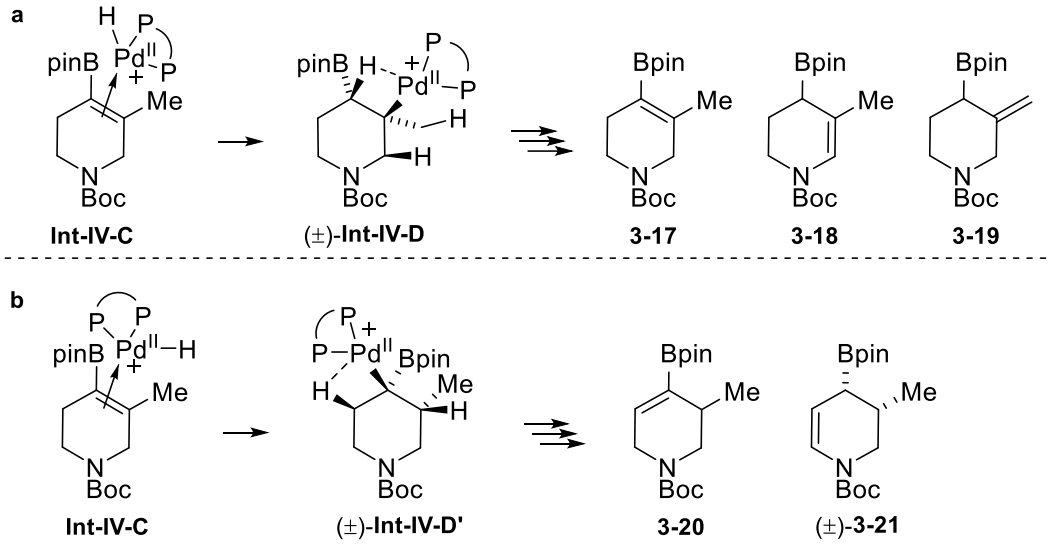

Figure 3-18. Possible borylated products from the methylated nonaflate.

3.8.4 Analysis of the potential reduction mechanisms of the alkenyl nonaflate

Based on the mechanism proposed in Section 3.7, many reasonable pathways can be envisioned to afford an overall reduction of the alkenyl nonaflate. For simplicity sake, three logical pathways will be discussed in this section. Furthermore, control reactions are proposed that could provide more conclusive evidence for an improved understanding of the borylative migration with other ring systems.

Mechanistically, the most straightforward explanation for the reduced products shown in Figure 3-17 is that the borylative migration mechanism is not affected by the changes in ring scaffold, but that the boronate products are more prone to protodeboronation than the pyranyl and piperidinyl scaffolds. An example of what that could look like mechanistically is shown in Scheme 3-14a, where amine coordination could promote an intermolecular protonation from the ammonium salt in solution. It is expected that the resulting ammonium boronate may not be stable, but could be further reduced by pinacolborane in solution to afford the ammonium salt and B_2pin_2. Control reactions can be easily envisioned to probe a protodeboronation pathway. For example, subjection of the alkenyl

boronates product(s) to the borylative migration reaction conditions would be a straightforward starting point, followed by checking reactivity in the presence of the amine and ammonium salt.

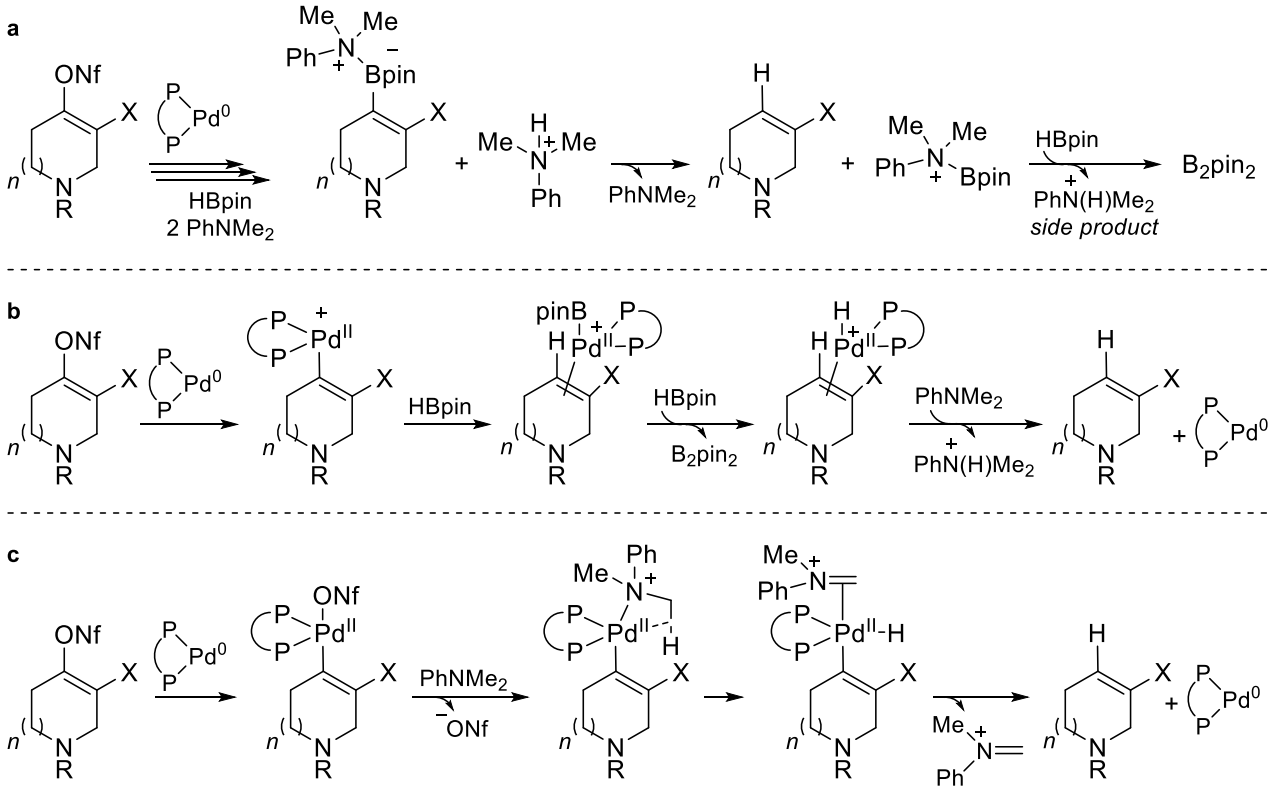

Scheme 3-14. Proposals for the observed reduced products by (a) protodeboronation (b) inversion of regioselectivity of the transmetallation or (c) protodematalation.

Alternatively, overall reduction could occur from inversion of the regioselectivity in the σ-bond metathesis step with pinacolborane post oxidative addition (Scheme 3-14b). An inverse in regioselectivity would cause the formation of a boronate-bound palladium complex. If the subsequent alkene insertion into the Pd-B bond in this complex is unfavourable, then many pathways could lead to the subsequent catalyst reduction. The palladium boronate complex could be deprotonated by dimethylaniline leading to products similar to the case in Scheme 3-14a. Alternatively, the Pd-Bpin intermediate could react with another equivalent of pinacolborane which would form a palladium hydride intermediate that would be quenched by the amine base, similarly

to that of the proposed catalytic cycle to form the allylic boronate of interest. A control reaction simply using D-Bpin would be very telling if this mechanistic scenario is at play.

Finally, a protometalation could occur after the oxidative addition (Scheme 3-14c). Considering the weak nucleophilicity of pinacolborane, it seems reasonable that coordination of dimethylaniline could compete, especially if either coordination of pinacolborane or the σ-bond metathesis is less favourable with certain substrates. After amine coordination, a β-hydride elimination would furnish the iminium and a palladium hydride. Subsequent reductive elimination would afford the overall reduced side product and regeneration of the catalyst. Although d_6-dimethylaniline would likely be difficult to obtain, a more simple control reaction would involve attempting the reaction in the absence of pinacolborane with a Pd(0) source.

Although the individual steps seem logical for all three pathways, the reason(s) for why there is such a drastic change in product distribution from the seemingly minor changes in the electrophiles remains unclear. Once the experimental studies described above are undertaken to clarify the mechanism at play, further calculations involving the unsuccessful scaffolds could provide important information to help substrate tailoring and a more successful outcome in subsequent optimizations of this reaction.

3.9 Summary

In summary, this chapter has presented evidence for a new mechanistic perspective of the borylative migration reaction using a combination of experimental and computational data. Experimental results have been obtained in support of a cationic palladium borylation pathway that has only been investigated computationally to-date with aryl iodides. The alkene isomerization involves a unique palladium hydride source, operating through a non-dissociative mechanism. Further insights have been obtained regarding the regio- and enantioselectivity of this reaction. With a new catalytic cycle

for the borylative migration deciphered, further studies involving the unsuccessful substrates from Section 3.2 could provide critical information in regard to expanding the substrate scope generality of this unique reaction. Finally, the efforts and conclusions described in this thesis chapter have the potential to provide further mechanistic insights in other metal-catalyzed borylation and palladium-catalyzed asymmetric methodologies.

3.10 Experimental

3.10.1 General information

Unless otherwise stated, all reactions were performed in flame-dried glassware under a nitrogen atmosphere. Diethyl ether (Et_2O) was distilled over sodium/benzophenone ketyl. Dioxane was distilled over sodium. Tetrahydrofuran (THF), toluene and DCM were purified using an MBraun MS SPS* solvent system. All other anhydrous solvents were purchased from Sigma Aldrich and used as received. All liquid amine and aniline bases were purchased from Sigma Aldrich or Combi-Blocks, distilled from calcium hydride and stored over potassium hydroxide before use. Pinacolborane (98%, HBpin) was purchased from Oakwood Chemicals and stored in a flame-dried pear-shaped flask in a –20 °C freezer under nitrogen atmosphere. 4-Piperidinone, HCl was purchased from Combi-Blocks and used as received. Palladium (II) acetate (99.95+%) was purchased from Strem. All other chemicals were purchased from Strem, Sigma Aldrich or Combi-Blocks and used as received. Piperidinyl allylic boronate (±)-**3-7** and alkenyl boronate **3-8** and allylboration product **3-18** were synthesized and characterized according to previously reported literature procedures.[4,3] Thin layer chromatography (TLC) was performed on silica gel 60 F254 plates and visualized using UV light, potassium permanganate ($KMnO_4$) and/or phosphomolybdic acid (PMA) stains. Flash chromatographic separations were performed with silica gel 60 using ACS grade solvents. Preparative thin-layer chromatography (pTLC) was performed on silica gel 60 F254

plates and visualized using UV light. ^{1}H NMR, ^{13}C NMR, ^{19}F NMR and ^{11}B NMR experiments were performed on 400 MHz, 500 MHz or 700 MHz instruments. The residual solvent ($CDCl_3$ or C_6H_6) protons (^{1}H) and carbons (^{13}C) were used as internal references. ^{1}H NMR data is presented as follows: chemical shift in ppm (δ) downfield from tetramethylsilane (multiplicity, coupling constant, integration). The following abbreviations are used in reporting the ^{1}H NMR data: s, singlet; br s, broad singlet; d, doublet; t, triplet; app t, apparent triplet; dd, doublet of doublet; m, multiplet. The error of coupling constants from ^{1}H NMR spectra is estimated to be 0.3 Hz. High-resolution mass spectra were recorded by the University of Alberta mass spectrometry services using electrospray ionization (ESI) techniques. Infrared (IR) experiments were performed using cast-film techniques with frequencies expressed in cm^{-1}. Optical rotations were measured using a 1 mL cell with a 10 cm length on a polarimeter by the University of Alberta analytical and instrumental laboratories. The enantiomeric excess ratios for optically enriched compounds were determined using a HPLC Agilent instrument with a Chiralpak IC or IB column.

3.10.2 Synthesis of borylative migration substrates

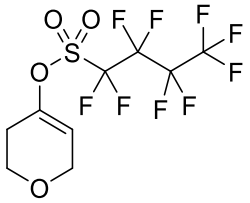

3,6-dihydro-2H-pyran-4-yl 1,1,2,2,3,3,4,4,4-nonafluorobutane-1-sulfonate (3-2): Following a modified literature procedure,[4] tetrahydro-4*H*-pyran-4-one (4.00 g, 40.0 mmol, 1.00 equiv) was dissolved in THF (80.0 mL, 0.500 M) and cooled to 0 °C. DBU (7.00 mL, 44.0 mmol, 1.10 equiv) was added followed by perfluorobutanesulfonyl fluoride (12.6 g, 42.0 mmol, 1.05 equiv) dropwise. The reaction was left to warm to room temperature in an ice bath overnight. The reaction was diluted

with ethyl acetate (50 mL) and water (50 mL), extracted with ethyl acetate three times (3 × 50 mL) and the combined organic phases were washed with brine then dried with anhydrous magnesium sulfate. The solution was filtered, concentrated *in vacuo* and purified by column chromatography (5% EtOAc/Hex, 1% Et_3N) to afford a clear, colourless oil (10.6 g, 69% yield): **^{1}H NMR** (700 MHz, $CDCl_3$) δ 5.85–5.81 (m, 1H), 4.26 (dt, *J* = 2.9, 2.9 Hz, 2H), 3.89 (t, *J* = 5.5 Hz, 2H), 2.46 (ttd, *J* = 5.5, 2.8, 1.4 Hz, 2H); **^{13}C NMR** (101 MHz, $CDCl_3$) δ 146.0 , 118.6 (t, *J* = 33.0 Hz), 117.0 , 115.7 (t, *J* = 33.0 Hz), 114.31 (t, *J* = 36.1 Hz), 109.9 (t, *J* = 36.1 Hz), 64.2 (d, *J* = 3.3 Hz), 64.0 (d, *J* = 3.7 Hz), 28.5 (d, *J* = 2.6 Hz); **^{19}F NMR** (377 MHz, $CDCl_3$) δ –80.8, –109.9, –121.1, –126.0; **HRMS** (EI) for $C_9H_7F_9O_4S$ calcd. 381.9921; found 381.9914.

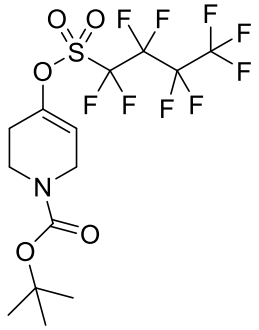

***tert*-butyl-4-(nonafluorobutylsulfonyloxy)-5,6-dihydropyridine-1(*2H*)-carboxylate (3-4)**: Following a modified literature procedure,[4] N-Boc-4-piperidone (3.98 g, 20.0 mmol, 1.00 equiv) was dissolved in THF (50.0 mL, 0.500 M) and cooled to 0 °C. DBU (3.40 mL, 11.0 mmol, 1.10 equiv) was added followed by perfluorobutanesulfonyl fluoride (6.36 g, 21.0 mmol, 1.05 equiv) dropwise. The reaction was left to warm to room temperature in an ice bath overnight. The reaction was diluted with ethyl acetate (50 mL) and water (50 mL), extracted with ethyl acetate three times (3 × 50 mL) and the combined organic phases were washed with brine then dried with anhydrous magnesium sulfate. The solution was filtered, concentrated *in vacuo* and purified by column chromatography (5% EtOAc/Hex, 1% Et_3N) to afford a clear, colourless oil, which solidified to a

white solid upon storing in a –20 °C freezer under argon atmosphere (8.86 g, 69% yield). The spectral data matched the literature: **^{1}H NMR** (400 MHz, $CDCl_3$) δ 5.77 (s, 1H), 4.11–3.99 (m, 2H), 3.63 (t, *J* = 5.7 Hz, 2H), 2.48–2.39 (m, 2H), 1.47 (s, 9H).

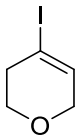

4-iodo-3,6-dihydro-2H-pyran (3-9): Following a modified literature procedure,[50] tetrahydro-4*H*-pyran-4-one (801 mg, 8.00 mmol, 1.00 equiv) was dissolved in EtOH (32 mL, 0.25 M), triethylamine (5.6 mL, 40 mmol, 5.0 equiv) and the reaction was cooled to 0 °C. Hydrazine (1M in THF, 40 mL, 40 mmol, 5.0 equiv) was added dropwise and the reaction was stirred at room temperature for one hour before the reaction was warmed to room temperature. The volatiles were carefully removed *in vacuo* before the residue was re-dissolved in DCM (50 mL, 0.16 M) and once again cooled to 0 °C. Iodine (≈ 6.10 g, 24.0 mmol, 3.0 equiv) was added in portions until in slight excess (cessation of nitrogen evolution, brown color not discharged). The reaction was warmed to room temperature and diluted in DCM (50 mL) and saturated aqueous sodium thiosulfate (50 mL), extracted with DCM three times (3 × 50 mL) and the combined organic phases were washed with water (2 × 50 mL), brine then dried with anhydrous sodium sulfate. The solution was filtered, concentrated *in vacuo*. The crude material was dissolved in toluene (16 mL, 0.50 M) and DBU (1.80 mL, 12.0 mmol, 1.50 equiv) then heated to 80 °C overnight. The reaction was cooled to room temperature, diluted with diethyl ether (20 mL) and 1M aqueous hydrochloric acid (20 mL). The aqueous phase was extracted with diethyl ether (3 × 20 mL) and the combined organic phases were washed with saturated aqueous sodium bicarbonate, water, brine and dried with anhydrous sodium sulfate. The reaction mixture was filtered and the volatiles were removed *in vacuo*. The crude reaction mixture was purified by column chromatography (25% DCM/Hex) to afford a pale yellow oil (1.14 g, 69% yield). All

characterization data matched the literature:[22] **^{1}H NMR** (400 MHz, $CDCl_3$, rotamers are present) δ 5.86–5.78 (m, 1H), 4.29–4.20 (m, 2H), 3.92–3.83 (m, 2H), 2.50–2.39 (m, 2H); **^{13}C NMR** (126 MHz, $CDCl_3$) δ 135.8, 90.5, 67.9, 65.8, 38.8; **HRMS** (EI) for C_5H_7OI calcd. 209.9542; found 209.9544.

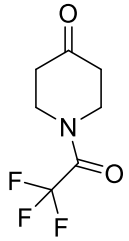

1-(2,2,2-Trifluoroacetyl)-4-piperidinone (3-10): Following a modified literature procedure,[2] 4-piperidone hydrochloride (2.00 g, 14.8 mmol, 1.00 equiv) was dissolved in DCM (40 mL, 0.37 M). Triethylamine (5.20 mL, 36.9 mmol, 2.50 equiv) was added and the reaction was cooled to 0 °C. trifluoroacetic anhydride (2.50 mL, 17.7 mmol, 1.20 equiv) was added dropwise and the reaction was left to warm to room temperature for 24 hours. The reaction was diluted with DCM (30 mL) and water (30 mL), extracted with DCM three times (3 × 30 mL) and the combined organic phases were washed with brine then dried with anhydrous magnesium sulfate. The solution was filtered, concentrated *in vacuo* and purified by column chromatography (20 to 25% EtOAc/Hex) to afford a white solid (1.28 g, 45% yield). All spectral data matches the literature:[51] **^{1}H NMR** (500 MHz, $CDCl_3$, rotamers are present) δ 3.96 (t, J = 6.4 Hz, 2H), 3.90 (t, J = 6.3 Hz, 2H), 2.64–2.49 (m, 4H); **^{13}C NMR** (126 MHz, $CDCl_3$, rotamers are present) δ 204.6, 155.9 (q, J = 37 Hz), 116.4 (q, J = 288 Hz), 44.1 (q, J = 3 Hz), 42.7, 41.0, 40.3; **^{19}F NMR** (469 MHz, $CDCl_3$) δ –69.1; **IR** (microscope, cm^{-1}) 2980, 2908, 1718, 1685, 1470, 1375, 1182, 1152, 1089; **HRMS** (EI) for $C_7H_8O_2F_3N$ calcd. 195.0507; found 195.0510.

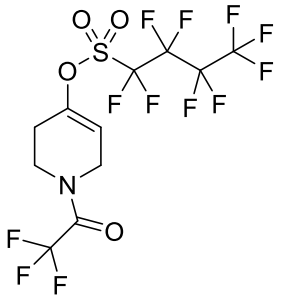

1-(2,2,2-trifluoroacetyl)-1,2,3,6-tetrahydropyridin-4-yl 1,1,2,2,3,3,4,4,4-nonafluorobutane-1-sulfonate (3-11): Following a modified literature procedure,[2] ketone **3-10** (1.28 g, 6.53 mmol, 1.0 equiv) was dissolved in THF (33 mL, 0.20 M) and cooled to –78 °C. LiHMDS (1.0 M in THF, 8.0 mL, 7.8 mmol, 1.20 equiv) was added and the reaction was stirred at room temperature for two hours. Perfluorobutanesulfonyl fluoride (2.17 g, 7.20 mmol, 1.10 equiv) was added dropwise and the reaction was left to warm to room temperature overnight. The reaction was diluted with EtOAc (25 mL) and saturated aqueous ammonium chloride (25 mL), extracted with EtOAc three times (3 × 25 mL) and the combined organic phases were washed with water and brine then dried with anhydrous magnesium sulfate. The solution was filtered, concentrated *in vacuo* and purified by column chromatography (5% EtOAc/Hex) to afford a light pale yellow solid (2.15 g, 69% yield): **^{1}H NMR** (500 MHz, $CDCl_3$, rotamers are present) δ 5.90–5.83 (m, 1H, rot A), 5.86–5.80 (m, 1H, rot B), 4.32–4.27 (m, 2H, rot A), 4.27–4.20 (m, 2H, rot B), 3.91 (t, *J* = 5.8 Hz, 2H, rot B), 3.81 (t, *J* = 5.8 Hz, 2H, rot A), 2.64–2.50 (m, 2H); **^{19}F NMR** (469 MHz, $CDCl_3$, rotamers are present) δ –69.3, –69.5, –80.7, –109.5, –120.9, –125.9; **IR** (microscope, cm^{-1}) 3049, 2979, 2908, 1718, 1687, 1470, 1374, 1268, 1183, 1089; **HRMS** (ESI-TOF) for $C_{11}H_7F_{12}NNaO_4S$ $(M + Na)^+$ calcd. 499.9796; found 499.9787.

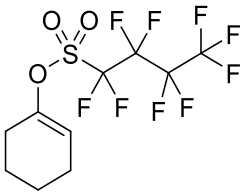

cyclohex-1-en-1-yl 1,1,2,2,3,3,4,4,4-nonafluorobutane-1-sulfonate (3-12): Following a similar procedure as for **3-11** using cyclohexanone (0.620 mL, 6.00 mmol, 1.00 equiv) was dissolved in THF (33 mL, 0.20 M) and cooled to 0 °C. LiHMDS (1.0 M in THF, 7.25 mL, 7.20 mmol, 1.20 equiv) was added and the reaction was stirred for one hour. Perfluorobutanesulfonyl fluoride (2.18 g, 7.20 mmol, 1.20 equiv) was added dropwise and the reaction was left to warm to room temperature overnight. The reaction was diluted with EtOAc (25 mL) and saturated aqueous ammonium chloride (25 mL), extracted with EtOAc three times (3 × 25 mL) and the combined organic phases were washed with water and brine then dried with anhydrous magnesium sulfate. The solution was filtered, concentrated *in vacuo* and purified by column chromatography (2.5% DCM/Hex + 0.5% Et_3N) to afford a clear, colourless oil (1.95 g, 85% yield). The spectral data matched the literature:[52]

^{1}H NMR (400 MHz, $CDCl_3$) δ 5.77 (td, J = 4.1, 1.9 Hz, 1H), 2.36–2.26 (m, 2H), 2.24–2.09 (m, 2H), 1.83–1.73 (m, 2H), 1.65–1.56 (m, 2H).

3.10.3 General procedure A: enantioselective borylation migration

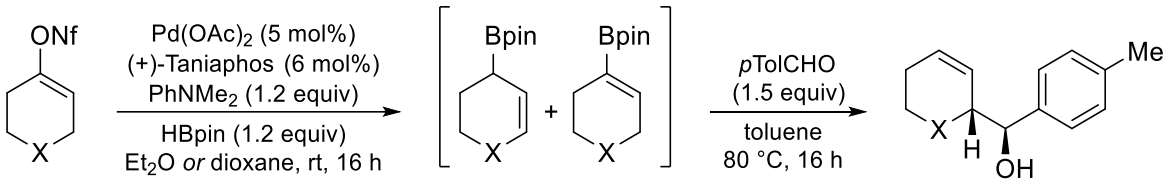

Following a modified literature procedure,[2] $Pd(OAc)_2$ (3.4 mg, 0.015 mmol, 5.0 mol%) and (+)-Taniaphos (12.4 mg, 0.018 mmol, 6.0 mol%) were dissolved in Et_2O or dioxane (4.8 mL, 0.063 M) and stirred for 20 minutes. $PhNMe_2$ (42 µL, 0.36 mmol, 1.2 equiv), HBpin (48 µL, 0.36 mmol, 1.2 equiv) and the alkenyl nonaflate (0.30 mmol, 1.0 equiv) were sequentially added and the reaction was left to stir at room temperature for 16 hours. The crude reaction mixture was sequentially filtered through a short silica plug with Et_2O (80 mL) and the volatiles were removed *in vacuo*. All ^{1}H NMR yields were determined by addition of 1,3,5-trimethoxybenzene (17 mg, 0.10 mmol, 0.33 equiv)

after the reaction was quenched. For reactions in which the allylboration was performed, the crude reaction mixture was transferred to a new flame-dried flask using toluene (0.20 M total) and *p*-tolualdehyde (66 µL, 0.45 mmol, 1.5 equiv) was added. The reaction was stirred at 80 °C for 16 hours. The volatiles were removed *in vacuo* and the crude reaction mixture was purified by column chromatography (eluent specified below).

3.10.4 General procedure B: racemic borylative migration

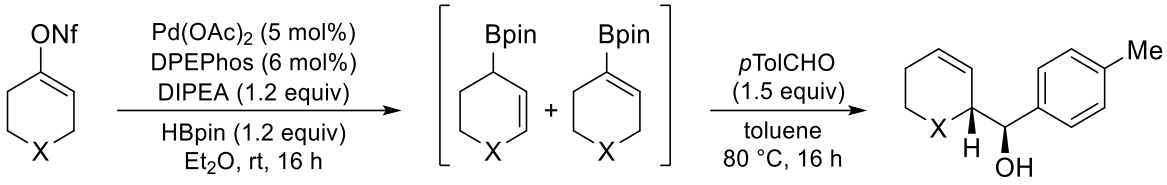

Following a modified literature procedure,[4] $Pd(OAc)_2$ (3.4 mg, 0.015 mmol, 5.0 mol%) and DPEPhos (9.7, 0.018 mmol, 6.0 mol%) were dissolved in Et_2O (4.8 mL, 0.063 M) and stirred for 20 minutes. DIPEA (58 µL, 0.36 mmol, 1.2 equiv), HBpin (48 µL, 0.36 mmol, 1.2 equiv) and the alkenyl nonaflate (0.30 mmol, 1.0 equiv) were sequentially added and the reaction was left to stir at room temperature for 16 hours. The crude reaction mixture was sequentially filtered through a short silica plug with Et_2O (80 mL) and the volatiles were removed *in vacuo*. For reactions in which the allylboration was performed, the crude reaction mixture was transferred to a new flame-dried flask using toluene (0.20 M total) and *p*-tolualdehyde (66 µL, 0.45 mmol, 1.5 equiv) was added. The reaction was stirred at 130 °C for two hours under microwave conditions or 80 °C for 16 hours. The volatiles were removed *in vacuo* and the crude reaction mixture was purified by column chromatography (eluent specified below).

3.10.5 Characterization of allylic and alkenyl boronates

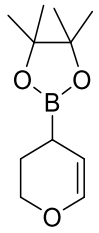

(±)-2-(3,4-dihydro-*2H*-pyran-4-yl)-4,4,5,5-tetramethyl-1,3,2-dioxaborolane (3-5): Synthesized following the general procedure B using **3-2** (115 mg, 0.300 mmol, 1.00 equiv). The crude reaction was purified by column chromatography (5% EtOAc/Hex) to afford a clear, colourless oil for characterization purposes (4 mg, 7% yield). Spectral data matched the literature:[3] **^{1}H NMR** (500 MHz, C_6D_6) δ 6.64 (dd, *J* = 6.3, 1.9 Hz, 1H), 5.04 (dd, *J* = 6.2, 3.7 Hz, 1H), 4.13 (ddd, *J* = 10.1, 7.0, 3.0 Hz, 1H), 3.99–3.91 (m, 1H), 2.09 (ddd, *J* = 12.6, 10.0, 7.0 Hz, 1H), 2.00–1.90 (m, 2H), 1.12 (s, 6H), 1.11 (s, 6H).

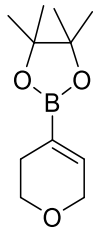

2-(3,6-dihydro-*2H*-pyran-4-yl)-4,4,5,5-tetramethyl-1,3,2-dioxaborolane (3-6): Following a modified literature procedure,[53] $Pd(dppf)Cl_2 \bullet CH_2Cl_2$ (109 mg, 0.144 mmol, 3.00 mol%), dppf (82.5 mg, 0.144 mmol, 3.00 mol%), bis(pinacolato)diboron (2.44 g, 9.60 mmol, 2.00 equiv), and potassium acetate (1.68 g, 16.8 mmol, 3.50 equiv) were dissolved in dioxane (10.7 mL, 0.449 M) and **3-2** (1.91 g, 4.8 mmol, 1.0 equiv) was added. The reaction was left to stir at 80 °C overnight. The reaction was cooled to room temperature, diluted in Et_2O and water (25 mL) and extracted with Et_2O (3 × 25 mL). The combined organic phases were washed with brine then dried with anhydrous sodium sulfate. The solution was filtered, concentrated *in vacuo* and purified by short silica plug

(1:4 EtOAc:Hex) and concentrated *in vacuo* to obtain **3-6** as a mixture with bis(pinolato)diboron. The mixture was dissolved in EtOAc (68 mL, 0.070 M) and a few drops of water were added followed by IBX (3.90 g, 13.9 mmol, 2.90 equiv). The reaction was heated to 80 °C with vigorous stirring for 3 hours. Upon cooled back to room temperature, the reaction mixture was filtered through a short silica plug (100% EtOAc) and the volatiles were removed *in vacuo*. The crude reaction mixture was purified by column chromatography (5% EtOAc/Hex) to afford a white solid (580 mg, 57% yield). The spectral data matched the literature:[3] **^{1}H NMR** (700 MHz, $CDCl_3$) δ 6.51–6.47 (m, 1H), 4.18–4.14 (m, 2H), 3.72 (t, *J* = 5.4 Hz, 2H), 2.22–2.16 (m, 2H), 1.23 (s, 12H).

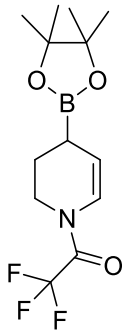

2,2,2-trifluoro-1-(4-(4,4,5,5-tetramethyl-1,3,2-dioxaborolan-2-yl)-3,4-dihydropyridin-1(2*H*)-yl)ethanone (3-13): Synthesized according to the general procedure B using **3-11** (476 mg, 1.00 mmol, 1.00 equiv). The crude material was purified by flash chromatography (7.5% EtOAc/Hex) to afford a clear, colourless oil (35 mg, 12% yield): **^{1}H NMR** (500 MHz, $CDCl_3$, rotamers are present) δ 7.03 (dd, *J* = 8.4, 2.1 Hz, 1H, rot A), 6.65 (dt, *J* = 8.3, 2.4 Hz, 1H, rot B), 5.43 (dd, *J* = 8.5, 3.6 Hz, 1H, rot A), 5.23 (dd, *J* = 8.3, 3.7 Hz, 1H, rot B), 3.83–3.67 (m, 2H), 2.05–1.83 (m, 3H), 1.24 (s, 12H); **^{13}C NMR** (126 MHz, $CDCl_3$, rotamers are present) δ 154.4 (q, *J* = 36 Hz), 153.9 (d, *J* = 37 Hz), 122.3, 121.8, 121.8, 121.8, 119.9 , 117.6 , 115.3, 115.2 , 113.4 , 83.9, 43.6, 43.6, 41.8, 24.8, 24.8 , 24.8, 24.7, 23.3, 22.7, 19.0 (br); **^{19}F NMR** (469 MHz, $CDCl_3$) δ –68.83, –69.1; **^{11}B NMR**

(160 MHz, $CDCl_3$) δ 32.5; **IR** (microscope, cm^{-1}) 2981, 1697, 1372, 1331, 1208, 1000; **HRMS** (EI) for $C_{13}H_{19}NO_3BF_3$ calcd. 305.1410; found 305.1402.

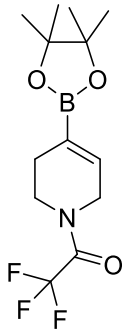

2,2,2-trifluoro-1-(4-(4,4,5,5-tetramethyl-1,3,2-dioxaborolan-2-yl)-5,6-dihydropyridin-1(2*H*)-yl)ethanone (3-14): Synthesized according to the general procedure B using **3-11** (476 mg, 1.00 mmol, 1.00 equiv). The crude material was purified by flash chromatography (7.5% EtOAc/Hex) to afford a clear, colourless oil (85 mg, 28% yield): **^{1}H NMR** (500 MHz, $CDCl_3$, rotamers are present) δ 6.50– 6.44 (m, 1H, rot A), 6.42–6.36 (m, 1H, rot B), 4.18–4.11 (m, 2H), 3.69 (t, *J* = 5.7 Hz, 2H, rot B), 3.62 (t, *J* = 5.6 Hz, 2H, rot A), 2.37–2.24 (m, 2H), 1.25 (s, 12H); **^{13}C NMR** (126 MHz, $CDCl_3$, rotamers are present) δ 155.8 (q, *J* = 36 Hz), 155.7 (q, *J* = 36 Hz), 136.7, 135.6, 128.4 (br), 116.5 (d, *J* = 288 Hz), 116.5 (q, *J* = 288 Hz), 83.8, 83.7, 45.4 (q, *J* = 4 Hz), 44.2, 42.8 (q, *J* = 3.6 Hz), 40.3, 26.6, 25.4, 24.8; **^{19}F NMR** (469 MHz, $CDCl_3$) δ –69.4, –69.6; **^{11}B NMR** (160 MHz, $CDCl_3$) δ 29.5; **IR** (microscope, cm^{-1}) 2984, 2918, 1700, 1643, 1392, 1331, 1209, 1151, 1022; **HRMS** (EI) for $C_{13}H_{19}NO_3BF_3$ calcd. 305.1410; found 305.1408.

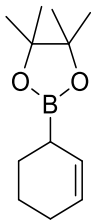

2-(cyclohex-2-en-1-yl)-4,4,5,5-tetramethyl-1,3,2-dioxaborolane (3-15): Synthesized according to the general procedure A using cyclohexenyl nonaflate **3-12** (114 mg, 0.300 mmol, 1.00 equiv).

Purification by column chromatography (20% DCM/hexanes) after the borylative migration step afforded compound **3-15** as a mixture with **3-16** as a clear, colourless oil for characterization purposes. Spectral data matched with the literature:[54] **^{1}H NMR** (500 MHz, $CDCl_3$) δ 5.7 –5.57 (m, 2H), 2.03–1.93 (m, 2H), 1.88–1.60 (m, 5H), 1.25 (s, 12H).

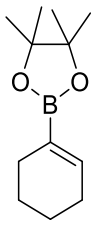

2-(cyclohex-1-en-1-yl)-4,4,5,5-tetramethyl-1,3,2-dioxaborolane (3-16): Synthesized using general procedure A. Isolated after the allylboration step by purification by column chromatography (2.5 to 5% EtOAc/Hex) to afford a clear, colourless oil (22 mg, 35% yield). The spectral data matched the literature:[55] **^{1}H NMR** (500 MHz, $CDCl_3$) δ 6.59–6.53 (m, 1H), 2.13–2.04 (m, 4H), 1.63–1.53 (m, 4H), 1.25 (s, 12H).

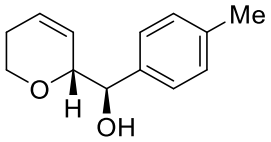

(*R*)-((*R*)-5,6-dihydro-2*H*-pyran-2-yl)(*p*-tolyl)methanol (3-17): Synthesized according to the general procedure A using **3-2** (112 mg, 0.300 mmol, 1.00 equiv) in Et_2O. The crude material was purified by flash chromatography (5 to 10% EtOAc/Hex) to afford a clear, colourless oil (35 mg, 63% yield). All characterization data matched the literature:[56] **^{1}H NMR** (400 MHz, $CDCl_3$) δ 7.27 (d, *J* = 7.4 Hz, 2H), 7.17 (d, *J* = 7.9 Hz, 2H), 5.95–5.84 (m, 1H), 5.36 (ddd, *J* = 10.4, 2.4, 2.1 Hz, 1H), 4.51 (d, *J* = 8.0 Hz, 1H), 4.15–4.09 (m, 2H), 4.04 (dt, *J* = 11.2, 4.7 Hz, 1H), 3.74 (ddd, *J* = 11.2, 8.3, 4.3 Hz, 1H), 3.09 (s, 1H), 2.35 (s, 3H), 2.33–2.15 (m, 1H), 2.10–1.97 (m, 1H); **^{13}C NMR** (101 MHz, $CDCl_3$) δ 137.8, 136.9, 129.1, 127.3, 126.7, 126.0, 78.1, 77.4, 77.1, 76.7, 76.3, 62.7,

25.2, 21.2; **HRMS** (ESI) for $C_{13}H_{16}NaO_2$ calcd. 227.1043; found 227.1041; **HPLC** (Chiralpak IB) 1:99 iso-propanol:hexanes, 0.5 mL/min, 20 °C, λ = 230 nm, T_{minor} = 15.5 min, T_{major} = 17.2 min, er = 95.1:4.9.

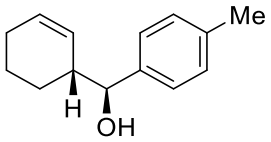

(±)-(*S*)-((*R*)-cyclohex-2-en-1-yl)(*p*-tolyl)methanol (3-19): Synthesized according to the general procedure A using **3-12** (107 mg, 0.300 mmol, 1.00 equiv) in Et_2O. The crude material was purified by flash chromatography (5% EtOAc/Hex) to afford a clear, colourless oil (11 mg, 19% yield): **^{1}H NMR** (400 MHz, $CDCl_3$) δ 7.23 (d, *J* = 8.0 Hz, 2H), 7.16 (d, *J* = 7.9 Hz, 3H), 5.80 (dt, *J* = 10.3, 3.9 Hz, 1H), 5.40–5.35 (m, 1H), 4.54 (d, *J* = 6.7 Hz, 1H), 2.53–2.44 (m, 1H), 2.35 (s, 3H), 2.04–1.95 (m, 2H), 1.84–1.67 (m, 2H), 1.59–1.44 (m, 2H); **^{13}C NMR** (126 MHz, $CDCl_3$) 140.0, 137.1, 130.2, 129.0, 128.1, 126.5, 77.4, 43.0, 29.8, 25.3, 24.1, 21.2; **IR** (microscope, cm^{-1}) 3408, 3023, 2926, 2859, 1514, 1447, 1028, 1016; **HRMS** (EI) for $C_{14}H_{16}$ (M–H_2O) calcd. 184.1252; found 184.1248; **HPLC** (Chiralpak IC) 3:97 iso-propanol:hexanes, 0.5 mL/min, 20 °C, λ = 220 nm, T_{minor} = 10.6 min, T_{major} = 11.6 min, er = 49.8:50.2.

3.10.6 General procedure for the kinetic experiments

<u>3 mol% palladium source:</u>

$Pd_2(dba)_3$●$CHCl_3$ (1.8 mg, 1.9 μmol, 3.0 mol%), (+)-Taniaphos (1.8 mg, 2.5 μmol, 4.0 mol%) and 1,3,5-trimethoxybenzene (3.6 mg, 21 μmol, 0.33 equiv) were added to an oven-dried J-Young NMR tube containing a small stir bar and capped with a septum which was evacuated and re-filled with

argon four times. Dry d_2-dichloromethane (0.75 mL) was added and the reaction mixture was stirred for 15 minutes. The small stir bar was quickly removed and the headspace of the NMR tube was flushed with argon for two minutes before resealing the tube with a septum. $PhNMe_2$ (10 µL, 79 µmol, 1.3 equiv) and HBpin (11 µL, 76 µmol, 1.2 equiv) were measured in separate gas-tight syringes and capped with a septum under nitrogen. Alkenyl nonaflate **3-4** (30.1 mg, 62.5 µmol, 1.00 equiv) was weighed into a tared gas-tight syringe and capped with a septum. Once the array parameters were set using a standard sample containing d_2-dichloromethane, $PhNMe_2$, HBpin and the alkenyl nonaflate **3-4** were sequentially added. The septum was quickly replaced with the J-Young NMR tube cap. The reaction mixture was shaken vigorously for ten seconds and the sample was inserted into the magnet. All measurements were acquired via continuous measurement arrays using a pre-acquisition delay (PAD) using Agilent instruments with the following parameters: steps = 120; starting value = 10; array increment = 0; nt = 4; ss = 0; pad[1] = 0. All spectra were phased, baseline-corrected, and the data obtained using VnmrJ software. The data was transferred to an excel spreadsheet and manipulated as required to obtained concentration over time by relative integration to the 1,3,5-trimethoxybenzene internal standard.

<u>0.3 mol% palladium source:</u>

$Pd_2(dba)_3 \bullet CHCl_3$ (1.8 mg, 1.9 µmol, 3.0 mol%) and (+)-Taniaphos (1.8 mg, 2.5 µmol, 4.0 mol%) and were added to round bottom flask and dissolved in dry d_2-dichloromethane (1.0 mL) and stirred for five minutes. An aliquot of the catalyst mixture (100 µL) was transferred to oven-dried J-Young NMR tube containing 1,3,5-trimethoxybenzene (3.6 mg, 21 µmol, 0.33 equiv) and a small stir bar, which was capped with a septum under argon. The mixture was diluted with dry d_2-dichloromethane (0.65 mL) and the reaction mixture was stirred for 15 minutes. The small stir bar was quickly removed and the headspace of the NMR tube was flushed with argon for two minutes after resealing

the tube with a septum. $PhNMe_2$ (10 µL, 79 µmol, 1.3 equiv) and HBpin (11 µL, 76 µmol, 1.2 equiv) were measured in separate gas-tight syringes and capped with a septum under nitrogen. Alkenyl nonaflate **3-4** (30.1 mg, 62.5 µmol, 1.00 equiv) was weighed into a tared gas-tight syringe and capped with a septum. Once the array parameters were set using a standard sample containing d_2-dichloromethane, $PhNMe_2$, HBpin and the alkenyl nonaflate **3-4** were sequentially added. The septum was quickly replaced with the J-Young NMR tube cap. The reaction mixture was shaken vigorously for ten seconds and the sample was inserted into the magnet. All measurements were acquired via continuous measurement arrays using a pre-acquisition delay (PAD) using Agilent instruments with the following parameters: steps = 180; starting value = 50; array increment = 0; nt = 4; ss = 0; pad[1] = 0. All spectra were phased, baseline-corrected, and the data obtained using VnmrJ software. The data was transferred to an excel spreadsheet and manipulated as required to obtained concentration over time by relative integration to the 1,3,5-trimethoxybenzene internal standard.

3.10.7 Details of the DFT calculations

The geometry optimizations were performed using the Gaussian 16 software package[57] with the M06[58] density functional, in combination with the 6-31G(d)[59] basis set for all atoms except palladium, for which LANL2DZ(ECP) was used.[60] Unless otherwise stated, the default (99,590) density grid was used for numerical integration in the calculations. The structures were optimized in the gas phase and include the Grimme dispersion correction using the original D3 damping function (D3(0)).[61] Harmonic vibrational frequencies were computed for all optimized structures to verify that they were either minima or transition states, possessing zero or one imaginary frequency, respectively. Single points energy calculations were performed using the M06 density functional, with the 6-31+G(d,p) basis set for all atoms except palladium, for which SDD(MWB28)[62] was used.

The single points were also performed using a solvation model (SMD) for 1,4-dioxane,[63] and include the Grimme dispersion correction using the original D3 damping function (D3(0). All the free energies (M06-D3(0)/6-31+G(d,p)SDD(Pd)SMD(1,4-dioxane)//M06-D3(0)/6-31G(d)) are reported in kcal mol^{-1}. They incorporate unscaled thermochemical corrections based on the vibrational analyses, using a temperature of 298.15 K and pressure of 1 atm. Additionally, the free energies were corrected to a 1M standard state using a +1.89 kcal mol^{-1} correction.

3.11 References

[1] a) J. Ding, D. G. Hall, *Angew. Chem. Int. Ed.* **2013**, *52*, 8069.; b) J. Ding, T. Rybak, D. G. Hall, *Nat. Commun.* **2014**, *5*, 5474.

[2] H. A. Clement, D. G. Hall, *Tetrahedron Lett.* **2018**, *59*, 4334.

[3] S. Lessard, F. Peng, D. G. Hall, *J. Am. Chem. Soc.* **2009**, *131*, 9612.

[4] Y.-R. Kim, D. G. Hall, *Org. Biomol. Chem.* **2016**, *14*, 4739.

[5] M. Murata, T. Oyama, S. Watanabe, Y. Masuda, *Synthesis* **2000**, *6*, 778.

[6] a) W. K. Chow, O. Y. Yuen, P. Y. Choy, C. M. So, C. Po Lau, W. T. Wong, F. Y. Kwong, *RSC Advances*, **2013**, *3*, 12518.; (b) T. Ishiyama, M. Murata, N. Miyaura, *J. Org. Chem.* **1995**, *60*, 7508.

[7] a) M. Murata, S. Watanabe, Y. Masuda, *J. Org. Chem.* **1997**, *62*, 6458.; b) M. Murata, S. Watanabe, Y. Masuda, *J. Org. Chem.* **2000**, *65*, 164.

[8] J. F. Hartwig *Organotransition Metal Chemistry - From Bonding to Catalysis*, 2nd edition; University Science Books: Mill Valley, California, 2010; pp 877–951.

[9] K. C. Lam, T. B. Marder, Z. Lin, *Organometallics* **2010**, *29*, 1849.

[10] M. Yamashita, K. Nozaki in *Synthesis and Application of Organoboron Compounds*, E. Fernández, A. Whiting, Chapter 1, Springer, 2015, 2–34.

[11] a) Y. Yamamoto, K. Nogi, H. Yorimitsu, A. Osuka, *ChemistrySelect* **2017**, *2*, 1723.; (b) M. Murata, T. Oda, Y. Sogabe, H. Tone, T. Namikoshi, S. Watanabe, *Chem. Lett.* **2011**, *40*, 962.

[12] a) Z.-D. Yang, R. Pal, G. L. Hoang, X. C. Zeng, J. M. Takacs, *ACS Catal.* **2014**, *4*, 763.; b) T. P. Pabst, J. V. Obligacion, E. Rochette, I. Pappas, P. J. Chirik, *J. Am. Chem. Soc.* **2019**, *141*, 15378.

[13] C. Pubill-Ulldemolins, A. Bonet, C. Bo, H. Gulyás, Elena Fernández, *Org. Biom. Chem.* **2010**, *8*, 2667.

[14] M. Satoh, Y. Nomoto, N. Miyaura, S. Suzuki, *Tetrahedron Lett.* **1989**, *30*, 3789.; b) Y. Matsumoto, M. Nalto, T. Hayashi, *Organometallics* **1992**, *11*, 2732.

[15] I. P. Beletskaya, A. V. Cheprakov, *Chem. Rev.* **2000**, *100,* 3009.

[16] D. Mc Cartney, P. J. Guiry, *Chem. Soc. Rev.*, **2011**, ***40***, 5122.

[17] A. Ashimori, B. Bachand, M. A. Calter, S. P. Govek, L. E. Overman, D. J. Poon, *J. Am. Chem. Soc.* **1998,** *120,* 6488.

[18] a) L. M. Alcazar-Roman, J. F. Hartwig, *Organometallics* **2002**, *21*, 491.; b) J. F. Hartwig *Organotransition Metal Chemistry - From Bonding to Catalysis*, 2nd edition; University Science Books: Mill Valley, California, 2010; pp 877–951.

[19] J. L. Hofstra, K. E. Poremba, A. M. Shimozono, S. E. Reisman, **2019**, *58*, 14901.

[20] D. H. R. Barton, R. E. O'Brien, S. Sternhell, *J. Chem. Soc.* **1962**, 470.

[21] a) D. P. Ojha, K. R. Prabhu, *Org. Lett.* **2015**, *17*, 18.; b) K. Lee, D. F. Wiemer, *Tetrahedron Lett.* **1993**, *34*, 2433.

[22] J. Son, T. W. Reidl, K. H. Kim, D. J. Wink, L. L. Anderson, *Angew. Chem. Int. Ed.* **2018**, *57*, 6597.

[23] G. J. Lovinger, M. D. Aparece, J. P. Morken, *J. Am. Chem. Soc.* **2017**, *139*, 3153.

[24] A. Jutand, Serge Négri, *Organometallics* **2003**, *22*, 4229.

[25] H. Xie, H. Zhang, Z. Lin, *Organometallics* **2013**, *32*, 2336.

[26] a) J. M. Dennis, N. A. White, R. Y. Liu, S. L. Buchwald, *ACS Catal.* **2019**, *9*, 3822,; b) S.-T. Kim, B. Pudasaini, M.-H. Baik, *ACS Catal.* **2019**, *9*, 6851.

[27] a) L. M. Alcazar-Roman, J. F. Hartwig, *Organometallics* **2002**, *21*, 491.; b) J. M. Dennis, N. A. White, R. Y. Liu, S. L. Buchwald, *J. Am. Chem. Soc.* **2018**, *140*, 4721.

[28] a) A. Milet, A. Dedieu, G. Kapteijn, G. van Koten, *Inorg. Chem.* **1997,** *36,* 3223.; b) Z. Lin, *Coord. Chem. Rev.* **2007**, *251*, 2280.

[29] V. Vasilenko, C. K. Blasius, L. H. Gade, *J. Am. Chem Soc.* **2018**, *140*, 9244.

[30] T. Kochi, S. Kanno, F. Kakiuchi, *Tetrahedron Lett.* **2019**, *60*, 150938.

[31] a) D. A. Petrone, I. Franzoni, J. Ye, J. F. Rodríguez, A. I. Poblador-Bahamonde, M. Lautens, *J. Am. Chem. Soc.* **2017**, *139*, 3546.; b) J. F. Rodríguez, K. I. Burton, I. Franzoni, D. A. Petrone, I. Scheipers, M. Lautens, *Org. Lett.* **2018**, *20*, 6915.

[32] P. Kisanga, L. A. Goj, R. A. Widenhoefer, *J. Org. Chem.* **2001,** *66,* 635.

[33] Examples with enol ethers: a) T. Moriya, A. Suzuki, N. Miyaura, *Tetrahedron Lett.* **1995**, *11*, 1887.; b) Y. Yamamoto, T. Miyairi, T. Ohmura, N. Miyaura, *J. Org. Chem.* **1999,** *64,* 296.

[34] Selected Pd-H examples: a) D. P. Ojha, K. Gadde, K. R. Prabhu, *J. Org. Chem.* **2017**, *82*, 4859.; b) T. Miura, J. Nakahashi, M. Murakami*, Angew. Chem. Int. Ed.* **2017**, *56*, 6989.

[35] a) B. J. Stokes, A. J. Bischoff, M. S. Sigman, *Chem. Sci.* **2014**, *4*, 2336.; b) H. H. Patel, M. S. Sigman, *J. Am. Chem. Soc.* **2015**, *137*, 3462.; c) R. J. DeLuca, B. J. Stokes, M. S. Sigman*, Pure Appl. Chem.* **2014**, *86*, 395.

[36] a) I. D. Hills, G. Fu, *J. Am. Chem. Soc.* **2004**, *126*, 13178.; b) D. A. Petrone, I. Franzoni, J. Ye, J. F. Rodríguez, A. I. Poblador-Bahamonde, M. Lautens, *J. Am. Chem. Soc.* **2017**, *139*, 3546.; c) P. Mamone, M. F. Grünberg, A. Fromm, B. A. Khan, L. J. Gooßen, *Org. Lett.* **2012**, *14*, 3716.

[37] H. Sommer, F. Juliá-Hernández, R. Martin, I. Marek, *ACS Cent. Sci.* **2018**, *4*, 153.

[38] K. Farshadfar, A. Chipman, M. Hosseini, B. F. Yates, A. Ariafard, *Organometallics* **2019**, *38*, 2953.

[39] K. Nilsson, A. Hallberg, *J. Org. Chem.* **1990**, *55*, 2464.

[40] a) D. G. Blackmond, *J. Am. Chem. Soc.* **2015**, *137*, 10852.; b) J. S. Mathew, M. Klussmann, H. Iwamura, F. Valera, A. Futran, E. A. Emanuelsson, D. G. Blackmond, *J. Org. Chem.* **2006**, *71*, 4711.

[41] C. D.-T. Nielsen, J. Burés, *Chem. Sci.*, **2019**, *10*, 348.

[42] J. Burés, *Angew. Chem. Int. Ed.* **2016**, *55*, 16084.

[43] R. D. Baxter, D. Sale, K. M. Engle, J.-Q. Yu, D. G. Blackmond, *J. Am. Chem. Soc.* **2012**, *134*, 4600.

[44] J. Burés, *Angew. Chem. Int. Ed.* **2016**, *55*, 2028.

[45] T. Rosner, J. Le Bars, A. Pfaltz, D. G. Blackmond, *J. Am. Chem. Soc.* **2001,** *123,* 1848.

[46] a) http://evans.rc.fas.harvard.edu/pdf/evans_pKa_table.pdf, accessed 07/10/2-19; b) *CRC Handbook of Tables for Organic Compound Identification*, Third Edition, CRC Press, Boca Raton, Florida, 1984, 438.

[47] a) T. Havashi, A. Kubo, F. Ozawa, *Pure & Appl. Chem.* **1992**, *64*, 421.; b) F. Ozawa, A. Kubo, Y. Matsumoto, T. Hayashi, *Organometallics* **1993**, *12*, 4188.; c) F. Ozawa, A. Kubo, T. Hayashi, *Tetrahedron Lett.* **1992**, *33*, 1485.

[48] K. K. Hii, T. D. W. Claridge, J. M. Brown, *Angew. Chem. Int. Ed. Engl.* **1997**, *9*, 984.

[49] S. Lessard, M.Sc. Dissertation, University of Alberta, **2009**.

[50] A. Fernández-Mateos, G. P. Coca, R. R. González, C. T. Hernández, *J. Org. Chem.* **1996**, *61*, 9097.

[51] P. Wessig, K. Möllnitz, *J. Org. Chem.* **2008**, *73*, 4452.

[52] S. Zhang, H. Neumann, M. Beller, *Chem. Commun.* **2019**, *55*, 5938.

[53] G. M. Gallego, R. Sarpong, *Chem. Sci.* **2012**, *3*, 1338.

[54] G. Dutheuil, N. Selander, K. J. Szabó, V. K. Aggarwal, *Synthesis* **2008**, *14*, 2293.

[55] N. Selander, B. Willy, K. J. Szabó, *Angew. Chem. Int. Ed.* **2010**, *49*, 4051.

[56] R. M. Al-Zoubi, D. G. Hall, *Mol. Divers.* **2014**, *18*, 701.

[57] Gaussian 16, Revision A.03, M. J. Frisch, G. W. Trucks, H. B. Schlegel, G. E. Scuseria, M. A. Robb, J. R. Cheeseman, G. Scalmani, V. Barone, B. Mennucci, G. A. Petersson, H. Nakatsuji, M. Caricato, X. Li, H. P. Hratchian, A. F. Izmaylov, J. Bloino, G. Zheng, J. L. Sonnenberg, M. Hada, M. Ehara, K. Toyota, R. Fukuda, J. Hasegawa, M. Ishida, T. Nakajima, Y. Honda, O. Kitao, H. Nakai, T. Vreven, J. A. Montgomery, Jr., J. E. Peralta, F. Ogliaro, M. Bearpark, J. J. Heyd, E. Brothers, K. N. Kudin, V. N. Staroverov, R. Kobayashi, J. Normand, K. Raghavachari, A. Rendell, J. C. Burant, S. S. Iyengar, J. Tomasi, M. Cossi, N. Rega, J. M. Millam, M. Klene, J. E. Knox, J. B. Cross, V. Bakken, C. Adamo, J. Jaramillo, R. Gomperts, R. E. Stratmann, O. Yazyev, A. J. Austin, R. Cammi, C. Pomelli, J. W. Ochterski, R. L. Martin, K. Morokuma, V. G. Zakrzewski, G. A. Voth, P. Salvador, J. J. Dannenberg, S. Dapprich, A. D. Daniels, Ö. Farkas, J. B. Foresman, J. V. Ortiz, J. Cioslowski, D. J. Fox, Gaussian, Inc., Wallingford CT, 2016.

[58] Y. Zhao, D. G. Truhlar, *Theor. Chem. Acc.* **2008**, *120*, 215.

[59] a) J. W. Hehre, R. Ditchfield, J. A. Pople, *J. Chem. Phys.* **1972**, *56*, 2257.; b) P. C. Hariharan, J. A. Pople, *Theor. Chim. Acta.* **1973**, *28*, 213.

[60] a) P. J. Hay, W. R. Wadt, *J. Chem. Phys.* **1985**, *82*, 284.; b) C. E. Check, T. O. Faust, J.M. Bailey, B. J. Wright, T. M. Gilbert, L. S. Sunderlin, *J. Phys. Chem. A* **2001**, *105*, 8111.

[61] S. Grimme, J. Antony, S. Ehrlich, H. Krieg, *J. Chem. Phys.* **2010**, *132*, 154104.

[62] M. Dolg, U. Wedig, H. Stoll, H. Preuß, *J. Chem. Phys.* **1987**, *86*, 866.

[63] A. V. Marenich, C. J. Cramer, D. G. Truhlar, *J. Phys. Chem. B* **2009**, *113*, 6378.

Chapter 4: Enantioselective Conjugate Borylation to Access Synthetically Versatile Cyclobutylboronates

4.1 Introduction

Cyclobutane rings are embedded in the structure of numerous natural products and medicines (Figure 4-1).[1] In drug discovery, cyclobutyl moieties are often employed to impose spatial pharmacophore rigidification and have also been identified as non-traditional bioisosteres of arenes.[2]

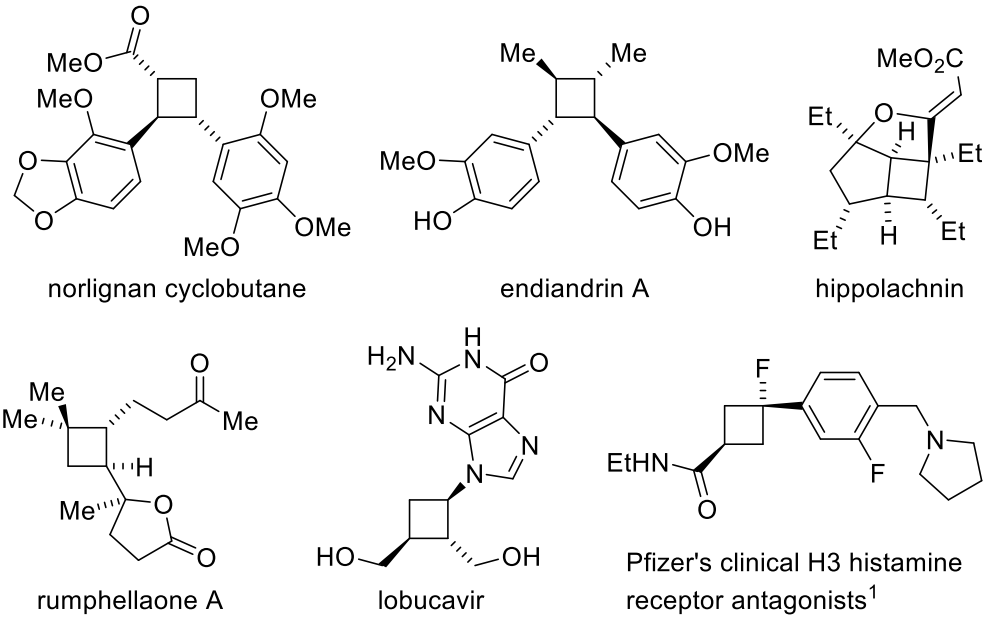

Figure 4-1. Examples of stereochemically complex cyclobutane-containing natural products and pharmaceutical drugs.

Compared to cyclopentane and cyclohexane homologs, relatively fewer synthetic methods exist to produce functionalized chiral cyclobutanes in high enantioselectivity.[3] One of the primary challenges for the enantioselectivite synthesis of cyclobutane rings is the inherent ring strain of the four membered rings. For comparison, a non-substituted cyclobutane ring contains a strain energy of 26.7 kcal mol^{-1}, whereas the strain energy contained in the cyclopentane homologue is 7.4 kcal

mol^{-1}.[4] The most common approach to cyclobutanes involves the use of [2+2] cycloaddition chemistry which has been explored extensively in an enantioselective fashion and typically results in specific fused ring systems.[5]

Owing to the versatility of the boronyl substituent as a precursor to C–O, C–N, C–C and C–X bonds, there is significant interest in the development of efficient methods to prepare chiral cyclobutylboronates in optically enriched form. Moreover, the boronyl unit can be employed as a potential handle to install a cyclobutyl unit into a medicinal scaffold via transition metal catalyzed Suzuki-Miyaura cross-coupling or O–/N–arylation.[6] However, stereoselective methods to prepare optically enriched cyclobutylboronates are scarce and generally limited in scope.[7]

A few diastereoselective approaches to enantioenriched cyclobutylboronates with chiral auxiliaries have been reported. Matteson and co-workers reported a multistep approach based on the stereospecific cyclization of a stabilized carbanion onto a chiral α-chloroboronic ester (Figure 4-2a).[8] Didier and co-workers disclosed an approach to alkylidenecyclobutanes through an allylic cyclobutenylboronate intermediate also using a chiral boronic ester and a Matteson homologation approach with cyclobutenyl zinc reagents (Figure 4-2b).[9] However, the the cyclobutenylboronate intermediates were not isolated and used directly in aldehyde allylboration chemistry furnishing the expected diastereoselectivity. Finally, Bach and co-workers reported an enantiofacial-selective photochemical [2+2] cycloaddition between an alkenyl boronate and isoquinolone promoted by a stoichiometric chiral hydrogen-bonding template (Figure 4-2c).[10]

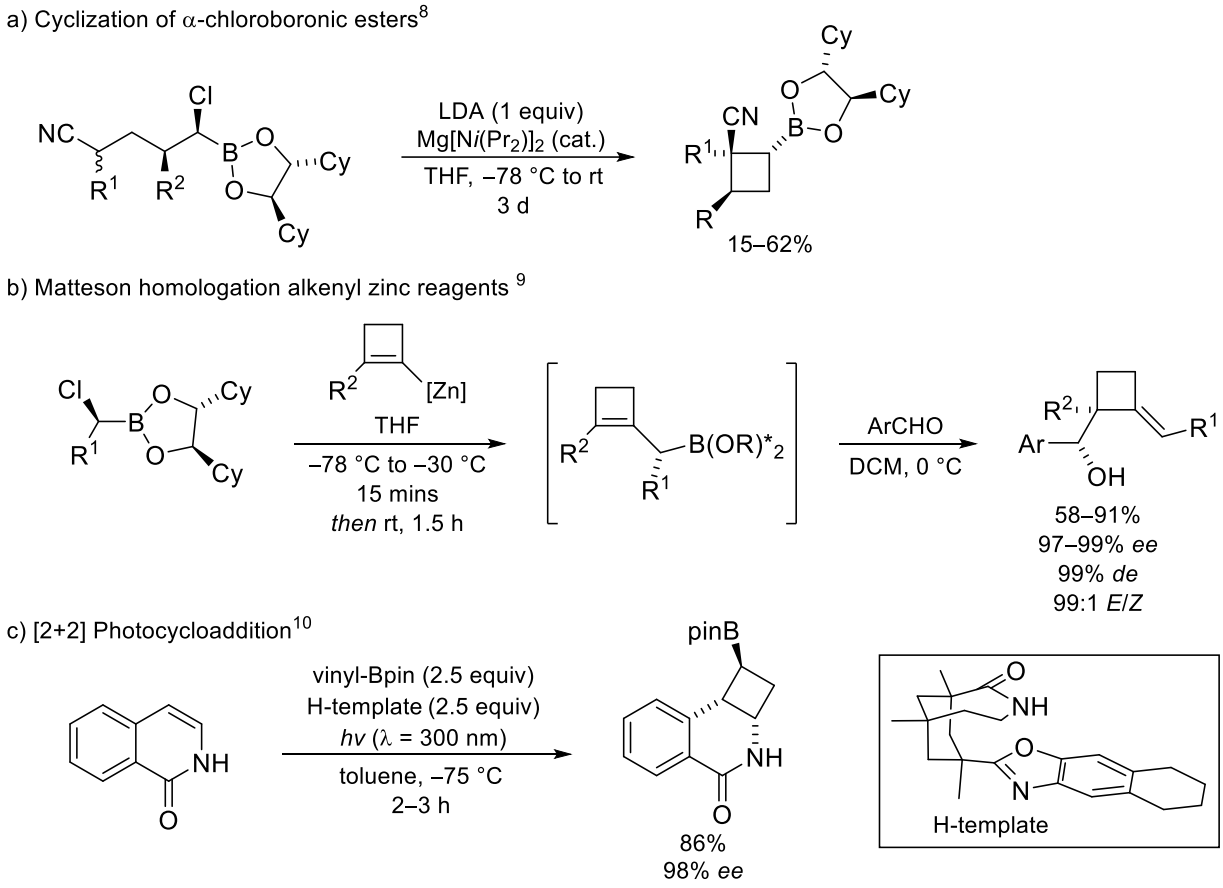

Figure 4-2. Stoichiometric approaches to enantioenriched cyclobutylboronates.

Reports of catalytic enantioselective methods are equally rare. A copper-catalyzed enantioselective formal hydroboration of symmetrical 2,4-disubstituted cyclobutenes was disclosed by Tortosa and co-workers (Figure 4-3a).[11] Because of its distinctive feature as a desymmetrization, this method is limited to symmetrically disubstituted cyclobutenes. Conversely, Yu and co-workers described a directed catalytic enantioselective C-H borylation of cyclobutyl carboxamides that provides cyclobutylboronates in high enantioselectivity with a distinct β-borylated amide substitution pattern due to the requirement of a directing group (Figure 4-3b).[12] Very recently, Lautens reported an enantioselective carboboration of ketones to access enantioenriched cyclobutanols (Figure 4-3c).[13] To-date, this type of boryl cyclization is limited to forming primary boronic ester-containing

products. Furthermore, Rajanbabu and co-workers described a cationic cobalt-catalyzed enantioselective cycloaddition furnishing cyclobutenylboronates in high enantioselectivity (Figure 4-3d).[14] Subsequent diastereoselective hydrogenation afforded an enantioenriched secondary cyclobutylboronate, with a similar substitution pattern to the work of Tortosa and co-workers (i.e. where $R^1 = R^2$).

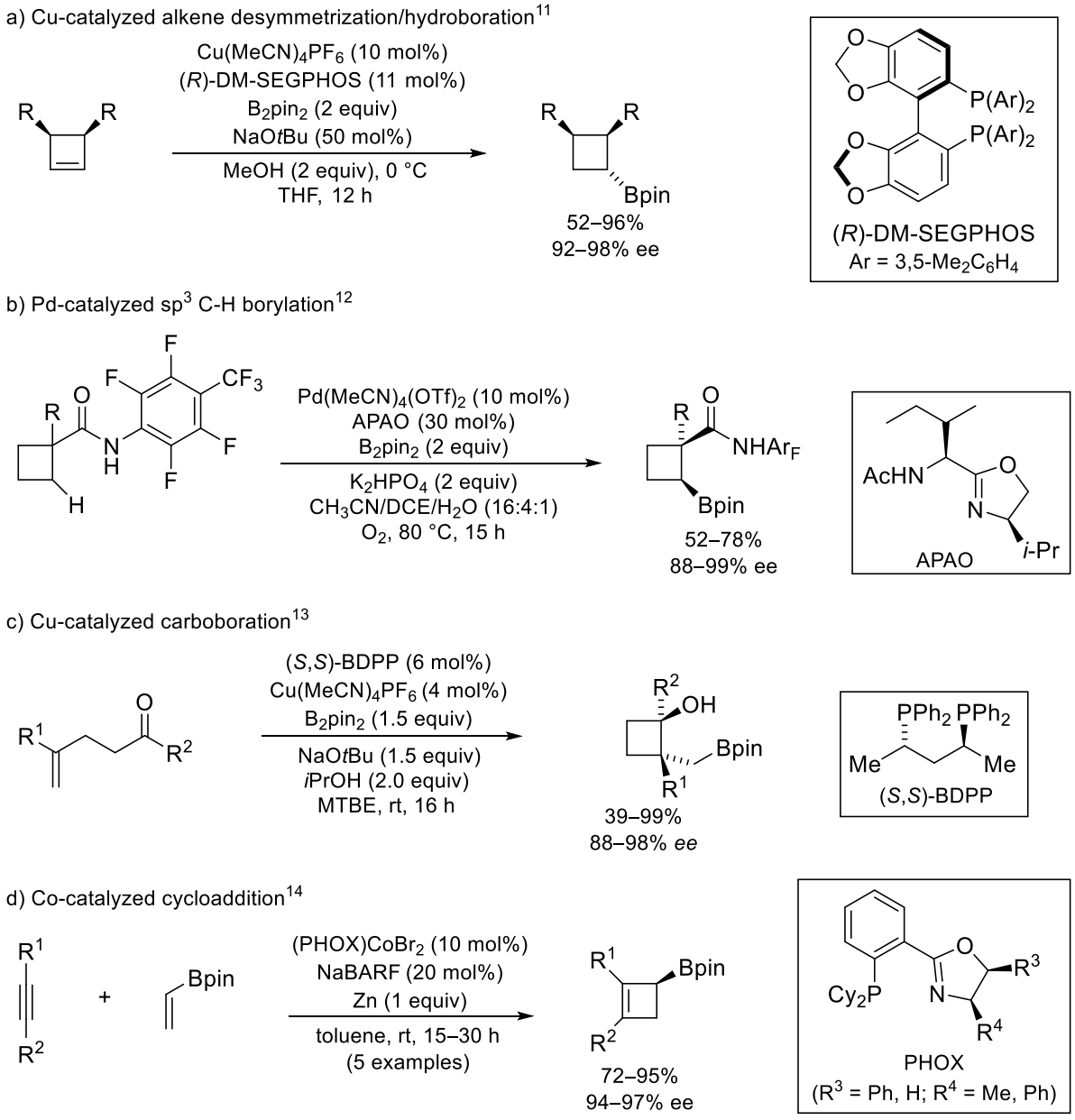

Figure 4-3. Catalytic enantioselective approaches to cyclobutylboronates.

4.2 Project objective

To develop a general, complementary approach to access cyclobutylboronates, our laboratory and collaborators at Pfizer envisioned using a copper-catalyzed conjugate borylation of cyclobutenones. Pioneering work by Hosomi, has shown that conjugate borylation provides an extremely efficient entry into optically enriched cyclopentyl- and cyclohexylboronates, however the cyclobutane equivalent is currently lacking in the literature.[15,16] To this end, we targeted the conjugate borylation of α,β-disubstituted cyclobutenones (Figure 4-4). Although 1,4-silyl cuprate additions to cyclobutenones had been reported,[17] to the best of our knowledge the enantioselective conjugate addition of cyclobutenones had yet to be disclosed.[18] The borylated products would be the first example of enantioenriched tertiary cyclobutylboronates and would also allow access to polysubstituted cyclobutanones, for which catalytic enantioselective approaches remain scarce (see Section 4.6.1).[19,20] Furthermore, with an additional ketone group present, the expected products have the potential to undergo bidirectional functionalizations, making them excellent medicinal chemistry intermediates. For example, a diastereoselective nucleophilic attack of the ketone in the conjugate borylation product could yield a densely functionalized cyclobutanol with three contiguous stereocenters.

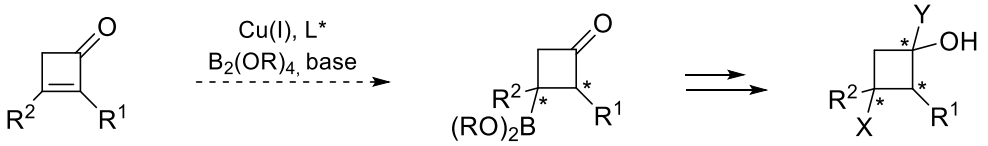

Figure 4-4. Envisioned conjugate borylation of α,β-disubstituted cyclobutenones.

4.3 Synthesis of unsymmetrical α,β-unsaturated cyclobutenones

4.3.1 Developed procedure

Considering the importance of methylation in medicinal chemistry[21] and the structural simplicity of a methyl substituent, we were particularly interested in targeting the borylation of α-methyl-β-

aryl/heteroaryl cyclobutenones (i.e. R^1 = Ph, R^2 = Me, **4-1**) as model substrates (Figure 4-4). Although cyclobutenones have proven to be useful substrates in various contexts,[18] a general preparative method for the synthesis of unsymmetrically disubstituted alkene derivatives was lacking in the literature. Therefore, a general approach for the synthesis of the desired conjugate borylation substrates had to first be developed.

Our approach towards accessing cyclobutenone **4-1** centered on a [2+2] cycloaddition between a keteniminium intermediate and phenylacetylene, followed by hydrolysis and subsequent alkene isomerization. Ghosez and co-workers had previously reported the regioselective [2+2] cycloaddition between phenylacetylene and the corresponding keteniminium reagent formed *in situ* from triflic anhydride and *N*,*N*-dimethylpropionamide. Hydrolysis of the iminium was achieved with 0.10 M aqueous sodium hydroxide, albeit no information regarding temperature, time, nor the equivalents of base was provided (Scheme 4-1a).[22] Once a procedure similar to that of Scheme 4-1a was established, it was envisioned that the desired tetrasubstituted cyclobutanone **4-1** could be obtained by a subsequent isomerization to the thermodynamically favored tetrasubstituted alkene. A single example existed of a cyclobutenone alkene isomerization using TMEDA and acetic acid in ethanol, however without a procedure or yield (Scheme 4-1b).[23]

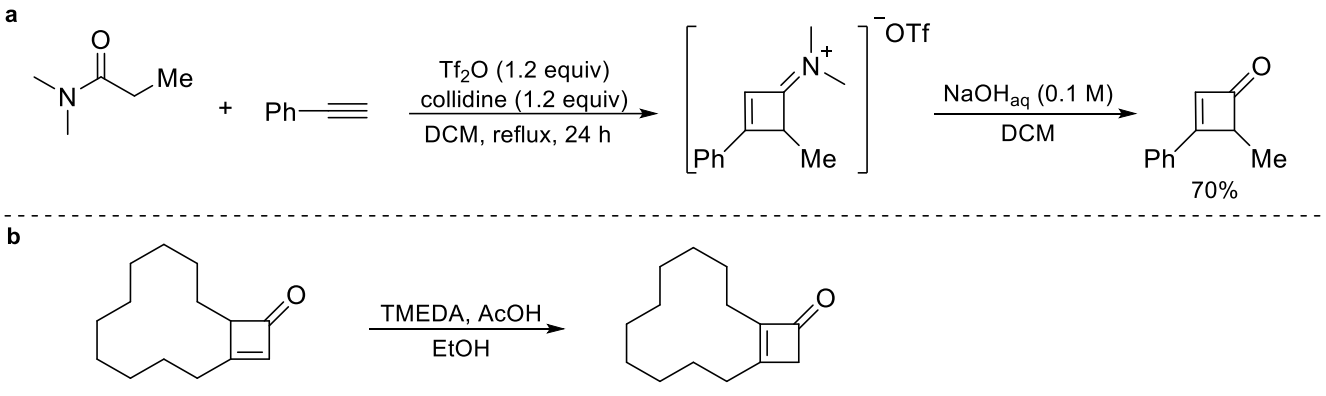

Scheme 4-1. Literature precedence of (a) ketenium 2+2 cycloaddition with phenylacetylene and hydrolysis[22] (b) cyclobutenone alkene isomerization.[23]

With the starting point outlined above, the cycloaddition, hydrolysis and alkene isomerization process was optimized by Dr. Michele Boghi and Rory McDonald, leading to the overall three step process shown in Table 4-1. Varying mixtures of tri- and tetrasubstituted alkene regioisomers were observed after the hydrolysis step. Full conversion to the tetrasubstituted alkene product was achieved under mild conditions in the presence of catalytic KO*t*Bu and ethanol. Notably, the developed approach allowed for the synthesis of **4-1** on a 50 mmol scale with a 44% yield over three steps. The reaction sequence was expanded to the synthesis of a number of other β-arylated cyclobutanones, generally affording moderate to good yields ranging from 30–50% over three steps (Table 4-1).

One advantage of the process shown in Table 4-1 is the commercial prevalence of both the acetylene and amide precursors. All arylacetylene derivatives were purchased from standard commercial sources, except for the tosyl indole cyclobutenone **4-19**. In this case, the starting material was obtained by a known two-step protocol involving indole tosyl protection followed by a Sonogashira coupling with trimethylsilylacetylene (Scheme 4-2). [24] In terms of the amide reagent, *N*,*N*-dimethylpropionamide (R^1 = Me) is readily available, whereas the other dimethyl amide derivatives were made in one step from the carboxylic acid, following standard protocols with thionyl chloride and amine-HCl salts.[25]

Table 4-1. Substrate scope for the synthesis of α,β-disubstituted cyclobutenones

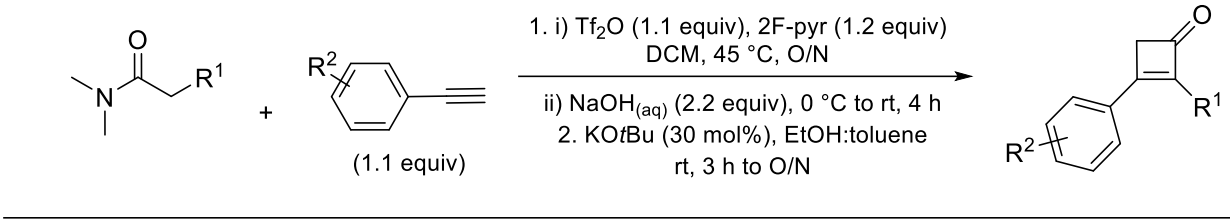

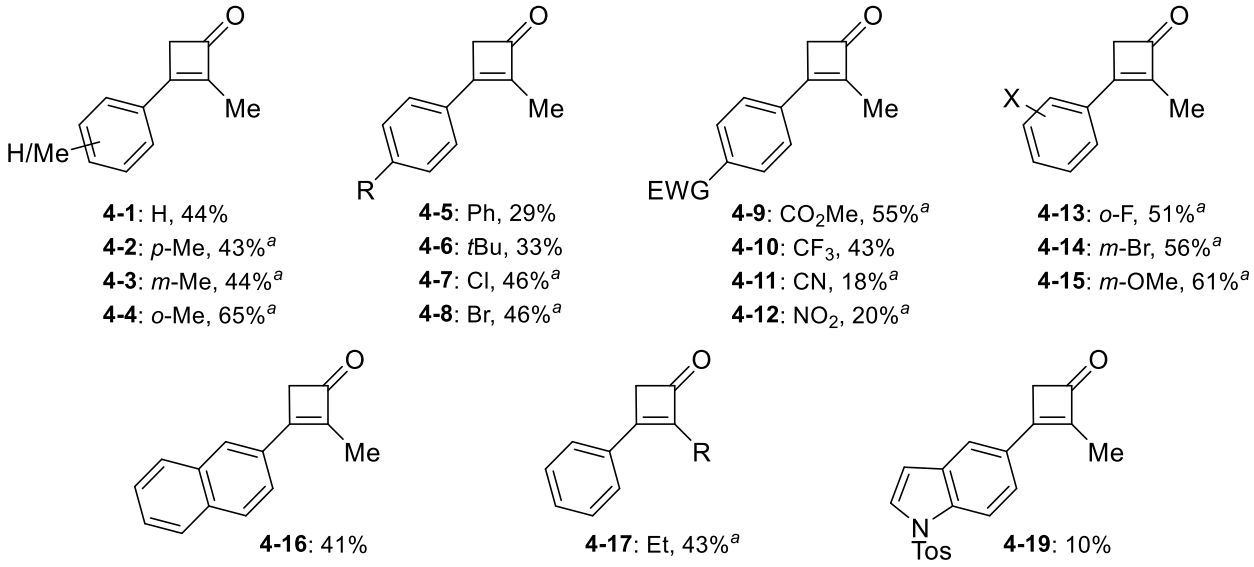

Isolated yields by column chromatography after two steps. [a]The reaction was performed and product characterized by Rory McDonald. All other dervatives were synthesized and characterized by the author of this thesis.

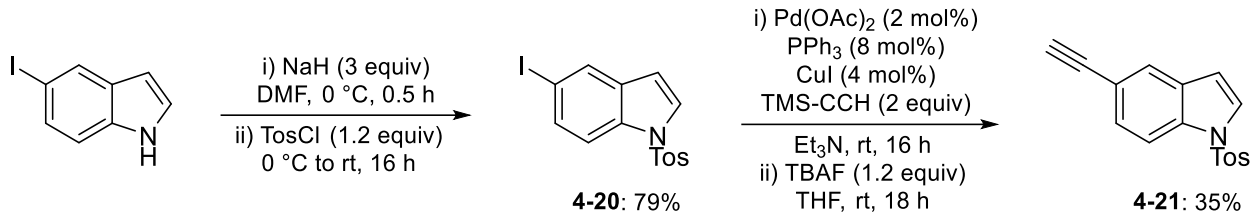

Scheme 4-2. Synthesis of the tosyl indole acetylene precursor.

Although the developed reaction sequence provides a general approach to the desired cyclobutenones for conjugate borylation, many limitations still exist. For example, whereas a *meta* methoxy arylacetylene derivative was well tolerated to afford cyclobutenone **4-4** in a high 65% yield over three steps, *para* electron donating substituents (e.g. *para* methoxy or dimethylamine) and coordinating heterocycles (e.g. 2-pyridine and thiophene) afforded complex mixtures. Furthermore, aliphatic acetylenes were incompatible with the basic hydrolysis step. If the limitation of hydrolysis of aliphatic acetylenes could be overcome, the reaction sequence has the potential to access unsymmetrical dialkyl cyclobutenones without issues of regioselectivity in the [2+2] cycloaddition. The regioselective synthesis of unsymmetrically α,β-dialkyl cyclobutenones are currently inaccessible by other means. Notably, a triflic acid promoted hydrolysis may be a potentially feasible approach to issue of hydrolysis, in analogy to Jiao's method (described in the following section).

4.3.2 Acetonitrile activation – Jiao's [2+2] approach to cyclobutenones

Jiao and co-workers recently described an elegant complementary synthesis of disubstituted cyclobutenones using a novel triflic anhydride mediated [2+2] cycloaddition between activated acetonitrile and internal, unsymmetrically disubstituted alkynes (Scheme 4-3a).[26] The reported isolated yields are very comparable to our approach described in Table 4-1 (e.g. a 45% yield was reported for **4-1** compared to 44% yield in Table 4-1). No issues of regioselectivity were reported in cases where terminal arylylacetylenes or alkyl-aryl disubstituted internal alkynes were used. In contrast, examples using dialkyl substituted alkynes showed regioselectivities of up to 5:1. Furthermore, terminal alkyl acetylenes did not provide an efficient reaction. Although the method developed by Jiao and co-workers requires internal disubstituted alkynes, which are not as commercially prevalent as terminal acetylenes, the advantage of this procedure features a mild work-up suitable for base-sensitive substituents and β-alkyl cyclobutenones. This acetonitrile activation

approach was utilized for the synthesis of bis(4-phenylpropyl) substrate **4-23**, which allowed the inclusion of a dialkyl cyclobutenone in the scope of the conjugate borylation reaction of interest in this study.

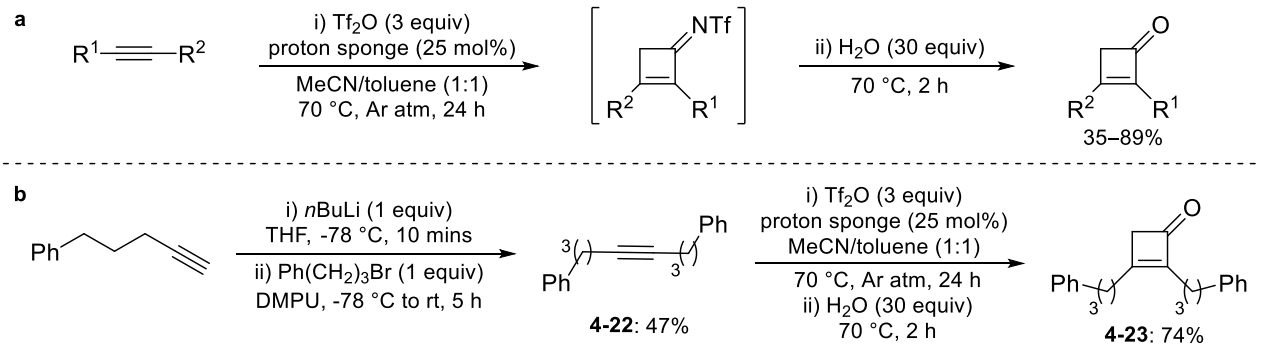

Scheme 4-3. (a) [2+2] Cycloaddition of acetonitrile reported by Jiao and co-workers[26] (b) application of Jiao's method for the synthesis of dialkyl cyclobutenone **4-23**.

4.4 Optimization of the conjugate borylation reaction

4.4.1 High throughput ligand screening results

Although enantioselective conjugate borylations of β-substituted cyclopentenones and cyclohexenones have been successfully realized,[27,28] the steric congestion in tetrasubstituted alkenes makes their borylation a significant challenge. In fact, to the best of our knowledge, no example of catalytic enantioselective conjugate borylation of a tetrasubstituted alkene exists in the literature.[29] To surmount this challenge we envisioned using a ligand high-throughput screening (HTS) approach. Notably, ligand optimization using HTS has recently been demonstrated to be effective in addressing notoriously difficult cases of catalytic enantioselective hydrogenations of tetrasubstituted alkenes.[30]

With an efficient access to **4-1** developed, HTS of a library of 118 chiral ligands was explored by our collaborators at Pfizer, in the lab of Dr. Neal W. Sach. Using similar conditions to that previously reported by Tortosa and co-workers,[11] the ligand screening for the conjugate borylation of **4-1** was

undertaken in a glovebox on a 2 μmol scale using $Cu(MeCN)_4PF_6$ as the copper(I) source with NaO*t*Bu as base in THF at 25 °C (see Experimental Section 4.10.6 for more details).[31] The full screening results are shown in Tables 4-2 and 4-3, with a graphical summary in Figure 4-4. Over half of the ligands screened (72 ligands, 61%) were found to give no observable conversion under the conditions used (Table 4-2). Many ligand scaffolds that are commonly used in enantioselective conjugate borylation of ketones and esters such as Josiphos, SEGPHOS, Mandyphos, BINAP and MeO-BIPHEP derivatives were completely ineffective for the conjugate borylation of **4-1**.[32,33]

Table 4-2. List of ligands that led to no observable conversion of **4-1**.

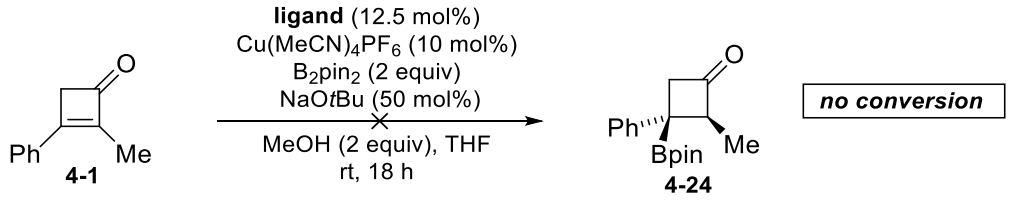

Entry	Ligand	Entry	Ligand	Entry	Ligand
1	cis-Aindanol	25	Naud SL-N014-1	49	(*R*)-Tol-SDP
2	(+)-TsCYDN	26	(*R*)-Josiphos SL-J002-1	50	(*R*)-(+)-Cl-MeO-BIPHEP
3	(*S*)-BINOL	27	SL-J502-1	51	Walphos SL-W002-1
4	(*S*,*S*)-*N*-Ms-1,2-DPEN	28	(*R*)-Josiphos SL-J009-1	52	SL-J014-2
5	Box Ligand 2	29	(*S*)-Me-f-KetalPhos	53	(*R*)-Josiphos SL-J011-1
6	Box Ligand 3	30	(*Ra*,*S*)-Ph-Bn-SIPHOX	54	(*R*)-(+)-TolBINAP
7	Box Ligand 4	31	SL-J014-1	55	(*R*)-DIFLUORPHOS
8	Box Ligand 5	32	(*R*)-(+)-MeO-BIPHEP	56	CTH-(*R*)-3,5-xylyl-PHANEPHOS
9	Box Ligand 8	33	(*R*)-SDP	57	2,2-BNDMDiE
10	Box Ligand 9	34	SL-J452-2	58	SL-J007-1
11	Box Ligand 10	35	TCI2	59	(*R*)-DM-SEGPHOS
12	Box Ligand 11	36	(*R*)-Josiphos SL-J004-1	60	(*S*)-BINAPINE
13	Box Ligand 12	37	(*R*)-C4-Tunephos	61	(*R*)-(+)-XylBINAP
14	(*R*)-Monophos	38	Naud SL-N008-2	62	(*R*)-Xylyl-P-Phos
15	Box Ligand 13	39	(*R*)-Josiphos SL-J004-1	63	(*Ra*,*S*)-DTB-Bn-SIPHOX
16	Box Ligand 15	40	(1)-(*S*)-SEGPHOS	64	Mandyphos SL-M002-1
17	(*R*,*R*)-*i*Pr-DUPHOS	41	(*S*)-Methyl BoPhoz	65	(*R*)-Josiphos SL-J006-1
18	PPM	42	catASium T1	66	SL-J008-1
19	Box Ligand 16	43	(*R*)-BINAP	67	Trifer
20	Nauds-*i*Pr Ligand	44	Salen	68	Mandyphos SL-M009-1
21	JoSPOphos 1	45	(*R*)-SYNPHOS	69	Walphos SL-W008-1
22	Naud SL-N012-2	46	(*R*)-Josiphos SL-J001-1	70	Walphos SL-W005-2
23	SL-J212-1	47	SL-J216-2	71	(*R*)-DTBM-SEGPHOS
24	(+)-Ph-Et-Monophos	48	CTH-(*S*)-P-Phos	72	SL-M004-2

No conversion based on HPLC analysis (see Experimental Section 4.10.6).

The results regarding the ligands that did lead to significant conversion are listed in Table 4-3 and are sorted by increasing enantioselectivity. In general, both the conversion and enantioselectivity were quite limited. The highest conversion is in the case of (*R*,*R*)-Me-BPE leading to just under 60% conversion, yet only 13% *ee* (entry 14). Out of 118 ligands, only two afforded over 50% *ee* (entries 46–47) with the second highest *ee* resulting from using Me-BPF with 15% conversion and 69% *ee* (entry 46). Remarkably, ligand scaffolds that were efficient for the copper-catalyzed borylation of cyclopentenones and cyclohexenones were inadequate with cyclobutenone **4-1**. For example, QuinoxP***** (entry 35) and Taniaphos (entry 30) led to -21% *ee* and 28% *ee* of cyclobutylboronate **4-24**, respectively.[16,27]

Table 4-3. List of ligands that led to observable conversion of **4-1**.

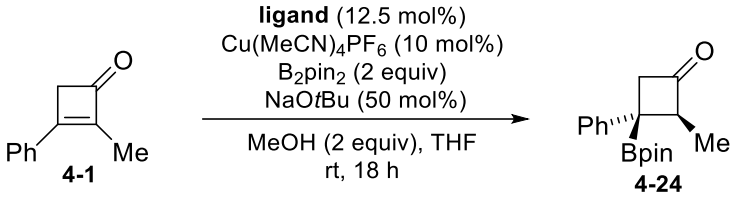

Entry	Ligand	conv.[a]	*ee*[a]	Entry	Ligand	conv.[a]	*ee*[s]
1	SaxS,S-BOBPHOS	25	3	25	(*R*,*R*)-Chiraphos	28	18
2	SL-J425-2	11	5	26	JoSPOphos 2	44	20
3	SL-J015-1	36	5	27	(*R*,*R*)-Me-DuPhos	57	21
4	SL-J505-1	34	6	28	t-BuDPPPO	37	21
5	Naud SL-N004-1	11	–6	29	TCI1	14	21
6	Walphos SL-W004-1	17	–6	30	Taniaphos SL-T002-1	25	–21
7	ChenPhos	52	7	31	catASium MNXylF(*R*)	17	21
8	SL-J418-1	25	–9	32	(*S*,*S*)-DIOP	39	–22
9	Josiphos SL-J404-2	21	–10	33	(*S*)-Phanephos	11	23
10	CTH-(R)-BINAM	47	11	34	(*R*)-Xyl-SDP	10	25
11	(2)-Xanthphos	33	11	35	(*R*,*R*)-QuinoxP*	16	27
12	(*R*,*R*)-DIPAMP	33	12	36	Box Ligand 14	12	30
13	(*S*,*S*)-DACH-pyridyl TROST	12	12	37	(*S*,*S*)-TsDPEN	12	33
14	(*R*,*R*)-Me-BPE	59	13	38	(*R*,*R*)-NORPHOS	29	37
15	(*R*,*R*)-DACH-naphthyl Trost ligand	15	14	39	P(Ph$_3$)-Chiral	54	–37
16	SL-J005-2	15	15	40	(*R*,*R*)-Et-DUPHOS	50	39
17	Box Ligand 1	18	15	41	(*R*,*R*,*S*,*S*)-DUANPHOS	51	44
18	Walphos SL-W022-2	39	15	42	*N*,*N*-DTsCHN	14	45
19	Buwen Ligand	12	15	43	Naud SL-N011-2	10	46
20	(*R*)-Binam-P	38	16	44	(*S*,*S*,*R*,*R*)-TangPhos	44	49
21	Pfizer Ligand	16	16	45	(*S*,*S*)-f-Binaphane	37	49
22	(2*R*)-*i*Pr-BPE	13	17	46	(*S*,*S*)-Me-BPF	15	69
23	Box Ligand 6	13	18	47	**(*S*,*S*)-BDPP**	54	88
24	Groton BINOL Ligand 1	12	18				

[a]The conversion and enantiomeric excess are reported as percentages by chiral HPLC (see Experimental Section 3.10).

The HTS results clearly highlight the notorious challenge provided by the cyclobutenone substrate **4-1** (Figure 4-5). The low efficiency of many commonly used chiral ligands in this reaction confirms the great value of a HTS screening approach to establish a reasonable starting point for the conjugate borylation of **4-1**. By far, the highest enantioselectivity was obtained with (*S*,*S*)-BDPP, leading to the formation of **4-24** as a single diastereomer in 55% conversion and 88% *ee* (Figure 4-5a). Most of the remaining material was leftover **4-1**, leaving room for further optimization. Importantly,

BDPP is a commercially available ligand from standard sources, such as Sigma-Aldrich and Strem Chemicals. It is also notable that the BDPP ligand scaffolds have been used in a limited number of recent reports regarding enantioselective copper-catalyzed borylation chemistry, most notably in the work of Ito and co-workers for the conjugate borylation of indole-2-carboxylates.[13,34]

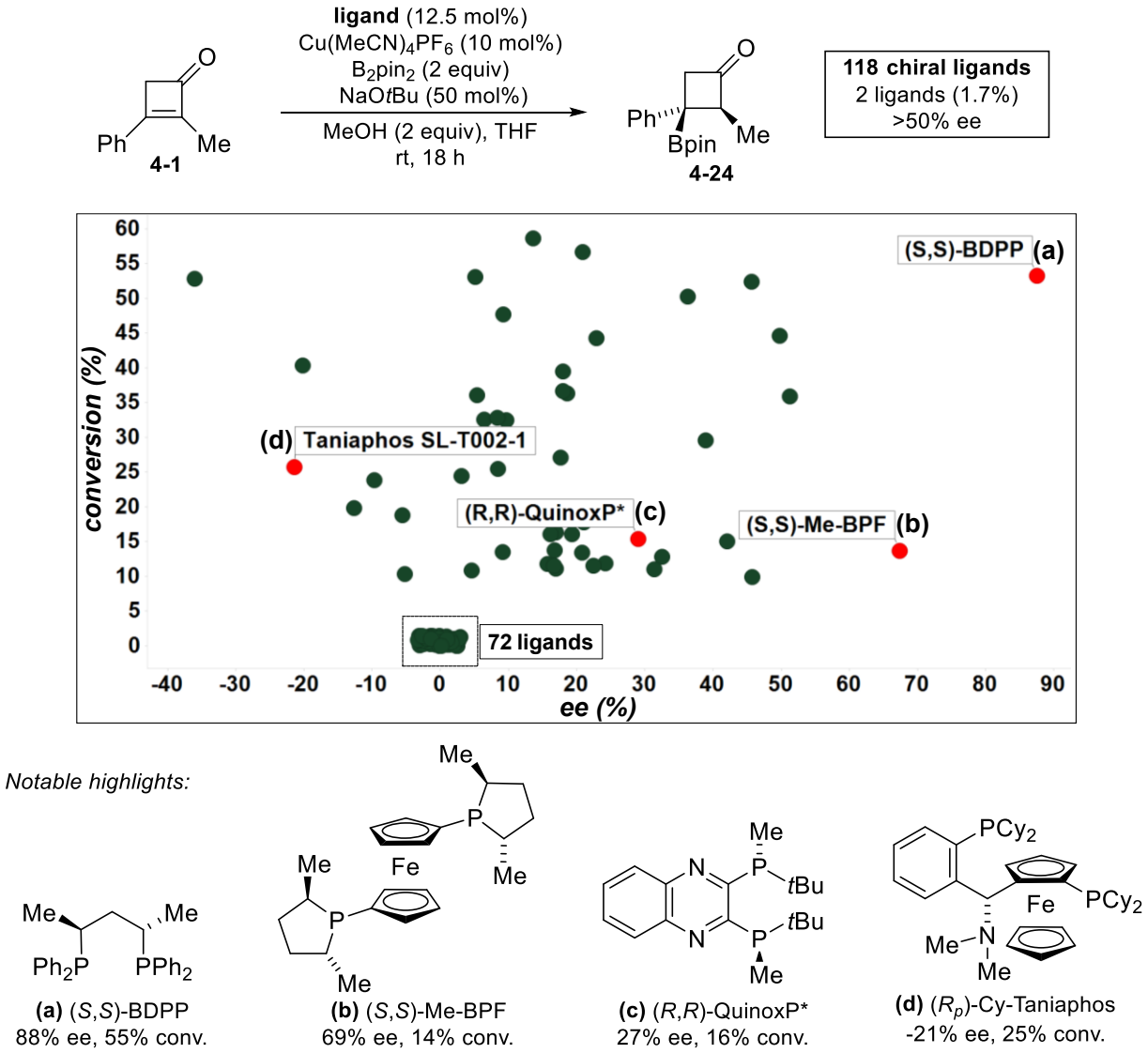

Figure 4-5. Summary of HTS results for ligand optimization. The data points are slightly skewed for visualization purposes. See Tables 4-2 and 4-3 for complete results.

4.4.2 Optimization of the alcohol and base

With BDPP identified as the optimal ligand, validation of the HTS conditions and screening of the remaining reaction parameters was undertaken. It was found that the major diastereomer could be separated by column chromatography purification. Importantly, there was no loss of enantioselectivity with full consumption of cyclobutenone **4-1** when the reaction was performed at 0 °C to room temperature with 5 mol% catalyst on a standard 0.3 mmol reaction scale (Table 4-4, entry 1). Increasing the steric bulk of the alcohol did not improve the diastereoselectivity, nor the enantioselectivity, except in the case of *t*BuOH, which led to a messy crude reaction (entries 1–4). A less sterically hindered base resulted in a slightly lower yield, yet LiO*t*Bu produced a cleaner reaction and higher diastereoselectivity than its sodium and potassium equivalents (entries 7–10).

Table 4-4. Variation of the alcohol and base.

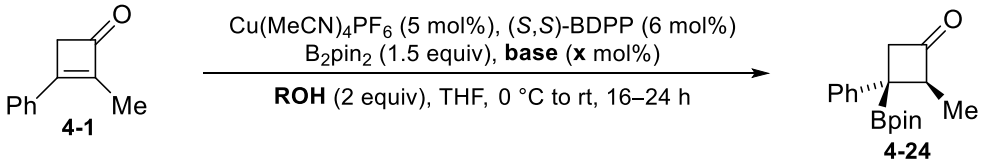

Entry	ROH	base (**x**)	Yield of d_1[a]	Ratio d_1 : d_2[a]	*ee*[b]
1	MeOH	NaO*t*Bu (50)	70%	6.9 : 1	92%
2	EtOH	NaO*t*Bu (50)	67%	6.9 : 1	92%
3	*i*PrOH	NaO*t*Bu (50)	68%	7 : 1	91%
4	tBuOH	NaO*t*Bu (50)	53%	1 : 0	94%
5	MeOH	NaO*t*Bu (20)	63%	4 : 1	91%
6	MeOH	NaO*t*Bu (100)	43%	3 : 1	—
7	MeOH	KO*t*Bu (50)	51%	3.5 : 1	—
8	MeOH	NaOMe (50)	57%	4.4 : 1	90%
9	MeOH	NaO*t*Pn (50)	42%	3.5 : 1	90%
10	**MeOH**	**LiO*t*Bu (40)**	**82%**	**9 : 1**	**91%**

[a] Determined by relative integration by ^{1}H NMR of the crude reaction mixture with dibromomethane as an internal standard. [b] *ee* of the isolated major diastereomer (d_1) by chiral HPLC.

4.4.3 Optimization of the solvent

A number of solvents were screened to try to improve the diastereo- and enantioselectivity (Table 4-5). Common ethereal and aromatic solvents resulted in lower yields and similar or slightly lower enantioselectivity (entries 1–8). Acetonitrile resulted in a very clean reaction with a high 17:1 dr, albeit with a lower conversion and enantioselectivity (entry 9). Attempts to use a mixed MeCN:THF solvent system improved the diastereoselectivity, but the enantioselectivity remained eroded (entry 10) compared to reactions in THF. The strongly coordinating solvent, DMF, resulted in a very messy crude reaction mixture and low dr (entry 11). Maintaining the reaction at 0 °C did not improve the enantioselectivity (entry 12). Interestingly, the reaction was very clean and highly diastereoselective when performed under air, however the enantioselectivity decreased to only 65%, supporting the requirement for oxygen-free reaction conditions (entry 13).

Table 4-5. Variation of the solvent.

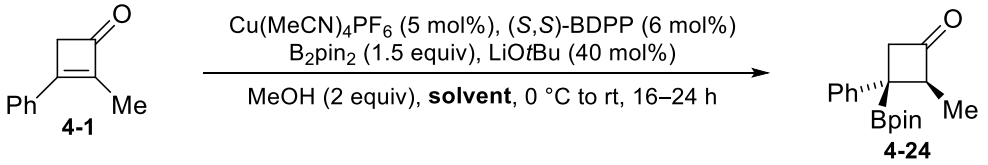

Entry	Solvent	Yield of d_1[a]	Ratio d_1 : d_2[a]	*ee*[b]
1	**THF**	**82%**	**9 : 1**	**91%**
2	2-Me-THF	56%	9 : 1	91%
3	Dioxane	57%	17 : 1	85%
4	Et_2O	50%	8 : 1	93%
5	CPME	60%	8 : 1	91%
6	MTBE	55%	12 : 1	89%
7	Toluene	59%	10 : 1	89%
8	Chlorobenzene	77%	10 : 1	82%
9[c]	MeCN	43%	17 : 1	67%
10[d,e]	10% MeCN in THF	86%	15 : 1	87%
11	DMF	29%	3 : 1	N.D.
12[f]	THF	63%	7 : 1	90%
13[e,g]	THF	86%	15 : 1	65%

[a] Determined by relative integration by ^{1}H NMR of the crude reaction mixture with dibromomethane as an internal standard. [b] *ee* of the isolated major diastereomer (d_1) by chiral HPLC. [c] 62% conversion of **4-1**. [d] 3 h

reaction time. [e]The reaction was performed by Rory M[c]Donald. [f]The reaction was performed at 0 °C. [g]The reaction was set up under ambient conditions.

4.4.4 Brief screening of the copper source, ligand and diboron reagent

Although the HTS identified BDPP as the most promising ligand scaffold, the copper source and a few structurally related ligands were not included in the initial screen and needed to be examined (Table 4-6). Changing the Cu(I) source to CuTC and CuCl lowered the yield and enantioselectivity, respectively (entries 2–3). Both the more sterically bulky *meta* xyl-BDPP derivative and (*R*)-PROPHOS did not improve the enantioselectivity, with the latter having very inefficient enantiomeric induction (entries 5–6). Surprisingly, excess B_2pin_2 was detrimental to the yield with multiple unidentified side products forming (entry 7). Although full conversion was observed when the diboron source was changed to the neopentyl variant, no desired product was isolated (entry 8). Finally, using the optimal parameters of Table 4-5 and 1.4 equivalents of B_2pin_2, the reaction was complete after 3 hours and provided more reproducible results when a sealed vessel with a tight cap was used rather than a septum (entry 9). Overall, the optimized reaction allowed for formation of the desired borylated product **4-24** in a high ^{1}H NMR yield (96%), with excellent diastereoselectivity (16:1 dr) and very statisfactory enantioselectivity (90% *ee*). The absolute and relative configuration of cyclobutylboronate **4-24** and other analogs was assigned based on the X-ray analysis of an optically enriched crystalline sample after derivatization of cyclobutylboronate **4-24** (cf. Scheme 4-4).

Table 4-6. Variation of the copper source, ligand and diboron reagent.

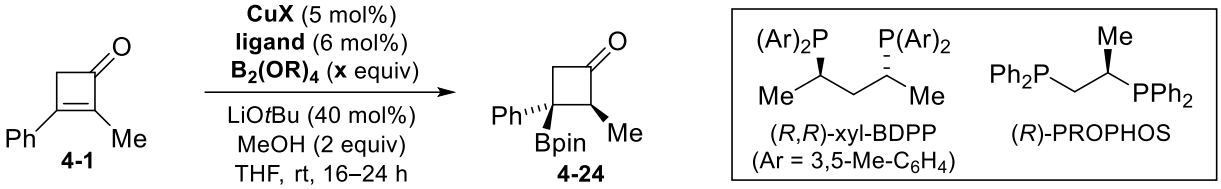

Entry	CuX	ligand	$B_2(OR)_4$(x)	Yield of d_1[a]	Ratio d_1 : d_2[a]	*ee*[b]
1	$Cu(MeCN)_4PF_6$	(*S*,*S*)-BDPP	B_2pin_2 (1.5)	82%	9 : 1	91%
2	Cu(TC)	(*S*,*S*)-BDPP	B_2pin_2 (1.5)	24%	3 : 1	N.D.
3	CuCl	(*S*,*S*)-BDPP	B_2pin_2 (1.5)	80%	9 : 1	85%
4	$Cu(MeCN)_4PF_6$	(*R*,*R*)-xyl-BDPP	B_2pin_2 (1.5)	57%	6 : 1	-71%
5	$Cu(MeCN)_4PF_6$	(*R*)-PROPHOS	B_2pin_2 (1.5)	71%	13 : 1	-31%
6[c]	$Cu(MeCN)_4PF_6$	(*S*,*S*)-BDPP	B_2pin_2 (1.1)	48%	6 : 1	N.D.
7	$Cu(MeCN)_4PF_6$	(*S*,*S*)-BDPP	B_2pin_2 (2.0)	28%	6 : 1	N.D.
8[d]	$Cu(MeCN)_4PF_6$	(*S*,*S*)-BDPP	$B_2(neop)_2$ (1.4)	—	—	—
9[e]	**$Cu(MeCN)_4PF_6$**	**(*S*,*S*)-BDPP**	**B_2pin_2 (1.4)**	**96%**	**16 : 1**	**90%**

[a]Determined by relative integration by ^{1}H NMR of the crude reaction mixture with dibromomethane as an internal standard. [b]*ee* of the isolated major diastereomer (d_1) by chiral HPLC. [c]60% conversion of **4-1**. [d]No desired product was obtained after a water deactivated silica plug as per the general procedure B (see Experimental Section). [e]3 h reaction time, sealed vial.

4.5 Substrate scope

A representative scope of the conjugate borylation is displayed in Table 4-7. In general, the isolated yields after a short silica plug purification are moderate to high (44–94%). Due to a slight instability to silica, in some cases the ^{1}H NMR yield is significantly higher than the isolated yield. For all entries, the product was fully characterized after a second purification by column chromatography to afford a single diastereomer.

Table 4-7. Substrate scope of the stereoselective conjugate borylation.

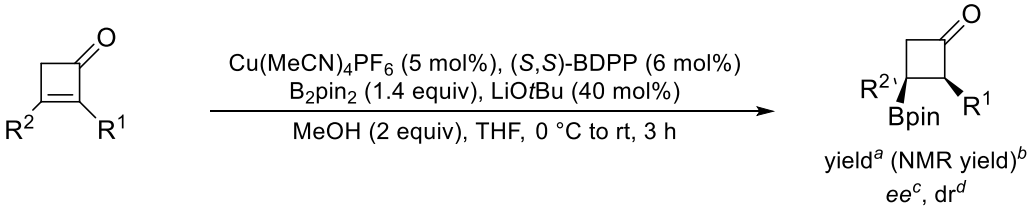

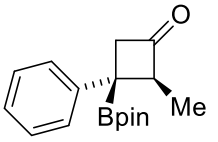

4-24: 76% (96%)
90% *ee*, 18:1 dr[e]

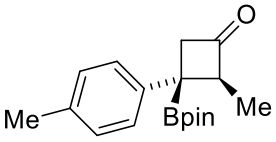

4-25: 86% (99%)
91% *ee*, >20:1 dr[f]

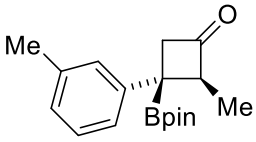

4-27: 59% (69%)
86% *ee*, >20:1 dr[e]

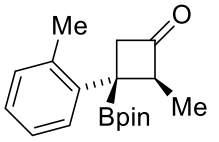

4-28: 43% (65%)
86% *ee*, >20:1 dr[e]

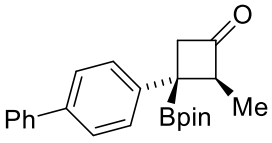

4-29: 58% (70%)
90% *ee*, 12:1 dr

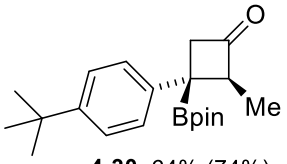

4-30: 64% (74%)
95% *ee*, 8:1 dr

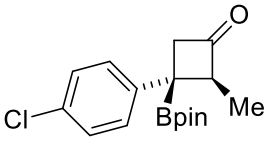

4-31: 70% (70%)
90% *ee*, >20:1 dr[e]

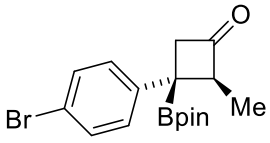

4-32: 61% (79%)
90% *ee*, 20:1 dr[e]

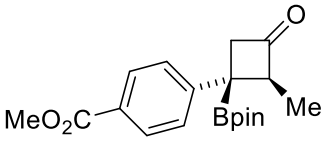

4-33: 54% (74%)
83% *ee*, >20:1 dr

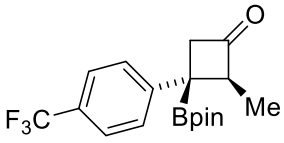

4-34: 55% (90%)
80% *ee*, >20:1 dr

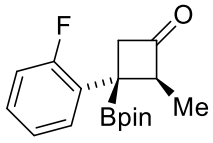

4-35: 76% (79%)
82% *ee*, >20:1 dr[e]

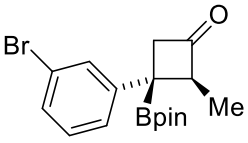

4-36: 66% (81%)
79% *ee*, 18:1 dr

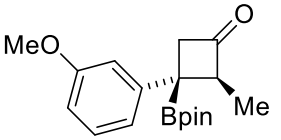

4-37: 43% (55%)
87% *ee*, 10:1 dr[e]

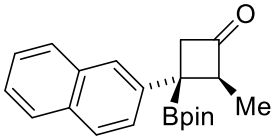

4-38: 88% (96%)
90% *ee*, >20:1 dr

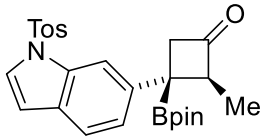

4-39: 69% (80%)
94% *ee*, 11:1 dr[g]

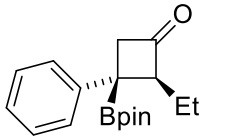

4-40: 76% (76%)
90% *ee*, 8:1 dr[e]

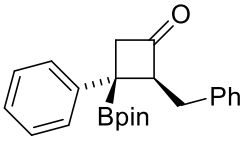

4-41: 80% (83%)
83% *ee*, >20:1 dr[e,g]

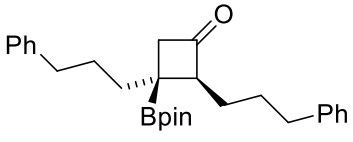

4-42: 94% (99%)
96% *ee*, 5:1 dr[g]

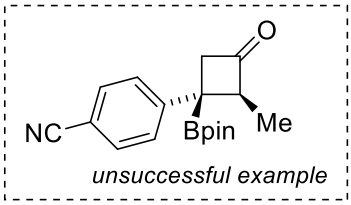

[a] Isolated yield after column chromatography with water deactivated silica. [b] ^{1}H NMR yield of the major diastereomer from the crude reaction mixture by integration of CH_2Br_2 as an internal standard. [c] Determined by chiral HPLC of the major diastereomer. [d] dr was determined by relative Me group peak height in the ^{1}H NMR after the first column. [e] The reaction was performed and product characterized by Rory McDonald. [f] The

ketone of **4-25** was reduced to the boryl alcohol **4-26** for chiral HPLC analysis. [g]10 mol% $Cu(MeCN)_4PF_6$, 11 mol% (*S*,*S*)-BDPP.

4.5.1 Electronic and steric effects of the β-aryl ring

The substrate scope generally focused on varying the sterics and electronics of the β-aryl ring. Screening of all three tolyl substrates showed the general steric effect of the different substitution patterns. The reaction is not significantly affected by the presence of a methyl group at the *para* position (**4-25**), however, for both *meta* and *ortho* substitution the enantioselectivity decreased slightly to 86% *ee* (**4-27** and **4-28**). Larger *para* hydrocarbon substituents are well tolerated such as phenyl (**4-29**) and *t*Bu (**4-30**). Furthermore, the synthetically useful *para* chlorine (**4-31**) and bromine (**4-32**) derivatives were obtained in 90% *ee,* allowing for the potential of further elaboration of the aryl ring.

In contrast, the use of electron withdrawing aryl rings such as *para* methyl ester (**4-33**), trifluoromethyl (**4-34**) and *ortho* fluoro (**4-35**) functionalities eroded the enantioselectivity to 80–83% *ee*. All attempts to improve the enantioselectivity with these substrates were unsuccessful, which included cooling the reaction temperature and increasing the catalyst loading. Furthermore, *meta* substitution led to varying results of only 79% *ee* with bromine (**4-36**) and 87% *ee* with a methoxy group and a notably lower ^{1}H NMR yield of 55% and dr of 10:1 (**4-37**). Conversely, a 2-napthyl derivative was obtained in a very high efficiency with 90% *ee* (**4-38**). Although the inclusion of heterocycles was largely limited by the substrate synthesis, a tosyl protected indole (**4-39**) was successfully accessed with an excellent 94% *ee*.

4.5.2 α-Alkyl and β-alkyl variation

Variation at the α-position was also briefly examined, with ethyl and benzyl substitution leading to quite different results. The *ee* remained high at 90% with an α-ethyl group (**4-40**), yet a lower 8:1 dr

was observed. Conversely, a diminished 83% *ee* was obtained the case of α-benzyl substitution (**4-41**) with over 20:1 dr. The reason for the large discrepancy in the enantioselectivity between **4-40** and **4-41** is unclear at this time, yet some sort of π-stacking interactions from the benzyl group may be at play. Finally, a symmetrical dialkyl substrate (**4-42**) resulted in a highly efficient reaction with 94% isolated yield and 96% *ee*, yet with a lower dr of 5:1. The high enantiopurity of **4-42** suggests the potential for the conjugate borylation to be quite general, especially if new and effective methods to access non-symmetrical dialkyl cyclobutenones are developped.

4.5.3 *para* Nitrile substrate: proposals for the observed alkene reduction

Surprisingly, when a *para* nitrile aryl group was used, protodeboronation was the major product observed in the crude reaction mixture. One can envision two pathways by which the reduced side product could be obtained – conjugate borylation followed by protodeboronation (Figure 4-6a) or conjugate addition to the α-position of the cyclobutenone following by protonation of the resulting enolate (Figure 4-6b).[35] Considering the strong electronic withdrawing nature of the nitrile group, the latter option is preferred. Furthermore, the relative amount of reduced side product was affected by the ligand (BDPP or the achiral Xantphos), which would more clearly align with the α-borylation pathway. For example, in the case of methyl ester (±)-**4-33**, the reduced side product was an inseparable impurity using the standard racemic conditions, whereas under the standard enantioselective conditions, reduction was not observed. Of course, further control reactions and product characterization would be required for more conclusive evidence, especially considering the base also varies between the enantioselective and racemic (15% NaO*t*Bu) conditions.

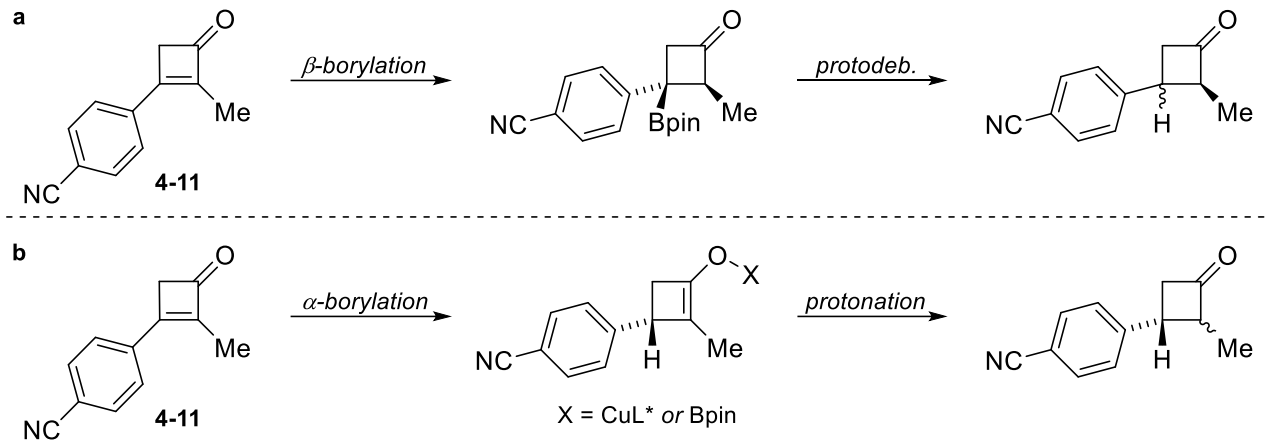

Figure 4-6. Potential rational for alkene reduction by (a) β-borylation or (b) α-borylation.

4.6 Functionalization of cyclobutylboronate 4-24

4.6.1 Potential for keto-cyclobutylboronates as versatile synthetic building blocks

Although the copper-catalyzed conjugate borylation is a well-established approach to organoboron compounds,[33,35] an appealing aspect of this methodology is the potential for bidirectional functionalization of the resulting enantioenriched products. Furthermore, both cyclobutanones and cyclobutanes have proven to be useful synthons in catalysis and for the synthesis of bioactive molecules.[4,36] In this case, the developed conjugate borylation provides access to novel enantioenriched non-fused trisubsituted cyclobutanones, for which only a limited number of examples exist (Figure 4-7). Both Ryu, Dong and their co-workers recently reported catalytic enantioselective approaches to trisubstituted cyclobutanones and displayed the synthetic utility of the obtained products.[20] Furthermore, tertiary enantioenriched boronic esters are of increasing importance in the literature, allowing the potential conversion to C-O, C-N, C-F, C-H and C-C bonds with increasing generality (c.f. Chapter 1.3).[37]

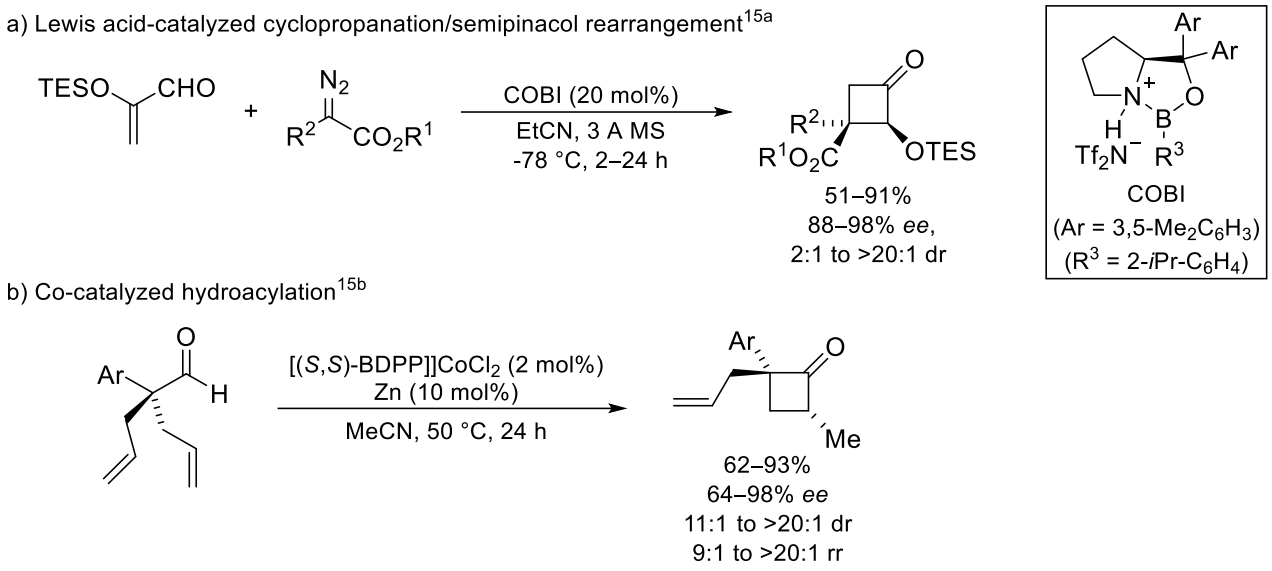

Figure 4-7. Recently reported catalytic enantioselective approaches to trisubstituted cyclobutanones.

4.6.2 Ketone functionalization

Ketone reduction of cyclobutylboronate **4-24** allows formation of a secondary alcohol. It was presumed that if a large, mild reductant was used, then steric differentiation between the two faces of the ketone would be more likely.[20a] Indeed, reduction with L-selectride occurred cleanly to afford the desired product **4-43** as a single diastereomer by NMR analysis (>20:1 dr). Furthermore, protection of the secondary alcohol as a *para* bromo-benzoyl ester from an enantioenriched sample of diboryl alcohol **4-43** allowed confirmation of the relative and absolute stereochemistry of the cyclobutylboronate product **4-44** by X-ray crystallographic analysis. The stereochemistry suggests that the diastereoselectivity of both the conjugate borylation and ketone reduction may be sterically controlled by the large boronic ester group. For a more detailed discussion in regard to the diastereoselectivity of this developed conjugate borylation method, see Section 3.7.

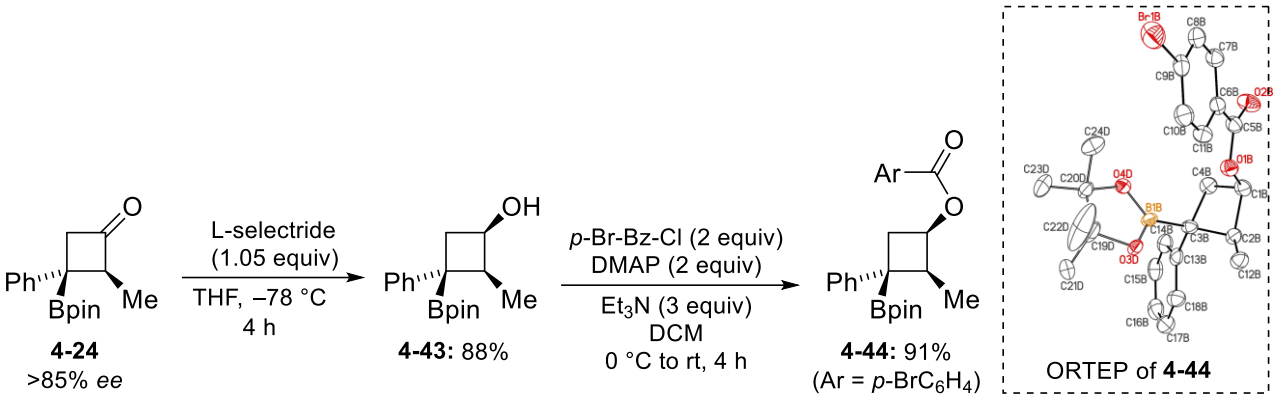

Scheme 4-4. Diastereoselective ketone reduction with L-selectride and ORTEP of ester **4-44**.

With an efficient ketone reduction to afford the borylated cyclobutanol **4-43** and the stereochemistry confirmed, reduction to the other alcohol diastereomer was sought. Based on literature precedence from Doyle and co-workers it was expected that DIBALH may result in the desired diastereoselectivity, but this was not found to be the case (Table 4-8, entry 1).[20] Conversely, sodium borohydride resulted in opposite diastereoselectivity (entry 2), allowing optimization for the isolation of **4-45** as a single diastereomer in 85% yield (entry 4).

Table 4-8. Optimization of the ketone reduction to obtain the boryl alcohol epimer.

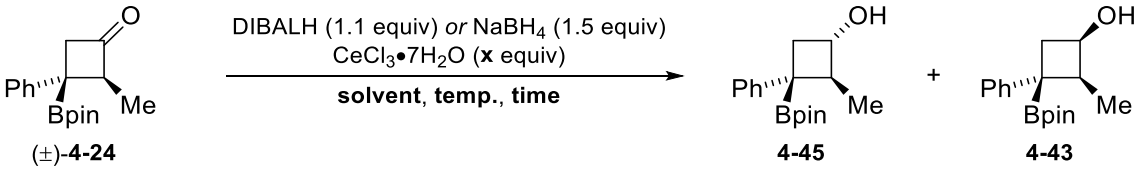

Entry	Reductant	x	solvent, temp., time	**4-45**:**4-43**[a]	isolated yield[b]
1	DIBALH	—	THF, 0 °C, 1 h	2:6	—
2	$NaBH_4$	—	MeOH, rt, O/N	3:1	—
3	$NaBH_4$	1.0	MeOH, rt, O/N	6:1	—
4	**$NaBH_4$**	**1.5**	**EtOH, –78 °C to rt, O/N**	**14:1**	**85%**

[a] Determined by ^{1}H NMR relative integration of the crude reaction mixture. [b] **4-45** was isolated as a single diastereomer by NMR (>20:1 dr) after column chromatography.

Based on the success of chemoselective ketone reduction to afford cyclobutanols **4-43** and **4-45**, it was expected that Grignard addition should also be a feasible application of the borylated cyclobutannones. However, a brief screening with vinyl magnesium bromide showed that decomposition was likely competing. The desired product **4-46** was only obtained in a 24% isolated yield, yet close to 90% conversion was observed by crude ^{1}H NMR (Scheme 4-5). In contrast, phenylmagnesium resulted in a clean reaction and an 86% isolated yield of **4-47** as a single diastereomer. The diastereomer obtained was assigned in anology to the reduction with L-selectride. The discrepancy between the efficiency of the two Grignard reagents is proposed to be due to the relative extent of coordination to the sterically conjested pinacolboronate. It is possible that significant coordination of the smaller vinyl nucleophile could lead to various decomposition pathways and a messier overall reaction. Furthermore, the ease of a borate formation with vinyl magnesium bromide, relative to phenylmagnesium bromide is in agreement with some carbon-carbon bond forming results described in Section 3.6.4.

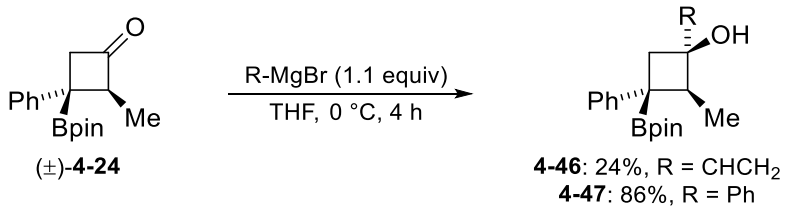

(±)-**4-24**

4-46: 24%, R = $CHCH_2$
4-47: 86%, R = Ph

Scheme 4-5. Chemoselective Grignard addition of **4-24**.

Finally, it was envisioned that either the ketone or alcohol functional groups of **4-24** and **4-43** could allow an efficient stereoselective entry to amine-containing cyclobutane products. Thus, reductive amination of **4-24** with *N*-methylbenzylamine and sodium triacetoxyborohydride under standard conditions seemed to lead to a 1:1 mixture of diastereomers after partial purification. Alternatively, a Mitsunobu attempt under standard reaction conditions with **4-43**, *N*-methyl-2-nitro-benzenesulfonamide and triphenylphosphine did not lead to any observable product after partial

purification of the crude reaction mixture. Therefore, no further attempts were made in regard to the amination of the ketone or alcohol in **2-34** and **4-43**, respectively.

4.6.3 Boron oxidation

Stereospecific oxygenation of aliphatic pinacol boronic esters is a standard and reliable application of organoboron compounds. In fact, the reaction is commonly used for isolation and purification of reaction products in reports of enantioselective approaches to alkylboronates. Interestingly, it was found that direct oxygenation of the conjugate borylation product **4-24** under standard conditions resulted in the ring-opened diketone **4-48** as the major product (Scheme 4-6). Considering similar issues were not reported in the oxygenation of 5- and 6-membered ring conjugate borylation products,[16,27] the observed ring opening to afford **4-48** is likely strain-promoted and further favoured by the formation of a carbonyl stabilized anion.[20b] The described reasoning is supported by the fact that oxidation of **4-43** worked as expected to afford diol **4-49** under similar conditions in 97% yield (Scheme 4-6).

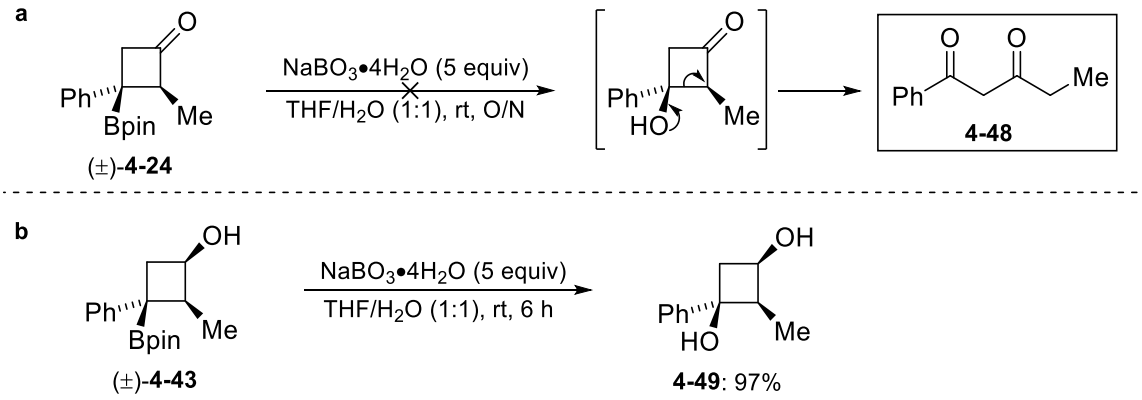

Scheme 4-6. Oxygenation attempts of (a) conjugate borylation product **4-24** (b) boryl alcohol **4-43**.

Unlike oxygenation, amination of boronates is a much less reliable reaction. Mild reaction conditions were recently reported for the amination of tertiary boronic esters by Morken and co-workers using methoxyamine and potassium *tert*-butoxide.[38] However, Morken's method has not

been extended to benzylic tertiary boronic esters to-date, reportedly due to issues of competing protodeboronation. Therefore, it was not surprising that all attempts to apply Morken's method to substrate **4-42** were unsuccessful. Furthermore, amination attempts involving *in situ* formation of the more reactive dichloroborane with using a ketal protected substrate were also found to be unproductive.[39]

4.6.4 Boron to carbon bond formation to afford carbon quaternary centers

Although the Suzuki-Miyaura cross-coupling is one of the most powerful $C_{sp}{}^2$-$C_{sp}{}^2$ bond forming reactions in organic chemistry, the extension to sp^2-sp^3 couplings is notoriously difficult, and even more so with tertiary boronates.[40,41] All attempts of palladium-catalyzed Suzuki-Miyaura cross-coupling of the conjugate borylation product **4-24** or its derivatives have been unsuccessful.

Other than the Suzuki-Miyaura cross-coupling, very few stereoselective transition metal catalyzed transformations of tertiary benzylic boronates have been reported. One notable exception is the rhodium-catalyzed addition of trifluoroborates to *para* nitrobenzaldehyde and *para* benzonitrile reported by Aggarwal and Ros.[42] With a view to attempt this transformation, the synthesis of trifluoroborate **4-50** was achieved in high yield (Figure 4-8). The trifluoroborate was then successfully applied in the synthesis of diketone **4-51** after a subsequent DMP oxidation, however as a mixture of diastereomers in 5:1 dr.[43] Based on the work of Aggarwal and Ros, it is expected that the rhodium-catalyzed addition of tertiary benzylic potassium trifluoroborates to aldehydes occurs with complete retention of stereochemistry, which has been recently further supported by Takacs and co-workers.[42,43] Therefore, it is being proposed that stereoretention at the benzylic position is most likely and that epimerization at the methyl center results in a mixture of diastereomers of the product. Methyl epimerization is further supported by the fact that the dr of the diastereomeric mixture of diketone **4-51** changed from 5:1 to 3:1 dr after sitting in $CDCl_3$ at room

temperature for less than a week. Selective 1D NOESY excitation experiments of the methyl group of each diastereomer suggests that the methyl group is *syn* to the nitro aryl keto group in the major diastereomer and *anti* in the minor.

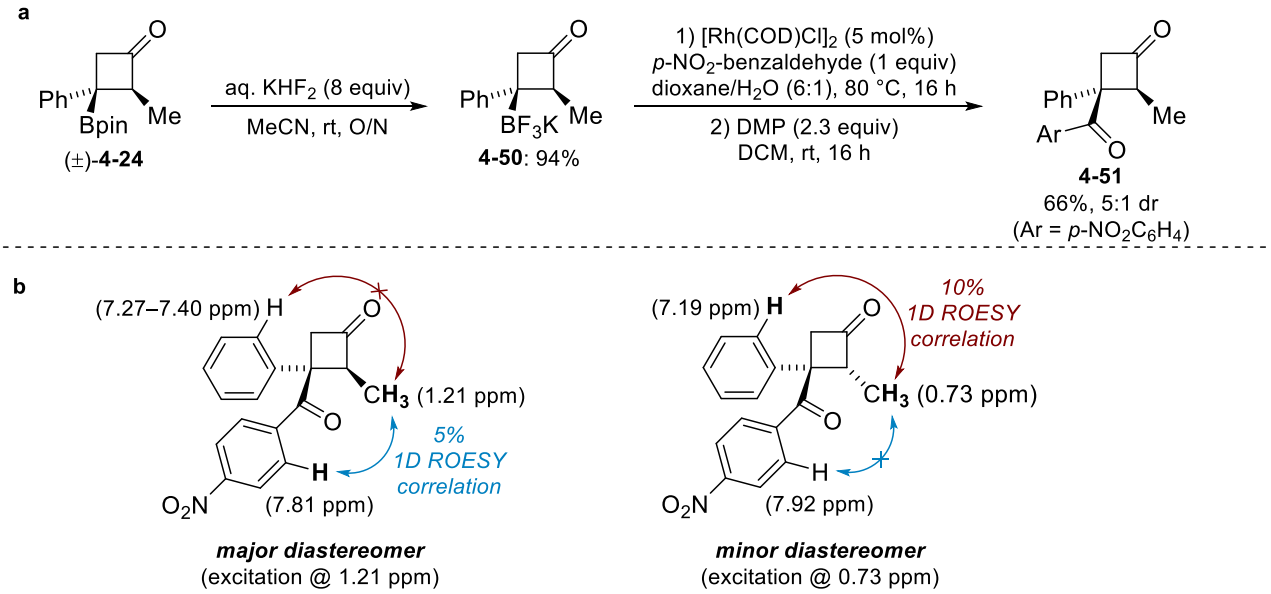

Figure 4-8. (a) Rh-catalyzed addition to *p*-NO_2-benzaldehyde (b) confirmation of the relative stereochemistry.

Due to the aforementioned lack of general transition metal-catalyzed functionalizations, the attention to C–C bond forming reactions was turned to lithiation-borylation approaches. For these studies, ketal substrate **4-52** was used, which was accessed from **4-24** under mild conditions (Scheme 4-7). After extensive screening, it was found that Zweifel olefination, acetylation and alkynylation were all applicable transformations to substrate **4-52**. Both the Zweifel olefination and acetylation worked reasonably well in over 50% yield without further optimization (Scheme 4-7).[44]

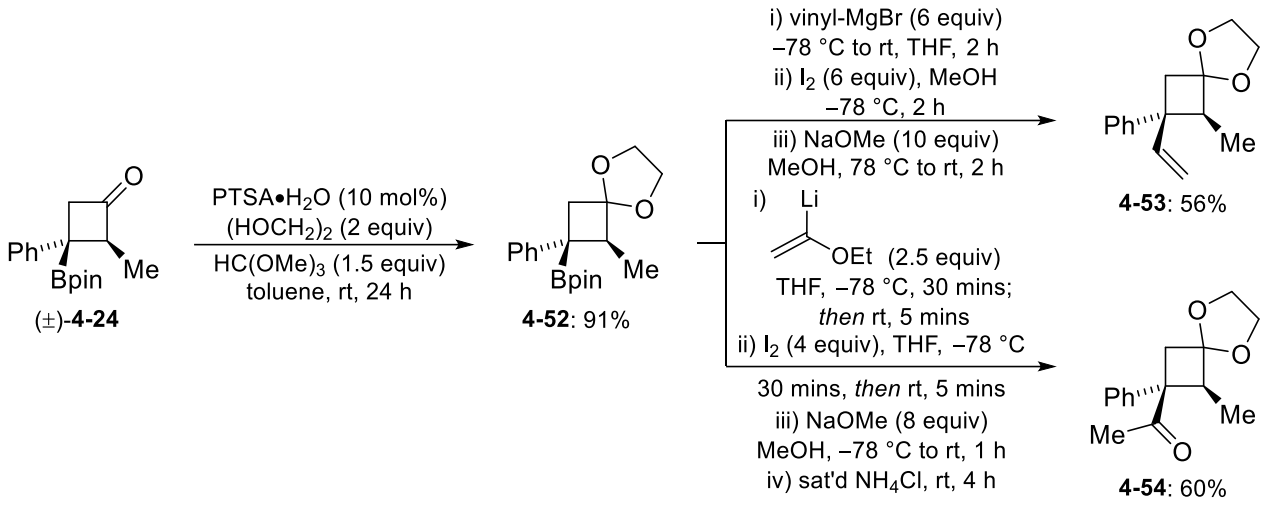

Scheme 4-7. Zweifel olefination and acetylation of boryl ketal **4-52**.

Conversely, the alkynylation required a small temperature screening for an efficient reaction. The alkynylation methodology is a two-step process involving a Zweifel olefination with alkenyl carbamate **4-55** and subsequent elimination of the alkenyl carbamate intermediate to furnish the desired terminal alkyne.[45] It was found that briefly warming the reaction to –40 °C was essential for borate formation in the Zweifel olefination step to form alkenyl carbamate **4-56**; only about 15% conversion was observed when the temperature was held at –78 °C.[19] Furthermore, although the elimination step went to full conversion, a large amount of decomposition was observed when the elimination was performed at 0 °C (Scheme 4-8a). However, simply holding the temperature at –20 °C allowed a much cleaner reaction and the development of an efficient alkynylation process with a 74% overall yield of quaternary ethynyl cyclobutane **4-57** (Scheme 4-8b).

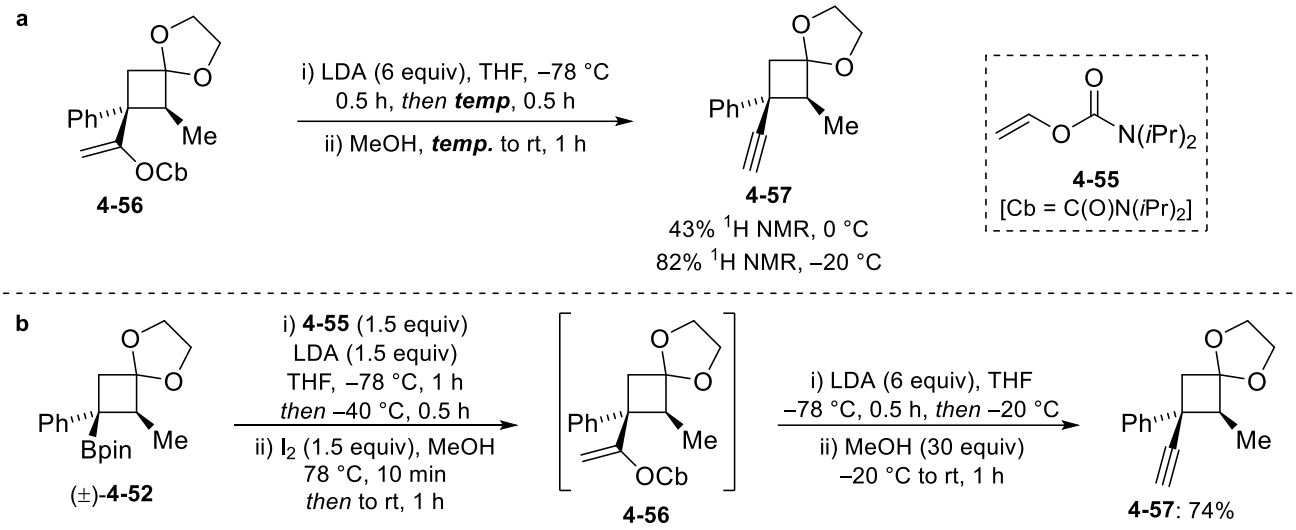

Scheme 4-8. (a) Optimization of the elimination step (b) optimized process for acetylene **4-57**.

Further attempts of other C–C bond variations, such as furanylation, pyridinylation and Matteson homologation were unsuccessful.[46] Notably, difficulties in conversion was met in the case of both the pyridinylation and Matteson homologation. In particular, a number of variations of the Matteson homologation were attempted, yet all experiments led only to the formation of small amounts of a complex mixture when conversion was achieved.[43,47] The fact that only two of the mentioned lithiation-borylation C–C bond forming reactions worked without further modifications or suffering from low efficiency highlights a lack in substrate generality that many of these transformations seem to be amenable to.

4.6.5 Protodeboronation

To-date, the stereoselective protodeboronation of tertiary boronates is largely limited to a 2010 report by Aggarwal and co-workers using benzylic and (bis)benzylic tertiary pinacolboronates.[48] A small screening of reaction conditions for the protodeboronation of **4-24** following Aggarwal's protocol indicated that the reaction's efficiency was quite dependent on the reaction temperature and

time. Overall it was found that over 50% yield of the protodeboronated product **4-58** could be achieved as a mixture of diastereomers in about a 10:1 dr (Scheme 4-9a). The *trans* relative stereochemistry was confirmed by comparing the NMR spectra with that of the *cis* cyclobutanone **4-59**, which had been previously synthesized and characterized by Dr. Michele Boghi from our laboratory (Scheme 4-9b).

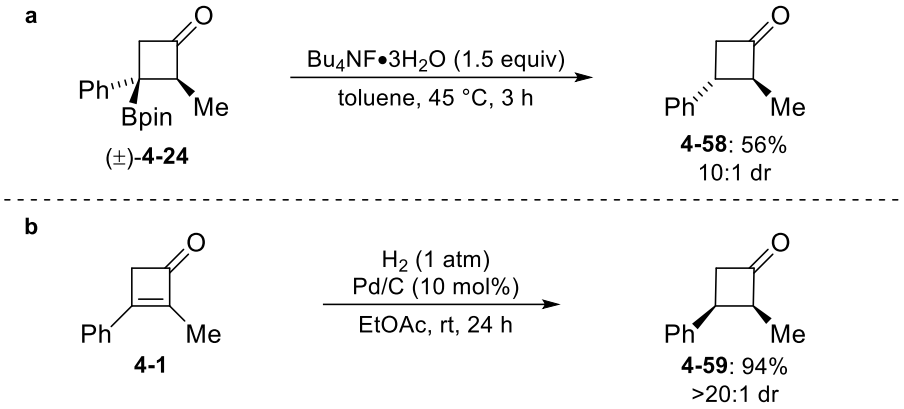

Scheme 4-9. (a) Protodeboronation of **4-24** (b) synthesis of the *syn* diastereomer for confirmation of relative stereochemistry.

4.6.6 Summary of successful applications

The synthetic potential and versatility of the bifunctional cyclobutylboronate products is summarized in Figure 4-9. Unless otherwise noted, all products were obtained as a single diastereomer according to ^{1}H NMR analysis. Remarkably, chemoselective functionalization of the ketone or boronic ester is possible in some cases. It is clear that the developed conjugate borylation allows access to synthetically versatile borylated cyclobutanones, which can be used as intermediates for the synthesis of a variety of novel cyclobutane-containing scaffolds, including ones quaternary stereocenters.

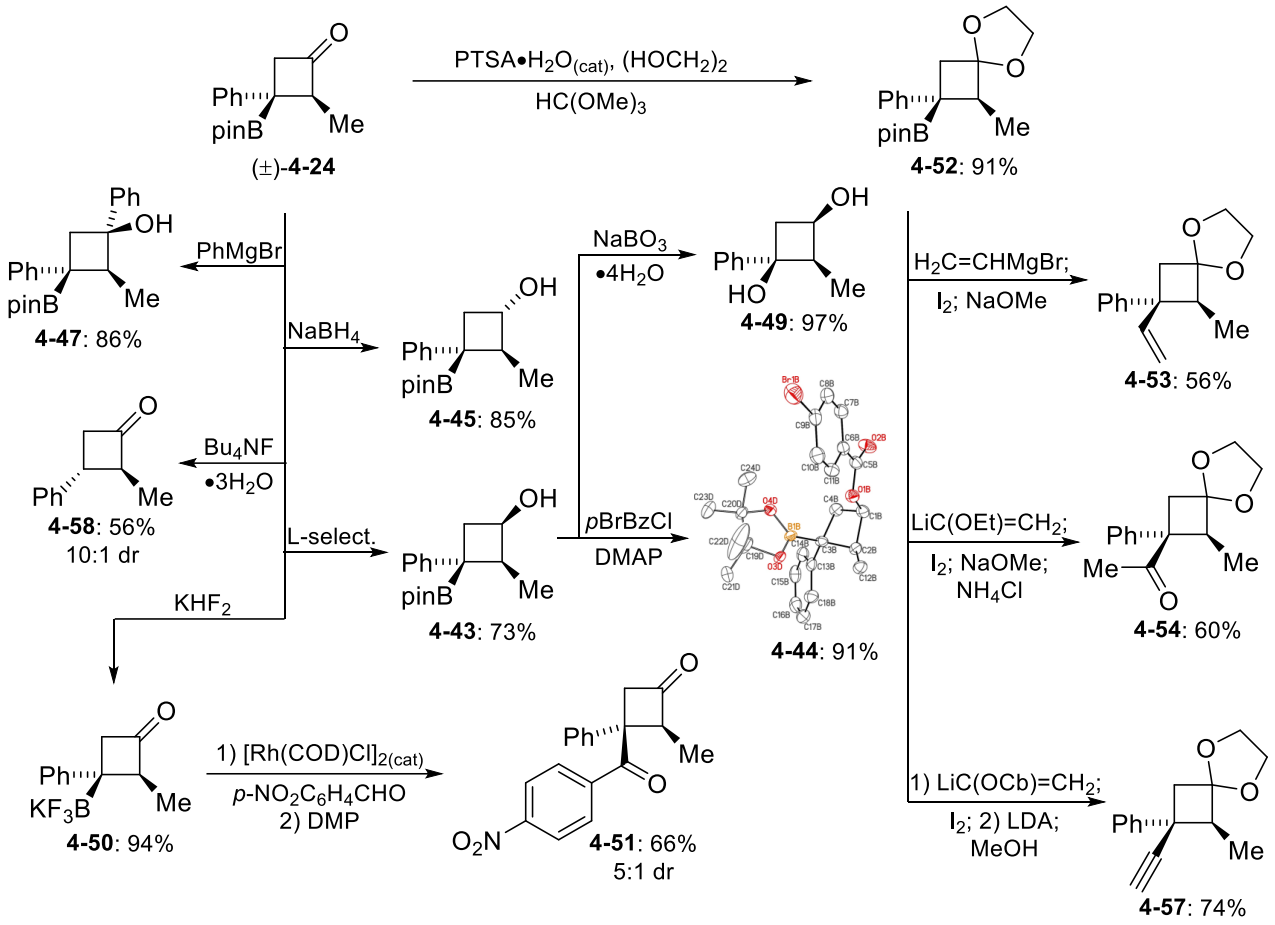

Figure 4-9. Summary of successful synthetic applications of **4-24**. For exact reaction conditions, the reader is referred to the sections above.

4.7 Proposed rational for the observed diastereoselectivity

As mentioned above, the stereochemistry of all of the cyclobutylboronate products were assigned based on X-ray analysis of the *para* benzoyl ester derivative **4-44** (c.f. Scheme 4-4). Confirmation of the relative stereochemistry allows an analysis of the preferred diastereoselectivity observed in this conjugate borylation methodology. The generally accepted mechanism for the conjugate borylation of ketones is shown in Figure 4-10.[49] The accepted diastereo-determining step is an alcohol-promoted proto-decupration of the borylated copper enolate. Therefore, the observed diastereoselectivity can be rationalized from either an irreversible kinetically-controlled proto-

decupration step or a thermodynamically-controlled epimerization after release of the borylated ketone.

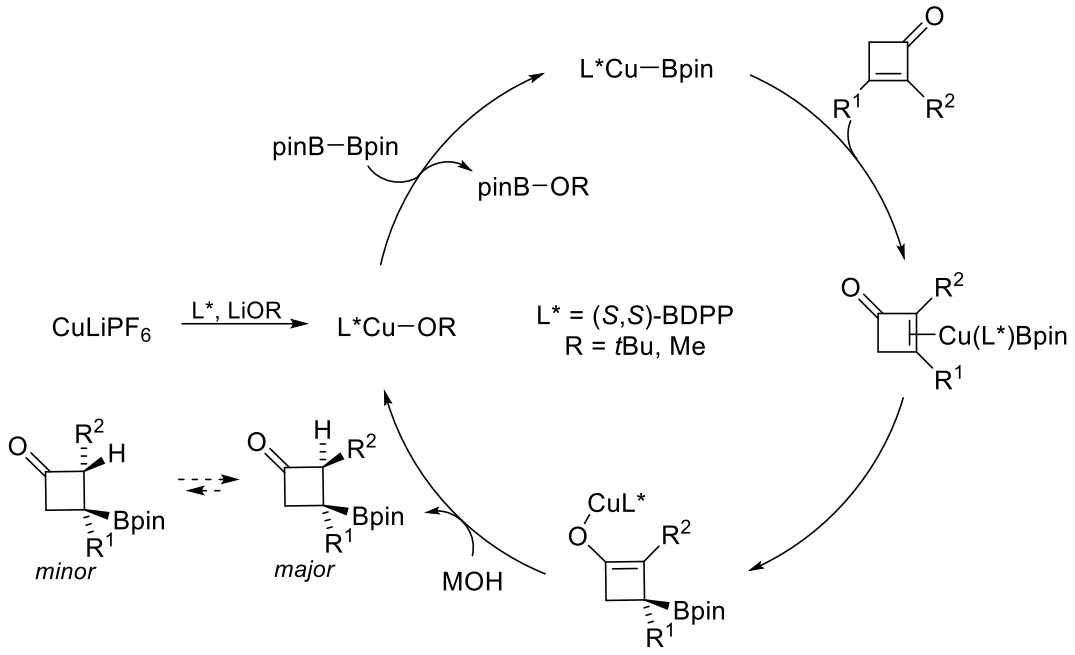

Figure 4-10. General mechanistic steps for the conjugate borylation of ketones.

To probe the two options described above, cyclobutylboronate **4-24** was subjected to the reaction conditions as a diastereomeric mixture with a low 3:1 dr (Scheme 4-10). The experiment showed an insignificant change in the diastereomeric ratio, suggesting that epimerization of **4-24** does not occur under the reaction conditions. The slight discrepancy in the diastereoselectivity is attributed to decomposition of **4-24**, considering the small reaction scale.

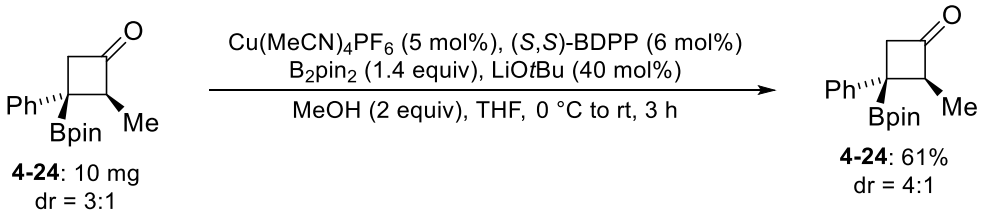

Scheme 4-10. Epimerization control experiment.

With the information provided in Scheme 4-10, the observed diastereoselectivity is likely rationalized by a non-reversible sterically-controlled proto-decupration step of the copper enolate

(Figure 4-11). Considering that the globular pinacolboronate substituent is significantly larger than the flat phenyl group, it is reasonable to propose that the approach of methanol *syn* to the phenyl group is kinetically favourable. Conversely, if the alcohol approaches from the same side as the large Bpin group, the approach may be more sterically congested leading to formation of the minor diastereomer. Notably, Ito and co-workers recently proposed a related model of pinacol boronic ester diastereocontrol in their work regarding the conjugate borylation of indoles (c.f. Chapter 1, Scheme 1-11).[50]

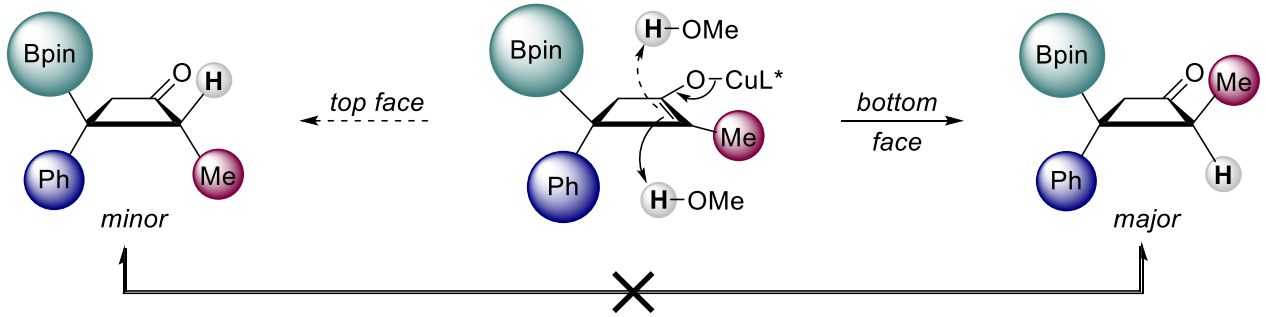

Figure 4-11**.** Proposed stereochemical model of the proto-decupration step.

Moreover, ground state gas phase calculations of each diastereomer using an AM1 model (Spartan chemistry software) suggests that the two diastereomers are similar in energy, with the minor diastereomer determined to be more stable by 1.1 kcal mol^{-1}. In theory, the calculations suggests that epimerization could lead to a ratio of **4-24** favouring the minor diastereomer. However, all attempts to epimerize the major diastereomer were ineffective and either led to no epimerization or competing decomposition of **4-24**.[51]

4.8 Conjugate borylation of cyclobutenoates

4.8.1 Project design

During our studies towards the conjugate borylation to access cyclobutylboronates, cyclobutenoates were also viewed as viable substrates to afford enantioenriched cyclobutylboronates. In particular,

it was envisioned that the borylated products have the potential to serve as efficient Suzuki-Miyaura cross-coupling partners for the late-stage introduction of enantioenriched cyclobutane scaffolds (Figure 4-12). Relevant literature precedence exists of carbonyl-promoted Suzuki-Miyaura cross-coupling of secondary boronates.[12,41] Furthermore, the successful coupling of a secondary potassium cyclobutyl trifluoroborate salt with aryl chlorides was reported by Molander and Gormisky.,[52]

The conjugate borylation products of Figure 4-12 are structurally related to the cyclobutylboronates reported in Yu's C–H borylation approach (c.f. Figure 4-3b). However, the ester products would be more synthetically appealing than Yu's polyfluorinated amide, which is a directing group required in the C–H borylation. In the report from Yu and co-workers, deprotection of the amide was achieved subsequently to boronate functionalization using quite harsh conditions ($BF_3{\cdot}OEt_2$, MeOH, 110 °C, 48 h). Furthermore, it is possible that both cyclobutylboronate diastereomers may be accessible in the proposed conjugate borylation approach, either from inverting the diastereocontrol in the proto-decupration step, or epimerization of the resulting borylated ester.

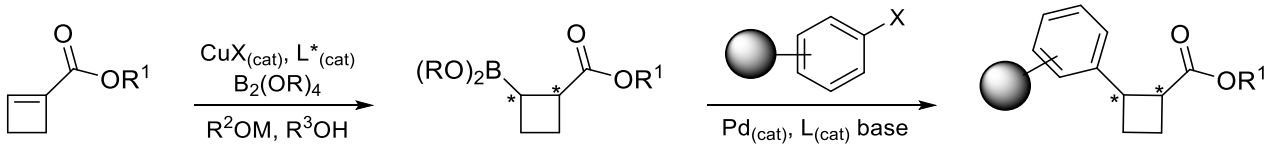

Figure 4-12. Project design for the conjugate borylation of cyclobutenoates.

4.8.2 Development of a novel cyclobutenoate substrate

The initial starting point for the substrate design focused on the synthesis of known α,β-unsaturated cyclobutenoate esters. Synthesis of benzyl ester **4-62** was achieved following a modified literature procedure (Scheme 4-11).[53] Notably, due to the carcinogenicity of carbon tetrachloride, an α-bromination procedure in benzene was developed, which required purification by distillation. Although the subsequent initial results of the racemic conjugate borylation of **4-62** were promising,

it was found that the cyclobutenoate ester was prone to polymerization in our hands. However, a simple modification to the more sterically hindered benzhydrol ester (**4-63**) afforded the use of a much more stable substrate for optimization of the conjugate borylation reaction. The synthetic protocol allowed the synthesis of two grams of benzhydrol ester **4-63** as a white solid, which was found to be stable over several months at room temperature.

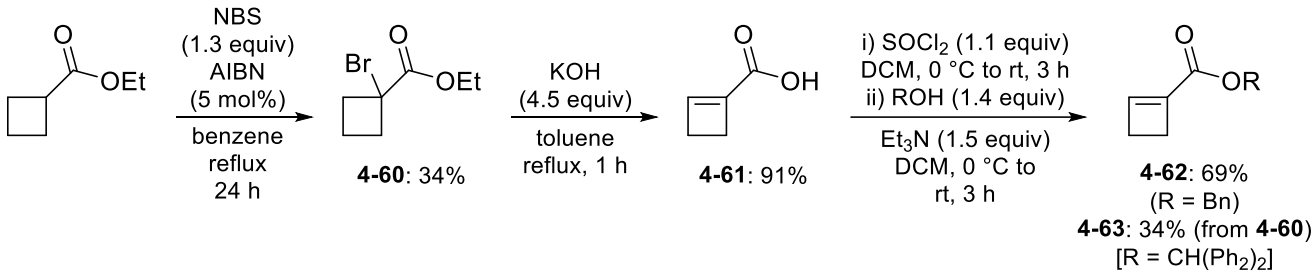

Scheme 4-11. Synthesis of cyclobutenoate starting material.

4.8.3 Initial conjugate borylation results

With an appropriate substrate identified, cyclobutenoate **4-63** was subject to previously reported, racemic borylation conditions reported by Tortosa and co-workers.[11] The reaction went to full conversion and was found to be quite clean, albeit with a low diastereoselectivity of about 3:1 dr by ^{1}H NMR integration (Scheme 4-12a).. The isolated yield was moderate likely due to instability on silica, but a small amount of 10:1 dr of each diastereomer was achieved for characterization purposes Samples of (±)-**4-64** were submitted to the Pfizer collaborators for HTS of chiral ligands, in a similar manner to the HTS screen previously described for cyclobutenone **4-1** (c.f. Section 3.4.1). From the HTS screening, a commercially available Naud ligand was identified to afford the highest enantioselectivity. The reaction was found to be reproducible on a standard reaction scale to provide **4-64** in a high 85% ^{1}H NMR yield, yet a 1:1 dr (Scheme 4-12b). The reproducibility of this reaction was used as a starting point for a new graduate student, Mr. Kevin Nguyen. The reproducibility of the enantioselective reaction has since been achieved on a standard reaction scale and was confirmed

to provide product **4-64** in over 90% *ee* for further development. Further optimization along with a study of synthetic transformations of **4-64** are currently in progress in the Hall Laboratory.

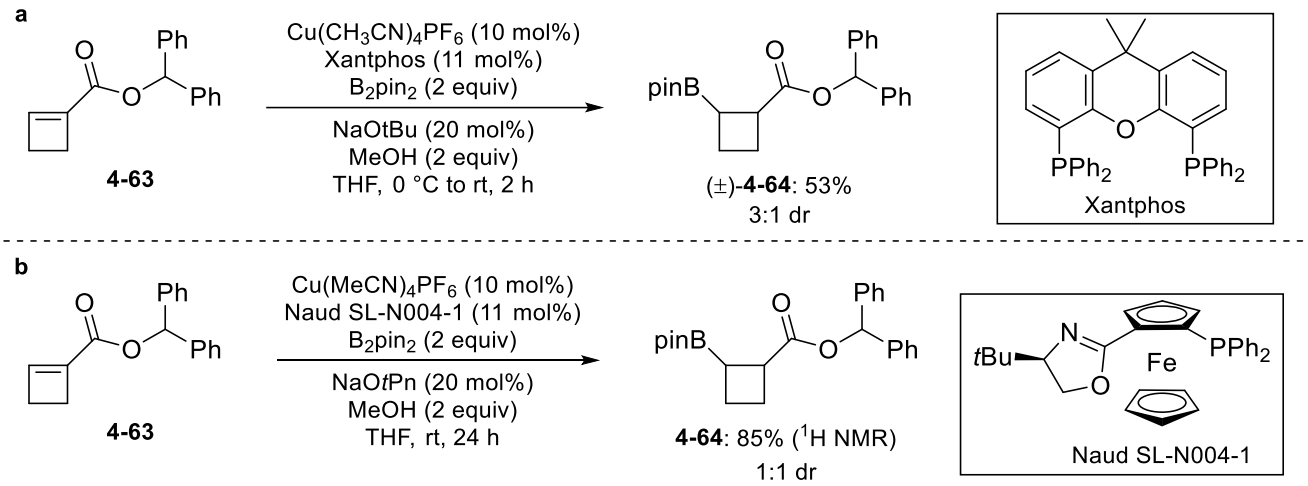

Scheme 4-12. Initial (a) racemic and (b) enantioselective conjugate borylation results of cyclobutenoate **4-63**.

4.9 Summary

In summary, a catalytic enantioselective approach to novel tertiary cyclobutylboronates by conjugate borylation of α-alkyl,β-aryl/alkyl cyclobutenones has been successfully developed. Vital to this advance include a new and practical access to unsymmetrically disubstituted cyclobutenones **4-1** and the application of HTS of 118 chiral ligands to identify an efficient starting point to optimize the desired reaction in up to 96% *ee*. Both the ketone and boronic ester moieties in cyclobutylboronate **4-24** can be transformed orthogonally, in high stereoselectivity, to access novel cyclobutane scaffolds of potential pharmaceutical interest. The successful application of the conjugate borylation to cyclobutenones suggests a promising platform for a general access to numerous enantioenriched non-fused cyclobutane rings. Furthermore, promising initial results regarding the borylation of novel cyclobutenoate substrate **4-63** has allowed a starting point for further investigations of the conjugate borylation approach to novel cyclobutylboronate scaffolds.

4.10 Experimental

4.10.1 General methods

Unless otherwise indicated, all reactions were performed under a nitrogen or argon atmosphere using glassware that was washed thoroughly and flame-dried in vacuo prior to use. DCM, toluene and DMF were used directly from an MBraun Solvent Purification System. Acetonitrile, DMPU and triethylamine were purchased from Sigma Aldrich and distilled from calcium hydride before use. THF was obtained from an MBraun Solvent Purification System, and was freeze-pump-thawed for three cycles and stored under nitrogen before use (only when used for the enantioselective conjugate borylation). Methanol (reagent grade, 99%) was dried over 3Å molecular sieves before use and stored under nitrogen. Bis(pinacolato)diboron (reagent grade 97%) was purchased from Combi-Blocks Inc., and recrystallized from pentanes prior to use. Thionyl chloride was purchased from Sigma Aldrich, and distilled prior to use. Triflic anhydride was purchased from Oakwood Chemicals (reagent grade 99.5%) was used as received and stored in a flame-dried flask under nitrogen. The triflic anhydride was distilled over phosphorous pentoxide if the liquid turned dark brown in colour. Ethyl vinyl ether was dried with calcium hydride and filtered immediately before use. *n*-Butyllithium and *tert*-butyllithium were titrated with diphenylacetic acid (recrystallized from toluene) before use. *N*,*N*-Dimethylbutanamide and *N*,*N*-dimethylbenzenepropanamide were made in one step from the carboxylic acid, following standard protocols with thionyl chloride and dimethylamine hydrochloride.[54] All other reagents were purchased from Sigma Aldrich, Combi-Blocks or Strem Chemicals and used without further purification. The pure cyclobutylboronate products were found to be stable over several months when stored in a -20 °C freezer under argon atmosphere.

Thin layer chromatography (TLC) was performed on Merck Silica Gel 60 F254 plates, and visualized with UV light, $KMnO_4$, and PMA stain. Flash chromatography was performed on ultra-pure silica gel 230-400 mesh. Nuclear magnetic resonance (NMR) spectra were recorded on Agilent/Varian INOVA-400, INOVA-500, INOVA-600, or INOVA-700 MHz instruments. The residual solvent ($CDCl_3$, CD_3CN, $(CD_3)_2CO$) proton (^1H) and carbon (^{13}C) signals were used as internal references. ^1H NMR data is presented as follows: chemical shift in ppm (δ) downfield from tetramethylsilane (multiplicity, coupling constant, integration). The following abbreviations are used in reporting the ^1H NMR data: s, singlet; br s, broad singlet; d, doublet; t, triplet; dd, doublet of doublet; m, multiplet. The error of coupling constants from ^1H NMR spectra is estimated to be 0.3 Hz. High resolution mass spectra were recorded by the University of Alberta Mass Spectrometry Services Laboratory using either electron impact (EI) ion source with double focusing sector analyzer (Kratos Analytical MS-50G), or electrospray (ESI) ion source with orthogonal acceleration TOF analyzer (Agilent Technologies 6220 oaTOF). Infrared spectra (performed on a Nicolet Magna-IR 750 instrument equipped with a Nic-Plan microscope) and optical rotations (performed using a Perkin-Elmer 241 polarimeter) were recorded by the University of Alberta Analytical and Instrumentation Laboratory. Optical rotations were measured using a 1 mL cell with a 1 cm length. The enantiomeric excess for chiral compounds were determined using a HPLC Agilent instrument with a Chiralpak IC/AS or Chiralcel OD column using specific conditions indicated for each individual compounds. Melting points (m.p.) of solids were measured on a melting point apparatus and are uncorrected.

4.10.2 General procedure A: synthesis of α,β-disubstituted cyclobutenones (Table 4-1)

N-*N*-dimethylpropionamide (*N*,*N*-DMP, 1.00 equiv) was dissolved in DCM (0.20 or 0.50 M) in a flame-dried 4-neck round bottom flask equipped with a condenser. 2-Fluoropyridine (1.20 equiv)

and the alkyne (1.20 equiv) were sequentially added to the reaction mixture followed by triflic anhydride dropwise (Tf_2O, 1.10 equiv). The reaction was heated to reflux overnight before cooling to 0 °C. Sodium hydroxide (0.60 or 1.0 M, 2.2 equiv) was added and the reaction was left to stir vigorously for 4 h in an ice bath. The reaction mixture was quenched with 1M HCl and transferred to a seperatory funnel. The layers were separated and the aqueous layer was extracted three times with DCM. The combined organic layers were washed with saturated sodium bicarbonate, water, brine and dried with magnesium sulfate, filtered, and concentrated *in vacuo*. The crude oil was filtered through a short silica plug (15% ethylacetate/hexanes), and the fractions were combined and re-concentrated *in vacuo*, providing a mixture of cyclobutenone regioisomers as a yellow oil. The cyclobutenone regioisomers were dissolved in ethanol (0.20 M). In cases where the crude reaction mixture was insoluble in 100% EtOH, toluene was added (up to 1:1 EtOH:toluene) – in these cases the solvent system is specified for each compound. Potassium *tert*-butoxide (1.0 M, 0.30 equiv) was added dropwise to the solution and the reaction was left to stir at room temperature for 4–16 h. The light orange solution was quenched by addition of saturated ammonium chloride, diluted with ethyl acetate and the layers were separated. The aqueous layer was extracted with ethyl acetate three times, and the combined organic layers were washed with water, brine and dried with sodium sulfate, filtered, and concentrated in vacuo giving the crude cyclobutenone as an oil or solid, which was purified by flash column chromatography using the eluent specified below for each compound.

4.10.3 Characterization of the α,β-disubstituted cyclobutenones 4-1 to 4-19

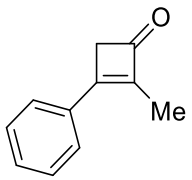

2-methyl-4-phenylcyclobut-2-enone (4-1): Prepared according to general procedure A with *N,N*-DMP (5.5 mL, 50 mmol, 1.0 equiv), phenylacetylene (6.5 mL, 60 mmol, 1.2 equiv), 2-fluoropyridine (5.5 mL, 60 mmol, 1.2 equiv), Tf_2O (10 mL, 55 mmol, 1.1 equiv) and potassium *tert*-butoxide (15 mL, 0.30 equiv). The crude material was purified by flash chromatography (5% ethyl actetate/hexanes) to provide a white-yellow solid (3.51 g, 44% yield over three steps). All spectral data matched the literature:[26] **mp =** 57.8–59.1 °C; **^{1}H NMR** (500 MHz, $CDCl_3$) δ 7.64–7.56 (m, 2H), 7.55–7.45 (m, 3H), 3.46 (q, *J* = 2.3 Hz, 2H), 2.01 (t, *J* = 2.4 Hz, 3H); **^{13}C NMR** (125 MHz, $CDCl_3$) δ 190.0, 163.5, 141.0, 132.8, 131.0, 129.2, 129.0, 48.2, 9.4; **IR** (cast film, $CHCl_3$ cm^{-1}) 3070, 2918, 1750, 1616, 1447, 1348, 1068; **HRMS** (EI) for $C_{11}H_{10}O$ calcd. 158.0732; found 158.0732.

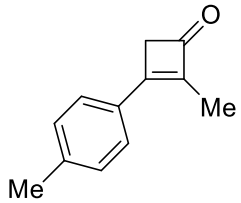

2-methyl-4-(*p*-tolyl)cyclobut-2-enone (4-2): Prepared according to general procedure A with *N,N*-DMP (0.81 mL, 7.3 mmol, 1.0 equiv), 4-ethynyltoluene (1.0 g, 8.8 mmol, 1.2 equiv), 2-fluoropyridine (0.76 mL, 8.8 mmol, 1.2 equiv), Tf_2O (1.4 mL, 8.1 mmol, 1.1 equiv) and potassium *tert*-butoxide (2.2 mL, 0.30 equiv). The crude material was purified by flash chromatography (5% ethyl actetate/hexanes) to provide a white solid (522 mg, 41% yield over three steps): **mp =** 84.8–86.0 °C; **^{1}H NMR** (500 MHz, $CDCl_3$) δ 7.54–7.42 (m, 2H), 7.35–7.28 (m, 2H), 3.43 (q, *J* = 2.4 Hz, 2H), 2.43 (s, 3H), 1.99 (t, *J* = 2.4 Hz, 3H); **^{13}C NMR** (125 MHz, $CDCl_3$) δ 190.1, 163.6, 141.7,

139.9, 130.2, 129.7, 129.2, 48.1, 21.7, 9.4; **IR** (cast film, $CHCl_3$ cm^{-1}) 3013, 2945, 1747, 1619, 1448, 1345, 1011; **HRMS** (EI) for $C_{12}H_{12}O$ calcd. 172.0888; found 172.0888.

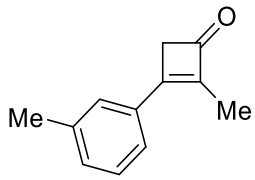

2-methyl-4-(*m*-tolyl)cyclobut-2-enone (4-3): Prepared according to general procedure A with *N,N*-DMP (0.26 mL, 2.6 mmol, 1.0 equiv), 4-ethynyltoluene (0.31 g, 2.7 mmol, 1.1 equiv), 2-fluoropyridine (0.26 mL, 3.1 mmol, 1.2 equiv), Tf_2O (0.50 mL, 2.8 mmol, 1.1 equiv) and potassium *tert*-butoxide (0.78 mL, 0.30 equiv). The crude material was purified by flash chromatography (5% ethyl actetate/hexanes) to provide a white solid (192 mg, 44% yield over three steps): **mp** = 41.1–42.3 °C; **^{1}H NMR** (500 MHz, $CDCl_3$) δ 7.44–7.35 (m, 3H), 7.33–7.26 (m, 1H), 3.44 (q, J = 2.3 Hz, 2H), 2.43 (s, 3H), 2.00 (t, J = 2.3 Hz, 3H); **^{13}C NMR** (125 MHz, $CDCl_3$) δ 190.2, 163.8, 140.8, 138.7, 132.8, 131.8, 129.8, 128.8, 126.4, 48.2, 21.4, 9.4; **IR** (cast film, $CHCl_3$ cm^{-1}): 3045, 2918, 1753, 1624, 1425, 1348, 1085; **HRMS** (EI) for $C_{12}H_{12}O$ calcd. 172.0888; found 172.0888.

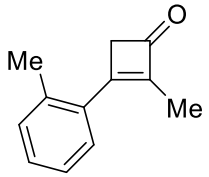

2-methyl-4-(*o*-tolyl)cyclobut-2-enone (4-4): Prepared according to general procedure A with *N,N*-DMP (0.56 mL, 5.0 mmol, 1.0 equiv), 2-ethynyltoluene (0.70 g, 6.0 mmol, 1.2 equiv), 2-fluoropyridine (0.52 mL, 6.0 mmol, 1.2 equiv), Tf_2O (1.0 mL, 5.5 mmol, 1.1 equiv) and potassium *tert*-butoxide (1.5 mL, 0.30 equiv). The crude material was purified by flash chromatography (5% ethyl actetate/hexanes) to provide a white solid (564 mg, 65% yield over three steps): **mp** = 63.8–64.7 °C; **^{1}H NMR** (500 MHz, $CDCl_3$) δ 7.45 (dd, J = 7.6, 1.5 Hz, 1H), 7.37–7.22 (m, 3H), 3.59 (q,

J = 2.4 Hz, 2H), 2.45 (s, 3H), 1.89 (t, *J* = 2.4 Hz, 3H); **^{13}C NMR** (125 MHz, $CDCl_3$) δ 190.6, 165.8, 143.6, 137.0, 132.4, 131.4, 130.4, 129.1, 126.0, 51.7, 21.1, 9.5; **IR** (cast film, $CHCl_3$ cm^{-1}): 3057, 2967, 1741, 1592, 1447, 1337, 1017; **HRMS** (EI) for $C_{12}H_{12}O$ calcd. 172.0888; found 172.0888.

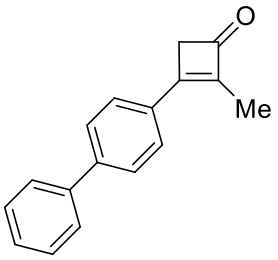

4-([1,1'-biphenyl]-4-yl)-2-methylcyclobut-2-enone (4-5): Prepared according to general procedure A with *N*,*N*-DMP (0.71 mL, 6.4 mmol, 1.0 equiv), 4-ethynyl-1,1'-biphenyl (1.2 g, 6.7 mmol, 1.1 equiv), 2-fluoropyridine (0.67 mL, 7.7 mmol, 1.2 equiv), Tf_2O (1.1 mL, 7.1 mmol, 1.1 equiv) and potassium *tert*-butoxide (2.0 mL, 0.30 equiv)) with 3.3:1 EtOH:toluene (0.15 M) for the alkene migration step. The crude material was purified by flash chromatography (2.5 to 5 to 10% ethyl actetate/hexanes) to provide a yellow solid (436 mg, 29% yield over three steps): **mp =** 131.7–133.2 °C; **^{1}H NMR** (500 MHz, $CDCl_3$) δ 7.77–7.71 (m, 2H), 7.70–7.61 (m, 4H), 7.52–7.45 (m, 2H), 7.44–7.37 (m, 1H), 3.49 (q, *J* = 2.3 Hz, 2H), 2.05 (t, *J* = 2.4 Hz, 3H); **^{13}C NMR** (126 MHz, $CDCl_3$) 190.0, 163.1, 143.7, 141.0, 140.0, 131.7, 129.7, 129.1, 128.2, 127.6, 127.2, 48.3, 9.5; **IR** (cast film, $CHCl_3$ cm^{-1}) 3056, 3029, 2959, 2918, 2856, 2810, 1766, 1737, 1615, 1410, 1400, 1338, 1093, 839, 771; **HRMS** (EI) for $C_{17}H_{14}O$ calcd. 234.1045; found 234.1044.

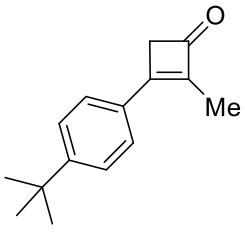

4-(4-(*tert*-butyl)phenyl)-2-methylcyclobut-2-enone (4-6): Prepared according to general procedure A with *N*,*N*-DMP (0.66 mL, 6.0 mmol, 1.0 equiv), 1-(1,1-dimethylethyl)-4-ethynyl-

benzene (1.0 g, 6.3 mmol, 1.1 equiv), 2-fluoropyridine (0.70 mL, 7.2 mmol, 1.2 equiv), Tf_2O (1.1 mL, 6.6 mmol, 1.1 equiv) and potassium *tert*-butoxide (1.8 mL, 0.30 equiv). The crude material was purified by flash chromatography (5% ethyl actetate/hexanes) to provide a yellow solid (427 mg, 33% yield over three steps): **mp =** 53.4–55.0 °C; **^{1}H NMR** (500 MHz, $CDCl_3$) δ 7.60–7.48 (m, 4H), 3.43 (q, J = 2.3 Hz, 2H), 1.99 (t, J = 2.4 Hz, 3H), 1.36 (s, 9H); **^{13}C NMR** (126 MHz, $CDCl_3$) δ 190.2, 163.6, 154.8, 140.2, 130.2, 129.2, 126.0, 48.1, 35.2, 31.2, 9.4; **IR** (cast film, $CHCl_3$ cm^{-1}) 2963, 2912, 1757, 1621, 1407, 1341, 1112, 1010, 837; **HRMS** (EI) for $C_{15}H_{18}O$ calcd. 214.1358; found 214.1355.

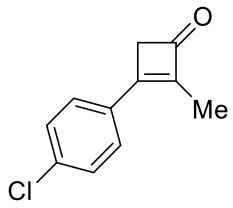

4-(4-chlorophenyl)-2-methylcyclobut-2-enone (4-7): Prepared according to general procedure A with *N,N*-DMP (0.81 mL, 7.4 mmol, 1.0 equiv), 1-ethynyl-4-chlorobenzene (1.2 g, 8.8 mmol, 1.2 equiv), 2-fluoropyridine (0.76 mL, 8.8 mmol, 1.2 equiv), Tf_2O (1.4 mL, 8.1 mmol, 1.1 equiv) and potassium *tert*-butoxide (2.2 mL, 0.30 equiv). The crude material was purified by flash chromatography (5% ethyl actetate/hexanes) to provide a yellow solid (643 mg, 46% yield over three steps): **mp =** 111.7–113.2 °C; **^{1}H NMR** (400 MHz, $CDCl_3$) δ 7.55–7.44 (m, 4H), 3.45 (q, J = 2.3 Hz, 2H), 1.99 (t, J = 2.3 Hz, 3H); **^{13}C NMR** (176 MHz, $CDCl_3$) δ 189.5, 162.0, 141.5, 137.0, 131.2, 130.3, 129.3, 48.3, 9.4; **IR** (cast film, $CHCl_3$ cm^{-1}) 3056, 2945, 1748, 1623, 1444, 1338, 1090; **HRMS** (EI) for $C_{11}H_9ClO$ calcd. 192.0342; found 192.0339.

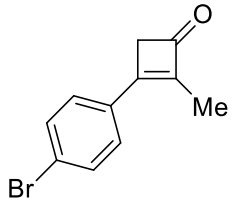

4-(4-bromophenyl)-2-methylcyclobut-2-enone (4-8): Prepared according to general procedure A with *N,N*-DMP (0.66 mL, 5.9 mmol, 1.0 equiv), 1-ethynyl-4-bromobenzene (1.1 g, 6.2 mmol, 1.2 equiv), 2-fluoropyridine (0.55 mL, 6.2 mmol, 1.2 equiv), Tf_2O (1.1 mL, 6.5 mmol, 1.1 equiv) and potassium *tert*-butoxide (2.4 mL, 0.40 equiv). The crude material was purified by flash chromatography (5% ethyl actetate/hexanes) to provide a white solid (643 mg, 46% yield over three steps): **mp =** 112.3–113.0 °C; **^{1}H NMR** (400 MHz, $CDCl_3$) δ 7.67–7.60 (m, 2H), 7.47–7.40 (m, 2H), 3.45 (q, *J* = 2.3 Hz, 2H), 1.99 (t, *J* = 2.3 Hz, 3H); **^{13}C NMR** (176 MHz, $CDCl_3$) δ 189.6, 162.1, 141.8, 132.3, 131.7, 130.5, 125.6, 48.3, 9.5; **IR** (cast film, $CHCl_3$ cm^{-1}) 3055, 2941, 2909, 1754, 1622, 1583, 1337, 1070, 1007, 831, 726; **HRMS** (EI) for $C_{11}H_9O^{79}Br$ calcd. 235.9837; found 235.9840.

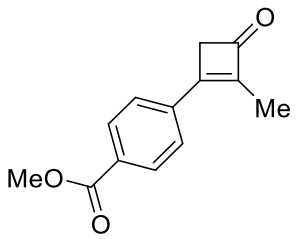

methyl 4-(2-methyl-4-oxocyclobut-1-en-1-yl)benzoate (4-9): Prepared according to general procedure A with *N,N*-DMP (0.64 mL, 5.7 mmol, 1.0 equiv), 4-ethynylbenzoic acid methyl ester (1.0 g, 6.2 mmol, 1.1 equiv), 2-fluoropyridine (0.65 mL, 7.5 mmol, 1.2 equiv), Tf_2O (1.1 mL, 6.2 mmol, 1.1 equiv) and potassium *tert*-butoxide (1.7 mL, 0.30 equiv) with 9:1 MeOH:toluene (0.06 M) for the alkene migration step. The crude material was purified by flash chromatography (5% ethyl actetate/hexanes) to provide a yellow solid (672 mg, 55% yield over three steps): **mp =** 139.0–140.6 °C; **^{1}H NMR** (700 MHz, $CDCl_3$) δ 8.18–8.13 (m, 2H), 7.67–7.62 (m, 2H), 3.96 (s, 3H), 3.51 (q, *J* = 2.3 Hz, 2H), 2.04 (t, *J* = 2.3 Hz, 3H); **^{13}C NMR** (175 MHz, $CDCl_3$) δ 189.7, 166.2, 161.9, 143.4, 136.5, 131.7, 130.0, 128.9, 52.4, 48.4, 9.5; **IR** (cast film, $CHCl_3$ cm^{-1}) 2953, 2919, 1746, 1716, 1618, 1276, 1107; **HRMS** (EI) for $C_{13}H_{12}O_3$ calcd. 216.0786; found 216.0787.

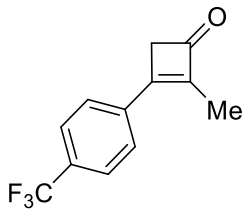

2-methyl-4-(4-(trifluoromethyl)phenyl)cyclobut-2-enone (4-10): Prepared according to general procedure A with *N*,*N*-DMP (0.73 mL, 6.6 mmol, 1.0 equiv), 1-ethynyl-4-(trifluoromethyl)-benzene (1.2 g, 7.0 mmol, 1.1 equiv), 2-fluoropyridine (0.70 mL, 8.0 mmol, 1.2 equiv), Tf_2O (1.3 mL, 7.3 mmol, 1.1 equiv) and potassium *tert*-butoxide (2.0 mL, 0.30 equiv). The crude material was purified by flash chromatography (2.5 to 5% ethyl actetate/hexanes) to provide a yellow solid (651 mg, 43% yield over three steps): **mp =** 75.3–76.4 °C; **^{1}H NMR** (500 MHz, $CDCl_3$) δ 7.75 (d, *J* = 8.2 Hz, 2H), 7.68 (d, *J* = 8.2 Hz, 2H), 3.50 (q, *J* = 2.3 Hz, 2H), 2.03 (t, *J* = 2.3 Hz, 3H); **^{13}C NMR** (101 MHz, $CDCl_3$, ^{19}F decoupled) δ 189.5, 161.5, 143.6, 135.8, 132.2, 129.2, 125.9, 123.7, 48.5, 9.5; **^{19}F NMR** (376 MHz, $CDCl_3$) δ -63.0; **IR** (cast film, $CHCl_3$ cm^{-1}) 3108, 3067, 2917, 1761, 1623, 1614, 1411, 1327, 1153, 1122, 1067, 845; **HRMS** (EI) for $C_{12}H_9OF_3$ calcd. 226.0606; found 226.0607.

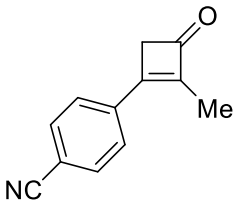

4-(2-methyl-4-oxocyclobut-1-en-1-yl)benzonitrile (4-11): Prepared according to general procedure A with *N,N*-DMP (0.87 mL, 7.2 mmol, 1.0 equiv), 4-ethynylbenzonitrile (1.2 g, 7.9 mmol, 1.1 equiv), 2-fluoropyridine (0.75 mL, 8.6 mmol, 1.2 equiv), Tf_2O (1.4 mL, 7.9 mmol, 1.1 equiv) and potassium *tert*-butoxide (2.1 mL, 0.30 equiv) with 1.1:1 EtOH:toluene (0.04 M) for the alkene migration step. The crude material was purified by flash chromatography (5% ethyl actetate/hexanes) to provide a yellow solid (240 mg, 18% yield over three steps): **mp =** 184.0–184.7 °C; **^{1}H NMR** (500 MHz, $CDCl_3$) δ 7.77 (d, *J* = 3.57 8.5 Hz, 2H), 7.65 (d, *J* = 8.5 Hz), 3.49 (q, *J* =

2.5 Hz, 2H), 2.03 (t, J = 2.5 Hz, 3H);**^{13}C NMR** (175 MHz, $CDCl_3$) δ 189.1, 160.7, 144.7, 136.5, 132.6, 129.2, 118.1, 113.9, 48.5, 9.6; **IR** (cast film, $CHCl_3$ cm^{-1}) 3089, 2968, 2227, 1751, 1618, 1342, 848; **HRMS** (EI) for $C_{15}H_{12}O$ calcd. 183.0684; found 183.0687.

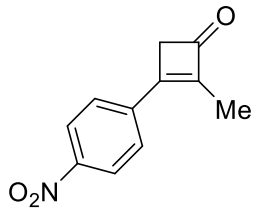

2-methyl-4-(4-nitrophenyl)cyclobut-2-enone (4-12): Prepared according to general procedure A with *N,N*-DMP (0.75 mL, 6.2 mmol, 1.0 equiv), 4-ethynylnitrobenzene (1.2 g, 6.8 mmol, 1.1 equiv), 2-fluoropyridine (0.65 mL, 7.4 mmol, 1.2 equiv), Tf_2O (1.1 mL, 6.8 mmol, 1.1 equiv) and potassium *tert*-butoxide (3.1 mL, 0.50 equiv) with 5% DCM in EtOH (0.03 M) for the alkene migration step. The crude material was purified by flash chromatography (5% ethyl actetate/hexanes) to provide an orange-red solid (251 mg, 20% yield over three steps): **mp =** 172.2–173.3 °C; **^{1}H NMR** (500 MHz, $CDCl_3$) δ 8.38–8.32 (m, 1H), 7.77–7.70 (m, 1H), 3.55 (q, J = 2.3 Hz, 1H), 2.07 (t, J = 2.3 Hz, 2H); **^{13}C NMR** (125 MHz, $CDCl_3$) δ 189.1, 160.3, 148.5, 145.3, 138.3, 129.7, 124.2, 48.8, 9.7; **IR** (cast film, $CHCl_3$ cm^{-1}): 3104, 2963, 1755, 1620, 1517, 1349, 855; **HRMS** (EI) for $C_{11}H_9NO_3$ calcd. 203.0582; found 203.0584.

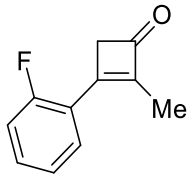

4-(2-fluorophenyl)-2-methylcyclobut-2-enone (4-13): Prepared according to general procedure A with *N,N*-DMP (0.76 mL, 6.9 mmol, 1.0 equiv), 1-ethynyl-2-fluorobenzene (1.0 g, 8.3 mmol, 1.2 equiv), 2-fluoropyridine (0.72 mL, 8.3 mmol, 1.2 equiv), Tf_2O (1.3 mL, 7.6 mmol, 1.1 equiv) and

potassium *tert*-butoxide (2.1 mL, 0.30 equiv). The crude material was purified by flash chromatography (5% ethyl actetate/hexanes) to provide a brown solid (624 mg, 51% yield over three steps): **mp =** 57.6–58.1 °C; **^{1}H NMR** (500 MHz, $CDCl_3$) δ 7.53–7.42 (m, 2H), 7.29–7.23 (m, 1H), 7.17 (ddd, *J* = 10.7, 8.3, 1.1 Hz, 1H), 3.54 (qd, *J* = 2.3, 1.3 Hz, 2H), 1.96 (dt, *J* = 3.4, 2.4 Hz, 3H); **^{13}C NMR** (101 MHz, $CDCl_3$, ^{19}F decoupled) δ 190.8, 160.4, 158.2, 143.8, 132.9, 130.7, 124.5, 120.9, 116.4, 50.0, 9.6; **^{19}F NMR** (376 MHz, $CDCl_3$) δ –108.5; **IR** (cast film, $CHCl_3$ cm^{-1}): 3057, 2967, 1756, 1619, 1458, 1333, 1015; **HRMS** (EI) for $C_{11}H_9FO$ calcd. 176.0637; found 176.0639.

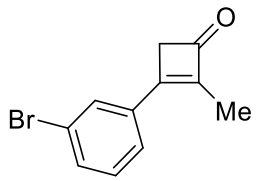

4-(4-bromophenyl)-2-methylcyclobut-2-enone (4-14): Prepared according to general procedure A with *N*,*N*-DMP (0.59 mL, 5.4 mmol, 1.0 equiv), 1-bromo-4-ethynyl-benzene (1.0 g, 5.6 mmol, 1.1 equiv), 2-fluoropyridine (0.60 mL, 6.4 mmol, 1.2 equiv), Tf_2O (1.0 mL, 5.6 mmol, 1.1 equiv) and potassium *tert*-butoxide (1.6 mL, 0.30 equiv). The crude material was purified by flash chromatography (5% ethyl actetate/hexanes) to provide a pale yellow solid (709 mg, 56% yield over three steps): **mp =** 81.6–82.1 °C **^{1}H NMR** (500 MHz, $CDCl_3$) δ 7.70 (dd, *J* = 7.7, 7.7 Hz, 1H), 7.60 (ddd, *J* = 8.0, 2.0, 1.0 Hz, 1H), 7.52 (ddd, *J* = 7.8, 1.3, 1.3 Hz, 1H), 7.38 (dd, *J* = 7.9, 7.9 Hz 1H), 3.46 (q, *J* = 2.3 Hz, 2H), 2.01 (t, *J* = 2.3 Hz, 3H); **^{13}C NMR** (126 MHz, $CDCl_3$) δ189.5, 161.7, 142.6, 134.7, 133.7, 131.8, 130.5, 127.6, 123.1, 48.4, 9.5; **IR** (cast film, $CHCl_3$ cm^{-1}): 3057, 2955, 2920, 1752, 1622, 1424, 1342, 786, 683; **HRMS** (EI) for $C_{11}H_9{}^{79}BrO_2$ calcd. 235.9837; found 235.9835.

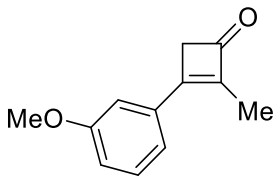

4-(4-methoxyphenyl)-2-methylcyclobut-2-enone (4-15): Prepared according to general procedure A with *N,N*-DMP (0.76 mL, 6.9 mmol, 1.0 equiv), 4-ethynylanisole (1.0 g, 7.6 mmol, 1.1 equiv), 2-fluoropyridine (0.71 mL, 8.3 mmol, 1.2 equiv), Tf_2O (1.3 mL, 7.6 mmol, 1.1 equiv) and potassium *tert*-butoxide (2.1 mL, 0.30 equiv). The crude material was purified by flash chromatography (5% ethyl actetate/hexanes) to provide a yellow solid (790 mg, 61% yield over three steps): **mp =** 61.5–63.1 °C; **^{1}H NMR** (500 MHz, $CDCl_3$) δ 7.41 (t, *J* = 7.9 Hz, 1H), 7.19 (dt, *J* = 7.7, 1.2 Hz, 1H), 7.07 (dd, *J* = 2.6, 1.6 Hz, 1H), 7.02 (ddd, *J* = 8.3, 2.6, 0.9 Hz, 1H), 3.86 (s, 3H), 3.43 (q, *J* = 2.3 Hz, 2H), 1.99 (t, *J* = 2.4 Hz, 3H); **^{13}C NMR** (126 MHz, $CDCl_3$) δ 190.0, 163.5, 159.9, 141.3, 134.0, 130.0, 121.7, 116.5, 114.4, 55.4, 48.3, 9.4; **IR** (cast film, $CHCl_3$ cm^{-1}): 3075, 2949, 1747, 1621, 1458, 1351, 1167, 1017; **HRMS** (EI) for $C_{12}H_{12}O_2$ calcd. 188.0837; found 188.0840.

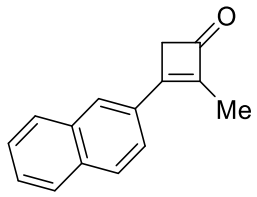

2-methyl-4-(naphthalen-2-yl)cyclobut-2-enone (4-16): Prepared according to general procedure A with *N,N*-DMP (0.73 mL, 6.6 mmol, 1.0 equiv), 2-ethynyl-naphthylene (1.1 g, 6.9 mmol, 1.1 equiv), 2-fluoropyridine (0.70 mL, 7.9 mmol, 1.2 equiv), Tf_2O (1.2 mL, 7.3 mmol, 1.1 equiv) and potassium *tert*-butoxide (2.0 mL, 0.30 equiv)) with 3.4:1 EtOH:toluene (0.15 M) for the alkene migration step. The crude material was purified by flash chromatography (2.5 to 5% to 7.5% ethyl actetate/hexanes) to provide a yellow solid (568 mg, 41% yield over three steps): **mp =** 146.4–147.3 °C; **^{1}H NMR** (500 MHz, $CDCl_3$) δ 7.98 (s, 1H), 7.96–7.90 (m, 2H), 7.90–7.87 (m, 1H), 7.75 (dd, *J* = 8.6, 1.7 Hz, 1H), 7.62–7.52 (m, 2H), 3.57 (q, *J* = 2.3 Hz, 2H), 2.10 (t, *J* = 2.3 Hz, 3H);**^{13}C NMR** (125 MHz, $CDCl_3$) δ 190.2, 163.5, 141.3, 134.2, 133.1, 130.4, 130.2, 129.0, 128.8, 128.1, 127.9,

127.1, 125.2, 48.4, 9.6; **IR** (cast film, $CHCl_3$ cm^{-1}): 3464, 3065, 3042, 2939, 2907, 2819, 1743, 1614, 1372, 1333, 1207, 824, 754; **HRMS** (EI) for $C_{15}H_{12}O$ calcd. 208.0888; found 208.0885.

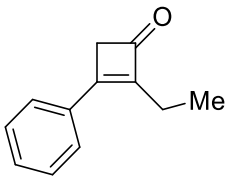

2-ethyl-4-phenylcyclobut-2-enone (4-17): Prepared according to general procedure A with *N,N*-dimethylbutanamide (1.2 g, 10 mmol, 1.0 equiv), phenylacetylene (1.3 mL, 12 mmol, 1.2 equiv), 2-fluoropyridine (1.0 mL, 12 mmol, 1.2 equiv), Tf_2O (1.9 mL, 11 mmol, 1.1 equiv) and potassium *tert*-butoxide (3.0 mL, 0.30 equiv). The crude material was purified by flash chromatography (5% ethyl actetate/hexanes) to provide a clear yellow oil (741 mg, 43% yield over three steps): **^{1}H NMR** (500 MHz, $CDCl_3$) δ 7.60–7.56 (m, 2H), 7.53–7.45 (m, 3H), 3.45 (t, J = 1.7 Hz, 2H), 2.47 (qt, J = 7.6, 1.7 Hz, 2H), 1.23 (t, J = 7.6 Hz, 3H); **^{13}C NMR** (125 MHz, $CDCl_3$) δ 190.0, 162.4, 146.7, 132.8, 131.0, 129.2, 129.0, 48.4, 18.3, 11.5; **IR** (cast film, $CHCl_3$ cm^{-1}): 3057, 2978, 1748, 1613, 1448, 1353, 1068; **HRMS** (EI) for (m/z) $C_{12}H_{12}O$ calcd. 172.0888; found 172.0888.

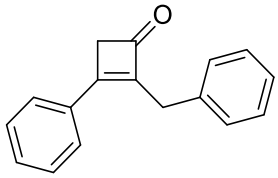

2-benzyl-4-phenylcyclobut-2-enone (4-18): Prepared according to general procedure A with *N,N*-dimethylbenzenepropanamide (4.0 g, 23 mmol, 1.0 equiv), phenylacetylene (3.0 mL, 27 mmol, 1.2 equiv), 2-fluoropyridine (2.3 mL, 27 mmol, 1.2 equiv), Tf_2O (4.0 mL, 25 mmol, 1.1 equiv) and potassium *tert*-butoxide (7.0 mL, 0.30 equiv). The crude material was purified by flash chromatography (5% ethyl actetate/hexanes) to provide an orange solid (1.65 g, 31% yield over three steps): **mp** = 45.8–46.5 °C; **^{1}H NMR** (500 MHz, $CDCl_3$) δ 7.61 (m, 2H), 7.50 (m, 3H), 7.32

(m, 4H), 7.24 (m, 1H), 3.83 (s, 2H), 3.57 (t, J = 1.5 Hz, 2H); **^{13}C NMR** (125 MHz, $CDCl_3$) δ 189.5, 164.2, 142.9, 137.0, 132.3, 131.3, 129.4, 129.0, 128.7, 128.4, 126.6, 48.6, 30.4; **IR** (cast film, $CHCl_3$ cm^{-1}): 3061, 2911, 1749, 1613, 1448, 1350, 1071; **HRMS** (EI) for $C_{17}H_{14}O$ calcd. 234.1045; found 234.1040.

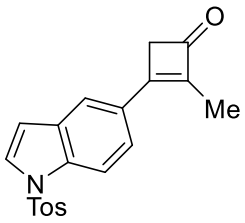

2-methyl-4-(1-tosyl-1H-indol-5-yl)cyclobut-2-enone (4-19): Prepared according to general procedure A with *N,N*-DMP (0.33 mL, 3.0 mmol, 1.1 equiv), indole acetylene **4-21** (840 mg, 2.8 mmol, 1.0 equiv), 2-fluoropyridine (0.30 mL, 3.4 mmol, 1.2 equiv), Tf_2O (0.53 mL, 3.1 mmol, 1.1 equiv) and potassium *tert*-butoxide (1.0 mL, 0.35 equiv). The crude material was purified by flash chromatography (15% to 20% ethyl actetate/hexanes) to provide a light yellow solid (98 mg, 10% yield over three steps): **mp =** 137.6–139.3 °C; **^{1}H NMR** (700 MHz, $CDCl_3$) δ 8.10 (d, J = 8.6 Hz, 1H), 7.81 – 7.76 (m, 2H), 7.73 (d, J = 1.6 Hz, 1H), 7.65 (d, J = 3.7 Hz, 1H), 7.58 (dd, J = 8.7, 1.7 Hz, 1H), 7.25 (s, 1H), 6.74 (d, J = 3.6 Hz, 1H), 3.47 (q, J = 2.4 Hz, 2H), 2.36 (s, 3H), 2.02 (t, J = 2.4 Hz, 3H); **^{13}C NMR** (125 MHz, $CDCl_3$) δ 189.8, 163.7, 145.5, 139.9, 135.8, 135.1, 131.1, 130.1, 128.3, 127.8, 126.9, 125.5, 122.9, 114.0, 109.2, 48.3, 21.7, 9.4; **IR** (cast film, $CHCl_3$ cm^{-1}): 3470, 3122, 2961, 2925, 1743, 1614, 1416, 1173, 1120, 988, 703; **HRMS** (EI) for $C_{20}H_{17}O_3SN$ calcd. 351.0929; found 351.0929.

4.10.4 Synthesis of tosyl indole aryl acetylene 4-21

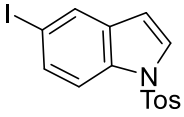

5-iodo-1-tosyl-1*H*-indole (4-20): Prepared according to a previously reported procedure with slight modification.[55] Sodium hydride (1.23 g, 60% dispersion in mineral oil, 31.0 mmol, 3.00 equiv) was added to a solution of 5-iodo-1-*H*-indole (2.49 g, 10.3 mmol, 1.00 equiv) in DMF (13.0 mL, 0.800 M) at 0 °C and left to stir at that temperature for 30 minutes. A solution of 4-methylbenzene-1-sulfonyl chloride (2.36 g, 12.4 mmol, 1.50 equiv) was added dropwise over ten minutes as a solution in DMF (13.0 mL, 0.400 M total). The reaction was left to warm to room temperature overnight in an ice bath. The reaction was diluted in 25 mL of saturated sodium bicarbonate and ethyl acetate, extracted three times. The combined organic phases were washed with 25 mL of water four times, brine and dried with magnesium sulfate, filtered and concentration *in vacuo*. The crude material was purified by flash chromatography (0% to 1.5% ethyl actetate/hexanes) to provide a white solid (3.20 g, 79% yield). All spectral data matched the literature: **^{1}H NMR** (500 MHz, $CDCl_3$) δ 7.87 (s, 1H), 7.78–7.68 (m, 3H), 7.60–7.54 (m, 1H), 7.52 (d, *J* = 3.7, 1.8 Hz, 1H), 7.23 (d, *J* = 7.8 Hz, 2H), 6.57 (d, *J* = 3.3 Hz, 1H), 2.35 (s, 3H).

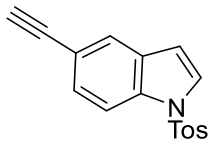

5-ethynyl-1-tosyl-1*H*-indole (4-21): Prepared according to a previously reported procedure with slight modification.[56] Aryl iodide **4-20** (3.18 g, 8.00 mmol, 1.00 equiv) was dissolved in dried triethylamine (25 mL, 0.33 M) at room temperature under argon atmosphere. $Pd(OAc)_2$ (37 mg, 0.16 mmol, 2 mol%), PPh_3 (168 mg, 0.64 mmol, 8.0 mol%), CuI (61 mg, 0.32 mmol, 4.0 mol%) then trimethylsilylacetylene (2.30 mL, 16.0 mmol, 2.0 equiv) were sequentially added and the reaction was flushed with argon for five minutes. The reaction was left to stir at room temperature overnight. The volatiles were removed *in vacuo* and the crude solid was dissolved in 25 mL of diethyl ether and water and extracted three times with diethyl ether. The combined organic phases were washed

with brine and dried with sodium sulfate, filtered and concentration *in vacuo*. The crude material was newly dissolved in a solution of TBAF (1M in THF, 16 mL, 2.0 equiv) at room temperature and stirred for 18 hours. The reaction was diluted in 25 mL of ethyl acetate and water and extracted three times with ethyl acetate. The combined organic phases were washed with brine, dried with magnesium sulfate and filtered. The volatiles were removed *in vacuo* and the crude reaction mixture was purified by flash chromatography (2.5% to 10% ethyl actetate/hexanes) to provide a white solid (840 mg, 35% yield). All spectral data matched the literature: **^{1}H NMR** (500 MHz, $CDCl_3$) δ 7.93 (d, *J* = 8.6 Hz, 1H), 7.77–7.72 (m, 2H), 7.67 (d, *J* = 1.6 Hz, 1H), 7.58 (d, *J* = 3.7 Hz, 1H), 7.42 (dd, *J* = 8.6, 1.6 Hz, 1H), 7.23 (d, *J* = 8.0 Hz, 1H), 6.62 (d, *J* = 3.7 Hz, 1H), 3.02 (s, 1H), 2.35 (s, 3H).

4.10.5 Synthesis of dialkyl cyclobutanone 4-23

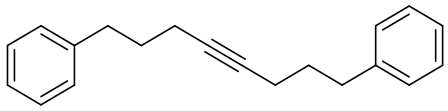

1,8-diphenyl-4-octyne (4-22): Prepared according to a previously reported procedure with slight modification.[57] 4-Pentyn-1-ylbenzene (1.76 g, 12.2 mmol, 1.00 equiv) was dissolved in THF (17 mL, 0.72 M) at room temperature and cooled to -78 °C. *n*-Butyllithium (4.70 mL, 12.2 mmol, 1.0 equiv) was added dropwise at -78 °C and the reaction was stirred for 10 minutes. 4-Bromo-1-phenylpropane (2.46 g, 12.3 mmol, 1.01 equiv) was added dropwise at -78 °C as a solution of DMPU (8.5 mL, 1.4 M). The dry ice/acetone bath was removed and the reaction was stirred at room temperature for five hours. The reaction was diluted with 25 mL of hexanes and saturated ammonium chloride and the aqueous phase was extracted three times with hexanes. The combined organic phases were washed with brine and dried with sodium sulfate, filtered and concentration *in vacuo*. The crude reaction mixture was purified by flash chromatography (0 to 5% DCM/hexanes) to provide a clear, colourless oil (1.50 g, 47% yield). All spectral data matched the literature: **^{1}H**

NMR (700 MHz, $CDCl_3$) δ 7.33–7.25 (m, 4H), 7.24–7.15 (m, 6H), 2.74 (t, *J* = 7.7 Hz, 4H), 2.20 (tt, *J* = 7.2, 2.4 Hz, 4H), 1.87–1.78 (m, 4H).

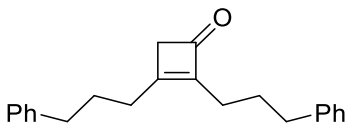

2,4-bis(4-phenylpropyl)cyclobut-2-enone (4-23): The substrate was synthesized following a literature procedure with slight modifications.[26] Proton sponge (291 mg, 1.38 mmol, 0.250 equiv) was dissolved in toluene (28 mL, 0.20 M) and acetonitrile (28 mL, 0.20 M) under an atmosphere of argon. Alkyne **4-22** (1.44 g, 5.50 mmol, 1.00 equiv) and triflic anhydride (2.80 mL, 16.5 mmol, 3.00 equiv) were subsequently added and the reaction mixture was left to stir at 70 °C. After 24 hours, distilled water (3.00 mL, 165 mmol, 30,0 equiv) was added and the reaction was stirred at 70 °C for another two hours. Upon cooling to room temperature, the reaction was diluted in ethyl acetate and water, and extracted with ethyl acetate three times. The combined organic layers were washed with brine, dried with magnesium sulfate, filtered and concentrated in vacuo. The crude material was purified by flash chromatography (2.5 to 5% ethyl actetate/hexanes) to provide a yellow oil (1.24 g, 74% yield): **^{1}H NMR** (400 MHz, $CDCl_3$) δ 7.37–7.15 (m, 10H), 3.10 (tt, *J* = 1.8, 1.0 Hz, 2H), 2.69 (t, *J* = 7.6 Hz, 2H), 2.63 (t, *J* = 7.6 Hz, 2H), 2.55 (t, *J* = 7.6 Hz, 2H), 2.11 (t, *J* = 7.6 Hz, 2H), 1.99–1.80 (m, 4H); **^{13}C NMR** (101 MHz, $CDCl_3$) δ 189.8, 172.2, 147.9, 141.7, 141.1, 128.5, 128.4, 128.4, 128.3, 126.1, 125.8, 49.3, 35.6 (2C), 29.2, 28.7, 27.8, 23.1; **IR** (cast film, $CHCl_3$ cm^{-1}): 3061, 3026, 2963, 2859, 1754, 1634, 1496, 1453, 1029, 745, 699; **HRMS** (EI) for $C_{22}H_{24}O$ calcd**.** 304.1827; found 304.1828.

4.10.6 HTS screening procedure and analysis

General screening procedure:

In an inert atmosphere (glove box with < 20 ppm O_2 and < 20 ppm H_2O), $Cu(MeCN)_4PF_6$ (0.040 M solution in MeCN, 5.0 µL, 0.2 µmol, 0.1 equiv) was first dispensed before evaporation to dryness. To the resulting residue was added (*S*,*S*)-BDPP (0.050 M solution in toluene, 5.0 µL, 0.25 µmol, 0.125 equiv,) and THF (50.0 µL, 0.080 M) added. The reaction was stirred for 1 hour before the THF was evaporated to dryness. To the resulting residue was added bis(pinacolato)diboron (0.040 M solution in THF, 100 µL, 4 µmol, 2.0 equiv). The reaction was stirred for 15 minutes before NaOtBu (0.20 M solution in THF, 5.0 µL, 1 µmol, 0.50 equiv,) was added. After a further 15 minutes a solution of **1a** (0.40 M solution in THF, 5.0 µL, 2 µmol, 1.0 equiv) was added followed by MeOH (0.040 M solution in THF, 100 µL, 4 µmol, 2.0 equiv). The reaction vial was crimp sealed to the glove-box environment before being stirred overnight at 25 °C. After 18 hours the vials were diluted with MeCN (200 µL), mixed, centrifuged before being analyzed directly by SFC/MS.

SFC/MS analysis:

SFC/MS analysis used a mobile phase of CO_2 with 2% isopropanol for 1.0 minute on two Chiralpak IG-U, 3.0 x 50 mm, 1.6 µm columns in series maintained at 25 °C with a flow rate of 2.0 ml/min and 160 bar back pressure. Detection modes of UV 215 nm and atmospheric pressure chemical ionization (APCI) were monitored (positive scan mode from 100-650 Da with single ion monitoring at m/z = 287 Da) for 1.0µL injections made directly from reaction mixtures. In addition, a 2-40% isopropanol over 1.0 minute gradient was added at 1.0 minutes to flush any unrelated reaction materials from the column. Analysis by SFC/MS at 215 nm. First and second integrated peaks are enantiomer products of **4-24** (MW = 287+ve). Peak at 1.806 min is remaining **4-1** (MW = 159+ve). Peaks at 1.434, and 1.961 min are internal standard 1 (from ketone **4-1** stock solution)

and internal standard 2 [from bis(pinacolato)diboron stock solution] and are not related to the reaction. 55% conversion, 88% *ee.*

4.10.7 General procedure B: enantioselective cyclobutenone conjugate borylation

To a flame-dried 5.0 mL microwave vial was added (2*S*,4*S*)-2,4-bis(diphenylphosphino)pentane (7.9 mg, 0.018 mmol, 0.060 equiv), tetrakis(acetonitrile)copper(I) hexafluorophosphate (5.6 mg, 0.015 mmol, 0.050 equiv), and bis(pinacolato)diboron (107 mg, 0.420 mmol, 1.40 equiv). The microwave vial was then capped, evacuated and backfilled with argon four cycles. THF (0.60 mL) was added to the vial and the mixture was stirred for 15 min forming a clear colourless solution. The reaction was cooled to 0 °C in an ice-water bath. Lithium tert-butoxide (1.0 M, 120 µL, 0.12 mmol, 0.40 equiv) was added dropwise and the reaction stirred for 10 minutes forming a yellow-brown solution. The corresponding cyclobutenone (0.30 mmol, 1.00 equiv) in 0.30 mL of THF was added to the vial dropwise, followed immediately by dropwise addition of methanol (25 µL, 0.60 mmol, 2.0 equiv). The flask which contained the cyclobutenone was further rinsed with THF and added to the reaction in three 0.3 mL portions until the final reaction concentration was 0.20 M (unless otherwise specified). The ice bath was subsequently removed and the reaction was stirred for 3 hours at room temperature. The reaction was diluted with 15 mL of diethyl ether and poured into 15 mL of saturated ammonium chloride in a separatory funnel. The layers were separated, and the aqueous was extracted with diethyl ether three times. The combined organic layers were washed brine, dried with sodium sulfate, filtered and concentrated *in vacuo*. The crude ^{1}H NMR yield was determined with dibromomethane as an internal standard (26 mg, 0.15 mmol, 0.5 equiv). The crude reaction mixture was purified by a 35 wt% water deactivated silica plug (7.5 g of silica, eluent specified below).[58] The diastereoselectivity of the isolated products was determined by the relative peak height of the corresponding methyl protons for which had signals consistently around 1.40 and 0.75 ppm

for the major and minor diastereomers, respectively. For products **4-39**, **4-40** and **4-41**, the dr was estimated by relative peak height of the pinacol methyl groups. A second purification using regular flash chromatography (eluent specified below) allowed isolation of the major diastereomer for full characterization purposes. The cyclobutylboronate products were found to be stable over several months when stored in a vial under argon atmosphere in a –20 °C freezer. The racemic borylated products were made following the same general procedure with Xantphos (6 mol%), NaO*t*Bu (15 mol%) and a 16–24 hour reaction time.

4.10.8 Characterization of the cyclobutylboronate products 4-24 to 4-42

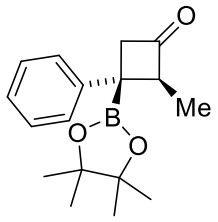

(2*S*,3*R*)-2-methyl-4-phenyl-4-(4,4,5,5-tetramethyl-1,3,2-dioxaborolan-2-yl)cyclobutanone (4-24): Prepared according to general procedure B with **4-1** (48 mg, 0.30 mmol, 1.0 equiv). The crude material was purified by flash chromatography (1:20 ethyl actetate:hexanes, water deactivated silica) to provide a white solid (65 mg, 76% yield, dr 16:1). A second purification by flash chromatography (1:20 ethyl acetate:hexanes) allowed isolation of a pure diastereomer for characterization purposes: **mp =** 46.2–47.5 °C; **^{1}H NMR** (400 MHz, $CDCl_3$) δ 7.36–7.29 (m, 2H), 7.24–7.17 (m, 3H), 3.58 (qdd, *J* = 7.3, 2.2, 2.2 Hz, 1H), 3.52 (dd, *J* = 16.6, 2.3 Hz, 1H), 3.22 (dd, *J* = 16.6, 2.1 Hz, 1H), 1.41 (d, *J* = 7.4 Hz, 3H), 1.19 (s, 6H), 1.16 (s, 6H); **^{13}C NMR** (126 MHz, $CDCl_3$) δ 209.1, 128.4, 126.2, 125.6, 84.3, 64.2, 53.5, 24.8, 24.7, 13.1 (the boron-bound carbon was not detected due to quadrupolar relaxation of boron); **^{11}B NMR** (128 MHz, $CDCl_3$) δ 33.2; **IR** (cast film, $CHCl_3$ cm^{-1}): 3066, 2981, 1773, 1320, 1143; **HRMS** (EI) for (M^+–CO) $C_{16}H_{23}BO_2$calcd.

258.1786; found 258.1794; **[α]$_D^{20}$**: –86.5 (c= 0.371, $CHCl_3$); **HPLC** (Chiralpak IC): 1:99 iso-propanol:hexanes, 0.5 mL/min, 20 °C, λ = 220 nm, T_{minor} = 14.2 min, T_{major} = 15.3 min, er = 95.0:5.0.

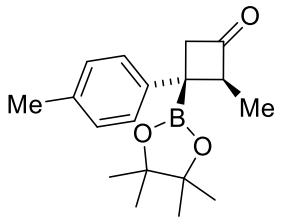

(2*S*,3*R*)-2-methyl-4-(4,4,5,5-tetramethyl-1,3,2-dioxaborolan-2-yl)-4-(p-tolyl)cyclobutanone (4-25): Prepared according to general procedure B with **4-2** (51 mg, 0.30 mmol, 1.0 equiv). The crude material was purified by flash chromatography (1:20 ethyl actetate:hexanes, water deactivated silica) to provide a white solid (76 mg, 86% yield, dr >20:1). A second purification by flash chromatography (1:20 ethyl acetate:hexanes) allowed isolation of a pure diastereomer for characterization purposes: **mp =** 50.7–52.3 °C; **^{1}H NMR** (500 MHz, $CDCl_3$) δ 7.12 (dd, *J* = 8.2, 8.2 Hz, 4H), 3.59–3.44 (m, 2H), 3.19 (d, *J* = 16.4 Hz, 1H), 2.33 (s, 3H), 1.40 (d, *J* = 7.4 Hz, 3H), 1.19 (s, 6H), 1.16 (s, 6H); **^{13}C NMR** (126 MHz, $CDCl_3$) δ 209.2, 144.2, 135.0, 129.1, 126.0, 84.2, 64.2, 53.6, 24.8, 24.7, 21.1, 13.1 (the boron-bound carbon was not detected due to quadrupolar relaxation of boron); **^{11}B NMR** (128 MHz, $CDCl_3$) δ 33.1; **IR** (cast film, $CHCl_3$ cm^{-1}) 3046, 2982, 2930, 1782, 1380, 1372, 1324, 1138, 857, 815; **HRMS** (EI) for $C_{18}H_{25}BO_3$calcd. 300.1897; found 300.1899; **[α]$_D^{20}$** –96.1 (c = 0.160, $CHCl_3$).

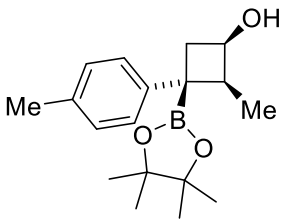

(1*R*,2*S*,3*R*)-2-methyl-4-(4,4,5,5-tetramethyl-1,3,2-dioxaborolan-2-yl)-4-(p-tolyl)cyclobutanol (4-26): For enantiomeric excess determination, cyclobutylboronate **4-25** (42 mg, 0.15 mmol, 1.0

equiv) was reduced following the procedure for alcohol **4-43**. The crude reaction mixture was purified by flash chromatography (10% ethyl acetate/hexanes) to afford a white solid as single diastereomer by ^{1}H NMR (36 mg, 86% yield, >20:1 dr): **^{1}H NMR** (500 MHz, $CDCl_3$) δ 7.09–7.05 (m, 2H), 7.03–6.97 (m, 2H), 4.27–4.18 (m, 1H), 3.11 (d, *J* = 9.7 Hz, 1H), 2.80 (dq, *J* = 7.2, 7.2 Hz, 1H), 2.31 (s, 3H), 1.28 (d, *J* = 7.3 Hz, 3H), 1.23 (s, 6H), 1.21 (s, 6H); **^{13}C NMR** (126 MHz, $CDCl_3$) δ 145.6, 134.0, 128.7, 125.6, 84.1, 68.7, 46.1, 39.3, 24.8, 24.7, 21.1, 12.9 (the boron-bound carbon was not detected due to quadrupolar relaxation of boron); **^{11}B NMR** (128 MHz, $CDCl_3$) δ 33.9; **IR** (cast film, $CHCl_3$ cm^{-1}): 3429, 3017, 2977, 2927, 1511, 1358, 1305, 1145, 1124, 860; **HRMS** (EI) for (M^+-H_2O) $C_{18}H_{25}BO_2$calcd. 284.1948; found 284.1944; **[α]$_D^{20}$** –68.3 (c = 0.210, $CHCl_3$); **HPLC** (Chiralpak IC) 5:95 iso-propanol:hexanes, 0.7 mL/min, 20 °C, λ = 220 nm, T_{minor} = 7.1 min, T_{major} = 8.0 min, er = 95.5:4.5.

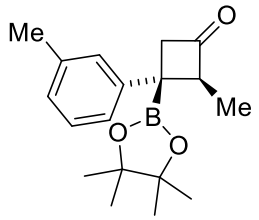

(2*S*,3*R*)-2-methyl-4-(4,4,5,5-tetramethyl-1,3,2-dioxaborolan-2-yl)-4-(m-tolyl)cyclobutanone (4-27): Prepared according to general procedure B with **4-3** (52 mg, 0.30 mmol, 1.0 equiv). The crude material was purified by flash chromatography (1:20 ethyl actetate:hexanes, water deactivated silica) to provide a clear, colourless oil (53 mg, 59% yield, dr 16:1). A second purification by flash chromatography (1:20 ethyl acetate:hexanes) allowed isolation of a pure diastereomer for characterization purposes: **^{1}H NMR** (500 MHz, $CDCl_3$) δ 7.24–7.18 (m, 1H), 7.04–6.97 (m, 3H), 3.57 (qdd, *J* = 7.3, 2.8, 2.0 Hz, 1H), 3.50 (dd, *J* = 16.6, 2.3 Hz, 1H), 3.20 (dd, *J* = 16.6, 2.2 Hz, 1H), 2.36 (s, 3H), 1.41 (d, *J* = 7.4 Hz, 3H), 1.19 (s, 6H), 1.16 (s, 6H); **^{13}C NMR** (126 MHz, $CDCl_3$) δ 209.2, 147.1, 137.8, 128.2, 126.8, 126.3, 123.3, 84.2, 64.0, 53.6, 24.8, 24.7, 21.6, 13.1 (the boron-

bound carbon was not detected due to quadrupolar relaxation of boron); **^{11}B NMR** (128 MHz, $CDCl_3$) δ 33.0; **IR** (cast film, $CHCl_3$ cm^{-1}): 2980, 2929, 1775, 1323, 1167; **HRMS** (EI) for $C_{18}H_{25}BO_3$calcd. 300.1897; found 300.1888; **[α]$_D^{20}$** –68.3 (c= 0.446, $CHCl_3$); **HPLC** (Chiralpak IC) 5:95 iso-propanol:hexanes, 0.7 mL/min, 20 °C, λ = 220 nm, T_{minor} = 6.4 min, T_{major} = 6.7 min, er = 93.0:7.0.

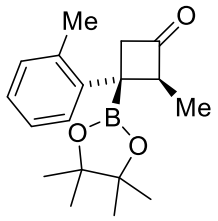

(2*S*,3*R*)-2-methyl-4-(4,4,5,5-tetramethyl-1,3,2-dioxaborolan-2-yl)-4-(o-tolyl)cyclobutanone (4-28): Prepared according to general procedure B with **4-4** (52 mg, 0.30 mmol, 1.0 equiv). The crude material was purified by flash chromatography (1:20 ethyl actetate:hexanes, water deactivated silica) to provide a clear, colourless oil (39 mg, 43% yield, dr >20:1). A second purification by flash chromatography (1:20 ethyl acetate:hexanes) allowed isolation of a pure diastereomer for characterization purposes: **^{1}H NMR** (600 MHz, $CDCl_3$) δ 7.22–7.12 (m, 4H), 3.72 (qdd, *J* = 7.4, 2.0, 2.0 Hz, 1H), 3.54 (dd, *J* = 16.1, 2.0 Hz, 1H), 3.01 (dd, *J* = 16.1, 1.8 Hz, 1H), 2.22 (s, 3H), 1.42 (d, *J* = 7.3 Hz, 3H), 1.22 (s, 6H), 1.19 (s, 6H);**^{13}C NMR** (176 MHz, $CDCl_3$) δ 209.0, 145.1, 135.6, 130.7, 126.0, 125.9, 125.6, 84.3, 61.8, 54.5, 25.0, 24.9, 20.6, 12.4 (the boron-bound carbon was not detected due to quadrupolar relaxation of boron); **^{11}B NMR** (128 MHz, $CDCl_3$) δ 33.6; **IR** (cast film, $CHCl_3$ cm^{-1}): 2979, 2932, 1779, 1381, 1142; **HRMS** (EI) for $C_{18}H_{25}BO_3$ calcd. 300.1897; found 300.1888; **[α]$_D^{20}$** –117.9 (c= 0.442, CHCl3); **HPLC** (Chiralpak IC) 5:95 iso-propanol:hexanes, 0.7 mL/min, 20 °C, λ = 220 nm, T_{minor} = 7.5 min, T_{major} = 8.8 min, er = 92.7:7.3.

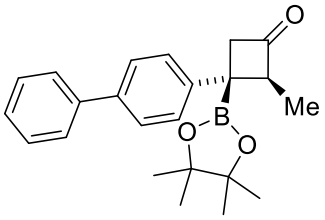

(2*S*,3*R*)-4-([1,1'-biphenyl]-4-yl)-2-methyl-4-(4,4,5,5-tetramethyl-1,3,2-dioxaborolan-2-yl)cyclobutanone (4-29): Prepared according to general procedure B with **4-5** (70 mg, 0.30 mmol, 1.0 equiv). The crude material was purified by flash chromatography (1:20 ethyl actetate:hexanes, water deactivated silica) to provide a white solid (62 mg, 58% yield, dr 12:1). A second purification by flash chromatography (1:20 ethyl acetate:hexanes) allowed isolation of a pure diastereomer for characterization purposes (39 mg, 36% overall yield): **mp =** 136.1–137.0 °C; **^{1}H NMR** (500 MHz, $CDCl_3$) δ 7.64–7.52 (m, 4H), 7.43 (t, *J* = 7.7 Hz, 2H), 7.37–7.27 (m, 3H), 3.62 (qdd, *J* = 7.3, 2.1, 2.1 Hz, 1H), 3.54 (dd, *J* = 16.6, 2.3 Hz, 1H), 3.26 (dd, *J* = 16.6, 2.2 Hz, 1H), 1.44 (d, *J* = 7.4 Hz, 3H), 1.21 (s, 6H), 1.18 (s, 6H); **^{13}C NMR** (126 MHz, $CDCl_3$) δ 208.9, 146.3, 140.9, 138.4, 128.8, 127.1, 127.1, 127.0, 126.6, 84.3, 64.3, 53.6, 24.8 (2C), 13.1 (the boron-bound carbon was not detected due to quadrupolar relaxation of boron); **^{11}B NMR** (160 MHz, $CDCl_3$) δ 33.2; **IR** (cast film, $CHCl_3$ cm^{-1}): 2979, 2929, 1781, 1488, 1373, 1326, 1140, 857, 825; **HRMS** (EI) for $C_{23}H_{27}O_3B$ calcd. 362.2053; found 362.2056; **$[\alpha]_D^{20}$** -82.9 (*c* = 0.190, $CHCl_3$); **HPLC** (Chiralcel OD) 1:99 iso-propanol:hexanes, 0.5 mL/min, 20 °C, λ = 254 nm, T_{minor} = 24.2 min, T_{major} = 26.0 min, er = 95.0:5.0.

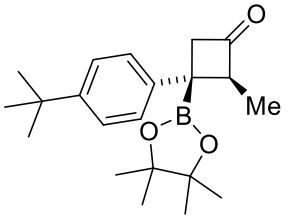

(2*S*,3*R*)-4-(4-(tert-butyl)phenyl)-2-methyl-4-(4,4,5,5-tetramethyl-1,3,2-dioxaborolan-2-yl)cyclobutanone (4-30): Prepared according to general procedure B with **4-6** (62 mg, 0.30 mmol,

1.0 equiv). The crude material was purified by flash chromatography (1:20 ethyl actetate:hexanes, water deactivated silica) to provide a white solid (64 mg, 64% yield, dr 8:1). A second purification by flash chromatography (1:20 ethyl acetate:hexanes) allowed isolation of a pure diastereomer for characterization purposes: **mp =** 81.3–82.0 °C; **^{1}H NMR** (500 MHz, $CDCl_3$) δ 7.39–7.29 (m, 2H), 7.20–7.09 (m, 2H), 3.57 (ddq, *J* = 7.3, 2.1, 2.1 Hz, 1H), 3.49 (dd, *J* = 16.6, 2.3 Hz, 1H), 3.21 (dd, *J* = 16.6, 2.2 Hz, 1H), 1.39 (d, *J* = 7.4 Hz, 3H), 1.32 (s, 9H), 1.19 (s, 6H), 1.17 (s, 6H); **^{13}C NMR** (126 MHz, $CDCl_3$) δ 209.4, 148.2, 143.9, 125.8, 125.3, 84.2, 64.2, 53.6, 34.4, 31.4, 24.9, 24.7, 13.0 (the boron-bound carbon was not detected due to quadrupolar relaxation of boron); **^{11}B NMR** (160 MHz, $CDCl_3$) δ 32.9; **IR** (cast film, $CHCl_3$ cm^{-1}): 2967, 2870, 1781, 1461, 1356, 1323, 1142, 858, 829; **HRMS** (EI) for $C_{21}H_{31}O_3B$calcd. 342.2366; found 342.2367; **$[\alpha]_D^{20}$** –79.4 (*c* = 0.460, $CHCl_3$); **HPLC** (Chiralcel OD) 2:98 iso-propanol:hexanes, 0.5 mL/min, 20 °C, λ = 230 nm, T_{major} = 9.7 min, T_{minor} = 11.5 min, er = 97.5:2.5.

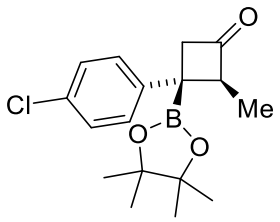

(2*S*,3*R*)-4-(4-chlorophenyl)-2-methyl-4-(4,4,5,5-tetramethyl-1,3,2-dioxaborolan-2-yl)cyclobutanone (4-31): Prepared according to general procedure B with **4-7** (58 mg, 0.30 mmol, 1.0 equiv). The crude material was purified by flash chromatography (1:20 ethyl actetate:hexanes, water deactivated silica) to provide a yellow solid (67 mg, 70% yield, dr >20:1). A second purification by flash chromatography (1:20 ethyl acetate:hexanes) allowed isolation of a pure diastereomer for characterization purposes: **mp =** 50.6–53.1 °C; **^{1}H NMR** (500 MHz, $CDCl_3$) δ 7.28 (dt, *J* = 8.4, 2.8 Hz, 2H), 7.02 (dt, *J* = 8.4, 2.8 Hz, 2H), 3.53 (m, 2H), 3.18 (dd, *J* = 16.4 Hz, 2.0 Hz, 1H), 1.40 (d, *J* = 7.2 Hz, 3H), 1.17 (s, 6H), 1.15 (s, 6H); **^{13}C NMR** (125 MHz, $CDCl_3$) δ 208.3,

131.3, 128.4, 127.5, 84.4, 64.4, 53.4, 24.8, 24.7, 24.6, 13.0 (the boron-bound carbon was not detected due to quadrupolar relaxation of boron); **^{11}B NMR** (128 MHz, $CDCl_3$) δ 33.2; **IR** (cast film, $CHCl_3$ cm^{-1}): 2979, 2930, 1782, 1492, 1141; **HRMS** (EI) for $C_{17}H_{22}BClO_3$ calcd. 320.1351; found 320.1351; **[α]$_D^{20}$** –70.9 (c= 0.391, $CHCl_3$); **HPLC** (Chiralpak IC) 5:95 iso-propanol:hexanes, 0.7 mL/min, 20 °C, λ = 220 nm, T_{minor} = 6.7, T_{major} = 7.8 min, er = 95.2:4.8**.**

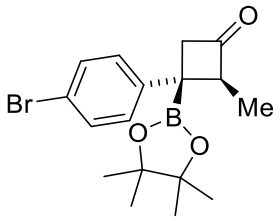

(2*S*,3*R*)-4-(4-bromophenyl)-2-methyl-4-(4,4,5,5-tetramethyl-1,3,2-dioxaborolan-2-yl)-cyclobutanone (4-32): Prepared according to general procedure B with **4-8** (69 mg, 0.30 mmol, 1.0 equiv). The crude material was purified by flash chromatography (1:20 ethyl actetate:hexanes, water deactivated silica) to provide a white solid (65 mg, 61% yield, dr 20:1). A second purification by flash chromatography (1:20 ethyl acetate:hexanes) allowed isolation of a pure diastereomer for characterization purposes: **mp =** 66.3–67.5 °C; **^{1}H NMR** (500 MHz, $CDCl_3$) δ 7.47–7.40 (m, 2H), 7.12–7.04 (m, 2H), 3.57–3.45 (m, 2H), 3.18 (dd, *J* = 16.9, 2.1 Hz, 1H), 1.40 (d, *J* = 7.4 Hz, 3H), 1.19 (s, 6H), 1.16 (s, 6H); **^{13}C NMR** (126 MHz, $CDCl_3$) δ 208.2, 146.3, 131.4, 128.0, 119.4, 84.5, 64.4, 53.4, 24.8, 24.8, 13.0 (the boron-bound carbon was not detected due to quadrupolar relaxation of boron); **^{11}B NMR** (160 MHz, $CDCl_3$) δ 33.0; **IR** (cast film, $CHCl_3$ cm^{-1}) 2979, 2929, 1781, 1488, 1373, 1326, 1140, 857, 825; **HRMS** (EI) for $C_{17}H_{22}O_3B^{79}Br$ calcd. 364.0845; found 364.0850; **[α]$_D^{20}$** –84.9 (*c* = 0.190, $CHCl_3$); **HPLC** (Chiralpak IC) 1:99 iso-propanol:hexanes, 0.5 mL/min, 20 °C, λ = 230 nm, T_{minor} = 17.5 min, T_{major} = 21.5 min, er = 93.8:6.1.

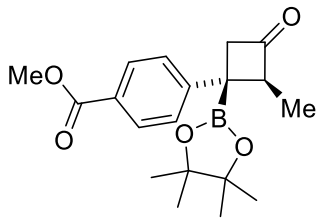

methyl 4-((1*R*,2*S*)-2-methyl-4-oxo-1-(4,4,5,5-tetramethyl-1,3,2-dioxaborolan-2-yl)cyclobutyl) benzoate (4-33): Prepared according to general procedure B with **4-9** (65 mg, 0.30 mmol, 1.0 equiv), the overall reaction concentration was 0.15 M. The crude material was purified by flash chromatography (1:10 ethyl actetate:hexanes, water deactivated silica) to provide a white solid (56 mg, 54% yield, dr > 20:1). A second purification by flash chromatography (10:1 ethyl acetate:hexanes) allowed isolation of a pure diastereomer for characterization purposes: **mp** = 106.8–108.5 °C; **^{1}H NMR** (500 MHz, $CDCl_3$) δ 8.02–7.96 (m, 2H), 7.29–7.26 (m, 2H), 3.91 (s, 3H), 3.62–3.50 (m, 2H), 3.24 (dd, *J* = 16.5, 2.0 Hz, 1H), 1.43 (d, *J* = 7.4 Hz, 3H), 1.18 (s, 6H), 1.15 (s, 6H); **^{13}C NMR** (126 MHz, $CDCl_3$) δ 208.1, 167.1, 152.8, 129.7, 127.6, 126.2, 84.5, 64.3, 53.4, 52.1, 24.8, 24.7, 13.1 (the boron-bound carbon was not detected due to quadrupolar relaxation of boron); **^{11}B NMR** (128 MHz, $CDCl_3$) δ 32.9; **IR** (cast film, $CHCl_3$ cm^{-1}) 2979, 2932, 1781, 1723, 1609, 1436, 1373, 1279, 1141, 1108, 859; **HRMS** (EI) for $C_{19}H_{25}O_5B$ calcd. 344.1795; found 344.1795; **$[\alpha]_D^{20}$** –93.0 (*c* = 0.200, $CHCl_3$); **HPLC** (Chiralpak IC): 10:90 iso-propanol:hexanes, 0.5 mL/min, 20 °C, λ = 254 nm, T_{minor} = 25.2 min, T_{major} = 27.0 min, er = 91.6:8.4.

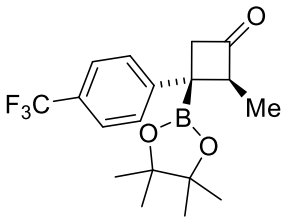

(2*S*,3*R*)-2-methyl-4-(4,4,5,5-tetramethyl-1,3,2-dioxaborolan-2-yl)-4-(4-(trifluoromethyl)phenyl)-cyclobutanone (4-34): Prepared according to general procedure B with

4-10 (66 mg, 0.30 mmol, 1.0 equiv). The crude material was purified by flash chromatography (1:20 ethyl actetate:hexanes, water deactivated silica) to provide a white solid (56 mg, 55% yield, dr > 20:1). A second purification by flash chromatography (1:20 ethyl acetate:hexanes) allowed isolation of a pure diastereomer for characterization purposes: **mp =** 73.7–75.3 °C; **^{1}H NMR** (500 MHz, $CDCl_3$) δ 7.63–7.51 (m, 2H), 7.37–7.29 (m, 2H), 3.63–3.48 (m, 2H), 3.23 (dd, *J* = 16.5, 1.9 Hz, 1H), 1.43 (d, *J* = 7.3 Hz, 3H), 1.20 (s, 6H), 1.17 (s, 6H); **^{13}C NMR** (101 MHz, $CDCl_3$, ^{19}F decoupled) δ 207.8, 151.4, 127.9, 126.5, 125.3, 124.4, 84.6, 64.5, 53.4, 24.8 (2C), 13.1 (the boron-bound carbon was not detected due to quadrupolar relaxation of boron); **^{11}B NMR** (160 MHz, $CDCl_3$) δ 33.0; **IR** (cast film, $CHCl_3$ cm^{-1}) 2981, 2933, 1783, 1618, 1355, 1327, 1165, 1141, 1123, 1070, 857, 838; **HRMS** (EI) for $C_{18}H_{22}O_3BF_3$calcd. 354.1614; found 354.1616; **$[\alpha]_D^{20}$** –68.1 (*c* = 0.230, $CHCl_3$); **HPLC** (Chiralpak IC) 1:99 iso-propanol:hexanes, 0.5 mL/min, 20 °C, λ = 220 nm, T_{minor} = 10.9 min, T_{major} = 11.7 min, er = 90.4:9.6.

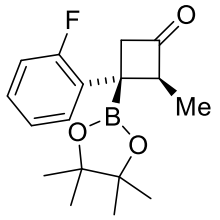

(2*S*,3*R*)-4-(2-fluorophenyl)-2-methyl-4-(4,4,5,5-tetramethyl-1,3,2-dioxaborolan-2-yl)cyclobutanone (4-35): Prepared according to general procedure B with **4-13** (53 mg, 0.30 mmol, 1.0 equiv). The crude material was purified by flash chromatography (1:20 ethyl actetate:hexanes, water deactivated silica) to provide a yellow solid (70 mg, 76% yield, dr >20:1). A second purification by flash chromatography (1:20 ethyl acetate:hexanes) allowed isolation of a pure diastereomer for characterization purposes: **mp =** 56.3–57.8 °C; **^{1}H NMR** (500 MHz, $CDCl_3$) δ 7.24–7.17 (m, 2H), 7.15–7.10 (m, 1H), 7.07–7.00 (m, 1H), 3.64 (qdd, *J* = 7.5 Hz, 2.0 Hz, 1.9 Hz, 1H), 3.53 (dt, J = 16.7 Hz, 2.0 Hz, 1H), 3.12 (dd, *J* = 17.0 Hz, 1.0 Hz, 1H), 1.37 (d, *J* = 7.3 Hz, 3H),

1.20 (s, 6H), 1.18 (s, 6H); **^{13}C NMR** (101 MHz, $CDCl_3$,^{19}F decoupled) δ 208.8, 161.0, 133.9, 127.5, 127.0, 124.0, 115.4, 84.4, 62.0, 54.0, 24.8, 24.7, 12.2 (the boron-bound carbon was not detected due to quadrupolar relaxation of boron); **^{11}B NMR** (128 MHz, $CDCl_3$) δ 33.2; **^{19}F NMR** (376 MHz, $CDCl_3$) δ –113.8; **IR** (cast film, $CHCl_3$ cm^{-1}) 2980, 2932, 1782, 1358, 1142; **HRMS** (EI) for $C_{17}H_{22}BFO_3$calcd. 304.1646; found 304.1651; **[α]$_D^{20}$** –88.5 (c= 0.602, $CHCl_3$); **HPLC** (Chiralpak IC) 1:99 iso-propanol:hexanes, 0.5 mL/min, 20 °C, λ = 220 nm, T_{minor} = 13.5 min, T_{major} = 15.2 min, er = 90.8:9.2**.**

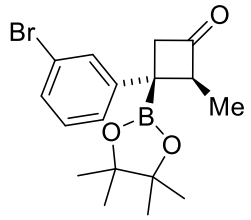

(2*S*,3*R*)-4-(4-bromophenyl)-2-methyl-4-(4,4,5,5-tetramethyl-1,3,2-dioxaborolan-2-yl)cyclobuta-none (4-36): Prepared according to general procedure B with **4-14** (70 mg, 0.30 mmol, 1.0 equiv). The crude material was purified by flash chromatography (1:20 ethyl actetate:hexanes, water deactivated silica) to provide a white solid (46 mg, 43% yield, dr > 20:1). A second purification by flash chromatography (1:20 ethyl acetate:hexanes) allowed isolation of a pure diastereomer for characterization purposes: **mp** = 85.4–87.1 °C; **^{1}H NMR** (400 MHz, $CDCl_3$) δ 7.38–7.30 (m, 2H), 7.22–7.09 (m, 2H), 3.62–3.45 (m, 2H), 3.19 (dd, *J* = 16.6, 2.1 Hz, 1H), 1.40 (d, *J* = 7.4 Hz, 3H), 1.20 (s, 6H), 1.17 (s, 6H); **^{13}C NMR** (126 MHz, $CDCl_3$) δ 208.1, 150.0, 129.9, 129.2, 128.8, 125.0, 122.5, 84.5, 64.3, 53.5, 24.8 (2C), 13.0 (the boron-bound carbon was not detected due to quadrupolar relaxation of boron); **^{11}B NMR** (128 MHz, $CDCl_3$) δ 33.0; **IR** (cast film, $CHCl_3$ cm^{-1}) 2979, 2932, 1781, 1723, 1609, 1436, 1373, 1353, 1279, 1141, 1109, 858, 830; **HRMS** (EI) for $C_{17}H_{22}O_3B^{79}Br$ calcd. 364.0845; found 364.0849; **[α]$_D^{20}$** –56.4 (*c* = 0.170, $CHCl_3$);

HPLC (Chiralpak IC) 10:90 iso-propanol:hexanes, 0.5 mL/min, 20 °C, λ = 220 nm, T_{minor} = 7.9 min, T_{major} = 8.8 min, er = 89.0:11.0.

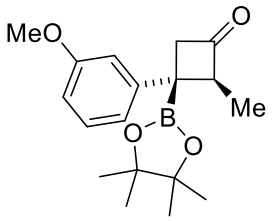

(2*S*,3*R*)-4-(4-methoxyphenyl)-2-methyl-4-(4,4,5,5-tetramethyl-1,3,2-dioxaborolan-2-yl)cyclobuta-none (4-37): Prepared according to general procedure B with **4-15** (57 mg, 0.30 mmol, 1.0 equiv). The crude material was purified by flash chromatography (1:20 ethyl actetate:hexanes, water deactivated silica) to provide a yellow solid (41 mg, 43% yield, dr 10:1). A second purification by flash chromatography (1:20 ethyl acetate:hexanes) allowed isolation of a pure diastereomer for characterization purposes: **mp =** 72.6–74.2 °C; **^{1}H NMR** (500 MHz, $CDCl_3$) δ 7.28–7.21 (m, 1H), 6.81 (d, *J* = 7.9 Hz, 1H), 6.78–6.71 (m, 2H), 3.82 (s, 3H), 3.58 (qdd, *J* = 7.1, 2.1, 2.1 Hz, 1H), 3.49 (dd, *J* = 16.7, 2.3 Hz, 1H), 3.22 (dd, *J* = 16.6, 2.2 Hz, 1H), 1.40 (d, *J* = 7.4 Hz, 3H), 1.19 (s, 6H), 1.17 (s, 6H); **^{13}C NMR** (126 MHz, $CDCl_3$) δ 209.0, 159.5, 148.9, 129.3, 118.7, 112.6, 110.4, 84.3, 64.1, 55.2, 53.5, 24.8, 24.7, 13.0 (the boron-bound carbon was not detected due to quadrupolar relaxation of boron); **^{11}B NMR** (128 MHz, $CDCl_3$) δ 32.0; **IR** (cast film, $CHCl_3$ cm^{-1}) 2979, 2931, 1779, 1355, 1141; **HRMS** (EI) for $C_{18}H_{25}BO_4$ calcd. 316.1846; found 316.1847; **$[\alpha]_D^{20}$** –63.1 (c = 0.204, $CHCl_3$); **HPLC** (Chiralpak IC): 5:95 iso-propanol:hexanes, 0.7 mL/min, 20 °C, λ = 220 nm, T_{minor} = 9.0 min, T_{major} = 9.9 min, er = 93.5:6.5.

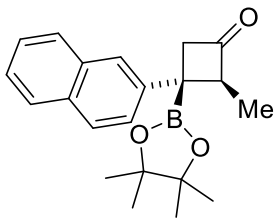

(2*S*,3*R*)-2-methyl-4-(naphthalen-2-yl)-4-(4,4,5,5-tetramethyl-1,3,2-dioxaborolan-2-yl)cyclobuta-none (4-38): Prepared according to general procedure B with **4-16** (61 mg, 0.30 mmol, 1.0 equiv). The crude material was purified by flash chromatography (1:15 ethyl actetate:hexanes, water deactivated silica) to provide a white solid (86 mg, 88% yield, dr > 20:1). A second purification by flash chromatography (1:20 ethyl acetate:hexanes) allowed isolation of a pure diastereomer for characterization purposes: **mp =** 155.7–157.2 °C; **^{1}H NMR** (500 MHz, $CDCl_3$) δ 7.89–7.75 (m, 3H), 7.62 (s, 1H), 7.46 (app dt, *J* = 19.1, 7.1 Hz, 2H), 7.37 (d, *J* = 8.4 Hz, 1H), 3.69 (q, *J* = 7.6 Hz, 1H), 3.61 (d, *J* = 16.7 Hz, 1H), 3.34 (d, *J* = 16.6 Hz, 1H), 1.49 (d, *J* = 7.4 Hz, 3H), 1.19 (s, 6H), 1.16 (s, 6H); **^{13}C NMR** (126 MHz, $CDCl_3$) δ 208.9, 144.7, 133.4, 131.7, 128.1, 127.7, 127.6, 126.1, 125.7, 125.4, 123.6, 84.3, 64.2, 53.5, 24.8, 24.7, 13.2 (the boron-bound carbon was not detected due to quadrupolar relaxation of boron); **^{11}B NMR** (128 MHz, $CDCl_3$) δ 33.1; **IR** (cast film, $CHCl_3$ cm^{-1}) 3054, 2979, 2930, 1775, 1357, 1325, 1138, 859, 751; **HRMS** (EI) for $C_{21}H_{25}BO_3$ calcd. 336.1897; found 336.1904; **[α]$_D^{20}$** –83.6 (*c* = 0.260, $CHCl_3$); **HPLC** (Chiralpak IC) 3:97 iso-propanol:hexanes, 0.5 mL/min, 20 °C, λ = 254 nm, T_{minor} = 15.9 min, T_{major} = 20.2 min, er = 94.9:5.1.

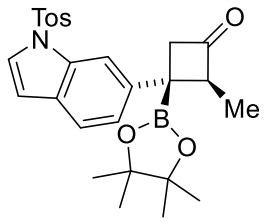

(2*S*,3*R*)-2-methyl-4-(4,4,5,5-tetramethyl-1,3,2-dioxaborolan-2-yl)-4-(1-tosyl-1*H*-indol-5-yl)cyclo-butanone (4-39): Prepared according to general procedure B with **4-19** (53 mg, 0.15 mmol, 1.0 equiv), the overall reaction concentration was 0.10 M. The crude material was purified by flash chromatography (1:10 ethyl actetate:hexanes, water deactivated silica) to provide a white solid (49 mg, 69% yield, dr = 10:1). A second purification by flash chromatography (1:10 ethyl acetate:hexanes) allowed isolation of a pure diastereomer for characterization purposes: **mp =**

174.2–176.0 °C; **^{1}H NMR** (500 MHz, $CDCl_3$) 7.92 (d, *J* = 8.6 Hz, 1H), 7.77 (d, *J* = 8.1 Hz, 2H), 7.54 (d, *J* = 3.7 Hz, 1H), 7.35 (d, *J* = 1.9 Hz, 1H), 7.22 (d, *J* = 8.0 Hz, 2H), 7.16 (dd, *J* = 8.6, 1.9 Hz, 1H), 6.61 (d, *J* = 3.7 Hz, 1H), 3.61–3.49 (m, 2H), 3.20 (dd, *J* = 16.5, 2.1 Hz, 1H), 2.34 (s, 3H), 1.42 (d, *J* = 7.4 Hz, 3H), 1.17 (s, 12H), 1.13 (s, 6H); **^{13}C NMR** (126 MHz, $CDCl_3$) δ 208.9, 144.9, 142.4, 135.5, 133.1, 130.8, 129.9, 126.9, 126.6, 123.5, 118.3, 113.4, 109.0, 84.3, 64.3, 53.9, 24.8, 24.7, 21.6, 13.1 (the boron-bound carbon was not detected due to quadrupolar relaxation of boron); **^{11}B NMR** (128 MHz, $CDCl_3$) δ 33.1; **IR** (cast film, $CHCl_3$ cm^{-1}): 3142, 2979, 2929, 1778, 1458, 1372, 1325, 1175, 1133, 753, 673; **HRMS** (EI) for $C_{26}H_{30}BO_5SN$calcd. 479.1938; found 479.1941; **[α]$_D^{20}$**: –60.3 (c= 0.230, $CHCl_3$); **HPLC** (Chiralpak IB) 5:95 iso-propanol:hexanes, 0.5 mL/min, 20 °C, λ = 254 nm, T_{minor} = 16.0 min, T_{major} = 19.7 min, er = 97.1:2.9.

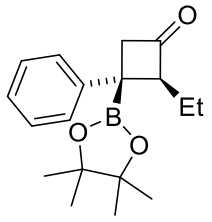

(2*S*,3*R*)-2-ethyl-4-phenyl-4-(4,4,5,5-tetramethyl-1,3,2-dioxaborolan-2-yl)cyclobutanone (4-40): Prepared according to general procedure B with **4-17** (51 mg, 0.30 mmol, 1.0 equiv). The crude material was purified by flash chromatography (1:20 ethyl actetate:hexanes, water deactivated silica) to provide a white solid (68 mg, 76% yield, dr 8:1). A second purification by flash chromatography (1:20 ethyl acetate:hexanes) allowed isolation of a pure diastereomer for characterization purposes: **mp =** 45.3–46.1 °C; **^{1}H NMR** (500 MHz, $CDCl_3$) δ 7.36–7.29 (m, 2H), 7.25–7.16 (m, 3H), 3.53 (dd, *J* = 16.8, 2.4 Hz, 1H), 3.45 (dddd, *J* = 9.2, 7.0, 2.4, 2.4 Hz, 1H), 3.17 (dd, *J* = 16.8, 2.4 Hz, 1H), 2.01–1.85 (m, 1H), 1.80 (ddq, *J* = 14.5, 7.4, 7.4 Hz, 1H), 1.19 (s, 6H), 1.16 (s, 6H), 1.16 (t, *J* = 7.5 Hz, 3H); **^{13}C NMR** (126 MHz, $CDCl_3$) δ 209.4, 147.2, 128.3, 126.3,

125.5, 84.2, 71.0, 53.8, 24.7, 24.7, 22.4, 13.0 (the boron-bound carbon was not detected due to quadrupolar relaxation of boron); **^{11}B NMR** (128 MHz, $CDCl_3$) δ 33.1; **IR** (cast film, $CHCl_3$ cm^{-1}) 3063, 2978, 1780, 1354, 1141; **HRMS** (EI) for $C_{18}H_{25}BO_3$calcd. 300.1897; found 300.1894; **$[\alpha]_D^{20}$** –82.8 (*c* = 0.500, $CHCl_3$); **HPLC** (Chiralpak IC) 5:95 iso-propanol:hexanes, 0.7 mL/min, 20 °C, λ = 210 nm, T_{minor} = 4.9 min, T_{major} = 5.3 min, er = 94.9:5.1.

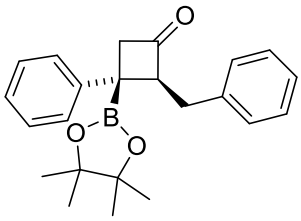

(2*S*,3*R*)-2-benzyl-4-phenyl-4-(4,4,5,5-tetramethyl-1,3,2-dioxaborolan-2-yl)cyclobutanone (4-41): Prepared according to general procedure B with **4-18** (70 mg, 0.30 mmol, 1.0 equiv). The crude material was purified by flash chromatography (1:20 ethyl actetate:hexanes, water deactivated silica) to provide a yellow oil (87 mg, 80% yield, dr >20:1). A second purification by flash chromatography (1:20 ethyl acetate:hexanes) allowed isolation of a pure diastereomer for characterization purposes: **^{1}H NMR** (500 MHz, $CDCl_3$) δ 7.38–7.34 (m, 2H), 7.33–7.28 (m, 2H), 7.27–7.20 (m, 3H), 7.18–7.12 (m, 1H), 7.08–7.03 (m, 2H), 3.77 (dddd, *J* = 8.0, 5.7, 2.1, 2.1 Hz, 1H), 3.51 (dd, *J* = 16.4, 2.1 Hz, 1H), 3.26 (dd, *J* = 14.4, 8.4 Hz, 1H), 3.20 (dd, *J* = 16.4, 1.9 Hz, 1H), 3.10 (dd, *J* = 14.4, 5.7 Hz, 1H), 1.24 (s, 6H), 1.21 (s, 6H); **^{13}C NMR** (126 MHz, $CDCl_3$) δ 207.1, 146.7, 140.0, 129.1, 128.8, 128.6, 128.3, 126.3, 125.6, 84.4, 70.5, 53.7, 34.8, 24.8 (2C) (the boron-bound carbon was not detected due to quadrupolar relaxation of boron); **^{11}B NMR** (128 MHz, $CDCl_3$) δ 33.4; **IR** (cast film, $CHCl_3$ cm^{-1}) 3082, 2979, 1779, 1356, 1140; **HRMS** (EI) for $C_{23}H_{27}BO_3$calcd. 362.2053; found 362.2051; **$[\alpha]_D^{20}$** –10.7 (*c* = 0.840, $CHCl_3$); **HPLC** (Chiralpak IB) 1:99 iso-propanol:hexanes, 0.5 mL/min, 5 °C, λ = 210 nm, T_{minor} = 7.4 min, T_{major} = 8.3 min, er = 91.5:8.5.

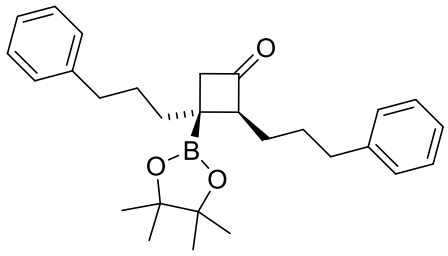

(2*S*,3*R*)-2,4-bis(4-phenylpropyl)-4-(4,4,5,5-tetramethyl-1,3,2-dioxaborolan-2-yl)cyclobutanone (4-42): Prepared according to general procedure B with **4-23** (90 mg, 0.30 mmol, 1.0 equiv). The crude material was purified by flash chromatography (20:1 ethyl actetate:hexanes, water deactivated silica) to provide a white solid (119 mg, 94% yield, dr = 5:1). A second purification by flash chromatography (1:20 ethyl acetate:hexanes) allowed isolation of a pure diastereomer for characterization purposes: **mp =** 46.6–47.8 °C; **^{1}H NMR** (500 MHz, $CDCl_3$)) δ 7.32–7.22 (m, 4H), 7.22–7.12 (m, 6H), 3.08 (dd, *J* = 16.9, 2.5 Hz, 1H), 2.87 (dddd, *J* = 7.9, 5.3, 2.6, 2.6 Hz, 1H), 2.74–2.50 (m, 6H), 1.88 (td, *J* = 12.1, 5.1 Hz, 1H), 1.82–1.43 (m, 6H), 1.22 (s, 6H), 1.21 (s, 6H); **^{13}C NMR** (126 MHz, $CDCl_3$) δ 210.2, 142.3, 142.1, 128.5, 128.3 (3C), 125.8 (2C), 83.9, 69.4, 52.1, 40.4, 36.3, 36.0, 29.7, 29.6, 28.1, 25.2, 24.9. (the boron-bound carbon was not detected due to quadrupolar relaxation of boron); **^{11}B NMR** (160 MHz, $CDCl_3$) δ 34.3; **IR** (cast film, $CHCl_3$ cm^{-1}): 3026, 2978, 2978, 2932, 2857, 1773, 1453, 1381, 1318, 1142, 249, 699; **HRMS** (EI) for $C_{28}H_{37}BO_3$calcd. 432.2836; found 432.2840; **$[\alpha]_D^{20}$** –18.8 (*c* = 0.330, $CHCl_3$); **HPLC** (Chiralpak IC) 1:99 iso-propanol:hexanes, 0.5 mL/min, 20 °C, λ = 220 nm, T_{minor} = 14.9 min, T_{major} = 17.8 min, er = 98.2:1.8.

4.10.9 Ketone functionalization products

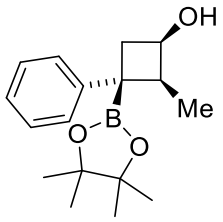

(±)-(1*RS*,2*SR*,3*RS*)-2-methyl-4-phenyl-4-(4,4,5,5-tetramethyl-1,3,2-dioxaborolan-2-yl)cyclobutanol (4-43): The reaction was performed following a literature procedure with slight modification.[20b] Compound **4-24** (113 mg, 0.400 mmol, 1.00 equiv) was dissolved in THF (2.0 mL, 0.20 M) and cooled to -78 °C. L-selectride (1.0 M in THF, 0.42 mL, 0.41 mmol, 1.1 equiv) was added dropwise and the reaction was left to stir at -78 °C for 4 h. After allowing the mixture to warm to room temperature, the mixture was diluted with 10 mL of diethyl ether and saturated ammonium chloride. The aqueous phase was extracted with diethyl ether three times. The combined organic layers were washed with brine, dried with magnesium sulfate, filtered and the solvent was removed in vacuo. The crude reaction mixture was purified by flash chromatography (1:10 ethyl acetate:hexanes) to afford a white solid as a single diastereomer by ^{1}H NMR (101 mg, 88% yield, dr > 20:1): **mp =** 42.0–43.5 °C; **^{1}H NMR** (400 MHz, $CDCl_3$) δ 7.31–7.22 (m, 2H), 7.16–7.07 (m, 3H), 4.32–4.11 (m, 1H), 3.09 (d, *J* = 9.7 Hz, 1H), 2.83 (dq, *J* = 7.2, 7.2 Hz, 1H), 2.52 (dd, *J* = 12.2, 6.5 Hz, 1H), 2.43 (dd, *J* = 12.2, 2.4 Hz, 1H), 1.30 (d, *J* = 7.3 Hz, 3H), 1.22 (s, 6H), 1.21 (s, 6H); **^{13}C NMR** (126 MHz, $CDCl_3$) δ 148.8, 128.0, 125.7, 124.7, 84.2, 68.8, 46.1, 39.2, 24.8, 24.7, 13.0 (the boron-bound carbon was not detected due to quadrupolar relaxation of boron); **^{11}B NMR** (160 MHz, $CDCl_3$) δ 33.6; **IR** (cast film, $CHCl_3$ cm^{-1}) 2979, 2932, 1781, 1723, 1609, 1436, 1373, 1353, 1279, 1141, 1109, 858, 830; **HRMS** (EI) for $C_{17}H_{23}O_2B$ $[M–H_2O]^+$calcd. 270.1791; found 270.1793.

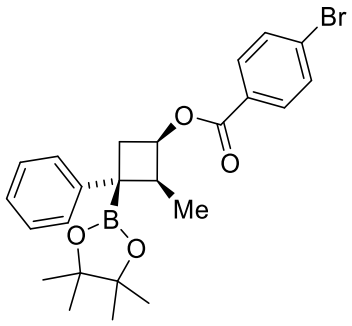

(1*R*,2*S*,3*R*)-2-methyl-4-phenyl-4-(4,4,5,5-tetramethyl-1,3,2-dioxaborolan-2-yl)cyclobutyl 4-bromo-benzoate (4-44): The reaction was performed following a literature procedure with slight modification.[59] Boronic ester **4-43** (29 mg, 0.10 mmol, 1.0 equiv, >85% *ee*) and 4-dimethylaminopyridine (28 mg, 0.23 mmol, 2.3 equiv) were dissolved in DCM (1.0 mL, 0.10 M) and cooled to 0 °C. Triethylamine (0.040 mL, 0.29 mmol, 2.9 equiv) and 4-bromobenzoyl chloride (52 mg, 0.24 mmol, 2.4 equiv) were sequentially added. The reaction was flushed with nitrogen and then stirred at 0 °C for 30 minutes. The ice bath was then removed and the reaction was stirred at room temperature for a total of 4 hours. The reaction was diluted with 5.0 mL of DCM and 5.0 mL of saturated ammonium chloride. The aqueous phase was extracted three times with DCM. The combined organic phase was washed brine and dried with magnesium sulfate, filtered and the volatiles were removed in vacuo. The crude reaction mixture was purified by flash chromatography (2.5% ethylacetate/hexanes) to afford a white solid (41 mg, 91% yield): **mp** = 69.2–70.1 °C; **^{1}H NMR** (500 MHz, $CDCl_3$) δ 8.00–7.93 (m, 2H), 7.62–7.55 (m, 2H), 7.33– 7.27 (m, 2H), 7.26–7.21 (m, 2H), 7.17–7.11 (m, 1H), 5.33 (ddd, *J* = 7.3, 7.2, 5.0 Hz, 1H), 3.20–3.10 (m, 1H), 2.89 (ddd, *J* = 12.3, 5.0, 0.9 Hz, 1H), 2.69 (ddd, *J* = 12.3, 7.0, 2.0 Hz, 1H), 1.35 (d, *J* = 7.3 Hz, 3H), 1.14 (s, 6H), 1.11 (s, 6H); **^{13}C NMR** (176 MHz, $CDCl_3$) δ 165.5, 146.9, 131.6, 131.2, 129.5, 128.2, 128.0, 126.0, 125.0, 83.6, 71.4, 44.8, 35.8, 29.8, 24.8, 24.5, 13.6; **^{11}B NMR** (128 MHz, $CDCl_3$) δ 32.9; **IR** (cast film, CH_3Cl cm^{-1}) 3058, 2977, 2931, 1722, 1591, 1357, 1312, 1272, 1173, 1144, 1119, 1013, 852, 758; **HRMS** (ESI) for $C_{24}H_{28}B^{79}BrNaO_4$ $[M+Na]^+$calcd. 493.1156; found 493.1156. Crystals

suitable for X-ray analysis were obtained from vapour diffusion of benzene into a solution of **4-44** dissolved in a minimal amount of methanol.

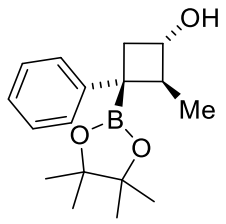

(±)-(1*SR*,2*SR*,3*RS*)-2-methyl-4-phenyl-4-(4,4,5,5-tetramethyl-1,3,2-dioxaborolan-2-yl)cyclobutanol (4-45): The reaction was performed following a literature procedure with slight modification.[20] Compound **4-24** (57 mg, 0.20 mmol, 1.0 equiv) and cerium(III) chloride heptahydrate (112 mg, 0.300 mmol, 1.50 equiv) were dissolved in EtOH (2.0 mL, 0.10 M) and cooled to -78 °C. Sodium borohydride (11 mg, 0.3 mmol, 1.5 equiv) was added as a solution in EtOH (2.0 mL, 0.050 M total) dropwise and the reaction was left to warm from -78 °C to room temperature overnight in a dry ice/acetone bath. The reaction was diluted with 10 mL of ethyl acetate and distilled water. The aqueous phase was extracted with ethyl acetate three times. The combined organic layers were washed with brine, dried with sodium sulfate, filtered and the solvent was removed in vacuo. The crude reaction mixture was purified by flash chromatography (15% ethyl acetate/hexanes) to afford a white solid as a single diastereomer by ^{1}H NMR (51 mg, 85% yield, dr >20:1): **mp =** 71.5–72.5 °C; **^{1}H NMR** (400 MHz, $CDCl_3$) δ 7.32–7.20 (m, 2H), 7.17–7.04 (m, 3H), 4.01–3.82 (m, 1H), 2.95 (dd, *J* = 9.9, 7.1 Hz, 1H), 2.37 (dq, *J* = 7.2, 7.2 Hz, 1H), 1.86 (dd, *J* = 10.0, 8.3 Hz, 1H), 1.57 (d, *J* = 6.2 Hz, 1H), 1.38 (d, *J* = 6.9 Hz, 3H), 1.19 (s, 6H), 1.17 (s, 6H); **^{13}C NMR** (126 MHz, $CDCl_3$) δ 149.0, 128.1, 125.6, 124.8, 83.6, 71.1, 52.2, 40.8, 24.8, 24.7, 17.5 (the boron-bound carbon was not detected due to quadrupolar relaxation of boron); **^{11}B NMR** (128 MHz, $CDCl_3$) δ 33.4; **IR** (cast film, $CHCl_3$ cm^{-1}) 3325, 3082, 3058, 2978, 2934m 1598, 1446, 1357, 1311, 1144, 1126, 1086, 847, 699; **HRMS** (EI) for $C_{17}H_{23}O_2B$ $[M–H_2O]^+$calcd. 270.1791; found 270.1796.

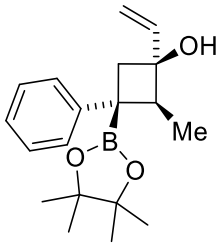

(±)-(1*SR*,2*SR*,3*RS*)-2-methyl-3-phenyl-3-(4,4,5,5-tetramethyl-1,3,2-dioxaborolan-2-yl)-1-vinyl-cyclobutanol: The reaction was performed following a literature procedure with slight modification.[20a] Compound **4-24** (57 mg, 0.20 mmol, 1.0 equiv) was dissolved in THF (1.0 mL, 0.20 M) and cooled to 0 °C. Vinylmagnesium bromide (1.00 M in THF, 210 µL, 0.210 mmol, 1.05 equiv) was added dropwise and the reaction was left to stir at 0 °C to for 4 hours. The solution was warmed to room temperature and then diluted with 10 mL of ethyl acetate and distilled water. The aqueous phase was extracted with ethyl acetate three times. The combined organic layers were washed with water, brine, dried with magnesium sulfate, filtered and the solvent was removed *in vacuo*. The crude reaction mixture was purified by flash chromatography (5% ethyl acetate/hexanes) to afford a clear, colourless oil, as a single diastereomer by ^{1}H NMR (14 mg, 24% yield, dr > 20:1): **^{1}H NMR** (500 MHz, $CDCl_3$) δ 7.31–7.23 (m, 2H), 7.17–7.07 (m, 3H), 5.85 (dd, *J* = 17.2, 10.7 Hz, 1H), 5.20 (dd, *J* = 17.2, 1.6 Hz, 1H), 5.00 (dd, *J* = 10.7, 1.6 Hz, 1H), 3.35 (s, 1H), 2.70 (q, *J* = 7.2 Hz, 1H), 2.60 (d, *J* = 11.7 Hz, 1H), 2.38 (d, *J* = 11.7 Hz, 1H), 1.27 (d, *J* = 7.2 Hz, 3H), 1.22 (s, 6H), 1.21 (s, 6H); **^{13}C NMR** (126 MHz, $CDCl_3$) δ 149.0, 142.9, 128.1, 125.6, 124.8, 112.2, 84.1, 75.5, 50.5, 43.8, 29.8, 24.7, 24.6, 12.; **^{11}B NMR** (128 MHz, $CDCl_3$) δ 33.9.

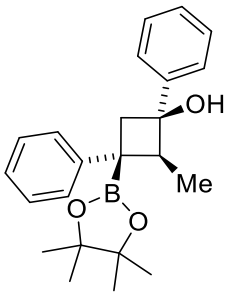

(±)-(1*RS*,2*SR*,3*RS*)-2-methyl-1,4-diphenyl-4-(4,4,5,5-tetramethyl-1,3,2-dioxaborolan-2-yl)cyclo-butanol (4-47): The same reaction procedure was followed as for vinyl Grignard product **4-46** using compound **4-24** (57 mg, 0.20 mmol, 1.0 equiv) and phenylmagnesium bromide (0.80 M in THF, 270 μL, 0.22 mmol, 1.1 equiv). The crude reaction mixture was purified by flash chromatography (5% ethyl acetate/hexanes) to afford a clear, colourless oil, as a single diastereomer by ^{1}H NMR (63 mg, 86% yield, dr > 20:1): **^{1}H NMR** (500 MHz, $CDCl_3$) δ 7.50–7.37 (m, 2H), 7.30 (q, *J* = 7.6 Hz, 4H), 7.25–7.19 (m, 1H), 7.19–7.09 (m, 3H), 3.62 (s, 1H), 3.02 (q, *J* = 7.1 Hz, 1H), 2.86 (d, *J* = 11.7 Hz, 1H), 2.70 (d, *J* = 11.7 Hz, 1H), 1.39 (d, *J* = 7.1 Hz, 3H), 1.26 (s, 6H), 1.25 (s, 6H); **^{13}C NMR** (126 MHz, $CDCl_3$) δ 148.9, 145.9, 128.1, 128.1, 126.8, 125.7, 125.1, 124.9, 84.2, 76.5, 51.9, 44.9, 24.8, 24.7, 12.7 (the boron-bound carbon was not detected due to quadrupolar relaxation of boron); **^{11}B NMR** (160 MHz, $CDCl_3$) δ 33.9; **IR** (cast film, $CHCl_3$ cm^{-1}): 3484, 3058, 3024, 2977, 2928, 1447, 1363, 1134, 996.5, 700; **HRMS** (EI) for $C_{17}H_{23}O_2B$ $[M–H_2O]^+$calcd. 346.2104; found 346.2105.

4.10.10 Products from boron functionalizations

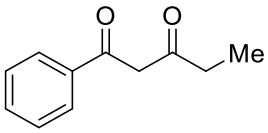

1-phenyl-1,4-pentanedione (4-48): A crude reaction mixture of the racemic conjugate borylation product was subjected to oxidation conditions following the same procedure as for diol **4-49**. The

crude reaction mixture was purified by flash chromatography (5% to 20% ethyl acetate/hexanes) to afford a clear, colourless oil for characterization purposes. The spectral data matched the literature, emitting the enol proton reportedly @ 16.11 ppm due to the use of δ 11.0 to -1.0 chemical shift range in the experiment:[60] **^{1}H NMR** (500 MHz, $CDCl_3$) δ (enol form) = 7.91– 7.80 (m, 2H), 7.56–7.49 (m, 1H), 7.48–7.39 (m, 2H), 6.18 (s, 1H), 2.47 (q, *J* = 7.5 Hz, 2H), 1.22 (t, *J* = 7.5 Hz, 3H); (keto form) = 7.98–7.92 (m, 0.12 H), 7.62–7.57 (m, 0.06 H), 4.10 (s, 0.12H), 2.62 (q, *J* = 7.3 Hz, 0.12 H), 1.09 (t, *J* = 7.2 Hz, 0.20 H) (the rest of the signals are overlapped by the signals of the major form); **^{13}C NMR** (126 MHz, $CDCl_3$) δ (enol form) = 198.0, 183.1, 135.1, 132.2, 128.6, 127.0, 95.5, 32.5, 9.8; (keto form) = 204.9, 194.1, 133.8, 128.8, 128.7, 53.7, 36.8, 7.6; **HRMS** (ESI) for $C_{11}H_{12}O_2Na$ $[M+Na]^+$calcd. 199.0730; found 199.0734.

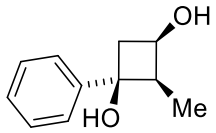

(±)-(1*SR*,2*RS*,3*RS*)-2-methyl-1-phenylcyclobutane-1,4-diol (4-49): Boronic ester **4-43** (55 mg, 0.20 mmol, 1.0 equiv) was dissolved in THF (1.0 mL, 0.20 M) under atmospheric conditions to provide a clear, colourless solution. Sodium perborate tetrahydrate (154 mg, 1.00 mmol, 5.00 equiv) was added followed by water (1.0 mL, 0.20 M). The reaction flask was capped with a stopper and stirred for six hours at room temperature. The mixture was diluted with 10.0 mL of ethyl acetate and 5.0 mL of water. The aqueous phase was extracted three times with 20 mL of ethyl acetate. The combined organic phases were washed brine and dried with sodium sulfate, filtered and the volatiles were removed in vacuo. The crude reaction mixture was purified by flash chromatography (1:2 to 1:1 ethyl acetate:hexanes) to afford a white solid (33 mg, 97% yield): **mp =** 118.9–119.8 °C; **^{1}H NMR** (500 MHz, d_6-acetone) δ 7.51–7.44 (m, 2H), 7.34–7.27 (m, 2H), 7.22–7.17 (m, 1H), 4.28–4.16 (m, 1H), 4.06 (s, 1H), 3.83 (d, *J* = 5.9 Hz, 1H), 2.85–2.69 (m, 2H), 2.24 (dd, *J* = 12.4, 5.4 Hz,

1H), 1.13 (d, J = 7.2 Hz, 3H); **^{13}C NMR** (176 MHz, d_6-acetone) δ 148.6, 128.8, 127.2, 125.8, 74.2, 64.0, 48.2, 46.2, 8.1; **IR** (cast film, CH_3Cl cm^{-1}): 3324, 3061, 3037, 2976, 2942, 2911, 1602, 1497, 1447, 1413, 1323, 1300, 1236, 1153, 986, 913, 849, 767, 699; **HRMS** (ESI) for $C_{11}H_{14}NaO_2$ $[M+Na]^+$calcd. 201.0886; found 201.0884.

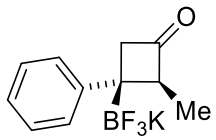

potassium (±)-trifluoro((1*RS*,2*SR*)-2-methyl-4-oxo-1-phenylcyclobutyl)borate (4-50): The reaction was performed following a literature procedure with slight modifications.[61] Compound **4-24** (57 mg, 0.20 mmol, 1.0 equiv) was dissolved in acetonitrile (3.3 mL, 0.060 M) at room temperature. A saturated aqueous solution of potassium hydrogenfluoride (4.5 M, 0.36 mL, 1.6 mmol, 8.0 equiv) was added dropwise. The reaction was left to stir at room temperature overnight. The volatiles were removed in vacuo and the dried crude reaction mixture was washed through a celite plug with 100% acetone, the volatiles were once again in vacuo and the white solid was left under high vacuum overnight. The resulting solid was triturated with hexanes to afford a white solid (50 mg, 94% yield): **mp =** N/A (decomposition ≥ 185 °C); **^{1}H NMR** (400 MHz, CD_3CN) δ 7.24–7.11 (m, 4H), 7.05–6.95 (m, 1H), 3.07 (q, J = 6.0 Hz, 1H), 2.98 (d, J = 15.8 Hz, 1H), 2.78 (d, J = 15.6 Hz, 1H), 1.30 (d, J = 6.1 3H); **^{13}C NMR** (101 MHz, CD_3CN) δ 213.1, 155.4, 128.1, 127.2, 124.2, 63.1, 53.4, 12.7 (the boron-bound carbon was not detected due to quadrupolar relaxation of boron); **^{11}B NMR** (128 MHz, CD_3CN) δ 4.0; **^{19}F NMR** (377 MHz, CD_3CN) δ –145.3; **IR** (cast film, MeOH cm^{-1}) 3565, 3056, 3028, 2968, 2932, 2874, 1757, 1599, 1490, 1217, 996, 952, 703; **HRMS** (ESI) for $C_{11}H_{11}OBF_3$ $[M]^-$calcd. 227.0861; found 227.0859.

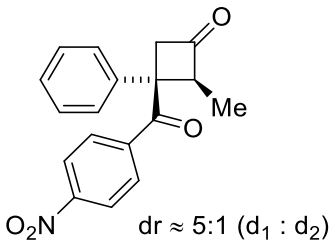

(±)-(2*SR*,3*SR*)-2-methyl-4-(4-nitrobenzoyl)-4-phenylcyclobutanone (4-51): The reaction was performed following a literature procedure with slight modification.[42,43] Trifluoroborate **4-50** (86 mg, 0.30 mmol, 1.5 equiv), *p*-nitrobenzaldehyde (31 mg, 0.20 mmol, 1.0 equiv) and 1,5-cyclooctadienerhodium(I) chloride dimer were dissolved in dioxane (1.0 mL, 0.20 M) and degassed water (0.17 mL, 1.2 M). The reaction mixture was heated to 80 °C for 16 hours. The reaction was cooled to room temperature and quenched with about 3 mL of saturated ammonium chloride and extracted with 25 mL of ethyl acetate three times. The combined organic layers were washed with brine, dried with sodium sulfate, filtered and the volatiles were removed in vacuo. The crude reaction mixture was purified by column chromatography (10 to 20% ethyl acetate/hexanes) to afford a mixture of stereoisomers. The resulting oil was dissolved in DCM and added to a solution of Dess Martin periodinane (200 mg, 0.45 mmol, 2.25 equiv) in DCM (10 mL total, 0.020 M). The reaction was stirred at room temperature overnight before the volatiles were once again removed in vacuo. The crude reaction mixture was filtered through a silica plug (15% ethylacetate/hexanes), which was subsequently further purified by column chromatograpghy (7.5 to 10% ethylacetate/hexanes) to afford a clear colourless oil (42 mg, 66% yield, 5:1 dr, d_1:d_2): **^{1}H NMR** (600 MHz, CD_3Cl) δ 8.19–8.15 (m, 2H, d_2), 8.15–8.09 (m, 2H, d_1), 7.94–7.89 (m, 2H, d_2), 7.83–7.76 (m, 2H, d_1), 7.40–7.34 (m, 2H, d_1+d_2), 7.34–7.31 (m, 1H, d_2), 7.31–7.27 (m, 3H, d_1), 7.19–7.14 (m, 1H, d_2), 4.47 (qdd, *J* = 7.3, 3.3, 1.7 Hz, 1H, d_2), 4.39 (dd, *J* = 17.5, 2.0 Hz, 1H, d_1), 4.25–4.15 (m, 1H, d_1), 3.82 (dd, *J* = 17.0, 1.8 Hz, 1H, d_2), 3.52 (dd, *J* = 17.1, 3.3 Hz, 1H, d_2), 3.12 (dd, *J* = 17.5, 4.6 Hz, 1H, d_1), 1.21 (d, *J* = 7.6 Hz, 3H, d_1), 0.73 (d, *J* = 7.3 Hz, 3H, d_2); **^{13}C NMR** (126 MHz, CD_3Cl) δ 205.6 (d_1),

205.3 (d_2), 197.8 (d_1), 197.3 (d_2), 150.0 (d_2), 149.7 (d_1), 141.6 (d_1), 141.0 (d_1), 138.3 (d_2), 136.0 (d_2), 131.1 (d_2), 130.7 (d_1), 129.7 (2C, d_1+d_2), 128.2 (d_2), 128.0 (d_1), 126.6 (d_2), 126.2 (d_1), 123.7 (d_2), 123.5 (d_1), 61.6 (d_2), 61.1 (d_1), 56.9 (d_1), 53.2 (d_2), 53.0 (d_1), 51.7 (d_2), 12.2 (d_1), 10.2 (d_2); **IR** (cast film, $CHCl_3$ cm^{-1}) 3051, 2970, 2930, 1788, 1683, 1604, 1526, 1349, 1247, 1009, 863, 702; **HRMS** (EI) for $C_{18}H_{15}O_4N$ calcd. 309.1001; found 309.0996.

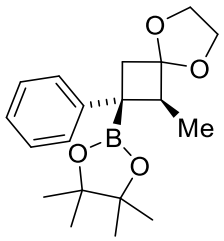

(±)-4,4,5,5-tetramethyl-2-((1*SR*,2*RS*)-1-methyl-2-phenyl-5,8-dioxaspiro[3.4]octan-2-yl)-1,3,2-dioxaborolane (4-52): The reaction was performed following a literature procedure with slight modifications.[62] Ketone **4-24** (152 mg, 0.520 mmol, 1.00 equiv) was dissolved in toluene (3.0 mL, 0.18 M). Ethylene glycol (0.090 mL, 1.6 mmol, 3.0 equiv), trimethyl orthoformate (0.090 mL, 0.82 mmol, 1.5 equiv) and *p*-toluenesulfonic acid monohydrate (10 mg, 0.053 mmol, 0.10 equiv) were sequentially added to the reaction mixture. The sides of the RBF was further rinsed with toluene (2.3 mL, 0.10 M total) and the headspace of the flask was flushed with nitrogen for a few minutes before allowing the reaction to stir at room temperature for 24 hours. The volatiles were removed in vacuo and the mixture was dissolved in 15 mL of ethyl acetate and saturated sodium bicarbonate. The aqueous phase was extracted with ethyl acetate three times. The combined organic layers were washed with water, brine, dried with sodium sulfate, filtered and the solvent was removed in vacuo. The crude reaction mixture was purified by flash chromatography (5% ethylacetate/hexanes) to afford white solid (160 mg, 91% yield): **mp =** 97.3–98.6 °C; **^{1}H NMR** (400 MHz, $CDCl_3$) δ 7.28–7.21 (m, 2H), 7.20–7.14 (m, 2H), 7.14–7.07 (m, 1H), 4.03–3.94 (m, 1H), 3.93–3.82 (m, 3H), 2.88–2.76 (m, 2H), 2.35 (dd, *J* = 11.3, 0.9 Hz, 1H), 1.30 (d, *J* = 7.2 Hz, 3H), 1.16 (s, 6H), 1.14 (s, 6H);

^{13}C NMR (176 MHz, $CDCl_3$) δ 147.8, 128.1, 125.9, 124.9, 107.7, 83.4, 64.5, 64.3, 52.1, 43.0, 24.5, 24.4, 12.5 (the boron-bound carbon was not detected due to quadrupolar relaxation of boron); **^{11}B NMR** (128 MHz, $CDCl_3$) δ 33.0; **IR** (cast film, solid cm^{-1}) 3054, 2978, 2941, 2902, 2879, 1597, 1426, 1354, 1314, 1275, 1165, 1115, 1045, 855, 702; **HRMS** (EI) for $C_{19}H_{27}O_4B$ calcd. 330.2002; found 330.2003.

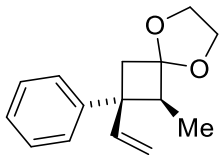

(±)-(1*SR*,2*SR*)-1-methyl-2-phenyl-2-vinyl-5,8-dioxaspiro[3.4]octane (4-53): The reaction was performed following a literature procedure with slight modification.[47a,63] Ketal **4-52** (66 mg, 0.20 mmol, 1.0 equiv) was dissolved in THF (2.0 mL, 0.10 M) and the reaction was cooled to -78 °C. Vinylmagnesium bromide (1.0 M in THF, 1.2 mL, 1.2 mmol, 6.0 equiv) was added dropwise. The dry ice/acetone bath was removed and the reaction mixture was left to stir at room temperature for two hours. The reaction was again cooled to -78 °C and iodine (305 mg, 1.2 mmol, 6.0 equiv) was added dropwise as a solution in methanol (3.0 mL, 0.40 M). The reaction was then left to stir at room temperature for two hours. The reaction mixture was once again cooled to -78 °C before sodium methoxide (104 mg, 2 mmol, 10 equiv) was added dropwise as a solution in methanol (3.0 mL, 0.67 M). The reaction was left to stir at room temperature for two hours. The reaction was diluted with 20 mL of diethyl ether and saturated sodium thiosulfate. The aqueous phase was extracted with diethyl ether and the combined organic phases were washed with water, brine and dried with sodium sulfate, filtered and the volatiles were removed in vacuo. The crude reaction mixture was purified by flash chromatography (5% diethyl ether in hexanes) to afford a clear, colourless oil (26 mg, 56% yield): **^{1}H NMR** (700 MHz, $CDCl_3$) δ 7.31 (t, *J* = 7.7 Hz, 2H), 7.22–7.17 (m, 1H), 7.15–7.11 (m, 2H), 6.31 (dd, *J* = 17.3, 10.6 Hz, 1H), 5.08 (dd, *J* = 10.6, 1.5 Hz, 1H),

4.52 (dd, J = 17.3, 1.5 Hz, 1H), 4.02 (ddd, J = 7.6, 6.3, 6.3 Hz, 1H), 3.97–3.91 (m, 1H), 3.89–3.82 (m, 2H), 3.12 (q, J = 7.2 Hz, 1H), 2.70 (d, J = 12.7 Hz, 1H), 2.67 (d, J = 12.4 Hz, 1H), 1.16 (d, J = 7.3 Hz, 3H); **^{13}C NMR** (176 MHz, $CDCl_3$) δ 147.9, 142.8, 128.1, 126.6, 125.9, 114.7, 107.4, 64.9, 64.2, 51.4, 45.7, 43.8, 10.0; **IR** (cast film, CH_3Cl cm^{-1}) 3083, 3059, 2955, 2881, 1623, 1601, 1496, 1446, 1276, 1061, 1043, 1011, 764, 701; **HRMS** (EI) for $C_{15}H_{18}O_2$calcd. 230.1307; found 230.1308.

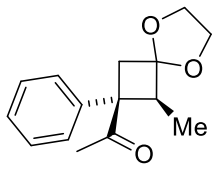

(±)-1-((1*SR*,2*SR*)-1-methyl-2-phenyl-5,8-dioxaspiro[3.4]octan-2-yl)ethanone (4-54): The reaction was performed following a literature procedure with slight modifications.[47a] *tert*-Butyllithium (1.46 M in hexanes, 343 µL, 0.500 mmol, 2.50 equiv) was added dropwise to a solution of ethyl vinyl ether (0.080 mL, 0.80 mmol, 4.0 equiv) in THF (2.6 mL, 0.19 M) at -78 °C. The clear yellow solution was stirred for 30 mins at -78 °C then 0 °C for 30 mins. The reaction was cooled back to -78 °C and boronic ester **11** (66 mg, 0.20 mmol, 1.0 equiv) was added dropwise as a solution in THF (1.1 mL, 0.19 M). The reaction was stirred for 30 mins at -78 °C, then warmed to room temperature and stirred for 5 mins longer (about 20 mins total). The reaction was again cooled to -78 °C and iodine (203 mg, 0.800 mmol, 4.00 equiv) was added dropwise as a solution in THF (2.1 mL, 0.38 M). The reaction was stirred for 30 mins at -78 °C, then once again warmed to room temperature and stirred for 5 mins (about 20 mins total). The reaction mixture was once again cooled to -78 °C before sodium methoxide (87 mg, 1.6 mmol, 8.0 equiv) was added dropwise as a solution in methanol (2.7 mL, 0.60 M). The dry ice/acetone bath was removed and the reaction was left to stir at room temperature for one hour. An aqueous saturated solution of ammonium chloride (2.6 mL, 0.079M relative to **11**) was added and the reaction was left to stir at room temperature for four hours. About 5 mL of saturated sodium thiosulfate was added and the aqueous phase was extracted

with 20 mL of diethyl ether three times. The combined organic phases were washed with water, brine and dried with magnesium sulfate, filtered and the volatiles were removed in vacuo. The crude reaction mixture was purified by flash chromatography (5 to 10% ethylacetate/hexanes) to afford an impure clear, colourless oil. A second flash chromatography purification (100% DCM) afforded a clear, colourless oil (29 mg, 60% yield): **^{1}H NMR** (700 MHz, $CDCl_3$) 7.37–7.31 (m, 2H), 7.25–7.21 (m, 3H), 4.03–3.97 (m, 1H), 3.89–3.81 (m, 3H), 3.47 (d, J = 12.6 Hz, 1H), 3.32 (qd, J = 7.4, 2.0 Hz, 1H), 2.38 (dd, J = 12.7, 2.0 Hz, 1H), 1.92 (s, 3H), 1.24 (d, J = 7.5 Hz, 3H); **^{13}C NMR** (126 MHz, $CDCl_3$) 206.7, 143.8, 128.7, 126.9, 126.7, 106.2, 65.0, 64.4, 54.7, 51.1, 42.5, 28.6, 11.3; **IR** (cast film, CH_3Cl cm^{-1}) 30.86, 2960, 1704, 1598, 1494, 1447, 1352, 1289, 1048, 1011, 949, 702; **HRMS** (ESI) for $C_{15}H_{18}NaO_3$ $[M+Na]^+$calcd. 269.1148; found 269.1150.

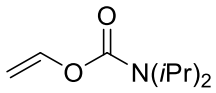

(±)-(1*SR*,2*RS*)-2-ethynyl-1-methyl-2-phenyl-5,8-dioxaspiro[3.4]octane (4-55): The reaction was performed following a literature procedure with slight modification.[64] *n*-Butyllithium (2.1 M in hexanes, 7.30 mL, 15.0 mmol, 1.5 equiv) was added dropwise to THF (7.80 mL, 1.30 M) at 0 °C. The ice bath was removed and the solution was left to stir at room temperature for 20 hours. *N,N*-diisopropyl carbamoyl chloride (1.63 g, 10.0 mmol, 1.00 equiv) was added dropwise as a solution in DMPU (8.0 mL, 1.3 M) at 0 °C. The ice bath was removed and the reaction was stirred for 4 hours at room temperature. The reaction was diluted in 25 mL of diethyl ether and saturated aqueous ammonium chloride and the aqeous phase was extracted three times with diethyl ether. The combined organic phases were washed with water twice, brine, dried with magnesium sulfate, filtered and the volatiles were removed *in vacuo*. The crude reaction mixture was purified by flash chromatography (2.5% ethyl acetate/hexanes) to afford a clear, colourless oil (1.02 g, 60% yield). The spectral data matched that previously reported:[65] **^{1}H NMR** (700 MHz, $CDCl_3$) 7.22 (dd, J =

14.0, 6.3 Hz, 1H), 4.72 (dd, *J* = 14.0, 1.6 Hz, 1H), 4.38 (dd, *J* = 6.4, 1.4 Hz, 1H), 4.14 – 3.63 (m, 2H), 1.22 (d, *J* = 8.9 Hz, 12H).

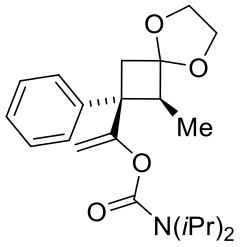

(±)-(1*SR*,2*RS*)-2-ethynyl-1-methyl-2-phenyl-5,8-dioxaspiro[3.4]octane (4-56): The reaction was performed following a literature procedure with slight modification.[19] *n*-Butyllithium (2.0 M in hexanes, 0.15 mL, 0.30 mmol, 1.5 equiv) was added dropwise to a solution of *N*,*N*-diisopropylamine (50.0 µL, 0.357 mmol, 1.78 equiv) in THF (0.35 mL, 0.086 M) at -78 °C. Boronate **4-52** (66 mg, 0.20 mmol, 1.0 equiv) was added dropwise as a solution in THF (1.0 mL, 0.20 M) followed by vinyl *N*,*N*-diisopropylcarbamate (51 mg, 0.30 mmol, 1.5 equiv). The reaction was stirred for 1 hour at -78 °C, then warmed to -40 °C (acetonitrile/dry ice bath) and stirred for 30 mins. The reaction was again cooled to -78 °C and iodine (76 mg, 0.30 mmol, 1.5 equiv) was added dropwise as a solution in methanol (1.7 mL, 0.18 M). The reaction was stirred for 10 mins at -78 °C, then warmed to room temperature for 1 hour. About 5 mL of saturated aqueous solution of sodium thiosulfate was added and the aqeous phase was extracted three times with 10 mL of diethyl ether. The combined organic phases were washed with brine, dried with magnesium sulfate and filtered through a short silica plug, which was rinse with about 50 mL of diethyl ether. The crude reaction mixture was purified by flash chromatography (10 to 25% diethyl ether/hexanes) to afford a clear, colourless oil for partial characterization purposes: **^{1}H NMR** (500 MHz, $CDCl_3$) δ 7.29–7.22 (m, 4H), 7.17–7.12 (m, 1H), 4.98–4.93 (m, 2H), 3.95 (ddd, *J* = 7.6, 6.7, 5.8 Hz, 1H), 3.93–3.83 (m, 2H), 3.85– 3.78 (m, 2H), 3.53 (br s, 1H), 3.26 (ddd, *J* = 7.3, 1.9, 1.9 Hz, 1H), 3.00 (d, *J* = 13.1 Hz, 1H), 2.60 (dd, *J* = 13.3, 2.0 Hz, 1H), 1.26 (d, *J* = 7.4 Hz, 3H), 1.23–0.92 (m, 12H).; **^{13}C NMR** (176 MHz, $CDCl_3$, rotamers are

present) δ 156.4, 151.9, 146.6, 127.9, 127.2, 126.1, 106.8, 102.4, 77.2, 77.1, 76.9, 64.9, 64.0, 50.5, 46.6, 46.3, 45.6, 45.2, 21.0, 20.8, 20.5, 20.4, 11.0.

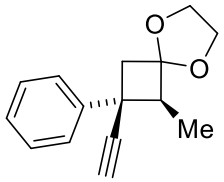

(±)-(1*SR*,2*RS*)-2-ethynyl-1-methyl-2-phenyl-5,8-dioxaspiro[3.4]octane (4-57): The reaction was performed following the same procedure as for alkenyl carbamate **4-56.** The crude reaction mixture was dried under high vacuum for 20 minutes. The yellow oil was dissolved in THF (2 mL, 0.1 M) and added dropwise to a freshly prepared solution of LDA (1.2 mmol, 6.0 equiv) stirring at -78 °C in THF (2.0 mL, 0.6 M). After 10 minutes, the reaction was allowed to stir at -20 °C for 30 mins. Methanol (0.60 mL, 0.33 M) was added dropwise. The cooling bath was removed after 10 minutes and the reaction was left to stir at room temperature for 1 hour. About 20 mL of saturated ammonium chloride was added and the aqueous phase was extracted three times with 20 mL of ethyl aceetate. The combined organic phases were washed with brine and dried with sodium sulfate, filtered and the volatiles were removed in vacuo. The crude reaction mixture was purified by flash chromatography (2.5% ethyl acetate/hexanes) to afford a white solid (33 mg, 74% yield): **mp** = 53.7–54.2 °C; **^{1}H NMR** (500 MHz, $CDCl_3$) δ 7.51–7.45 (m, 2H), 7.39–7.29 (m, 2H), 7.26–7.21 (m, 1H), 4.07 (ddd, *J* = 7.8, 6.3, 6.3 Hz, 1H), 3.98 (ddd, *J* = 7.8, 6.8, 5.9 Hz, 1H), 3.92–3.85 (m, 2H), 2.98 (qd, *J* = 7.0, 1.3 Hz, 1H), 2.88 (dd, *J* = 12.6, 1.4 Hz, 1H), 2.81 (d, *J* = 12.6 Hz, 1H), 2.50 (s, 1H), 1.25 (d, *J* = 7.1 Hz, 3H); **^{13}C NMR** (126 MHz, $CDCl_3$) δ 144.7, 128.5, 126.7, 125.7, 106.7, 86.5, 73.1, 65.2, 64.4, 53.6, 48.8, 37.0, 10.3; **IR** (cast film, CH_3Cl cm^{-1}) 3287, 3060, 3026, 2956, 2925, 2887, 2111, 1778, 1727, 1600, 1448, 1288, 1047, 1013, 760, 699; **HRMS** (EI) for $C_{15}H_{15}O_2$ $[M-H]^+$calcd. 227.1072; found 227.1071.

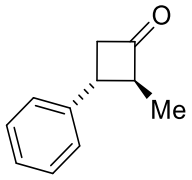

***anti*-2-methyl-4-phenylcyclobutanone (4-58):** The reaction was performed following a literature procedure with slight modification.[48] Compound **4-24** (58 mg, 0.20 mmol, 1.0 equiv) and tetrabutylammonium fluoride trihydrate (95 mg, 0.30 mmol, 1,5 equiv) were dissolved in toluene (2.0 mL, 0.10 M). The reaction was heated to 45 °C for three hours. The solution was then allowed to cool back to room temperature before the crude reaction mixture was flitlered through a short silica plug and eluted with about 10 mL of ethyl acetate. The crude reaction mixture was purified by flash chromatography (2% ethylacetate/hexanes) to afford a clear, colourless oil (18 mg, 56% yield, dr 9.5:1): **^{1}H NMR** (500 MHz, $CDCl_3$) δ 7.41–7.34 (m, 2H), 7.34 7.30 (m, 2H), 7.30–7.23 (m, 1H), 3.45–3.37 (m, 1H), 3.33 (ddd, *J* = 16.9, 8.9, 2.1 Hz, 1H), 3.26 (ddd, *J* = 17.0, 8.5, 2.4 Hz, 1H), 3.16 (q, *J* = 8.5 Hz, 1H), 1.31 (d, *J* = 7.2 Hz, 3H); **^{13}C NMR** (166 MHz, $CDCl_3$) δ 209.2, 142.9, 128.8, 126.8, 126.5, 62.8, 51.8, 37.8, 13.3; **IR** (cast film, $CHCl_3$ cm^{-1}): 3029, 2965, 2927, 1784, 1603, 1497, 1454, 1145, 1032, 736, 699; **HRMS** (EI) for $C_{11}H_{12}O$ calcd. 160.0888; found 160.0887.

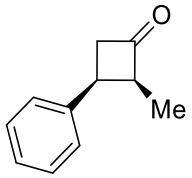

***syn*-2-methyl-4-phenylcyclobutanone (4-59):** Cyclobutenone **4-1** (36 mg, 0.13 mmol, 1.0 equiv) and palladium (13 mg, 10% Pd on activated carbon, 0.012 mmol, 10 mol%) were dissolved in ethyl acetate (1.0 mL, 0.20 M) and purged with hydrogen gas for about five minutes. The needle was then removed from the solution and left in the reaction headspace while stirring at room temperature overnight. The crude reaction mixture was filtered through celite to afford a clear, colourless oil (19

mg, 94% yield): **^{1}H NMR** (400 MHz, $CDCl_3$) δ 7.38–7.31 (m, 2H), 7.29–7.22 (m, 1H), 7.20–7.15 (m, 2H), 3.78 (ddd, *J* = 9.9, 9.9, 5.1 Hz, 1H), 3.75–3.64 (m, 1H), 3.51 (ddd, *J* = 17.6, 9.7, 3.8 Hz, 1H), 3.21 (ddd, *J* = 17.7, 5.1, 2.1 Hz, 1H), 0.78 (d, *J* = 7.3 Hz, 3H); **^{13}C NMR** (126 MHz, $CDCl_3$) δ 211.1, 139.6, 128.5, 128.0, 126.7, 59.0, 50.0, 33.3, 10.1; **HRMS** (EI) for $C_{11}H_{12}O$ calcd. 160.0888; found 160.0885.

4.10.11 Synthesis of cyclobutenoate substrates

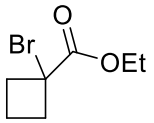

1-bromocyclobutane-1-carboxylate (4-60): The reaction was performed following a literature procedure with slight modification.[66] Ethyl cyclobutanecarboxylate (7.69 g, 60.0 mmol, 1.00 equiv) was dissolved in benzene (300 mL, 0.200 M) at room temperature. N-bromosuccinimide (16.1 g, 90.0 mmol, 1.50 equiv) and α,α′-azoisobutyronitrile (520 mg, 3.0 mmol, 5 mol%) were sequentially added and the reaction was heated to 80 °C for four hours. The crude reaction mixture was cooled to room temperature and the volatiles were removed *in vacuo*. The crude solid was re-dissolved in 100 mL of ethyl acetate and water and the aqueous phase was extracted three times. The combined organic phass were washed with brine and dried with sodium sulfate, filtered and the volatiles were removed *in vacuo*. The crude reaction mixture was filtered through a silica plug with 10% diethyl ether/hexanes and once again the volatiles were removed *in vacuo*. The crude oil was purified by simple distillation under high vacuum (≈ 0.3 mmg Hg). Ethyl cyclobutanecarboxylate distilled first at 50 °C (about 30 °C thermometer reading), while the desired product distilled from 65 to 110 °C (about 45 °C thermometer reading) to afford a clear, colourless oil (4.24 g, 34% yield). The spectral

data matched the literature:[66] **^{1}H NMR** (400 MHz, $CDCl_3$) δ 4.22 (q, *J* = 7.1 Hz, 2H), 2.95–2.81 (m, 2H), 2.65–2.52 (m, 2H), 2.26–2.10 (m, 1H), 1.90–1.77 (m, 1H), 1.28 (t, *J* = 7.1 Hz, 3H).

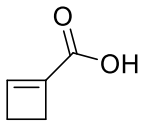

1-cyclobutene-1-carboxylic acid (4-61): The reaction was performed following a literature procedure with slight modification.[67] Crushed potassium hydroxide (5.21 g, 92.4 mmol, 4.5 equiv) was dissolved in toluene (50 mL, 0.41 M) at 110 °C. Upon cooling to room temperature, 1-bromocyclobutane **4-60** (4.25 g, 20.5 mmol, 1.00 equiv) as a solution in toluene (17 mL, 0.3 M total). The reaction was stirred at reflux for 1 hour before being allowed to cool back to room temperature. The crude reaction mixture was diluted with about 60 mL of water and the aqueous phase was washed twice with 40 mL of pentanes. The aqueous layer was acidified to pH ≈ 3.0 with 30% aqueous sulfuric acid. The acidified aqueous phase was subsequently extracted with 40 mL of diethyl ether four times. The combined organic phases were dried with sodium sulfate, filtered and the volatiles were removed *in vacuo*. The crude reaction mixture was purified by column chromatography (5% MeOH/DCM) to afford a white solid (1.71 g, 91% yield). The dried solid was stored at -20 °C and used as soon as possible to avoid decomposition. The spectral data matched the literature:[67] **^{1}H NMR** (500 MHz, $CDCl_3$) δ 9.71 (br s, 1H), 6.93 (t, *J* = 1.3 Hz, 1H), 2.75 (t, *J* = 3.2 Hz, 2H), 2.52–2.49 (m, 2H); **^{13}C NMR** (126 MHz, $CDCl_3$) δ 166.6, 149.7, 138.2, 29.0, 27.3.

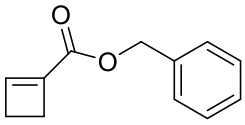

benzyl cyclobut-1-enecarboxylate (4-62): The reaction was performed following a literature procedure with slight modification.[67] Carboxylic acid **4-61** (326 mg, 3.30 mmol, 1.00 equiv) was dissolved in DCM (3.2 mL, 1.0 M) and cooled to 0 °C. Thionyl chloride (0.27 mL, 3.6 mmol, 1.1

equiv) was added dropwise at 0 °C then the reaction was warmed to room temperature and stirred for three hours. The volatiles were *in vacuo*, then the reaction was newly dissolved in DCM (3.2 mL, 1.0 M). The solution was cooled to -20 °C before DIPEA (0.87 mL, 5.0 mmol, 1.5 equiv) and benzyl alcohol (0.48 mL, 4.6 mmol, 1.4 equiv) were added. The reaction was left to warm to room temperature overnight. The crude reaction mixture was diluted with about 10 mL of 1M aqueous HCl and DCM and the aqueous phase was extracted three times. The combined organic phases were washed twice with 10 mL of 5% $NaHCO_3$, water, brine then dried with sodium sulfate, filtered and the volatiles were removed *in vacuo*. The crude reaction mixture was purified by column chromatography (50% DCM/hexanes) to afford a clear, colourless oil (432 mg, 69% yield). The spectral data matched the literature:[53] **^{1}H NMR** (500 MHz, $CDCl_3$) δ 7.45–7.30 (m, 5H), 6.81 (t, *J* = 1.3 Hz, 1H), 5.18 (s, 2H), 2.78–2.72 (m, 2H), 2.52–2.43 (m, 2H).

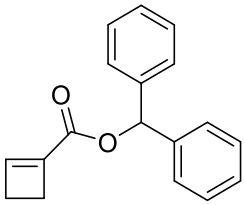

benzyl cyclobut-1-enecarboxylate (4-63): The reaction was performed following the same procedure as described for benzyl ester **4-62** with crude carboxylic acid **4-61** (23 mmol scale, 1.00 equiv) with triethylamine (4.5 mL, 32.2 mmol, 1.4 equiv), diphenylmethanol (5.15 g, 27.6 mmol, 1.2 equiv). The alcohol and base were added in the second step at 0 °C. The crude reaction mixture was purified by column chromatography (25 to 30% DCM/hexanes) to afford a white solid (2.07 g, 34% yield over 2 steps, from **4-60**): **^{1}H NMR** (500 MHz, $CDCl_3$) δ 7.40–7.31 (m, 8H), 7.31–7.26 (m, 2H), 6.94 (s, 1H), 6.89 (t, *J* = 1.2 Hz, 1H), 2.81–2.76 (m, 2H), 2.53–2.47 (m, 2H); **^{13}C NMR** (126 MHz, $CDCl_3$) δ 161.1, 147.3, 140.4, 138.6, 128.5, 127.9, 127.2, 76.3, 29.2, 27.3; **HRMS** (EI) for $C_{18}H_{16}O_2$ calcd. 264.1150; found 264.1151.

4.10.12 Borylated benzhydrol ester

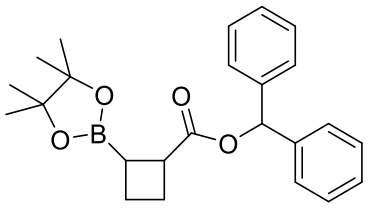

benzhydryl 2-(4,4,5,5-tetramethyl-1,3,2-dioxaborolan-2-yl)cyclobutanecarboxylate (4-64): Xantphos (13 mg, 0.022 mmol, 11 mol%), tetrakis(acetonitrile)copper(I) hexafluorophosphate (8 mg, 0.02 mmol, 10 mol%), and bis(pinacolato)diboron (102 mg, 0.30 mmol, 2.0 equiv) was dissolved in THF (0.70 mL) and the mixture was stirred for 15 min. The reaction was cooled to 0 °C in an ice-water bath. Sodium tert-butoxide (2.0 M, 20 µL, 0.040 mmol, 20 mol%) was added dropwise followed by cyclobutene **4-63** (52 mg, 0.20 mmol, 1.00 equiv) as a solution in 0.40 mL of THF and methanol (16 µL, 0.40 mmol, 2.0 equiv) dropwise. The flask which contained cyclobutene **4-63** was further rinsed with THF and added to the reaction in portions until the final reaction concentration was 0.20 M. The ice bath was subsequently removed and the reaction was stirred for 2 hours at room temperature. The reaction was diluted with 15 mL of diethyl ether and poured into 15 mL of saturated ammonium chloride in a separatory funnel. The layers were separated, and the aqueous was extracted with diethyl ether three times. The combined organic layers were washed brine, dried with sodium sulfate, filtered and concentrated *in vacuo*. The crude reaction mixtire was purified by column chromatography (5% ethyl acetate/hexanes) for characterization purposes (41 mg, 53% yield). Samples obtained with about a dr ≈ 10:1 and 1:10 were used for spectral characterization purposes: **^{1}H NMR** (700 MHz, $CDCl_3$) δ (major diastereomer) 7.39–7.34 (m, 4H), 7.34–7.29 (m, 4H), 7.28–7.23 (m, 2H), 6.85 (s, 1H), 3.30 (dd, *J* = 8.8, 8.8 Hz, 1H), 2.40 (ddd, *J* = 11.4, 9.1, 9.1 Hz, 1H), 2.25–2.16 (m, 2H), 2.04–1.93 (m, 2H), 1.26 (s, 12H); (minor diastereomer 7.37–7.28 (m, 8H), 7.28–7.21 (m, 2H), 6.87 (s, 1H), 3.39 (dd, *J* = 9.3, 9.3 Hz, 1H), 2.39–2.33 (m,

1H), 2.30 (dddd, J = 14.5, 11.2, 7.2, 1.9 Hz, 1H), 2.23–2.17 (m, 1H), 2.11–1.99 (m, 2H), 1.13 (s, 6H), 1.12 (s, 6H); **^{13}C NMR** (176 MHz, $CDCl_3$) δ (major diastereomer): 174.3, 140.7 (2C), 128.5, 128.4, 127.8, 127.7, 127.1, 126.9, 83.4, 76.5, 39.4, 25.1, 24.8, 24.8, 20.1; δ (minor diastereomer): 174.7, 140.8, 140.6, 128.4, 128.4, 127.7 (2C), 127.3, 127.2, 83.3, 76.5, 40.1, 29.8, 25.2, 24.8, 24.7, 20.3; **^{11}B NMR** (160 MHz, $CDCl_3$) δ (major diastereomer): 33.0; (minor diastereomer): 33.3; **HRMS** (ESI) for $C_{24}H_{29}NaO_4B$ calcd. 415.2051; found 415.2055.

The enantioenriched boronate **4-64** was made following the general procedure B using Naud SL-N004-1 (8 mg, 0.017 mmol, 11 mol%), tetrakis(acetonitrile)copper(I) hexafluorophosphate (6 mg, 0.0015 mmol, 10 mol%), and bis(pinacolato)diboron (76 mg, 0.30 mmol, 2.0 equiv), sodium tert-pentoxide (1.4 M in THF, 22 μL, 0.030 mmol, 20 mol%), cyclobutene **4-63** (40 mg, 0.15 mmol, 1.0 equiv) and THF (1.5 mL, 0.10 M) for a 24 hour reaction time. Crude ^{1}H NMR with dibromomethane internal standard (12.3 mg, 0.071, 0.5 equiv) indicated a 39% and 46% ^{1}H NMR yield of the major and minor diastereomer from above respectively (dr ≈ 1.2 : 1.0). Further purification and analysis by chiral HPLC was undertaken by Mr. Kevin Nguyen and Hao Fu.

4.11 References

[1] a) Review of cyclobutane-containing natural products: V. M. Dembitsky, *Phytomedicine* **2014**, *21*, 1559.; b) T. T. Wager, B. A. Pettersen, A. W. Schmidt, D. K. Spracklin, S. Mente, T. W. Butler, H. Howard, Jr, D. J. Lettiere, D. M. Rubitski, D. F. Wong, F. M. Nedza, F. R. Nelson, H. Rollema, J. W. Raggon, J. Aubrecht, J. K. Freeman, J. M. Marcek, J. Cianfrogna, K. W. Cook, L. C. James, L. A. Chatman, P. A. Iredale, M. J. Banker, M. L. Homiski, J. B. Munzner, R. Y. Chandrasekaran, *J. Med. Chem.* **2011**, *54*, 7602.

[2] Rigidification: a) M. L. Wrobleski, G. A. Reichard, S. Paliwal, S. Shah, H.-C. Tsui, R. A. Duffy, J. E. Lachowicz, C. A. Morgan, G. B. Varty, N.-Y. Shiha, *Bioorg. Med. Chem. Lett.* **2006,** *16*, 3859.; b) Bioisostere: A. F. Stepan, C. Subramanyam, I. V. Efremov, J. K. Dutra, T. J. O'Sullivan, K. J. DiRico, W. S. McDonald, A. Won, P. H. Dorff, C. E. Nolan, S. L. Becker, L. R. Pustilnik, D. R. Riddell, G. W. Kauffman, B. L. Kormos, L. Zhang, Y. Lu, S. H. Capetta, M. E. Green, K. Karki, E. Sibley, K. P. Atchison, A. J. Hallgren, C. E. Oborski, A. E. Robshaw, B. Sneed, C. J. O'Donnell, *J. Med. Chem.* **2012**, *55*, 3414.; c) K. C. Nicolaou, D. Vourloumis, S. Totokotsopoulos, A. Papakyriakou, H. Karsunky, H. Fernando, J. Gavrilyuk, D. Webb, A. F. Stepan, *ChemMedChem* **2016**, *11*, 31.

[3] M. Weng, P. Lu, *Org. Chem. Front.* **2018**, *5*, 254.

[4] T. Seiser, T. Saget, D. N. Tran, N. Cramer, *Angew. Chem. Int. Ed.* **2011**, *50*, 7740.

[5] a) S. Poplata, A. Tröster, Y.-Q. Zou, T. Bach, *Chem. Rev.* **2016**, *116*, 9748.; b) Y. Xu, M. L. Conner, M. K. Brown*, Angew. Chem. Int. Ed.* **2015**, *54*, 11918.

[6] D. G. Hall, Chapter 1 in *Boronic Acids*, 2nd Edition: D. G. Hall, **2011**, Wiley: Weinheim, 1–133.

[7] V. Martín-Heras, A. Parra, M. Tortosa, *Synthesis* **2018**, *50*, 470.

[8] H.-W. Man, W. S. Hiscox, D. S. Matteson, *Org. Lett.* **1999**, *1*, 379.

[9] M. Eisold, G. M. Kiefl, D. Didier, *Org. Lett.* **2016**, *18*, 3022.

[10] S. C. Coote, T. Bach, *J. Am. Chem. Soc.* **2013**, *135*, 14948.

[11] M. Guisán-Ceinos, A. Parra, V. Martín-Heras, M. Tortosa, *Angew. Chem. Int. Ed.* **2016**, *128*, 7038; *Angew. Chem.* **2016**, *128*, 7083.

[12] J. He, Q. Shao, Q. Wu, J.-Q. Yu, *J. Am. Chem. Soc.* **2017**, *139*, 3344.

[13] A. Whyte, B. Mirabi, A. Torelli, L. Prieto, J. Bajohr, M. Lautens, *ACS Catal.* **2019**, *9*, 9253.

[14] M. M. Parsutkar, V. V. Pagar, T. V. RajanBabu, *J. Am. Chem. Soc.* **2019**, *141*, https://doi.org/10.1021/jacs.9b07885.

[15] H. Ito, H. Yamanaka, J. Tateiwa, A. Hosomi, *Tetrahedron Lett.* **2000**, *41*, 6821.

[16] X. Feng, J. Yun, *Chem. Commun.* **2009**, 6577.

[17] M. Murakami, Y. Miyamoto, Y. Ito, *J. Am. Chem. Soc.* **2001,** *123,* 6441.

[18] P. Chen, G. Dong, *Chem. Eur. J.* **2016**, *22*, 18290.

[19] For a recent approach to prepare non-chiral tertiary cyclobutylboronates, see: A. Fawcett, T. Biberger, V. K. Aggarwal, *Nat. Chem.* **2019**, *11*, 117.

[20] For recent enantioselective syntheses of non-fused cyclobutanones: a) S. Y. Shim, Y. Choi, D. H. Ryu, *J. Am. Chem. Soc.* **2018**, *140*, 11184.; b) D. K. Kim, J. Riedel, R. S. Kim, V. M. Dong, *J. Am. Chem. Soc.* **2017**, *139*, 10208.

[21] E. J. Barreiro, A. E. Kümmerle, C. A. Fraga, *Chem. Rev.* **2011**, *111*, 5215.

[22] C. Schmidt, S. Sahraoui-Taleb, E. Differding, C. G. Dehass-De Lombaert, L. Ghosez, *Tetrahedron Lett.* **1984**, *25*, 5043.

[23] R. L. Danheiser, S. Savariar, *Tetrahedron Lett.* **1987**, *28*, 3299.

[24] S.-L. Shi, S. L. Buwchwald, *Nat. Chem.* **2015**, *7*, 38.

[25] A. L. Fuentes de Arriba, E. Lenci, M. Sonawane, O. Formery, D. J. Dixon, *Angew. Chem. Int. Ed.* **2017**, *56*, 3655.

[26] Q. Qin, X. Luo, J. Wei, Y. Zhu, X. Wen, S. Song, N. Jiao, *Angew. Chem. Int. Ed.* **2019**, *58*, 4376.

[27] I. H. Chen, L. Yin, W. Itano, M. Kanai, M. Shibasaki, *J. Am. Chem. Soc.* **2009**, *131*, 11664.

[28] S. Radomkit, A. Hoveyda, *Angew. Chem. Int. Ed.* **2014**, *53*, 3387.

[29] One exa**mp**le of racemic β-borylation of tetrasubstituted enoate using Ni catalysis can be found in: K. Hirano, H. Yorimitsu, K. Oshima, *Org. Lett.* **2007**, *9*, 5031.

[30] a) J. R. Calvin, M. O. Frederick, D. L. Laird, J. R. Remacle, S. A. May, *Org. Lett.* **2012**, *14*, 1038.;

b) M. Christensen, A. Nolting, M. Shevlin, M. Weisel, P. E. Maligres, J. Lee, R. K. Orr, C. W. Plummer, M. T. Tudge, L. C. Ca**mp**eau, R. T. Ruck, *J. Org. Chem.* **2016**, *81*, 824.

[31] D. Perera, J. W. Tucker, S. Brahmbhatt, C. J. Helal, A. Chong, W. Farrell, P. Richardson, N. W. Sach, *Science* **2018**, *359*, 429.

[32] A. D. Calow, A. Whiting, *Org. Biomol. Chem.* **2012**, *10*, 5485.

[33] S. Lee, J. Yun, in *Synthesis and Application of Organoboron Co**mp**ounds*, E. Fernández, A. Whiting, Chapter 3, Springer, 2015, 73–92.

[34] a) K. Kubota, K. Hayama, H. Iwamoto, H. Ito, *Angew. Chem. Int. Ed.* **2015**, *54*, 8809.; b) K. Kubota, Y. Watanabe, K. Hayama, H. Ito, *J. Am. Chem. Soc.* **2016**, *138*, 4338.; c) K. Kato, K. Hirano, M. Miura *Chem. Eur. J.* **2018**, *24*, 5775.

[35] J.-B. Chen, A. Whiting, *Synthesis* **2018**, *50*, 3843.

[36] X. Sun, Y. Sun, Y. Rao, *Curr. Org. Chem.* **2016**, *20*, 1878.

[37] C. Sandford, V. K. Aggarwal, *Chem. Commun.* **2017**, *53*, 5481.

[38] a) S. N. Mlynarski, A. S. Karns, J. P. Morken, *J. Am. Chem. Soc.* **2012**, *134*, 16449.; b) E. K. Edelstein, A. C. Grote, M. D. Palkowitz, J. P. Morken, *Synlett* **2018**, *29*, 1749.

[39] a) V. Bagutski, T. G. Elford, V. K. Aggarwal, *Angew. Chem. Int. Ed.* **2011**, *50*, 1080.; b) D. S. Matteson, G. Y. Kim, *Org. Lett.,* **2002**, *4*, 2153.; c) C. G. Watson, A. Balanta, T. G. Elford, S. Essafi, J. N. Harvey, V. K. Aggarwal, *J. Am. Chem. Soc.* **2014**, *136*, 17370.

[40] H.-Y. Sun, D. G. Hall in *Synthesis and Application of Organoboron Co**mp**ounds*, E. Fernández, A. Whiting, Chapter 7, Springer, 2015, 221–242.

[41] J. P. Rygus, C. M. Crudden, *J. Am. Chem. Soc.* **2017**, *139*, 18124.

[42] A. Ros, V. K. Aggarwal, *Angew. Chem. Int. Ed.* **2009**, *48*, 6289.

[43] A. J. Bochat, V. M. Shoba, J. M. Takacs, *Angew. Chem. Int. Ed.* **2019**, *58*, 9434.

[44] R. J. Armstrong, V. K. Aggarwal, *Synthesis* **2017**, *49*, 3323.

[45] Y. Wang, A. Noble, E. L. Myers, V. K. Aggarwal, *Angew. Chem. Int. Ed.* **2016**, *55*, 4270.

[46] a) A. Fawcett, T. Biberger, V. K. Aggarwal, *Nat. Chem.* **2014**, *6*, 584.; b) J. Llaveria, D. Leonori, V. K. Aggarwal, *J. Am. Chem. Soc.* **2015**, *137*, 10958.

[47] a) R. P. Sonawane, V. Jheengut, C. Rabalakos, R. Larouche-Gauthier, H. K. Scott, V. K. Aggarwal, *Angew. Chem. Int. Ed*. **2011**, *50*, 3760.; b) M. Silvi, V. K. Aggarwal, *J. Am. Chem. Soc.* **2019**, *141*, 9511.; c) J. A. Myhill, C. A. Wilhelmsen, L. Zhang, J. P. Morken, *J. Am. Chem. Soc.* **2018**, *140*, 15181.

[48] S. Nave, R. P. Sonawane, T. G. Elford, V. K. Aggarwal, *J. Am. Chem. Soc.* **2010**, *132*, 17096.

[49] H.-S. Sim, X. Feng, J. Yun, *Chem. Eur. J.* **2009**, *15*, 1939.

[50] K. Kubota, K. Hayama, H. Iwamoto, H. Ito, *Angew. Chem. Int. Ed.* **2015**, *54*, 8809.

[51] a) B. Darses, A. E. Greene, J.-F. Poisson, *J. Org. Chem.* **2012**, *77*, 1710.; b) W. R. Gutekunst, P. S. Baran, *J. Org. Chem.* **2014**, *79*, 2430.

[52] G. A. Molander, P. E. Gormisky, *J. Org. Chem.* **2008**, *73*, 7481.

[53] Y.-J. Chen, T.-J. Hu, C.-G. Feng, G.-Q. Lin, *Chem. Commun.,* **2015**, *51*, 8773.

[54] a) Á. L. Fuentes de Arriba, E. Lenci, M. Sonawane, O. Formery, D. J. Dixon, *Angew. Chem. Int. Ed.* **2017**, *56*, 3655; *Angew. Chem.* **2017**, *129*, 3709.; b) V. Tona, A. de la Torre, M. Padmanaban,

S. Ruider, L. González, N. Maulide, *J. Am. Chem. Soc.* **2016**, *138*, 8348.; c) W. Yao, X. Ma, L. Guo, X. Jia, A. Hua, Z. Huang, *Tetrahedron Lett.* **2016**, *57*, 2919.

[55] G. Chen, T. Shigenari, P. Jain, Z. Zhang, Z. Jin, J. He, S. Li, C. Mapelli, M. M. Miller, M. A. Poss, P. M. Scola, K.-S. Yeung, J.-Q. Yu, *J. Am. Chem. Soc.* **2015**, *137*, 3338.

[56] S.-L. Shi, S. L. Buchwald, *Nat. Chem.* **2015**, *7*, 38.

[57] Y. Kawasaki, Y. Ishikawa, K. Igawa, K. Tomooka, *J. Am. Chem. Soc.* **2011**, *133*, 20712.

[58] C. Li, J. Wang, L. M. Barton, S. Yu, M. Tian, D. S. Peters, M. Kumar, A. W. Yu, K. A. Johnson, A. K. Chatterjee, M. Yan, P. S. Baran, *Science*, **2017**, *356*, 1045.

[59] Y. Tan, S. Luo, D. Li, N. Zhang, S. Jia, Y. Liu, W. Qin, C. E. Song, H. Yan, *J. Am. Chem. Soc.* **2017**, *139*, 6431.

[60] P. Šimůnek, M. Svobodová, V. Bertolasi, V. Macháčeka, *Synthesis* **2008**, *11*, 1761.

[61] J. C. Lee, R. McDonald, D. G. Hall, *Nat. Chem.* **2011**, *3*, 894.

[62] M. Sutter, *Tetrahedron Lett.* **1989**, *30*, 5417.

[63] S. Chakrabarty, J. M. Takacs, *J. Am. Chem. Soc.* **2017**, *139*, 6066.

[64] A. M. Fournier, J. Clayden, *Org. Lett.* **2012**, *14*, 142.

[65] N. J. Webb, S. P. Marsden, S. A. Raw, *Org. Lett.* **2014**, *16*, 4718.

[66] M. E. Jung, G. Deng, *J. Org. Chem.* **2012**, *77*, 11002.

[67] A. Song, K. A. Parker, N. S. Sampson, *J. Am. Chem. Soc.* **2009**, *131*, 3444.

Chapter 5: Conclusions and Future Perspectives

Throughout the past decade, organoboron compounds have become increasingly important targets in organic methodology due to their low toxicity, stability and Lewis acidity. In regard to enantioenriched alkyl boronic esters, these favourable properties have led to a flourishing area of catalytic enantioselective methods to access linear hydrocarbon-based boronates. In comparison, approaches to enantioenriched cyclic boronates are relatively limited (Chapter 1) and many opportunities exist to acccess novel variants of these building blocks, with increased functionality. The research described in this thesis has presented innovative approaches to enantioenriched seven and four membered cyclic boronates, as well as provided a detailed discussions regarding mechanistic considerations.

In Chapter 2, the borylative migration reaction was expanded to a new ring system for the first time, specifically the 7-membered azepane ring. Considering that the subsequent allylboration provided a mixture of diastereomers, further investigations in regards to catalytic allylboration reactions are merited. It has been shown that both Lewis acids (LA) and Brønsted acids (BA) can catalyze allylboration reactions to improve diastereoselectivity, which could be applicable to the azepanyl allylic boronate (Scheme 5-1a). Furthermore, considering the low diastereoselectivity, it may be possible to invert the diastereoselectivity in favour of the minor diastereomer observed in thermal allylboration reactions. Alternatively, formation of the corresponding borinic ester *in situ* may improve the diastereoselectivity. Moreover, considering that both the α- and β-selective Suzuki-Miyaura cross-coupling have been reported by our group for the corresponding piperidine system, the azepanyl allylic boronate has the potential to provide efficient reactivity under similar conditions (Scheme 5-1b). Finally, many of the stereoselective applications reported for other C–B bond

functionalizations described in Section 1.3 have the potential to form C–O, C–N, C–C and C–X bonds from the novel azepanyl allylic boronate obtained.

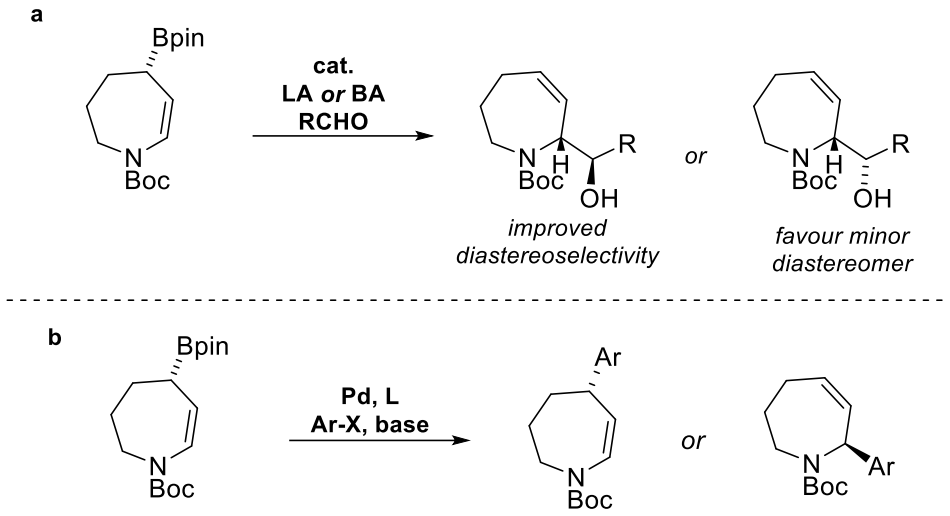

Scheme 5-1. Opportunities for further functionalization of the enantioenriched allylic boronic ester.

In Chapter 3, the combination of experimental and DFT studies provided insight regarding the mechanism of the borylative migration reaction with the pyranyl- and piperidinyl-based scaffolds. The mechanistic studies provide a new perspective of the borylative migration catalytic cycle. Considering that a cationic palladium catalyst is involved, there may be an appropriate additive to improve the enantioselectivity and chemoselectivity of the reaction, leading to more generally applicable conditions. Furthermore, the mechanistic information obtained can provide the opportunity for more logically-designed electrophiles in the future, such as a symmetrical difluoro or dimethyl 6-membered ring system as that shown in Scheme 5-2. Finally, considering the inverse relation observed between pK_{aH} and *ee*, there may be an amine base with a lower pK_{aH} than $PhNMe_2$ that could hold the potential for increased enantioselectivity. In this regard, concluding the mechanistic studies by tying up the loose ends described in Chapter 3 could be very helpful in the quest to develop a more general borylative migration reaction.

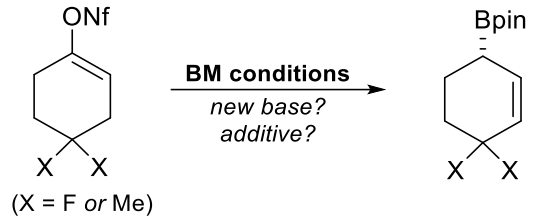

Scheme 5-2. Potential diversification of the borylative migration.

Finally in Chapter 4, a copper-catalyzed conjugate borylation was developed for α,β-disubstituted cyclobutenones. The results described in this initial study suggest that a conjugate borylation approach to cyclobutylboronates has the potential to be relatively general. Specifically, if the issues of hydrolysis could be resolved for the dialkyl cyclobutenones, then the expansion of the conjugate borylation to a variety of new substrates should be possible (Scheme 5-3a). In contrast, the use of functionalized non-aryl substitutents merits further investigation, such as a β-silyl group (Scheme 5-2b). Successful development of the conjugate borylation of β-silyl substrate would introduce a third synthetic handle in the borylated products. Also, it has been shown that electrophiles other than methanol can be used in conjugate borylation reactions. In particular, if an electrophilic carbon source such as an aldehyde or allyl bromide could be applied in the conjugate borylation, further avenues for substrate functionalization can be envisioned(Scheme 5-2c). Finally, successful Suzuki-Miyaura cross-coupling of the conjugate borylation products would allow a mild and general approach to enantioenriched cyclobutane rings containing a quaternary carbon. In particular, the combination of nickel and iridium photocatalysts have shown to be capable of coupling sterically hindered tertiary boronates through a single electron transmetallation process. In theory, the α-stereocenter set by the conjugate borylation could control the diastereoselectivity of the coupling process and retain the enantioenrichment in the arylated product. Reduction of the ketone to avoid ring opening and formation of the trifluoroborate salt may be beneficial for a productive reaction.

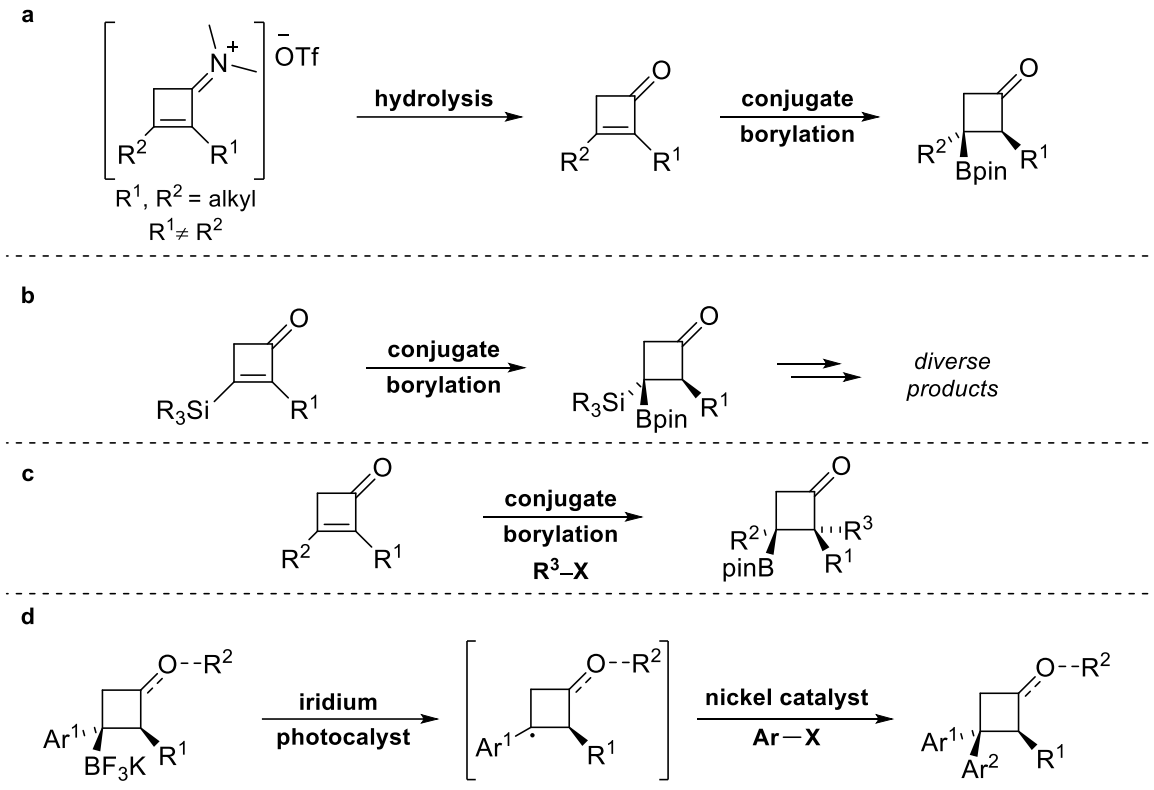

Scheme 5-3. Avenues for expansion of the developped conjugate borylation reaction.

Although the toolbox of enantioenriched borylated scaffolds is continuously growing, approaches for the synthesis of functionalized enantioenriched cyclic boronates are still in the early stages of development. The research in this thesis describes only a small contribution to a field of increasing interest and utility. Futher innovations in the development of the synthesis and application of cyclic chiral boronates will provide more versatile building blocks available for the utility in organic chemistry, with the ultimate goal of accessing novel chemical space for medicinal chemistry purposes.

Bibliography

1. A. Ashimori, B. Bachand, M. A. Calter, S. P. Govek, L. E. Overman, D. J. Poon, *J. Am. Chem. Soc.* **1998,** *120,* 6488.
2. A. D. Calow, A. Whiting, *Org. Biomol. Chem.* **2012**, *10*, 5485.
3. A. F. Stepan, C. Subramanyam, I. V. Efremov, J. K. Dutra, T. J. O'Sullivan, K. J. DiRico, W. S. McDonald, A. Won, P. H. Dorff, C. E. Nolan, S. L. Becker, L. R. Pustilnik, D. R. Riddell, G. W. Kauffman, B. L. Kormos, L. Zhang, Y. Lu, S. H. Capetta, M. E. Green, K. Karki, E. Sibley, K. P. Atchison, A. J. Hallgren, C. E. Oborski, A. E. Robshaw, B. Sneed, C. J. O'Donnell, *J. Med. Chem.* **2012**, *55*, 3414.
4. A. Fawcett, T. Biberger, V. K. Aggarwal, *Nat. Chem.* **2014**, *6*, 584.
5. A. Fernández-Mateos, G. P. Coca, R. R. González, C. T. Hernández, *J. Org. Chem.* **1996**, *61*, 9097.
6. A. Guzman-Martinez, A. H. Hoveyda, *J. Am. Chem. Soc.* **2010**, *132*, 10634.
7. A. J. Bochat, V. M. Shoba, J. M. Takacs, *Angew. Chem. Int. Ed.* **2019**, *58*, 9434.
8. A. Jutand, Serge Négri, *Organometallics* **2003**, *22*, 4229.
9. A. L. Fuentes de Arriba, E. Lenci, M. Sonawane, O. Formery, D. J. Dixon, *Angew. Chem. Int. Ed.* **2017**, *56*, 3655.
10. A. López-Pérez, M. Segler, J. Adrio, J. C. Carretero, *J. Org. Chem.* **2011**, *76*, 1945.
11. A. M. Fournier, J. Clayden, *Org. Lett.* **2012**, *14*, 142.
12. A. McKillop, W. R. Sanderson, *Tetrahedron* **1995**, *51*, 6145.
13. A. Nortcliff, J. C. Moody, *Bioorg. Med. Chem.* **2015**, 2730.
14. A. Ros, V. K. Aggarwal, *Angew. Chem. Int. Ed.* **2009**, *48*, 6289.
15. A. Song, K. A. Parker, N. S. Sampson, *J. Am. Chem. Soc.* **2009**, *131*, 3444.

16. A. V. Marenich, C. J. Cramer, D. G. Truhlar, *J. Phys. Chem. B* **2009**, *113*, 6378.

17. A. Whyte, B. Mirabi, A. Torelli, L. Prieto, J. Bajohr, M. Lautens, *ACS Catal.* **2019**, *9*, 9253.

18. A. Whyte, K. I. Burton, J. Zhang, M. Lautens, *Angew. Chem. Int. Ed.* **2018**, *57*, 13927.

19. B. Chen, P. Cao, Y. Liao, M. Wang, J. Liao, *Org. Lett.* **2018**, *20*, 1346.

20. B. Darses, A. E. Greene, J.-F. Poisson, *J. Org. Chem.* **2012**, *77*, 1710.

21. B. Drouillat, I. V. Dorogan, M. Kletskii, O. N. Burov, F. Couty, *J. Org. Chem.* **2016**, *81*, 6677.

22. J. Zhou, Y.-Y. Yeung, *Org. Lett.* **2014**, *16*, 2134.

23. B. H. Lipshultz, D. J. Buzard, R. W. Vivian, *Tetrahedron Lett.* **1999**, *40*, 6871.

24. H. Kotsuki, P. K. Datta, H. Hayakawa, H. Suenaga, *Synthesis* **1995**, *11*, 1348.

25. B. J. Huffman, R. A. Shenvi, *J. Am. Chem. Soc.* **2019**, *141*, 3332.

26. B. J. Stokes, A. J. Bischoff, M. S. Sigman, *Chem. Sci.* **2014**, *4*, 2336.

27. B. Potter, A. A. Szymaniak, E. K. Edelstein, J. P. Morken, *J. Am. Chem. Soc.* **2014**, *136*, 17918.

28. B. S. Collins, C. M. Wilson, E. L. Myers, *Angew. Chem. Int. Ed.* **2017**, *56*, 11700.

29. B. Subramanian, M. Jack, N. M. Leon, R. Roopa, S. Irina, T. Vincent, *Genelabs Tech Inc.* **2010**, *US2010204265 (A1).*

30. C. D.-T. Nielsen, J. Burés, *Chem. Sci.*, **2019**, *10*, 348.

31. C. Diner, K. J. Szabó, *J. Am. Chem. Soc.* **2016**, *139*, 2.

32. C. E. Check, T. O. Faust, J.M. Bailey, B. J. Wright, T. M. Gilbert, L. S. Sunderlin, *J. Phys. Chem. A* **2001**, *105*, 8111.

33. C. G. Watson, A. Balanta, T. G. Elford, S. Essafi, J. N. Harvey, V. K. Aggarwal, *J. Am. Chem. Soc.* **2014**, *136*, 17370.

34. C. Li, J. Wang, L. M. Barton, S. Yu, M. Tian, D. S. Peters, M. Kumar, A. W. Yu, K. A. Johnson, A. K. Chatterjee, M. Yan, P. S. Baran, *Science*, **2017**, *356*, 1045.

35. C. M. Crudden, D. Edwards, *Eur. J. Org. Chem.* **2003**, 4695.

36. C. Pubill-Ulldemolins, A. Bonet, C. Bo, H. Gulyás, Elena Fernáandez, *Org. Biom. Chem.* **2010**, *8*, 2667.

37. C. Sandford, V. K. Aggarwal, *Chem. Commun.* **2017**, *53*, 5481.

38. C. Schmidt, S. Sahraoui-Taleb, E. Differding, C. G. Dehass-De Lombaert, L. Ghosez, *Tetrahedron Lett.* **1984**, *25*, 5043.

39. https://labs.chem.ucsb.edu/zakarian/armen/11---bond dissociationenergy.pdf, accessed August 5th, 2019.

40. Conhydrine review: C. Bhat, S. T. Bugde, S. G. Tilve, *Synthesis* **2014**, *46*, 2551.

41. *CRC Handbook of Tables for Organic Compound Identification*, Third Edition, CRC Press, Boca Raton, Florida, 1984, 438.

42. C-Y., Wang, J. Derosa, M. R. Biscoe, *Chem. Sci.* **2015**, *6*, 5105.

43. D. A. Petrone, I. Franzoni, J. Ye, J. F. Rodríguez, A. I. Poblador-Bahamonde, M. Lautens, *J. Am. Chem. Soc.* **2017**, *139*, 3546.

44. D. G. Blackmond, *J. Am. Chem. Soc.* **2015**, *137*, 10852.

45. D. G. Brown, J. Boström, *J. Med. Chem.* **2016**, *59*, 4443.

46. D. G. Hall, Chapter 1 in *Boronic Acids*, 2nd Edition: D. G. Hall, **2011**, Wiley: Weinheim, 1–133.

47. D. G. Hall, T. Rybak, T. Verdelet, *Acc. Chem. Res.* **2016**, *49*, 2489.

48. D. G. Wishka, M. Bédard, K. E. Brighty, R. A. Buzon, R. K. A. Farley, M. W. Fichtner, G. S. Kauffman, J. Kooistra, J. G. Lewis, H. O'Dowd, I. J. Samardjiev, B. Samas, G. Yalamanchi, M. C. Noe, *J. Org. Chem.* **2011**, *76*, 1937.;

49. D. H. R. Barton, R. E. O'Brien, S. Sternhell, *J. Chem. Soc.* **1962**, 470.

50. D. K. Kim, J. Riedel, R. S. Kim, V. M. Dong, *J. Am. Chem. Soc.* **2017**, *139*, 10208.

51. D. Kong, S. Han, G. Zi, G. Hou, J. Zhang, *J. Org. Chem.* **2018**, *83*, 1924.

52. D. Männig, H. Nöth, *Angew. Chem. Int. Ed.* **1985**, *10*, 878.

53. D. Mc Cartney, P. J. Guiry, *Chem. Soc. Rev.*, **2011**, ***40***, 5122.

54. D. Nishikawa, K. Hirano, M. Miura, *J. Am. Chem. Soc.* **2015**, *137*, 15620.

55. D. P. Ojha, K. R. Prabhu, *Org. Lett.* **2015**, *17*, 18.;

56. D. Perera, J. W. Tucker, S. Brahmbhatt, C. J. Helal, A. Chong, W. Farrell, P. Richardson, N. W. Sach, *Science* **2018**, *359*, 429.

57. D. S. Matteson, G. Y. Kim, *Org. Lett.,* **2002**, *4*, 2153.

58. D.-W. Gao, Y. Xiao, M. Liu, Z. Liu, M. K. Karunananda, J. S. Chen, K. M. Engle, *ACS Catal.* **2018**, *8*, 3650.

59. E. Cini, G. Bifulco, G. Menchi, M. Rodriquez, M. Taddei, *Eur. J. Org. Chem.* **2012**, 2133.

60. E. J. Barreiro, A. E. Kümmerle, C. A. Fraga, *Chem. Rev.* **2011**, *111*, 5215.

61. E. K. Edelstein, A. C. Grote, M. D. Palkowitz, J. P. Morken, *Synlett* **2018**, *29*, 1749.

62. E. Vitaku, D. T. Smith, J. T. Njardarson, *J. Med. Chem.* **2014**, *57*, 10257.

63. E. W. Ng, K-H. Low, P. Chiu, *J. Am. Chem. Soc.* **2018**, *140*, 3537.

64. E. Yamamoto, Y. Takenouchi, T. Ozaki, T. Miya, H. Ito, *J. Am. Chem. Soc.* **2014**, *136*, 16515.

65. F. Lovering, J. Bikker, C. Humblet, *J. Med. Chem.* **2009**, *52*, 6752.

66. F. Lovering, *Med. Chem. Commun.* **2013**, *4*, 515..

67. F. Ozawa, A. Kubo, T. Hayashi, *Tetrahedron Lett.* **1992**, *33*, 1485.

68. F. Ozawa, A. Kubo, Y. Matsumoto, T. Hayashi, *Organometallics* **1993**, *12*, 4188.

69. G. A. Molander, P. E. Gormisky, *J. Org. Chem.* **2008**, *73*, 7481.

70. G. Barker, P. O'Brien, K. R. Campos, *Org. Lett.* **2010**, *12*, 4176.

71. G. Chen, T. Shigenari, P. Jain, Z. Zhang, Z. Jin, J. He, S. Li, C. Mapelli, M. M. Miller, M. A. Poss, P. M. Scola, K.-S. Yeung, J.-Q. Yu, *J. Am. Chem. Soc.* **2015**, *137*, 3338.

72. G. Dutheuil, N. Selander, K. J. Szabó, V. K. Aggarwal, *Synthesis* **2008**, *14*, 2293.

73. G. J. Lovinger, M. D. Aparece, J. P. Morken, *J. Am. Chem. Soc.* **2017**, *139*, 3153.

74. G. L. Hoang, J. M. Takacs, *Chem. Sci.* **2017**, *8*, 4511.

75. G. L. Hoang, Z-D. Yang, S. M. Smith, R. Pal, J. L. Miska, D. E. Pérez, L. S. Pelter, X. C. Zeng, J. M. Takacs, *Org. Lett.* **2015**, *17*, 940.

76. G. M. Gallego, R. Sarpong, *Chem. Sci.* **2012**, *3*, 1338.

77. G. Ohanessian, Y. Six, J. Y. Lallemand, *Bull. Soc. Chim. Fr.* **1996**, *133*, 1143.

78. G. Zheng, A. M. Smith, X. Huang, K. L. Subramanian, K. B. Siripurapu, A. Deaciuc, C.-G. Zhan, L. P. Dwoskin, *J. Med. Chem.* **2013**, *56*, 1693.

79. G.-F. Zha, K. P. Rakesh, H. M. Manukumar, C. S. Shantharam, S. Long, *Eur. J. Med. Chem.* **2019**, *162*, 465.

80. Gaussian 16, Revision A.03, M. J. Frisch, G. W. Trucks, H. B. Schlegel, G. E. Scuseria, M. A. Robb, J. R. Cheeseman, G. Scalmani, V. Barone, B. Mennucci, G. A. Petersson, H. Nakatsuji, M. Caricato, X. Li, H. P. Hratchian, A. F. Izmaylov, J. Bloino, G. Zheng, J. L. Sonnenberg, M. Hada, M. Ehara, K. Toyota, R. Fukuda, J. Hasegawa, M. Ishida, T. Nakajima, Y. Honda, O. Kitao, H. Nakai, T. Vreven, J. A. Montgomery, Jr., J. E. Peralta, F. Ogliaro, M. Bearpark, J. J. Heyd, E. Brothers, K. N. Kudin, V. N. Staroverov, R. Kobayashi,

J. Normand, K. Raghavachari, A. Rendell, J. C. Burant, S. S. Iyengar, J. Tomasi, M. Cossi, N. Rega, J. M. Millam, M. Klene, J. E. Knox, J. B. Cross, V. Bakken, C. Adamo, J. Jaramillo, R. Gomperts, R. E. Stratmann, O. Yazyev, A. J. Austin, R. Cammi, C. Pomelli, J. W. Ochterski, R. L. Martin, K. Morokuma, V. G. Zakrzewski, G. A. Voth, P. Salvador, J. J. Dannenberg, S. Dapprich, A. D. Daniels, Ö. Farkas, J. B. Foresman, J. V. Ortiz, J. Cioslowski, D. J. Fox, Gaussian, Inc., Wallingford CT, 2016.

81. H. C. Brown, K. S. Bhat, P. K. Jadhav, *J. Chem. Soc. Perkin Trans. 1* **1991**, 2633.
82. H. H. Patel, M. S. Sigman, *J. Am. Chem. Soc.* **2015**, *137*, 3462.
83. H. Ito, H. Yamanaka, J. Tateiwa, A. Hosomi, *Tetrahedron Lett.* **2000**, *41*, 6821.
84. H. Ito, *Pure Appl. Chem.* **2018**, *90*, 703.
85. H. Ito, S. Ito, Y. Sasaki, K. Matsuura, M. J. Sawamura, *J. Am. Chem. Soc.* **2007**, *129*, 14856.
86. H. Ito, S. Kunii, M. Sawamura, *Nat. Chem.* **2010**, *2*, 972.
87. H. Ito, T. Miya, M. Sawamura, *Tetrahedron Lett.* **2012**, *68*, 3423.
88. H. Ito, T. Okura, K. Matsuura, M. Sawamura, *Angew. Chem. Int. Ed.* **2010**, *49*, 560.
89. H. L. Sang, S. Yu, S. Ge, *Org. Chem. Front.* **2018**, *5*, 1284.
90. H. Lachance, D. G. Hall, *Org. React*. **2008**, ***73***, 1–574.;
91. H. Lee, J. Yun, *Org. Lett.* **2018**, *20*, 7961.
92. H. Li, Y. Blériot, C. Chantereau, J.-M. Mallet, M. Sollogoub, Y. Zhang, E. Rodríguez-García, P. Vogel, J. Jiménez-Barbero, P. Sinaÿ, *Org. Biomol. Chem.* **2004**, *2*, 1492.
93. H. Liu, C. Sun, N.-K. Lee, R. F. Henry, D. L. Lee, *Chem. Eur. J.* **2012**, *18*, 11889.
94. H. Sommer, F. Juliá-Hernández, R. Martin, I. Marek, *ACS Cent. Sci.* **2018**, *4*, 153.
95. H. Wang, H. Matsuhashi, B. D. Doan, S. N. Goodman, X. Ouyang, W. M. Clark, *Tetrahedron* **2009**, *65*, 6921.

96. H. Xie, H. Zhang, Z. Lin, *Organometallics* **2013**, *32*, 2336.

97. H.-S. Sim, X. Feng, J. Yun, *Chem. Eur. J.* **2009**, *15*, 1939.

98. H.-W. Man, W. S. Hiscox, D. S. Matteson, *Org. Lett.* **1999**, *1*, 379.

99. H.-Y. Sun, D. G. Hall in *Synthesis and Application of Organoboron Compounds*, E. Fernández, A. Whiting, Chapter 7, Springer, 2015, 221–242.

100. http://evans.rc.fas.harvard.edu/pdf/evans_pKa_table.pdf, accessed 07/10/2-19.

101. H-Y. Sun, D. G. Hall in *Synthesis and Application of Organoboron Compounds*, E. Fernández, A. Whiting, Chapter 7, Springer, 2015, 221–242.

102. H-Y. Sun, K. Kubota, D. G. Hall, *Chem. Eur. J.* **2015**, *21*, 19186.

103. I. D. Hills, G. Fu, *J. Am. Chem. Soc.* **2004**, *126*, 13178.

104. I. Dragutan, V. Dragutan, C. Mitan, H. C. Vosloo, L. Delaude, A. Demonceau, *Belstein J. Org. Chem.* **2011**, *7*, 699.

105. I. G. Smilović, E. Casas-Arcé, S. J. Roseblade, U. Nettekoven, A. Zanotti-Gerosa, M. Kovačevič, Z. Časar, *Angew. Chem. Int. Ed.* **2012**, *51*, 1014.

106. I. H. Chen, L. Yin, W. Itano, M. Kanai, M. Shibasaki, *J. Am. Chem. Soc.* **2009**, *131*, 11664.

107. I. P. Beletskaya, A. V. Cheprakov, *Chem. Rev.* **2000**, *100,* 3009.

108. I.-H. Chen, L. Yin, W. Itano, M. Kanai, M. Shibasaki, *J. Am. Chem. Soc.* **2009**, *131*, 11664.

109. J. A. Schiffner, K. Müther, M. Oestreich, *Angew. Chem. Int. Ed.* **2010**, *49*, 1194.

110. J. B. Morgan, S. P. Miller, J. P. Morken, *J. Am. Chem. Soc.* **2003**, *125*, 8702.

111. J. Burés, *Angew. Chem. Int. Ed.* **2016**, *55*, 16084.

112. J. Burés, *Angew. Chem. Int. Ed.* **2016**, *55*, 2028.

113. J. C. Green, M. V. Joannou, S. A. Murray, J. M. Zanghi, S. J. Meek, *ACS Catal.* **2017**, *7*, 4441.

114. J. C. Lee, D. G. Hall, *J. Am. Chem. Soc.* **2010**, *132*, 5544.

115. J. C. Lee, R. McDonald, D. G. Hall, *Nat. Chem.* **2011**, *3*, 894.

116. J. Ding, D. G. Hall, *Angew. Chem. Int. Ed.* **2013**, *52*, 8069.

117. J. Ding, T. Rybak, D. G. Hall, *Nat. Commun.* **2014**, *5*, 5474.

118. J. F. Hartwig *Organotransition Metal Chemistry - From Bonding to Catalysis*, 2nd edition; University Science Books: Mill Valley, California, 2010; pp 877–951.

119. J. F. Rodríguez, K. I. Burton, I. Franzoni, D. A. Petrone, I. Scheipers, M. Lautens, *Org. Lett.* **2018**, *20*, 6915.

120. J. He, Q. Shao, Q. Wu, J.-Q. Yu, *J. Am. Chem. Soc.* **2017**, *139*, 3344.

121. J. Högermeier, H.-U. Ressig, *Adv. Synth. Catal.* **2009**, *351*, 2747.

122. J. K. Park, H. H. Lackey, B. A. Ondrusek, D. T. McQuade, *J. Am. Chem. Soc.* **2011**, *133*, 2410.

123. J. L. Hofstra, K. E. Poremba, A. M. Shimozono, S. E. Reisman, **2019**, *58*, *https://doi.org/10.1002/anie.201906815.*

124. J. L.-Y. Chen, V. K. Aggarwal, *Angew. Chem. Int. Ed.* **2014**, *53*, 10992.

125. J. Llaveria, D. Leonori, V. K. Aggarwal, *J. Am. Chem. Soc.* **2015**, *137*, 10958.

126. J. M. Bentley, D. C. Brookings, J. A. Brown, T. P. Cain, P. T. Chovatia, A. M. Foley, E. O. Gallimore, L. J. Gleave, A. Heifetz, H. T. Horsley, M. C. Hutchings *et al.*, *UCB Pharma SA* **2014**, WO204009295 (A1).

127. J. M. Dennis, N. A. White, R. Y. Liu, S. L. Buchwald, *ACS Catal.* **2019**, *9*, 3822,

128. J. M. Dennis, N. A. White, R. Y. Liu, S. L. Buchwald, *J. Am. Chem. Soc.* **2018**, *140*, 4721.

129. J. P. G. Rygus, C. M. Crudden, *J. Am. Chem. Soc.* **2017**, *139*, 18124.

130. J. R. Calvin, M. O. Frederick, D. L. Laird, J. R. Remacle, S. A. May, *Org. Lett.* **2012**, *14*, 1038.

131. J. R. Coombs, L. Zhang, J. P. Morken, *J. Am. Chem. Soc.* **2014**, *136*, 16140.

132. J. S. Mathew, M. Klussmann, H. Iwamura, F. Valera, A. Futran, E. A. Emanuelsson, D. G. Blackmond, *J. Org. Chem.* **2006**, *71*, 4711.

133. J. Son, T. W. Reidl, K. H. Kim, D. J. Wink, L. L. Anderson, *Angew. Chem. Int. Ed.* **2018**, *57*, 6597.

134. J. W. Hehre, R. Ditchfield, J. A. Pople, *J. Chem. Phys.* **1972**, *56*, 2257.

135. J. W. Lehmann, I. T. Crouch, D. J. Blair, M. Trobe, P. Wang, J. Li, M. D. Burke, *Nat. Commun.* **2019**, *10*, 1263.

136. J. Y. Renard, J. Y. Lallemand, *Bull. Soc. Chim. Fr.* **1996**, *133*, 143.

137. J.-B. Chen, A. Whiting, *Synthesis* **2018**, *50*, 3843.

138. K. C. Lam, T. B. Marder, Z. Lin, *Organometallics* **2010**, *29*, 1849.

139. K. C. Nicolaou, D. Vourloumis, S. Totokotsopoulos, A. Papakyriakou, H. Karsunky, H. Fernando, J. Gavrilyuk, D. Webb, A. F. Stepan, *ChemMedChem* **2016**, *11*, 31.

140. K. Farshadfar, A. Chipman, M. Hosseini, B. F. Yates, A. Ariafard, *Organometallics* **2019**, *38*, 2953.

141. K. Hirano, H. Yorimitsu, K. Oshima, *Org. Lett.* **2007**, *9*, 5031.

142. K. Hong, J. P. Morken, *J. Org. Chem.* **2011**, *76*, 9102.

143. K. K. Hii, T. D. W. Claridge, J. M. Brown, *Angew. Chem. Int. Ed. Engl.* **1997**, *9*, 984.

144. K. Kato, K. Hirano, M. Miura *Chem. Eur. J.* **2018**, *24*, 5775.

145. K. Kato, K. Hirano, M. Miura, *Angew. Chem. Int. Ed.* **2016**, *55*, 14400.

146. K. Kubota, K. Hayama, H. Iwamoto, H. Ito, *Angew. Chem. Int. Ed.* **2015**, *54*, 8809.

147. K. Kubota, S. Osaki, M. Jin, H. Ito, *Angew. Chem. Int. Ed.* **2017**, *56*, 6646.

148. K. Kubota, Y. Watanabe, H. Ito, *Adv. Synth. Catal.* **2016**, *358*, 2379.

149. K. Kubota, Y. Watanabe, K. Hayama, H. Ito, *J. Am. Chem. Soc.* **2016**, *138*, 4338.

150. K. Lee, D. F. Wiemer, *Tetrahedron Lett.* **1993**, *34*, 2433.

151. K. Li, J. Ou, S. Gao, *Angew. Chem. Int. Ed.* **2016**, *55*, 14778.

152. K. M. Kuhn, T. M. Champagne, S. H. Hong, W.-H. Wei, A. Nickel, C. W. Lee, S. C. Virgil, R. H. Grubbs, R. L. Pederson, *Org. Lett.* **2010**, *12*, 984.

153. K. Nilsson, A. Hallberg, *J. Org. Chem.* **1990**, *55*, 2464.

154. K. Semba, T. Fujihara, J. Terao, Y. Tsuji, *Tetrahedron* **2015**, *71,* 2183.

155. K. Toribatake, H. Nishiyama, *Angew. Chem. Int. Ed.* **2013**, *52*, 11011.

156. L. Jiang, P. Cao, M. Wang, B. Chen, B. Wang, J. Liao, *Angew. Chem. Int. Ed.* **2016**, *55*, 13854.

157. L. M. Alcazar-Roman, J. F. Hartwig, *Organometallics* **2002**, *21*, 491.

158. L. Yan, J. P. Morken, *Org. Lett.* **2019**, *21*, 3760.

159. L. Yan, Y. Meng, F. Haeffner, R. M. Leon, M. P. Crockett, J. P. Morken, *J. Am. Chem. Soc.* **2018**, *140*, 3663.

160. L. Zhang, Z. Zuo, X. Wan, Z., *J. Am. Chem. Soc.* **2014**, *136*, 15501.

161. L-A. Chen, A. R. Lear, P. Gao, M. K. Brown, *Angew. Chem. Int. Ed.* **2019**, *58*, 10956.

162. M. Christensen, A. Nolting, M. Shevlin, M. Weisel, P. E. Maligres, J. Lee, R. K. Orr, C. W. Plummer, M. T. Tudge, L. C. Ca**mp**eau, R. T. Ruck, *J. Org. Chem.* **2016**, *81*, 824.

163. M. Dolg, U. Wedig, H. Stoll, H. Preuß, *J. Chem. Phys.* **1987**, *86*, 866.

164. M. E. Jung, G. Deng, *J. Org. Chem.* **2012**, *77*, 11002.

165. M. Eisold, G. M. Kiefl, D. Didier, *Org. Lett.* **2016**, *18*, 3022.

166. M. Guisán-Ceinos, A. Parra, V. Martín-Heras, M. Tortosa, *Angew. Chem. Int. Ed.* **2016**, *128*, 7038; *Angew. Chem.* **2016**, *128*, 7083.

167. M. L. Wrobleski, G. A. Reichard, S. Paliwal, S. Shah, H.-C. Tsui, R. A. Duffy, J. E. Lachowicz, C. A. Morgan, G. B. Varty, N.-Y. Shiha, *Bioorg. Med. Chem. Lett.* **2006,** *16*, 3859.

168. M. M. Parsutkar, V. V. Pagar, T. V. RajanBabu, *J. Am. Chem. Soc.* **2019**, *141*, 15367.

169. M. Murakami, Y. Miyamoto, Y. Ito, *J. Am. Chem. Soc.* **2001,** *123,* 6441.

170. M. Murata, S. Watanabe, Y. Masuda, *J. Org. Chem.* **1997**, *62*, 6458.

171. M. Murata, S. Watanabe, Y. Masuda, *J. Org. Chem.* **2000**, *65*, 164.

172. M. Murata, T. Oda, Y. Sogabe, H. Tone, T. Namikoshi, S. Watanabe, *Chem. Lett.* **2011**, *40*, 962.

173. M. Murata, T. Oyama, S. Watanabe, Y. Masuda, *Synthesis* **2000**, *6*, 778.

174. M. Royzen, G. P. Yap, J. M. Fox, *J. Am. Chem. Soc.* **2008**, *130*, 3760.

175. M. Satoh, Y. Nomoto, N. Miyaura, S. Suzuki, *Tetrahedron Lett.* **1989**, *30*, 3789.

176. M. Silvi, V. K. Aggarwal, *J. Am. Chem. Soc.* **2019**, *141*, 9511.

177. J. A. Myhill, C. A. Wilhelmsen, L. Zhang, J. P. Morken, *J. Am. Chem. Soc.* **2018**, *140*, 15181.

178. M. Sutter, *Tetrahedron Lett.* **1989**, *30*, 5417.

179. M. Weng, P. Lu, *Org. Chem. Front.* **2018**, *5*, 254.

180. M. Yamashita, K. Nozaki in *Synthesis and Application of Organoboron Compounds*, E. Fernández, A. Whiting, Chapter 1, Springer, 2015, 2–34.

181. N. A. Meanwell, *Chem. Res. Toxicol* **2016**, *29*, 564.

182. N. Bailey, P. L. Pickering, D. M. Wilson, *Glaxo Group LTD.* **2006**, WO2006097691 (A1).

183. N. Hu, G. Zhao, Y. Zhang, X. Liu, G. Li, W. Tang, *J. Am. Chem. Soc.* **2015**, *137*, 6746.

184. N. J. Webb, S. P. Marsden, S. A. Raw, *Org. Lett.* **2014**, *16*, 4718.

185. N. Kim, J. T. Han, D. H. Ryu, J. Yun, *Org. Lett.* **2017**, *19*, 6144.

186. N. Matsuda, K. Hirano, T. Satoh, M. Miura, *J. Am. Chem. Soc.* **2013**, *135*, 4934.

187. N. Selander, B. Willy, K. J. Szabó, *Angew. Chem. Int. Ed.* **2010**, *49*, 4051.

188. N. Vicker, J. M. Day, H. V. Bailey, H. Wesley, A. M. R. Gonzalez, C. M. Sharland, J. M. Reed, A. Purohit, B V. Potter, *Sterix LTD* **2007**, WO2007003934 (A2).

189. P. C. Hariharan, J. A. Pople, *Theor. Chim. Acta.* **1973**, *28*, 213.

190. P. Chen, G. Dong, *Chem. Eur. J.* **2016**, *22*, 18290.

191. P. Hommes, C. Fischer, C. Lindner, H. Zipse, H.-U. Reissig, *Angew. Chem. Int. Ed.* **2014**, *53*, 7647.

192. P. J. Hay, W. R. Wadt, *J. Chem. Phys.* **1985**, *82*, 284.

193. P. Kisanga, L. A. Goj, R. A. Widenhoefer, *J. Org. Chem.* **2001,** *66,* 635.

194. P. Krogsgaard-Larsen, H. Hjeds, *Acta Chem. Scand.* **1976**, *30b*, 884.

195. P. Mamone, M. F. Grünberg, A. Fromm, B. A. Khan, L. J. Gooßen, *Org. Lett.* **2012**, *14*, 3716.

196. P. Šimůnek, M. Svobodová, V. Bertolasi, V. Macháčeka, *Synthesis* **2008**, *11*, 1761.

197. P. Singh, S. K. Manna, G. Panda, *Tetrahedron*, **2014**, *70*, 1363.

198. P. V. Ramachandran, P. D. Gagare, D. R. Nicponski, in *Comprehensive Organic Synthesis II*, 2nd Edition, P. Knochel, Allylborons, Elsevier, 2014, 1–71.

199. P. Wessig, K. Möllnitz, *J. Org. Chem.* **2008**, *73*, 4452.

200. P. Y. Renard, P. Y. Lallemand, *Tetrahedron: Asymmetry* **1996**, *7*, 2523.

201. P. Zheng, X. Han, J. Hu, X. Zhao, T. XU, *Org. Lett.* **2019**, *21*, 6040.

202. Q. I. Churches, C. A. Hutton in *Boron Reagents in Synthesis*, Adiel Coca, Chapter 11, Oxford University Press, 2011, 357–377.

203. Q. Qin, X. Luo, J. Wei, Y. Zhu, X. Wen, S. Song, N. Jiao, *Angew. Chem. Int. Ed.* **2019**, *58*, 4376.

204. R. D. Baxter, D. Sale, K. M. Engle, J.-Q. Yu, D. G. Blackmond, *J. Am. Chem. Soc.* **2012**, *134*, 4600.

205. R. D. Taylor, M. MacCoss, A. D. Lawson, *J. Med. Chem.*, **2014**, *57*, 5854.

206. R. J. DeLuca, B. J. Stokes, M. S. Sigman*, Pure Appl. Chem.* **2014**, *86*, 395.

207. R. Kojima, S. Akiyama, H. Ito, *Angew. Chem. Int. Ed.* **2018**, *57*, 7196.

208. R. L. Danheiser, S. Savariar, *Tetrahedron Lett.* **1987**, *28*, 3299.

209. R. M. Al-Zoubi, D. G. Hall, *Mol. Divers.* **2014**, *18*, 701.

210. R. P. Sonawane, V. Jheengut, C. Rabalakos, R. Larouche-Gauthier, H. K. Scott, V. K. Aggarwal, *Angew. Chem. Int. Ed*. **2011**, *50*, 3760.

211. R. Sakae, K. Hirano, T. Satoh, M. Miura, *Angew. Chem. Int. Ed.* **2015**, *54*, 613.

212. V. M. Dembitsky, *Phytomedicine* **2014**, *21*, 1559.

213. T. T. Wager, B. A. Pettersen, A. W. Schmidt, D. K. Spracklin, S. Mente, T. W. Butler, H. Howard, Jr, D. J. Lettiere, D. M. Rubitski, D. F. Wong, F. M. Nedza, F. R. Nelson, H. Rollema, J. W. Raggon, J. Aubrecht, J. K. Freeman, J. M. Marcek, J. Cianfrogna, K. W. Cook, L. C. James, L. A. Chatman, P. A. Iredale, M. J. Banker, M. L. Homiski, J. B. Munzner, R. Y. Chandrasekaran, *J. Med. Chem.* **2011**, *54*, 7602.

214. S. Akiyama, K. Kubota, M. S. Mikus, P. H. Paioti, F. Romiti, Q. Liu, Y. Zhou, A. H. Hoveyda, H. Ito, *Angew. Chem. Int. Ed.* **2019**, *58*, 11998.

215. S. C. Coote, T. Bach, *J. Am. Chem. Soc.* **2013**, *135*, 14948.

216. S. C. Jonnalagadda, P. Suman, A. Patel, G. Jampana, A. Colfer, in *Boron Reagents in Synthesis*, **2016**, 1st Edition, A. Coca, Chapter 3, Oxford University Press: Washington DC, 67.

217. S. C. Söderman, A. L. Schwan, *J. Org. Chem.* **2012**, *77*, 10978.

218. S. Chakrabarty, H. Palencia, M. D. Morton, R. O. Carr, J. M. Takacs, *Chem. Sci.*, **2019**, *10*, 4854.

219. S. Chakrabarty, J. M. Takacs, *ACS Catal.* **2018**, *8*, 10530.

220. S. Chakrabarty, J. M. Takacs, *J. Am. Chem. Soc.* **2017**, *139*, 6066.

221. S. E. Denmark, H. M. Chi, *J. Am. Chem. Soc.* **2014**, *136*, 8915.

222. S. Grimme, J. Antony, S. Ehrlich, H. Krieg, *J. Chem. Phys.* **2010**, *132*, 154104.

223. S. Kwok, M.Sc. Dissertation, University of Alberta, **2016**.

224. S. L. Schreiber, *Science* **2000**, *287*, 1964.

225. S. Lee, J. Yun, in *Synthesis and Application of Organoboron Compounds*, E. Fernández, A. Whiting, Chapter 3, Springer, 2015, 73–92.

226. S. Lessard, F. Peng, D. G. Hall, *J. Am. Chem. Soc.* **2009**, *131*, 9612.

227. S. Lessard, M.Sc. Dissertation, University of Alberta, **2009**.

228. S. M. Thullen, D. M. Rubush, T. Rovis, *Synlett* **2017**, *28*, 2755.

229. S. N. Mlynarski, A. S. Karns, J. P. Morken, *J. Am. Chem. Soc.* **2012**, *134*, 16449.

230. S. Namirembe, J. P. Morken, *Chem. Soc. Rev.* **2019**, *48*, 3464.

231. S. Nave, R. P. Sonawane, T. G. Elford, V. K. Aggarwal, *J. Am. Chem. Soc.* **2010**, *132*, 17096.

232. S. P. Roy, S. K. Chattopadhyay, *Tetrahedron Lett.* **2008**, *49*, 5498.;

233. S. Poplata, A. Tröster, Y.-Q. Zou, T. Bach, *Chem. Rev.* **2016**, *116*, 9748.

234. S. R. Sardini, M. K. Brown, *J. Am. Chem. Soc.* **2017**, *139*, 9823.

235. S. Radomkit, A. H. Hoveyda, *Angew. Chem. Int. Ed.* **2014**, *53*, 3387.

236. S. Radomkit, Z. Liu, A. Closs, M. S. Mikus, A. H. Hoveyda, *Tetrahedron* **2017**, *73*, 5011.

237. S. Trudeau, J. B. Morgan, M. Shrestha, J. P. Morken, *J. Org. Chem.* **2005**, *70*, 9538.

238. S. Y. Shim, Y. Choi, D. H. Ryu, *J. Am. Chem. Soc.* **2018**, *140*, 11184.

239. S. Zhang, H. Neumann, M. Beller, *Chem. Commun.* **2019**, *55*, 5938.

240. S. Zhao, T. Gensch, B. Murray, Z. L. Niemeyer, M. S. Sigman, M. R. Biscoe, *Science* **2018**, *362*, 670.

241. S.-L. Shi, S. L. Buwchwald, *Nat. Chem.* **2015**, *7*, 38.

242. S.-T. Kim, B. Pudasaini, M.-H. Baik, *ACS Catal.* **2019**, *9*, 6851.

243. D. P. Ojha, K. Gadde, K. R. Prabhu, *J. Org. Chem.* **2017**, *82*, 4859.

244. T. G. Elford, D. G. Hall in *Boronic Acids*, **2011**, 2nd edition, D. G. Hall, Chapter 8, Wiley-VCH Verlag & Co. KGaA, Weinheim, Germany, 393.

245. T. Havashi, A. Kubo, F. Ozawa, *Pure & Appl. Chem.* **1992**, *64*, 421.

246. T. Ishiyama, M. Murata, N. Miyaura, *J. Org. Chem.* **1995**, *60*, 7508.

247. T. Kan, T. Fujimoto, S. Ieda, Y. Asoh, H. Kitaoka, T. Fukuyama, *Org. Lett.* **2004**, *16*, 2729.

248. T. Kochi, S. Kanno, F. Kakiuchi, *Tetrahedron Lett.* **2019**, *60*, 150938.

249. T. Miura, J. Nakahashi, M. Murakami*, Angew. Chem. Int. Ed.* **2017**, *56*, 6989.

250. T. Moriya, A. Suzuki, N. Miyaura, *Tetrahedron Lett.* **1995**, *11*, 1887.

251. T. P. Pabst, J. V. Obligacion, E. Rochette, I. Pappas, P. J. Chirik, *J. Am. Chem. Soc.* **2019**, *141*, 15378.

252. T. Rosner, J. Le Bars, A. Pfaltz, D. G. Blackmond, *J. Am. Chem. Soc.* **2001,** *123,* 1848.

253. T. Rybak, D. G. Hall, *Org. Lett.* **2015**, *17*, 4156.

254. T. Seiser, T. Saget, D. N. Tran, N. Cramer, *Angew. Chem. Int. Ed.* **2011**, *50*, 7740.

255. T. Seki; S. Tanaka, M. Kitamura, *Org. Lett.* **2012**, *14*, 608.

256. V. Bagutski, T. G. Elford, V. K. Aggarwal, *Angew. Chem. Int. Ed.* **2011**, *50*, 1080.

257. V. M. Shoba, N. C. Thacker, A. J. Bochat, J. M. Takacs, *Angew. Chem. Int. Ed.* **2016**, *55*, 1465.

258. V. Martín-Heras, A. Parra, M. Tortosa, *Synthesis* **2018**, *50*, 470.

259. V. Tona, A. de la Torre, M. Padmanaban, S. Ruider, L. González, N. Maulide, *J. Am. Chem. Soc.* **2016**, *138*, 8348.

260. W. J. Jang, S. M. Song, J. H. Moon, J. Y. Lee, J. Yun, *J. Am. Chem. Soc.* **2017**, *139*, 13660.

261. W. K. Chow, O. Y. Yuen, P. Y. Choy, C. M. So, C. Po Lau, W. T. Wong, F. Y. Kwong, *RSC Advances*, **2013**, *3*, 12518.

262. W. R. Gutekunst, P. S. Baran, *J. Org. Chem.* **2014**, *79*, 2430.

263. W. Yao, X. Ma, L. Guo, X. Jia, A. Hua, Z. Huang, *Tetrahedron Lett.* **2016**, *57*, 2919.

264. X. Chen, Z. Cheng, J. Guo, Z. Lu, *Nat. Commun.* **2018**, *9*, 3939.

265. X. Feng, H. Jeon, J. Yun, *Angew. Chem. Int. Ed.* **2013**, *52*, 3989.

266. X. Feng, J. Yun, *Chem. Commun.* **2009**, 6577.

267. X. Gao, D. G. Hall, *J. Am. Chem. Soc.* **2003**, *125*, 9308.

268. X. Li, C. Wang, J. Song, Z. Yang, G. Zi, G. Hou, *J. Org. Chem.* **2019**, *84*, 8638.

269. X. Sun, Y. Sun, Y. Rao, *Curr. Org. Chem.* **2016**, *20*, 1878.

270. X.-M. Zhang, Y.-Q. Tu, F.-M. Zhang, H. Shao, X. Meng, *Angew. Chem. Int. Ed.* **2011**, *50*, 3916.

271. Y. Cai, X-T. Yang, S-Q. Zhang, F. Li, Y-Q. Li, L-X. Ruan, X. Hong, S-L. Shi, *Angew. Chem. Int. Ed.* **2018**, *57*, 1376.

272. Y. Ge, X-Y. Cui, S. M. Tan, H. Jiang, J. Ren, N. Lee, R. Lee, C-H. Tan, *Angew. Chem. Int. Ed.* **2019**, *58*, 2382.

273. Y. Kawasaki, Y. Ishikawa, K. Igawa, K. Tomooka, *J. Am. Chem. Soc.* **2011**, *133*, 20712.

274. Y. Luo, S. M. Wales, S. E. Korkis, I. D. Roy, W. Lewis, H. W. Lam, *Chem. Eur. J.* **2018**, *24*, 8315.

275. Y. Matsumoto, M. Nalto, T. Hayashi, *Organometallics* **1992**, *11*, 2732.

276. Y. Sasaki, C. Zhong, M. Sawamura, H. Ito, *J. Am. Chem. Soc.* **2010**, *132*, 1226.

277. Y. Takenouchi, R. Kojima, R. Momma, H. Ito, *Synlett* **2017**, *28*, 270.

278. Y. Tan, S. Luo, D. Li, N. Zhang, S. Jia, Y. Liu, W. Qin, C. E. Song, H. Yan, *J. Am. Chem. Soc.* **2017**, *139*, 6431.

279. Y. Wang, A. Noble, E. L. Myers, V. K. Aggarwal, *Angew. Chem. Int. Ed.* **2016**, *55*, 4270.

280. Y. Wei, T. Singer, H. Mayr, G. N. Sastry, H. Zipse, *J. Comput. Chem.* **2007**, *2*, 291.

281. Y. Xi, J. F. Hartwig, *J. Am. Chem. Soc.* **2016**, *138*, 6703.

282. Y. Xu, M. L. Conner, M. K. Brown*, Angew. Chem. Int. Ed.* **2015**, *54*, 11918.

283. Y. Yamamoto, K. Nogi, H. Yorimitsu, A. Osuka, *ChemistrySelect* **2017**, *2*, 1723.;

284. Y. Yamamoto, T. Miyairi, T. Ohmura, N. Miyaura, *J. Org. Chem.* **1999,** *64,* 296.

285. Y. Zhao, D. G. Truhlar, *Theor. Chem. Acc.* **2008**, *120*, 215.

286. Y.-J. Chen, T.-J. Hu, C.-G. Feng, G.-Q. Lin, *Chem. Commun.,* **2015**, *51*, 8773.

287. Y.-R. Kim, D. G. Hall, *Org. Biomol. Chem.* **2016**, *14*, 4739.

288. Z. Bai, S. Zheng, Z. Bai, F. Song, H. Wang, Q. Peng, G. Chen, G. He, *ACS Catal.* **2019**, *9*, 6502.

289. Z. Han, G. Liu, X. Zhang, A. Li, X-Q. Dong, X. Zhang, *Org. Lett.* **2019**, *21*, 3923.

290. Z.-D. Yang, R. Pal, G. L. Hoang, X. C. Zeng, J. M. Takacs, *ACS Catal.* **2014**, *4*, 763.

Appendices

Appendix 1: Selected copies of NMR spectra

^{1}H NMR for the *N*Boc nonaflate **2-6** ($CDCl_3$, 400 MHz, 60 °C)

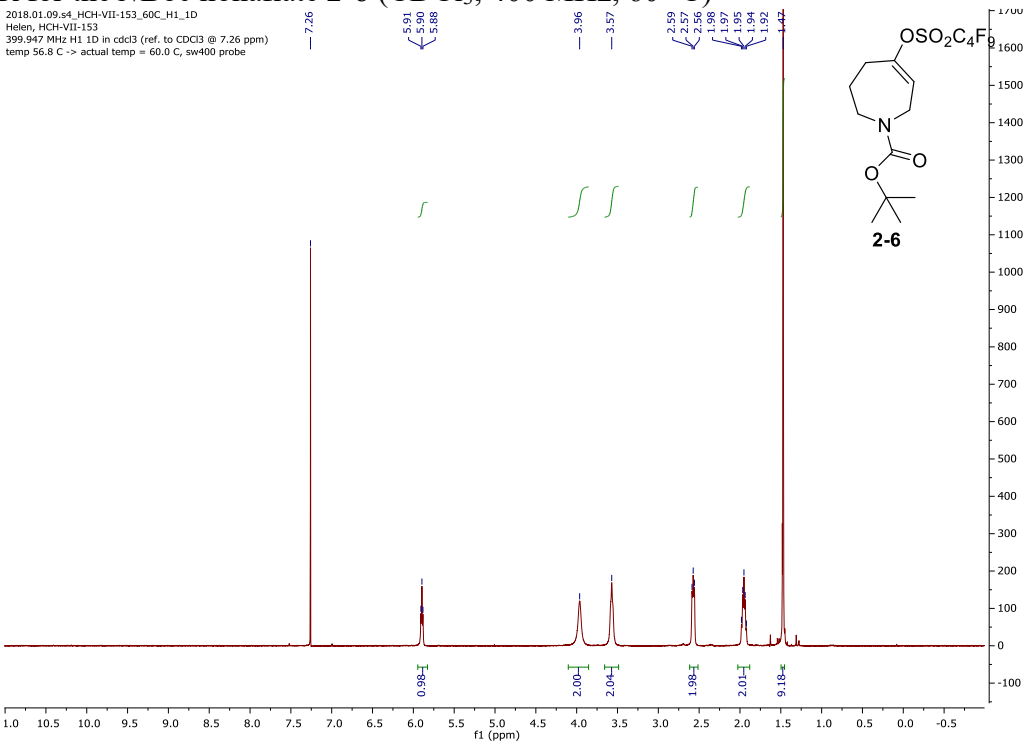

^{1}H NMR for allylic boronate **2-14** (C_6D_6, 500 MHz), rotamers are present

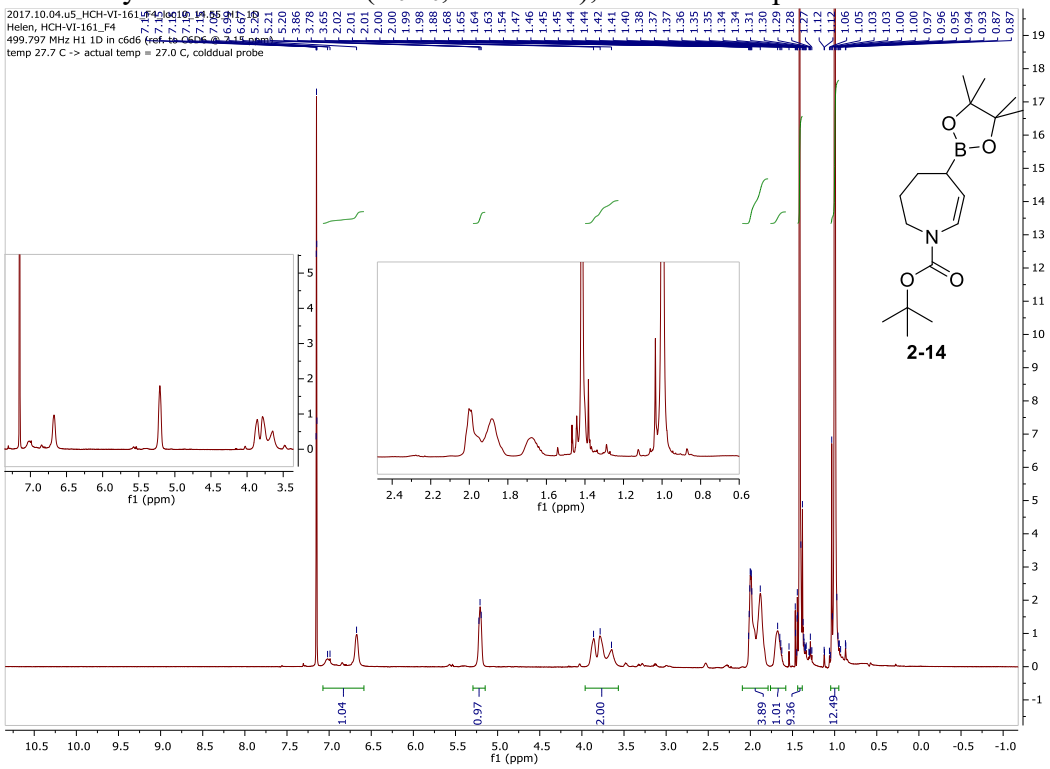

^{13}C NMR for allylic boronate **2-14** ($CDCl_3$, 126 MHz,)

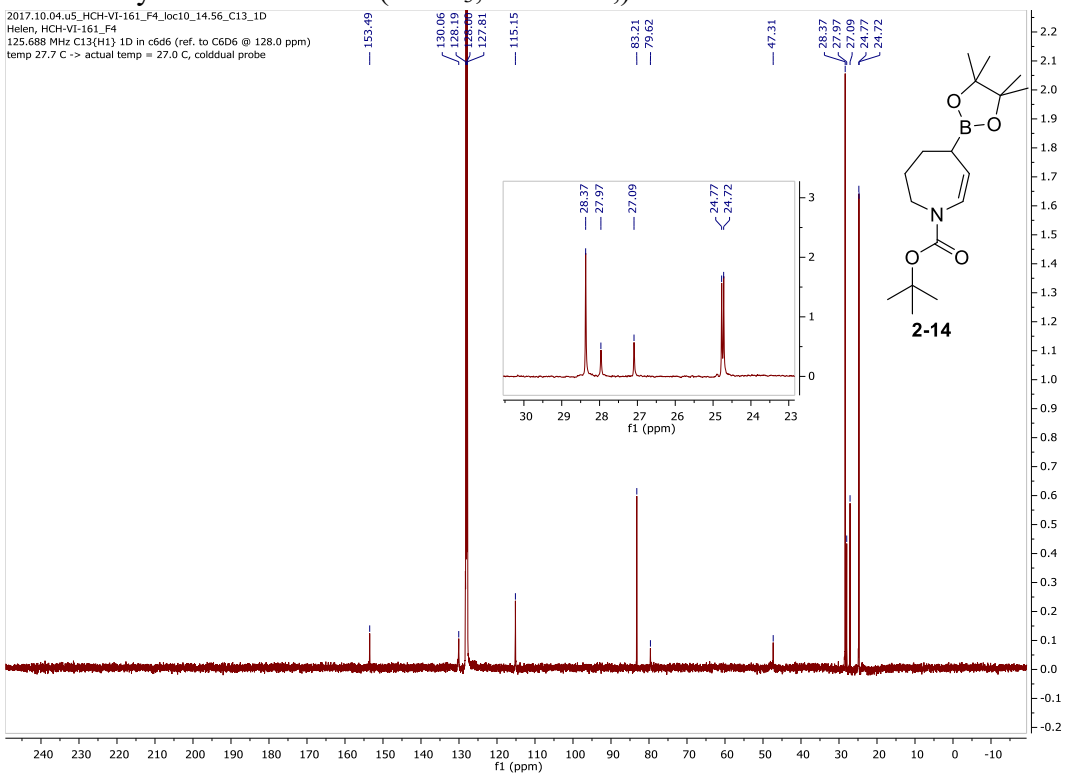

^{1}H NMR for alkenyl boronate **2-36** (C_6D_6, 400 MHz), rotamers are present

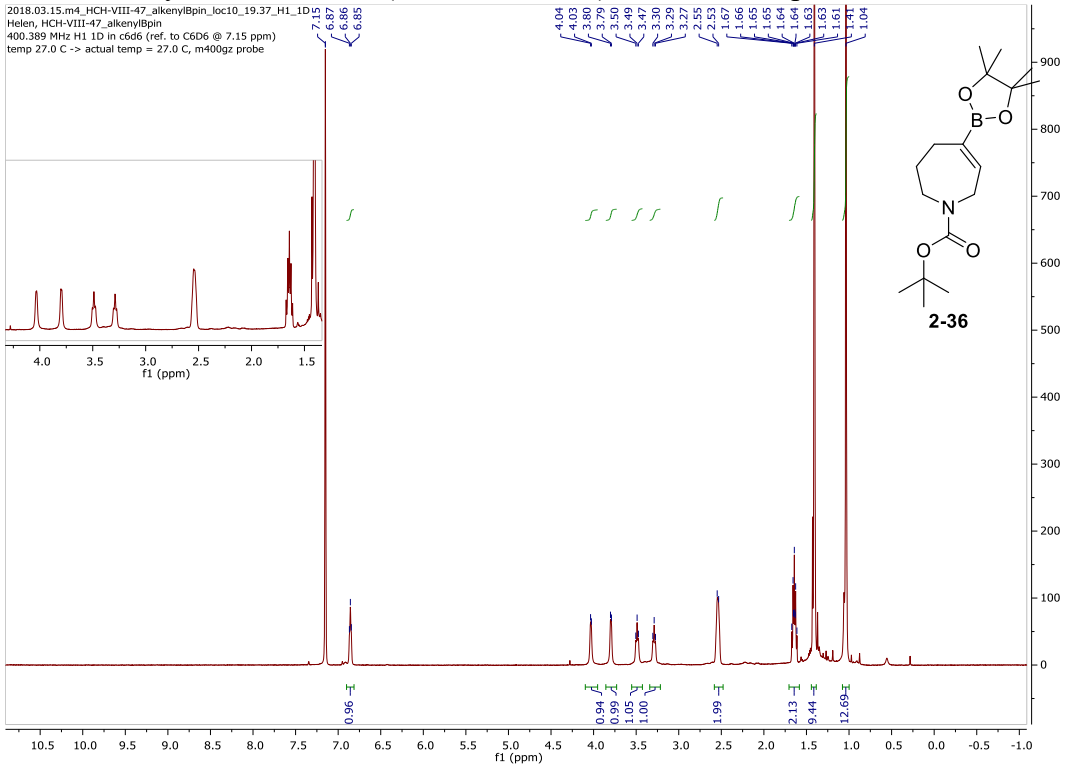

^{13}C NMR for alkenyl boronate **2-36** ($CDCl_3$, 126 MHz)

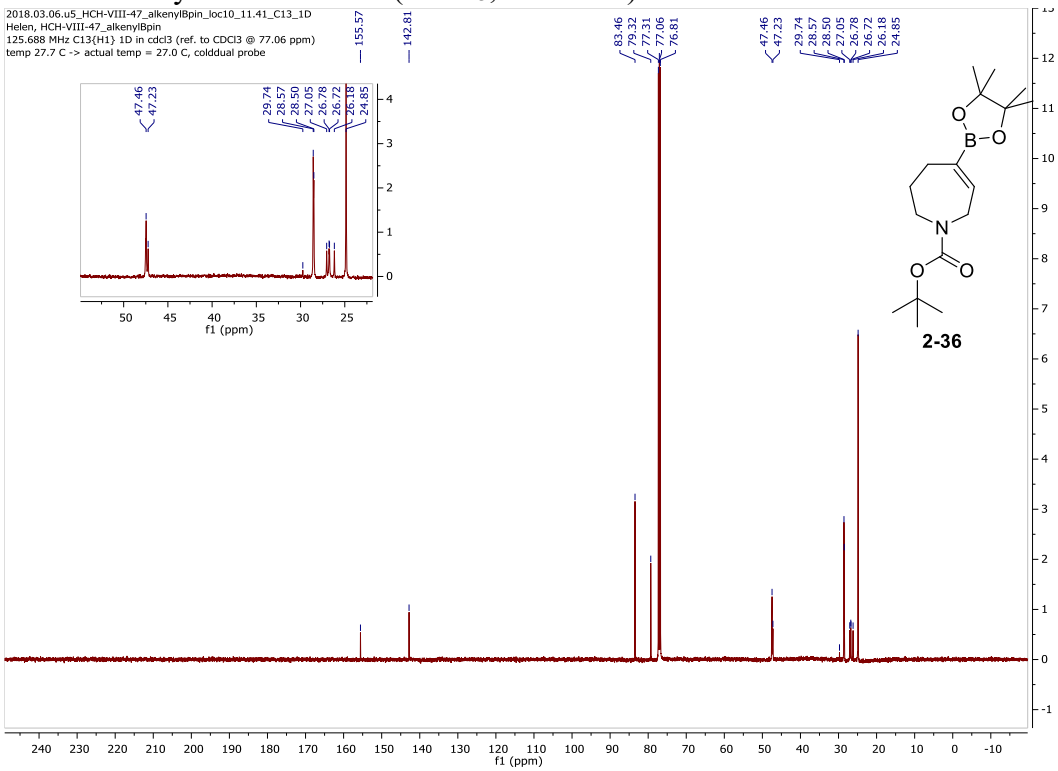

^{1}H NMR for enamide **2-37** (C_6D_6, 400 MHz), rotamers are present

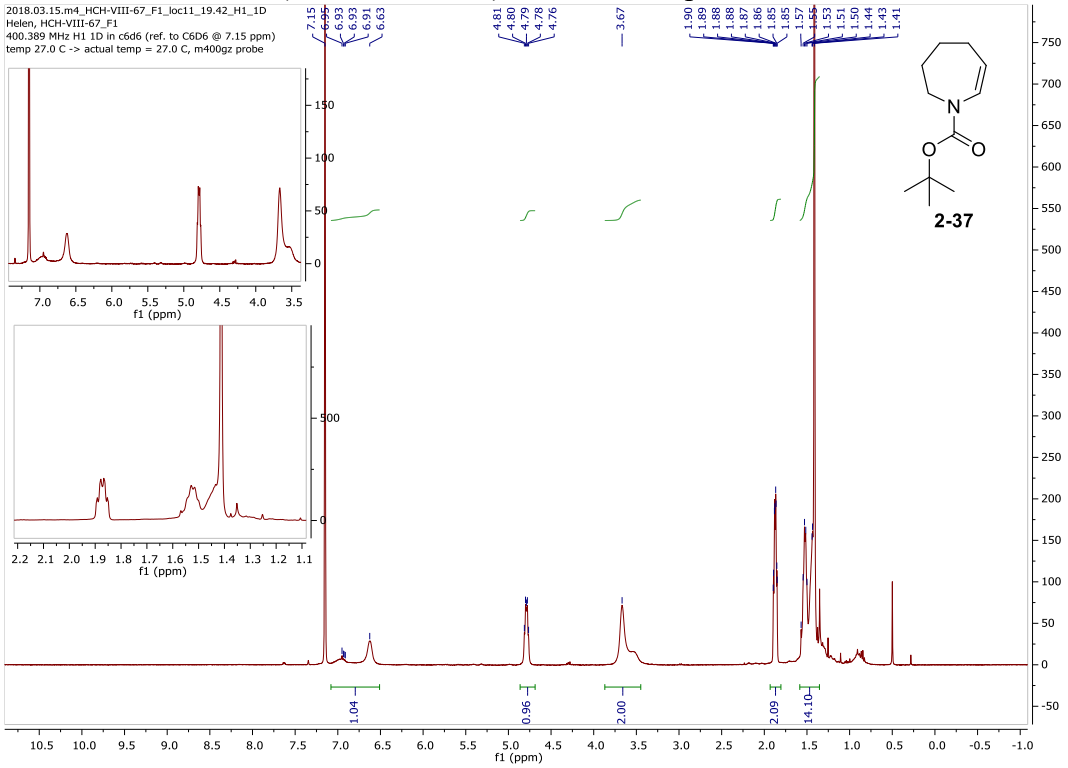

^{13}C NMR for enamide **2-37** ($CDCl_3$, 126 MHz), rotamers are present

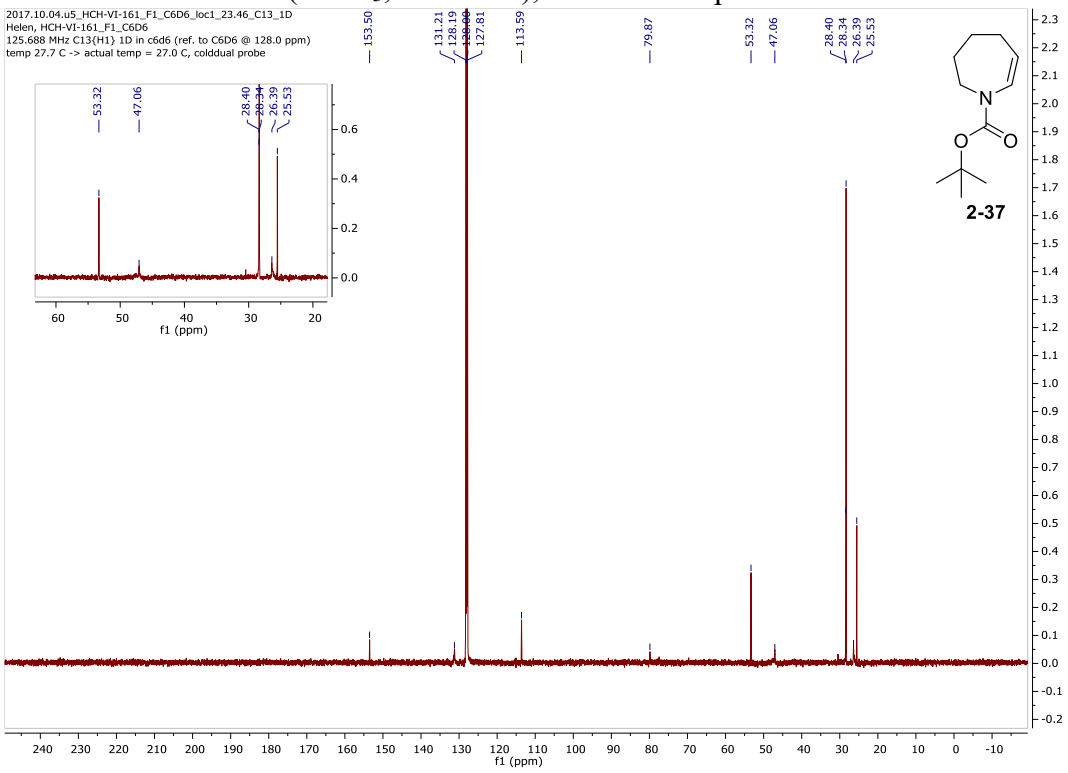

^{1}H NMR for tolyl allylboration product **2-15** (CD_3OD, 500 MHz), rotamers are present

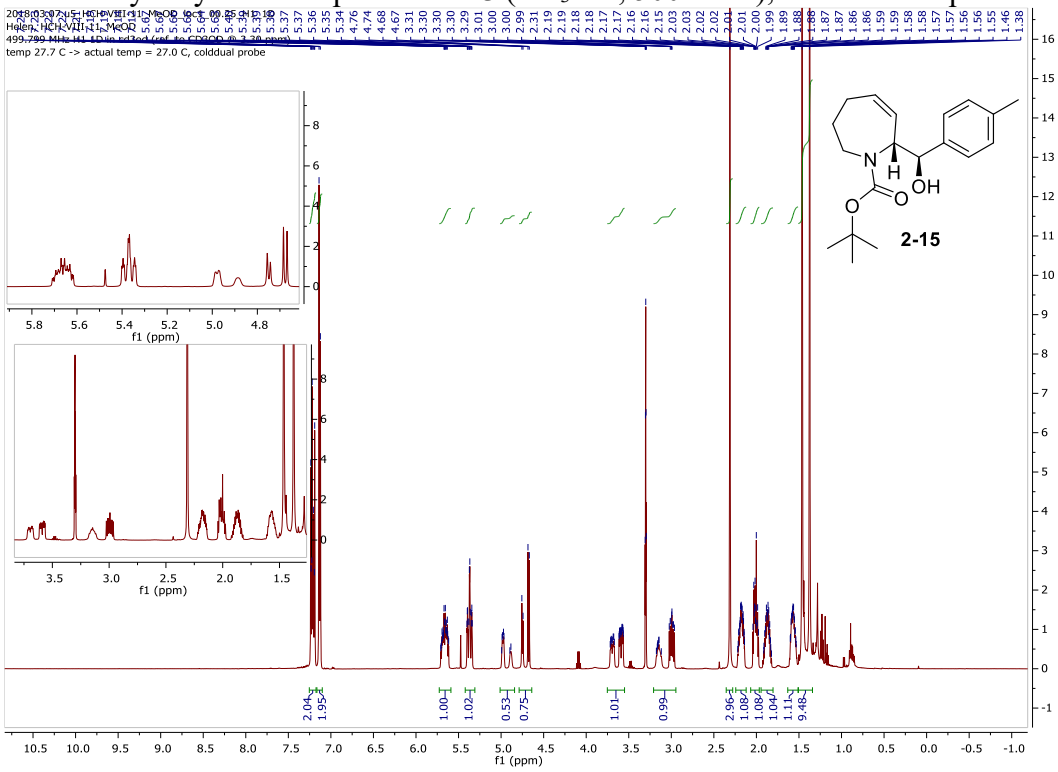

^{13}C NMR for tolyl allylboration product **2-15** (CD_3OD, 126 MHz), rotamers are present

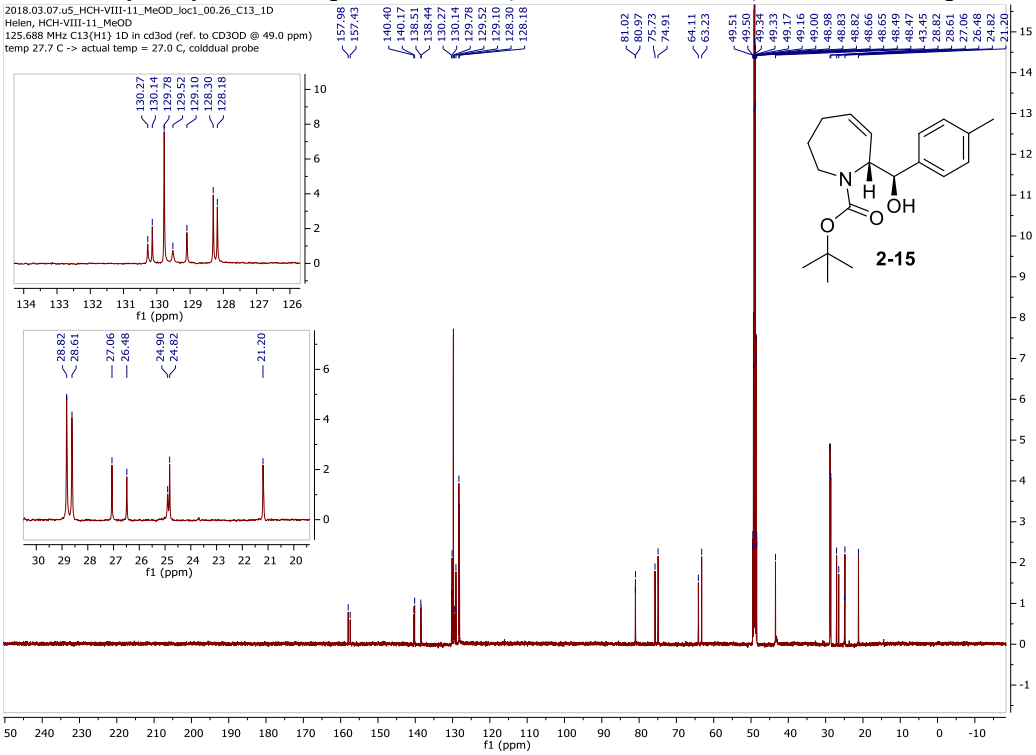

^{1}H NMR for furanyl allylboration product **2-38** (CD_3OD, 500 MHz), rotamers are present

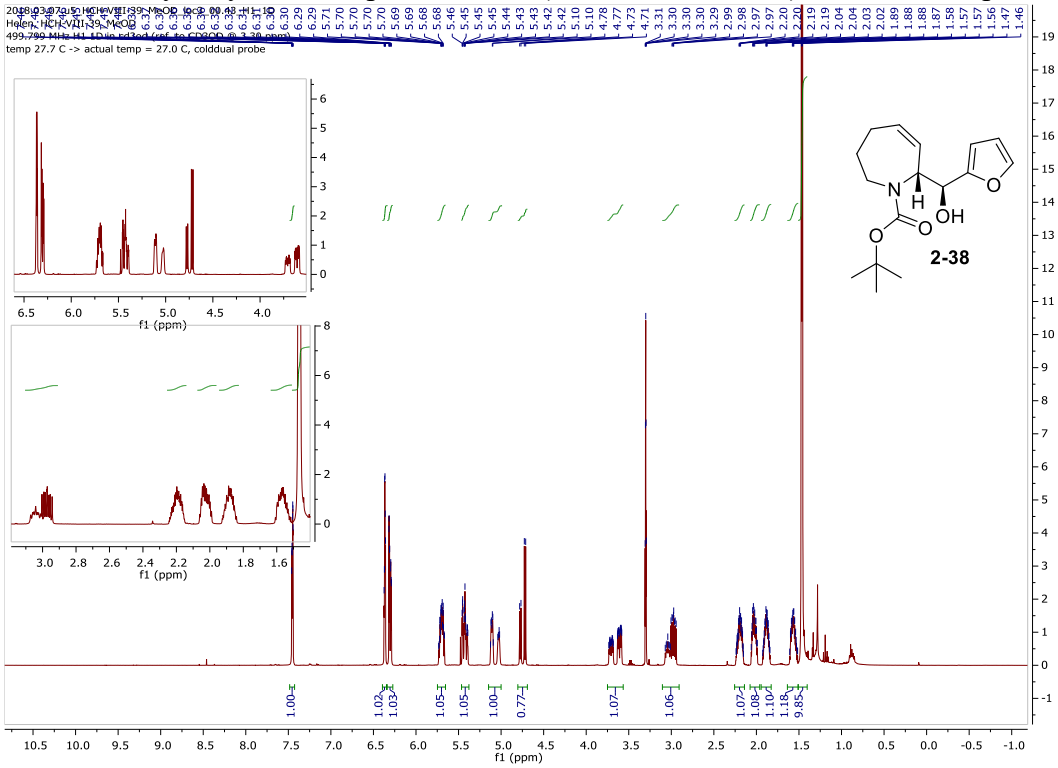

^{13}C NMR for furanyl allylboration product **2-38** (CD_3OD, 126 MHz), rotamers are present

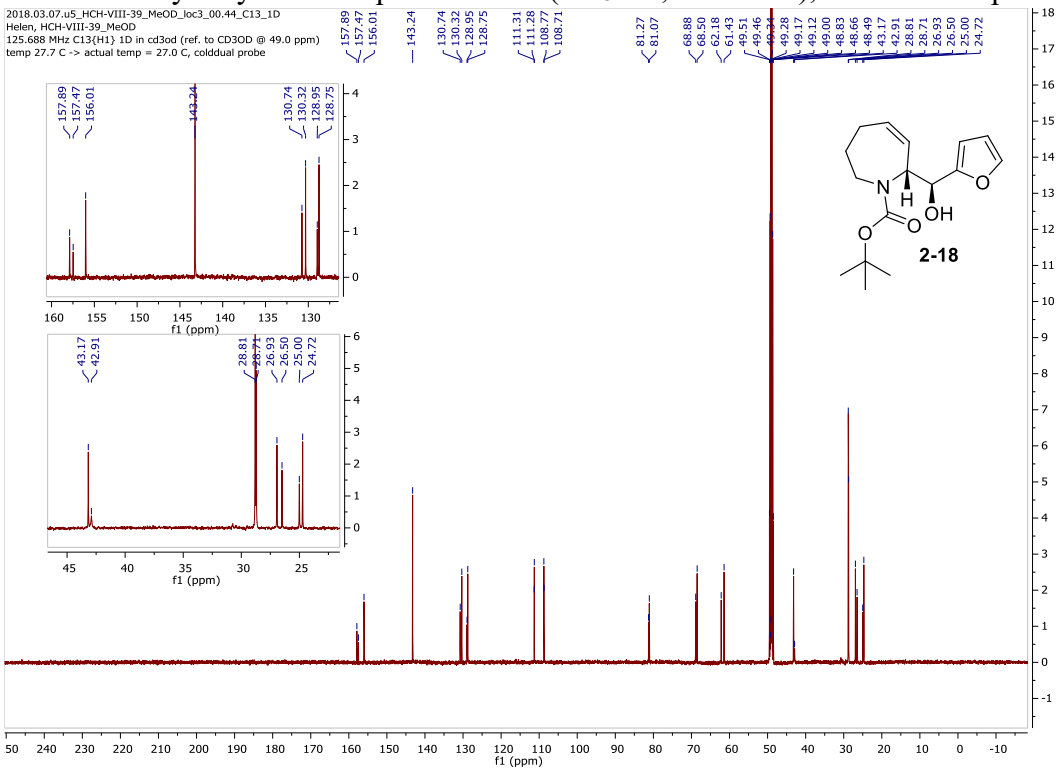

^{1}H NMR for hydrocinnamyl product **2-39** (CD_3OD, 500 MHz), rotamers are present, dr ≈ 5.5 : 1

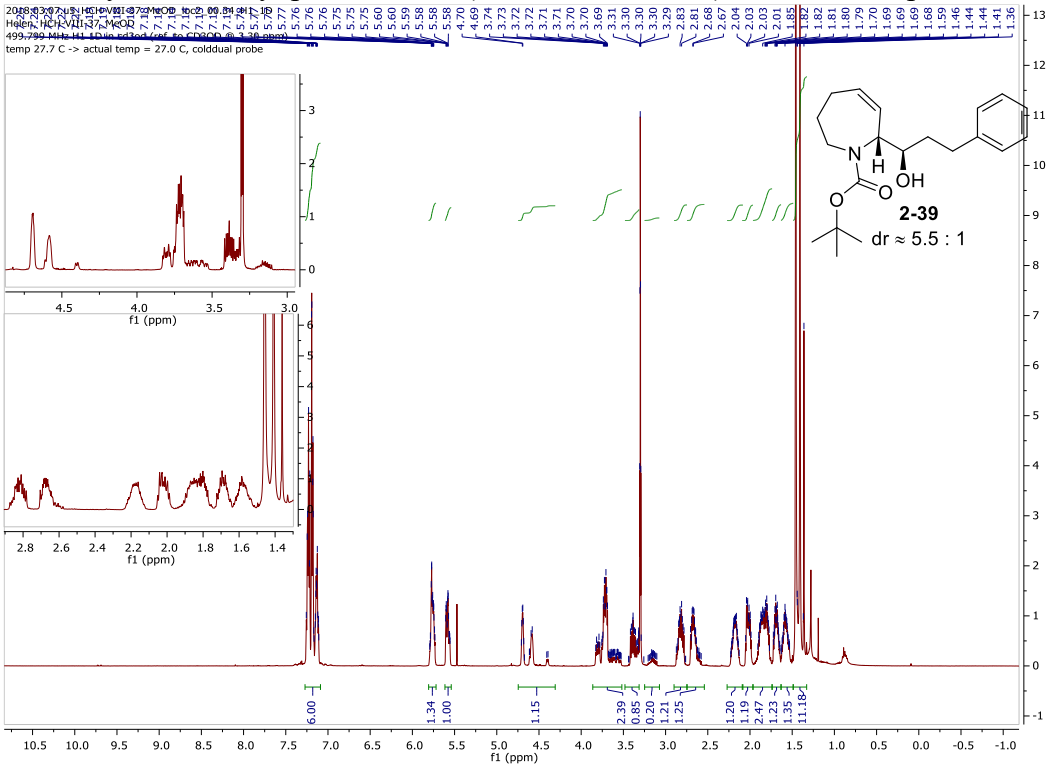

^{13}C NMR for hydrocinnamyl product **2-39** (CD_3OD, 126 MHz), rotamers are present

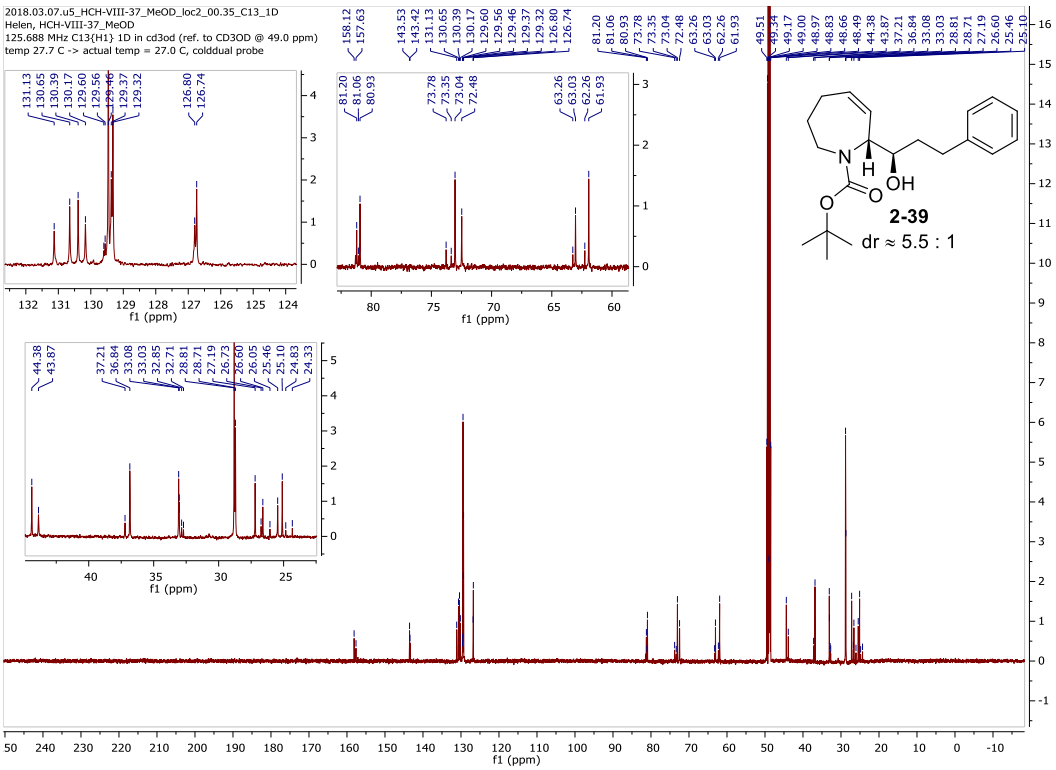

^{1}H NMR for major diastereomer **2-39a** (CD_3OD, 500 MHz), rotamers are present

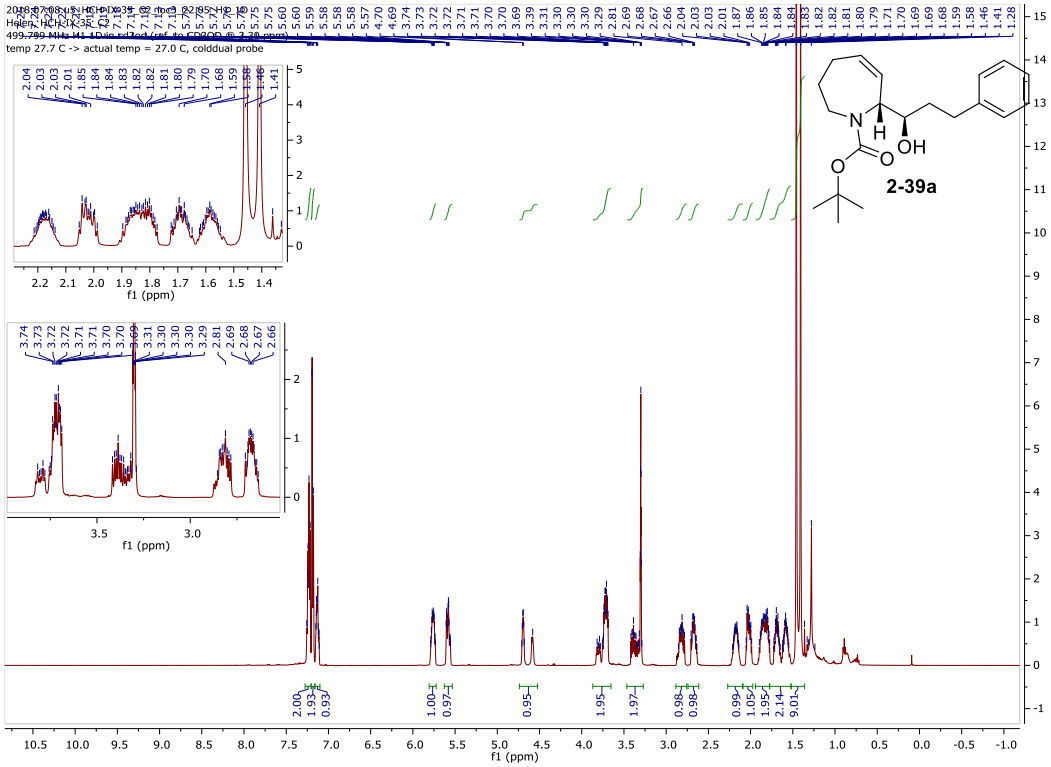

^{13}C NMR for major diastereomer **2-39a** (CD_3OD, 126 MHz), rotamers are present

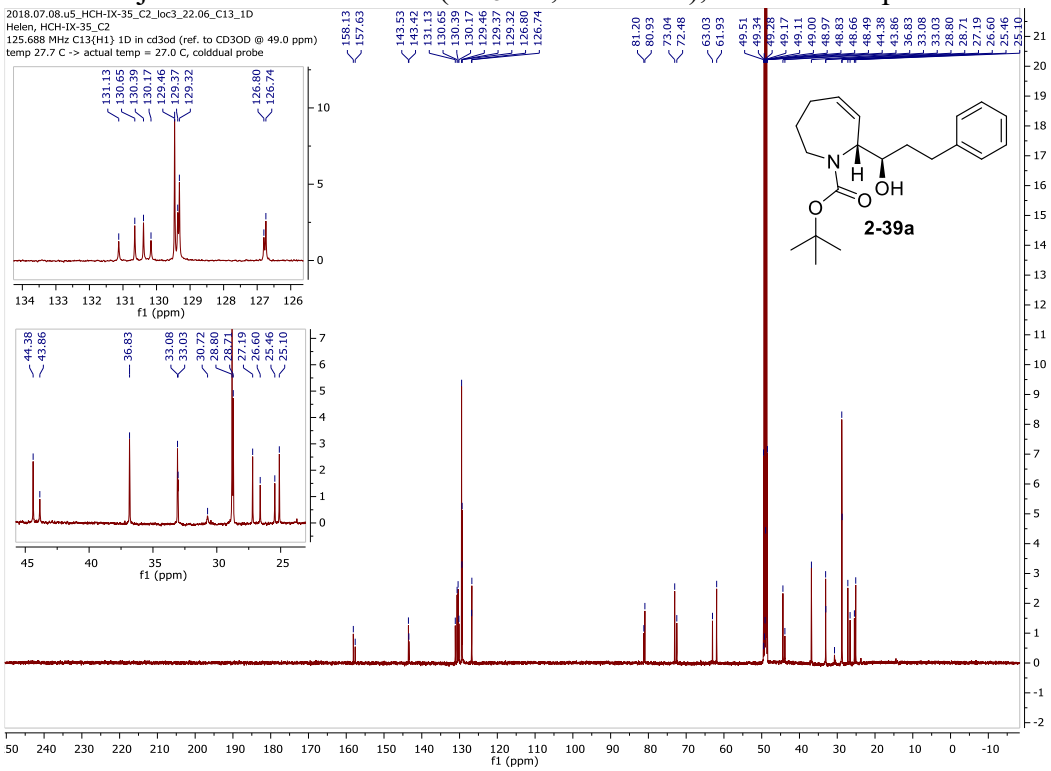

^{1}H NMR for minor diastereomer **2-39b** (CD_3OD, 500 MHz), rotamers are present

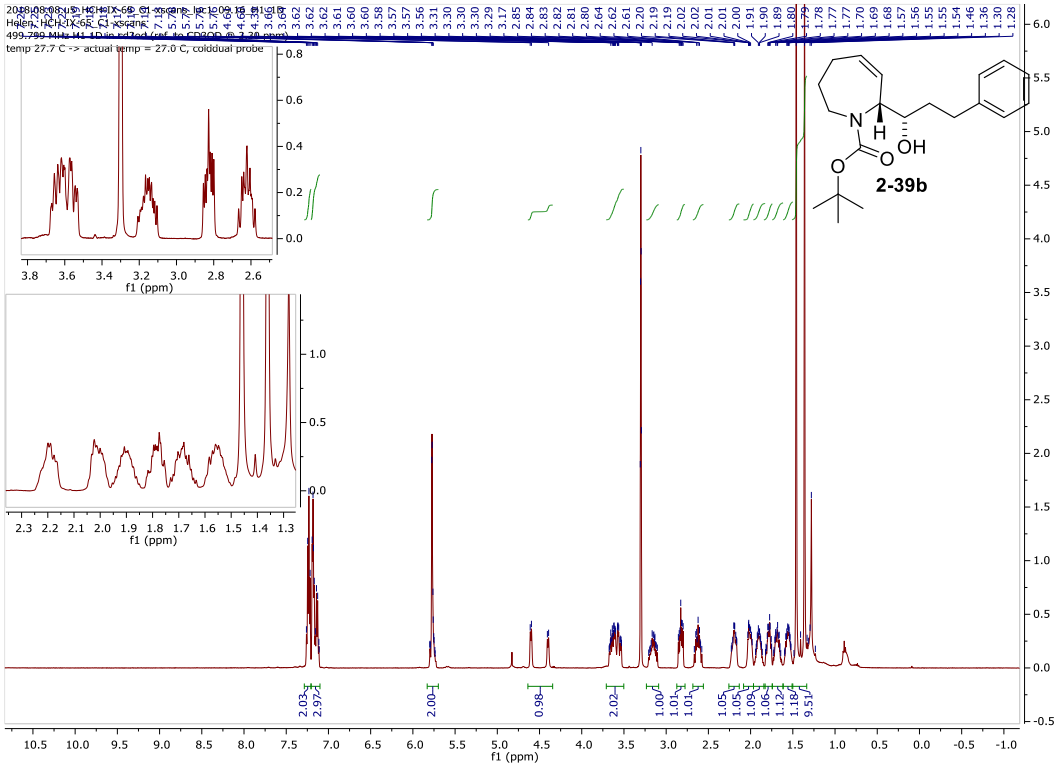

^{13}C NMR for minor diastereomer **2-39b** (CD_3OD, 126 MHz), rotamers are present

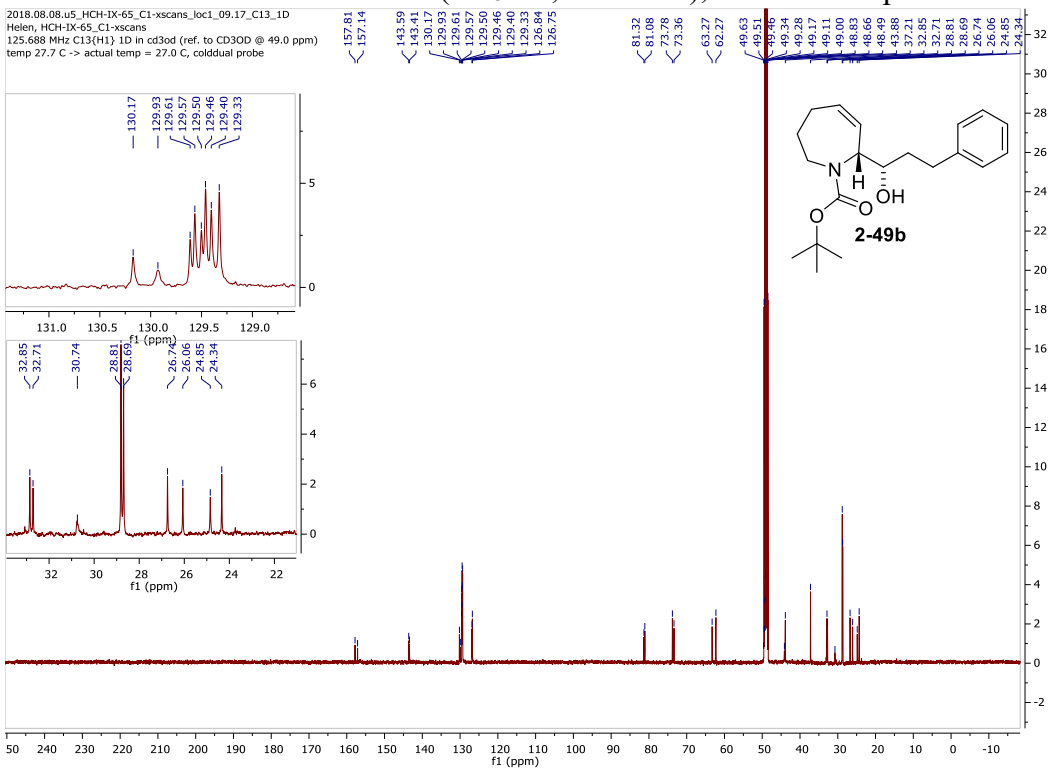

^{1}H NMR for carbamate major diastereomer **2-42a** (CD_3OD, 500 MHz)

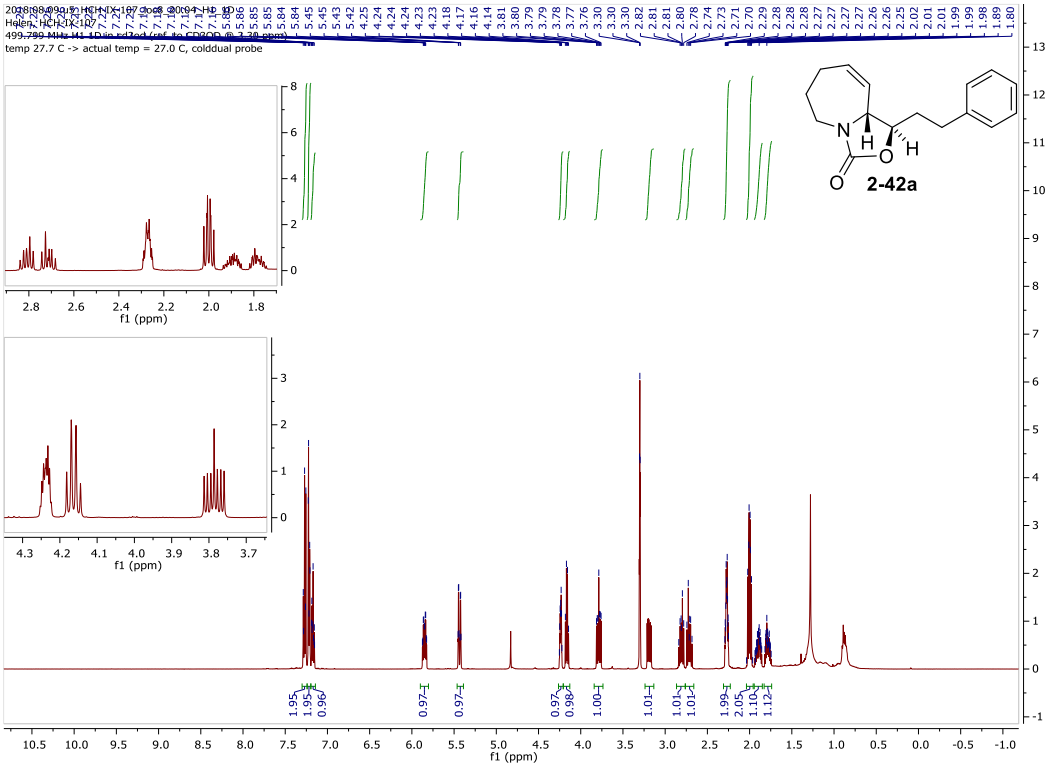

^{13}C NMR for carbamate major diastereomer **2-42a** (CD_3OD, 126 MHz)

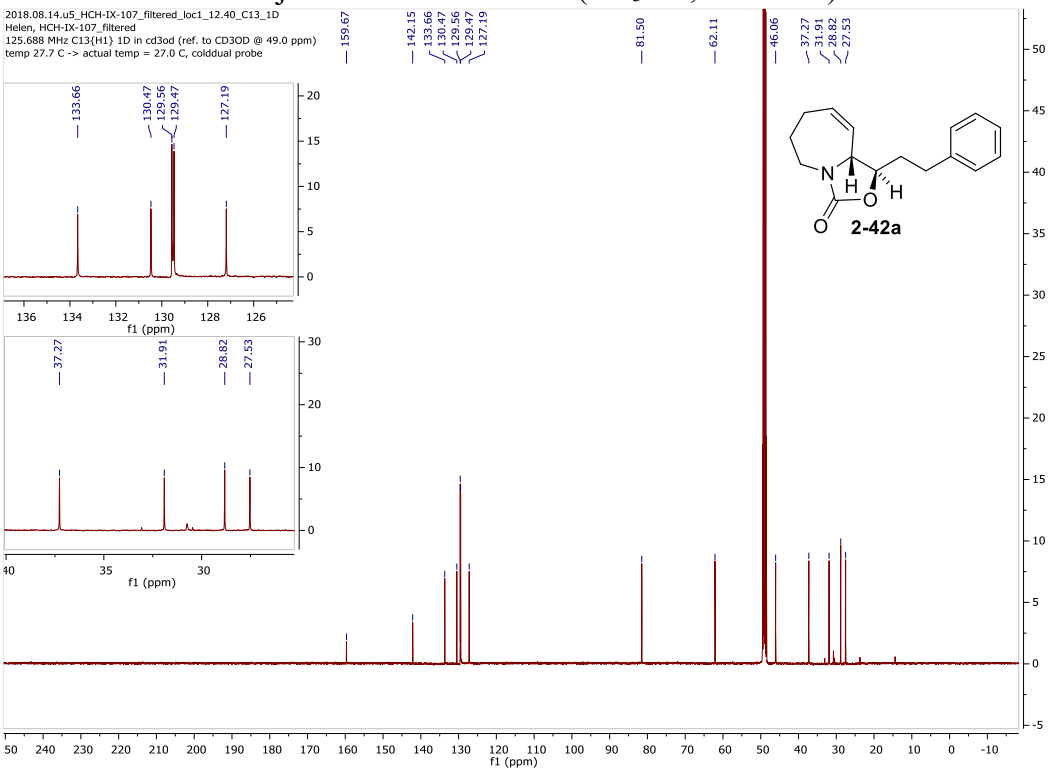

gCOSY NMR for carbamate **2-42a** (CD_3OD, 700 MHz)

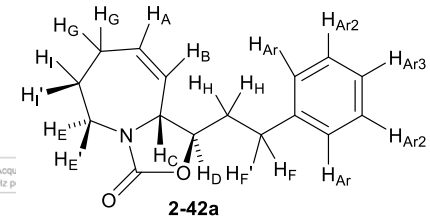

2-42a

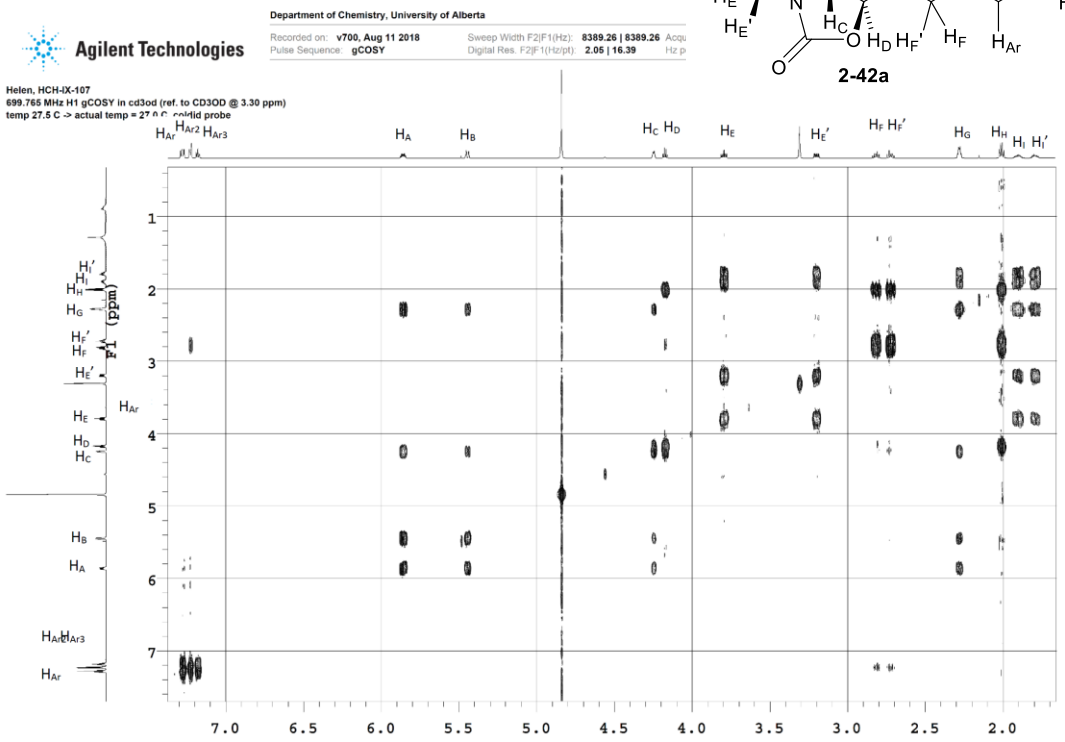

2D ROESY for carbamate **2-42a** (CD_3OD, 700 MHz)

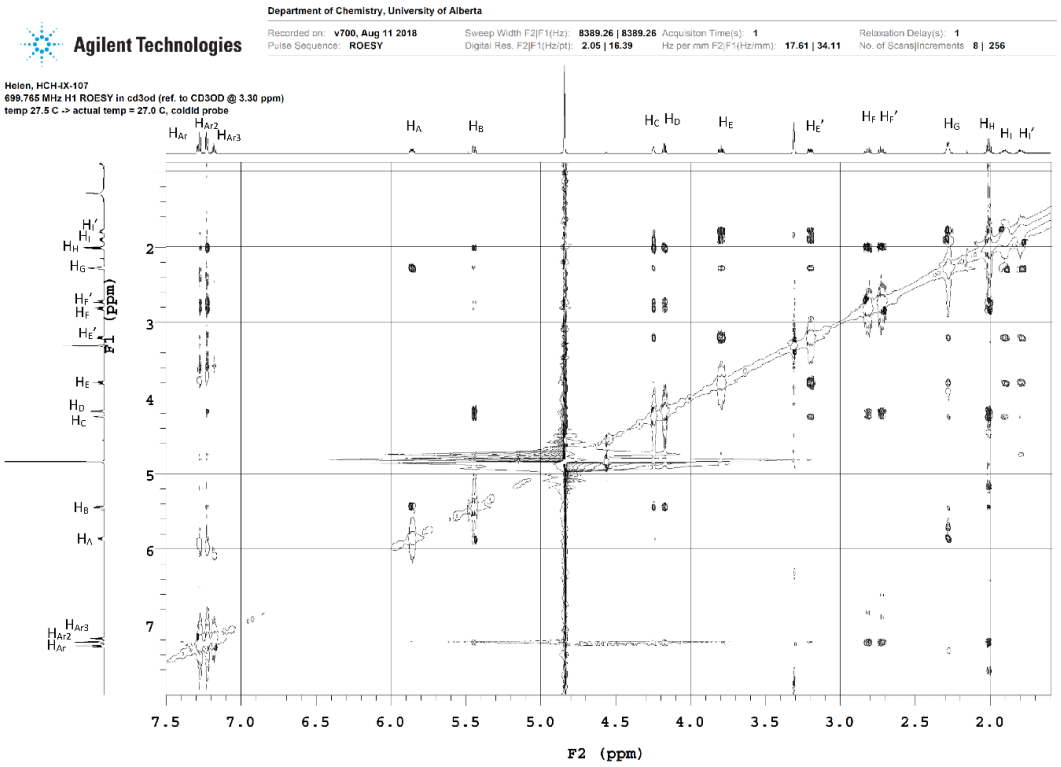

1D ROESY for carbamate **2-42a** – selective excitation at 3.20 ppm (CD_3OD, 600 MHz)

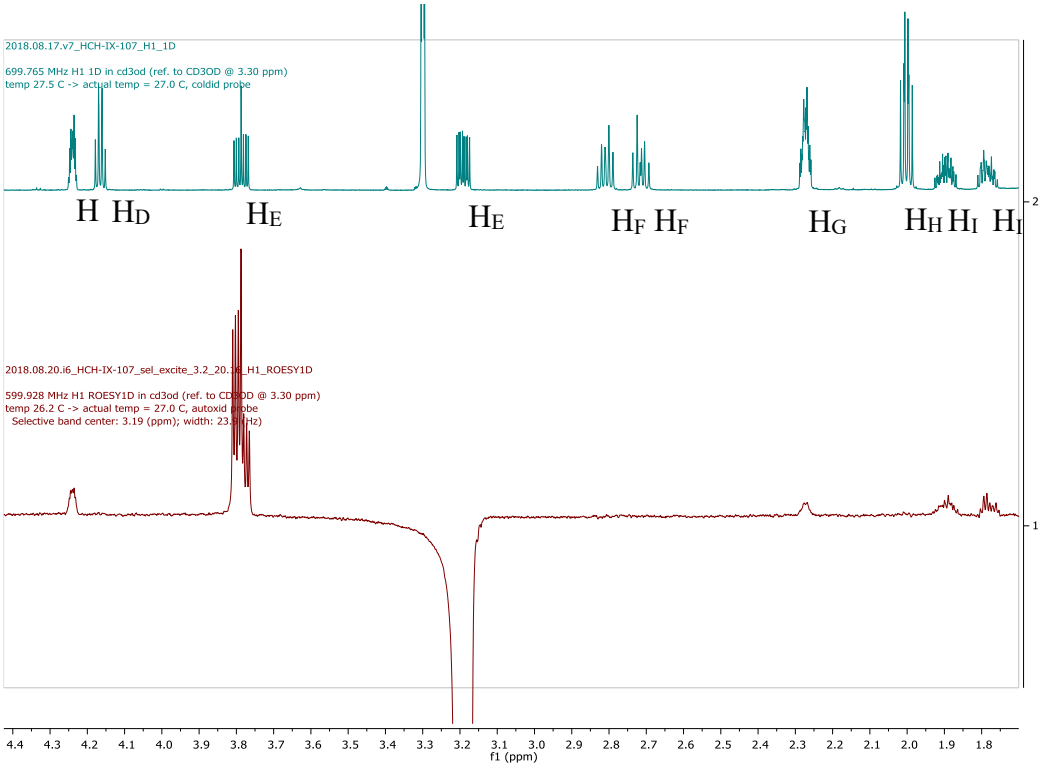

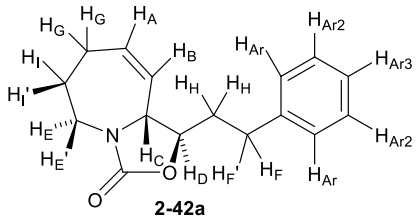

2-42a

^{1}H NMR for hydrocinnamyl minor diastereomer **2-42b** ($CDCl_3$, 500 MHz)

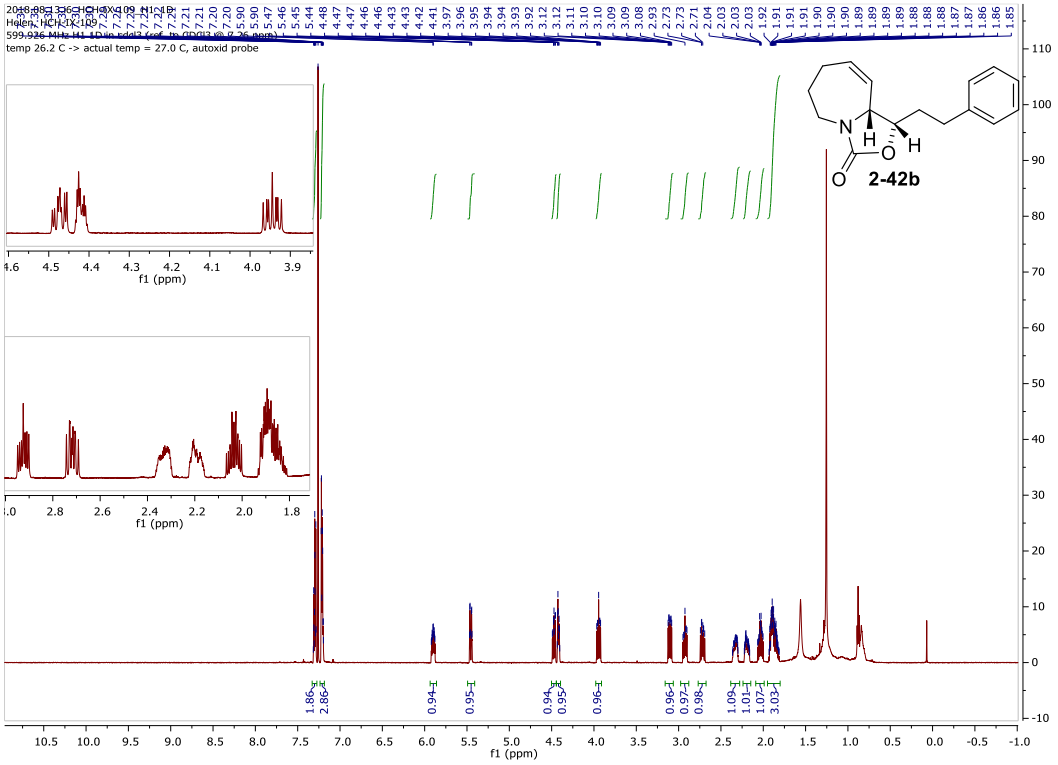

^{13}C NMR for hydrocinnamyl minor diastereomer **2-42b** ($CDCl_3$, 126 MHz)

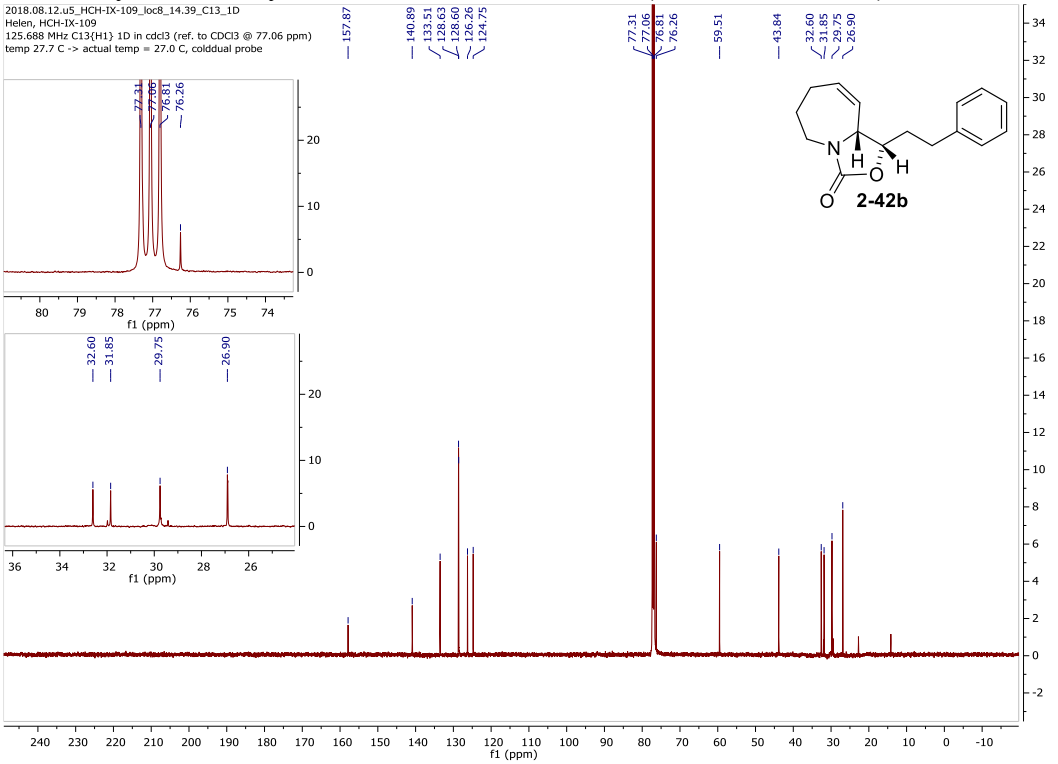

gCOSY NMR for carbamate **2-42b** ($CDCl_3$, 700 MHz)

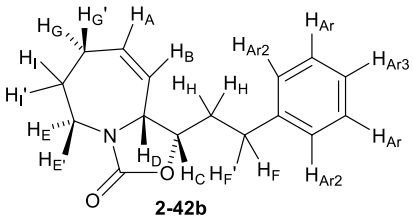

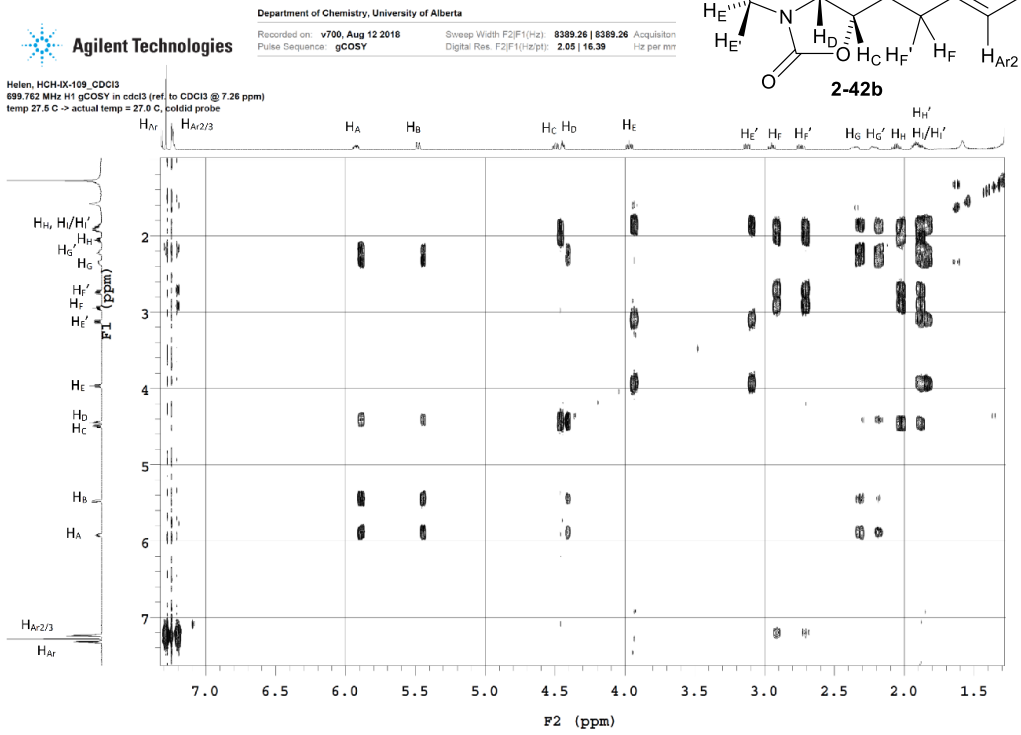

2D ROESY for carbamate **2-42b** ($CDCl_3$, 700 MHz)

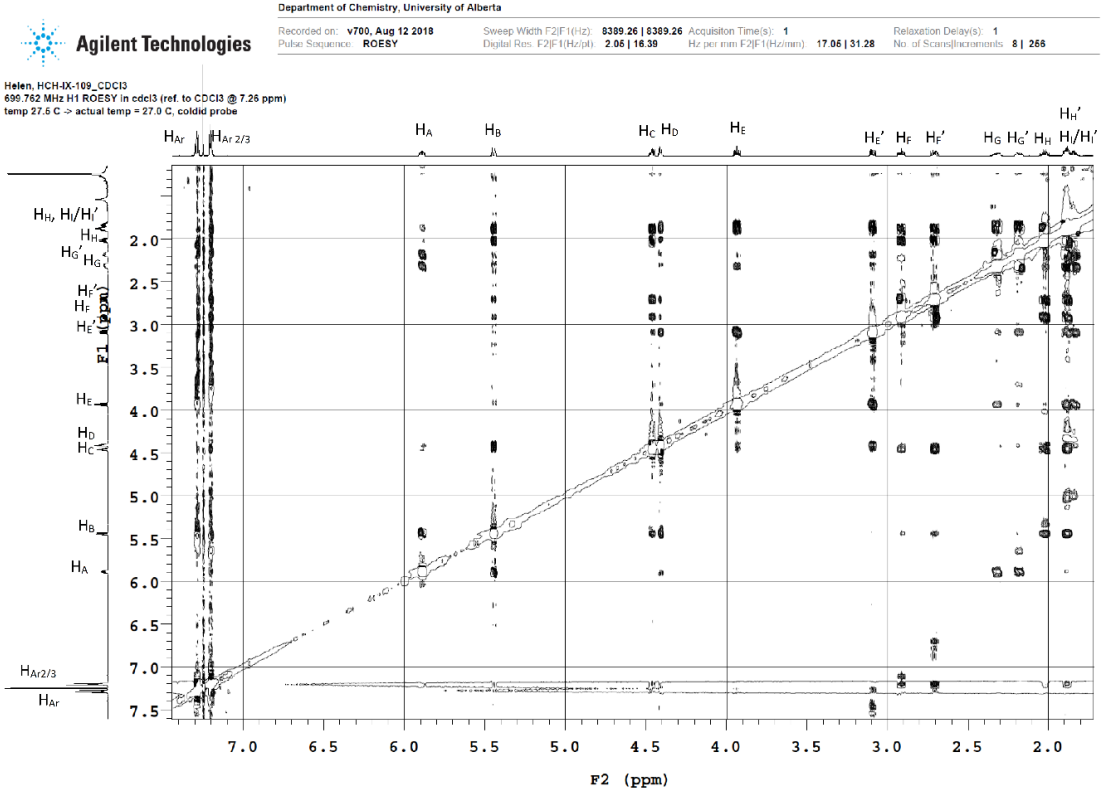

1D ROESY for carbamate **2-42b** – selective excitation at 3.12 ppm (CD_3OD, 600 MHz)

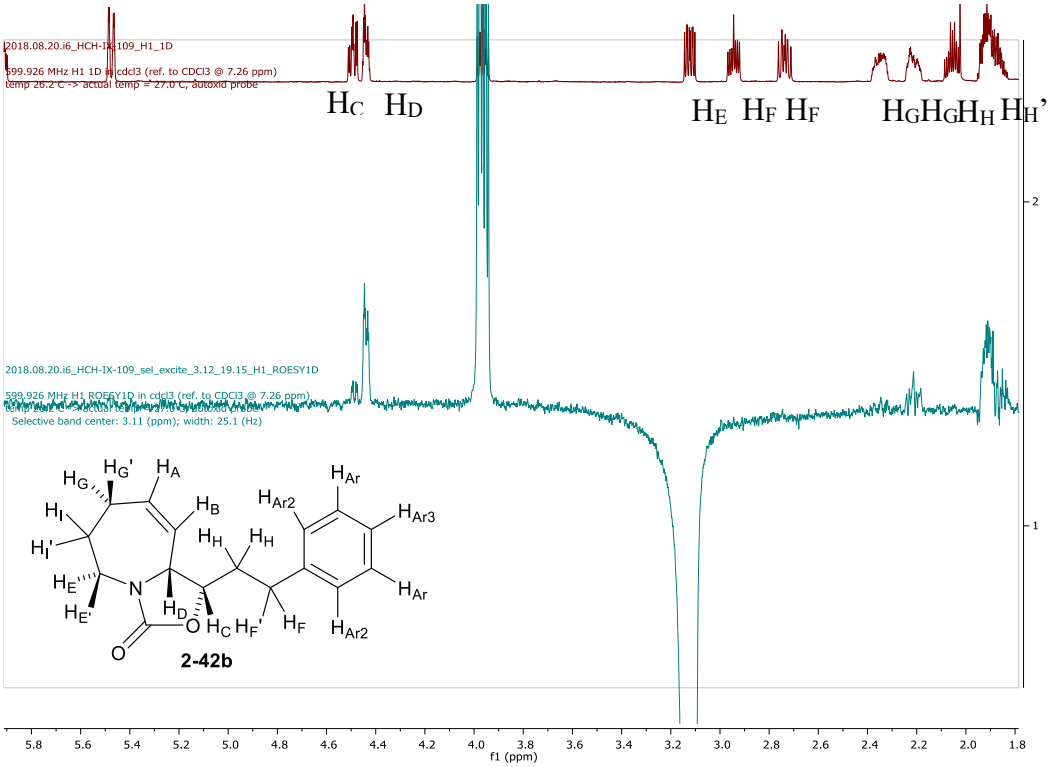

1D ROESY for carbamate **2-42b** – selective excitation at 3.12 ppm (CD_3OD, 600 MHz)

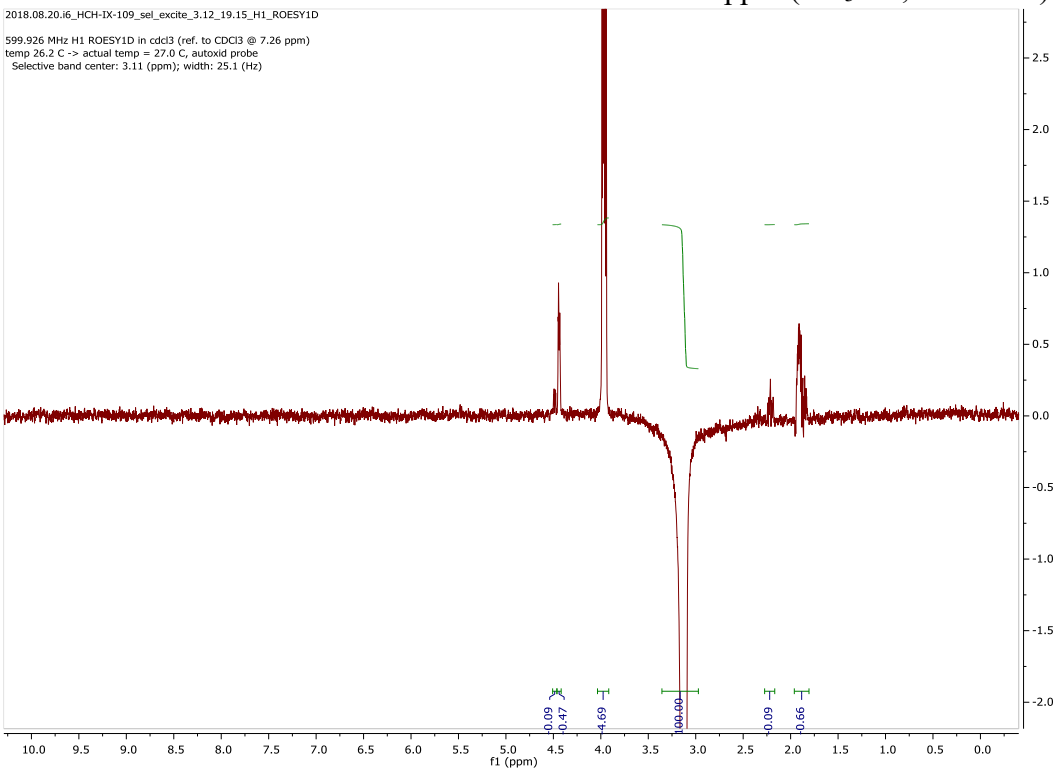

^{1}H NMR for pyranyl nonaflate **3-2** ($CDCl_3$, 700 MHz)

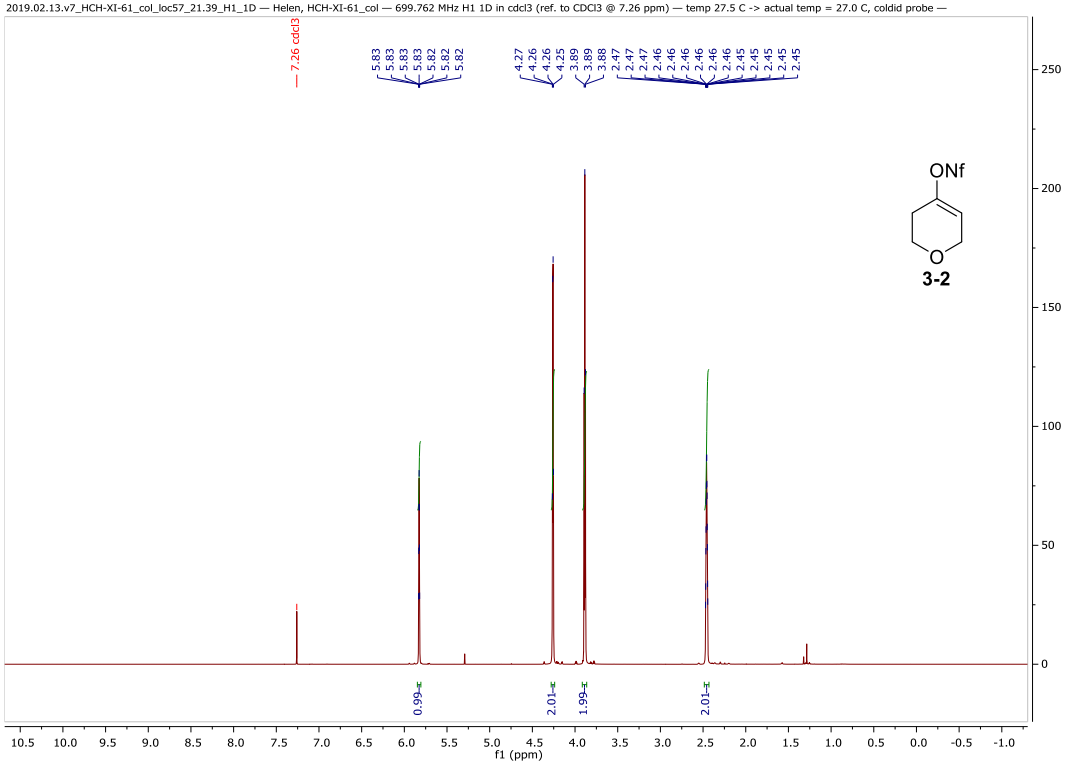

^{13}C NMR for pyranyl nonaflate **3-2** ($CDCl_3$, 101 MHz)

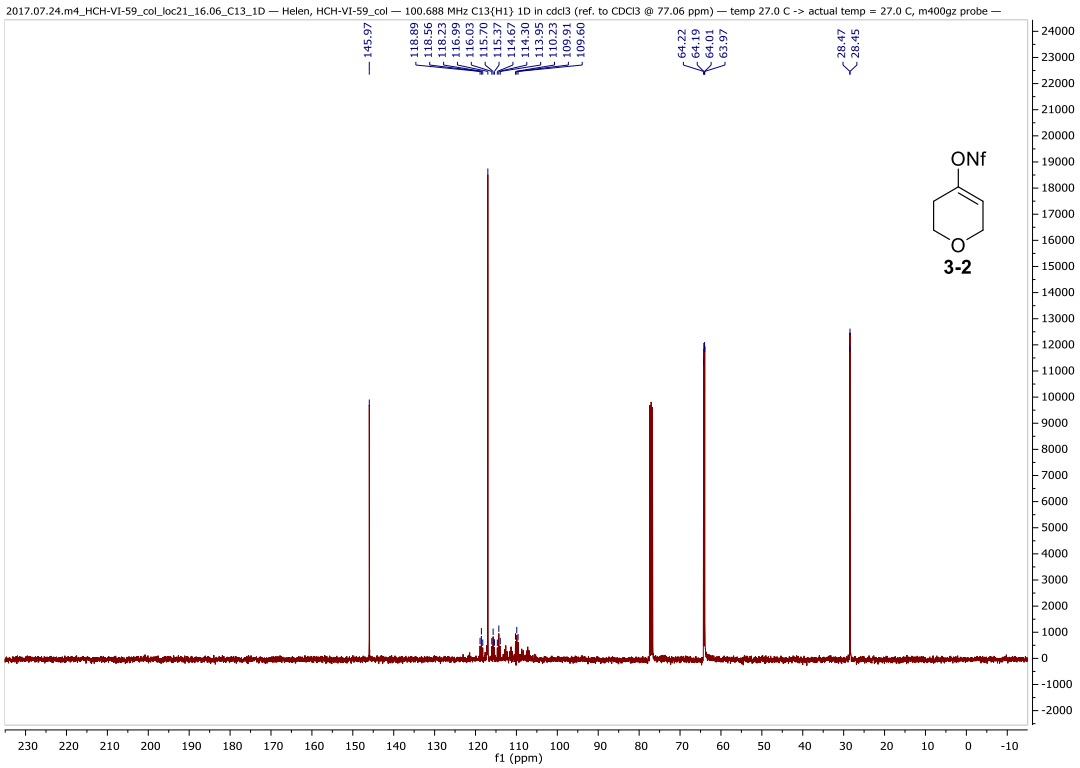

^{1}H NMR for trifluoroacetamide nonaflate **3-11** ($CDCl_3$, 500 MHz)

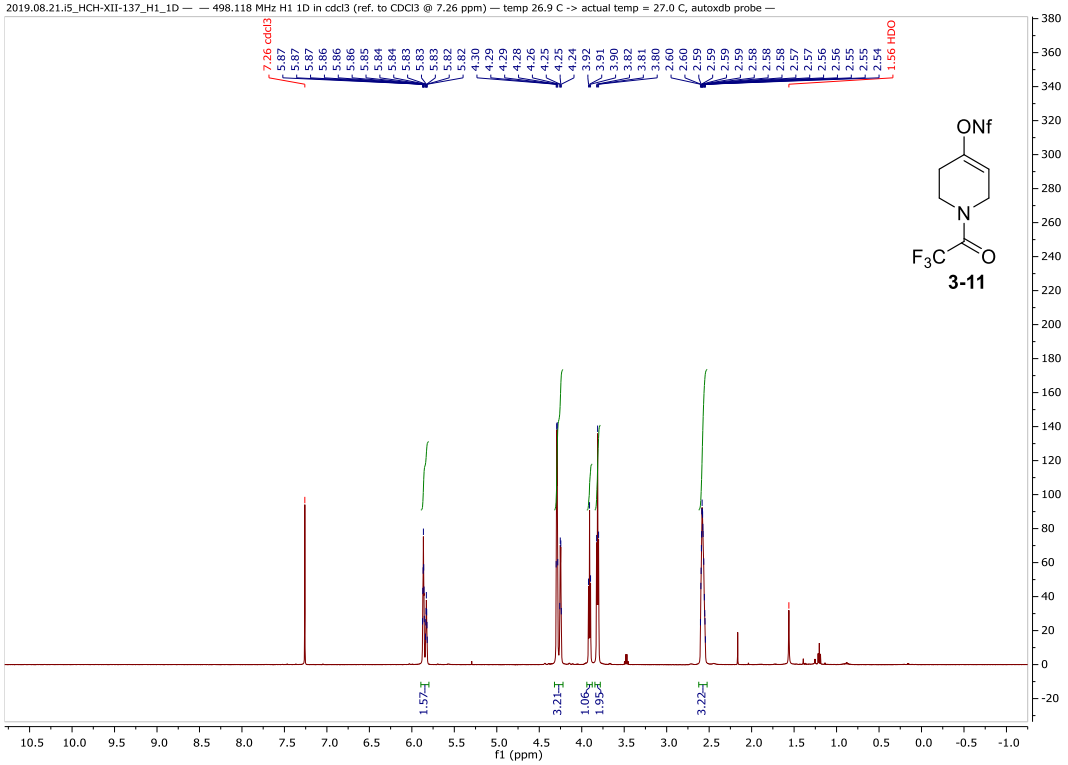

^{19}F NMR for trifluoroacetamide nonaflate **3-11** ($CDCl_3$, 469 MHz)

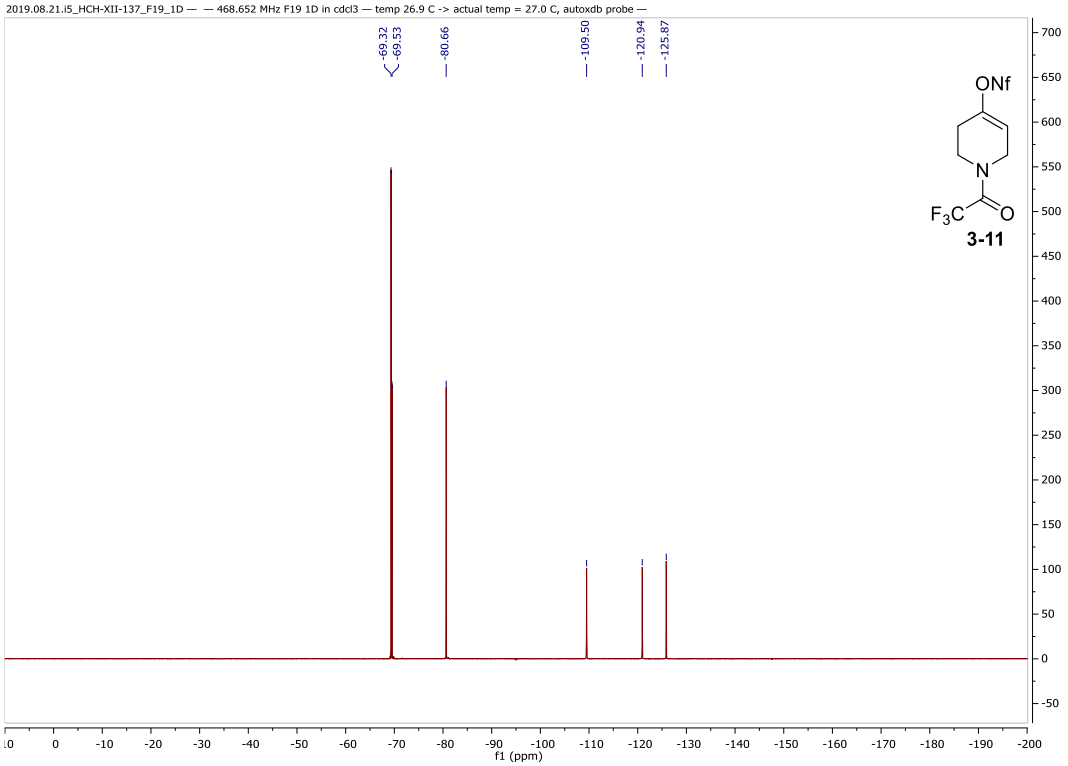

^{1}H NMR for trifluoroacetamide allylic boronate **3-13** ($CDCl_3$, 500 MHz)

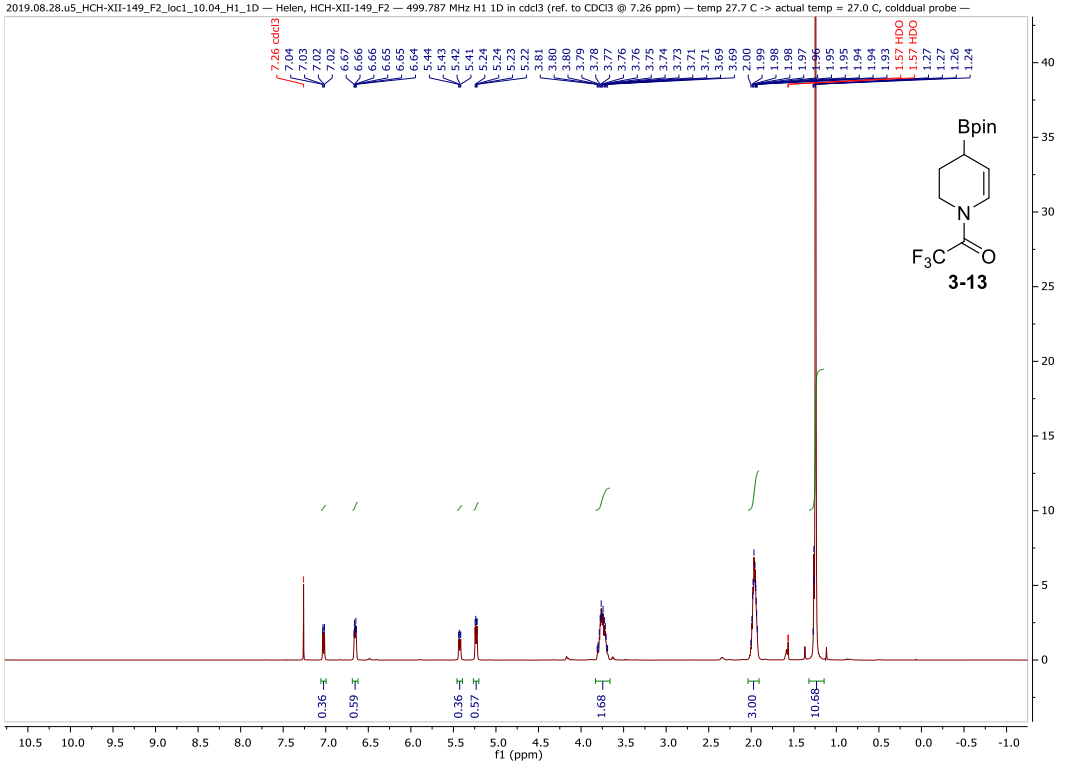

^{13}C NMR for trifluoroacetamide allylic boronate **3-13** ($CDCl_3$, 126 MHz)

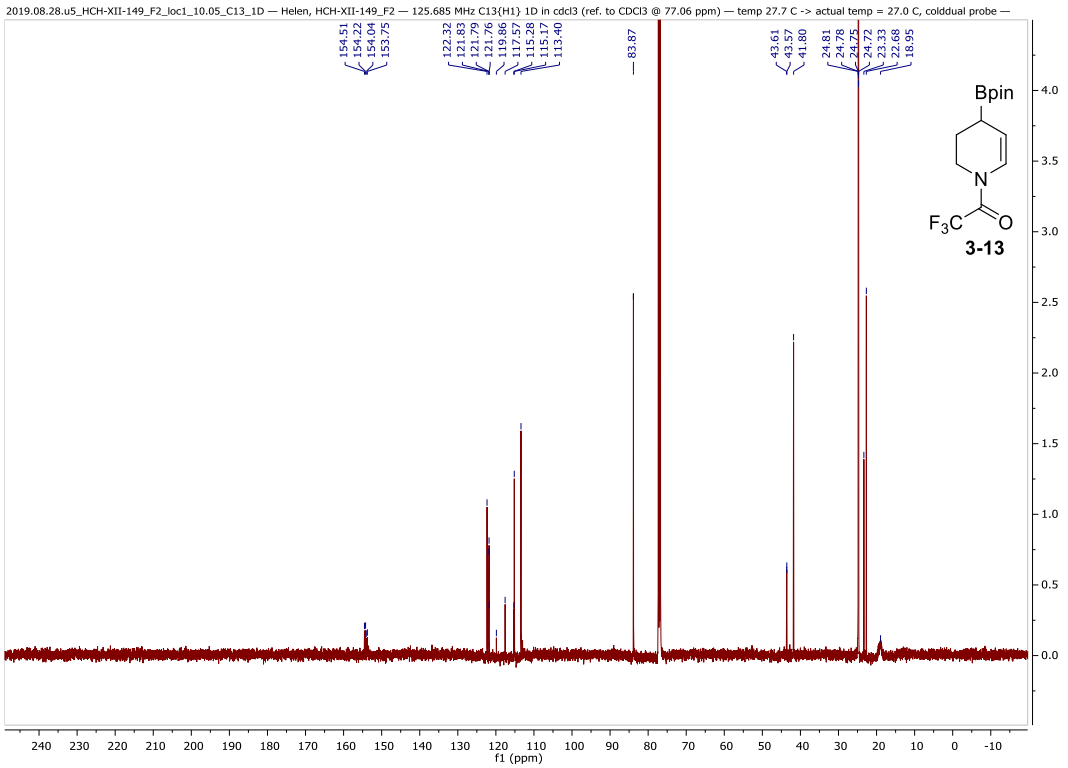

^{1}H NMR for trifluoroacetamide alkenyl boronate **3-14** ($CDCl_3$, 500 MHz)

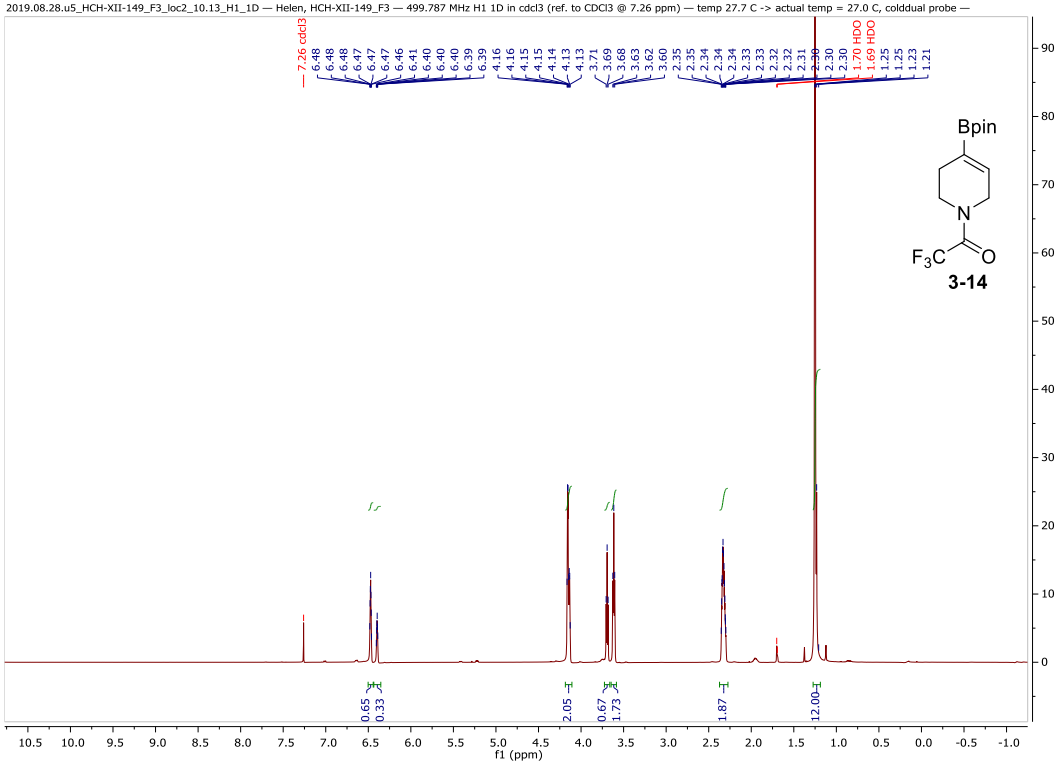

^{13}C NMR for trifluoroacetamide alkenyl boronate **3-14** ($CDCl_3$, 126 MHz)

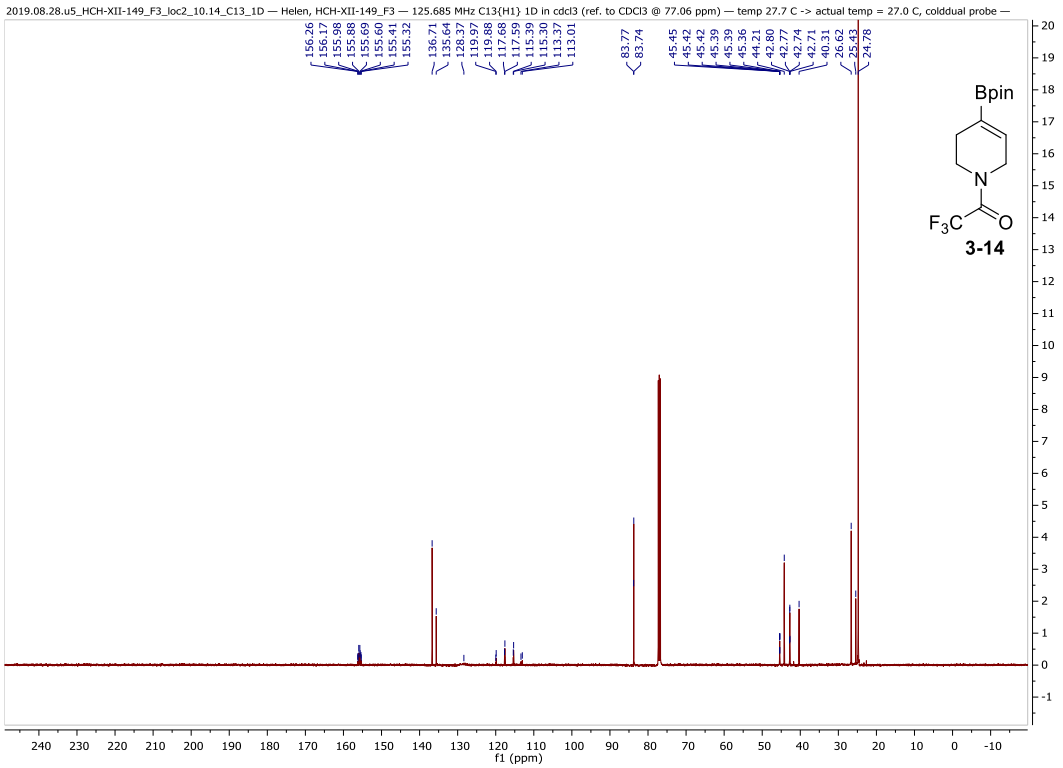

^{1}H NMR for pyranyl tolyl product **3-17** ($CDCl_3$, 500 MHz)

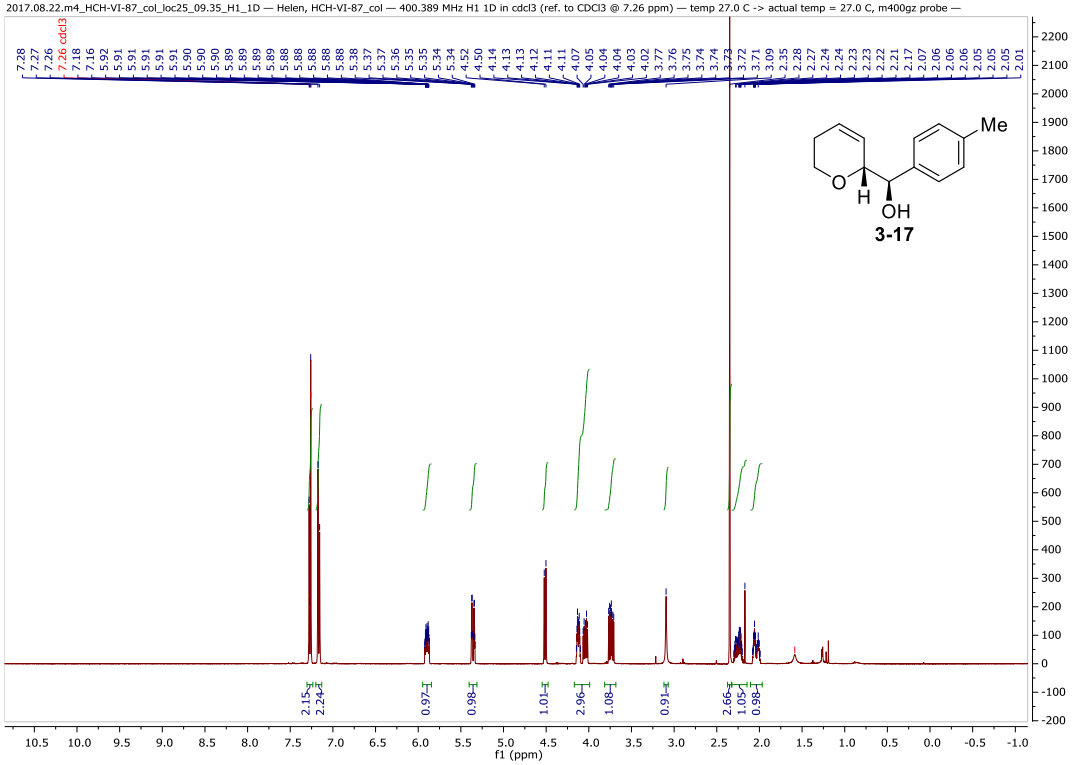

^{13}C NMR for pyranyl tolyl product **3-17** ($CDCl_3$, 126 MHz)

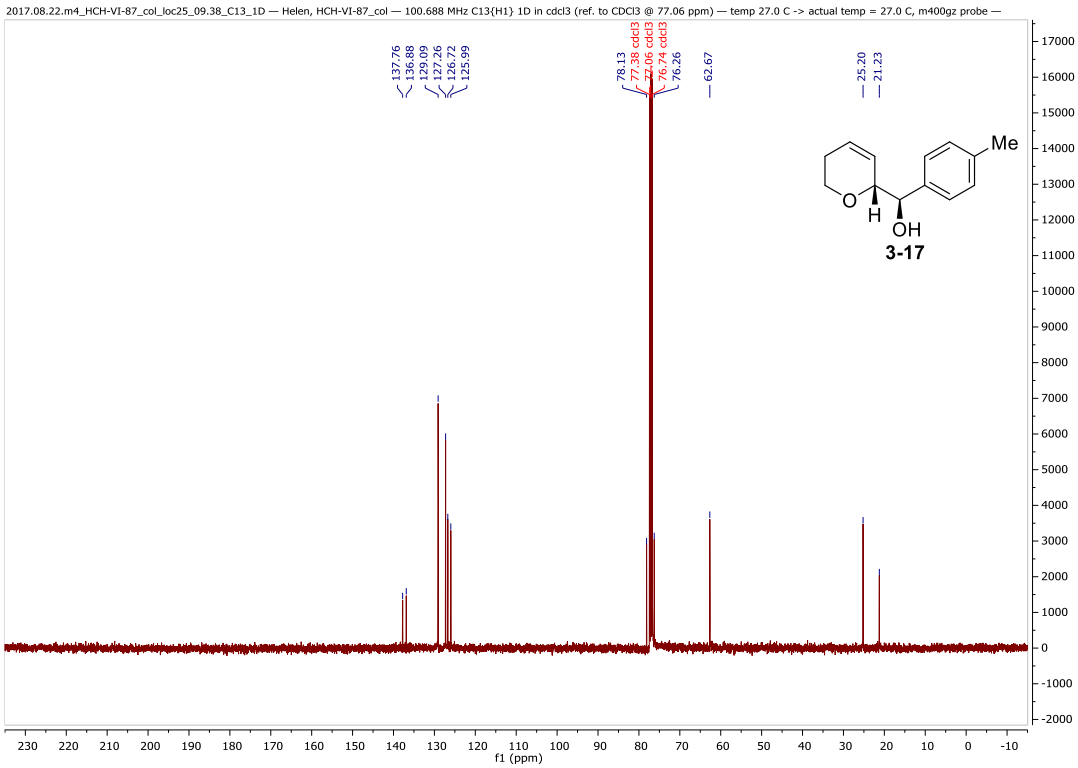

^{1}H NMR for cyclohexyl tolyl product **3-19** ($CDCl_3$, 500 MHz)

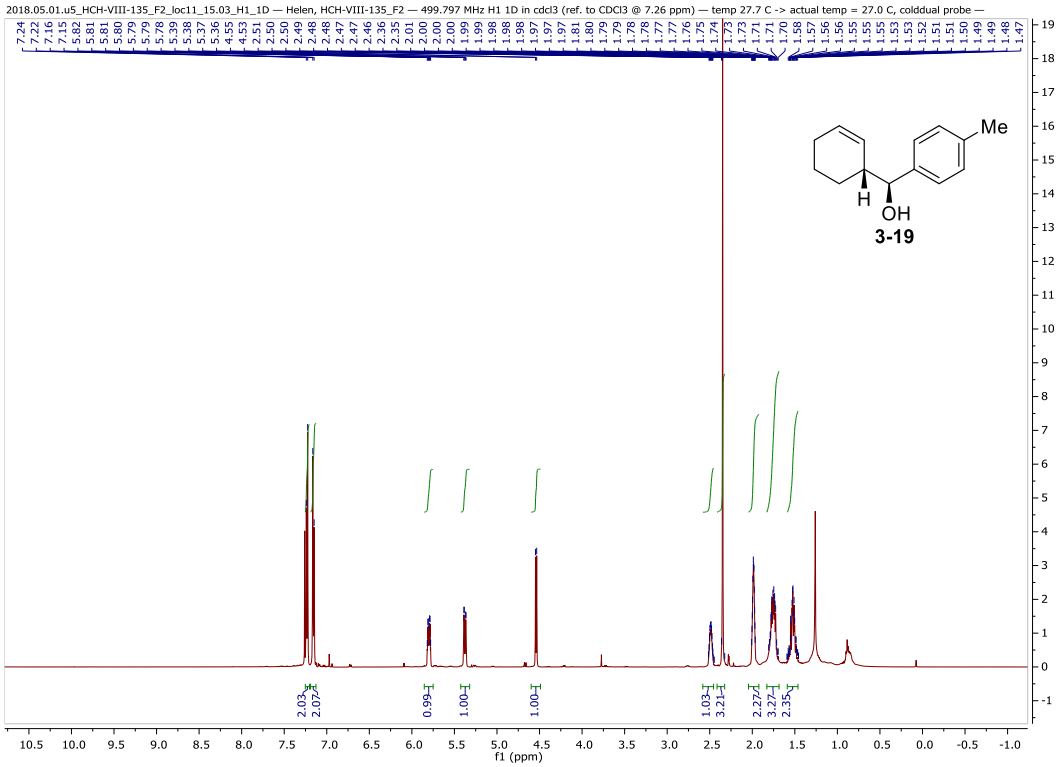

^{13}C NMR for cyclohexyl tolyl product **3-19** ($CDCl_3$, 126 MHz)

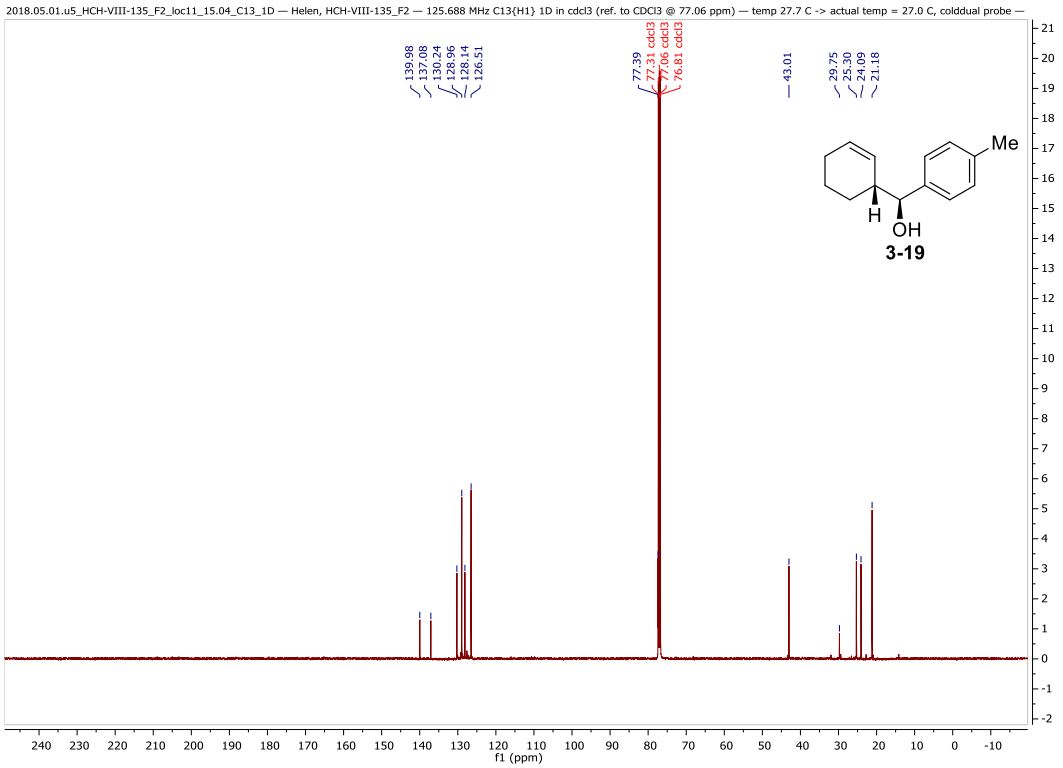

^{1}H NMR of cyclobutenone **4-1** ($CDCl_3$, 500 MHz)

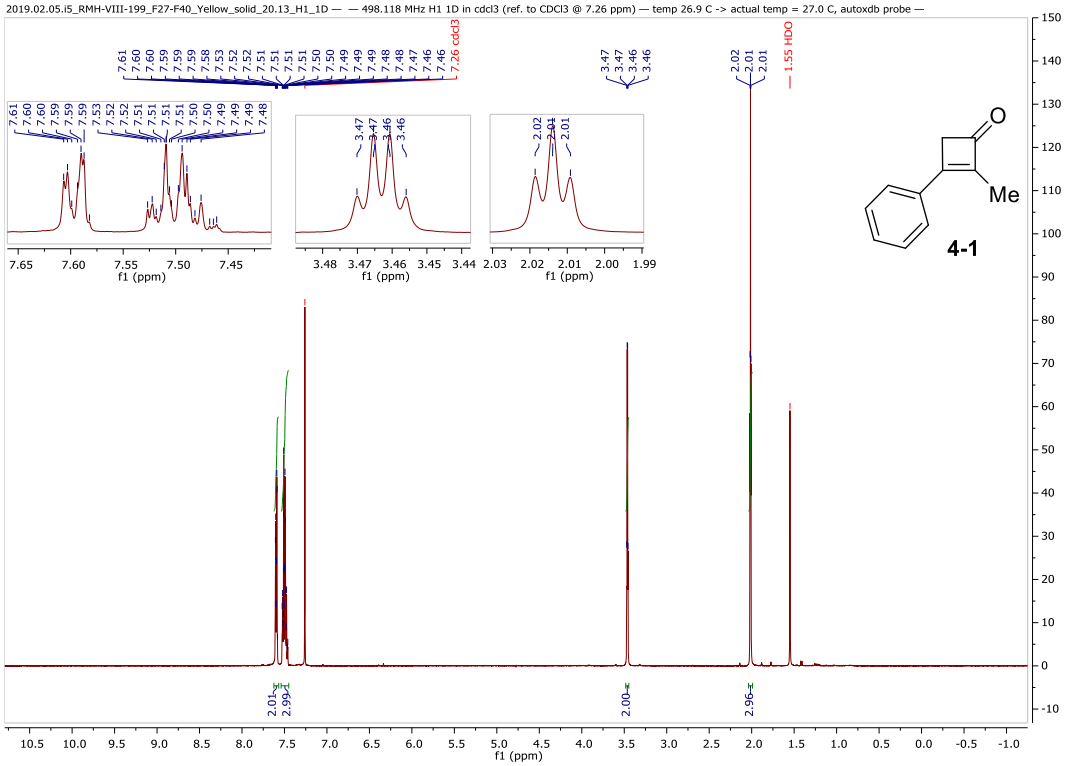

^{13}C NMR of cyclobutenone **4-1** ($CDCl_3$, 126 MHz)

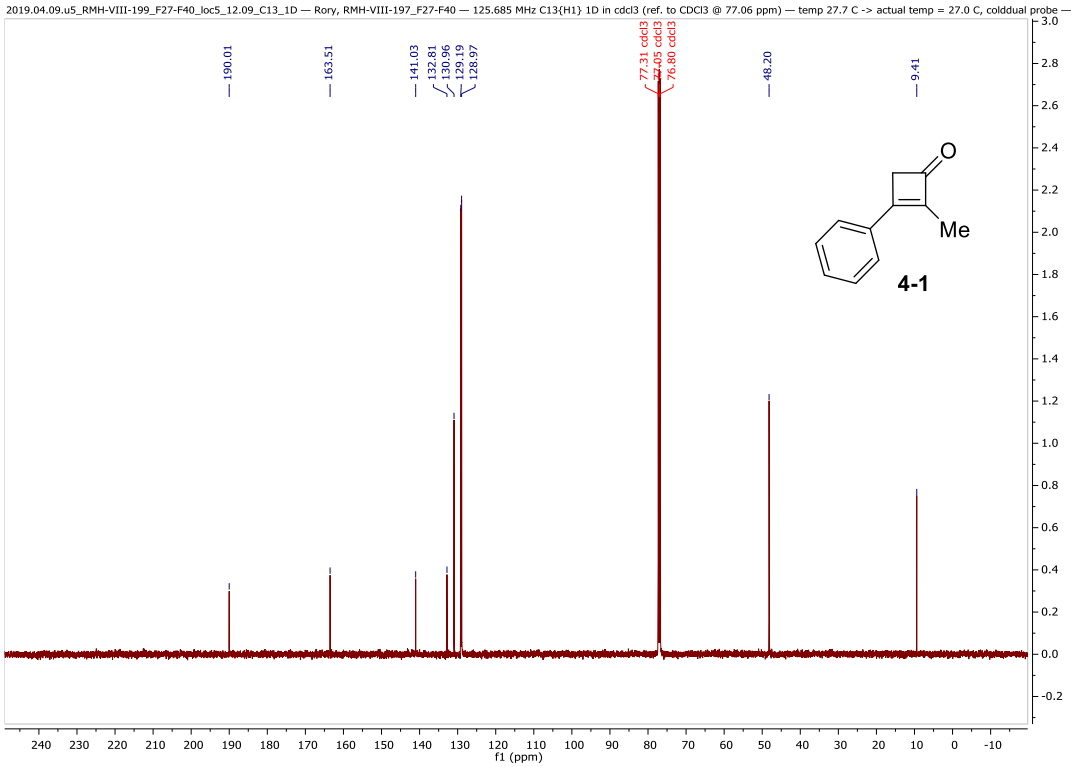

^{1}H NMR of cyclobutylboronate **4-24** ($CDCl_3$, 400 MHz)

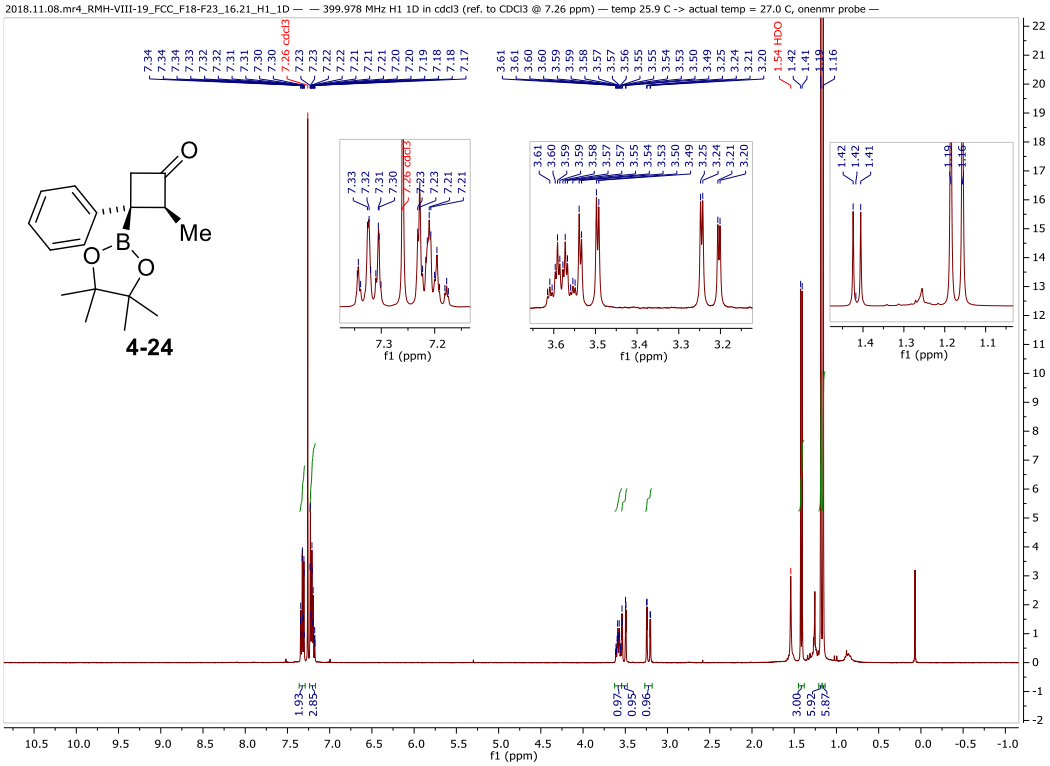

^{13}C NMR of cyclobutylboronate **4-24** ($CDCl_3$, 126 MHz)

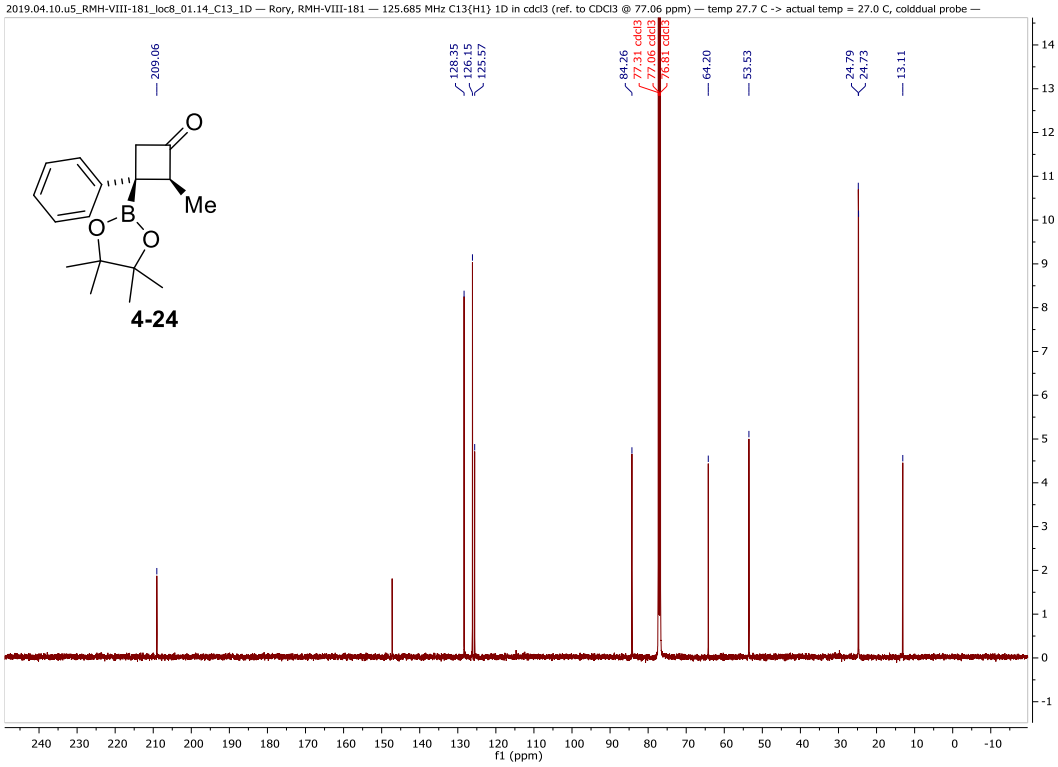

^{1}H NMR of alcohol **4-45** ($CDCl_3$, 400 MHz)

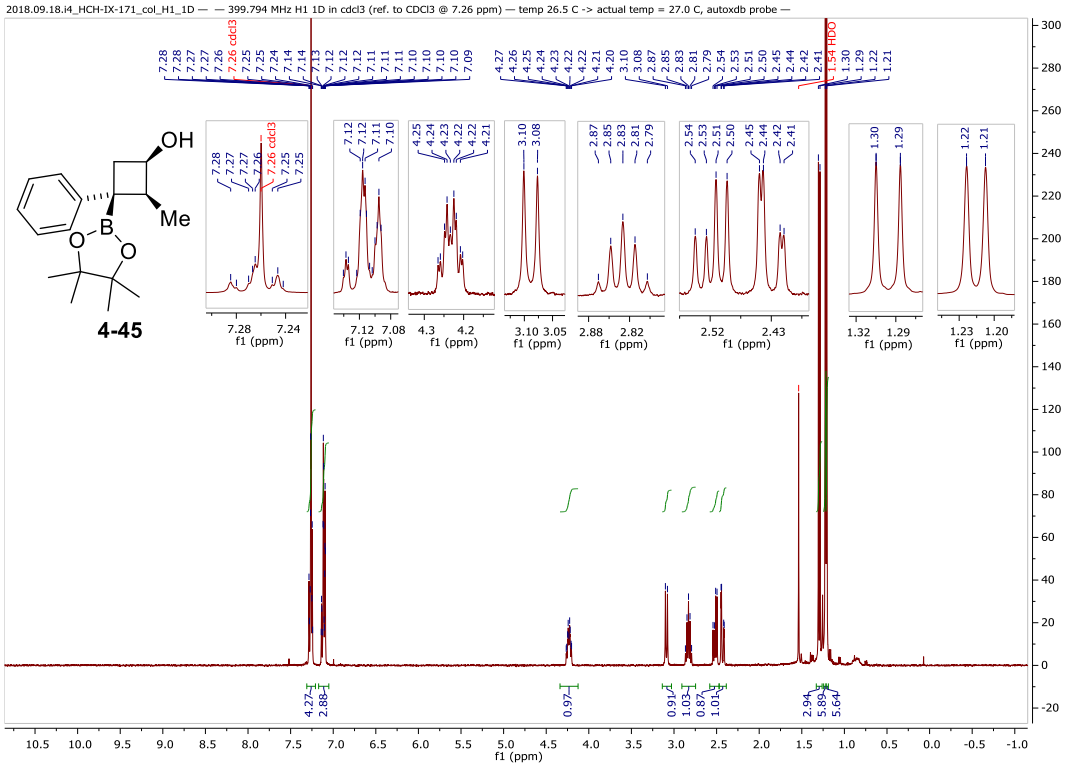

^{13}C NMR of alcohol **4-45** ($CDCl_3$, 126 MHz)

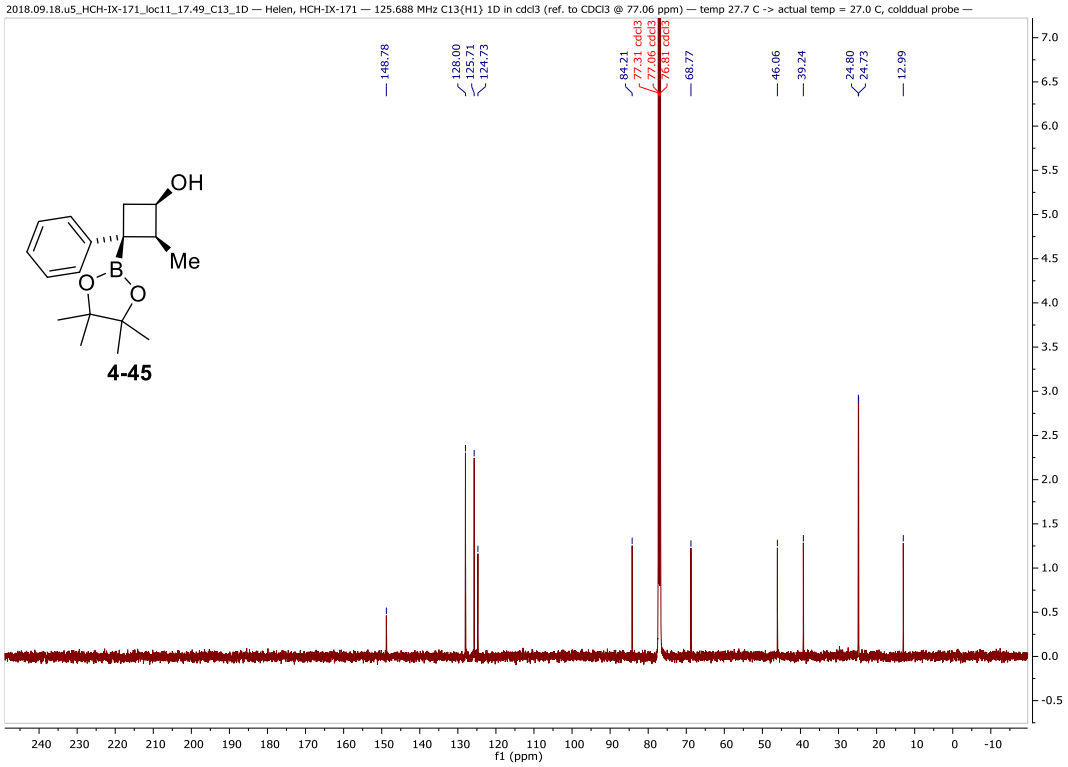

^{1}H NMR of tertiary alcohol **4-47** ($CDCl_3$, 500 MHz)

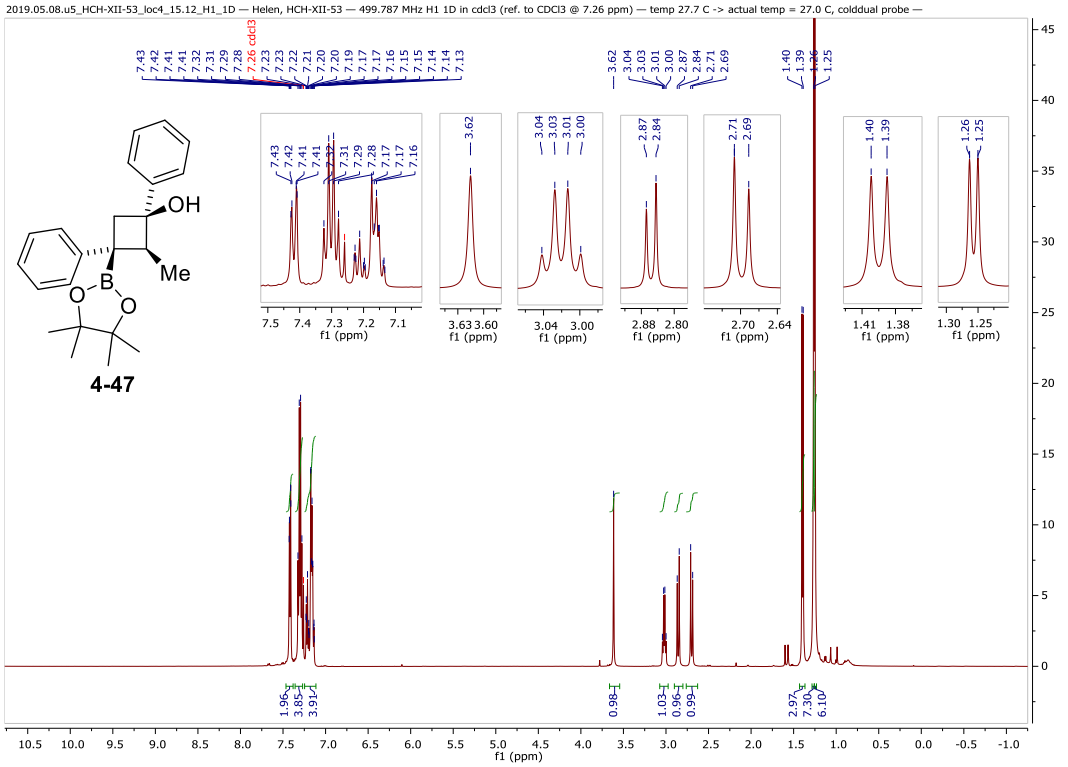

^{13}C NMR of tertiary alcohol **4-47** ($CDCl_3$, 126 MHz)

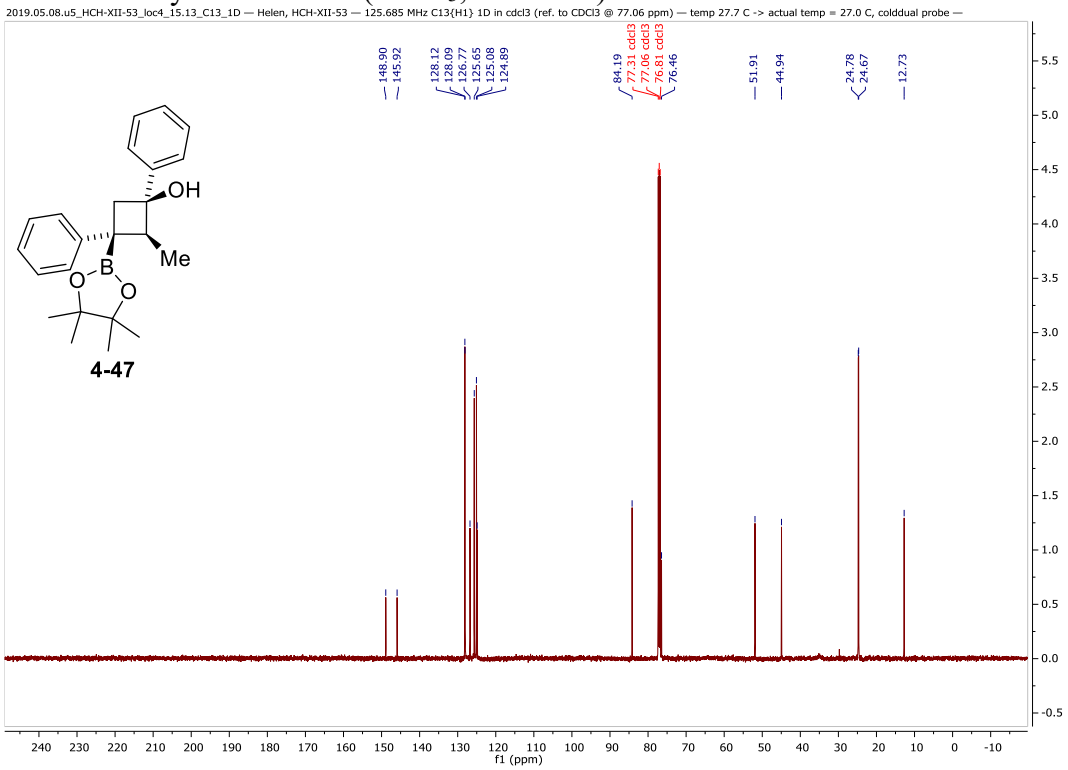

^{1}H NMR of diol **4-49** (d_6-Ac, 500 MHz)

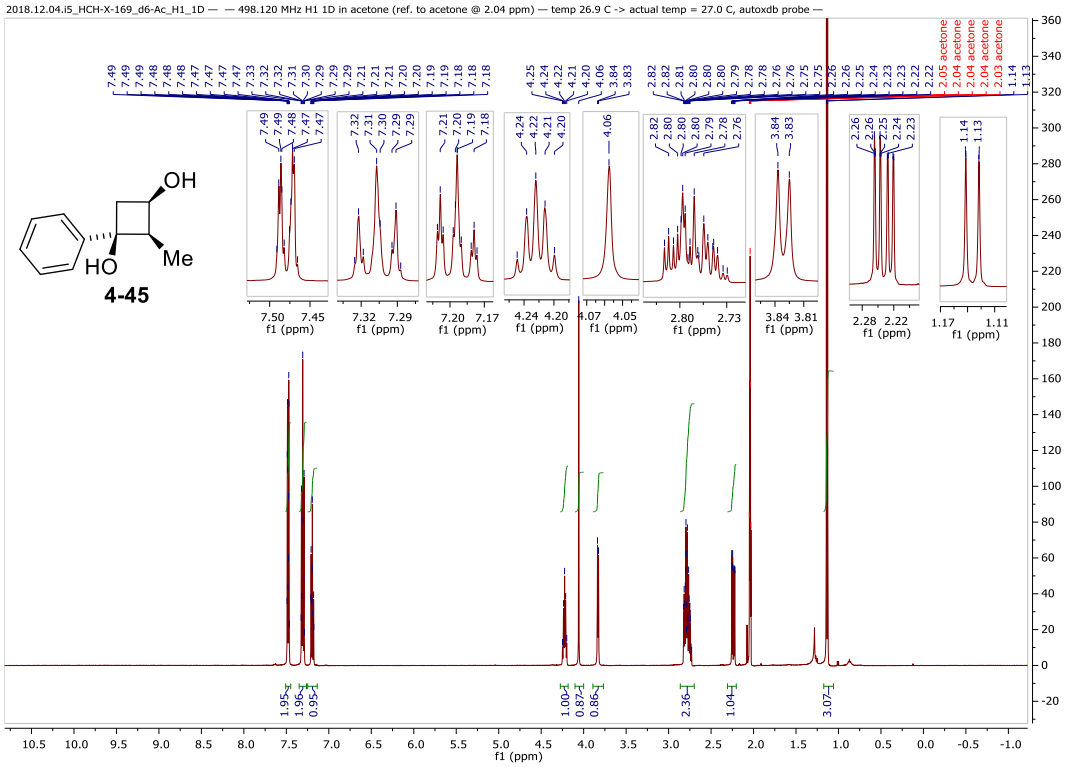

^{13}C NMR of diol **4-49** (d_6-Ac, 176 MHz)

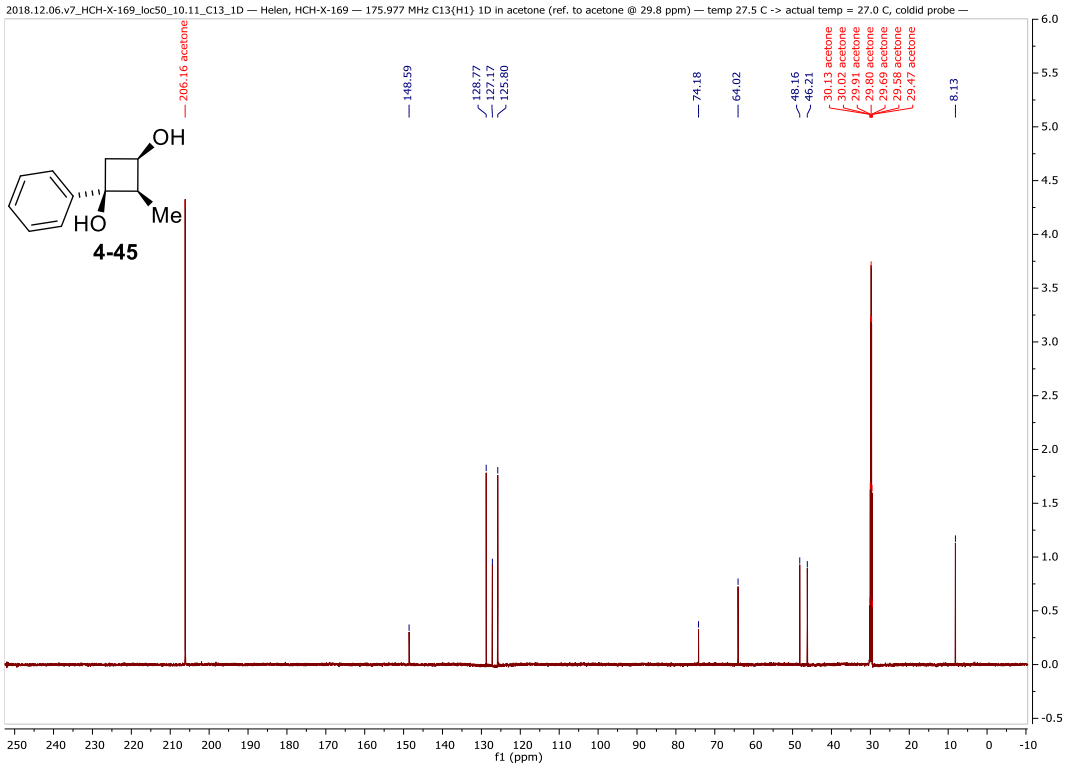

^{1}H NMR of *anti* disubstituted cyclobutanone **4-58** ($CDCl_3$, 500 MHz)

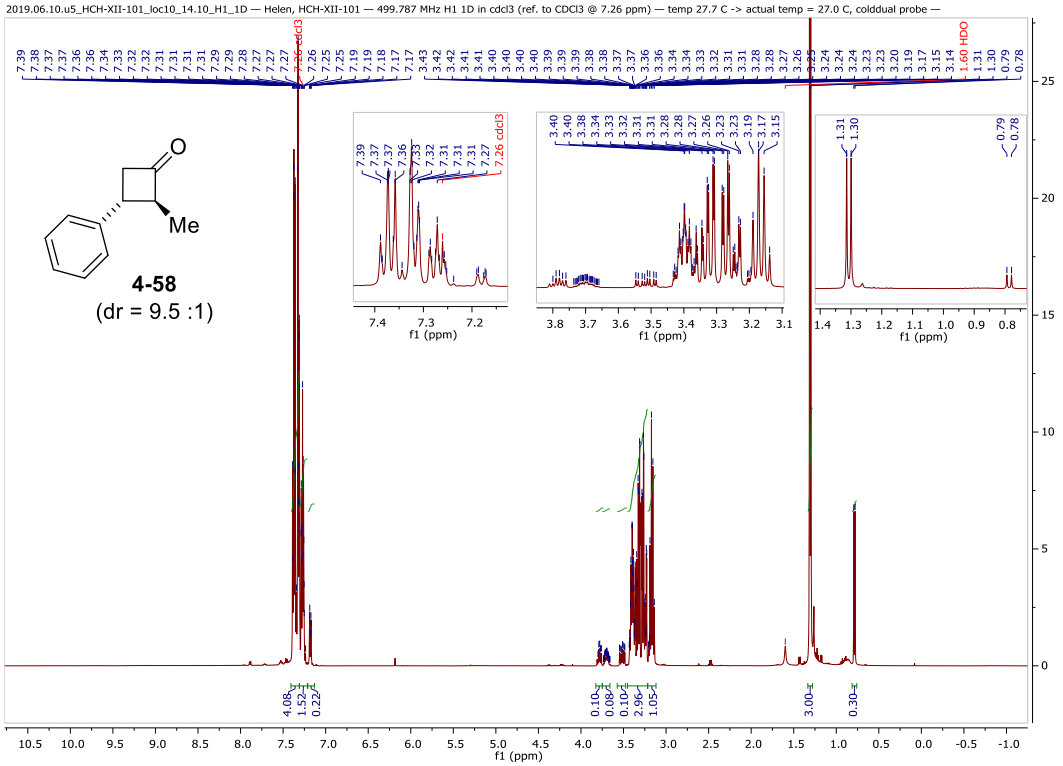

^{13}C NMR of *anti* disubstituted cyclobutanone **4-58** ($CDCl_3$, 126 MHz)

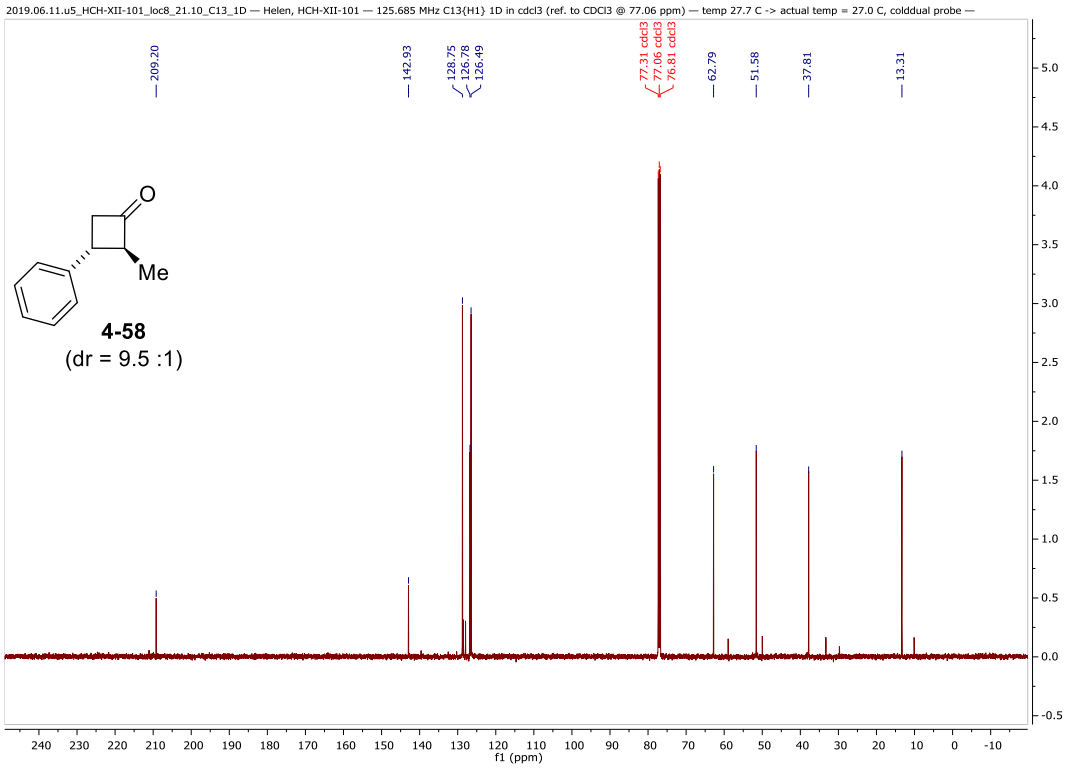

^{1}H NMR of ketal **4-52** ($CDCl_3$, 400 MHz)

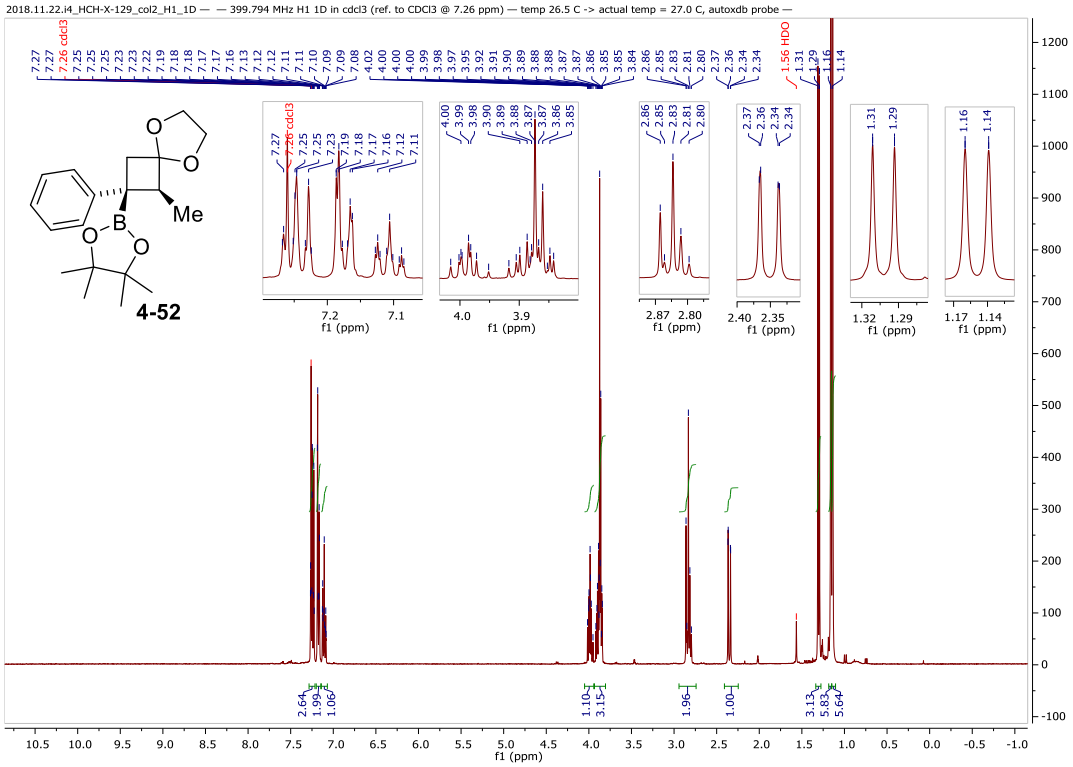

^{13}C NMR of ketal **4-52** ($CDCl_3$, 176 MHz)

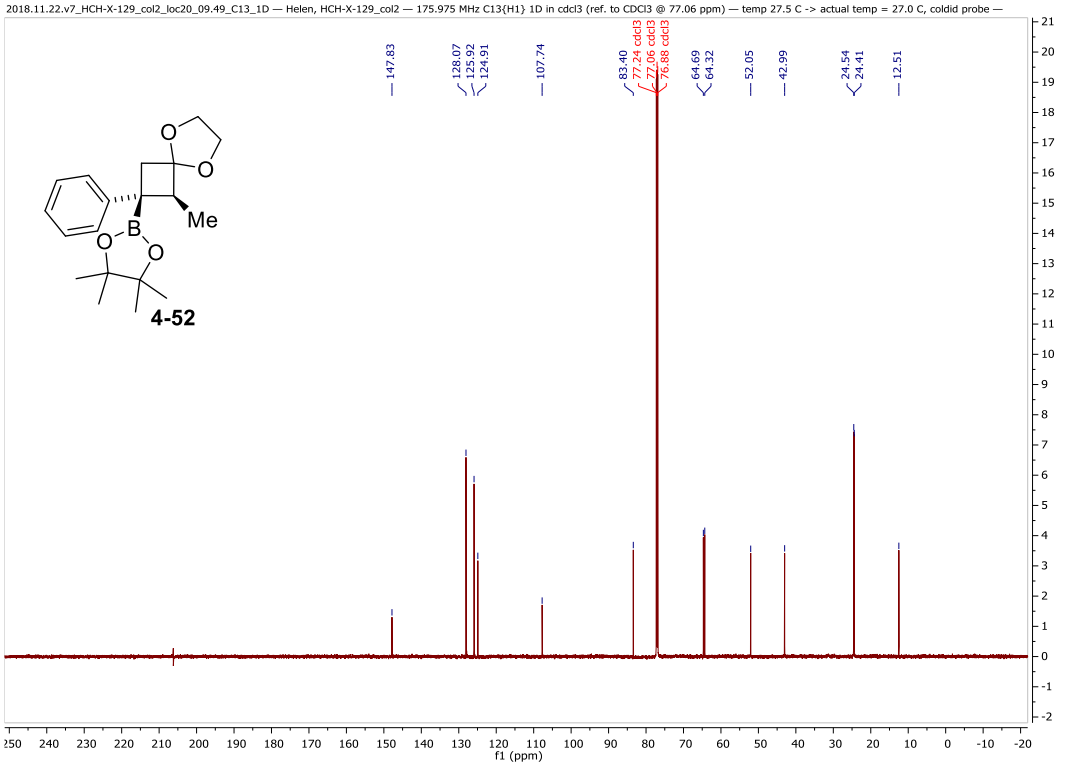

^{1}H NMR of olefin **4-53** ($CDCl_3$, 700 MHz)

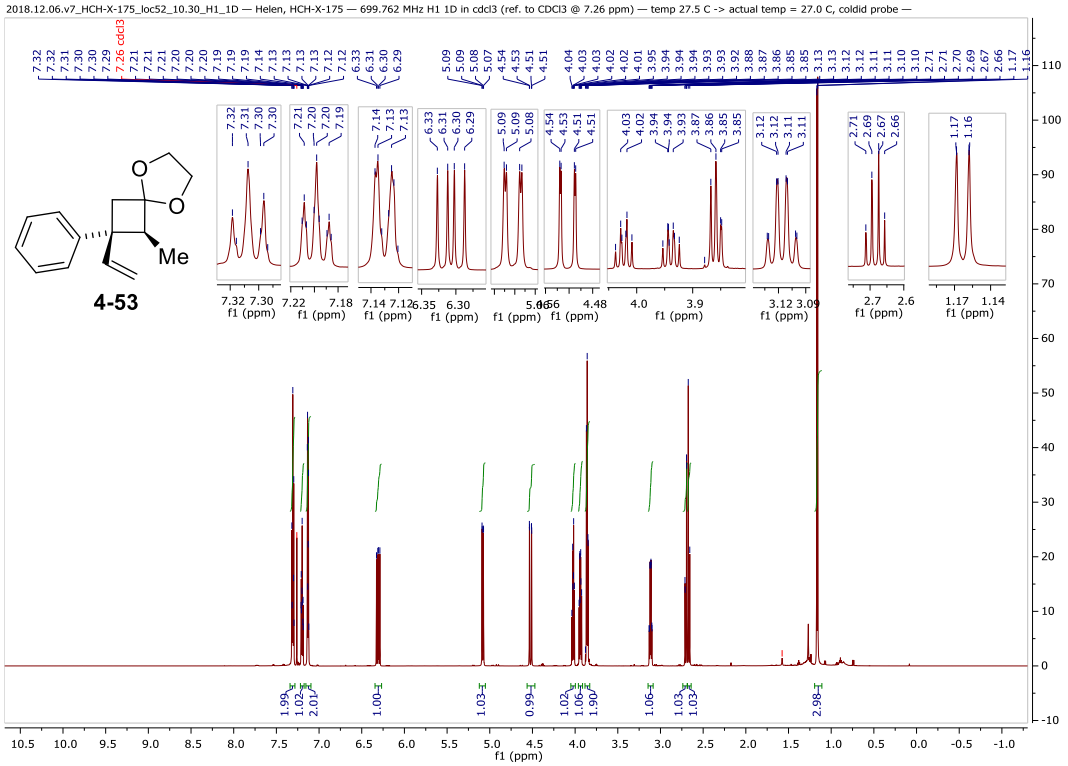

^{13}C NMR of olefin **4-53** ($CDCl_3$, 176 MHz)

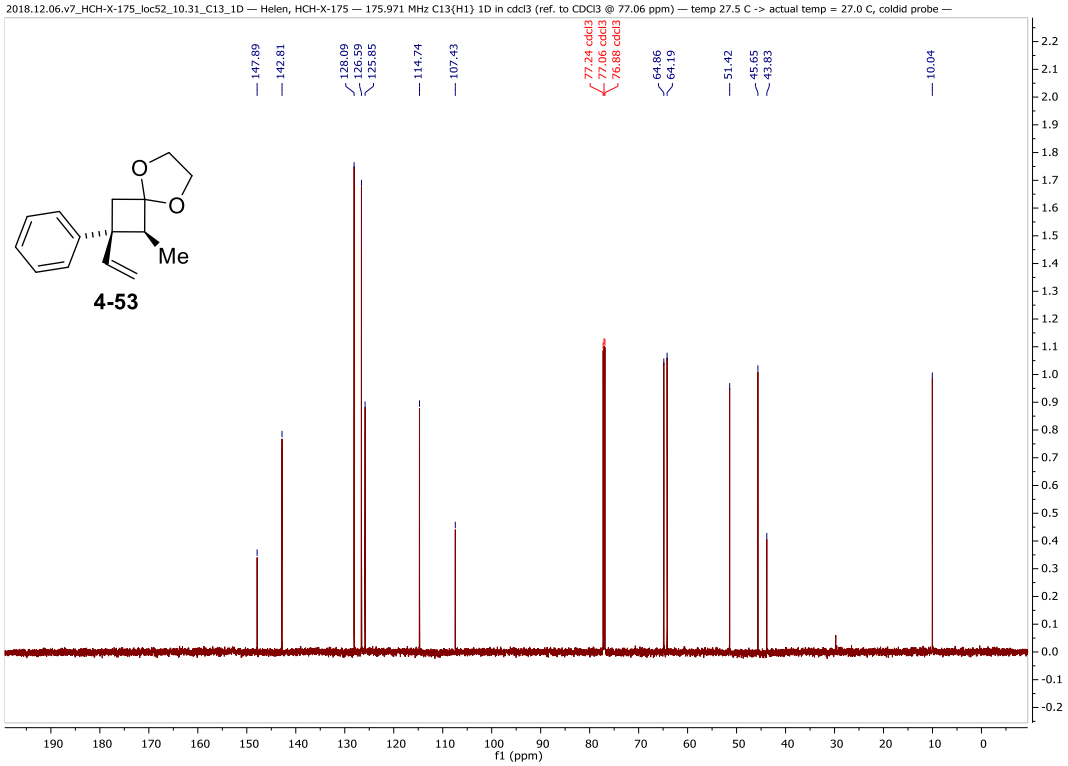

^{1}H NMR of cyclobutenoate **4-63** ($CDCl_3$, 500 MHz)

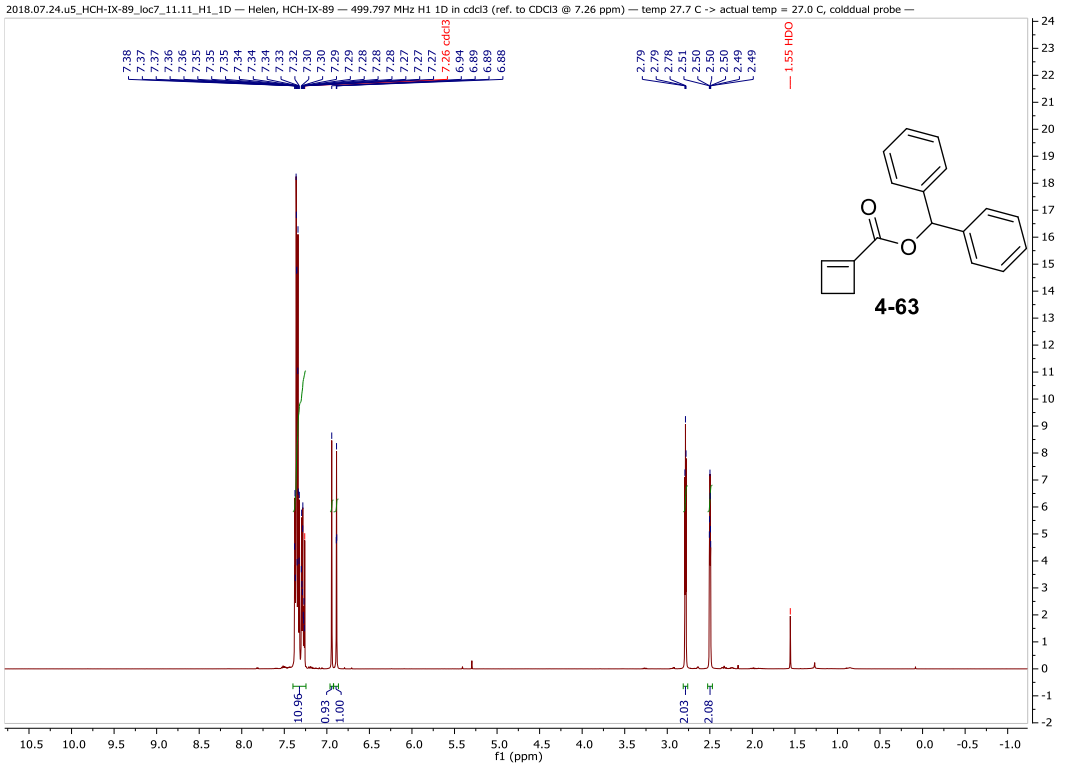

^{13}C NMR of cyclobutenoate **4-63** ($CDCl_3$, 126 MHz)

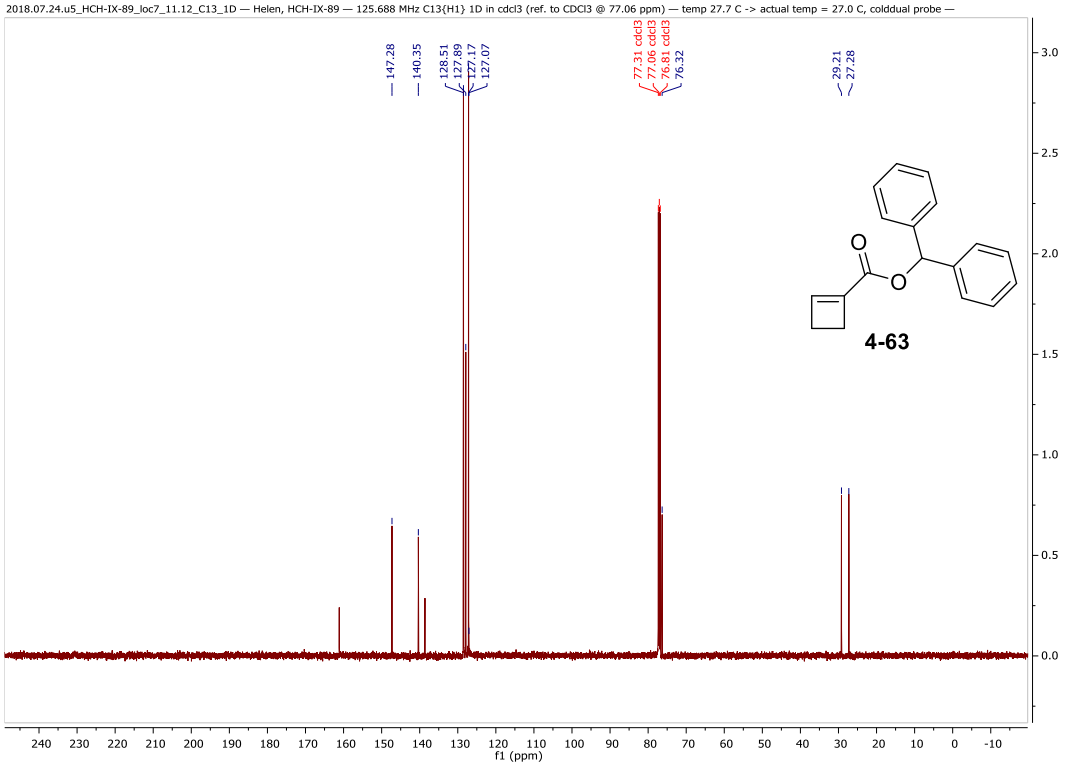

^{1}H NMR of cyclobutenoate **4-64** major diastereomer ($CDCl_3$, 500 MHz)

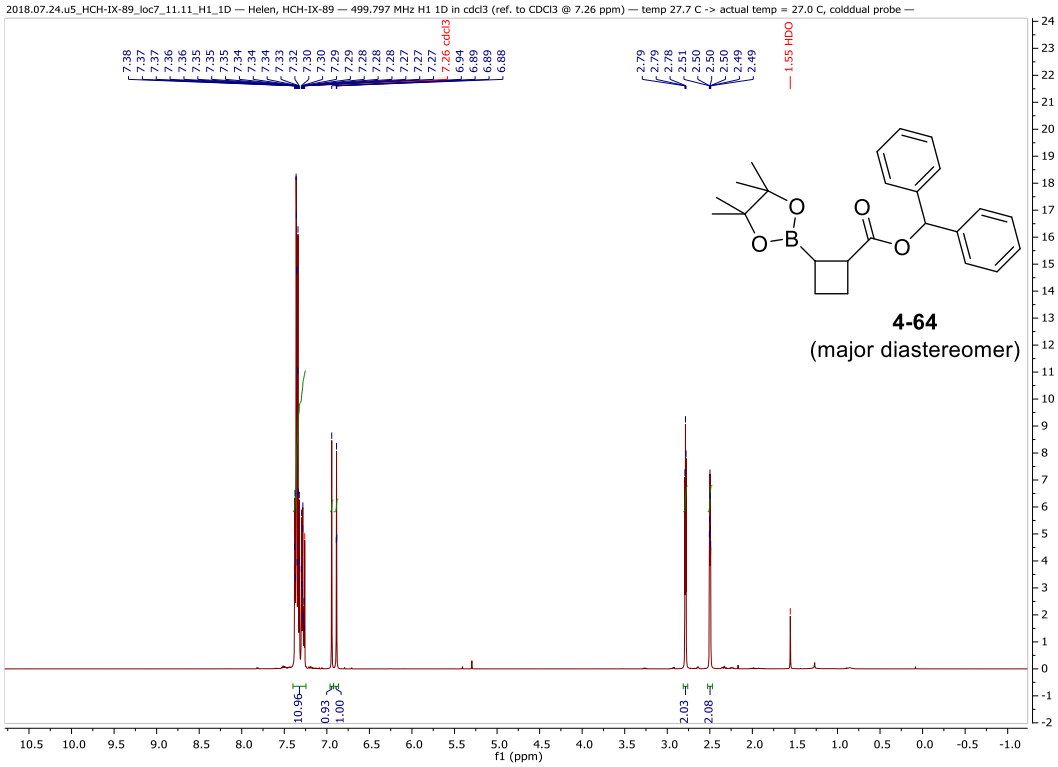

^{13}C NMR of cyclobutenoate **4-64** major diastereomer ($CDCl_3$, 176 MHz)

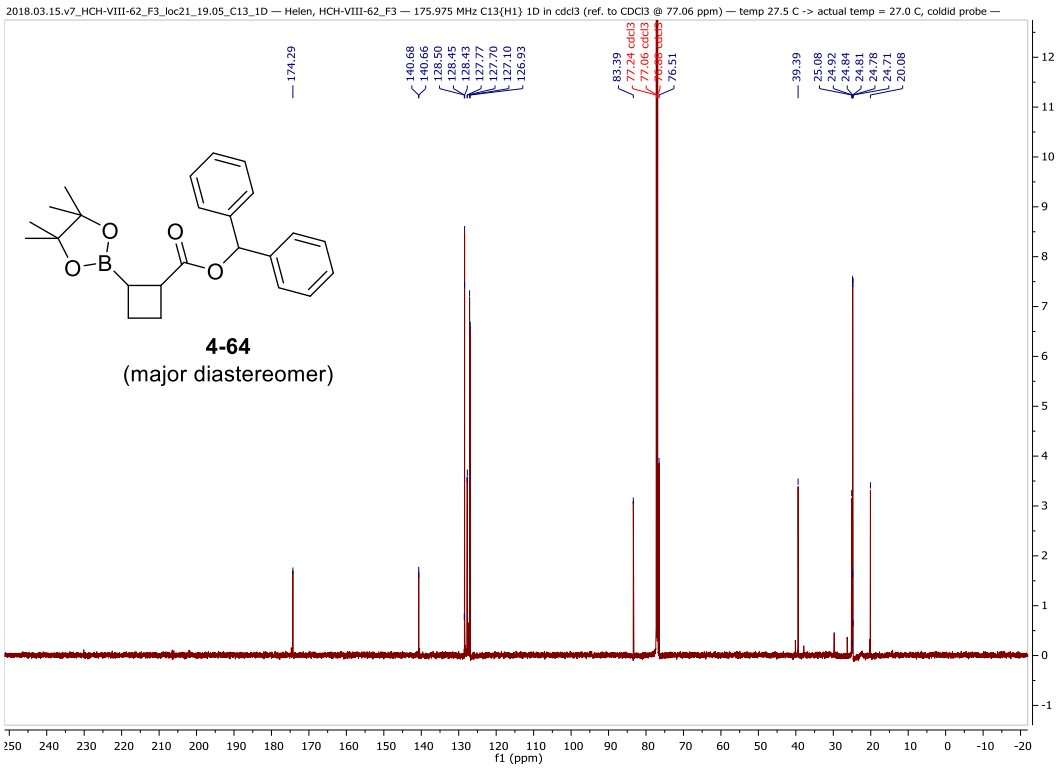

^{1}H NMR of cyclobutenoate **4-64** minor diastereomer (700 MHz)

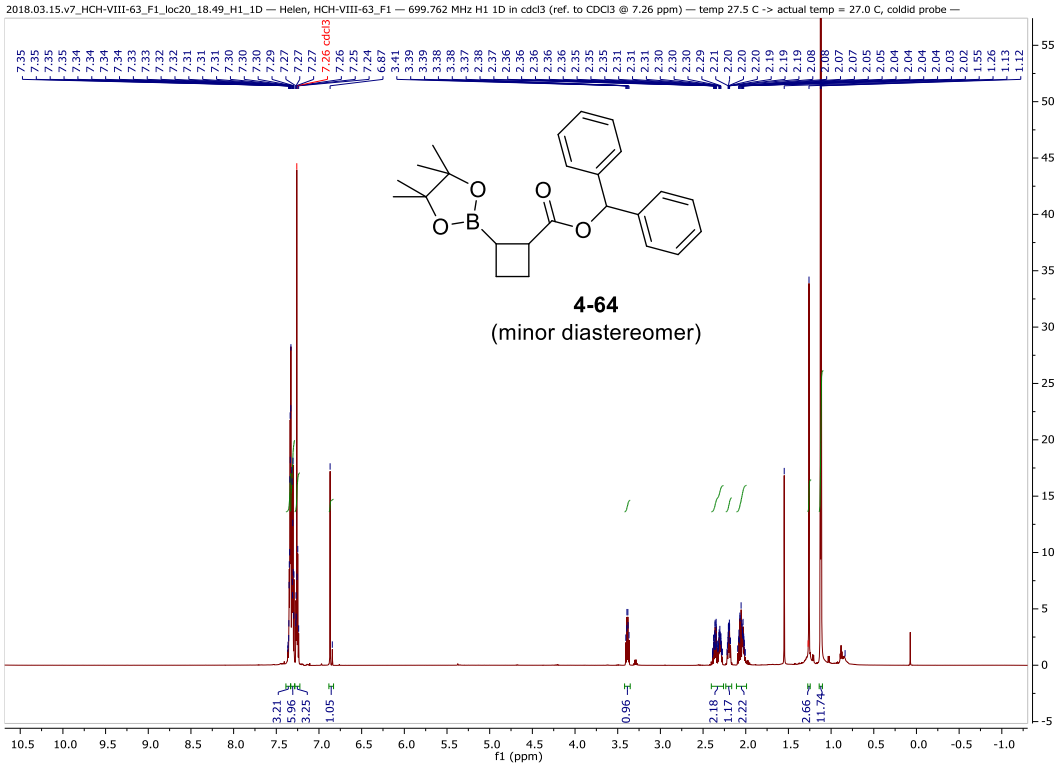

^{13}C NMR of cyclobutenoate **4-64** minor diastereomer (176 MHz)

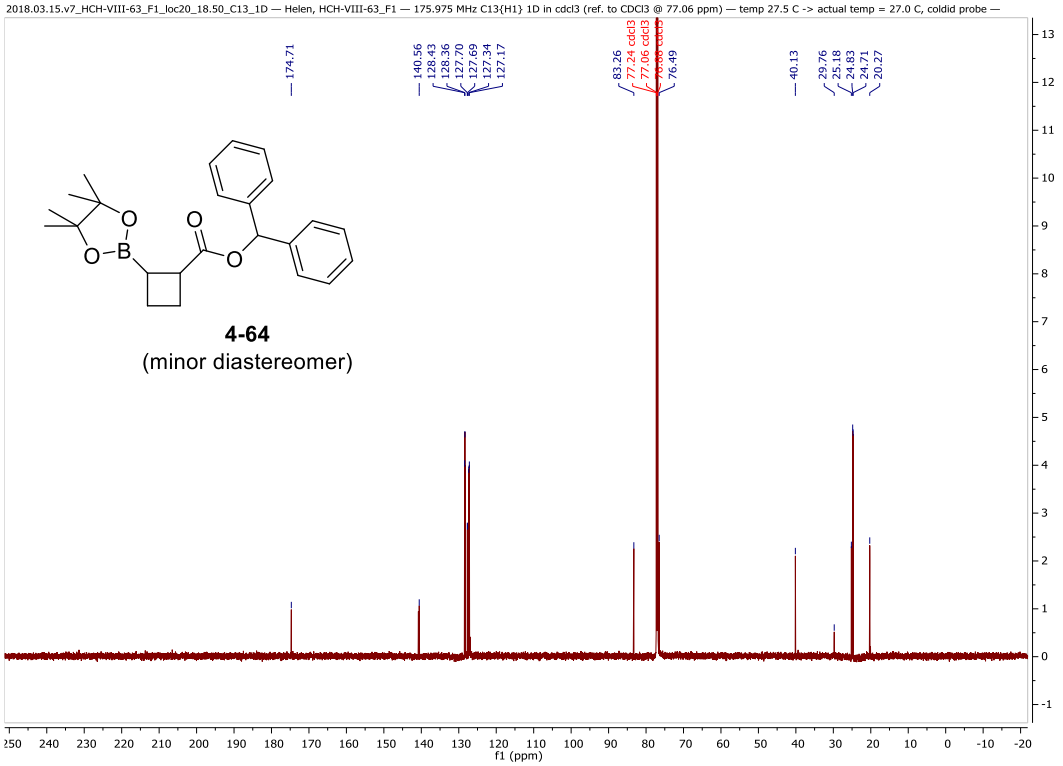

Appendix 2: Select chromatograms for HPLC measurements

HPLC data for racemic (top) and optically enriched (bottom) for compound **2-15**

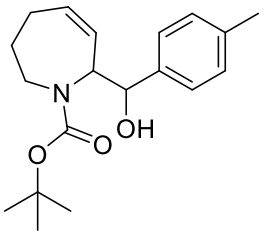

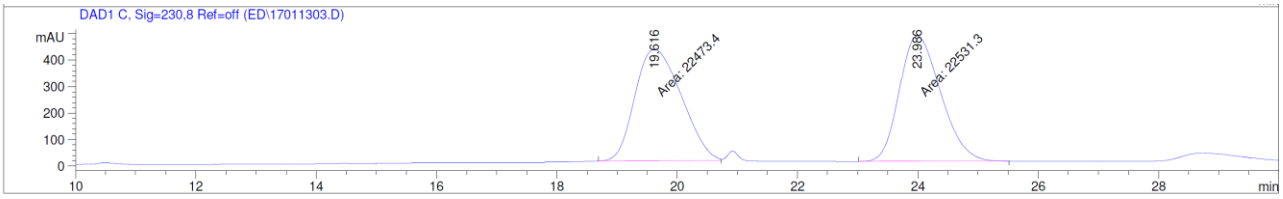

Signal 2: DAD1 C, Sig=230,8 Ref=off

Peak #	RetTime [min]	Type	Width [min]	Area [mAU*s]	Height [mAU]	Area %
1	19.616	MM	0.8926	2.24734e4	419.64597	49.9357
2	23.986	MM	0.7960	2.25313e4	471.75006	50.0643
Totals :				4.50047e4	891.39603	

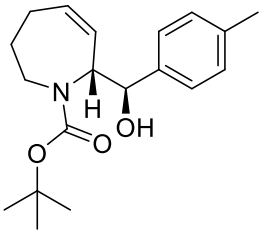

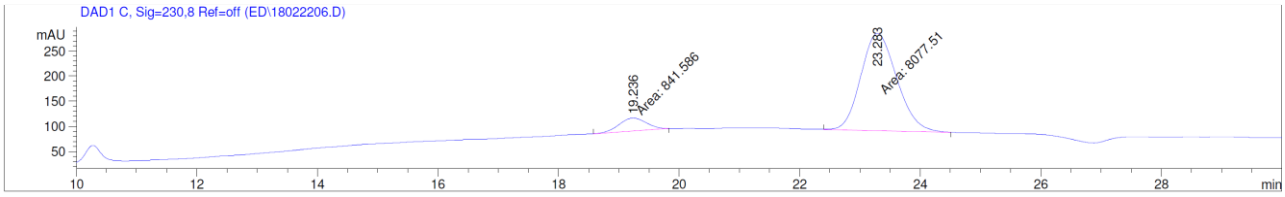

Signal 2: DAD1 C, Sig=230,8 Ref=off

Peak #	RetTime [min]	Type	Width [min]	Area [mAU*s]	Height [mAU]	Area %
1	19.236	MM	0.5373	841.58612	26.10493	9.4358
2	23.283	MM	0.6939	8077.51074	194.00479	90.5642
Totals :				8919.09686	220.10972	

Chromatogram for semi preparative HPLC purification of **2-39**

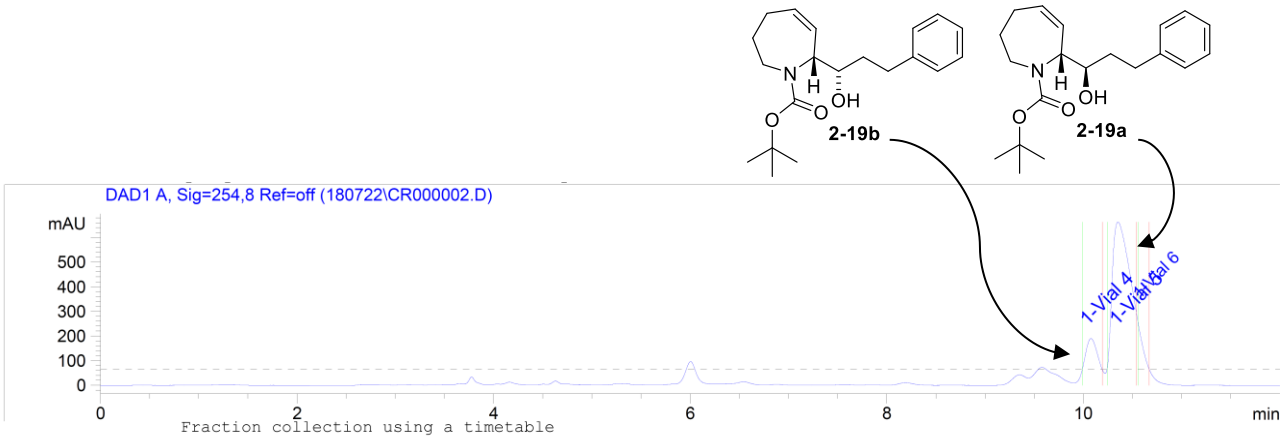

Fraction collection using a timetable

Frac #	Well #	Location	Volume [µl]	BeginTime [min]	EndTime [min]	Reason	Mass
1	1	1-Vial 4	620.00	9.9894	10.1910	DAD1	
2	1	1-Vial 5	908.13	10.2402	10.5379	DAD1	
3	1	1-Vial 6	364.37	10.5540	10.6704	DAD1	

HPLC trace for racemic **3-17** (top) and enantioenriched **3-17** (bottom)

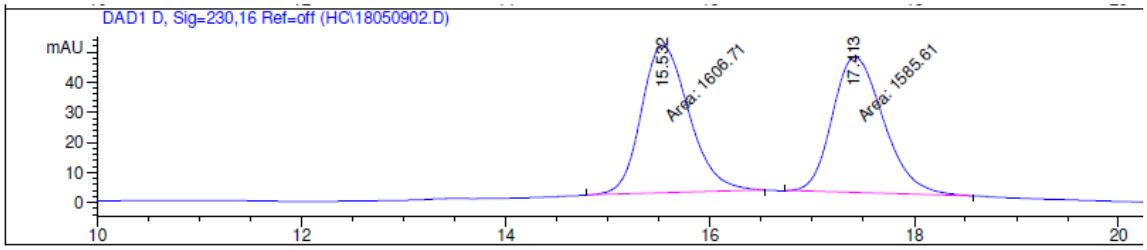


```
================================================================================
                            Area Percent Report
================================================================================
Signal 2: DAD1 D, Sig=230,16 Ref=off

Peak RetTime Type  Width     Area      Height     Area
  #   [min]        [min]   [mAU*s]     [mAU]       %
----|-------|----|-------|----------|----------|--------|
   1  15.532 MM    0.5436 1606.70898   49.25897  50.3305
   2  17.413 MM    0.5840 1585.60681   45.25505  49.6695
```

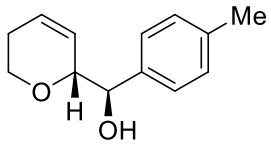

(±)-3-17

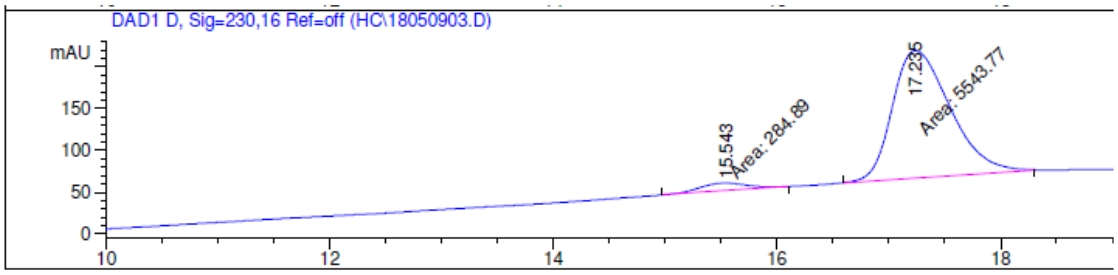


```
================================================================================
                            Area Percent Report
================================================================================
Signal 2: DAD1 D, Sig=230,16 Ref=off

Peak RetTime Type  Width     Area      Height     Area
  #   [min]        [min]   [mAU*s]     [mAU]       %
----|-------|----|-------|----------|----------|--------|
   1  15.543 MM    0.5045  284.89005    9.41219   4.8877
   2  17.235 MM    0.6025 5543.77490  153.34457  95.1123
```

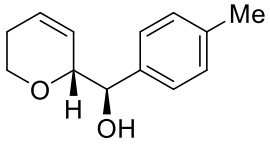

3-17

HPLC trace for racemic **3-19** (top) and enantioenriched **3-19** (bottom)

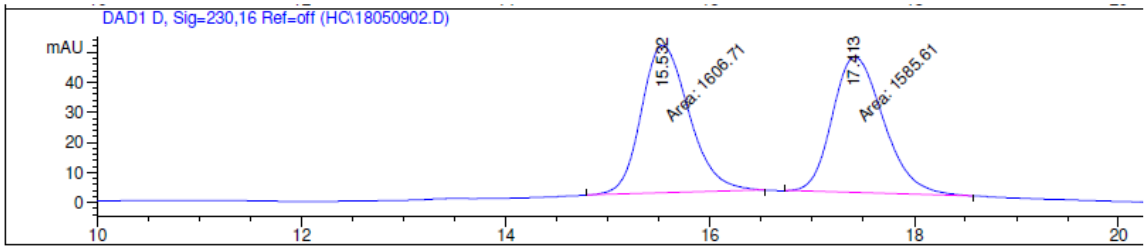


```
================================================================================
                            Area Percent Report
================================================================================
Signal 2: DAD1 D, Sig=230,16 Ref=off

Peak RetTime Type  Width     Area      Height     Area
  #   [min]        [min]   [mAU*s]     [mAU]       %
----|-------|----|-------|----------|----------|--------|
   1  15.532 MM    0.5436 1606.70898   49.25897  50.3305
   2  17.413 MM    0.5840 1585.60681   45.25505  49.6695
```

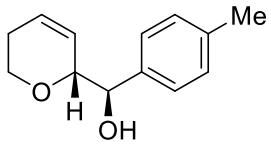

(±)-3-17

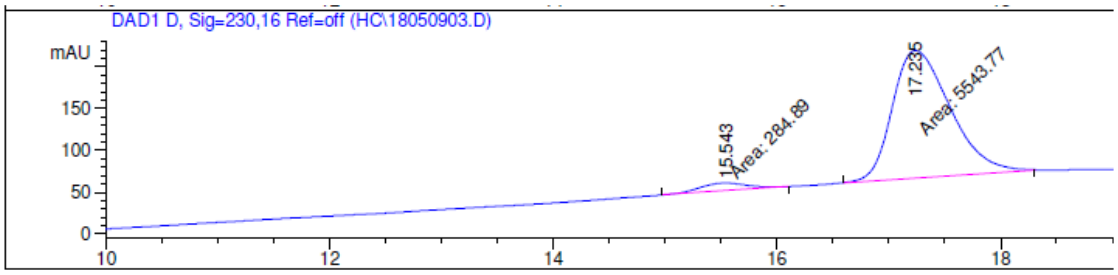


```
================================================================================
                            Area Percent Report
================================================================================
Signal 2: DAD1 D, Sig=230,16 Ref=off

Peak RetTime Type  Width     Area      Height     Area
  #   [min]        [min]   [mAU*s]     [mAU]       %
----|-------|----|-------|----------|----------|--------|
   1  15.543 MM    0.5045  284.89005    9.41219   4.8877
   2  17.235 MM    0.6025 5543.77490  153.34457  95.1123
```

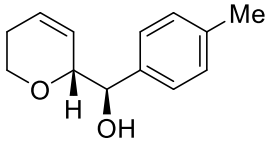

3-17

HPLC trace for racemic **4-24** (top) and enantioenriched **4-24** (bottom)

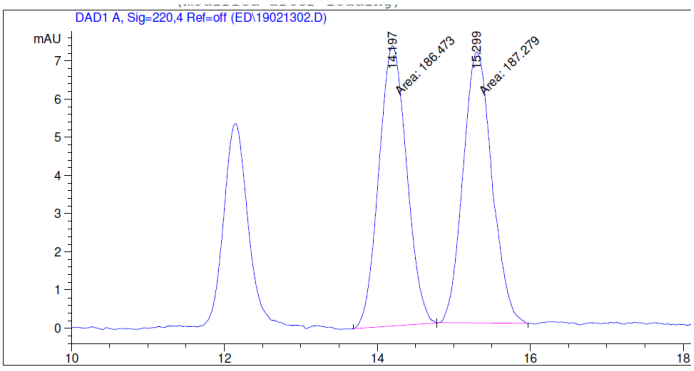

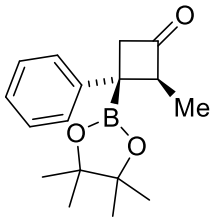

(±)-4-24

```
================================================================================
                            Area Percent Report
================================================================================

Sorted By             :      Signal
Multiplier            :      1.0000
Dilution              :      1.0000
Use Multiplier & Dilution Factor with ISTDs


Signal 1: DAD1 A, Sig=220,4 Ref=off

  Peak RetTime Type  Width     Area      Height     Area
    #   [min]        [min]   [mAU*s]     [mAU]       %
  ----|-------|----|-------|----------|----------|--------|
     1  14.197 MM    0.4234  186.47258    7.34037  49.8922
     2  15.299 MM    0.4393  187.27870    7.10538  50.1078

  Totals :                   373.75128   14.44575
```

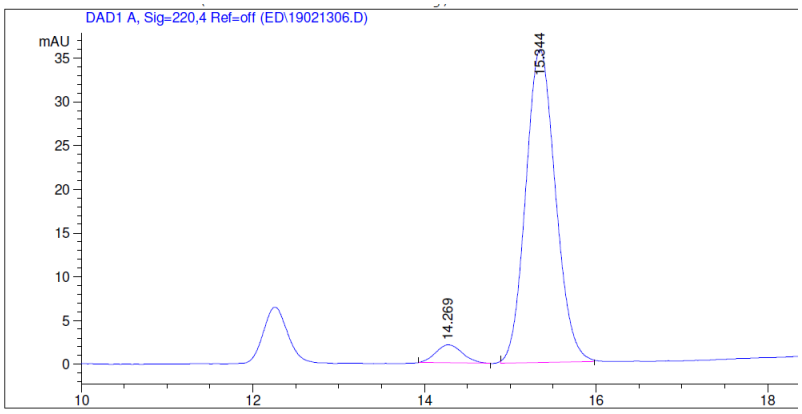

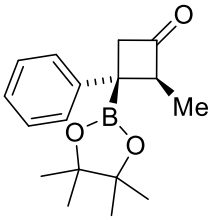

4-24

```
================================================================================
                            Area Percent Report
================================================================================

Sorted By             :      Signal
Multiplier            :      1.0000
Dilution              :      1.0000
Use Multiplier & Dilution Factor with ISTDs


Signal 1: DAD1 A, Sig=220,4 Ref=off

  Peak RetTime Type  Width     Area      Height     Area
    #   [min]        [min]   [mAU*s]     [mAU]       %
  ----|-------|----|-------|----------|----------|--------|
     1  14.269 BP    0.3079   44.85875    2.07745   4.9351
     2  15.344 BB    0.3715  864.11157   35.80891  95.0649

  Totals :                   908.97032   37.88637
```

HPLC trace for racemic **4-30** (top) and enantioenriched **4-30** (bottom)

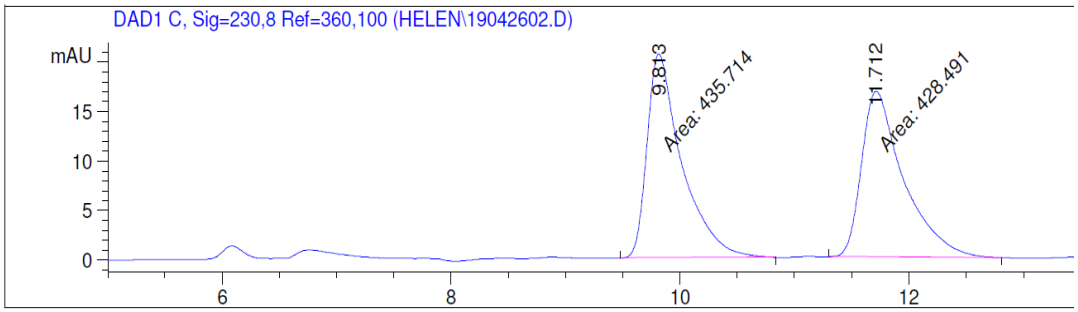


```
=====================================================================
                      Area Percent Report
=====================================================================

Sorted By             :      Signal
Multiplier            :      1.0000
Dilution              :      1.0000
Use Multiplier & Dilution Factor with ISTDs

Signal 2: DAD1 C, Sig=230,8 Ref=360,100

 Peak RetTime Type  Width     Area      Height     Area
   #   [min]        [min]   [mAU*s]     [mAU]       %
----|-------|----|-------|----------|----------|--------|
   1   9.813 MM    0.3520  435.71402   20.62930  50.4179
   2  11.712 MM    0.4267  428.49100   16.73705  49.5821

 Totals :                  864.20502   37.36635
```

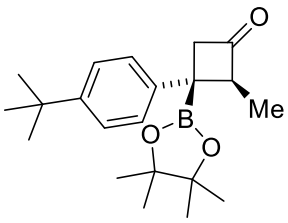

(±)-4-30

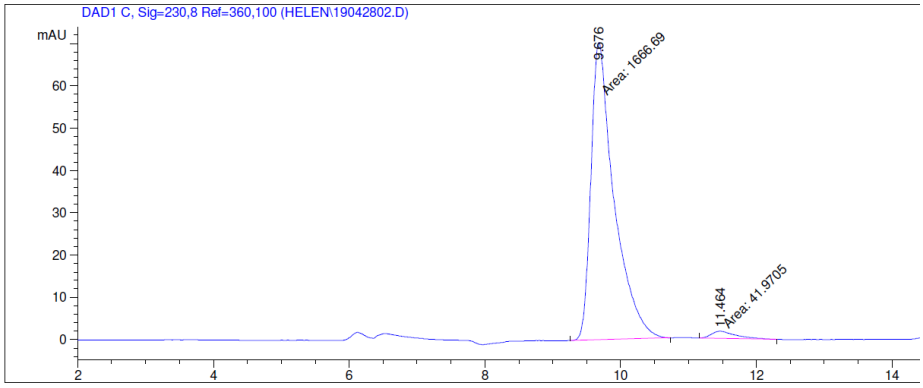


```
=====================================================================
                      Area Percent Report
=====================================================================

Sorted By             :      Signal
Multiplier            :      1.0000
Dilution              :      1.0000
Use Multiplier & Dilution Factor with ISTDs


Signal 1: DAD1 C, Sig=230,8 Ref=360,100

 Peak RetTime Type  Width     Area      Height     Area
   #   [min]        [min]   [mAU*s]     [mAU]       %
----|-------|----|-------|----------|----------|--------|
   1   9.676 MM    0.3950 1666.69250   70.31990  97.5437
   2  11.464 MM    0.4154   41.97052    1.68409   2.4563

 Totals :                 1708.66303   72.00399
```

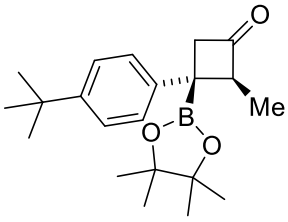

4-30

HPLC trace for racemic **4-33** (top) and enantioenriched **4-33** (bottom)

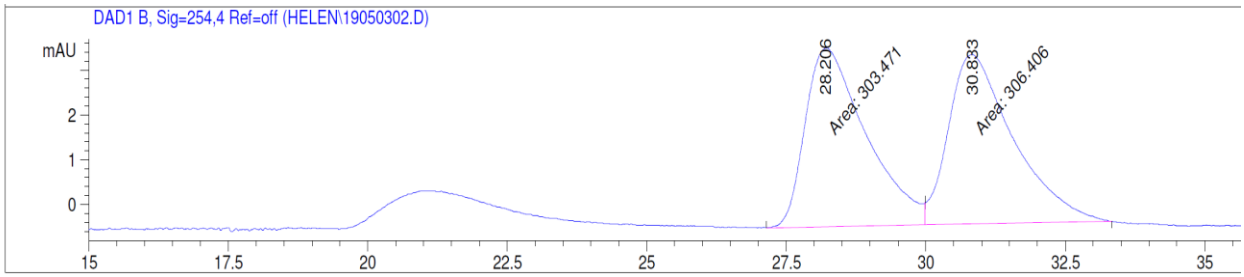


```
=====================================================================
                      Area Percent Report
=====================================================================

Sorted By             :      Signal
Multiplier            :      1.0000
Dilution              :      1.0000
Use Multiplier & Dilution Factor with ISTDs

 Signal 2: DAD1 B, Sig=254,4 Ref=off

 Peak RetTime Type  Width     Area      Height     Area
   #   [min]       [min]   [mAU*s]     [mAU]       %
----|-------|----|-------|----------|----------|--------|
   1  28.206 MF    1.2674  303.47095    3.99082  49.7594
   2  30.833 FM    1.3469  306.40610    3.79164  50.2406

 Totals :                  609.87704    7.78246
```

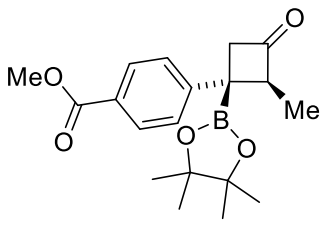

(±)-4-33

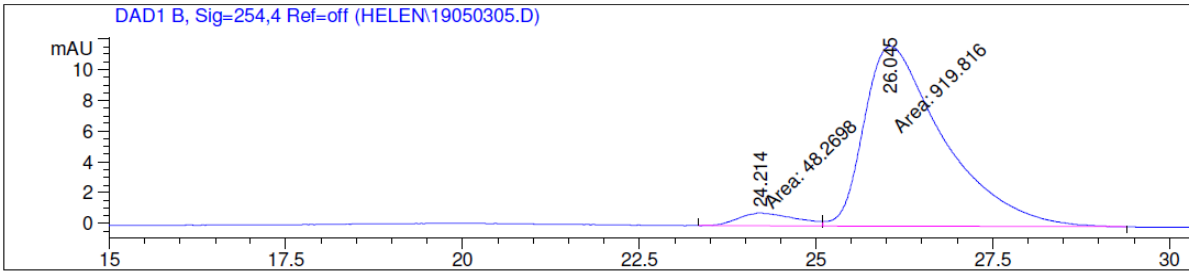


```
=====================================================================
                      Area Percent Report
=====================================================================

Sorted By             :      Signal
Multiplier            :      1.0000
Dilution              :      1.0000
Use Multiplier & Dilution Factor with ISTDs

 Signal 2: DAD1 B, Sig=254,4 Ref=off

 Peak RetTime Type  Width     Area      Height     Area
   #   [min]       [min]   [mAU*s]     [mAU]       %
----|-------|----|-------|----------|----------|--------|
   1  24.214 MF    0.9598   48.26979 8.38206e-1   4.9861
   2  26.045 FM    1.3080  919.81616   11.72012  95.0139

 Totals :                  968.08595   12.55832
```

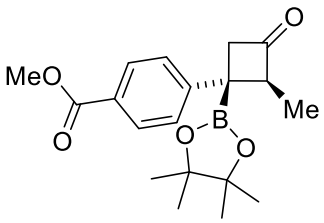

4-33

HPLC trace for racemic **4-42** (top) and enantioenriched **4-42** (bottom)

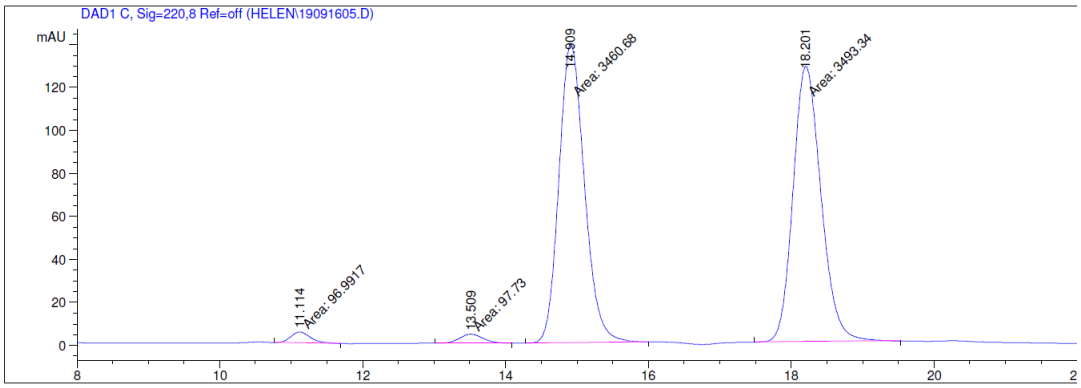


```
================================================================================
                          Area Percent Report
================================================================================

Signal 1: DAD1 C, Sig=220,8 Ref=off

Peak RetTime Type  Width     Area      Height     Area
  #   [min]        [min]   [mAU*s]     [mAU]      %
----|-------|----|-------|----------|----------|--------|
   1  11.114 MM    0.3203   96.99172    5.04744   1.3568
   2  13.509 MM    0.3883   97.73005    4.19441   1.3671

Peak RetTime Type  Width     Area      Height     Area
  #   [min]        [min]   [mAU*s]     [mAU]      %
----|-------|----|-------|----------|----------|--------|
   3  14.909 MM    0.4144 3460.68140  139.18147  48.4097
   4  18.201 MM    0.4542 3493.33667  128.19507  48.8665
```

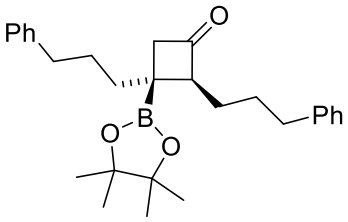

(±)-4-42

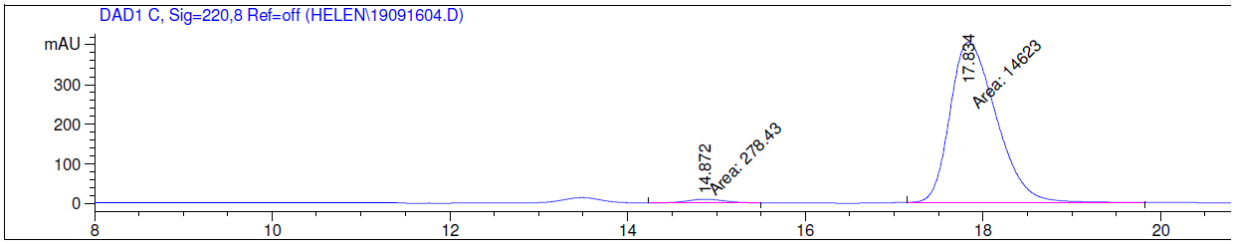


```
================================================================================
                          Area Percent Report
================================================================================

Signal 2: DAD1 C, Sig=220,8 Ref=off

Peak RetTime Type  Width     Area      Height     Area
  #   [min]        [min]   [mAU*s]     [mAU]      %
----|-------|----|-------|----------|----------|--------|
   1  14.872 MF    0.4960   278.42990    9.35556   1.8685
   2  17.834 FM    0.6022 1.46230e4   404.71014  98.1315
```

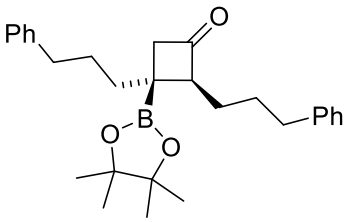

4-42

Appendix 3: X-ray crystal structure report

X-ray crystallographic data of compound 2-41

XCL Code: DGH1808 **Date:** 28 May 2018
Compound: 7-[hydroxy(4-methylphenyl)methyl]-2,3,4,7-tetrahydro-1*H*-azepinium chloride
Formula: $C_{14}H_{20}ClNO$
Supervisor: D. G. Hall **Crystallographer:** M. J. Ferguson

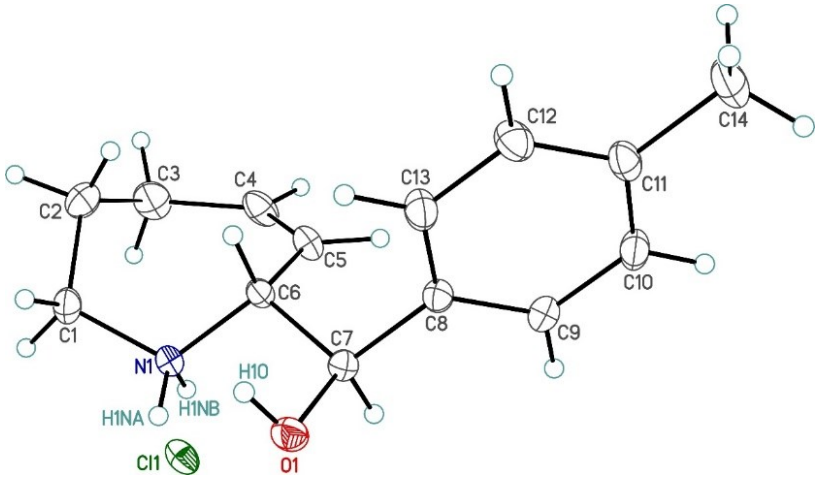

Perspective view of the 7-[hydroxy(4-methylphenyl)methyl]-2,3,4,7-tetrahydro-1H-azepinium chloride molecule showing the atom labelling scheme. Non-hydrogen atoms are represented by Gaussian ellipsoids at the 30% probability level. Hydrogen atoms are shown with arbitrarily small thermal parameters.

Crystallographic data (excluding structure factors) for the structures in this paper have been deposited with the Cambridge Crystallographic Data Centre as supplementary publication nos. CCDC 1848056. Copies of the data can be obtained, free of charge, on application to CCDC, 12 Union Road, Cambridge CB2 1EZ, UK, (fax: +44-(0)1223-336033 or e-mail: deposit@ccdc.cam.ac.Uk).

X-ray crystallographic data of compound 4-44

XCL Code: DGH1811 **Date:** 19 September 2018

Compound: 2-methyl-3-phenyl-3-(4,4,5,5-tetramethyl-1,3,2-dioxaborolan-2-yl)cyclobutyl 4-bromobenzoate

Formula: $C_{24}H_{28}BBrO_4$

Supervisor: D. Hall **Crystallographer:** Y. Zhou

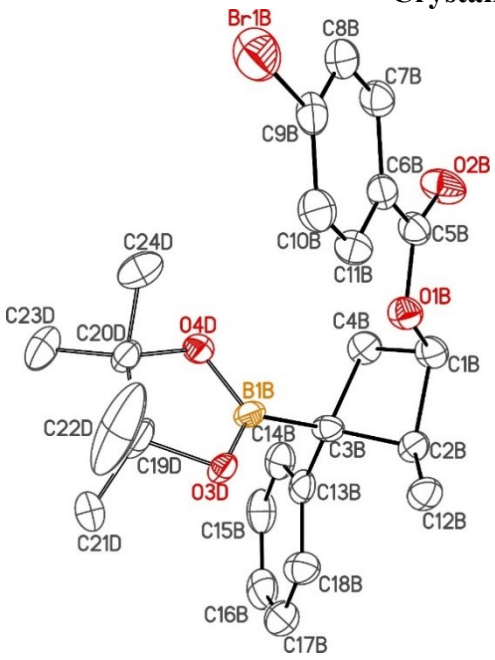

Perspective view of the second of two crystallographically independent 2-methyl-3-phenyl-3-(4,4,5,5-tetramethyl-1,3,2-dioxaborolan-2-yl)cyclobutyl-4-bromobenzoate (*moiety B*) showing the atom labelling scheme. For the clarification, another part (*Part 2*) of the disorder units of *moiety B* are shown. Non-hydrogen atoms are represented by Gaussian ellipsoids at the 30% probability level.

Crystallographic data (excluding structure factors) for the structures in this paper have been deposited with the Cambridge Crystallographic Data Centre as supplementary publication nos. CCDC 1941055. Copies of the data can be obtained, free of charge, on application to CCDC, 12 Union Road, Cambridge CB2 1EZ, UK, (fax: +44-(0)1223-336033 or e-mail: deposit@ccdc.cam.ac.Uk).